

750  
ANNALS OF THE NEW YORK ACADEMY OF SCIENCES

VOLUME 125, ART. 2      PAGES 249-772

## FORMS OF WATER IN BIOLOGIC SYSTEMS

*Conference Cochairmen*

JOSEPH F. SAUNDERS and JOHN E. FLYNN

### AUTHORS

H. J. BERENDSEN, T. G. OWE BERG, P. R. CAMP, J. F. CATCHPOOL, J. CLIFFORD, J. D. DAVIES, G. F. DOEBBLER, W. DROST-HANSEN, I. R. FENICHEL, H. FERNANDEZ-MORAN, H. S. FRANK, F. FRANKS, M. T. GONDER, E. H. GRANT, R. I. N. GREAVES, G. W. GROSS, O. HECHTER, F. HEINMETS, S. B. HOROWITZ, R. S. KIBLER, A. LEAF, G. NING LING, B. J. LUYET, A. P. MACKENSIE, N. V. B. MARSDEN, P. MAZUR, P. J. MEINICK, C. MIGCHELSEN, M. D. PERSIDSKY, B. A. PETHICA, V. RICHARDS, A. P. RINFRET, R. R. SAKAIDA, J. F. SAUNDERS, H. A. SCHERAGA, H. P. SCHWAN, W. A. SENIOR, V. SMITH, W. A. SOANES, D. T. WARNER.

*Editor*

HAROLD E. WHIPPLE



NEW YORK  
PUBLISHED BY THE ACADEMY

October 13, 1965

N66-87875  
(ACCESSION NUMBER)  
527  
CP 78739  
(INACA CN OR INX OR AD NUMBER)  
FACILITY FORM 602

# THE NEW YORK ACADEMY OF SCIENCES

(Founded in 1817)

## BOARD OF TRUSTEES

J. JOSEPH LYNCH, S. J., *Chairman of the Board*

<i>Class of 1962-1966</i>		
HILARY KOPROWSKI	HARDEN F. TAYLOR	G. W. MERCK
<i>Class of 1963-1965</i>		
W. STUART THOMPSON	EDMUND J. BLAKE, JR.	HUGH CULLMAN
<i>Class of 1964-1967</i>		
HENRY C. BRECK	LEON SHIMKIN	LOWELL WADMOND
<i>Class of 1965-1968</i>		
GORDON Y. BILLARD	FREDERICK A. STAHL	BORIS PREGEL
EMERSON DAY, <i>President of the Academy</i>		
J. JOSEPH LYNCH, S.J., <i>Past President</i>		
CHARLES W. MUSHETT, <i>Past President</i>		
EUNICE THOMAS MINER, <i>Executive Director</i>		

## SCIENTIFIC COUNCIL, 1965

EMERSON DAY, <i>President</i>		
JACOB FELD, <i>President-Elect</i>		
J. J. BURNS, <i>Vice-President</i>	MINORU TSUTSUI, <i>Vice-President</i>	
ANDRES FERRARI <i>Recording Secretary</i>	ROSS F. NIGRELLI <i>Corresponding Secretary</i>	
<i>Elected Councilors</i>		
RHODES W. FAIRBRIDGE	1963-1965	L. WILLIAM MAX
ALBERT S. GORDON	1964-1966	WALTER E. TOLLES
N. HENRY MOSS	1965-1967	H. CHRISTINE REILLY

EUNICE THOMAS MINER, *Executive Director*

### SECTION OF BIOLOGICAL AND MEDICAL SCIENCES

GABRIEL G. NAHAS, *Chairman* HERMAN COHEN, *Vice-Chairman*

#### DIVISION OF ANTHROPOLOGY

JEROME BRIGGS, *Chairman* ANNEMARIE DE WAAL MALEFIJT, *Vice-Chairman*

#### DIVISION OF INSTRUMENTATION

CARL BERKLEY, *Chairman* MYRON W. LESLIE, *Vice-Chairman*

#### DIVISION OF MICROBIOLOGY

EUGENE L. DULANEY, *Chairman* EUGENE R. L. GAUGHRAN, *Vice-Chairman*

#### DIVISION OF PSYCHOLOGY

JOSEPH F. KUBIS, *Chairman* VIRGINIA STAUDT SEXTON, *Vice-Chairman*

#### DIVISION OF ENVIRONMENTAL SCIENCES

IRVING J. SELIKOFF, *Chairman* E. CUYLER HAMMOND, *Vice-Chairman*

### SECTION OF CHEMICAL SCIENCES

EMIL J. MORICONI, *Chairman* ROBERT ROUSE, *Vice-Chairman*

#### DIVISION OF BIOCHEMISTRY

PAUL GREENGARD, *Chairman* BERT N. LA DU, JR., *Vice-Chairman*

#### DIVISION OF ORGANOMETALLIC CHEMISTRY

WILLIAM J. CONSIDINE, *Chairman* MINORU TSUTSUI, *Vice-Chairman*

#### DIVISION OF POLYMER SCIENCE

FRANCIS MICHELOTTI, *Chairman* E. H. IMMERGUT, *Vice-Chairman*

### SECTION OF GEOLOGICAL SCIENCES

LEWIS G. WEEKS, *Chairman* BRUCE C. HEEZEN, *Vice-Chairman*

### SECTION OF PHYSICAL SCIENCES

MORRIS H. SHAMOS, *Chairman* BERNARD KRAMER, *Vice-Chairman*

#### DIVISION OF BIOPHYSICS

ROSALYN YALOW, *Chairman* IRA PULLMAN, *Vice-Chairman*

#### DIVISION OF ENGINEERING

I. B. LASKOWITZ, *Chairman* JULIAN D. TEBO, *Vice-Chairman*

#### DIVISION OF MATHEMATICS

AUBREY W. LANDERS, *Chairman* CHARLES LEWIS, S.J., *Vice-Chairman*

### SECTION OF PLANETARY SCIENCES

HAROLD L. STOLOV, *Chairman* RICHARD M. SCHOTLAND, *Vice-Chairman*

The Sections and Divisions hold meetings regularly, one evening each month, during the academic year, October to May, inclusive. All meetings are held at the building of The New York Academy of Sciences, 2 East Sixty-third Street, New York, New York 10021.

Conferences are also held at irregular intervals at times announced by special programs.



ANNALS OF THE NEW YORK ACADEMY OF SCIENCES

VOLUME 125, ART. 2      PAGES 249-772

*Editor*  
HAROLD E. WHIPPLE

October 13, 1965

*Managing Editor*  
HURD HUTCHINS

FORMS OF WATER IN BIOLOGIC SYSTEMS\*

*Conference Cochairmen*  
JOSEPH F. SAUNDERS and JOHN E. FLYNN

---

CONTENTS

Introductory Remarks. <i>By</i> JOSEPH F. SAUNDERS. . . . .	251
The Effect of Solutes on the Structure of Water and its Implications for Protein Structure. <i>By</i> HAROLD A. SCHERAGA. . . . .	253
Hydrophobic Hydration and the Effect of Hydrogen Bonding Solutes on the Structure of Water. <i>By</i> FELIX FRANKS. . . . .	277
Diffusional Specificity in Water. <i>By</i> I. ROBERT FENICHEL AND SAMUEL B. HOROWITZ. . . . .	290
Bonds in Water and Aqueous Solutions. <i>By</i> T. G. OWE BERG. . . . .	298
The Formation of Ice at Water-Solid Interfaces. <i>By</i> P. R. CAMP. . . . .	317
Electrical Properties of Bound Water. <i>By</i> H. P. SCHWAN. . . . .	344
The Effect of Various Biologic Compounds on Proton Conductivity and Activation Energy in Ice. <i>By</i> F. HEINMETS. . . . .	355
Hydration Structure of Fibrous Macromolecules. <i>By</i> H. J. C. BERENDSEN AND C. MIGCHELSEN. . . . .	365
Ion Incorporation and Activation Energies of Conduction in Ice. <i>By</i> GERARDO WOLFGANG GROSS. . . . .	380
Mechanism of the Electrical Conductivity in Ice. <i>By</i> C. JACCARD. . . . .	390
The Physical State of Water in Living Cell and Model Systems. <i>By</i> GILBERT NING LING. . . . .	401
The Structure of Water Neighboring Proteins, Peptides and Amino Acids as Deduced from Dielectric Measurements. <i>By</i> EDWARD H. GRANT. . . . .	418
Solute Behavior in Tightly Cross-Linked Dextran Gels. <i>By</i> N. V. B. MARSDEN. . . . .	428
N.M.R. and Raman Properties of Water in Colloidal Systems. <i>By</i> J. CLIFFORD, B. A. PETHICA, W. A. SENIOR. . . . .	458

\*This series of papers is the result of a conference entitled *Forms of Water in Biologic Systems*, held by The New York Academy of Sciences on October 5, 6, 7 and 8, 1964, under No 6-729(33-20-001).

The Effects on Biologic Systems of Higher-Order Phase Transitions in Water. By WALTER DROST-HANSEN.....	471
Phase Transitions Encountered in the Rapid Freezing of Aqueous Solutions. By B. J. LUYET.....	502
Factors Affecting the Mechanism of Transformation of Ice Into Water Vapor in the Freeze-Drying Process. By ALAN P. MACKENZIE.....	522
Separate Effects of Freezing, Thawing and Drying Living Cells. By R.I.N. GREAVES AND J. D. DAVIES.....	548
Transport Properties of Water. By ALEXANDER LEAF.....	559
Diffusion and the Transport of Organic Nonelectrolytes in Cells. By SAMUEL B. HOROWITZ AND I. ROBERT FENICHEL.....	572
The Hydrate Microcrystal Theory of Anesthesia. By J. F. CATCHPOOL.....	595
A Proposed Water-Protein Interaction and Its Application to the Structure of the Tobacco Mosaic Virus Particle. By DONALD T. WARNER.....	605
Intracellular Water Structure and Mechanisms of Cellular Transport. By OSCAR HECHTER.....	625
Rapid Freezing and Thawing of Blood. By R. R. SAKAIDA, G. F. DOEBBLER, R. S. KIBLER, A. P. RINFRET.....	647
The Role of Cell Membranes in the Freezing of Yeast and Other Single Cells. By PETER MAZUR.....	658
New Approaches in Measuring the Linear Rate of Ice Crystallization in Water and Aqueous Solutions. By MAXIM D. PERSIDSKY AND VICTOR RICHARDS..	677
Enzyme Patterns of Tumors Demonstrated Histochemically in Cryostat Sections. By P. J. MELNICK.....	689
Chemical and Morphologic Changes in the Prostate Following Extreme Cooling. By MAURICE J. GONDER, WARD A. SOANES, VERNON SMITH.....	716
Summation and General Discussion.....	730
H. S. FRANK.....	730
H. FERNÁNDEZ-MORÁN.....	739
GENERAL.....	754

*Copyright, 1965, by The New York Academy of Sciences.*

*All rights reserved. Except for brief quotations by reviewers, reproduction of this publication in whole or in part by any means whatever is strictly prohibited without written permission from the publisher.*

## INTRODUCTORY REMARKS

Joseph F. Saunders

*Bioscience Programs Division,  
National Aeronautics and Space Administration,  
Washington, D.C.*

We are deeply grateful to The New York Academy of Sciences, the National Aeronautics and Space Administration and the Office of Naval Research for sponsoring this worthy conference.

Our program is one that we consider to be the interdisciplinary type, including basic and applied studies of the complexity of water in its various forms. At first, we thought of devoting this meeting to the field of cryobiology. Later, however, we decided that we should not limit the scope of the conference to the study of water as ice, but to extend our discussion to the physiochemical and biologic parameters governing the role of water in living systems. We hoped for a meeting of biologists, chemists, physicists, clinicians and engineers so that the exchange of views and ideas would shed more light on the complexity of water.

Most of us consider water as a homogeneous fluid with definite physical properties subject to variation or alteration as a function of temperature and pressure. We know that water is indispensable for the maintenance of normal metabolic activity. We appreciate, too, that disturbances occur in water metabolism with and without consistent alterations in other metabolic processes. For instance, in many diseased states, there is an imbalance in water metabolism without any significant disturbance in electrolyte metabolism. On the other hand, during the rapid freezing of biologic systems such as erythrocytes, water is transformed into ice with simultaneous dehydration and concentration of electrolytes in the tissue.

Many cryobiologists believe that the manner of freezing of living systems is irrelevant, so long as a protective substance is added to the medium. There are still those who assume that, because of their structure, many substances act as water or as substitutes for water during freezing and lyophilization. Perhaps this conference may tend to illuminate such concepts.

With the advent of numerous new physicochemical techniques, we find that water is not the simple, homogeneous substance we once assumed it to be. Depending on its environment or substrate, if you will, such properties of water as total energy, ionic mobility, viscosity, dielectric behavior and position among molecular fluids are subject to obvious as well as subtle changes. We often wonder how microorganisms can survive at  $-70^{\circ}\text{C}$ . and lower, perhaps. Is there a "built in" protective mechanism against damage from ice formation?

Why is it possible to preserve blood indefinitely at temperatures as low as those provided by cryogenic gases? Certainly rapid freezing to avoid massive destruction by ice formation is not the only answer.

What is the source of water or mechanism(s) by which an organism obtains water from a hydrocarbon environment?

How does water contribute to the molecular architecture of living systems not only in adult form, but in embryonic form? Water must be the medium upon which unique cellular morphology is dependent. Perhaps it is water that is the directing or orienting force in the morphogenic development of tissue specificity, membrane structure and function, and biochemical functionality.

Cellular transport, oxygen transfer in respiratory pigments, photosynthesis and every other process we can think of depend upon water. Yet, the fundamental mechanisms by which water regulates life processes continue to be evasive so as to handicap us in our quest for understanding life.

We hope that this conference will serve to clarify and elucidate at least a few of the problems associated with the ubiquitous water molecule.

We believe that experimental data will be presented to confirm some of the theoretical values established for some of the parameters of water behavior. Finally, we wish that the papers will engender broad discussion of problems, and new ideas which result in new and significant avenues of approach to our understanding of the structure and function of water in living systems.

# THE EFFECT OF SOLUTES ON THE STRUCTURE OF WATER AND ITS IMPLICATIONS FOR PROTEIN STRUCTURE\*

Harold A. Scheraga

*Department of Chemistry,  
Cornell University, Ithaca, N. Y.*

The properties of aqueous solutions depend largely on the interaction of water with the dissolved solute. In order to provide a statistical mechanical treatment of such systems it is necessary to have a model for water and for the influence of the solute and solvent components on each other. A very fruitful discussion of the properties of aqueous solutions, which provides a basis for the formulation of appropriate models, has recently been presented by Frank and Wen.<sup>1,2</sup>

It is necessary to distinguish between polar and nonpolar solutes since the nature of their interaction with water differs. Frank and Wen<sup>1,2</sup> have discussed both types of systems. However, from a statistical mechanical point of view, most of the recent progress has been made in the field of solutions of nonpolar solutes. Therefore, this paper will be confined to such systems.† We will consider here the recent developments in our understanding of the structure of water and the influence of nonpolar solutes on it; also, we will discuss a related topic of considerable current interest — the interaction between nonpolar groups of proteins in water, the so-called “hydrophobic bond”.<sup>4</sup> This interaction is of considerable importance in the stability of proteins in aqueous solution.

## *Structures of Liquid H<sub>2</sub>O and D<sub>2</sub>O*

The structural features of liquid water depend primarily on the ability of the water molecule to participate in any number of hydrogen bonds, up to a maximum of four, by utilizing its two hydrogens and the two lone pairs of its oxygen. There are many structures in which water achieves its maximum (tetra-) coordination, one of them being the ordinary form of ice<sup>5</sup> which exists at 0°C. and 1 atm. pressure. The ice lattice is a rather open one, accounting for the fact that its density is lower than that of liquid water at the melting point.

When ice melts, there still exists a high degree of hydrogen bonding in the resulting liquid. The history of theories of water structure is essen-

\*This work was supported by a research grant (AI-0473) from the National Institute of Allergy and Infectious Diseases of the National Institutes of Health, U. S. Public Health Service, and by a research grant (GB-2238) from the National Science Foundation.

†A statistical mechanical treatment of aqueous salt solutions is being attempted<sup>3</sup>; the work is not yet complete. However, see “Note added in proof” at end of this paper.

tially a story of the various forms in which this hydrogen bonding was envisaged as existing; the modern view, emphasizing extensive hydrogen bonding, was initiated by Bernal and Fowler.<sup>6</sup> Two recent surveys of theories of water structure have been presented elsewhere.<sup>7,8</sup> From these considerations,<sup>7</sup> the "flickering cluster" concept proposed by Frank and Wen<sup>1,2</sup> was selected and used by Nemethy and Scheraga<sup>7,9</sup> as a basis to develop theories of liquid  $\text{H}_2\text{O}$  and  $\text{D}_2\text{O}$ .

Frank and Wen<sup>1,2</sup> have argued that the formation of a hydrogen-bonded dimer of two  $\text{H}_2\text{O}$  molecules makes it easier to form additional hydrogen bonds with other  $\text{H}_2\text{O}$  molecules because of the contribution (to the partially covalent hydrogen bond) of a resonant form having a partial charge separation. In other words, the formation of hydrogen bonds in the liquid is a cooperative phenomenon, i.e. the bonds are not made and broken singly but several at a time, thus producing short-lived "clusters" of highly hydrogen-bonded regions surrounded by nonhydrogen-bonded molecules. These clusters may be expected to be compact and nearly spherical in shape. On

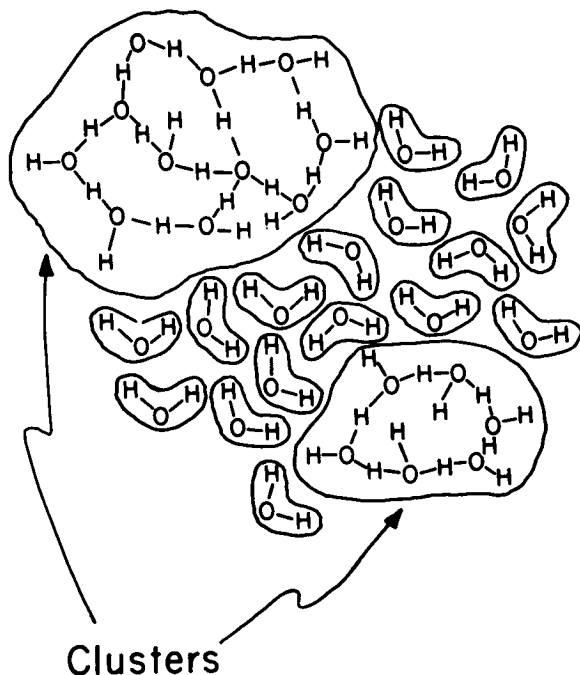


FIGURE 1. Schematic representation of liquid water, showing hydrogen-bonded clusters and unbonded molecules. The molecules in the interior of the clusters are tetracoordinated, but not drawn as such in this two-dimensional diagram (Nemethy & Scheraga<sup>7</sup>).

the basis of the Frank-Wen assumptions, no appreciable amount of small aggregates (dimers, trimers, etc.) will exist — only clusters and monomers. The model is represented in FIGURE 1. While there is probably a distribution of cluster sizes, the theory was developed on the assumption that all clusters are of uniform size, equal to the mean size, which varies with temperature.

Even though there are only two main structures, free molecules and clusters, the individual molecules may be distributed among five classes, depending on the number of hydrogen bonds in which they are involved. The monomeric species constitute one class, and there are four more classes of species in the cluster; inside the cluster there are tetrabonded species, while on the surface of the cluster there are tri-, di-, and mono-bonded species. An energy level can be assigned to each species, depending on the number of its hydrogen bonds, as shown in FIGURE 2. The ground state is occupied by tetracoordinated species; as hydrogen bonds are broken the upper states become populated. The state labeled "vapor" lies much higher on the energy scale and does not play a role in a theory of the liquid. Even though the "unbonded" molecules (i.e. the monomeric species) do

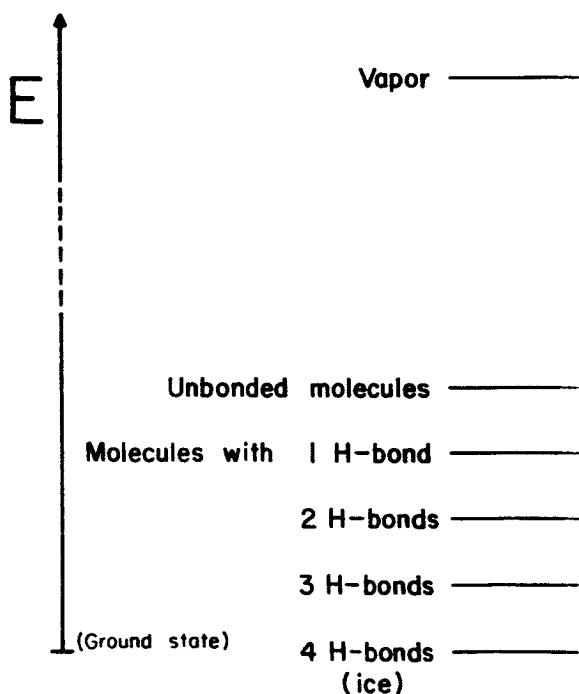


FIGURE 2. Schematic representation of energy levels for H<sub>2</sub>O molecules in liquid water (Nemethy & Scheraga<sup>7</sup>).

not participate in hydrogen bonding, they are still close enough in the liquid (unlike those in the vapor) to interact by dipole forces.

In order to completely define the state of the system, the populations of the various energy levels must be computed. For this purpose, it is necessary to specify the spacings of the levels. Consider first the difference in energy between the ground state (level 4) and that corresponding to the unbonded molecules (level u). In order to bring a molecule from level 4 to level u, four hydrogen bonds must be broken; but a molecule in level u has approximately eight neighbors<sup>7</sup> with which it interacts by dipole forces. Therefore, the separation between these two levels is the *difference* in the energy to break four hydrogen bonds and the dipole interaction energy with eight neighbors. This net energy was taken as an empirical parameter in the theory, obtained by fitting the resulting equations to experimental data for the thermodynamic properties of liquid water; the resulting value was a reasonable one, on the basis of current estimates of hydrogen bond energies and dipole interaction energies. In addition, a second parameter, the "free volume" for the translational motion of unbonded molecules, was introduced; it too was found to be a reasonable one, on the basis of known values of the free volume of many substances. The distance between levels 4 and u was divided up equally in order to obtain the location of levels 1, 2 and 3.

The populations of the various levels are not independent. For example, for a cluster containing a given number of molecules, the number on the surface is not independent of the number inside, i.e. there is a correlation between the number on the surface and the number inside, a kind of surface-to-volume ratio. These cluster correlations were put in the form of empirical equations (relating the mole fractions of the various species), obtained by building models of various sized clusters and counting the number of each species. With these cluster correlations and the Boltzmann principle, it was possible to write the partition function for the system, and evaluate it in order to calculate the populations of the levels and the thermodynamic parameters of the system. The internal motions of each species were represented by Einstein oscillator functions, using frequencies from infrared and Raman spectra.

The first result which emerged from the calculation is the cluster size. These data are shown in TABLE 1 and FIGURE 3 and provide a quantitative description for the model shown in FIGURE 1. The original papers<sup>7,9</sup> may be consulted for the other parameters describing the clusters (e.g. the mole fractions of the various species). From recent infrared spectroscopic studies, Buijs and Choppin<sup>10</sup> obtained structural parameters for liquid H<sub>2</sub>O, with values which appear to be similar to the theoretical ones.<sup>7</sup> The cluster sizes given in TABLE 1 are also compatible with data on the viscosity of water<sup>11,12</sup> and on the conductivity of aqueous solutions of electrolytes.<sup>12</sup>



TABLE 1  
TEMPERATURE-DEPENDENCE<sup>7,9</sup> OF CLUSTER SIZE,  $n_{cl}$ , AND THE MOLE FRACTION,  $x_u$ , OF NONHYDROGEN-BONDED MOLECULES, IN LIQUID  $H_2O$  AND  $D_2O$

t, °C.	$n_{cl}$		$x_u$	
	$H_2O$	$D_2O$	$H_2O$	$D_2O$
0	91	—	0.24	—
4	—	117	—	0.23
10	72	97	0.27	0.25
20	57	72	0.29	0.27
30	47	56	0.32	0.30
40	38	44	0.34	0.32
50	32	35	0.36	0.34
60	28	29	0.38	0.36

It is of interest to compare  $D_2O$  and  $H_2O$  at this point. The same theory is applicable to both systems; the only differences are in: (1) the hydrogen bond energy, (2) the vibrational frequencies, and (3) the masses and moments of inertia. The hydrogen bond energy was taken as 0.24 kcal./mole higher for  $D_2O$  than for  $H_2O$ , and the vibrational frequencies, masses and moments of inertia were taken in accord with theoretical values for isotopic substitution. The resulting cluster sizes in  $D_2O$  are also shown in TABLE 1 and FIGURE 3. It can be seen that more structural order exists in  $D_2O$  than in  $H_2O$  at a given temperature.

The partition function was also used to obtain the thermodynamic parameters. The calculated values of the free energy, enthalpy, and en-

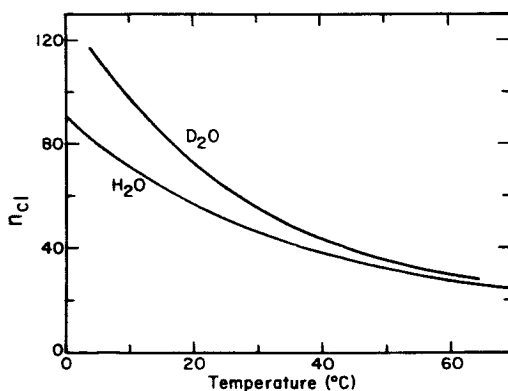


FIGURE 3. Sizes of clusters,  $n_{cl}$ , in liquid  $H_2O$  and  $D_2O$  as functions of temperature (Nemethy & Scheraga<sup>9</sup>).

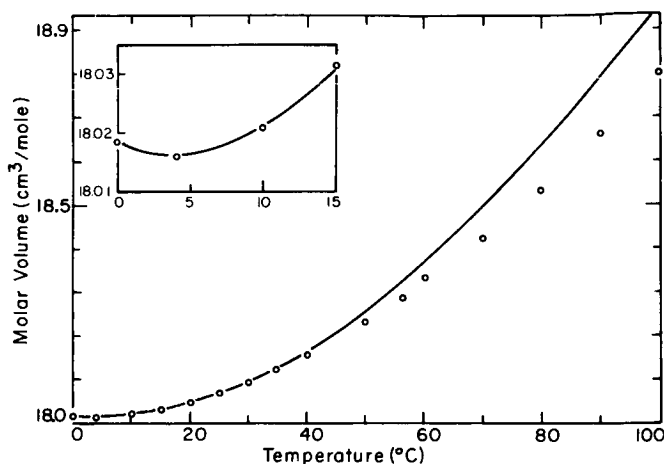


FIGURE 4. Comparison of calculated and experimental values of the molar volume of  $\text{H}_2\text{O}$  as function of temperature. The inset is an enlargement at low temperature. The agreement is within 0.5 per cent near  $70^\circ\text{C}$ . and much better at lower temperatures. (Nemethy & Scheraga<sup>7</sup>).

trophy of liquid  $\text{H}_2\text{O}$  agree with experimental data to within an error of less than three per cent. For liquid  $\text{D}_2\text{O}$  the overall average error is six per cent. The calculated temperature dependence of  $c_v$  for both  $\text{H}_2\text{O}$  and  $\text{D}_2\text{O}$  is too large. The calculated results agree well with the radial distribution curves derived from x-ray diffraction data.

The temperature dependence of the molar volumes of liquid  $\text{H}_2\text{O}$  and  $\text{D}_2\text{O}$  are shown in FIGURES 4 and 5, respectively; the inserts in these

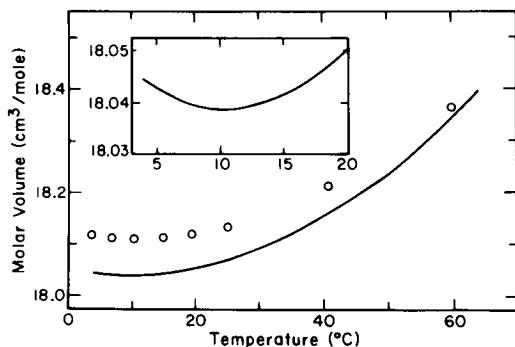


FIGURE 5. Comparison of calculated and experimental values of the molar volume of  $\text{D}_2\text{O}$  as function of temperature. The inset shows the calculated curve near the minimum at a larger scale. The relative error is within 0.4 per cent over the range from  $4^\circ$  to  $25^\circ\text{C}$ ., decreasing to 0.1 per cent at  $60^\circ\text{C}$ . (Nemethy & Scheraga<sup>11</sup>).

FIGURES are enlargements at low temperature. Aside from the behavior at low temperature, it is seen that the molar volume increases monotonically with temperature. If we ignore, for the moment, the variation of  $n_{cl}$  with temperature, i.e., if we assume that  $n_{cl}$  is constant at all temperatures, then a liquid consisting of clusters and unbonded molecules *should* show a monotonic rise in  $V$  with  $T$  because the volumes of ice-like clusters and normal unbonded liquids normally do increase with temperature. However, recognizing that  $n_{cl}$  does decrease with increasing temperature (See TABLE 1), it can be seen that, as the temperature is raised, molecules are removed from the open-spaced, low-density ice-like structure of the clusters and packed more densely (average coordination number of 8) in the unbonded liquid; this process contributes a *decrease* in molar volume with increasing temperature. The combination of this latter process together with the normal thermal expansion of the ice-like clusters and unbonded liquid gives rise to the curves of FIGURES 4 and 5, with minima at 4°C. and 11.2°C. for  $H_2O$  and  $D_2O$ , respectively. In order to compute the curves of FIGURES 4 and 5, one needs the data of TABLE 1 and the coefficients of thermal expansion for the ice-like clusters and unbonded liquid. For the clusters, the coefficient of expansion of ice (the same for  $H_2O$  and  $D_2O$ ), extrapolated into the liquid region, was used; for the unbonded liquid, an empirical equation (with three constants, obtained by fitting to experimental data on  $H_2O$ , and assumed to be the same for  $D_2O$ ), was used. The agreement between theory and experiment is excellent (see FIGURES 4 and 5), the errors being noted in the legends to the FIGURES. Especially noteworthy is the calculation of the minima at 4° and 10.2°C., for  $H_2O$  and  $D_2O$  respectively. Excellent agreement was also obtained between the calculated and observed compressibilities.

Given the success of the theory in accounting for the thermodynamic properties of both  $H_2O$  and  $D_2O$ , and the experimental confirmation of some of the parameters obtained by Buijs and Choppin,<sup>10</sup> we may regard the model as sufficiently accurate for its use in attempting to understand the effect of solutes on the structure of the liquid and on the properties of the resulting solutions. We, therefore, consider next the properties of aqueous solutions of hydrocarbons.

#### *Aqueous Solutions of Hydrocarbons*

In considering the properties of hydrocarbon solutions, we focus attention on the thermodynamic parameters for the processes in which one mole of hydrocarbon is transferred from the pure liquid (or from a nonpolar solvent) into a dilute aqueous solution. The resulting solutions are anomalous in that they are nonideal. If they were ideal we would expect the changes in volume and enthalpy to be zero and the changes in entropy and free energy to correspond to those for ideal mixing. Actually,<sup>4,13</sup> for hydro-

carbon solutions, the changes in volume and enthalpy are negative and there is a very large negative excess entropy change over the entropy of ideal mixing; this leads to a large positive  $\Delta F^\circ$  and hence to a low solubility because of the dominance of the entropy term over the enthalpy one.

Frank and Evans<sup>13</sup> proposed that the negative enthalpy and entropy terms are due to the ordering of the water by the hydrocarbon solute, i.e. while pure water contains "flickering clusters," the water in a hydrocarbon solution is even more highly hydrogen-bonded and ordered. If this explanation is accepted, the solubility data can be computed from theory.<sup>14</sup> However, before accepting the explanation, we should consider two questions: (1) *why* does the dissolving of hydrocarbon in water lead to an ordering of the water, and (2) why is the process accompanied by a decrease in volume?

In order to answer these two questions, consider first the structures shown in FIGURE 6. When a near-spherical cluster forms in pure water, it

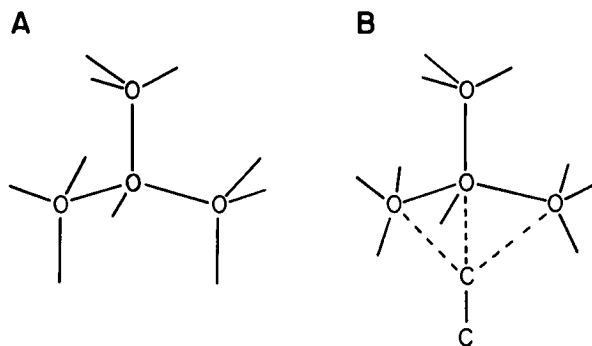


FIGURE 6. A. Fourfold coordination of a fully hydrogen-bonded water molecule in a cluster of the pure liquid. B. Increase in coordination number of the same molecule to five on introduction of a nonpolar solute nearest neighbor. The dotted lines do not correspond to bonds, but represent the increase in coordination (Nemethy & Scheraga<sup>14</sup>).

tends to have a convex surface. Therefore, a tetrabonded molecule will be inside the cluster, as shown in FIGURE 6A. The energy of such a molecule is determined only by the four neighbors to which it is hydrogen-bonded. The other molecules in the cluster are too far away to affect the energy of the given molecule; in fact, the energy level of the tetrabonded species in FIGURE 2 corresponds to a molecule with only four neighbors. On the other hand, when a "flickering cluster" forms next to a hydrocarbon molecule in dilute solution, the surface of the cluster can be concave in the neighborhood of the hydrocarbon; i.e. the hydrocarbon molecule can approach the given water molecule on the surface of the cluster, and thereby

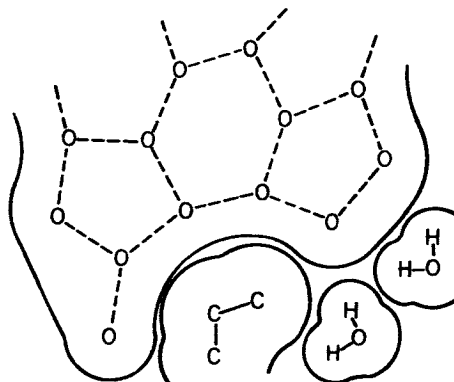


FIGURE 7. Schematic cross-section of a hydrogen-bonded water cluster near a hydrocarbon solute molecule, indicating the formation of a partial cage around the solute. The O-H...O hydrogen bonds are represented by broken lines. The heavy lines correspond to the surfaces defined by the van der Waals contact radii of the molecules involved (Nemethy & Scheraga<sup>14</sup>).

affect its energy (FIGURE 6B). Since the surface is concave, the surface water molecules can take part in four hydrogen bonds, with the hydrocarbon molecule as a fifth neighbor; in other words, the water molecule becomes pentacoordinated. The cluster, in essence, forms a partial cage around the hydrocarbon, as shown in FIGURE 7. The acquisition of a fifth neighbor lowers the energy of the tetrahydrogen-bonded molecule by an amount  $\Delta E_i$ , which depends on the van der Waals interaction energy between the water molecule and hydrocarbon molecule. An unbonded water molecule, on the other hand, already has a high coordination number in pure water. It can acquire a hydrocarbon neighbor only if the latter replaces a neighboring water molecule. By this process, a strong water-water dipole interaction is replaced by the much weaker water-solute induction and dispersion forces. Therefore, the energy of the unbonded water molecule will be raised by an amount  $\Delta E_r$ , which depends on the difference between the water-water interaction energy and the water-hydrocarbon interaction energy. Molecules with one to three hydrogen bonds, lying on the surface of clusters, also acquire a hydrocarbon neighbor by replacement of an unbonded water neighbor; hence their energy levels are also raised by  $\Delta E_r$ . We thus obtain the energy level diagram shown in FIGURE 8. The values of  $\Delta E_i$  and  $\Delta E_r$  are empirical parameters, obtained ultimately by fitting the theoretical equations to experimental data; when evaluated, they can be rationalized in terms of the known values of van der Waals and dipole interaction energies.

It is important to note that the only water molecules which occupy the new energy levels are those in the first layer around the hydrocarbon; all

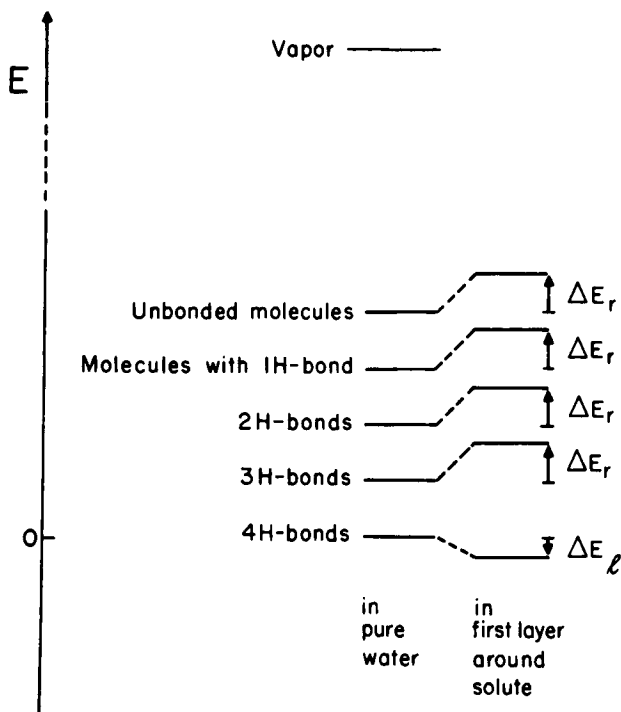


FIGURE 8. Schematic representation of the energy level changes occurring on transfer of water from the pure liquid to the structure next to a nonpolar solute. It should be emphasized that these shifts in energy levels occur only for water molecules in the first layer around the hydrocarbon (Nemethy & Scheraga<sup>14</sup>).

other water molecules occupy the old set of energy levels, i.e. the same ones which pertain to pure water. This is because van der Waals forces fall off very rapidly with distance; hence, only those water molecules immediately adjacent to a hydrocarbon molecule will have their energies affected. The number the water molecules in the first layer will depend, of course, on the size of the hydrocarbon.

Considering the new set of energy levels, it can be seen that there will be relatively more molecules in the lower states, compared to the old set of levels. Hence, in the presence of the hydrocarbon, there is a greater degree of hydrogen bonding and more ordering, as predicted by Frank and Evans.<sup>13</sup> In other words, the presence of the hydrocarbon in water affects the energies of those water molecules immediately adjacent to it in such a way as to favor the populating of the lower states, compared to the situation in pure water.

Since the hydrocarbon fills space which would be empty in an ordinary ice-like cluster (see FIGURES 6 and 7), there will be a decrease in volume

when hydrocarbon molecules are transferred from the pure liquid into water.

The concept of a partial cage derives from information on the crystal structures of hydrates of the rare gases and hydrocarbons.<sup>13</sup> In these structures there are large polyhedral cages (larger than the voids in ordinary ice) formed by tetra-hydrogen-bonded water molecules with cavities ranging in diameter from 5.2 to 6.9 Å. The hole in the cage is filled by a hydrocarbon molecule which effectively increases the coordination number of the water molecules in the wall of the cage to five. In the crystal, the solute molecules in neighboring cages act cooperatively in stabilizing the structure, since a given water molecule can interact with more than one solute molecule. However, in dilute solution, two solute molecules do not approach each other close enough to provide this cooperative interaction. Therefore, partial cages, rather than complete cages, will be encountered, i.e., one obtains the partial cage around a hydrocarbon, the partial cage being itself part of a larger cluster, as shown in FIGURE 7.

The calculation of the populations of the new set of levels was carried out as in the case of pure water, employing empirical cluster correlation equations and the Boltzmann principle to obtain the partition function.<sup>14</sup> It was thus possible to calculate the mole fractions of the various hydrogen bonded species in the first layer around the hydrocarbon. The increase in ice-likeness upon introduction of a hydrocarbon into water may be represented in terms of  $x_{HB}^c$ , the fraction of unbroken hydrogen bonds; these data are shown in FIGURE 9.

The partition function also yielded values of the standard free energies, enthalpies and entropies of solution for aliphatic and aromatic hydrocar-

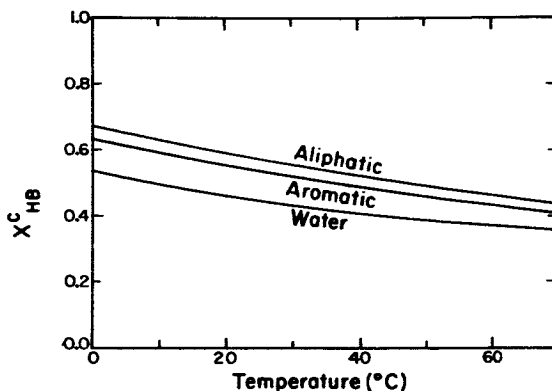


FIGURE 9. The increase in "ice-likeness" on introducing a solute into water.  $x_{HB}^c$  (referred to perfectly crystalline ice as having  $x_{HB} = 1$ ) is plotted against temperature for pure water, and for the *first layer of water* around molecules of saturated aliphatic and of aromatic hydrocarbons (Nemethy & Scheraga<sup>14</sup>).

bonds which are in good agreement with experimental data over the temperature range of 0° to 70°C. Estimates of the volume decreases on solution were also obtained. The dependence of the thermodynamic parameters on hydrocarbon size arises directly from the fact that, the larger the hydrocarbon molecule, the greater will be the number of water molecules in the first layer around it having their energies affected.

Recent experimental data<sup>16</sup> indicate that the solubilities of hydrogen containing hydrocarbons are similar, but not identical, in H<sub>2</sub>O and D<sub>2</sub>O. However, the theory of the solubility of hydrocarbons in D<sub>2</sub>O has not yet been completed.<sup>17</sup>

With the good agreement between the theoretical and experimental thermodynamic parameters for hydrocarbon solutions, we may have some confidence in the model, and proceed to use it to treat the interactions of hydrocarbons in solution, i.e., the hydrophobic bond.

#### *Formation of Hydrophobic Bonds*

The interaction of hydrocarbons in aqueous solution was at first thought to arise simply from the van der Waals forces between the hydrocarbon molecules.<sup>18</sup> However, Kauzmann<sup>19</sup> and Kirkwood<sup>20</sup> later pointed out that changes in the structure of water surrounding the nonpolar groups must play an important role in the formation of hydrophobic bonds. In fact, it was later shown<sup>21</sup> that the contribution from the van der Waals interaction between two hydrocarbon molecules is only about 45 per cent of the total free energy of formation of a hydrophobic bond at 25°C; of course, in the liquefaction of *pure* hydrocarbons, the van der Waals contribution is essentially the only one.

If two nonpolar side chains of a protein are in water, they will have an environment similar to that described in the previous section for hydrocarbons in water. When the nonpolar groups approach each other until they touch (within their van der Waals radii), there will be a decrease in the total number of water molecules in contact with them (see FIGURE 10). This can be considered as a *partial* reversal of the solution process discussed in the previous section. Therefore, if ice-like regions are found when hydrocarbons are introduced into water, the partial removal of hydrocarbon from water (i.e., formation of a hydrophobic bond) is accompanied by a melting of ice-like regions; also, the thermodynamic parameters for formation of hydrophobic bonds will have the opposite signs of those for the solution process. Formation of a hydrophobic bond involves not only these changes in water structure but also a van der Waals interaction between the two nonpolar side chains.

The same energy parameters, used to compute the properties of aqueous hydrocarbon solutions, were used to compute the thermodynamic parameters for the formation of hydrophobic bonds.<sup>21</sup> These calculations were



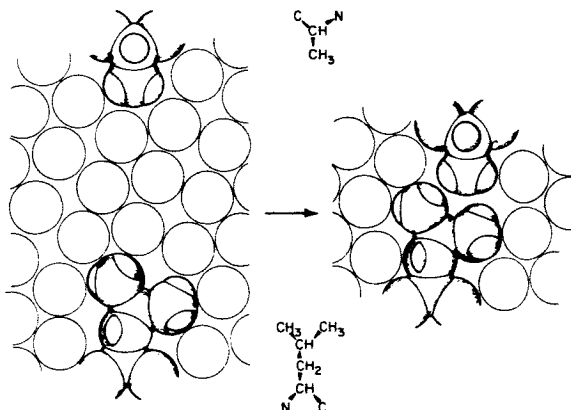


FIGURE 10. Schematic representation of the formation of a hydrophobic bond between two isolated side chains (alanine and leucine). The bond is formed through an approach of the two side chains until they touch, with a reduction of the number of nearest water neighbors. The extent of contact shown here is less than the maximum obtainable for the two side chains. Water molecules are shown only schematically, without indicating particular orientations or hydrogen-bonded networks (Nemethy & Scheraga<sup>21</sup>).

carried out for all possible pairs of side chains which normally occur in proteins, and for minimum and maximum degrees of contact between the partners forming the hydrophobic bond. A representative set of pairs of interactions is shown in FIGURE 11. The thermodynamic parameters for these pairs are listed in TABLE 2. More extensive tables of data are given in the original paper.<sup>21</sup> The ranges of values at 25°C. for interactions between all possible pairs of side chains are:  $\Delta F_{H\phi}^\circ = -0.2$  to  $-1.5$  kcal./mole,  $\Delta H_{H\phi}^\circ = +0.3$  to  $+1.8$  kcal./mole, and  $\Delta S_{H\phi}^\circ = +1.7$  to  $+11$  e.u.

It should be emphasized that these data apply to pair interactions. The calculations have also been carried out<sup>21</sup> for the bringing together of three nonpolar side-chains (originally surrounded by water, but now involved in a triple hydrophobic interaction). This process can be continued for higher multiple interactions, the asymptotic limit corresponding to the process in which many nonpolar groups are taken out of water and assembled into a nonpolar region. Thus, the calculated values approach those obtained for the solution of hydrocarbons in water, with of course the opposite sign. This emphasizes that it is erroneous to use hydrocarbon solubility data as a measure of the strength of hydrophobic bonds involving *pair* interactions; the solubility data pertain to the multiple interaction, rather than to the pair interaction.

It has already been mentioned that the solubilities of hydrogen-containing hydrocarbons are similar, but not identical,<sup>16</sup> in H<sub>2</sub>O and D<sub>2</sub>O. This

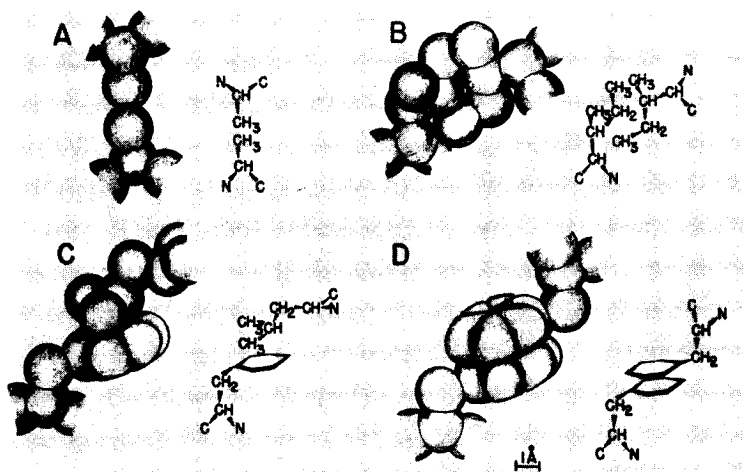


FIGURE 11. Illustrative examples of hydrophobic bonds between pairs of isolated side chains. The hydrogens are not indicated individually. Drawn to scale, but with the van der Waals radii reduced by 20 per cent for the sake of clarity. The structural formulas to the right of each space-filling drawing indicate the arrangement of the atoms. A, alanine-alanine bond (minimum strength); B, isoleucine-isoleucine bond (maximum strength); C, phenylalanine-leucine bond (maximum strength); D, phenylalanine-phenylalanine bond (maximum strength) (Nemethy & Scheraga<sup>21</sup>).

would suggest that the strengths of hydrophobic bonds between hydrogen-containing nonpolar side chains would be similar, but not identical, in  $H_2O$  and  $D_2O$ . Therefore, differences in the thermal stability of proteins in  $H_2O$  and in  $D_2O$  probably arise from isotopic effects on the strengths of hydrogen bonds, as well as from small differences in hydrophobic bond strengths in the two solvents. Differences in hydrophobic bond strength in  $H_2O$  and  $D_2O$  also give rise to differences in the critical concentration for formation of detergent micelles.<sup>16</sup>

TABLE 2  
THEORETICAL THERMODYNAMIC PARAMETERS<sup>21</sup> FOR FORMATION OF HYDROPHOBIC BONDS OF FIGURE 11 AT 25°C.

Side Chains	$\Delta F^\circ_{H\phi}$ kcal./mole	$\Delta H^\circ_{H\phi}$ kcal./mole	$\Delta S^\circ_{H\phi}$ e.u.
Alanine-alanine	-0.3	0.4	2.1
Isoleucine-isoleucine	-1.5	1.8	11.1
Phenylalanine-leucine	-0.4	0.9	4.7
Phenylalanine-phenylalanine	-1.4	0.8	7.5

*Experimental Verification of Theoretical Calculations*

It is worthwhile to consider next some experimental data which verify the theoretical calculations. In water, carboxylic acids bind to the nonpolar resin, cross-linked polystyrene, presumably with a contribution from a hydrophobic bond between the nonpolar part of the carboxylic acid and the nonpolar resin.<sup>22</sup> Subtracting the data for formic acid from those of the higher homologues, it is possible to obtain experimental data for the thermodynamic parameters for hydrophobic bond formation between the nonpolar groups involved. These are shown in TABLE 3.<sup>23</sup> It can be seen that there is very good agreement between the experimental and theoretical values.

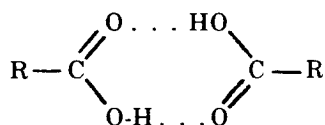
Urea was found to decrease the binding affinity of the resin for the carboxylic acid,<sup>22</sup> i.e., presumably urea reduces the strengths of hydrophobic bonds.

TABLE 3  
THERMODYNAMIC PARAMETERS<sup>23</sup> FOR HYDROPHOBIC BOND FORMATION BETWEEN THE NONPOLAR PARTS OF CARBOXYLIC ACIDS AND A POLYSTYRENE RESIN\* AT 4°C.

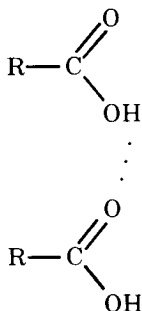
R groups of acid	Experimental			Theoretical		
	$\Delta F^\circ$ kcal./mole	$\Delta H^\circ$ kcal./mole	$\Delta S^\circ$ e. u.	$\Delta F^\circ$ kcal./mole	$\Delta H^\circ$ kcal./mole	$\Delta S^\circ$ e. u.
CH <sub>3</sub> -	-0.1	0.4	1.7	-0.2	0.5	2.5
CH <sub>3</sub> CH <sub>2</sub> -	-0.7	0.6	4.6	-0.7	0.7	4.9
CH <sub>3</sub> CH <sub>2</sub> CH <sub>2</sub> -	-1.4	1.1	8.9	-1.1	1.1	7.9

\*See original paper<sup>23</sup> for the assumption made about the nature of the binding site on the resin.

Another kind of experiment involves the dimerization of carboxylic acids in aqueous solutions, the presence of dimers being inferred from anomalies in the ionization behavior of these acids.<sup>24</sup> Recent analysis<sup>25</sup> of available data indicates that the dimerization constant increases with chain length, in contrast to the behavior in nonaqueous solutions and in the gas phase where it is essentially independent of chain length. This suggested that, whereas the dimer has the following structure in the gas phase:



it probably has the following structure, permitting hydrophobic bond formation between the R groups, in aqueous solution:



Subtracting the thermodynamic parameters for formic acid from those for the higher homologues eliminates the contribution from the hydrogen bond and yields data for pair interactions between like R groups; these are given in TABLE 4, where they are compared with theoretical values (computed on two different bases). The excellent agreement provides additional support for the validity of the theoretical calculations of the strengths of hydrophobic bonds.

As another example, we cite the use of the theoretical data to compute the lowering of the transition temperature for the thermal denaturation

TABLE 4  
FREE ENERGY OF HYDROPHOBIC BOND FORMATION<sup>25</sup> IN THE DIMERIZATION  
OF CARBOXYLIC ACIDS AT 25° C.

Side-Chain	$\Delta F_{H\phi}^{\circ}$ (kcal./mole)				
	Experimental*			Calculated†	
	(1)	(2)	(3)	(4)	(5)
CH <sub>3</sub> -	-0.79	-0.95	-0.80	-0.70	-0.70
CH <sub>3</sub> CH <sub>2</sub> -	-1.03	-1.06	-1.09	-0.90	-1.00
CH <sub>3</sub> CH <sub>2</sub> CH <sub>2</sub> -	-1.31	-1.47	-1.41	-1.15	-1.35
CH <sub>6</sub> H <sub>5</sub> CH <sub>2</sub> -	—	—	-1.57	-1.45	-1.63

\*These three columns correspond to three different sets of experimental data (see *Reference 25*).

†These two columns correspond to two slight variations in the theory (see *Reference 25*).

TABLE 5  
 LOWERING OF THE TRANSITION TEMPERATURE OF RIBONUCLEASE BY  
 ONE MOLAR SOLUTIONS OF ALIPHATIC ALCOHOLS<sup>26</sup>

Alcohol	Lowering of transition temperature over that in water (in °C.)	
	Experimental	Calculated
CH <sub>3</sub> OH	1.6	1.9
CH <sub>3</sub> CH <sub>2</sub> OH	3.1	3.3
CH <sub>3</sub> CH <sub>2</sub> CH <sub>2</sub> OH	7.1	6.0
CH <sub>3</sub> CH <sub>2</sub> CH <sub>2</sub> CH <sub>2</sub> OH	13.1	11.0

of ribonuclease caused by alcohols of varying chain length.<sup>26</sup> The calculations were based on the assumption that the R group of the alcohol binds to a similar nonpolar site of the denatured form of the protein, thereby favoring denaturation. The binding constants were computed from the theoretical values<sup>21</sup> of the hydrophobic bond strengths. The data are shown in TABLE 5. Again, the excellent agreement supports the validity of the theoretical calculations.

Finally, we may cite some experiments involving volume changes in aqueous solutions of nonpolar materials.<sup>27</sup> From experiments on the densities of aqueous solutions of alcohols, it was possible to obtain data for the

TABLE 6  
 VOLUME DECREASE (IN C.C./MOLE) ACCOMPANYING THE ADDITION OF  
 NONPOLAR GROUPS TO WATER

Group	-ΔV							
	0°C.		20°C.		40°C.		50°C.	
	Exp.	Theor.	Exp.	Theor.	Exp.	Theor.	Exp.	Theor.
CH <sub>3</sub>	1.1	1.9	1.2	1.5	1.2	1.3	1.3	1.1
C <sub>2</sub> H <sub>5</sub>	1.9	3.7	2.1	3.1	2.2	2.5	2.3	2.3
C <sub>3</sub> H <sub>7</sub>	2.9	5.6	3.1	4.6	3.3	3.8	3.5	3.4
C <sub>4</sub> H <sub>9</sub>	3.8	7.5	3.8	6.2	4.2	5.0	4.3	4.5

volume decrease accompanying the addition of nonpolar groups to water. Here again, the device of subtracting the data for the first member of a homologous series, in order to obtain the contribution of the nonpolar group, was used. The agreement between experimental and theoretical data is fairly good, especially at the higher temperatures (TABLE 6).

Of course, the volume change accompanying the formation of hydrophobic bonds will have the opposite, i.e., positive, sign. Such increases in volume are observed in association reactions<sup>28,29</sup> where hydrophobic bond formation may be involved.

In summary, it appears that we now have a sound theoretical and experimental basis for predicting the strengths of hydrophobic bonds between various nonpolar side-chains. In the remainder of this paper, we shall explore some of the implications of these known strengths of hydrophobic bonds.

#### *Some Implications for Protein Structure*

As with other noncovalent interactions, hydrophobic bonds can stabilize various conformations of polypeptide chains. For example, a hydrophobic bond between two nearby residues on an  $\alpha$ -helix can stabilize the helical structure<sup>21</sup> (see FIGURE 12). In the case of the  $\alpha$ -helical form of poly-L-alanine, the  $\beta$ -methyl group of an  $i^{\text{th}}$  residue can form a hydrophobic bond

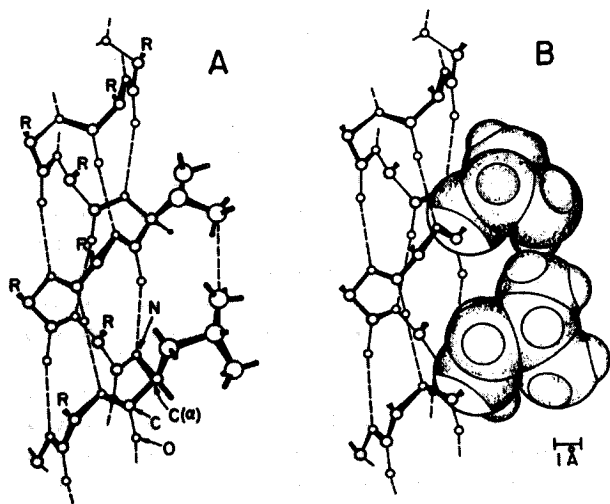


FIGURE 12. Hydrophobic bond between an  $i^{\text{th}}$  leucine residue and an  $(i + 4)$  valine residue on a right handed  $\alpha$ -helix composed of L-amino acids. (A) Skeletal drawing showing the positions of the atoms in the helix and in the side chains. (B) Space-filling model, with van der Waals radii drawn to scale (Nemethy & Scheraga<sup>21</sup>).

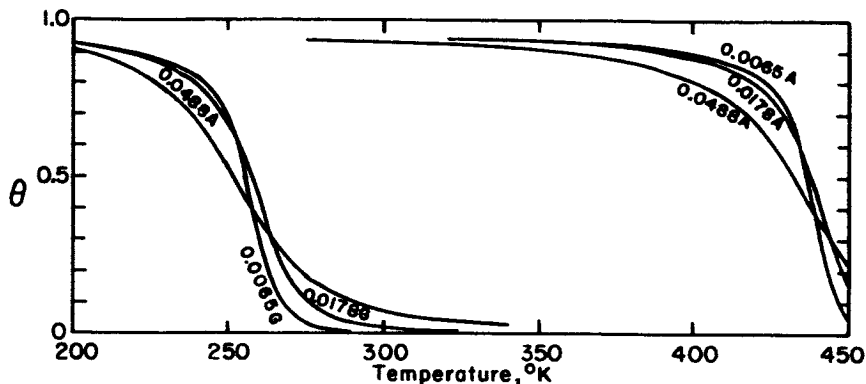


FIGURE 13. Computed curves for a helix-random coil transition for polyglycine (G) and poly-L-alanine (A) containing 100 residues. The various curves in each group correspond to different values of one of the parameters in the theory. The enthalpy of formation of the amide hydrogen bond was taken as  $-500$  cal. (Bixon *et al.*<sup>30</sup>).

with the  $\alpha$ -CH group on the  $(i+3)$  residue providing similar stabilization of the  $\alpha$ -helix<sup>21</sup> The effect of this hydrophobic bond on the stability of a helix can be seen by comparing calculated thermal transition curves<sup>30</sup> for polyglycine and poly-L-alanine (FIGURE 13). In agreement with these results, it was observed by Gratzer and Doty<sup>31</sup> that a poly-L-alanine helix of 175 residues could not be melted in water at  $95^{\circ}\text{C}$ . Calculations and experimental results indicated that *very short* poly-L-alanine helices can be melted in water.<sup>30</sup>

Recently, the effect of hydrophobic bonding in the random coil form of poly-L-alanine was taken into account in the theory of the helix-coil transition.<sup>32</sup> Such hydrophobic bonds tends to partially compensate for the stability provided in the helical form. However, the possibility of internal breaks in the helix was taken into account in those cases where the break would be favored by interactions between the side-chains of the neighboring helical sections produced by bending the chain at the break in the helix.<sup>32</sup> Such interacting helices exhibit quite sharp transition curves, more like those observed in proteins, rather than the broad transitions characteristic of single, noninteracting helices.

Because of the positive sign of  $\Delta H_{H\phi}$  it is possible to observe anomalies in transition curves, reflecting an increased stability with increasing temperature in a limited temperature range. Such anomalies have been observed by Fasman *et al.*<sup>33</sup> and accounted for<sup>32</sup> in terms of hydrophobic interactions in a system of interacting helices. This explanation may also account for the lability of some enzymes at low temperature and their stability at higher temperatures.<sup>34,35</sup>

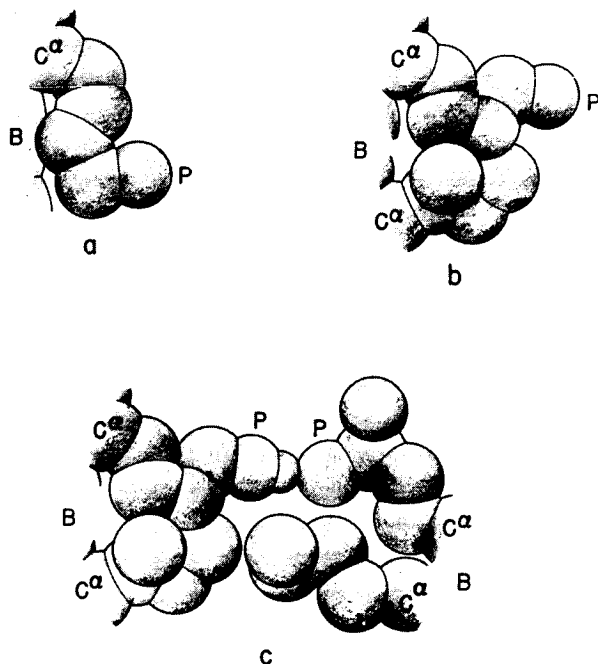


FIGURE 14. Schematic representation of various hydrophobic interactions of a polar side chain with its surroundings. B refers to the backbone, P to the polar head, and  $C^\alpha$  to the  $\alpha$ -carbon. (a) Interaction of a lysine side chain with the backbone. (b) Interaction of a lysine side chain with a nearby isoleucine side chain. (c) Interaction of two polar side chains (lysine and glutamic acid), engaged in hydrogen-bonding, with two nonpolar side chains (isoleucine and leucine, respectively). A hydrophobic bond is also formed between the two nonpolar side chains (Nemethy *et al.*<sup>36</sup>).

Nonpolar groups can be of importance in the behavior of polar side chains.<sup>36</sup> For example, the nonpolar part of a lysine side chain may interact with the nonpolar part of the backbone of a polypeptide chain (FIGURE 14a) or with a neighboring nonpolar group (FIGURE 14b); in either case, the polar head is in contact with water. In FIGURE 14c it can be seen how a lysine-glutamic acid hydrogen bond can be stabilized by interactions between the nonpolar groups. Interactions of this kind have been found in the myoglobin molecule, in which the polar parts of a lysyl and glutamyl residue form a hydrogen bond, while the nonpolar parts of these side chains lie against the molecule with no water in the intervening space.<sup>37</sup>

Hydrophobic bonds can also play a role in the association of proteins and other large molecules. Even though most association reactions are accompanied by increases in enthalpy (characteristic of hydrophobic bond formation), they are nevertheless favored because of large increases in en-



tropy<sup>38</sup> (also characteristic of hydrophobic bond formation). Examples of such association are the protein of tobacco mosaic virus<sup>28</sup> and biocolloids.<sup>39</sup> These are in contrast to the association of fibrin monomer,<sup>40</sup> which is accompanied by a decrease in enthalpy, probably due to the formation of intermolecular hydrogen bonds.

### Summary

On the basis of a recent theory of water structure<sup>7</sup> it is now possible to understand the effect of nonpolar solutes thereon.<sup>14</sup> We still lack a quantitative theory for the effect of ions and polar materials on water structure, but current work<sup>3</sup> on this problem may yield fruitful results. A significant consequence of the theory of aqueous hydrocarbon solutions is the availability of theoretical thermodynamic parameters for pair and multiple interactions between nonpolar groups in water<sup>21</sup> (hydrophobic bonds). These theoretical data have recently been verified by a series of experimental investigations. As a result, it is possible to understand, on a quantitative basis, the contribution of hydrophobic bonding to protein stability and reactivity.

### Note Added in Proof

Recently,<sup>3</sup> progress has been made in refining the theory for liquid H<sub>2</sub>O and D<sub>2</sub>O and in obtaining a theory of dilute aqueous solutions of electrolytes.

In the more recent theory, five energy levels, corresponding to the possible states of hydrogen bonding, are still maintained, and no a priori requirement is introduced for the existence of clusters. The statistical weight,  $s_i$ , for each state is

$$s_i = f_i \exp(-E_i/RT)$$

where  $f_i$  is a product of six vibrational terms corresponding to the six degrees of freedom of the molecule.

$$f_i = \prod_{i=1}^6 [1 - \exp(-h\nu_i/kT)]^{-1}$$

and  $E_i$  is energy of the  $i^{\text{th}}$  state, taking the tetra-bonded level as the zero of the energy scale.

The total partition function for one mole of water is

$$Z_{\text{total}} = \sum_{x_i} g \prod_{i=u}^4 (s_i)^{x_i} N_0$$

where  $g$  is a combinatorial factor,  $x_i$  is the mole fraction of the  $i^{\text{th}}$  species, and  $N_0$  is Avogadro's number. The partition function is replaced by its maximum term, obtained by differentiating  $Z_{\text{total}}$  with respect to the  $x_i$ 's.

$$Z_{\text{max}} = \left( \sum_{i=u}^4 s_i \right)^{N_0}$$

$Z_{\max}$  is then a function of the 30 vibrational frequencies and the 5 energies  $E_i$ .

In evaluating  $Z_{\max}$  it is assumed that the three translational frequencies for each  $f_i$  are equal and the three librational frequencies for each  $f_i$  are equal, and that the frequencies for  $D_2O$  are related to the corresponding ones for  $H_2O$  by the appropriate isotopic mass ratios. Thus, for the treatment of  $H_2O$  and  $D_2O$  there are effectively 10 frequencies and 5 energy levels as variables.

The assignment of the frequencies is a difficult task, especially since only the translational and librational frequencies of the tetra-bonded level can be assigned with confidence ( $210\text{ cm}^{-1}$  for the translational and a value between  $650$  and  $800\text{ cm}^{-1}$  for the librational frequencies; the choice between  $650$  and  $800$  is not too critical). The only restriction placed on the other frequencies is that they be no higher than those for the tetra-bonded species.

From the work of Buijs and Choppin,<sup>10</sup> it appears that the difference in energy between the levels for the tetra-bonded and un-bonded species is about  $2.7\text{ kcal/mole}$ . Therefore, we demand that this energy must lie between  $2.5$  and  $3.0\text{ kcal/mole}$  and, further, that the positions of the other three levels may be varied but remain ordered between the lowest and highest levels. The same energy levels are used for both  $H_2O$  and  $D_2O$ . We then have 8 frequencies and 4 energies as variables, which are required to lie within certain ranges.

The results for the thermodynamic properties of water indicate good agreement between theory and experiment; in particular, there is a considerable improvement, over the previous theory,<sup>7</sup> in the agreement for the heat capacity data. In contrast to the previous theory,<sup>7</sup> the mole fraction of unbonded water is considerably lower, being about  $0.07$  for  $H_2O$  at room temperature instead of the previous value of about  $0.3$ .

With this model for liquid  $H_2O$ , we have been able to compute the properties of infinitely dilute solutions of electrolytes. For this purpose we have made use of the hypothesis of Frank and Wen<sup>1</sup> that the water around an ion may be divided into three regions: (1) The inner hydration layer consisting of the nearest neighbors of the ion; the number of water molecules in this layer will vary between 4 and 8, depending on the ion size. It is only for the water molecules in this layer that the electric field due to the ion is the dominant influence. (2) An intermediate region in which the structure of the liquid is altered because of the geometrical arrangements of the molecules in the inner layer. (3) Unaffected liquid, the same as in pure  $H_2O$ .

The water molecules in region 1 may participate in only three hydrogen bonds because the ion occupies a position which would prevent a fourth

bond from forming. We treat the positions of these four energy levels as variables. In region 2 there are five such variables.

With this model, we have been able to reproduce the thermodynamic data for the alkali halides at infinite dilution.

### References

1. H. S. FRANK & W. Y. WEN. 1957. *Disc. Faraday Soc.* **24**: 133.
2. H. S. FRANK. 1958. *Proc. Roy. Soc. (London)*. **A247**: 481.
3. J. H. GRIFFITH & H. A. SCHERAGA. Work in progress.
4. W. KAUZMANN. 1959. *Adv. Protein Chem.* **14**: 1.
5. W. H. BARNES. 1929. *Proc. Roy. Soc. (London)*. **A125**: 670.
6. J. D. BERNAL & R. H. FOWLER. 1933. *J. Chem. Phys.* **1**: 515.
7. G. NEMETHY & H. A. SCHERAGA. 1962. *J. Chem. Phys.* **36**: 3382.
8. J. L. KAVENAU. 1964. *Water and Solute-Water Interactions*. Holden-Day, Inc., San Francisco, Calif.
9. G. NEMETHY & H. A. SCHERAGA. 1964. *J. Chem. Phys.* **41**: 680.
10. K. BUIJS & G. R. CHOPPIN. 1963. *J. Chem. Phys.* **39**: 2035.
11. A. A. MILLER. 1963. *J. Chem Phys.* **38**: 1568.
12. R. A. HORNE & R. A. COURANT. 1964. *J. Phys. Chem.* **68**: 1258.
13. H. S. FRANK & M. W. EVANS. 1945. *J. Chem. Phys.* **13**: 507.
14. G. NEMETHY & H. A. SCHERAGA. 1962. *J. Chem. Phys.* **36**: 3401.
15. M. V. STACKELBERG *et al.* 1954. *Z. Elektrochem.* **58**: 25, 40, 99, 104, 162; 1958 **62**: 130.
16. G. C. KRESHECK, H. SCHNEIDER & H. A. SCHERAGA. *J. Phys. Chem.* In press.
17. G. NEMETHY & H. A. SCHERAGA. Work in Progress. 1964.
18. K. U. LINDERSTRØM - LANG. 1952. *Proteins and Enzymes*. Lane Medical Lectures. :57. Stanford Univ. Press, Stanford, Cal.
19. W. KAUZMANN. 1954. *A Symposium on the Mechanism of Enzyme Action*. W. D. McElroy & B. Glass, Eds. :70. Johns Hopkins University Press, Baltimore, Md.
20. J. G. KIRKWOOD. Reference 19. :16.
21. G. NEMETHY & H. A. SCHERAGA. 1962. *J. Phys. Chem.* **66**: 1773; 1963 **67**: 2888.
22. I. Z. STEINBERG & H. A. SCHERAGA. 1962. *J. Am. Chem. Soc.* **84**: 2890.
23. H. SCHNEIDER, G. C. KRESHECK & H. A. SCHERAGA. 1965. *J. Phys. Chem.* **69**, 1310.
24. A. KATCHALSKY, H. EISENBERG & S. LIFSON. 1951. *J. Am. Chem. Soc.* **73**: 5889.
25. E. E. SCHRIER, M. POTTLE & H. A. SCHERAGA. 1964. *J. Am. Chem. Soc.* **86**: 3444.
26. E. E. SCHRIER, R. T. INGWALL & H. A. SCHERAGA. *J. Phys. Chem.* **69**, 298 1965.
27. M. E. FRIEDMAN & H. A. SCHERAGA. To be submitted.
28. M. A. LAUFFER. 1962. *Molecular Basis of Neoplasia*: 180. Univ. of Texas Press. Austin, Tex.
29. F. FRANKS. Private communication.
30. M. BIXON, H. A. SCHERAGA & S. LIFSON. 1963. *Biopolymers*. **1**: 419.
31. W. B. GRATZER & P. DOTY. 1963. *J. Am. Chem. Soc.* **85**: 1193.
32. D. C. POLAND & H. A. SCHERAGA. *Biopolymers*. In press.
33. G. D. FASMAN, C. LINDBLOW & E. BODENHEIMER. 1964. *Biochemistry* **3**: 155.
34. M. E. PULLMAN, H. S. PENEFSKY, A. DATTA & E. RACKER. 1960. *J. Biol. Chem.* **235**: 3322.
35. D. J. GRAVES, R. W. SEALOCK & J. H. WANG. 1965. *Biochemistry*, **4**, 290.
36. G. NEMETHY, I. Z. STEINBERG & H. A. SCHERAGA. 1963. *Biopolymers* **1**: 43.

37. J. C. KENDREW. 1962. Brookhaven Symp. Biol. 15: 216.
38. I. Z. STEINBERG & H. A. SCHERAGA. 1963. J. Biol. Chem. 238: 172.
39. W. L. PETICOLAS. 1962. J. Chem. Phys. 37: 2323; 1964 40: 1463.
40. J. M. STURTEVANT, M. LASKOWSKI, JR., T. H. DONNELLY & H. A. SCHERAGA. 1955. J. Am. Chem. Soc. 77: 6168.

# HYDROPHOBIC HYDRATION AND THE EFFECT OF HYDROGEN BONDING SOLUTES ON THE STRUCTURE OF WATER

Felix Franks

*Department of Chemical Technology,  
Institute of Technology,  
Bradford, England*

Investigations into the thermodynamic properties of aqueous solutions of the noble gases and of hydrocarbons have contributed greatly to our understanding of the structure of liquid water. In recent years several attempts have been made to interpret the enthalpy and entropy of evaporation of hydrocarbons from aqueous solution in terms of particular structural models. Liquid water is regarded as a mixture of a quasicrystalline modification in which each molecule is capable of taking part in four tetrahedrally-oriented hydrogen bonds, and a nonhydrogen bonded molecular species, the properties of which are not very clearly defined. According to the gas hydrate type model put forward by H. S. Frank and A. S. Quist, the quasicrystalline structure resembles a clathrate lattice which is stabilized by the presence of interstitial monomeric  $\text{H}_2\text{O}$  molecules.<sup>1</sup> The model of G. Nemethy and H. A. Scheraga, on the other hand, provides for a distribution of ice-like clusters dispersed in a denser, nonhydrogen bonded form of water.<sup>2</sup> Both models have been partially successful in accounting for the observed enthalpies and entropies of evaporation of hydrocarbons from aqueous solution; the relevant data are given in TABLE 1. The introduction of a nonpolar solute molecule into liquid water is believed to be associated with a shift in the structural equilibrium in the direction of greater structuredness or ice-likeness of the water. This effect of nonpolar solutes on liquid water is sometimes referred to as "hydrophobic hydration" to distinguish it from the normal hydration which arises from strong interactions between molecular or ionic solutes and water. Evidence that the presence of a hydrocarbon may have a profound influence on the nature of the hydrogen bonds in liquid water has recently been advanced by J. Clifford and B. A. Pethica who studied the proton resonance spectra of aqueous solutions of sodium alkyl sulfates and alcohols of increasing chain lengths.<sup>3</sup>

The cluster model of Nemethy and Scheraga can account well for the properties of butane solutions but not for those of the smaller methane molecule, whereas the interstitial model of Frank and Quist can account for the thermodynamic functions associated with methane but not for those of molecules too large to be accommodated in the polyhedral cavities of the clathrate framework. From these observations it can be concluded that a realistic model of aqueous hydrocarbon solutions might provide both for

TABLE 1  
PARTIAL MOLAR ENTHALPIES AND ENTROPIES OF EVAPORATION AT INFINITE  
DILUTION OF HYDROCARBONS AND ALCOHOLS FROM AQUEOUS SOLUTION, AND  
ENTROPIES OF DISSOCIATION OF GAS HYDRATES

Solute	Solution*		Hydrate†	Solute	Solution*	
	$\Delta H_2$ kcal.	$\Delta S_2$ e. u.			$\Delta H_2$ kcal.	$\Delta S_2$ e. u.
CH <sub>4</sub>	3.2	32	46	CH <sub>3</sub> OH	11.2	35
C <sub>2</sub> H <sub>6</sub>	4.1	35	75	C <sub>2</sub> H <sub>5</sub> OH	12.9	41
C <sub>3</sub> H <sub>8</sub>	5.8	41	113	n-C <sub>3</sub> H <sub>7</sub> OH	14.4	47
				iso-C <sub>3</sub> H <sub>7</sub> OH	13.5	44
n-C <sub>4</sub> H <sub>10</sub>	6.1	42		n-C <sub>4</sub> H <sub>9</sub> OH	15.9	52
				sec-C <sub>4</sub> H <sub>9</sub> OH	15.1	49
iso-C <sub>4</sub> H <sub>10</sub>	5.4	40		iso-C <sub>4</sub> H <sub>9</sub> OH	15.2	50
				tert-C <sub>4</sub> H <sub>9</sub> OH	14.2	48

\*Evaporation from solution refers to 1 atm. pressure at 25° C. and unit mole fraction.

†Figures refer to the process Hydrate (s) + Gas (1 atm.) → n H<sub>2</sub>O(1). For CH<sub>4</sub> and C<sub>2</sub>H<sub>6</sub> n = 5.76, and for C<sub>3</sub>H<sub>8</sub> n = 17.

interstitial sites capable of accommodating solute and a more "normal" type of interaction between the solute and the nonbonded, dense water.<sup>4</sup>

Unfortunately the study of the thermodynamic properties of aqueous hydrocarbon solutions is subject to considerable experimental difficulties, because of the low solubilities involved; for the same reason enthalpies and heat capacities of solution cannot be determined calorimetrically. It is therefore of interest to study the behavior of aqueous solutions of compounds which, while possessing alkyl groups, are at the same time miscible with water. Aliphatic alcohols satisfy both these conditions. Indeed, they can be regarded either as hydrocarbons containing a solubilizing -OH groups or as water in which one hydrogen atom has been replaced by an alkyl group, and the highly abnormal behavior of alcohol-water mixtures very likely originates from the bifunctionality of the alcohol molecule. Both alcohols and water are associated by hydrogen bonding, but whereas water is able to form three-dimensional clusters, alcohols form only linear or cyclic aggregates,<sup>5,6</sup> in spite of the fact that the alcohol oxygen atom

has two unshared electron pairs. Thus the anomalous properties of alcohol-water mixtures must in some degree also arise from the coexistence of two mutually incompatible types of association. This is well illustrated by comparing the solution properties of monohydric alcohols with those of polyhydric alcohols and sugars. As the number of hydroxy groups in the molecule increases, so the anomalies observed in aqueous solutions become less marked, and sugar solutions, although far from ideal, do not exhibit the extremely complex behavior shown by the alkanols.

In a study of the physical properties of alcohol-water mixtures two concentration regions would appear to be of great interest. In dilute solutions of alcohols, the alcohol molecule must in some way affect the structure of liquid water, either by being incorporated into the existing structure without changing this a great deal, or by depolymerizing the three-dimensional clusters. On the other hand, in dilute solutions of water in alcohols the available evidence favors the view that water breaks up the alcohol aggregates and water-centered association may take place.

The present discussion is confined almost exclusively to dilute solutions of monohydric aliphatic alcohols, and from a review of the properties of such mixtures it is shown that the observed anomalies can be interpreted in terms of an interstitial model similar to that advanced for hydrocarbon solutions.<sup>1,4</sup>

#### *Partial Molar Volumes*

The complex concentration dependence of the density of dilute alcohol solutions is well known, and the partial molar volume ( $V_2$ ) curve for ethanol is to be found in many standard textbooks,<sup>8</sup> although usually no attempt is made to account for the negative values of  $(V_2^\circ - V_2^\circ)$ , where  $V_2^\circ$  is the partial molar volume at infinite dilution and  $V_2^\circ$  is the molar volume of the pure alcohol at the same temperature, or for the fact that  $(V_2 - V_2^\circ)$  becomes progressively more negative as the mole fraction of alcohol ( $x_2$ ) increases. To the knowledge of the author the only interpretation of the observed results is that by A. G. Mitchell and W. F. K. Wynne-Jones which invokes the breakdown of the structure of water by preferential hydrogen bonding between water and alcohol.<sup>9</sup>

FIGURE 1 shows the  $(\bar{V}_2 - V_2^\circ)$  versus  $x_2$  curves for some normal alcohols, ethylene glycol, and glycerol,<sup>10</sup> while FIGURE 2 shows a similar plot for the isomeric butanols.<sup>10</sup> A comparison of the behavior of the different alcohols illustrates several interesting points:

(1) for the *n*-alcohols —  $(\bar{V}_2 - V_2^\circ)$  increases with increasing chain length by about 2 ml. per mole  $\text{CH}_2$  groups,<sup>11</sup>

(2) the presence of more than one hydroxy group leads to a more normal behavior, i.e.,  $(\bar{V}_2 - V_2^\circ)$  is less negative and the minimum is less pronounced or is missing completely.

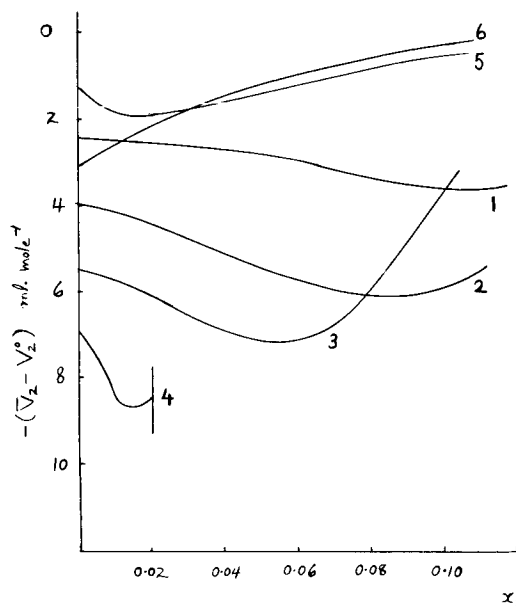


FIGURE 1. Partial molar volumes at 20° of aqueous (1) MeOH, (2) EtOH, (3) n-PrOH, (4) n-BuOH, (5) ethylene glycol, and (6) glycerol.

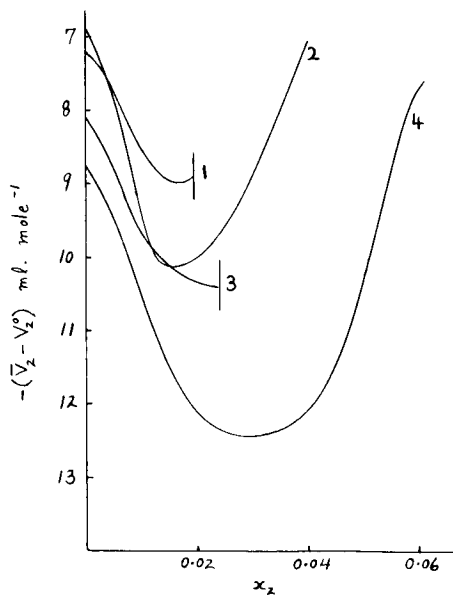


FIGURE 2. Partial molar volumes at 20° of aqueous solutions of the isomeric butyl alcohols: (1) normal, (2) secondary, (3) iso, and (4) tertiary. The vertical lines denote the miscibility limits.



(3) the concentration at which  $(\bar{V}_2 - V_2^\circ)$  passes through its minimum value depends on the size and shape of the alkyl group. Thus both butanol-1 and butanol-2 are derived from *n*-butane, and  $\bar{V}_2$  for both these compounds passes through a minimum at  $x_2 = 0.015$ ; on the other hand 2-methyl propanol-1 and 2-methyl propanol-2 are both derived from isobutane, and the minimum  $\bar{V}_2$  of 2-methyl propanol-2 is at  $x_2 = 0.03$ . The low solubility of 2-methyl propanol-1 ( $x_{2\text{sat}} = 0.021$  at  $20^\circ$ ) makes it impossible to ascertain the exact position of  $V_{2\text{min}}$ , but reference to FIGURE 2 shows that it is likely to be near  $x_2 = 0.03$ .

Negative partial molar volumes appear to be common to hydrocarbons<sup>12</sup> and have also been reported for electrolytes containing large hydrocarbon groups, such as the tetraalkyl ammonium halides<sup>13</sup> and sodium alkyl sulfates,<sup>14</sup> and as is the case with the alcohols,  $-(\bar{V}_2^\circ - V_2^\circ)$  increases with increase in the number of carbon atoms. These results give support to the interstitial solution model, i.e., the concept that the solute occupies vacant sites in a water quasilattice. Although solid clathrate hydrates of the alkyl-ammonium salts are known and have been extensively studied by G. A. Jeffrey and his colleagues,<sup>15</sup> the analogy with solid hydrates must not be pushed too far. Methane, ethane, propane, and isobutane form crystalline hydrates (see TABLE 1), but no hydrate is known of *n*-butane, yet no qualitative differences can be observed between the solution properties of *n*-butane and iso-butane or of *n*-butanol and isobutanol. Thus on a time scale of  $10^{-10}$ – $10^{-11}$  sec. (the dielectric relaxation time of water) sites capable of accommodating a *n*-butyl or even a *n*-dodecyl group may well exist in the liquid state.

The postulate of an interstitial solution can therefore account for the negative  $\bar{V}_2^\circ$  values but not for the fact that  $\bar{V}_2$  becomes more negative with rising concentration. This could arise from some form of cooperative interaction between quasicrystalline regions which are stabilized by the presence of interstitial hydrocarbon groups. The minimum in the  $\bar{V}_2$  ( $x_2$ ) curve, which has also been observed for tetraalkylammonium halides,<sup>13</sup> may well be a function of the hydrocarbon portion of the molecule or ion and could probably be observed in solutions of hydrocarbons, if the low solubilities did not make the determination of accurate densities almost impossible.

The question arises as to what is the function of the hydroxy group in such an interstitial solution, since it is this functional group which solubilizes the hydrocarbon. The alcohol oxygen atom could take the place of a water oxygen atom in the lattice and be bonded by one donor and one acceptor hydrogen bond. This causes a local disturbance in the ordered water structure, as is shown in FIGURE 3, but experiments with models indicate that this disorder need only extend over a short range. Enthalpies of mixing<sup>16</sup> and proton exchange rates<sup>17</sup> indicate that water-alcohol hydrogen

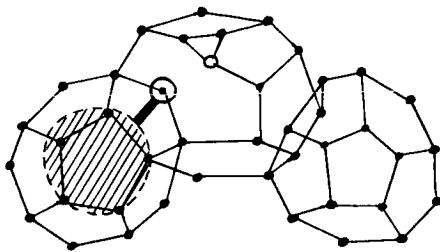


FIGURE 3. The alcohol molecule occupying an interstitial site in a clathrate framework and hydrogen bonded into the framework.  $\odot$  denotes the alcohol oxygen atom; the inability of the alcohol molecule to form more than two hydrogen bonds gives rise to a structural defect involving the water molecule shown by the open circle.

bonds are stronger than water-water bonds, and that the bond stability increases as does the base strength of the alcohol. Although the postulate that the alcohol oxygen atom is actually bonded into the water framework can account for the observed results, it may possibly contradict the recent findings that ethylene oxide forms a gas hydrate in which the guest molecule is not hydrogen bonded to the lattice, but that the solute behaves as an inert gas.<sup>18</sup> This result would appear to run counter to the accepted idea that miscibility with water arises from hydrogen bonding interactions, with the subsequent breakdown of the water structure.\*

#### *The Temperature of Maximum Density*

The phenomenon of the maximum density distinguishes water from all other liquids. It can be accounted for on the basis of the mixture model: both 'bulky' (ice-like) and 'dense' water possess their respective coefficients of expansion, but also a rise in temperature favors the degradation of 'bulky' to 'dense' water. Thus at the temperature of maximum density (TMD) the expansion is balanced by the thermal breakdown of the structured variety. Hence any process which affects the structural integrity of liquid water should produce a change in the TMD. The presence of a solute which forms an ideal solution with water must of necessity produce a lowering in the TMD,  $\Delta T_{\text{ideal}}$ . G. Wada and S. Umeda have calculated  $\Delta T_{\text{ideal}}$  by assuming the following expansibility functions for water and solute respectively:

\*Since the above was written, studies involving the dielectric properties of ethanol-water mixtures at low temperatures have prompted A. D. Potts and D. W. Davidson [J. Phys. Chem. 69: 996 (1965)] to state that a clathrate hydrate  $\text{C}_2\text{H}_5\text{OH} \cdot 17\text{H}_2\text{O}$  does in fact exist and is stable up to  $-73.5^\circ$ . It appears that the guest molecule does not enjoy the same freedom of rotation which is normally observed in gas hydrates, and the view is put forward that the hydroxy group is hydrogen bonded into the water lattice.

$$V_1^0(T) = a + bT + cT^2$$

$$\text{and } V_2^0(T) = a' + b'T$$

If there is a structural contribution involved in  $\Delta T_{\text{observed}}$ , then, assuming a zero volume of mixing,

$$\Delta T_{\text{observed}} = \Delta T_{\text{ideal}} + \Delta T_{\text{struct}}$$

For most solutes  $\Delta T_{\text{observed}}$  is negative, but for the aliphatic alcohols  $\Delta T_{\text{observed}}$  at low concentrations is positive and a function of the nature of the alkyl group; FIGURE 4 shows  $\Delta T_{\text{struct}}$  and  $\Delta T_{\text{observed}}$  for ethanol and tert-butanol. The maximum effect coincides with the inflexion in the  $\bar{V}_2(x_2)$  curve.

As a good approximation,  $\Delta T$  can be related to the apparent molal expansibility  $\phi_E$  by the relationship

$$\frac{\Delta T}{m} = -\phi_E \left( \frac{\partial^2 V}{\partial T^2} \right)^{-1}_{m=0, t=3.98^\circ}$$

where  $\phi_E = (\partial \phi_v / \partial T)_p$  and  $m$  is the molality.<sup>20</sup> Thus at the low concentrations ( $x_2 < 0.03$ ) where  $\Delta T$  is positive, aqueous solutions of alcohols should exhibit negative expansibilities. This has never actually been reported, although it has been pointed out that  $\phi_E$  at low concentrations is extremely small and increases rather suddenly above the concentration at which the inflexion in the  $\bar{V}_2(v_2)$  curve occurs.<sup>21</sup>

### Compressibility

Another property of water which would be affected by the presence of alkyl groups in interstitial sites is the adiabatic compressibility. This is

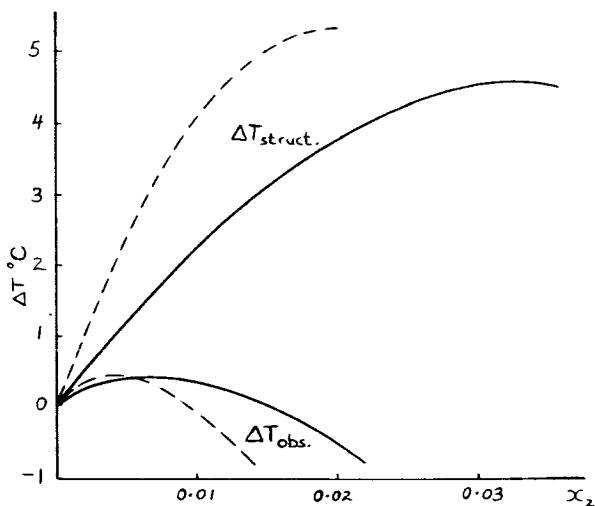


FIGURE 4. The observed and structural TMD of aqueous ethyl alcohol and tert.-butyl alcohol. ——— EtOH, — — — tert.-BuOH.

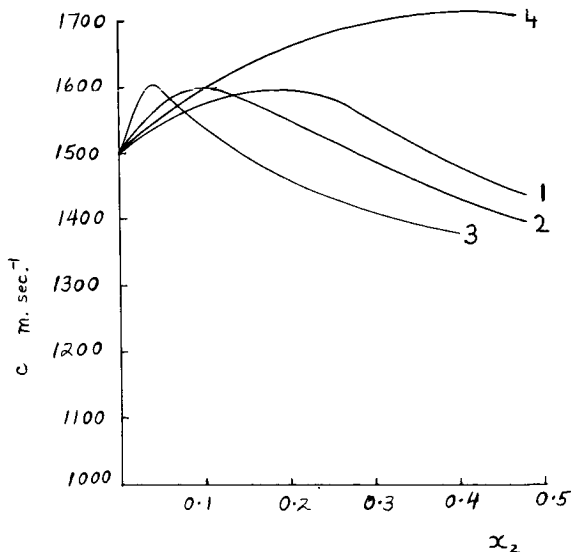


FIGURE 5. The velocity of sound in aqueous (1) MeOH, (2) EtOH, (3) n-PrOH, and (4) ethylene glycol. (After C. J. Burton, Ref. 22.)

conveniently obtained from a study of the velocity of sound,  $c$ , where

$$c^2 = -\frac{V}{M} \left( \frac{\partial P}{\partial V} \right)_s$$

FIGURE 5 shows the dependence of  $c$  on the composition for various water-alcohol mixtures,<sup>22</sup> and it is clear that here again the observed anomalies can be reconciled with the interstitial model, in that the mixture for which  $\bar{V}_2$  has a minimum value also has a minimum compressibility  $\beta$ . It also appears that for this mixture  $\beta$  is a constant, independent of temperature.<sup>23</sup>

Closely associated with  $\beta$  is the coefficient of sound absorption,  $\alpha$ , which is given by

$$\frac{2\alpha}{\nu^2} = \frac{8\pi^2\eta}{3\rho c}$$

where  $\nu$  is the frequency,  $\eta$  the viscosity, and  $\rho$  the density of the liquid. However, this classical relationship cannot account for the large absorption of sound by water.<sup>24</sup> The excess absorption has been associated with a relaxation (structural) compressibility which arises from the relaxation time of the clustered structures. By reference to FIGURE 6 it is seen that the water-alcohol mixtures have a very large concentration dependent excess sound absorption which cannot be interpreted in terms of simple complex formation,<sup>25</sup> but which, when considered alongside the other abnormal P-V-T properties of such mixtures, can be reconciled with

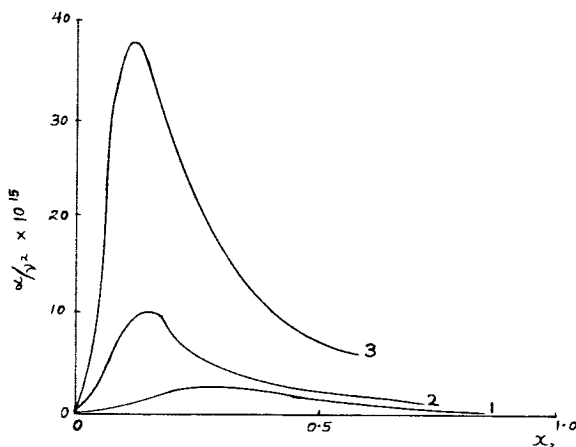


FIGURE 6. The ultrasound absorption coefficient at 20° in water - alcohol mixtures: (1) EtOH, (2) n-PrOH, (3) tert.-BuOH. (After C. J. Burton, Ref. 22.)

the existence of structural entities which are more stable than those existing in pure water. Such additional stability may be derived from the interstitial nature of the solution and from the comparatively strong hydrogen bonds formed between alcohol and water molecules.

#### *Thermodynamic Properties*

Although a study of the thermodynamic properties of solutions cannot yield unambiguous evidence for or against a given structural model, nevertheless for this model to be a realistic one, the qualitative nature of the thermodynamic parameters must be able to be reconciled with the assumptions on which the model is based. As has been pointed out earlier, in alcohol-water mixtures two competing processes are considered, involving, in water rich solutions, the promotion of structures more stable than that of water itself, and in alcohol rich mixtures, the depolymerization of linear and/or cyclic alcohol aggregates, possibly with the formation of water centered association complexes.

The enthalpies of mixing,  $\Delta H^M$ , of several water-alcohol systems are shown in FIGURE 7, and the standard enthalpies of evaporation  $\Delta H_2$ , from aqueous solution are included in TABLE 1. It is seen that  $\Delta H_2$  increases with the length of the hydrocarbon chain in a similar manner as for the hydrocarbons. The nature of the  $\Delta H^M(x_2)$  curves has been discussed by A. C. Brown and D. J. G. Ives in terms of the  $\Delta H^M(x_2)$  curves of two less complex systems.<sup>7</sup> For the system  $\text{Me}_2\text{CO}-\text{CHCl}_3$ , in which stable hydrogen bonded complexes exist,  $\Delta H^M$  is negative with a minimum at  $x_2 = 0.5$ . For the system  $\text{CH}_3\text{OH}-\text{CCl}_4$ , on the other hand,  $\Delta H^M$  is positive, because the alcohol aggregates are broken down. By the super-

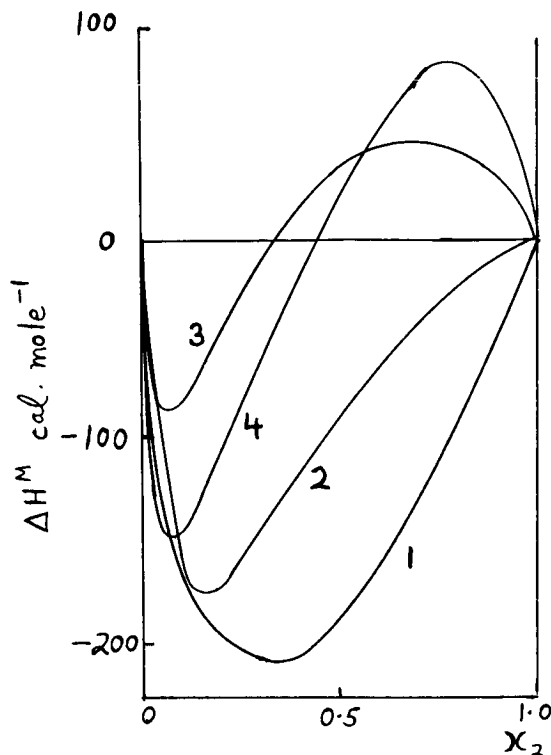


FIGURE 7. Enthalpies of mixing at 25° of water with (1) MeOH, (2) EtOH, (3) n-PrOH, and (4) tert.-BuOH.

position of the two plots a curve resembling that of a water-alcohol system is obtained. Thus we can regard the exothermic process as related to the formation of a stable, structural configuration which is not, however, formed at the expense of a breakdown in the liquid water structure, as has been previously suggested.<sup>7,9</sup> The endothermic process which is predominant in alcohol rich mixtures is due to a depolymerization and, as would be expected, it is accompanied by a large heat capacity change.

Although a study of the mixing functions cannot by itself provide any significant evidence for or against the existence of interstitial structures, a reference to TABLE 1 shows that a parallelism exists between  $\Delta H_2$  and  $\Delta S_2$  for the evaporation of hydrocarbons and alcohols from aqueous solution, and of hydrocarbon from solid hydrates. So far, no clathrate hydrates of alcohols have been reported, although D. N. Glew has speculated as to their existence.<sup>20</sup> Stable interstitial hydrates are known of ethylene oxide, tetrahydrofuran, and several amines, i.e. compounds which are miscible

with water, capable of forming hydrogen bonds, and yet do not appear to destroy the peculiar structure of water to any marked extent.

Finally the behavior of water-alcohol mixtures in relation to Raoult's Law should be considered: in spite of the negative enthalpy of mixing, implying strong interactions, the mixtures nevertheless show positive deviations from Raoult's Law, because of their large negative excess entropy of mixing. Most experimental determinations of the activity coefficients of such mixtures have been based on the determination of vapor pressures,<sup>16</sup> a method which is unsuitable for the study of very dilute solutions. Recently a very comprehensive investigation, involving the measurement of freezing points, enthalpies of mixing, and heat capacities of dilute aqueous solutions of the C<sub>1</sub>-C<sub>4</sub> alcohols, has revealed that under certain conditions, i.e. low temperatures and concentrations, these mixtures show negative deviations from Raoult's Law,<sup>27</sup> a hypothesis which had previously been advanced by F. Franks and D. J. G. Ives to account for the interfacial tensions of very dilute solutions of alcohols.<sup>28</sup> FIGURE 8 shows a typical case of this type of behavior; it is seen that at low temperatures the Raoult Law activity coefficient of water,  $f_1$ , decreases with rising alcohol concen-

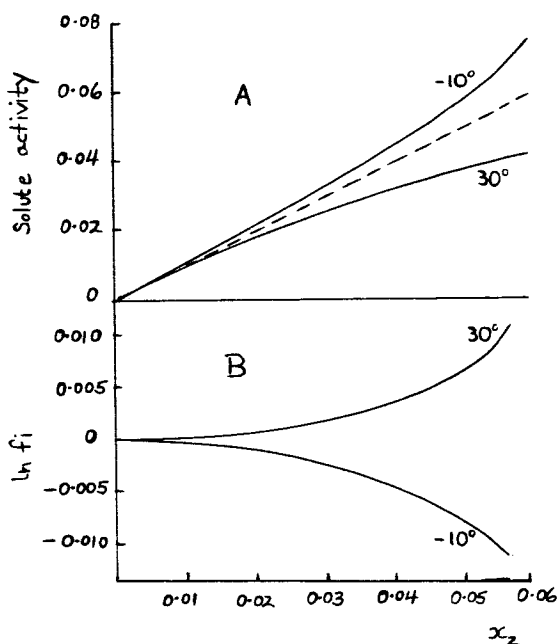


FIGURE 8. A. Activity of iso-PrOH compared to Henry's Law (*broken line*) as standard state. B. Raoult's Law activity coefficients of water in water - isopropyl alcohol mixtures as function of the alcohol mole fraction.

tration. The corresponding solute activity,  $a_2$ , therefore is greater than that predicted by Henry's Law. Eventually the  $a_2(x_2)$  curve cuts the Henry's Law reference line, and as  $x_2$  increases further, the behavior normally associated with water-alcohol mixtures is observed.

In this connection it is of interest to note that the behavior shown in FIGURE 8 should give rise to a lower consolute temperature (LCT). Although for the aliphatic alcohols the LCT would lie below the freezing point of the mixture, at low temperatures the solubilities of *n*-, iso-, and sec- butyl alcohols do indeed have negative temperature coefficients, and LCT's as high as 45° have been reported for water-glycol ether mixtures.<sup>29</sup>

### *Spectroscopic Properties*

Paradoxically, spectroscopic methods have not so far yielded much information about the nature of the hydrogen bonds and structural properties of water-alcohol mixtures. The infrared and Raman spectra are extremely complex, and at the time of writing the interpretation of such spectra for liquid water is still very much under discussion. In recent years several independent proton magnetic resonance (PMR) studies have led to mutually contradicting results, possibly because of the presence of small amounts of acidic impurities. W. G. Paterson and H. Spedding, as the result of an extensive study of proton exchange rates, found that the lifetime of a proton in a given position increases in the order  $\text{MeOH} \ll \text{EtOH} < \text{PrOH} < \text{n-BuOH} < \text{iso-BuOH} < \text{iso-PrOH} < \text{sec-BuOH} < \text{tert-BuOH}$ ,<sup>17</sup> thus underlining the acid-base nature of the hydrogen bond.

Finally of great interest is a recent study of the effect of alkyl groups on the water proton shift.<sup>3</sup> The observed shift of -0.02 p.p.m. per  $\text{CH}_2$  group at first sight indicates that hydrocarbon groups cause a net breaking of hydrogen bonds in water. However, this conclusion is based on the frequently made assumption that the hydrogen bond is of a purely electrostatic nature. The PMR results are quite consistent with other experimental observations on water-hydrocarbon and water-alcohol systems, if a covalent contribution to hydrogen bonding is invoked.<sup>30</sup> The association shift in the direction of a higher field could thus arise from an additional polarization of the hydrogen bond in the proximity of an interstitial (i.e. nonbonded) hydrocarbon group; this effect might be considered as the origin of the "icebergs," first postulated by H. S. Frank and M. W. Evans to account for the thermodynamic properties of aqueous solutions of nonelectrolytes,<sup>31</sup> and employed by later workers in the development of structural models for liquid water.<sup>1,2,4</sup>

### *References*

1. FRANK, H. S. & A. S. QUIST. 1961. *J. Chem. Phys.* **34**: 601.
2. NEMETHY, G. & H. A. SCHERAGA. 1962. *J. Chem. Phys.* **36**: 3382; 3401.
3. CLIFFORD, J. & B. A. PETHICA. 1964. *Trans. Faraday Soc.* **60**: 1483.



4. FRANK, H. S. & F. FRANKS. In preparation.
5. ZACHARIASEN, W. H. 1935. *J. Chem. Phys.* **3**: 158.
6. BERMAN, N. S. & J. J. MCKETTA. 1962. *J. Phys. Chem.* **66**: 1444.
7. BROWN, A. C. & D. J. G. IVES. 1962. *J. Chem. Soc.* : 1608.
8. PRIGOGINE, I. R. DEFAY. 1954. *Chemical Thermodynamics*, Longmans Green & Co., London, England. P. 11 ff.
9. MITCHELL, A. G. & W. F. K. WYNNE-JONES. 1953. *Disc. Faraday Soc.* **15**: 161.
10. FRANKS F. 1964. Unpublished results.
11. ALEXANDER, D. M. 1959. *J. Chem. Eng. Data* **4**: 252.
12. MASTERTON, W. L. 1954. *J. Chem. Phys.* **22**: 1830.
13. WEN, W. Y. & S. SAITO. 1964. *J. Phys. Chem.* **68**: 2639.
14. FRANKS, F. & H. T. SMITH. 1964. *J. Phys. Chem.* **68**: 3581.
15. McMULLAN, R. K. & G. A. JEFFREY. 1959. *J. Chem. Phys.* **31**: 1231.
16. BUTLER, J. A. V., D. W. THOMSON & W. H. MACLENNAN. 1933. *J. Chem. Soc.* : 674.
17. PATERSON, W. G. & H. SPEDDING. 1963. *Canad. J. Chem.* **41**: 714; 2472; 2477.
18. JEFFREY, G. A. 1964. Private communication.
19. WADA, G. & S. UMEDA. 1962. *Bull. Chem. Soc. Japan* **35**: 646.
20. FRANK, H. S. Unpublished work.
21. FRANKS, F. & H. H. JOHNSON. 1962. *Trans. Faraday Soc.* **58**: 656.
22. BURTON, C. J. 1948. *J. Acoust. Soc. Am.* **20**: 186.
23. GIACOMINI, A. 1942. *Acta Pontif. Acad. Sci.* **6**: 87.
24. HALL, L. 1948. *Phys. Rev.* **73**: 775.
25. SCHNEIDER, W. G. 1959. *Colloque Internat. Centre Nat. Recherche Sci. (Paris)*. **77**: 529.
26. GLEW, D. N. 1962. *Nature* **195**: 698.
27. KNIGHT, J. 1961. Ph.D. Thesis. Princeton University, Princeton, N. J.
28. FRANKS, F. & D. J. G. IVES. 1960. *J. Chem. Soc.* : 741.
29. LANDOLT - BOERNSTEIN. 1960. *Zahlenwerte und Funktionen*. **2**: 406. Springer. Berlin, Germany.
30. FRANK, H. S. & W. Y. WEN. 1957. *Disc. Faraday Soc.* **24**: 133.
31. FRANK, H. S. & M. W. EVANS. 1945. *J. Chem. Phys.* **13**: 507.

## DIFFUSIONAL SPECIFICITY IN WATER\*

I. Robert Fenichel and Samuel B. Horowitz

*Laboratory of Cellular Biophysics, Albert Einstein Medical Center,  
Philadelphia, Pa.*

The usual starting point in discussions of diffusion in very dilute aqueous solutions is the Stokes-Einstein equation

$$D_{12} = \frac{kT}{6\pi\eta_1 r_2} \quad (1)$$

where  $\eta_1$  is the solvent viscosity,  $r_2$  the radius of the diffusing solute, and  $D_{12}$  its diffusion coefficient, or the more general Sutherland equation<sup>1</sup>

$$D_{12} = \frac{kT}{6\pi\eta_1 r_2} \frac{1 + 3\eta_1/\beta_{12}r_2}{1 + 2\eta_1/\beta_{12}r_2} \quad (2)$$

where  $\beta_{12}$  is a coefficient of sliding friction.

Despite the limitations inherent in the derivation of these equations, they provide a fair description of diffusion of a large number of solutes in water. Quite good correlations of this data have been obtained by several equations of similar form, such as that of Wilke and Chang.<sup>2</sup>

$$D_{12} = \text{const} \frac{T}{\eta_1 V_{02}^{0.6}} \quad (3)$$

where  $V_{02}$  is the solute molar volume.

It is not commonly realized that the success of these equations is, in the light of current ideas of the equilibrium properties of liquid water, anomalous. The striking feature in Equations 1-3 is that, among different solutes,  $D_{12}$  depends on size only. In the derivation of Equation 1 for large solutes, this dependence is natural, since it is assumed that a large solute will carry an immobilized water shell, with shear occurring only between water molecules. In the case of small solutes, no shell exists,<sup>3</sup> and a dependence of  $D_{12}$  on size alone implies that water-solute interactions are independent of the chemical composition of the solute. Both theory and experiment<sup>4</sup> show that, even in the gaseous state, such independence is to be expected only if solvent and solute molecules behave like hard, perfectly elastic spheres. There is overwhelming evidence, from studies of the equilibrium properties of water and aqueous solutions, that a description in terms of a hard sphere model is inadequate. Strong, highly directional attractive forces — hydrogen bonds — exist in water, and solutes differ in their ability to form H-bonds with water molecules. One would

\*This work was supported in part by National Science Foundation Research Grant GB 1794 and by Public Health Service Research Grant GM 11070 from the Division of General Medical Sciences.

expect this variation to be reflected in  $D_{12}$ . Why, then, do Equations 1 and 3 fit the data for water so well?

An answer to this question is suggested by a comparative study of diffusion in parallel solvent systems, one containing water, and the other, formamide. In this study the self-diffusion coefficients, at very low concentration, of a variety of solutes were determined in swollen dextran gels containing about 80 per cent formamide or water. Details of technique and tabulations of experimental data have been presented elsewhere.<sup>5</sup> Comparison of the data in water-swollen gels with that available in liquid water showed the effect of the dextran matrix to be a constant factor independent of solute species:

$$D_{gel} = 0.65 D_{liquid} \quad (4)$$

The same will be assumed for the formamide gels. The data, corrected for this factor, may then be considered in terms of a frictional coefficient  $f_{12}$ , given by

$$D_{12} = \frac{kT}{f_{12}\eta_1 r_2} \quad (5)$$

where  $\eta_1$  is taken as the viscosity of pure formamide or water.

The frictional coefficient  $f_{12}$  as defined by Equation 5 incorporates the contributions to the overall frictional resistance not described by the solvent viscosity,  $\eta_1$  and the reciprocal first-power dependence on solute radius,  $r_2$ . Experimentally,  $f_{12}$  is found to vary, and this is expected on theoretical grounds.

A number of studies have shown that, as the size of the diffusing molecule relative to that of the solvent increases, the value of  $f_{12}$  increases.<sup>6,7</sup> For very large solutes,  $f_{12}$  has a value of about  $6\pi$ ; in self-diffusion in the pure liquid, in which the equation

$$D_1 = \frac{kT}{f_{11}\eta_1 r_1} \quad (6)$$

replaces Equation 5, the value of  $f_{11}$  is approximately  $4\pi$ , the Sutherland value for  $\beta = 0$ ; for solutes smaller than the solvent a smaller value yet is observed.<sup>8</sup> The origin of this variation with size is suggested by kinetic theory, in which molecular collisions and therefore transport coefficients are dependent upon molecular cross-sections,  $r_2^2$ , rather than radius,  $r_2$ . Also, the larger  $r_2$  relative to  $r_1$  (the molecular radius of the solvent), the greater the probability of multibody collisions; this also will make  $f_{12}$  an increasing function of  $r_2$ . The dimensions of  $D$  require that  $r_2$  enters as an inverse first power in Equation 5; the additional dependence of  $f_{12}$  on  $r_2$  must therefore be in terms of a reduced radius. The constancy of  $f_{11}$  observed in the self diffusion of pure liquids, over a wide range of values of  $r_1$ , supports the idea that the appropriate reduced radius is  $r_2/r_1$ .

The coefficient  $f_{12}$  also reflects the features of the interaction of solute and solvent molecules which are determined by their chemical composition. The solvent viscosity,  $\eta_{11}$ , is introduced in expressions for  $D$  under the assumption that the unit process and therefore the pertinent interactions are the same in diffusion and viscous flow. That this assumption is essentially correct for self diffusion in the pure liquid is shown by the constancy of  $f_{11}$ .<sup>3,9</sup> In the diffusion of solutes of different compositions, the coefficient  $f_{12}$  will reflect differences between the solute-solvent and solvent-solvent interactions, reduced, in part, to unit solute size by the presence of  $r_2$  in Equation 5. The stronger the solute-solvent interactions relative to solvent-solvent interactions, the larger will be  $f_{12}$ . A plot of  $f_{12}$  as a function of  $r_2/r_1$  should, therefore, reflect both the general increase in  $f_{12}$  with size

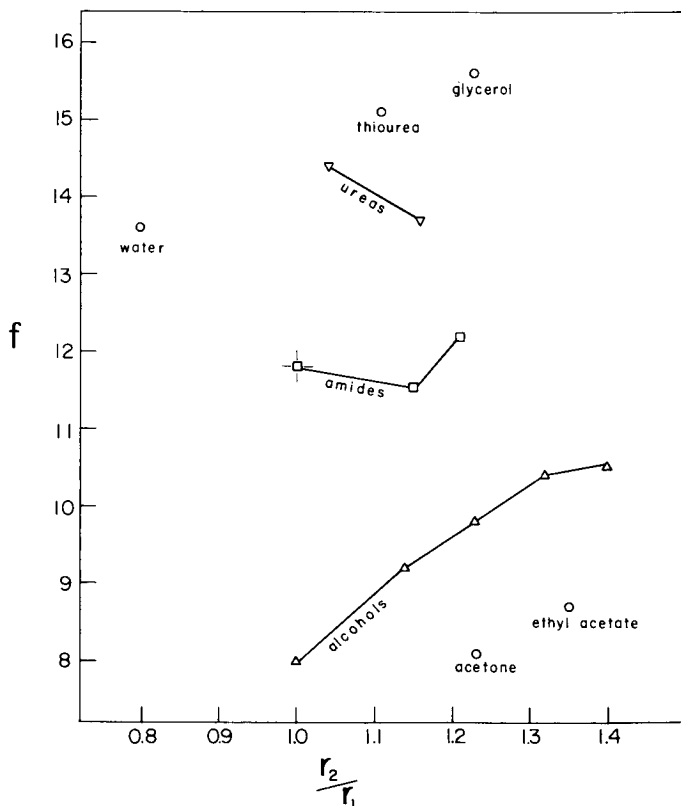


FIGURE 1. Frictional coefficients,  $f$ , for diffusion in formamide, at 15.3°C, as a function of  $r_2/r_1$ , the ratio of the molecular radii of solute and solvent. The amides are formamide, acetamide and propionamide; the alcohols are the primary alcohols through 1-pentanol; the ureas are urea and methyl urea.

and the specific variation due to the chemical interaction of the solute with the solvent.

In FIGURE 1, data for diffusion of 15 compounds in formamide-swollen dextran gels are presented as  $f_{12}$ , calculated from Equation 5, and  $f_{11}$ , from Equation 6, as a function of  $r_2/r_1$ . Values of  $r$  were determined from the molar volumes at 20°C.,  $V_0$ , using the formula

$$r = \frac{1}{2} \left( \frac{V_0}{N_0} \right)^{1/2}$$

where  $N_0$  is Avogadro's number.\*

The striking feature of FIGURE 1 is the dependence of  $f_{12}$  on the chemical nature of the diffusing solute. At any value of  $r_2/r_1$ ,  $f_{12}$  is larger the greater the H-bonding ability of the solute, judging by the number and strength<sup>10</sup> of H-bonding groups. Acetone and ethyl acetate, weak proton acceptors which are unable to donate protons, have, for their size, the smallest values of  $f_{12}$ . The alcohols have somewhat larger values, but even the largest alcohol studied (1-pentanol) does not have a value as large as  $f_{11}$ . Only the solutes able to form strong, multiple H-bonds — water, the ureas, thiourea, and glycerol — have  $f_{12}$  greater than  $f_{11}$ .

A general increase in  $f_{12}$  with  $r_2/r_1$ , as described above, is present, as can be seen most clearly among the alcohols and possibly in the series: water, urea, thiourea, glycerol. However, chemical specificity is great enough to reverse this trend in the pairs urea-methyl urea and formamide-acetamide. In the former pair, the increase of size by the addition of a methyl group is at the expense of an H-bonding site, and a large decrease of  $f_{12}$  is seen. In the latter pair, the addition is not to an H-bonding site, but steric and inductive effects may account for the small decrease in  $f_{12}$ .

These data confirm the idea that solute-solvent interaction, in the present case H-bonding, is an important determinant of diffusion and is reflected in  $f_{12}$ . One would expect this also in water. In FIGURE 2, the data for diffusion in water-swollen gels are presented. For a few solutes — acetone, ethyl acetate, and glycerol — a pattern of chemical specificity similar to that in formamide is seen. But for the other solutes, urea, thiourea, the amides, and the alcohols, virtually no chemical specificity is discernible; the dominant feature is the general rise of  $f_{12}$  with  $r_2/r_1$ .

\*There is an inherent difficulty in choosing a suitable volume from which to define  $r$  in the use of Stokes-Einstein type equations. This is due to the semi-empirical nature of the equations when applied to small solutes. Longsworth<sup>6</sup> has used the molar volume in solution, while other investigators have used the boiling point or LeBas molar volumes. In the absence of knowledge of how the interactions determining the differences in these volumes enter the unit diffusional process, no definitive basis for choice exists. In this work, we have used the molar volume of the pure solute near the temperature of the diffusion experiment; this is nearly equal to the volume in solution. The principle points to be made would not be affected by the use of boiling point volumes.

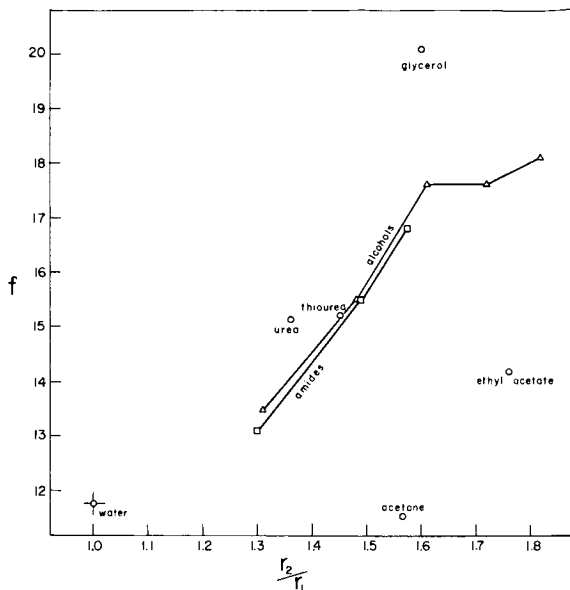


FIGURE 2. Frictional coefficients,  $f$ , for diffusion in water at 15°C as a function of  $r_2/r_1$ , the ratio of the molecular radii of solute and solvent. Amides and alcohols are as in FIGURE 1.

This apparent absence of specificity due to solute-solvent H-bonding in water, in contrast to formamide, is the anomaly referred to above. Its explanation lies principally in the fact that water not only can interact with solutes by H-bonding but also is capable of a special interaction with nonpolar radicals and solutes. Since the work of Frank and Evans,<sup>11</sup> a great deal of evidence, some discussed in the present symposium, has shown that increased association of water molecules occurs in the vicinity of a nonpolar solute or radical (eg., the alkyl chain of an alcohol), with the production of a stabilized domain, often referred to as an "iceberg." It seems reasonable to believe that these interactions will be reflected in  $f_{12}$ .

Several lines of evidence support this interpretation. Among solutes lacking a hydrocarbon chain (methanol, formamide, thiourea, urea, glycerol) the activation energy for diffusion,  $E$ , is in the range of 4.4–4.8 kcal., independently of size, and is similar to that for the self-diffusion of water, 4.4 kcal. On the other hand, iceberg-forming solutes such as 1-propanol, 1-butanol, and 1-pentanol have values of  $E$  in the range 5.4 to 5.9 kcal. This can be interpreted as the effect of the breakdown or "melting" of the icebergs as temperature increases, a process which, as attested by the high partial molar heat capacities of nonpolar solutes in aqueous solution,<sup>11</sup> is more sensitive to temperature than the normal water struc-

tures. Secondly, a close correlation can be shown<sup>5</sup> between  $D_{12}$  and the entropy of vaporization of the solute from water,  $\Delta S_v$ , a parameter which strongly reflects iceberg formation.

Because of the influence of icebergs on diffusion, the value of  $f_{12}$  will depend on contributions from both H-bonding groups and nonpolar groups. A reciprocal relation, however, exists between these groups: among solutes of equal size, the more H-bonding groups, the fewer nonpolar groups, and vice versa. Because of this reciprocity the observed specificity may be small even though the interactions strongly affect diffusion.

The solute interactions in water can be interpreted in greater detail by comparison of FIGURES 1 and 2. The values of  $f_{12}$  for weak H-bonding solutes common to both systems, the alcohols, acetone, and ethyl acetate, are shifted upward relative to  $f_{11}$  in going from formamide to water. This is consistent with the role of icebergs in the aqueous systems. The upward shift is not the same among all of these solutes, alcohols being more displaced than the ester and ketone. These differences are in agreement with the data on  $\Delta S_v$  of Frank and Evans which suggest that, per unit solute radius, the alcohols are better iceberg formers than acetone and ethyl acetate. The positions of the alcohols, acetone, and ethyl acetate in water, then, reflect both the better H-bonding ability of the alcohols, as judged from the formamide data, and their better iceberg forming ability as judged from the equilibrium data.

Among the stronger H-bonding solutes urea, thiourea, and glycerol, there is a different type of displacement in going from formamide to water. While  $f_{12}$  for glycerol relative to  $f_{11}$  is similar in the two systems, the values of  $f_{12}$  for urea and thiourea in water are depressed relative to those in formamide. An explanation for this may lie in the suggestion<sup>12</sup> that urea disorders water structure; this should also be applicable to thiourea, which is of similar structure. Such disordering would provide a third source of specificity, in addition to the H-bonding and iceberg formation already described. A similar effect of structure breaking on the mobility of monovalent cations has been observed;<sup>13</sup> it is accompanied by a decrease in the activation energy  $E$  to a value smaller than that of water itself. A comparable effect does not occur in the case of urea and thiourea, for which  $E$  is  $4.4 \pm 0.4$  kcal and  $4.7 \pm 0.3$  kcal, respectively, as compared to a value of  $4.4 \pm 0.4$  kcal for water. This indicates that the structure-breaking effect of these solutes is not large in comparison to their H-bonding interactions. This conclusion can be drawn also from the values of  $f_{12}$  for urea and thiourea, which are not small in comparison to those of, for example, the H-bonding and iceberg-forming alcohols.

The possibility of a successful analysis of diffusional behavior of small solutes in water and other liquids using a Stokes-Einstein type equation does not, unfortunately, throw much light on the nature of the diffusional

process. Attention is merely shifted to the fluidity, which, in itself, is one of the principal problems in the theory of liquids. Of the two types of approach to liquid theory, the "gas-like" and the "solid-like", the former is more readily adaptable to fluidity. In fact, the Stokes-Einstein form  $D\eta \propto kT/r$  is derivable from the Enskog dense gas theory. On the other hand, lattice theories more naturally account for the observation that fluidity and diffusion are activated processes in liquids,<sup>14</sup> having an exponential temperature dependence.

The problem, then, is two-sided: while the temperature dependence is solid-like, the Stokes-Einstein behavior is gas-like, and not derivable from lattice models unless gas-like features are introduced. Current ideas of the equilibrium properties of liquid water do little to resolve the problem. Since the work of Bernal and Fowler,<sup>15</sup> it has been customary to view liquid water as having, in greater or lesser degree, structure — i.e., solid-like features. The extent of structuring attributable to water is inversely related to the integrity of the structure — the more structure, the less solid-like it must be, so as to permit fluidity. While the conflict of these descriptions may, to some extent, reflect only differences in "averaging" over an assembly of water molecules, and so be resolved in a definitive liquid-state model, they nonetheless reflect the real possibility of important differences in the behavior of water resulting from small changes in local conditions. For example, in the "flickering cluster" model of Frank and Wen,<sup>16</sup> it is assumed that the overall transport reflects only that occurring in areas where clusters are broken down; the temperature dependence of transport reflects that of cluster size. For this to be so, there must be a large difference in, say, diffusion in an intact and in a broken cluster. A convenient description would be that diffusion in the intact cluster is "solid-like" while that in the broken cluster is "gas-like."

Since there has been almost no experimentation on diffusion in molecular crystals, we can only have a general idea of the characteristics of this "solid-like" diffusional component, though some attributes are clear. For example, it would not bear similarity to Stokes-Einstein behavior, which predicts a simple inverse size dependence among different solutes; as in the case of solids, a higher order dependence on size is to be expected.<sup>17</sup> In such a scheme, a very substantial difference in diffusional behavior, determined by thermal fluctuations, would occur in different zones in liquid water. The possibility that such differences are more than simply "model-making" becomes an important question in multicomponent systems in which interactions between water and very large solutes such as protein occur. Changes in the transport properties of water in such systems have long been recognized; the water is often referred to as "bound." The idea implicit in "binding" is that a strong, short-range interaction is responsible for changes in the transport properties, the analogue being, for example,



ionic hydration in salt solutions. An entirely different picture is suggested by "two-state" ideas of the structuring in water: that weaker interactions, perhaps on the order of  $kT$ , can produce substantial local changes in transport properties. The extent to which these changes are observable macroscopically depends upon the stability of these interactions to thermal fluctuation, relative to those in pure water. This stability is provided, not by the strength of the interaction, but by the great inertia of the macromolecular component. Moreover, (using again the cluster model) if, by virtue of such interactions, the clusters became sufficiently extensive, the macroscopic transport behavior would tend towards the "solid-like" rather than "gas-like" extreme. Inertial stabilization, with the emergence of "solid-like" behavior, are in fact seen in studies of water films at solid surfaces,<sup>18</sup> which are, in a sense, a large-scale analog of the macromolecule-water system.

1. SUTHERLAND, G. B. B. M. 1905. *Phil. Mag.* 9: 781.
2. WILKE, C. R. & P. CHANG. 1955. *Am. Inst. Chem. Engrs. J.* 1: 264.
3. DULLIEN, F. A. L. 1963. *Trans. Faraday Soc.* 59: 856.
4. HIRSCHFELDER, J. O., C. F. CURTISS & R. B. BIRD. 1954. *Molecular Theory of Gases and Liquids*. J. Wiley & Sons, Inc. New York, N. Y.
5. HOROWITZ, S. B. & I. R. FENICHEL. 1964. *J. Phys. Chem.* 68: 3378.
6. LONGSWORTH, L. G. 1955. *In Electrochemistry in Biology and Medicine*. T. Shedlovsky, Ed. : 225. J. Wiley & Sons, Inc. New York, N. Y.
7. POLSON, A. 1950. *J. Phys. Colloid Chem.* 54: 649.
8. HIMMELBLAU, D. M. 1964. *Chem. Rev.* 64: 527.
9. MCLAUGHLIN, E. 1959. *Trans. Faraday Soc.* 55: 28.
10. MIZUSHIMA, S. 1954. *Structure of Molecules and Internal Rotation*. Academic Press. New York, N. Y.
11. FRANK, H. S. & M. W. EVANS. 1945. *J. Chem. Phys.* 13: 507.
12. RUPLEY, J. A. 1964. *J. Phys. Chem.* 68: 2002.
13. WANG, J. H. 1954. *J. Phys. Chem.* 58: 686.
14. GLASSTONE, S., K. J. LAIDLER & H. EYRING. 1941. *The Theory of Rate Processes*. McGraw-Hill Book Co., Inc. New York, N. Y.
15. BERNAL, J. D. & R. H. FOWLER. 1933. *J. Chem. Phys.* 1: 515.
16. FRANK, H. S. & W. Y. WEN. 1957. *Disc. Faraday Soc.* 24: 133.
17. HOROWITZ, S. B. & I. R. FENICHEL. 1965. *This Annal.*
18. HENNIKER, J. C. 1949. *Rev. Mod. Phys.* 21: 322.

# BONDS IN WATER AND AQUEOUS SOLUTIONS

T. G. Owe Berg

*T. G. Owe Berg, Inc., Garden Grove, Calif.*

## *Introduction*

The molecules in liquid as well as in solid water, as distinguished from gaseous water, are held together by fairly strong intermolecular bonds. The bond strength, as measured by the heat of vaporization, is 10.5 kcal./mole for liquid water and 12 kcal./mole for solid water. This energy results from a difference in the electronic energy state of liquid and solid water as compared to gaseous water and also from some bond strain energy, which may amount to two or three kcal./mole. The intermolecular bonds are generally referred to as hydrogen bonds.

In aqueous solutions, the bonds may be affected by the solute, but the heat of water vaporization is relatively insensitive to the presence of a solute. It appears that the solute may affect the bond strain energy but not the electronic energy. There are some notable exceptions from this rule. Some solutes combine chemically with water to form hydrates or new species. Thus,  $\text{SO}_3$  gives  $\text{H}_2\text{SO}_4$  with  $\text{H}_2\text{O}$ .

It follows from this example already that the properties of aqueous solutions are strongly affected by the strength of the intermolecular bonds and by the distribution of the intermolecular bonds in the solution. This paper is primarily concerned with these effects.

A real solution, as contrasted to the ideal solution, is characterized by a preferential distribution of solvent and solute molecules. This effect results from a difference in size and shape between solvent and solute molecules and, occasionally, from a difference in chemical affinity between solvent and solute molecules. Such ordered structures are well known in the solid state, e.g., intermetallic compounds, and have been studied extensively by various techniques. A much used technique is dilatometry. Other such techniques are based upon changes in magnetic, electric and other properties in the ordering process.

The solid state is characterized by a rigid geometrical arrangement of the constituent atoms or molecules. This property makes it possible to study the structure of solids by means of x-ray or electron diffraction. This technique is much less useful in the study of the liquid state because the liquid structure lacks the rigid geometry. On the other hand, aqueous solutions may be studied conveniently by vapor pressure measurements, a technique that is rarely applicable to solid solutions.

At the present state of the art, the structure of a solution and the distribution of solvent and solute molecules in the solution cannot be predicted

on the basis of the constituent properties. These properties of solutions can be determined empirically only, e.g., by the techniques just referred to. The treatment of these properties in the following is, accordingly, empirical, although, of course, the structures determined by various techniques should agree among themselves and with the various physical and chemical properties as well as with general laws of thermodynamics and statistics.

### *The Structure of Liquid Water*

The coalescence of two water drops in contact with each other occurs through the formation of intermolecular bonds across the contact surface. A study of the coalescence process may therefore give information on the intermolecular bonds in water. Such a study has been undertaken.<sup>1</sup>

Two drops were mounted on thin platinum wires and pushed together. A voltage was applied between the wires. The event was followed by high-speed photography. FIGURE 1 shows the experimental set up. FIGURE 2 shows two typical frames. In one frame, the drops are in contact, and the contact surface is flattened as a result of deformation under the contact pressure. In the other frame, a narrow lens has been formed at the inter-

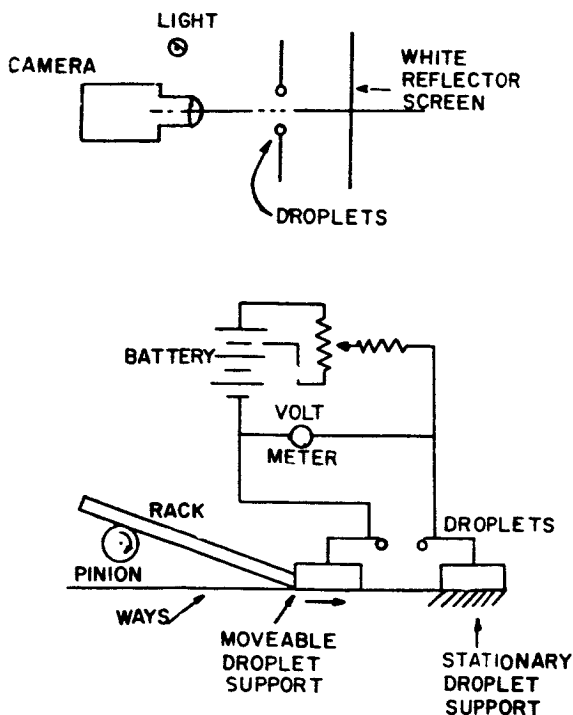


FIGURE 1. Experimental setup for observing drop coalescence.

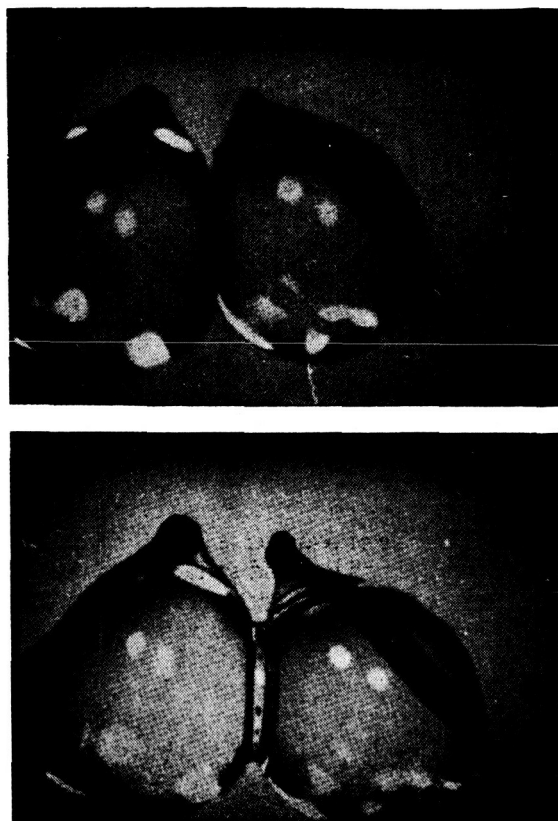


FIGURE 2. Flattening of drops and appearance of lens in coalescence.

face. This lens widens in later frames. The appearance of the lens is indication of coalescence.

The time delay  $t$ , of the order of 0.1 to 1 ms. in our experiments, between contact and coalescence was measured at various voltages  $V$ , between 1 and 10 volts. The product  $tV$  was found to be a constant as shown in FIGURE 3. Repeating the experiment with various alcohols instead of water, it was found that the product  $tV \sqrt{\epsilon - 1}$  is the same constant for all these liquids,  $\epsilon$  denoting the dielectric constant of the liquid. The time delay  $t$  depends thus upon the product of the induced dipole moment  $\mu = \sqrt{\epsilon - 1}$  of the bond and the applied electric field. Hence, coalescence is effected by the orientation of bond dipoles in the direction of the electric field across the interface. A similar case is encountered in electrolytic conduction, discussed later. In this case, transport of electricity is effected by charge transfer along intermolecular bonds, rate-determining being the

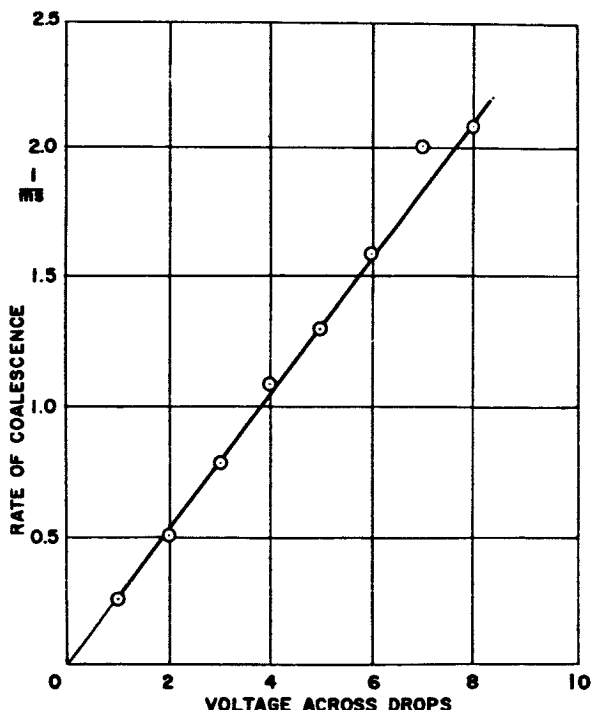


FIGURE 3. Rate of coalescence of water drops against voltage across the drops.

orientation of the bonds in the direction of the field. Results similar to those with a pair of drops were obtained when one drop was replaced by a piece of a solid.<sup>2</sup>

The results from the coalescence experiments give some information of intermolecular bonds in liquid water.

(a) All intermolecular bonds are engaged and none are broken. Bonds may be broken as a result of thermal fluctuations, but such broken bonds are rapidly reformed according to the original pattern. In particular, there are no free bonds sticking out of the surface of the water.

(b) The engagement of the bonds within the surface of the liquid must cause considerable straining of the bonds in the vicinity of the surface. This strain appears as surface tension.

Let us now consider the distribution of bonds within liquid water as compared to those in gaseous and solid water. Gaseous water consists of free independent  $\text{H}_2\text{O}$  molecules. Water vapor is close to the ideal gas. This state is a convenient reference state. Solid water may be considered as an aggregate of an infinite number of  $\text{H}_2\text{O}$  molecules held together by hydrogen bonds in a certain pattern. The geometry of this pattern has

been determined by x-ray diffraction.<sup>3</sup> The structure is tetrahedral, each H<sub>2</sub>O molecule being surrounded by four nearest neighbors, and the five H<sub>2</sub>O molecules being located at the center and at the corners of a tetrahedron.

There is x-ray evidence to the effect that the coordination number is four in liquid water too.<sup>4-7</sup> The smallest possible number of H<sub>2</sub>O molecules in liquid water is thus five. Let us assume that liquid water consists of aggregates of five H<sub>2</sub>O molecules, within which aggregates all the 10 bonds are engaged, although they are readily switched from one aggregate to another. This model permits us to calculate the entropies of fusion and vaporization.

The entropy of vaporization is the difference in bond entropy between liquid and gaseous water. This difference is readily calculated from the permutations of 10 hydrogen atoms in the aggregate as compared to that of two hydrogen atoms of five individual molecules. Thus,

$$\Delta S = \frac{1}{5} R \ln \left( \frac{2!}{10!} \right)^5 = -28.8 \text{ eu} \quad (1)$$

This compares very well with the experimental value  $\Delta S = -28.4$  eu.

The entropy of fusion is also readily calculated on the basis of the same model. In liquid water, a molecule A at the center of the tetrahedron, is bonded to four molecules B, at the corners of the tetrahedron, and the molecules B are bonded to one another by six hydrogen bonds. In solid water, the molecule A is bonded in the same manner, but each molecule B is bonded to three nearest neighbor molecules C outside the aggregate by a total of 12 hydrogen bonds between B and C molecules. When calculating the entropy of fusion, we may use a reference state in which all bonds, except those with the molecule A, are broken. Then entropy of fusion is thus

$$\Delta S = \frac{1}{5} R \ln \frac{6!}{12!} = -5.31 \text{ eu} \quad (2)$$

This is close to the experimental value  $\Delta S = -5.28$  eu.

The model under consideration is thus compatible with the entropy of liquid water formation from solid and from gaseous water, the structures of which are known.

An aggregate of five molecules has  $3 \times 5 - 6 = 9$  vibrational degrees of freedom each contributing 2 cal. to the specific heat.<sup>8</sup> The specific heat of an isolated aggregate is thus 18 cal. per five moles of H<sub>2</sub>O. If it is assumed that the rearrangement of bonds among the bonded aggregates makes each H<sub>2</sub>O molecule part of five aggregates, this gives 18 cal. per mole of H<sub>2</sub>O. Thus, the model is also compatible with the specific heat of liquid water. This is merely a corollary since the specific heat is deter-

mined by the structure and is, indeed, related to the entropy of the structure.

It is clear that this bonding in liquid water is associated with considerable bond strain as compared to solid water. The difference in bond strain energy is the heat of fusion.

#### *Electrical Conduction in Aqueous Solutions*

Electrical conduction in aqueous solutions is effected by charge transfer, or the propagation of an electronic disturbance, along hydrogen bonds. This mechanism, which seems to be generally accepted, was formulated in essence by von Grotthuss<sup>9</sup> in 1806. The rate-determining step in this process may conceivably be one among several, e.g., the orientation of bonds in the direction of the applied field, or the transfer of charge along the oriented bond. An analysis of the data shows that the former step is rate-determining.<sup>10</sup>

If  $c$  is the number of effective bonds and  $\mu$  is their dipole moment, the number of dipoles oriented in the direction of the field  $E$  is

$$c \frac{\mu E}{3 kT} e^{-\epsilon/kT} \quad (3)$$

where  $\epsilon$  denotes the activation energy of the orientation process. Denoting by  $p$  the charge transferred, the current is proportional to

$$p \frac{kT}{h} c \frac{\mu E}{3 kT} \frac{F'}{F} e^{-\epsilon/kT} \quad (4)$$

where  $F'$  and  $F$  are the partition functions for the activated state and the original state, respectively. This gives for the conductivity

$$\kappa = \frac{\partial i}{\partial E} = A c \frac{F'}{F} e^{-\epsilon/kT} \quad (5)$$

where  $A$  is a constant. Taking classical partition functions, this reduces to

$$\kappa = A c T^{-n} e^{\frac{\Delta S}{R}} e^{-\epsilon/RT} \quad (6)$$

where

$$n = \frac{\Delta C_p}{R} \quad (7)$$

and  $\Delta C_p$  is the change in specific heat. If the activated state contains an  $H_2O$  molecule whose bonds are all broken,  $\Delta C_p = 18$  and  $n = 9$ . The value of  $n$  can be determined by plotting the experimental values of  $\ln (\kappa T^n)$  against  $1/T$ . This plot should be linear. The best fit of the data for solutions of  $HCl$ ,  $HNO_3$ ,  $H_2SO_4$ , and  $HClO_4$  to a straight line is given by  $n=9$ . The value of  $\epsilon$  thus determined is approximately 8 kcal./mole. Both  $n$  and  $\epsilon$

are the same for these various solutes and also for all concentrations of the solutions. Hence, the rate-determining step is the orientation of a free  $\text{H}_2\text{O}$  molecule in the liquid.

The process may be studied in further detail by an analysis of the entropy  $\Delta S$ . Taking the equivalent conductivity

$$\Delta = \frac{\kappa}{c} \quad (8)$$

formula (6) gives

$$\ln \frac{\Delta}{\Delta_\infty} = \frac{\Delta S}{R} - \frac{\Delta S_\infty}{R} = \frac{\Delta S'}{R} \quad (9)$$

the subscript  $\infty$  denoting infinite dilution. Plots of  $\ln \Delta/\Delta_\infty$  against the mole fraction of solute are straight lines for all aqueous solutions for which data are available. The linear plot holds for NaCl solutions in the

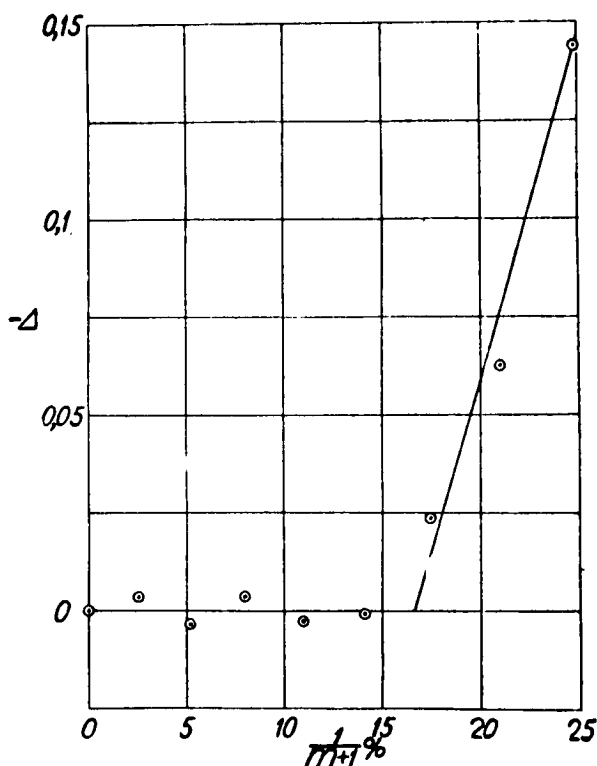


FIGURE 4. The plot of  $\ln \Delta$  against the mole fraction  $\frac{1}{m+1}$  of solute is a straight line. The deviation  $\Delta$  is plotted against  $\frac{1}{m+1}$  for HCl at 15° on the data of Kohlrausch.<sup>11</sup>



entire range of solubility, for HCl solutions up to 9 N, and for HClO<sub>4</sub> solutions up to 10 N solutions. FIGURES 4 and 5 show the deviations from the straight line for HCl and HClO<sub>4</sub> solutions against the mole fraction of solute.

For HCl and HNO<sub>3</sub> solutions, which are particularly simple and therefore convenient to treat in this short paper, the empirical formulae are

$$\text{HCl: } \ln \frac{\Delta}{\Delta_{\infty}} = 0.0001 - \frac{9.54}{m+1}, m > 5 \quad (10)$$

$$\text{HNO}_3: \ln \frac{\Delta}{\Delta_{\infty}} = -0.0411 - \frac{8.46}{m+1}, m > 9 \quad (11)$$

In these formulae,  $m$  denotes the number of H<sub>2</sub>O molecules per molecule of solute.

Let us consider an H<sub>2</sub>O molecule that is adjacent to a solute molecule and that has all its bonds with its four nearest neighbors broken. One of these neighbor molecules is a solute molecule, three of them are H<sub>2</sub>O molecules. The probability that the free H<sub>2</sub>O molecule makes a bond with the solute molecule is 1/4; the probability that it makes a bond with an H<sub>2</sub>O molecule is 3/4. The probability for the simultaneous occurrence of both these events is  $1/4 \times 3/4 = 3/16$ . To this corresponds an entropy

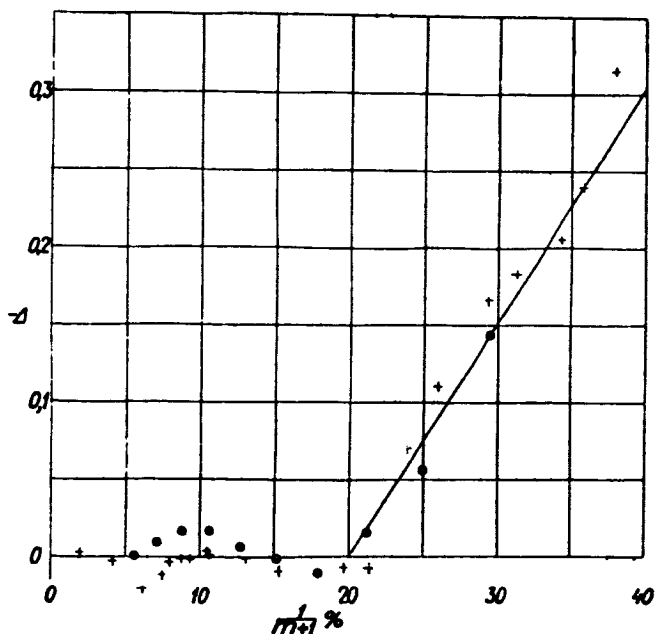


FIGURE 5. Same plot as in FIGURE 4 for HClO<sub>4</sub> at 25° on the data of Brickwedde<sup>12</sup> (○) and Linde<sup>13</sup> (+).

$$R \ln \frac{3}{16}$$

or, per H atom

$$\Delta S_0 = \frac{1}{2} R \ln \frac{3}{16} = R \ln 0.433 \quad (12)$$

The data give  $\Delta S_0 = R \ln 0.42$ .<sup>10</sup> The value of  $\Delta S'$  is

$$\Delta S' = \frac{N+1}{m+1} \Delta S_0 \quad (13)$$

when  $N$  is the number of  $H_2O$  molecules adjacent to the solute molecule. This number is  $N = 10$  for  $HCl$  and  $N = 9$  for  $HNO_3$  solutions. Inserting these values and  $\Delta S_0$  from formula (12) we obtain

$$HCl: \ln \frac{\Lambda}{\Lambda_\infty} = -\frac{9.2}{m+1}, m > 5 \quad (14)$$

$$HNO_3: \ln \frac{\Lambda}{\Lambda_\infty} = -\frac{8.5}{m+1}, m > 9 \quad (15)$$

in agreement with the empirical formulae (10) and (11).

It follows from this analysis that the rate of transportation of electricity through an aqueous solution is determined by the following process:

An  $H_2O$  molecule adjacent to a solute molecule has all its bonds with its neighbors broken and is reorientated in the direction of the applied electric field.

The charge transfer along the intermolecular bonds is comparatively rapid.

#### *Density and Vapor Pressure*

The mixing of two substances of different molecular size and shape causes a change in volume as compared to the two separate substances and also an ordered structure with respect to solvent and solute molecules. These two changes are not necessarily independent. Indeed, an analysis of aqueous solutions shows that the two effects are merely different features of the same phenomenon.

The volume change shows up directly in the specific volume or density of the solution; the ordered distribution of solvent and solute molecules shows up directly in the vapor pressure of the solvent. These two quantities are briefly discussed in this section.

Aqueous solutions of inorganic salts invariably show a volume contraction, and the vapor pressure of the solvent is therefore lower than that given by Raoult's law. The volume change is, as a rule, very small, but this does not reduce its significance. However, the experimental error in density measurements are frequently large enough to mask the phenomena involved. The data given in tables are frequently smoothed so as to further obscure the phenomena. However, even so the derivative of the density may be

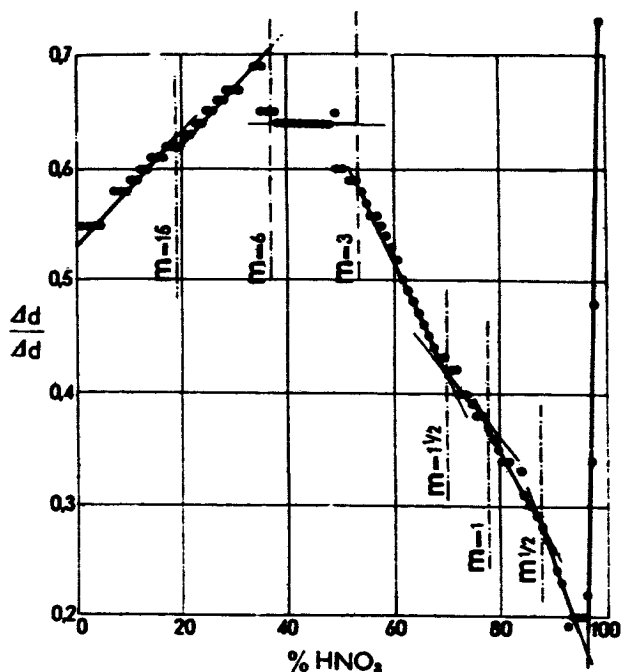


FIGURE 6. The derivative  $\frac{\Delta d}{\Delta g}$  of the density  $d$  for  $\text{HNO}_3$  solutions at  $20^\circ$  on the data in Hodgman's Handbook of Chemistry and Physics.

informative. FIGURE 6 shows the differential  $\Delta d/\Delta g$  against  $g$  for  $\text{HNO}_3$  solutions on the basis of the data given in Hodgman's handbook.<sup>14</sup> The denotations are  $d$  for density and  $g$  for solute concentration in per cent by weight. There are conspicuous changes in the plot at  $m = 1/10$ ,  $m = 1/2$ ,  $m = 1$ ,  $m = 1-1/2$ ,  $m = 3$ ,  $m = 6$ , and  $m = 15$ , corresponding to changes in the structure at these concentrations. FIGURE 7 shows the corresponding plot for  $\text{HCl}$  solutions on the data of Akerlöf and Teare.<sup>15</sup> It is noteworthy that the ordinate scales in FIGURE 6 and 7 differ by a factor of 20. The hydrates of  $m = 5$ ,  $m = 10$ , and  $m = 26$  are conspicuous in this plot.

The relative partial vapor pressure  $p$  of the solvent is the actual partial vapor pressure above the solution divided by that above the pure solvent. This quantity may be written in the form

$$p = e^{\Delta S/R} e^{-\Delta E/RT} \quad (16)$$

where  $\Delta S$  is the entropy of mixing and  $\Delta E$  is the energy of mixing.  $\Delta E$  may be determined from the slope of a plot of  $\ln p$  against  $1/T$ . The values

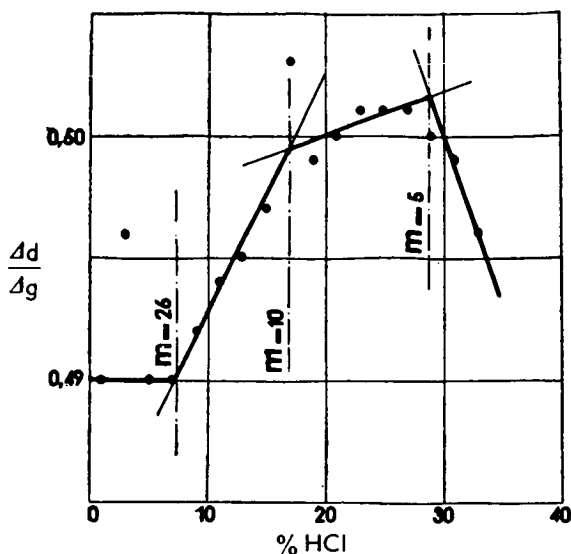


FIGURE 7. The derivative  $\frac{\Delta d}{\Delta g}$  of the density  $d$  for HCl solutions at  $20^\circ$  on the data of Akeröf and Teare.<sup>15</sup>

of  $\Delta E$  thus determined for HCl solutions are plotted against the concentration of the solute in FIGURE 8 and against  $10 - m$  ( $m+1$ )<sup>2</sup> in FIGURE 9. The latter plot is a straight line through the origin. Thus, for  $m > 10$ ,  $\Delta E > 0$ .

The entropy of mixing may be written in the form

$$\Delta S = \Delta S_0 + \frac{\Delta E}{T_0} \quad (17)$$

Hence, for  $T = T_0$ ,

$$p = e^{\Delta S_0 / R} \quad (18)$$

and since

$$\Delta S_0 = R \ln W \quad (19)$$

$W$  being the thermodynamic probability of the structural change in mixing,

$$p = W \quad (20)$$

The probability  $W$  may be defined as that of finding a solvent molecule on a given molecular site, or as the probability of finding a solvent molecule in a given volume element. The former definition pertains to the distribution of solute and solvent molecules relative to one another; the latter definition pertains to the volume change in mixing.

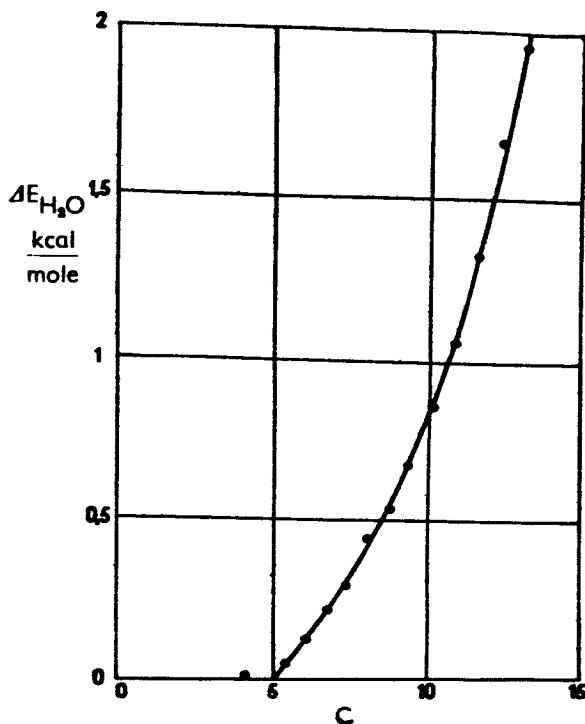


FIGURE 8. The relative heat of water vaporization  $\Delta E$  in HCl solutions as a function of the concentration  $c$  from the vapor pressure data of Yannakis.<sup>11</sup>

For the ideal solution, the former definition gives

$$W = \frac{m}{m+1} \quad (21)$$

i.e., the mole fraction of the solvent. The formula

$$p = \frac{m}{m+1} = 1 - \frac{1}{m+1} \quad (22)$$

is known as Raoult's law.

A plot of  $p$  against  $1/m+1$  very rarely has unit slope. Thus, for HCl solutions the data give

$$p = 1 - \frac{3}{m+1} = \frac{m-2}{m+1}, \quad m > 26 \quad (23)$$

This formula holds for  $m > 26$  only. For  $m < 26$ , there is a deviation  $\Delta p$  from this formula

$$\Delta p = p - \frac{m-2}{m+1} \quad (24)$$

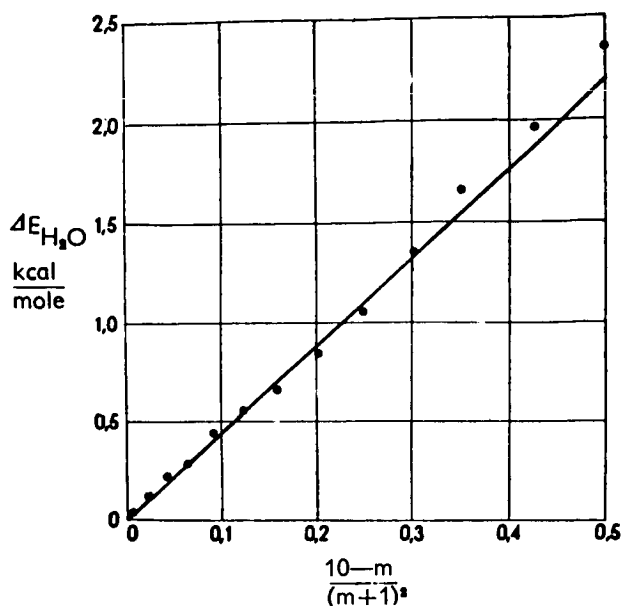


FIGURE 9. The data in FIGURE 8 plotted against  $\frac{10-m}{(m+1)^2}$ .

The data seem to start to deviate from formula (23) in the vicinity of  $m = 26$ . In order to investigate this matter in detail, the function

$\Delta p - \frac{3}{100} \frac{26-m}{m+1}$  is plotted against  $\frac{1}{m+1}$  in FIGURE 10. This plot in-

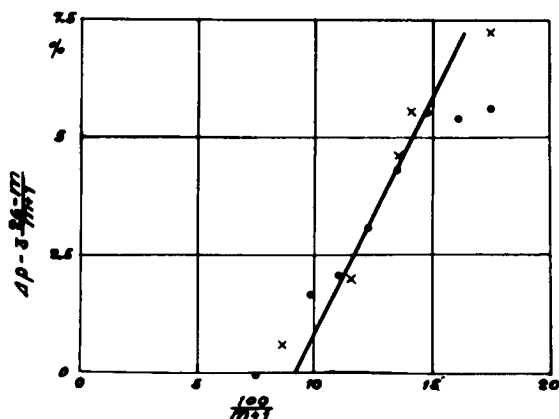


FIGURE 10.  $\Delta p - \frac{3}{100} \frac{26-m}{m+1}$  plotted against  $\frac{1}{m+1}$  for HCl from the vapor pressure data of Yannakis<sup>(11)</sup> (○) and Wrewsky *et al.*<sup>(11)</sup> (×).

icates that

$$\Delta p = \frac{3}{100} \frac{26-m}{m+1}, \quad 10 < m < 26 \quad (25)$$

and that

$$p = \frac{3}{100} \frac{26-m}{m+1} + \left( \frac{1}{m+1} - \frac{1}{11} \right), \quad 5 < m < 10 \quad (26)$$

The function

$$-\Delta p + \frac{3}{100} \frac{26-m}{m+1} + \left( \frac{1}{m+1} - \frac{1}{11} \right) \quad (27)$$

is plotted against  $\frac{1-\alpha}{m+1}$  in FIGURE 11 with

$$\begin{cases} \alpha = \frac{m}{5}, m = 5 \\ \alpha = 1, m = 5 \end{cases} \quad (28)$$

The data suggest a straight line through the origin, the slope of which is 2. Hence,

$$\Delta p = \frac{3}{100} \frac{26-m}{m+1} + \left( \frac{1}{m+1} - \frac{1}{11} \right) - 2 \frac{1-\alpha}{m+1}, \quad m < 5 \quad (29)$$

#### Salt Solutions

A brief reference will be made in this section to some properties of salt solutions. The NaCl solution is particularly simple and may serve to illustrate a few general principles.<sup>14</sup>

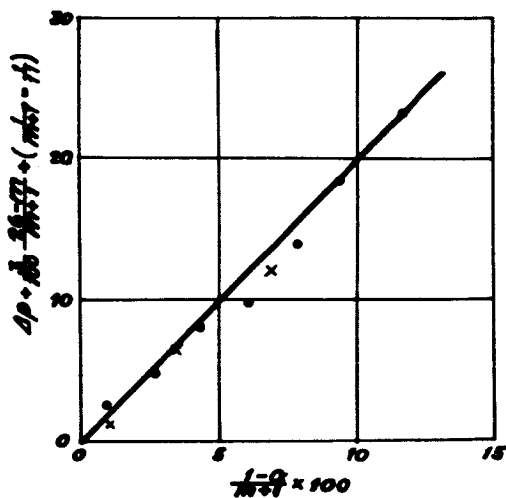


FIGURE 11.  $-\Delta p + \frac{3}{100} \frac{26-m}{m+1} + \left( \frac{1}{m+1} - \frac{1}{11} \right)$  plotted against  $\frac{1-\alpha}{m+1}$  for HCl.

TABLE 1  
SOLUBILITY OF NaCl IN AQUEOUS HCl

HCl mol./100 g.	NaCl solution	HCl	NaCl mole fractions	H <sub>2</sub> O	H <sub>2</sub> O + NaCl
					HCl + NaCl
0.0000	4.513	0.0000	9.950	90.050	10.055
0.0438	4.474	0.0960	9.838	90.065	10.057
0.0870	4.433	0.1913	9.720	90.059	10.068
0.1756	4.346	0.3853	9.5365	90.078	10.040
0.3610	4.151	0.7879	9.0593	90.153	10.075
0.9263	3.605	1.9935	7.7583	90.248	10.049
1.6677	2.889	3.5247	6.1060	90.369	10.017
2.6740	2.055	5.5529	4.2675	90.180	(9.618)
3.5670	1.408	7.3209	2.8898	89.789	(9.070)
				Average	10.053 ± 0.005

At saturation, a solution is at equilibrium with the precipitate. The free energy difference is then zero,

$$\Delta F = \Delta E - T \Delta S = 0 \quad (30)$$

The NaCl solution is peculiar by having  $\Delta E$  very close to zero so that  $\Delta S$  is also close to zero. Hence, there is no difference in structure between the solution and the precipitate. The precipitate is  $\text{NaCl} \cdot 2\text{H}_2\text{O}$ . The structure of this hydrate is known. The Na and Cl atoms are separated by the two  $\text{H}_2\text{O}$  molecules. The same structure should occur in the saturated solution.

TABLE 1 shows the solubility of NaCl at room temperature in the presence of HCl. The data in the last column show that

$$[\text{NaCl}] = \frac{1}{9} \left\{ [\text{H}_2\text{O}] - 10 [\text{HCl}] \right\} \quad (31)$$

Thus, each HCl molecule effectively removes ten  $\text{H}_2\text{O}$  molecules and reduces the solubility of NaCl correspondingly. This is in agreement with the coordination number found in vapor pressure data for HCl.

It appears, thus, that the NaCl solution consists of  $\text{NaCl} \cdot 2\text{H}_2\text{O}$  aggregates separated by  $\text{H}_2\text{O}$ . If the number of  $\text{H}_2\text{O}$  molecules is reduced so that they do not suffice to separate the aggregates, the aggregates combine and precipitate.

The same structure should result in the neutralization of HCl and NaOH solutions. The entropy of neutralization may be calculated on the assumption that the HCl molecule is surrounded by two layers of  $\text{H}_2\text{O}$ , each of five  $\text{H}_2\text{O}$  molecules, and that two of the five outer  $\text{H}_2\text{O}$  molecules are replaced by the NaOH molecule. Thus, we have a system of 10  $\text{H}_2\text{O}$  molecules, and the replacement of two adjacent  $\text{H}_2\text{O}$  molecules among five. The replacement may occur in 10 ways. The entropy is thus



$$\Delta S = 10 R \ln 10 = 46 \text{ eu} \quad (32)$$

The heat of neutralization at 18°C. is 13.8 kcal./mole. Neglecting the change in heat content and the corresponding entropy change, we have

$$\frac{\Delta E}{T} = \frac{13800}{291} = 47 = \sim \Delta S = 46 \text{ eu} \quad (33)$$

Thus, the Second Law of Thermodynamics holds for neutralization as well as for dissolution-precipitation at saturation.

### *Applications to Chemistry*

Chemical reactions in aqueous solutions are essentially a redistribution of inter- and intramolecular bonds. This process is promoted, if not effected, by bonds between H<sub>2</sub>O molecules and reactant molecules. Of course, the fact that a redistribution of bonds may occur does not ensure that it does occur. Whether it occurs or not, and which of all conceivable distributions results, are decided by the peculiar properties of the species involved. An instance of such a process is the formation of NaCl from HCl and NaOH discussed previously.

Dilute and concentrated acid solutions frequently behave as different chemical species. Thus, dilute nitric acid dissolves iron but not copper, and concentrated nitric acid dissolves copper but not iron; dilute nitric acid may form nitrates, concentrated nitric acid may form oxides or nitronium compounds. Similarly, dilute sulfuric acid attacks iron under evolution of hydrogen, concentrated sulfuric acid attacks iron, although slowly, under evolution of sulfur dioxide.

It appears that the HNO<sub>3</sub> molecule may split up into H + NO<sub>3</sub> or into OH + NO<sub>2</sub>, the former case applying to dilute solutions, the latter case to concentrated solutions. In terms of intermolecular bonds, an H atom or an OH group is transferred to the surrounding H<sub>2</sub>O through the means of intermolecular hydrogen bonds.

It is customary in chemistry and physical chemistry to write reaction formula with ions and electrons separately. From the point of view of kinetics, this is justified if the charge transfer is a slow process. However, the treatment of electrolytic conduction in *Electrical Conduction in Aqueous Solutions* shows that the charge transfer is rapid as compared to the orientation of bonds. Hence, the separation of ions and electrons in reaction formulae make the formulae unwieldy without adding to clarity or precision.

Returning now to the HNO<sub>3</sub> solutions, it is clear that the transfer of H from HNO<sub>3</sub> requires an intermolecular bond with H<sub>2</sub>O engaging this H atom. An acid molecule that satisfies this requirement is said to be dissociated, and the fraction of acid molecules satisfying this requirement is the degree of dissociation. Acid molecules not satisfying this requirement are said to be undissociated. These have their H atoms engaged in bonds

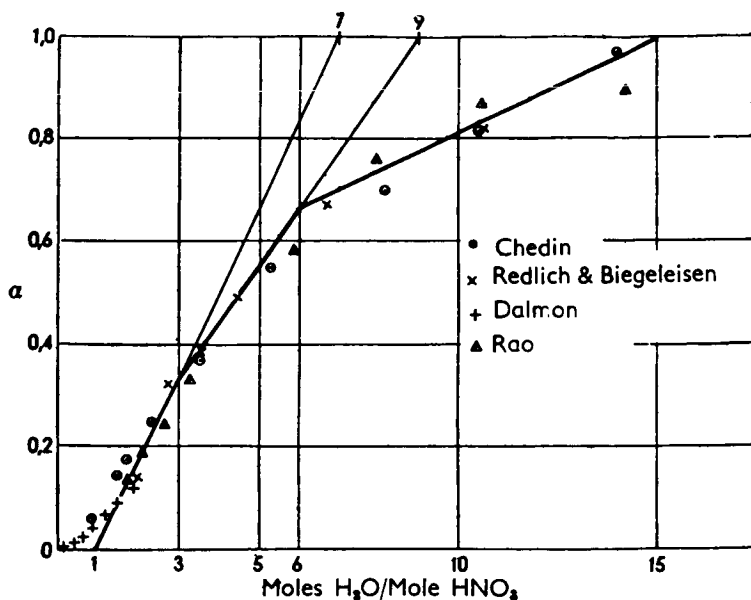


FIGURE 12. The degree of dissociation  $\alpha$  for  $HNO_3$ . The curve has been calculated from the structure. The data are those of Chedin,<sup>20</sup> Redlich and Biegeleisen,<sup>21</sup> Dalmon<sup>22</sup> and Rao.<sup>23</sup>

with other acid molecules, but they may well have the O atom, to which the H atom is attached, engaged in a hydrogen bond with  $H_2O$ .

The dissociation of an acid and thereby its chemical behavior is thus determined by the distribution of hydrogen bonds in the solution. Knowing the structure one may calculate the degree of dissociation  $\alpha$ . This has been

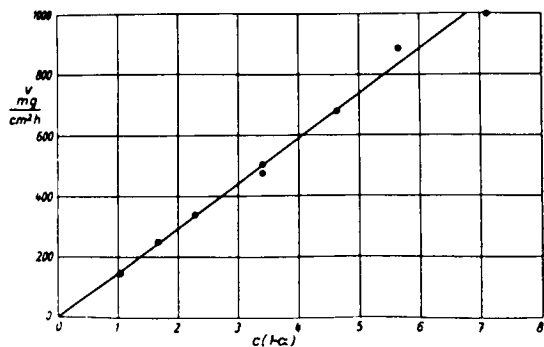


FIGURE 13. The rate of dissolution of copper in nitric acid as a function of the concentration of undissociated nitric acid,  $c(1-\alpha)$ .

done for various acids, e.g.,  $\text{HNO}_3$ ,<sup>17</sup>  $\text{H}_2\text{SO}_4$ ,<sup>18</sup>  $\text{HClO}_4$ ,<sup>19</sup>  $\text{H}_3\text{PO}_4$ ,<sup>19</sup> and  $\text{HCl}$ .<sup>19</sup> The result of such a calculation is shown in FIGURE 12 together with the results of Raman measurements. The data of Chédin are the most accurate among these data. They agree very well with the calculated values. FIGURE 13 shows a plot of the rate of dissolution of copper in nitric acid as a function of the concentration of undissociated  $\text{HNO}_3$ .<sup>24</sup> The values of  $\alpha$  for the abscissa were calculated from the structure.

### Conclusion

It follows from this brief summary of the properties of concentrated aqueous solutions that they are comparatively simply related to the structure of the solutions, i.e., the distribution of solute and solvent molecules with respect to each other. The structure may be derived from various properties, particularly vapor pressure and density. The basic physical and chemical properties may then be derived from the structure by means of elementary statistics. It should be admitted, however, that the systems treated in this paper have been selected because of their simplicity, and that other systems may be considerably more complex. This, however, does not affect the basic principles. It appears, indeed, that the physical chemistry of concentrated aqueous solutions is much simpler than that of dilute aqueous solutions.

### References

1. OWE BERG, T. G., G. C. FERNISH & T. A. GAUKLER. 1963. *J. Atmos. Sci.* **20**: 153.
2. OWE BERG, T. G., T. A. GAUKLER & L. A. SQUIRE. 1964. *Proc. Fallout Conf. AEC*.
3. WELLS, A. F. 1950. *Structural Inorganic Chemistry*. Oxford Univ. Press. Oxford, England.
4. FINBAK, C. & H. VIERVOLL. 1943. *Tids. Kjemi Bergvesen Met.* **3**: 36.
5. FINBAK, C. 1943. *Avhandl. Norske Videnskaps-Akad. Oslo, I Mat. Naturv. Klasse Nr. 3*.
6. FINBAK, C. 1944. *Avhandl. Norske Videnskaps-Akad. Oslo, I. Mat. Naturv. Klasse No. 6*.
7. VEIRVOLL, H. 1950. *Avhandl. Norske Videnskaps-Akad. Oslo, I. Mat. Naturv. Klasse, No. 2*.
8. GLASSTONE, S. 1947. *Textbook of Physical Chemistry*. D. Van Nostrand Co., Inc., New York, N. Y.
9. v. GROTHUSS, T. 1806. *Ann. Chim.* **58**: 54.
10. OWE BERG, T. G. 1953. *J. Chim. Phys.* **50**: 247.
11. LANDOLT-BÖRNSTEIN. 1923-1936. *Physik. Chem. Tabellen*, Berlin, Germany.
12. BRICKWEDDE, L. H. 1949. *J. Res. Nat. Bur. Stand.* **42**: 309.
13. LINDE, E. 1924. *Z. Elektrochem.* **30**: 55.
14. HODGMAN, C. D. 1963. *Handbook of Chemistry and Physics*. Chemical Rubber Pub. Co., Cleveland, Ohio.
15. ÅKERLÖF, G. & J. W. TEARE. 1938. *J. Am. Chem. Soc.* **60**: 1226.
16. OWE BERG, T. G. 1954. *Acta Chem. Scand.* **8**: 1.
17. OWE BERG, T. G. 1951. *Z. A. ANORG. Allgem. Chemi* **265**: 338.
18. OWE BERG, T. G. 1952. *Z. Anorg. Allgem. Chem.* **267**: 334.
19. OWE BERG, T. G. 1954. *Z. Anorg. Allgem. Chem.* **275**: 283.

20. CHÉDIN, J. 1937. *Ann. Chimie* **8**: 243.
21. REDLICH, O. & J. BIEGELEISEN. 1943. *J. Ann. Chem. Soc.* **65**: 1883.
22. DALMON, R. 1943. *Mém. Serv. Chim. l'État* **29**: 141.
23. RAO, N. R. 1941. *Indian J. Phys.* **25**: 185.
24. OWE BERG, T. G. 1951. *Z. Anorg. Allgem. Chem.* **265**: 332.

# THE FORMATION OF ICE AT WATER-SOLID INTERFACES

P. R. Camp

*U. S. Army Cold Regions Research and Engineering Laboratory  
Hanover, N. H.*

## INTRODUCTION

Despite its rather obvious importance in nature and its direct relation to metallurgical processes, the growth of ice from the liquid phase on solid surfaces has been studied very little. In fact, the process does not seem even to have been adequately described. The importance and neglect of surface growth have been pointed out by Shumski<sup>1</sup> who reviewed the confused and confusing state of affairs in 1955. Unfortunately, his own experiments gave little quantitative information and led him to assertions which we believe to be incorrect as will be developed later. Recently, Knight<sup>2</sup> has given a qualitative description of some forms of growth on several surfaces and some further review of the literature. He worked under difficult circumstances and here again inadequate data and poor control led to the formulation of hypotheses which seem unsupportable in the light of further experiment as will be shown. The rate of ice growth on a brass surface was studied as a function of temperature by Lindenmeyer.<sup>3</sup> However, he gave no information about how the measurements were performed and it is not clear exactly what it is he measured. No structural information is given. Hallett<sup>4</sup> has written on some aspects of the freezing of water at an air water interface as have Kumai and Itagaki.<sup>5</sup> Knight<sup>2</sup> has also commented on this matter. Luyet and Repatz<sup>6</sup> have described the patterns of ice in some aqueous solutions, but the role of the solid surface (glass) is not discussed.

In contrast to the situation as regards surface growth from the liquid phase both the problems of epitaxial growth from the vapor and of bulk growth from the liquid have been studied extensively. The demands of the electronics industry have given great impetus to the study of epitaxial growth of many substances and the interest of the meteorologists have stimulated much work on the epitaxial growth of ice from the vapor (see for example the work of B. J. Mason and his colleagues). The metallurgists, concerned with the growth dynamics of single crystals, have studied the growth of ice crystals from the melt, but here the perturbing effects of the surface have been regarded as a nuisance. Indeed, work on the growth of dynamics of ice grown in containers has been criticized<sup>7</sup> on the ground that the growth might be determined in part by the properties of the container walls.

With this state of affairs, it has seemed worthwhile to launch an experimental study of the way in which ice forms from the liquid on solid surfaces of various kinds. As a part of this program we have determined the principal structures which appear in the temperature range 0 to  $-5^{\circ}\text{C}$ . for three very different surfaces, aluminum, lucite and glass, and have measured the growth velocities of these structures as a function of interface temperature.

Two types of experiment will be discussed. The first, in which ice growing horizontally from a vertical wall is observed from above, was designed to permit observation of the growing interface and the ice behind it and thus the history of the growth of ice out from the wall. It established the existence of an initial ice film which spreads rapidly across the interface before appreciable growth normal to the interface has occurred and it showed that the form of the subsequent growth normal to the interface is for the most part determined by this initial film.

The second kind of experiment was designed for studying the properties of the initial layer of ice as it spreads across the interface. It permits the observation from above of a horizontal interface cooled from below. In this way, both the form of the initial growth and its velocity as it spreads over the interface can be determined.

#### VERTICAL WALL EXPERIMENTS

The vertical wall experiments were conducted with the apparatus shown in FIGURE 1. Essentially it is simply a pair of cells one wall of which is brass and serves as a heat sink. The other walls are lucite. On the wall opposite the brass is a small heater the purpose of which is to maintain a temperature gradient of the magnitude desired. The symmetry of the system allows two experiments to be run at the same time under nearly identical conditions. This is a useful arrangement when the effects of one parameter are to be studied. Then one cell serves as a control. The cells are illuminated from below with diffuse polarized light and photographed from above through a second polarized set for extinction when there is no ice in the system. Growth begins at the brass walls either by spontaneous nucleation or by touching a seed crystal to the water brass interface. With this apparatus, it is possible to follow the growth of the ice as it progresses out into the liquid.

Our first experiments gave what at the time were surprising results. Instantly upon nucleation a fan-shaped cluster of dendrites seemed to burst from the brass surface into the liquid. These seemed to appear simultaneously from all points of the liquid solid interface. The situation was similar for both the spontaneous and deliberately nucleated cases except that in the latter there were no dendrites in the region of nucleation and there was a pronounced tendency for those that appeared in other regions

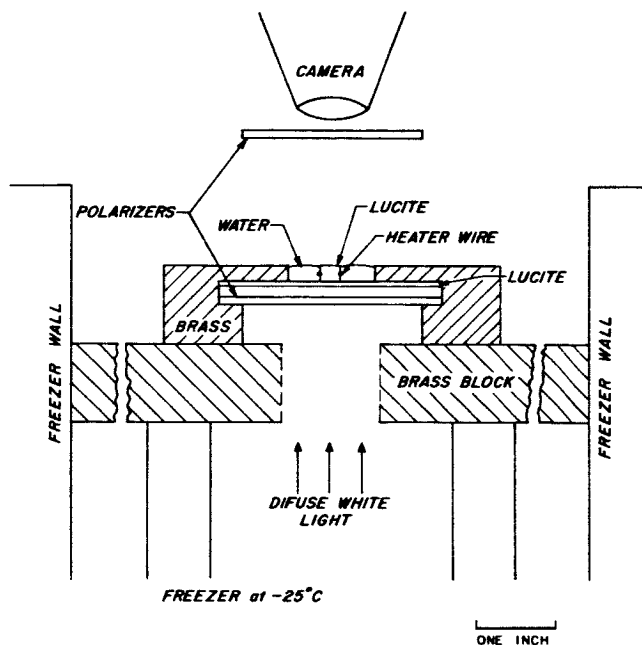


FIGURE 1. Apparatus used in the vertical wall experiments.

to lean away from the point of nucleation. These dendrites were correctly interpreted as resulting from a thin sheet of ice growing very rapidly over the interface and nucleating dendrites wherever the surface conditions were favorable. Subsequent experiments showed that the dendrites could be suppressed if the supercooling of the water was reduced. Moreover, at higher temperatures the process went more slowly and the dendrites first appeared near the site of nucleation and then further away. By suitable illumination, we were able to detect the surface layer moving across the brass surface. It is this surface layer which is the primary concern of the present paper.

Immediately after the dendrites had appeared, a solid sheet of ice grew slowly out from the brass. As it grew, the dendrites remelted until they were engulfed by the thickening ice sheet. From here on, columnar grains could be seen in the ice which continued to propagate across the cell in a regular way. The sequence of events is illustrated in FIGURES 2a and b which are photographs of the double cell taken at different stages of the experiment. The cell on the left in FIGURE 2a has just been nucleated and shows the dendrites as they first appear. The cell on the right was nucleated a minute or so earlier and shows the advancing wall of ice which has en-

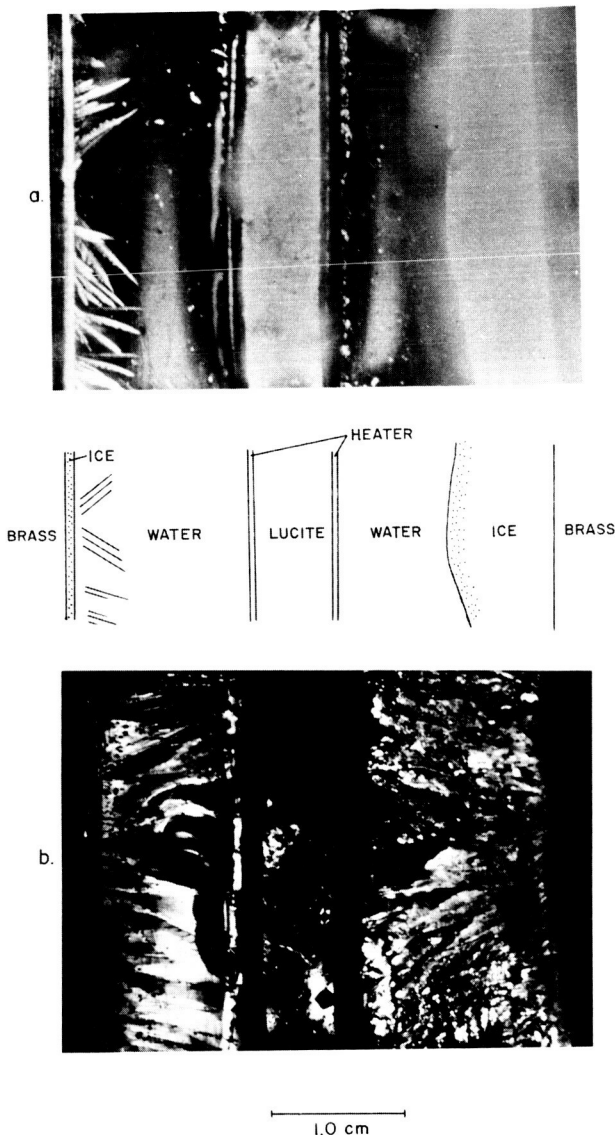


FIGURE 2. Different stages of development of ice in the vertical wall experiment. *Top left*: Dendrites have grown out into the water and an ice wall is just moving out from the brass. *Top right*: The dendrites have melted back and been overtaken by the advancing ice wall. *Bottom left and right*: The experiments of the top left and right after growth is complete.



gulfed the dendrites. FIGURE 2b shows the situation at a later stage when growth is nearly completed.

### HORIZONTAL EXPERIMENTS

It was apparent from the vertical cell experiments that the precursor, the initial growth along the interface, is the most important stage of growth on a solid surface. Accordingly a horizontal apparatus was built to enable us to study its characteristics. The nature of the surface interaction leading to this growth is unknown. However, the types of possible interaction seem to fall into three categories: electrical, molecular bonding, and thermal. Therefore, the materials chosen for study were a conductor, aluminum, and two insulators one which is not wet by water, lucite, and one which is, glass. The apparatus used for all three studies is very similar. That built for aluminum is shown in FIGURE 3.

A heavy aluminum plate is mounted a few inches below the top of a commercial chest-type freezer in which the air is circulated by means of a fan. This acts as a cold plate of fairly constant and uniform temperature. On this cold plate is mounted a shallow aluminum dish 7 x 11 x 1/2 inches milled out of a one-inch thick aluminum plate. Holes bored horizontally into the end of the plate accommodate thermocouples which measure the surface temperature and horizontal and vertical temperature gradients.

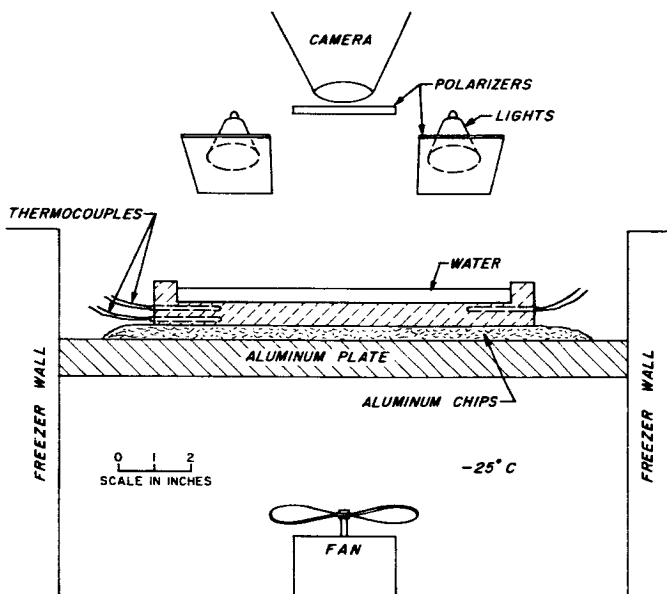


FIGURE 3. Apparatus used for photographing growth structures and measuring growth velocity.

Because air pockets, which inadvertently occur if the aluminum dish is set directly on the cold plate, lead to thermal gradients in the dish, it is thermally coupled to the cold plate by a bed of aluminum chips as shown. The inner wall of the dish is burnished with fine emery paper using lengthwise strokes to create a surface which will reflect polarized light in a diffuse manner without depolarization. The system is illuminated from the side with plane polarized light directed at an angle of about  $60^\circ$  to the surface and is photographed from above through a polarizer set for extinction when there is no ice in the system. Because the incident and reflected rays pass through the ice at different angles, some rotation of the plane of polarization occurs even when the optic axis of the ice is normal to the interface. In this way ice films only a few tens of microns thick can be seen and photographed. Multiple nucleation experiments were performed to show that the ice did not extend appreciably beyond the point at which it became visible.

The experiments were conducted by filling the dish to a depth of about 2 mm. with demineralized distilled water and allowing it to come to a fairly constant temperature. (The final temperature was controlled by varying the temperature of the water used.) When the proper temperature was reached, growth was initiated by plunging a single crystal seed of the desired orientation through the water to the interface. Except at temperatures close to  $0^\circ\text{C}$ ., growth commenced immediately upon touching the water-solid interface with an ice crystal. The interfacial growth which resulted depended both in structure and in velocity on the nature and temperature of the substrate and on the manner of nucleation. The growth was photographed at appropriate intervals by a rapid rewind 35 mm. still camera. Growth rates were measured by projecting the resulting photographs and plotting distance as a function of time. When thermal gradients were negligible and the growth of one structure was not impeded by another, the resulting graphs were straight lines the slopes of which gave the growth velocity. With this apparatus (aluminum) interface temperatures could be measured to  $\pm 0.1^\circ\text{C}$ . and growth rates to an accuracy of 5 to 10 per cent depending on the experiment.

#### RESULTS FOR ALUMINUM

For the growth of ice on aluminum, we find that at least two distinct growth modes occur depending on the amount of undercooling and the manner of nucleation. These are illustrated in FIGURE 4 which shows the structures characteristic of four different temperatures,  $-4^\circ\text{C}$ .,  $-1.6^\circ\text{C}$ .,  $-0.7^\circ\text{C}$ . and  $-0.2^\circ\text{C}$ . At the lower temperatures the structure is fine, many branched, and grows with the c-axis nearly perpendicular ( $\pm 10^\circ$ ) to the interface. However, little flecks of growth for which the c-axis makes a low angle with the interface also sometimes occur. At higher temperatures,

between 0 and  $1^\circ\text{C}$ ., a strikingly different structure develops as well.

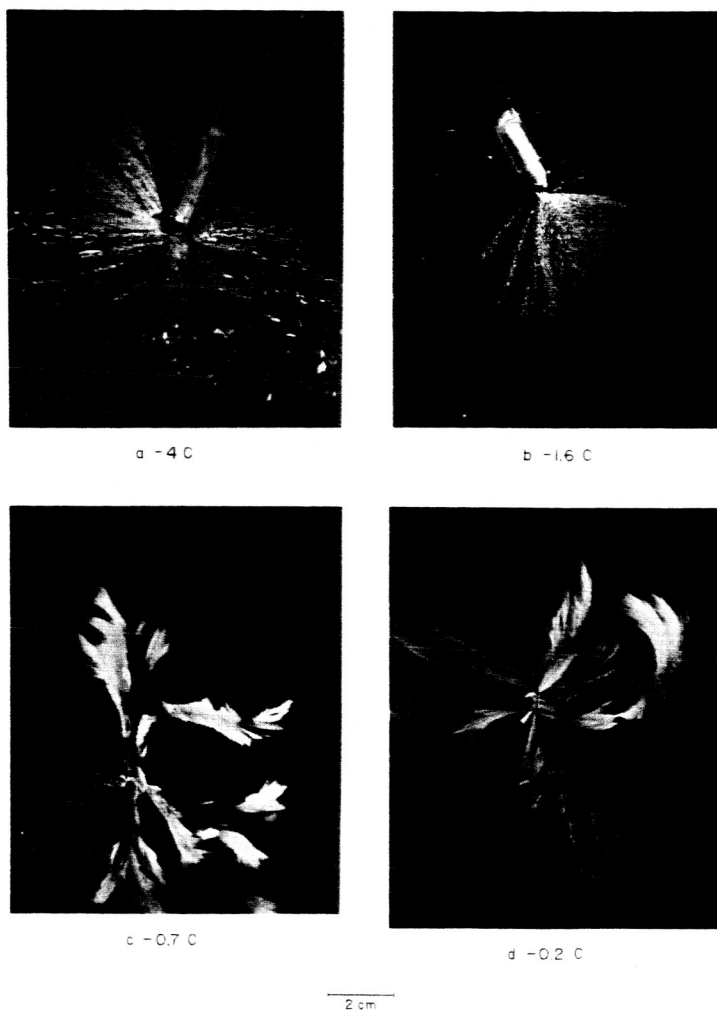


FIGURE 4. Growth structures appearing on aluminum at various temperatures, a.  $-4^{\circ}\text{C}$ ., b.  $-1.6^{\circ}\text{C}$ ., c.  $-0.7^{\circ}\text{C}$ ., d.  $-0.2^{\circ}\text{C}$ . Arrows indicate the direction of c-axis in the seed crystal.

This is characterized by better defined tightly bound feathers for which the c-axis makes a low angle to the interface. In the intermediate range it is possible to favor one kind of growth or the other by using a seed with c parallel or perpendicular to the plate.

The velocities for both modes of growth were measured and the results are plotted in FIGURE 5. For the mode with the c-axis nearly perpendicular to the surface, the data are plotted as circles. For the other, the data are

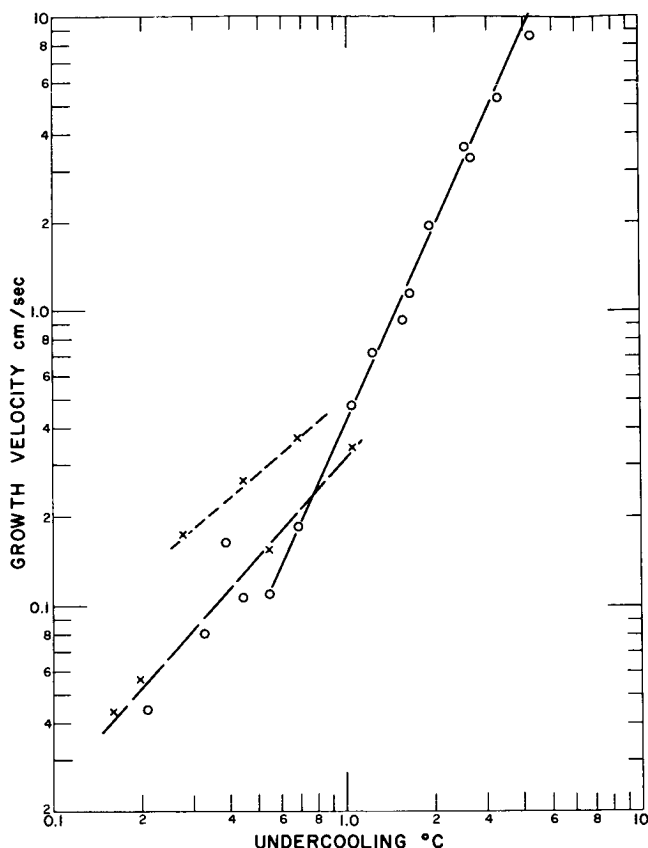


FIGURE 5. Growth velocity (cm./sec.) of ice on aluminum vs. undercooling ( $^{\circ}\text{C}.$ ). Circles indicate growth with  $c$ -axis nearly perpendicular to the interface. Crosses,  $x$ , indicate other modes for which the  $c$ -axis makes a small angle to the interface. (The points at  $3.3^{\circ}\text{C}.$  and  $4.3^{\circ}\text{C}.$  may be in error by  $\pm 0.3^{\circ}\text{C}.$ , the others by  $\pm 0.1^{\circ}\text{C}.$ ).

plotted as crosses. Within the limits of experimental error, the  $c$  perpendicular data can be summarized by

$$v = (0.42 \pm 0.1) \Delta t^{(2.2 \pm 0.1)} \text{ for } 5 > \Delta t > 0.8^{\circ}\text{C}. \quad (1)$$

Where  $v$  is the growth velocity in cm./sec.,  $\Delta t$  is the undercooling in  $^{\circ}\text{C}.$  and  $t$  is the centigrade temperature. Above about  $-1^{\circ}\text{C}.$  there seems to be systematic departure from Equation 1. Although this is in a region in which experimental errors are large, we believe that the departure is real. It should be noted that in this temperature region the  $c$  perpendicular growth structure becomes more open and rounded than at lower temperatures.

The data for the low angle growth are so scattered that it seems there must be some parameter not considered in our experiments which is important in determining the growth rate. We suspect that the scatter indicates the existence of at least two low angle modes and have indicated this by the dashed lines in FIGURE 5. The system was seeded with a single crystal whose *c*-axis was in the plane of the interface. These low angle structures grow along the interface at initial angles to the *c*-axis of the seed of 0, 30, 45, 60 and 90 degrees. It was first thought that the points of a given curve might correspond to specific angles of initial growth but no such relation was found. Nevertheless, it does appear possible to select the points belonging to a particular line on the basis of the appearance of the structure; the upper line resulting from a more curved and open structure than the lower.

However this may be, it is quite clear that the low angle mode, or modes, has a rate which exceeds that for the *c* perpendicular mode at high temperatures but which rises more slowly as temperature falls. Thus, given an opportunity to occur, either by deliberate nucleation or accidental re-nucleation at a surface imperfection, the low angle growth dominates at high temperatures and the *c* perpendicular growth dominates at lower temperatures. The cross over occurs at about  $-1^{\circ}\text{C}$ . Since the subsequent growth as the ice sheet thickens is conditioned by this initial growth, the final structure depends quite critically on the temperature at which growth first occurred. Thus, systems which are allowed to supercool slightly before freezing have a quite different final ice fabric from those which are frozen with some ice already present to prevent undercooling.

To date, we have been unable to measure accurately the orientation of the *c*-axis with respect to the interface as the growth progresses. However, in several cases we have remounted the sample on glass plates after growth was complete and measured the orientation of the more prominent grains. We find that the high angle grains are mostly between 75 and 85 degrees to the interface and the low angle grains are between zero and 50 degrees to the plate. Because extensive recrystallization and grain growth take place as the sample thickens and even after all the water is frozen, these measurements may not describe accurately the orientation of the initial growth.

The importance of grain growth in the early history of the growing process can be seen in FIGURES 6*a* and *b* which show the structures of FIGURES 4*a* and *d* as they appear 22 minutes and 16 minutes later respectively.

#### RESULTS FOR LUCITE

The lucite surface experiments were similar to those for aluminum in most respects. However, some changes were made. Because of the low



a.



b

10 cm

FIGURE 6. Grain development in the early stages of growth. (a) Same as FIGURE 4a but 22 minutes later. (b) Same as FIGURE 4c but 16 minutes later. In both the ice is about 3 mm. thick. Arrow indicates the direction of c-axis in the seed crystal.

thermal conductivity of lucite, it was found necessary to use a liquid bath instead of aluminum chips for thermal coupling between the cold plate and the lucite. With the chips we found it difficult to prevent serious temperature gradients from occurring. Also because of the low thermal conductivity we had to modify our method of measuring temperature. Instead of imbedding thermocouples in the lucite, we soldered fine wire thermocouples to 0.5 x 0.5 cm. pieces of 5 mil brass shimstock and cemented these to the inside of our lucite dish. The thickness of the whole assembly was about 0.3 mm. The dish itself was made of  $\frac{1}{8}$ " lucite with rubber walls built up around it. The bottom (outside) of the dish was sprayed with aluminum paint to provide a reflecting surface which did not destroy the polarization of the incident light.

The results for lucite are quite different from those for aluminum. Some characteristic structures are shown in FIGURES 7a, b, c, and d at temperatures of  $-5.8$ ,  $-2.6$ ,  $-1.2$  and  $-0.6^{\circ}\text{C}$ . respectively. Several different growth modes are apparent. At  $-5.8^{\circ}\text{C}$ . a mode with the c-axis nearly perpendicular to the surface is dominant but the details of the structure are quite different from those found on aluminum (FIGURE 4a). At  $-2.6^{\circ}\text{C}$ . there are at least two modes having c at a low angle to the interface. One of these is a very straight needle-shaped dendrite which appears to be a ribbon in the vertical plane. The second is a curved blade type structure the bottom side of which seems to spawn new curved dendrites for which the c-axis is almost perpendicular. These curved blades have their c-axes neither parallel to nor perpendicular to the surface and the angle it makes changes as the blade grows. One might suppose that these structures would eventually cover most of the surface. In fact this does not happen because the needles do not regenerate very extensively at the walls and the curved dendrites die out into c perpendicular structure. The result is that much of the surface becomes covered with c perpendicular growth. This growth is composed of a few main branches with long secondary branches (1 to 3 cm.) at  $60^{\circ}$  angles to the main stem spaced at very regular distances of between 0.5 and 1 mm. At moderate undercooling ( $\approx 2^{\circ}$ ) these large grids grow within the liquid as well as (presumably) at the interface. The result is that they overlap one another. As the ice on the interface thickens, these structures in the liquid melt and break up. One can even run a needle under a grid of this kind and remove it bodily. We believe that the interface becomes covered with a similar grid work although we cannot see it in the early stages because, as the ice sheet thickens, its plane is perpendicular to c in these regions even if the internal grids are manually removed soon after their formation.

FIGURE 8a, which is a photograph of the same experiment as FIGURE 7b, 140 seconds later, shows extensive gridwork of this kind north and west

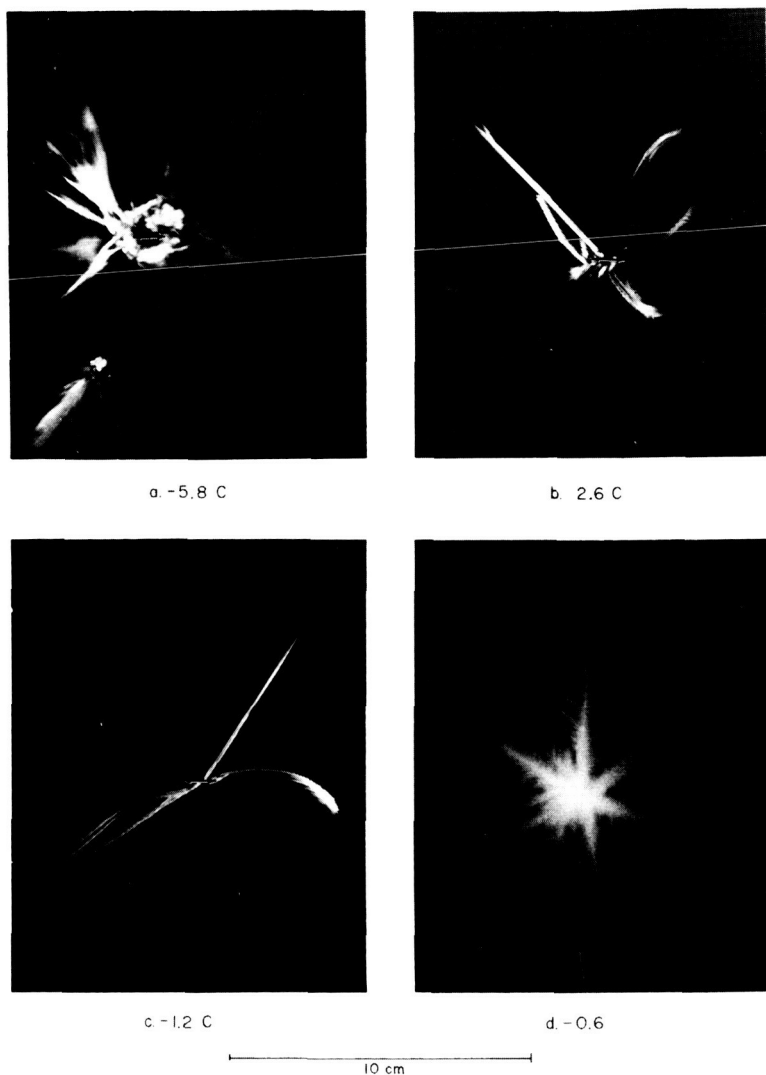


FIGURE 7. Growth structures appearing on lucite at various temperatures, (a)  $-5.8^{\circ}\text{C}$ ., (b)  $-2.6^{\circ}\text{C}$ ., (c)  $-1.2^{\circ}\text{C}$ ., (d)  $-0.6^{\circ}\text{C}$ . In b, the smaller straight member has been deliberately moved with a probe and broken in the middle as mentioned in the discussion. Arrows indicate the direction of c-axis in the seed crystal.





a



b

— 10 cm —

FIGURE 8. Later stages in the development of (a), FIGURE 7b (after 140 seconds) and (b) FIGURE 7c (after 15 minutes). Arrows indicate the direction of c-axis in the seed crystal.

of the northeast-southwest diagonal. It is very faint and may not show on reproduction.

At somewhat smaller undercoolings,  $-1.2^{\circ}\text{C}$ , the general features seem to be the same (see FIGURE 7c). However, here the internal gridwork does not appear and the bottom growth perpendicular to  $c$  is tree like with thicker trunks and shorter secondary branches with much tertiary structure. Some of this should be evident in FIGURE 8b which shows the structure of FIGURE 7c, 15 minutes later.

Finally at small undercoolings, the low angle curved structures terminate rather quickly in  $c$  perpendicular trees similar to that shown in FIGURE 7d ( $-0.6^{\circ}\text{C}$ ). In this same experiment a fine needle grew across the dish but it does not show on the reproduction.

A set of rate experiments similar to those for aluminum was run using lucite with the results shown in FIGURE 9. The mode with  $c$  perpendicular to the interface, plotted as circles, is seen to have a very well defined velocity-temperature relation.

$$v = 9.2 (\pm 0.4) \times 10^{-3} (\Delta t)^{2.8 \pm 0.08} \text{ cm./sec.}$$

over the temperature range  $-0.5$  to  $5.0^{\circ}\text{C}$ . As with aluminum, the rates for the low angle growth modes are more widely scattered. The crosses in FIGURE 9 represent the data for the straight spikes and the triangles those for the curved blades. It is interesting that although the  $c$  perpendicular structure grows much more slowly at small undercoolings than do the low angles modes, it is responsible for most of the subsequent growth. As mentioned earlier this is because the low angle modes fail to reproduce.

#### RESULTS FOR GLASS

The procedure for the glass-water interface experiments was the same as that for the lucite experiments. A glass cell was constructed and treated in the same manner as was the lucite cell. All of the cells used in these experiments were cleaned in alconox and rinsed with demineralized distilled water. Fresh water was used in each run. As has been mentioned, the lucite surface repelled water but the glass surface was wet by it.

The structures found on glass were surprisingly different from those on lucite. Representative cases are shown in FIGURES 10a, b, c, d. At an undercooling of  $3.7^{\circ}\text{C}$ ., the growth is coarse and vinelike with the branches of the vine made up apparently of short-curved crystal fibers having  $c$  axes which make low angles to the plane of the interface. When nucleation is provided by a crystal whose  $c$ -axis is parallel to the interface, the main trunk of the vine lies approximately perpendicular to  $c$ . As growth continues, the spaces between the branches of the vine fill in with ice of undetermined structure. The whole system seems highly disordered when viewed in detail and it is not surprising that as time goes on, grain

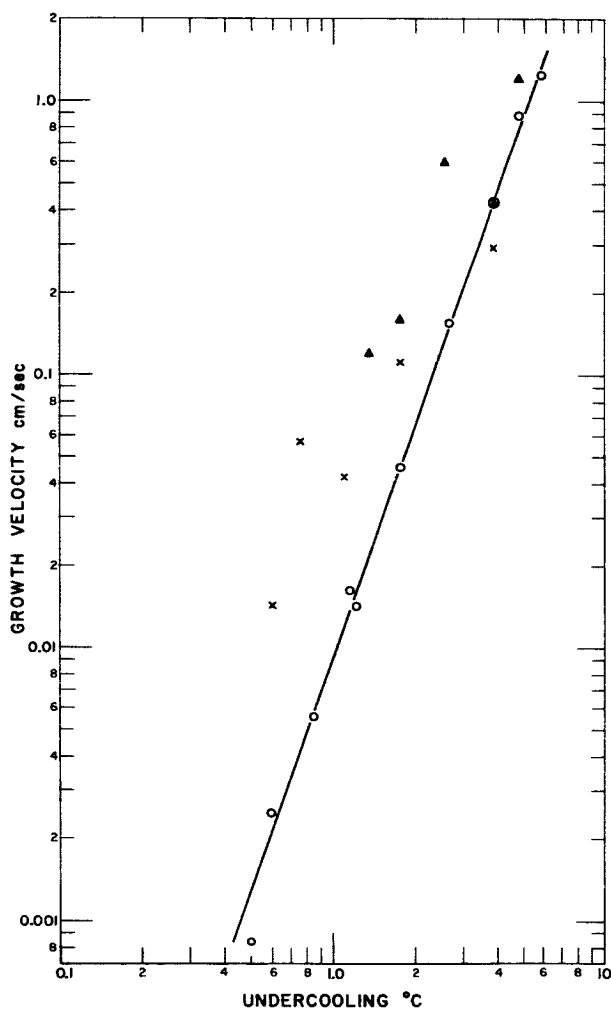


FIGURE 9. Growth velocity (cm./sec.) of ice on lucite vs. undercooling ( $^{\circ}\text{C}.$ ). Circles,  $\odot$ , indicate growth with  $c$  perpendicular to the interface. Crosses,  $x$ , indicate long straight spikes, Deltas,  $\Delta$ , indicate a curved blade type growth which starts out with the  $c$ -axis making a small angle to the interface. As the blade curves, the  $c$ -axis becomes more and more perpendicular to the surface until at the tip of the blade the  $c$  perpendicular growth takes over.

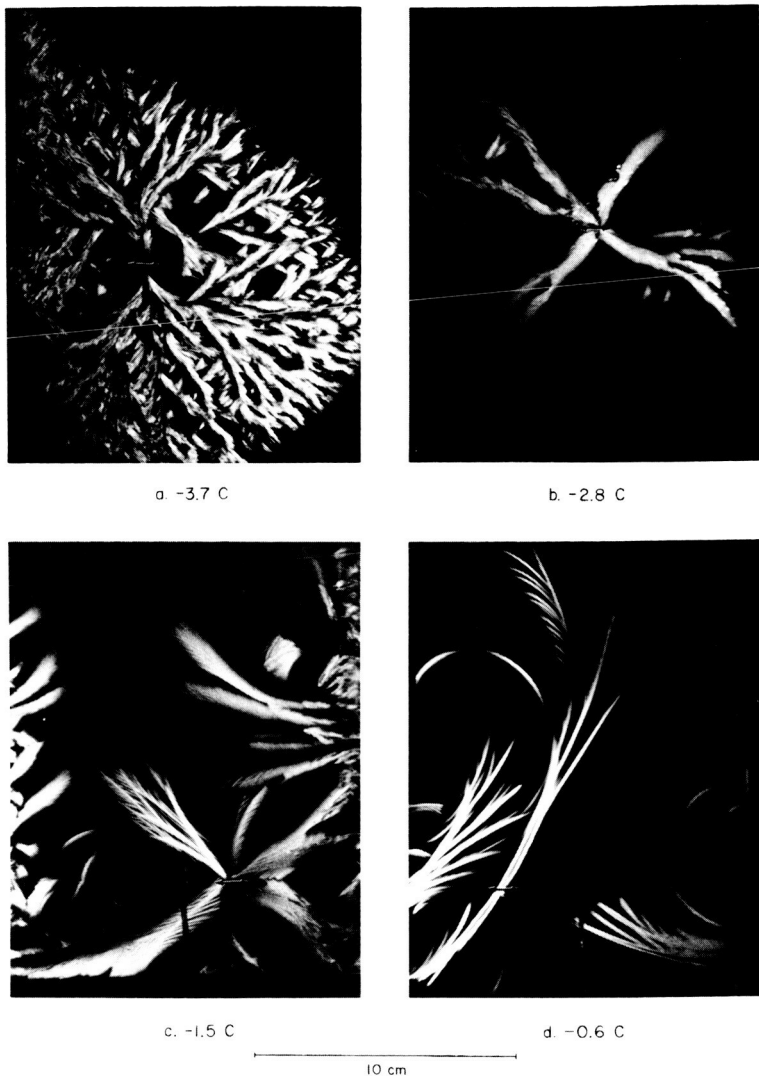
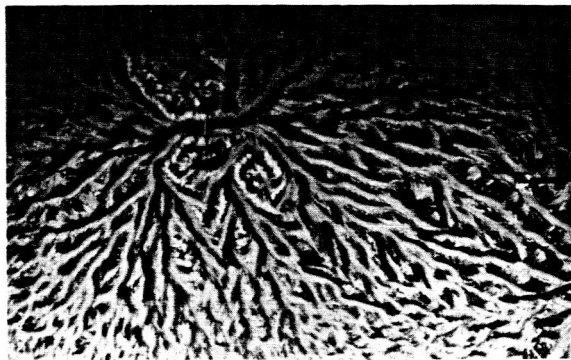


FIGURE 10. Growth appearing on glass at various temperatures: (a)  $-3.7^{\circ}\text{C}$ ., (b)  $-2.8^{\circ}\text{C}$ ., (c)  $-1.5^{\circ}\text{C}$ ., (d)  $-0.6^{\circ}\text{C}$ . Arrows indicate the direction of c-axis in the seed crystal.

growth occurs producing the slightly more ordered structure of FIG. 11a which shows the sample of FIGURE 10a eleven minutes later.

A slight increase in temperature to  $-2.8^{\circ}\text{C}$ . brings about a fairly dramatic change. It is a little as if the picture at  $-3.7^{\circ}\text{C}$ . had been magnified. The predominant structure is still vinelike but much larger and more



a.



b.



c.

10 cm

FIGURE 11. Later stages in the development of (a) FIGURE 10a (after 11 minutes), (b) FIGURE 10b (after seven minutes) and (c) FIGURE 10d (after three minutes). Arrows indicate the direction of c-axis in the seed crystal.

orderly. It is still hard to define the structures but after a longer time, as shown in FIGURE 11*b* taken seven minutes after FIGURE 10*b*, it is seen that the "bark" of the vine has peeled back here and there, and that the region partly enclosed by these curves has its *c*-axis tending toward perpendicular to the interface.

At somewhat higher temperatures,  $-1.5^{\circ}\text{C.}$ , as shown in FIGURE 10*d*, the structure begins to take new form. One, which we have called a type one growth, is made up of fine long-curved needles growing in a cluster. Another, which we have designated type two, comprises a dark band fringed on both sides with short fine feathers, all curving away from the black band in the direction of growth. These two types have been sketched in the legend of FIGURE 11. As growth continues, the type one structure seems to peel as did the vine structure and the interstices become filled with ice for which the *c* axis makes a high angle to the interface.

At still higher temperatures,  $-0.6^{\circ}\text{C.}$ , these structures seem to become sharper and more magnified and take on some new features. The type one structure becomes larger. It becomes difficult to say in some cases whether a long slim fiber is a needle or a part of a type one structure. Curved needles present a similar problem. These develop an abundance of small circular arcs which must have their *c* axes at a high angle to the interface. Much less of the total surface becomes covered with a low angle growth and consequently more high angle growth occurs. Some trace of the tree-like growth perpendicular to *c* so common to lucite begins to appear. The whole develops a striking beauty and complexity as is shown in FIGURE 11*c*, a photograph taken three minutes after that of FIGURE 10*d*.

The rate vs. temperature data for glass are plotted in FIGURE 12. At this time we have only limited amount of first quality data available. (Photographic measurements for which the temperature is accurately known). As a result many of the points have a rather large experimental error ( $\pm 0.2^{\circ}\text{C.}$  and  $\pm 20$  per cent in rate) and so the temperature characteristics are not as well defined as those for aluminum and lucite. This is particularly true of the behavior of the growth oriented with *c* perpendicular to the interface, indicated in FIGURE 12 by circles. Because the other growth fills space so readily, this is a very difficult mode to measure except at temperatures close to  $0^{\circ}\text{C.}$  for which the relative error in temperature becomes very large. Thus the fact that the four points fall rather nicely on a straight line must be regarded as fortuitous. None the less, it seems clear that the rates for the high angle growth are much smaller than those for the low angle growths except for undercoolings of less than  $0.2^{\circ}\text{C.}$  A novel feature here is that the rate of increase of velocity with undercooling seems to be less for the high angle growth than for the low angle growth, a reversal of the situation found for aluminum and lucite. This fact coupled with the tendency of the low angle growth to curve and

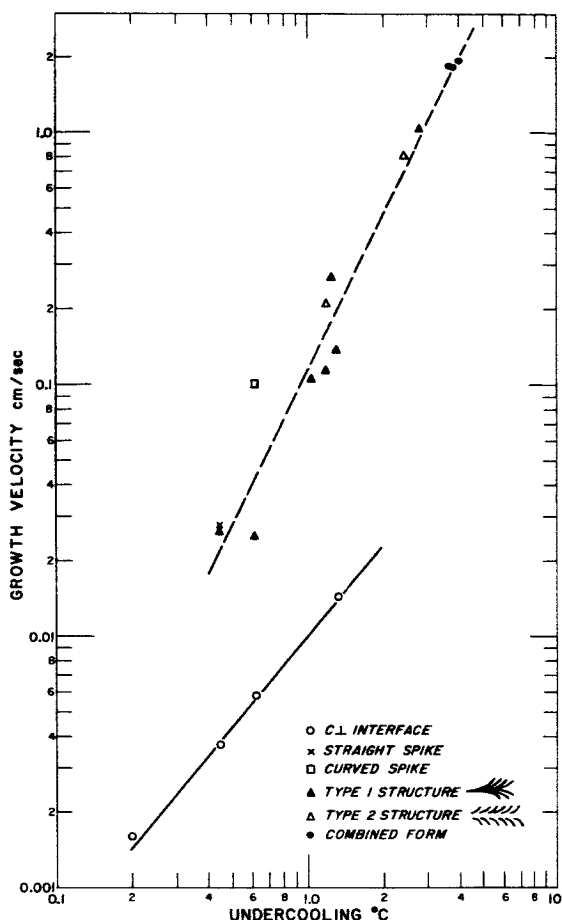


FIGURE 12. Growth velocity (cm./sec.) of ice on glass vs. undercooling ( $^{\circ}\text{C}.$ ). The symbols are explained in the legend. (As indicated in the text, these data are preliminary. Since we have not yet unraveled the temperature dependence of the low angle modes, a dashed line is drawn through all the data, weighted in accordance with the reliability of the individual experiments).

renucleate (for example the “peeling of the bark” at  $-3^{\circ}\text{C}.$  and the types I and II growth at  $-1^{\circ}\text{C}.$ ) lead to greater complexity in the glass patterns than in those for aluminum and lucite. Moreover, the selection among the various low angle modes apparently depends on more subtle details of nucleation than simply whether the c-axis of the seed is perpendicular to or parallel to the interface. It is this complexity which leads to the delightful intricacy of frost patterns on the window. If the growth velocity for the high angle mode on glass exceeded that for the low angle mode

in the 0 to  $-5^{\circ}\text{C.}$  range, winter mornings in a steamy kitchen would be much more prosaic.

In considering the data of FIGURE 12, one must bear in mind not only its somewhat tentative nature but the fact that it is sometimes difficult to assign to a given structure a name such as type I or curved spike and so forth, because these forms themselves change with temperature. Thus while we show points as straight spikes (X) or curved spikes ( $\square$ ) these may really be of the same species as type I. We hope in the near future to be able to resolve these matters. In the meantime we have summarized the low angle growth by the dashed line in FIGURE 12. In drawing it we have given the most weight to those points in which we have the most confidence. With the reservations mentioned above we find for the high angle growth

$$v = 0.01 (\pm 0.003) (\Delta t)^{1.2 (\pm 0.3)} \text{ cm./sec.}$$

and for the low angle growth

$$v = 0.12 (\pm 0.03) (\Delta t)^{2.1 (\pm 0.2)} \text{ cm./sec.}$$

#### DISCUSSION

When water freezes on aluminum, lucite, or glass because heat is extracted through the solid, the sequence of events is as follows: Upon nucleation at the interface (either deliberate or spontaneous) a thin layer of ice grows rapidly across it. This growth is not simple but depends both in structure and velocity on the temperature and nature of the interface and on the manner of nucleation. Subsequently, this ice sheet thickens and the kind of structure which grows depends on the nature of the initial layer. This initial layer may be very thin, not more than  $30\mu$ , or it may include structures which are bladelike, anchored to the solid along one edge and extending in width several millimeters out into the water. If the water is appreciably undercooled, dendrites may grow out into it from the surface. As the ice sheet thickens, the heat of fusion causes these dendrites to melt back and the blades to shrink in width.

The initial structure may occur by several different growth modes. It is convenient to divide these into two classes, those having their c-axis very nearly perpendicular to the interface and those whose c-axes make a small angle to the surface. In this latter category, we include those which change orientation as they grow so that they start out with their c-axes nearly parallel to the interface and gradually turn so that the c-axis becomes vertical. The c-perpendicular mode is well defined, which is reasonable because c perpendicular defines a unique crystal plane. However, there appear to be several different growth modes for which c is parallel to the interface or makes a small angle to it. This too is reasonable because even if the c-axis is parallel to the interface a unique crystal plane is not specified.



TABLE 1  
RATE PARAMETERS ASSUMING  $v = a(\Delta t)^m$  CM./SEC.

Surface material	a cm./sec.	m
High angle modes		
Aluminum	$0.42 \pm 0.04$	$2.2 \pm 0.1$
Lucite	$0.092 \pm 0.004$	$2.86 \pm 0.08$
Glass	$0.01 \pm 0.003$	$1.2 \pm 0.3$
Low angle modes*		
Aluminum, upper dashed line	0.51	0.85
Aluminum, lower dashed line	0.32	1.1
Lucite $\Delta$	0.66	1.9
Lucite x	0.45	1.4
Glass (average)	0.12	2.1
From Lindenmeyer <sup>3</sup>		
Brass 3°C. t 1°C.	0.18	2.6 (Approx. from graph)
Bulk Growth Hillig 1958 <sup>8†</sup>		
Growth 1 c	0.16	1.7
Growth 11c imperfect crystals	0.01	1.16 (Approx. from graph)

\*As is evident from the discussion in the text and the scatter of the points in FIGURES 5, 9, and 12 these data are quite tentative and one cannot properly assign error limits to them. The  $\Delta$  and x correspond to the use of these symbols in FIGURE 9.

†These data are for the growth of ice along thin 0.3 to 0.7 mm. diameter glass capillaries. The tube axis is the growth direction. Heat is extracted through the ice at ice water interface and thus this represents bulk growth not surface growth.

(However, it does appear that there are only a few important modes of this kind).

The rate data for the various surfaces and modes are summarized in TABLE 1. Those for the low angles modes are very tentative both because of the scatter of the data and the uncertainty of assignment as discussed earlier. For convenience the rate data of Lindenmeyer<sup>3</sup> for growth on brass and of Hillig<sup>8</sup> for bulk growth are also included. Although temperatures can be found at which the rate of growth for a low angle mode on aluminum is the same as that for a low angle mode on lucite or glass, this does not mean that one or more of these modes is independent of the substrate, because their temperature dependence is different. Thus, we must conclude

that the kind of surface does indeed affect the mode of surface growth and its rate. Even the low angle growth structures which are bounded on both flat sides by water seem to be effected by the kind of surface their bottom edge is touching. In this connection, it is interesting to note that for glass and lucite at small undercoolings (of the order of  $1^{\circ}\text{C}.$ ) none of the modes is rigidly bonded to the substrate. One can move a branch or a blade by pushing it with a glass probe. This is illustrated in FIGURE 7*b* in which the tip of the shorter of the two straight needles has been probed. The needle moved and then broke in the middle causing the discontinuity shown in the photograph.

Moreover, it is clear that the growth rate is not determined wholly (or perhaps even largely) by the thermal properties of the substrate. For example, this is evident from the fact that the rate for the high angle growth on lucite can be either greater or less than that on glass depending on the temperature. (The two curves cross). Moreover, we have performed preliminary experiments on a lucite dish half of which is covered with a very thin film of vacuum-deposited aluminum. The heat capacity of the aluminum film is too small to have a noticeable effect on the heat flow at the interface and yet the velocity of growth on the aluminized side is larger than that on the clear side, the velocity on the aluminized side being intermediate between that for plain lucite and plain aluminum.

It was mentioned in the introduction that the results of these investigations are in conflict with some of the observations of Knight.<sup>2</sup> One of these is his statement that, "when the nucleating crystal is oriented with its *c*-axis perpendicular to the plane of the surface ordinary more or less rounded dendritic growths of ice slowly cover the slide." This seems to imply that nucleation with a crystal whose *c*-axis is perpendicular to the interface results in purely *c*-perpendicular growth. On the contrary, we find that when the temperature is such that the velocity of a low angle mode is appreciably larger than that of the high angle mode, secondary nucleation of the low angle mode usually occurs. (Similarly if the growth velocity of the high angle mode exceeds that of the low angle structures, the high angle mode will be nucleated by a secondary process even though the *c*-axis of the seed was in the plane of the interface). For example, we have been unable to nucleate appreciable *c* perpendicular growth on glass below  $-1^{\circ}\text{C}.$  even though the *c*-axis of the seed was normal to the interface. Possibly this disagreement is a result of our rather different technique. He used a system in which a thin water film 0.05 mm. thick was sandwiched between two glass plates. We use a single free interface. A more serious conflict arises with regard to his assertion about curved dendrites that "the fundamental proposition regarding this curved growth is that the curvature is always such as to line up the fast growth direction parallel to the steepest temperature gradient" and his subsequent argument that the

curvature of a dendrite which makes an angle of less than  $90^\circ$  to the interface is because the heat of fusion liberated on the side of the acute angle to the interface is somewhat trapped by the surface and therefore growth is faster on the other side. We believe that he is correct in identifying curved growth as being of special interest but we must contest these two hypotheses with the following observations: (1) Curved growth (to be sure of a somewhat different structure) can occur on aluminum for which the surface is a much better heat sink than is glass. (2) Curved growth as well as long straight growth also occurs on lucite which is a poorer heat sink than glass. (3) In our experiments with a lucite surface half of which is covered by an evaporated aluminum film, curved dendrites which cross from one section to the other show a smaller radius of curvature on the aluminized section than on the plain Lucite section. (4) Curved growth on both lucite and glass, particularly at small undercoolings, frequently terminates in c perpendicular growth for which the growth velocity is less than that of the curved growth. (5) The thermal diffusivity of glass is higher than that of water and the contact coefficients are nearly the same. (6) The curved blades are in contact with water on both sides so the thermal properties of the substrate can hardly be important except where the blade joins it. Knight (FIGURE 4) shows this junction thickened to make an obtuse angle with the base on both sides of the dendrite. (7) In another experiment, we have deliberately created a large temperature gradient oblique to the path of these structures and observed no change in direction at all, merely a change in velocity.

Mention was also made in the introduction of the fact that our experiments are in conflict with some of the statements made by Shumski. His paper is rather diffuse and probably suffers in translation so it is often difficult to determine precisely what his theses are. However, one seems to be that before crystal growth commences on a visible scale, there are in the liquid, or on the surface, crystal embryos which normally are chaotically oriented. The effect of the surface is to exert an orienting influence on these. Growth then commences almost simultaneously at many of these sites and such order as occurs in the crystal is a result of the prenatal order of these embryos. On the contrary, our work and that of Knight both show that growth proceeds from a single point of nucleation and that this is the cause of the subsequent order in the crystal. (We are speaking here of the initial growth on the surface. Grain boundary migration and the wedging out of grains as growth proceeds of course may take place subsequently). He also appears to claim that the structure is dependent on the thickness of the undercooled layer of water adjoining the surface. For thin layers, c-perpendicular growth predominates and for thick layer the structure is more varied. However, all of our experiments were conducted under conditions such that there was a fairly thick layer of undercooled water

(several millimeters) and c-perpendicular could be made to dominate for all three surfaces. A particularly striking example is the growth on lucite. Another contention is that the temperature gradient in the water has an important influence on the resulting ice structure in the initial layer. He indicates that for zero temperature gradient the orientation of the crystals is chaotic and for a large positive temperature gradient the basal plane tends to become parallel to the interface. However, in our work the temperature gradients were small ( $< 1^{\circ}/\text{mm.}$ ) and we found that we could produce a surface c-perpendicular growth by varying other factors. We believe our experiments demonstrate that when heat is extracted through the substrate neither the thickness of the supercooled layer nor the temperature gradient at the moment of freezing is of particular importance to the structure of the interfacial ice, that the two dominant factors are the temperature of the interface and material of the substrate and that the manner of nucleation is important in certain temperature regions.

#### ACKNOWLEDGMENTS

It is a pleasure to thank Mr. Charles F. Barter and Mr. John Creamer for their help in conducting these experiments. I am also grateful to Dr. Walter Kiszénick for preparing the evaporated aluminum films.

#### REFERENCES

1. SHUMSKI, P. A. 1955. The growth of ice crystals on solid surfaces. *In* Vaprosy Geologii Azii (Problems of Geology in Asia). Acad. Sci. USSR Pub. House, Moscow : 565-595.
2. KNIGHT, C. A. 1962. Curved growth of ice on surfaces. *J. Ap. Phys.* 33(5) 1808-1815.
3. LINDENMEYER, C. S., G. T. ORROK, K. A. JACKSON & B. CHALMERS. 1957. Rate of growth of ice crystals in supercooled water. *J. Chem. Phys.* 27: 822.
4. HALLETT, J. 1960. Crystal growth and the formation of spikes in the surface of supercooled water. *J. Glac.* 3:(28): 698-704.
5. KUMAI, M. & K. ITAGAKI. 1954. Cinematographic study of ice crystal formation in water. Pub. No. 39, de l'Association Internationale d'Hydrologie (Assemblée generale de Rome, Tome IV) : 463-7.
6. LUYET, B. & G. RAPATZ. 1958. Patterns of ice formation in some aqueous solutions. *Biodynamica.* 8(156-158): 1-80.
7. CHALMERS, B. 1958. Growth of crystals of pure materials and of the solvents of solutions. *In* Growth and Perfection of Crystals. R. H. Doremus, B. W. Roberts and D. Trumbull, Eds. :300. John Wiley and Sons. London, England.
8. HILLIG, W. B. 1958. The kinetics of freezing of ice in the direction perpendicular to the basal plane. *In* Growth and Perfection of Crystals. R. H. Doremus, B. W. Roberts & D. Trumbull, Eds. : 350-360. John Wiley and Sons. London, England.

#### *Discussion of the Paper*

J. HALLETT (*Physics Department, Imperial College, London England*): Growth in the bulk liquid, in the absence of solid surfaces, may be studied\*

\*HALLETT, J. 1964. *J. Atmos. Sci.*

by insertion of an ice single crystal of selected orientation into the free surface of a water sample uniformly supercooled. As temperatures above about  $-5^{\circ}\text{C}$ . it has been found that growth follows the orientation of the nucleating crystal, in the form of thin dendrites (with  $60^{\circ}$  branches) growing parallel to the basal plane of the ice structure. Below this temperature, dendrites grow from the site of nucleation, in several directions, not necessarily related to the orientation of the seed crystal. With decrease of temperature, dendrite arms become narrower and more closely spaced, being  $\sim 10\mu$  at  $-10^{\circ}\text{C}$ . The crystallization velocity increases approximately as the square of supercooling being  $\sim 30\text{ cm. sec.}^{-1}$  at  $-20^{\circ}\text{C}$ . The presence of a solute has two effects: to change the habit of growth (relative velocity along different crystallographic directions) and to change (lower) the velocity of growth — molecules have a diffusion barrier to growth. When dendrites meet a solid surface (FIGURE 1) the form of growth changes strikingly to that already shown by Camp, and if the supercooling is sufficiently great, curved growth, and nucleation of new crystal growth directions may occur in addition. The surface may act in two ways — as a sink for release of latent heat and as a site to nucleate new crystals at the

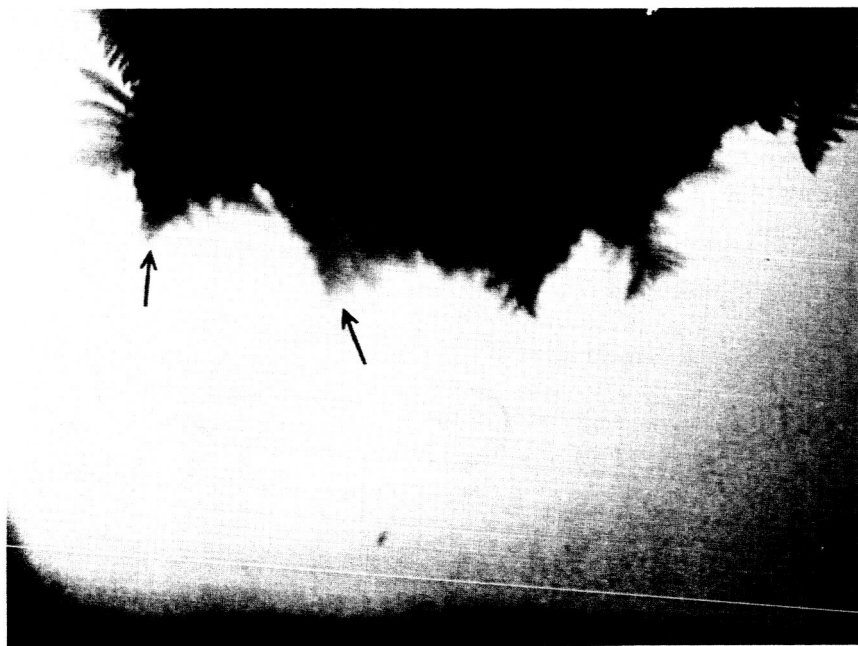


FIGURE 1a. Crystal growth in rabbit serum at  $-5^{\circ}\text{C}$ ., nucleated by a single crystal in the upper free surface. Growth (arrowed) in the bulk of the liquid occurs as dendrites with straight arms.



FIGURE 1*b*. As the dendrites meet the outer glass walls the velocity of propagation increases and the growth becomes curved.

interface with the crystal which grows from the bulk liquid. The crystallization velocity is therefore greater on the surface than in the bulk of the liquid.

In any closed system — a water or solution drop in air, a plant or animal cell — the final form of the ice (its spacial distribution) and its petrographic structure, will depend critically on the amount, and spacial distribution of supercooling before nucleation took place, and also on the distribution of nucleation sites. The form of crystals which grow first, into the supercooled liquid, will depend on the supercooling, and on the thermal and crystallographic characteristics of the membrane surface where nucleation occurs. Whether the growth is characteristic of the surface or the bulk liquid will also depend on the supercooling and, particularly, the cell dimensions. The second stage of freezing will depend entirely on the efficiency with which heat can be removed and how the shell of ice growing inwards from the periphery interacts with the initial growth of fine dendrites—separating the solute into small regions with dimensions related to dendrite size, which would be equivalent to the final spacial distribution of any eutectic which might form. Previous work has not been concerned with investigating cell damage in relation to this initial distribution of

ice — (which may change subsequently by recrystallization) and I would like to suggest that a full understanding of the processes responsible for cell damage will not be achieved until detailed studies of all stages of the freezing processes have been made.

As has been discussed in the text, our experiments seem to us to refute the idea that the surface acts merely as a heat sink or as a site for renucleation. Interfacial growth occurs on glass which is certainly not much better as a heat sink than is water and on lucite, which is worse. Very thin surface layers of foreign substances (e.g., aluminum on lucite) radically alter the velocity of interfacial growth. It appears that one must at least accept interfacial free energy as important in determining the characteristics of interfacial growth and probably even the more detailed aspects of the interfacial forces involved.

# ELECTRICAL PROPERTIES OF BOUND WATER

H. P. Schwan

*Electromedical Division, Moore School of Electrical Engineering,  
University of Pennsylvania, Philadelphia, Pa.*

Water bound to the surface of macromolecules is indicated whenever the physical properties of a macromolecular suspension cannot be readily accounted for by the properties of the suspending medium and those of the macromolecules. I shall report here some of the electrical properties of macromolecular suspensions observed at very high frequencies and whatever this may imply for the electrical properties of bound water. Essentially macroscopic and valid concepts will be applied in order to reduce experimental dielectric data to those of bound water. No detailed molecular interpretation will be attempted.

The dielectric properties of protein in electrolytes have been extensively investigated during the 1940's throughout the radio frequency range, primarily by Oncley and his associates (Oncley, 1942, 1943). Experimental data could be understood in terms of a sum of two Debye type relaxation mechanisms.

$$\epsilon^* = \epsilon_\infty + \sum_{\gamma=1,2} \frac{\Delta \epsilon}{1 + j \omega \tau_\gamma} \quad (1)$$

where  $\epsilon^* = \epsilon' - j \epsilon''$  is the complex dielectric constant and where the  $\tau_\gamma$  are time constants characteristic of the relaxation process responsible for the observed frequency dependence of  $\epsilon^*$ .  $\epsilon_\infty$  is the limit value of the dielectric constant  $\epsilon'$  approached at frequencies much higher than  $1/(2\pi\tau_2)$  and  $\epsilon_0 = \epsilon_\infty + \Delta\epsilon_1 + \Delta\epsilon_2$  the limit value at low frequencies. Typically, limit values were observed below 100 kc. and above 10 mc. A good fit of theory and experiment was achieved by approximating the shape of the individual polar macromolecule by an ellipsoid of revolution. This yields two relaxation time constants whose ratio is given by the axial ratio of the ellipsoid (Perrin, 1934). Oncley was also able to estimate amounts of water which must be assumed to rotate with the protein and hence is bound to its surface. Hydration values thus obtained fitted well with those established by other means, i.e. are in the range of 0.2 to 0.5 g. bound water per g. protein. Dipole moments calculated from the experimental data appeared quite reasonable. Oncley's interpretation of the dielectric data measured throughout the radio frequency range has not been seriously challenged even though other interpretations have been suggested (Jacobson 1955, Kirkwood & Shumaker 1952).

\*This investigation was supported by Office of Naval Research Contract Nonr 551 (05) and National Institutes of Health Grant H1253.



The changes which result from the addition of 1 g. protein to 100 cc. suspending medium are called dielectric increments if they are positive, and decrements if they are negative. Increments are observed at frequencies which are low in comparison to about 1 mc. and decrements at frequencies much above. Low frequency dielectric increment values permitted Oncley to determine protein dipole moments. High frequency dielectric decrements result from the fact that the dielectric constant of the hydrated protein is lower than that of the replaced electrolyte. However, the decrement values obtained by Oncley near 10 Mc. are not as low as one might predict if the dielectric constant of the hydrated protein is rather low in comparison with that of the replaced electrolyte.

Decrement values were also obtained during the 1950's at microwave frequencies above 1000 Mc. (Buchanan 1952). They are of a higher magnitude than those observed by Oncley and of reasonable magnitude if the dielectric constant of the hydrated protein is assumed to be very small compared to that of electrolytes. Clearly, another relaxation process is indicated at frequencies between those employed by Oncley and by Buchanan. Li and Schwan have determined the dielectric properties of hemoglobin in 1955 in the frequency range from 10 to 1000 Mc. (Li 1955; Schwan 1957). They observed a dispersion due to this anticipated relaxation effect. It is the purpose of this presentation to first summarize some of these results and then to interpret them.

#### *Material and Method*

Hemoglobin was prepared with toluene (Haurowitz, 1930). Investigations were also conducted on packed erythrocytes which were diluted with distilled water. It is known that the resultant erythrocyte ghost suspensions behave at frequencies above 100 Mc. exactly like hemoglobin of equal concentration since the ghost membranes are of negligible impedance and hence do not affect the dielectric properties (Fricke & Curtis 1935; Schwan 1957). Indeed, results obtained with hemoglobin and erythrocyte ghost suspensions were noted to provide the same information with regard to dielectric decrements. Data were taken at various concentrations. Measurements extended usually over the frequency range from 150 to 1000 Mc. and in some cases from 0.5 to 1000 Mc. They were repeated to check reproducibility.

The determination of the dielectric properties throughout the range from 150 to 1000 Mc. was conducted with a transmission line, operating in a resonance mode. Details have been given previously (Schwan & Li, 1955). Measurements from 0.5 to 150 Mc. were conducted using General Radio Bridges 1601A and 916A and a sample cell described elsewhere (Schwan, 1963, Figure 37). Dielectric constants were obtained accurate within about one half dielectric unit and electrical conductivities accurate within two

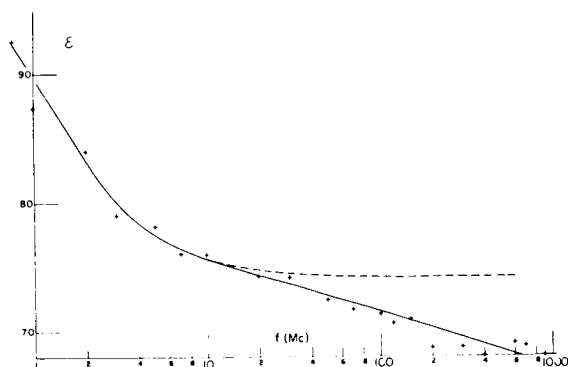


FIGURE 1. Frequency dependence of the dielectric constant  $\epsilon$  of a 10 per cent Hb — suspension.

to three per cent, depending on frequency and dielectric loss. All data were taken at about 25°C.

### Results

FIGURE 1 illustrates the frequency dependence of the dielectric constant  $\epsilon$  of a 10 per cent hemoglobin suspension. The steep slope of the curve which is drawn for a best smooth fit of the data represents the greater part of the radio frequency relaxation behavior mentioned above. The dashed curve extending above 20 Mc. illustrates the high-frequency behavior obtained from an extrapolation of the radio-frequency relaxation effect. Its deviation from the continually decreasing curve constitutes the evidence for an additional relaxation mechanism.

TABLE 1  
DIELECTRIC DECREMENT VALUES FOR HEMOGLOBIN FOR FOUR  
DIFFERENT CONCENTRATIONS

	100 Mc	300 Mc	600 Mc	900 Mc
5%	0.79	0.97	1.23	1.29
10%	0.75	0.87	0.98	1.08
15%	0.71	0.85	0.97	1.03
20%	0.71	0.8	0.86	0.88

Decrement values are given in terms of dielectric unit change per 1 g. Hb in 100 cc. Concentrations are given in terms of weight percentage. Accuracy  $\pm 0.05$ .

Dielectric decrement values have been calculated from the data given in FIGURE 1 and are given together with those for other concentrations in TABLE 1. The decrement values are fairly independent of concentration up to a weight percentage figure of about 10. As the concentration increases further, the frequency dependence becomes less pronounced. Clearly, the mechanism which is responsible for the observed relaxation behavior becomes less effective at higher concentration values, presumably due to macromolecular interaction. It is also apparent that the decrement values approach at low frequencies for all concentrations a value of about 0.8. This value is close to the one observed by Oncley at 10 Mc. (Oncley, 1942, 1943). The decrement value approaches 1.2 near 1000 Mc. This is identical within experimental error with the value observed by Buchanan *et al.* 1952.

Conductivity data are presented in FIGURE 5 and will be discussed later.

### *Interpretation of Results*

*A. Dielectric constant of hydrated hemoglobin molecule.* We proceed by lumping together whatever amount of water is bound to the individual macromolecule with the macromolecule per se and characterize the total polarization resulting from the hydrated protein by its effective dielectric constant  $\epsilon_e$ . It can be shown (Schwan, 1957) that this effective dielectric constant, the dielectric constant  $\epsilon_s$  of the suspending electrolyte and that of the suspension  $\epsilon$  are interrelated by

$$\frac{\epsilon - \epsilon_s}{\epsilon + 2\epsilon_s} = p \frac{\epsilon_e - \epsilon_s}{\epsilon_e + 2\epsilon_s} \quad (2)$$

where  $p$  stands for the volume fraction taken by the hydrated macromolecules. Equation 2 is the dielectric equivalent of an equation given for the conductivity of a suspension of spheres by Maxwell (1873). It is applicable at frequencies which are high enough so that capacitive currents are larger than conductive ones. The validity of Equation 2 presumes furthermore that deviations from spherical shape are not extreme and that the volume fraction  $p$  is small, say less than 0.3. The equation can be used to calculate the effective dielectric constant  $\epsilon_e$  of the hydrated hemoglobin molecule. However, an assumption has to be made as to the hydration value of the hemoglobin molecule in order to convert the known specific volume of hemoglobin and its concentration into  $p$ -values. The FIGURE 2 shows thus calculated  $\epsilon_e$ -values for two assumed hydration values of 0.3 and 0.4 g. H<sub>2</sub>O/g. Hb. The solid curves shown are obtained from the solid curve in FIGURE 1.

The effective dielectric constant of the hydrated protein undergoes a rather substantial change as the frequency varies from 10 to 1000 Mc. The dashed line indicates what level the effective dielectric constant would approach at low frequencies if the microwave relaxation process of interest here would completely describe the total frequency dependence of Hb. The

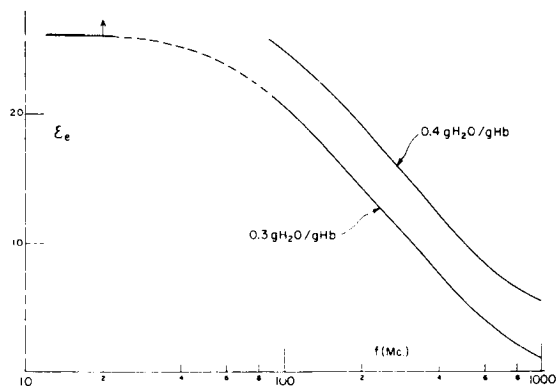


FIGURE 2. Frequency dependence of the effective dielectric constant of hydrated Hb — molecule  $\epsilon_e$  for two assumed hydration values.

magnitude of the dispersion of  $\epsilon_e$  is about 25 dielectric units and fairly independent on the assumed hydration value. This is demonstrated in FIGURE 3. Hydration and  $\epsilon_e$ -values are plotted against each other for three different frequencies. Most probable hydration values are between 0.3 and 0.4. At frequencies above 1000 Mc. a low dielectric constant of a few units is approached. However, below 100 Mc., a rather large value of more than 20 dielectric units characterizes the hydrated hemoglobin molecule.

The frequency dependance of the dielectric constant of the hydrated hemoglobin molecule can reflect either one of the two following processes:

1. Polar subgroups of the hemoglobin molecule are sufficiently free to rotate with the applied field at frequencies where the total molecule is no longer able to respond. The time constants indicated by the major frequency

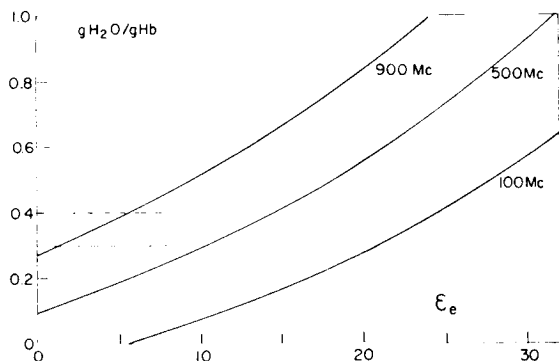


FIGURE 3. Amount of bound water versus the effective dielectric constant  $\epsilon_e$  of the hydrated Hb — molecule for three different frequencies.

range of change from 100 to 1000 Mc. are about 100-fold smaller than those characteristic of the rotation of the total hemoglobin. Since time constants are proportional to molecular volume, the molecular weight of the rotating subunits is probably about 100 times smaller than that of hemoglobin.

2. The water bound to the protein surface undergoes a corresponding change in dielectric properties.

The concentration dependance of the decrement demonstrated in TABLE 1 appears to favor the second hypothesis. In the first case this concentration dependance might be anticipated at concentration levels where the individual hemoglobin molecules could interact, i.e., above 30 per cent in weight. However, if hydration values are considered in the 0.3 to 0.5 g. H<sub>2</sub>O/g. Hb range, the volume of the hydrated protein is about 50 per cent larger than that of the unhydrated one. Thus, interaction would be definitely anticipated to occur at the 20 per cent level. It would occur at even lower levels if bound water structure extends further out than reflected by the average thickness which one would derive from the quoted hydration values.

*B. The dielectric constant of bound water.* The following equation has been used to calculate the dielectric constant of the hydration shell  $\epsilon_s$  from the effective dielectric constant of the hydrated protein  $\epsilon_e$  and assumed values of the protein per se  $\epsilon_p$ :

$$\frac{\epsilon_e - \epsilon_s}{\epsilon_s + 2\epsilon_s} = \left( \frac{R}{R+d} \right)^3 \frac{\epsilon_p - \epsilon_s}{\epsilon_p + 2\epsilon_s} \quad (3)$$

This equation is the dielectric counterpart of an equation involving conductivity terms and was given first by Maxwell (1873). It is applicable in the present case as has been shown by us above (Schwan, 1957).  $R$  is the radius of the protein and  $d$  the thickness of the shell of bound water. The equation assumes spherical shape. For other than spherical shape the factor 2 in the denominators is to be replaced by another, slightly different number (Fricke, 1925). Errors which are made by assuming spherical shape can be shown to be of no significance here.

FIGURE 4 gives values of the dielectric constant of bound water  $\epsilon_s$  as function of assumed dielectric constant of the protein  $\epsilon_p$ . Results for two hydration values are shown. All data in FIGURE 4 pertain to 100 Mc. and are appropriate conversion of the  $\epsilon_e$ -data previously given for 100 Mc. Two extreme cases are of particular interest:

1. For a low dielectric constant  $\epsilon_p$  of the hemoglobin molecule the value for the dielectric constant of bound water  $\epsilon_s$  is close to that of normal water. Furthermore, the value of  $\epsilon_s$  is rather independent of the hydration value assumed.

2. If the dielectric constant  $\epsilon_s$  is assumed small, unlikely large values of the protein dielectric constant  $\epsilon_p$  must be assumed. Clearly, such a combination of  $\epsilon_s$ ,  $\epsilon_p$ -values is less attractive than the one listed first.

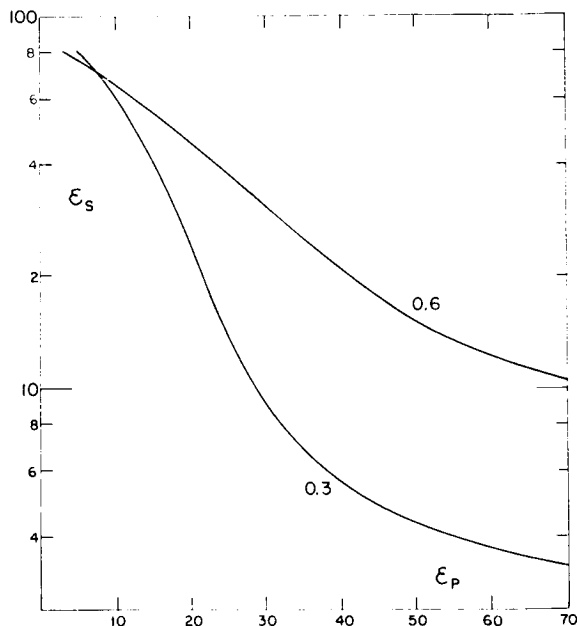


FIGURE 4. Dielectric constant of bound water  $\epsilon_s$  versus assumed dielectric constant  $\epsilon_p$  of Hb for two assumed hydration values.

In FIGURE 5 we have plotted the dielectric constant of bound water, giving preference to the first possibility, i.e., assuming that the dielectric constant  $\epsilon_p$  is reasonably small. The values for bound water are compared with those for normal "free" water and ice. Bound water relaxes at frequencies between those characteristic of the corresponding behavior of ice and normal water. Thus bound water appears to stand from a structural point of view

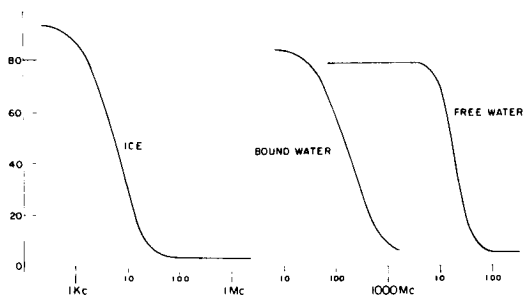


FIGURE 5. Frequency dependence of the dielectric constant of ice, bound and normal (free) water. All three curves have comparable limit values. The curve for bound water is less steep than the others.

between normal water and ice. The slope of the dispersion curve of bound water is flatter than that of ice and particularly that of water. Thus, a broader spectrum of time constants is involved in the relaxation behavior of bound water. This indicates variation in the characteristics of bound water associated with different activation energies.

*C. Conductivity.* Additional information can be gained from a study of the electrical conductivity  $\kappa$  of suspended proteins. The dielectric behavior of normal water and electrolytes at microwave frequencies can be characterized by one single time constant (Schwan, 1954) and, hence, by the following Debye equation

$$\epsilon^* = \epsilon_\infty + \frac{\epsilon_0 - \epsilon_\infty}{1 + j\omega\tau} \quad (4)$$

The subscripts 0 and  $\infty$  refer to limit values at low and high frequencies. The following conductivity equation is derived from this:

$$\kappa_w = \kappa_{ow} + (\kappa_\infty - \kappa_{ow}) \frac{(\omega\tau)^2}{1 + (\omega\tau)^2} \quad (5)$$

where a conductivity term  $\kappa_{ow}$  has been added to account for ionic and frequency independent contributions to  $\kappa_w$ . Furthermore, from Equation 4

$$\kappa_\infty - \kappa_{ow} = \frac{\epsilon_0 - \epsilon_\infty}{18 \cdot 10^{11}} f_c \quad (6)$$

The characteristic frequency  $f_c = 1/(2\pi\tau)$  of normal water is close to 19,000 Mc. at room temperature and the magnitude of its dispersion characterized by  $\epsilon_0 - \epsilon_\infty = 73$ . Hence for frequencies smaller than  $f_c$

$$\kappa_w - \kappa_{ow} = 0.76 (f/f_c)^2 \quad (7)$$

Consider next the conductivity  $\kappa$  of a suspension of protein molecules in an electrolyte. Let us assume for the moment that the electrical conductivity of the hydrated protein  $\kappa_p$  is very small in comparison with that of water. Then the Maxwell equation (1873)

$$\frac{\kappa - \kappa_w}{\kappa + 2\kappa_w} = p \frac{\kappa_p - \kappa_w}{\kappa_p + 2\kappa_w} \quad (8)$$

reduces to

$$\kappa = \kappa_w \left(1 - \frac{3}{2}p\right) \quad (9)$$

where  $\kappa$  is the conductivity of the suspension,  $\kappa_w$  that of the suspending medium and  $p$  the small volume fraction taken by the hydrated protein.

Combinations of Equations 7 and 9 gives us the microwave behavior of the conductance of a protein suspension, provided that the hydrated protein conductance is very small:

$$\kappa = \kappa_o + 0.76 \left(\frac{f}{f_c}\right)^2 \left(1 - \frac{3}{2}p\right) \quad (10)$$

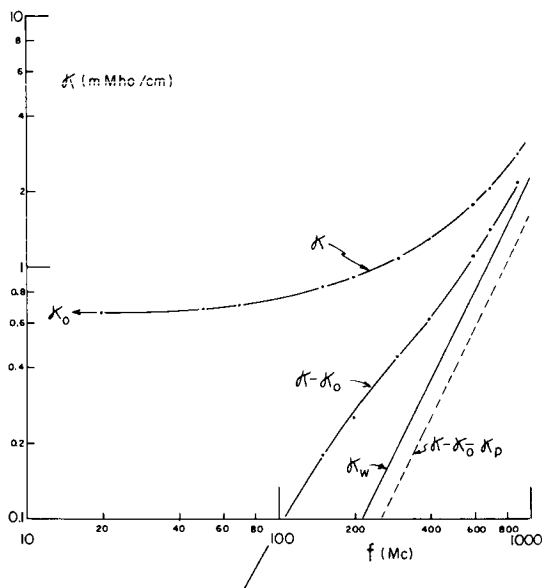


FIGURE 6. Frequency dependence of the conductance of 20 per cent HB ( $\kappa$ ) and water ( $\kappa_w$ ). A contribution  $\kappa_0$  is characteristic of hydrated Hb.

where  $\kappa_0 = \kappa_{ow} \left(1 - \frac{3}{2} p\right)$  is obviously the low frequency conductance of the protein solution. Thus  $\kappa - \kappa_0$  should vary with the square of the frequency and the protein curve  $\kappa - \kappa_0$  ought to be simply displaced against the corresponding electrolyte curve by a factor of  $1 - \frac{3}{2} p$ .

Conductivity data were obtained between 10 and 1000 Mc. with a technique previously described (Schwan & Li, 1955). A typical result is displayed in FIGURE 6.  $\kappa$  approaches a low frequency value  $\kappa_0$ , which is determined by the ionic content of the suspending phase.  $\kappa_w$  designates the conductivity of water, as calculated from the expression (7). Clearly, the curve for  $\kappa - \kappa_0$  is not running parallel to the curve  $\kappa_w$ . Furthermore, it is placed above instead below the  $\kappa_w$  - curve. Thus, the assumption of a negligible conductance of the hydrated protein is not valid. To predict the curve which results from a nonconducting hydrated molecule requires an assumption as to the hydration value in order to arrive at a figure for the volume fraction  $p$  occupied by the hydrated proteins. For a figure of 0.3 g.  $H_2O/g.$  Hb the dashed curve is obtained. The difference between the  $\kappa - \kappa_0$  curve and the dashed curve then must be due to a conductance contribution  $\kappa_0$  of the hydrated Hb-molecule. This difference appears to approach a value of 0.8 mMho/cm. at 1000 Mc., while the value at 100 Mc. is smaller than 0.1 mMho/cm.



Another independent estimate of  $\kappa_{\infty}$  and its variation between 100 and 1000 Mc. is obtained as follows. If the relaxation behavior of proteins could be described by a single relaxation time constant, Equation 6 would apply. This equation is often found to be quite useful in interrelating changes in conductance and dielectric constant with frequency even though the relaxation process involves a spectrum of time constants. In this case  $\tau$  is some average time constant. For the case under consideration, most of the frequency dependence observed appears to occur between 100 and 1000 Mc. Below 100 Mc. decrement values approach those noted by Oncley and further changes at lower frequencies are of a different origin not of interest here. Above 1000 Mc. on the other hand dielectric constant data approach those anticipated if the hydrated protein molecule has a low dielectric constant and a significant further decrease is, therefore, not possible. Thus, it is concluded that an average relaxation time constant corresponding to about 300 Mc. pertains. For the case of a 20 per cent Hb suspension, the dielectric decrement values quoted in TABLE 1 correspond to a change of four dielectric units over frequency range from 100 to 1000 Mc. Thus  $\kappa_{\infty} - \kappa_0$ , as calculated from Equation 6 ought to be near 0.6 mMho/cm., which is satisfactorily close to the estimate taken from FIGURE 5.

*D. Protein hydration determination from microwave conductivity.* Above outlined estimates of the conductance contribution which is caused by the hydrated hemoglobin molecule imply a new technique to determine bound water values. In essence the technique relies on a determination of the volume fraction taken by normal water as reflected by the placement of the  $\kappa - \kappa_0 - \kappa_{\infty}$  curve. The more this curve is situated differently from the one which characterizes free water alone ( $\kappa_w$ ), the greater is the volume taken by the hydrated molecules. The volume taken by bound water is obtained from the volume of the hydrated molecule by subtraction of the molecular volume. The proposed technique is presently not very accurate. Small errors in the conductance  $\kappa$  reflect in larger errors in  $p$  and the volume taken by bound water. For example, if one assumes that either  $\kappa$  or  $\kappa_{\infty}$  indicated in FIGURE 5 at 900 Mc. would differ from the values previously used by 0.1 mMho/cm. (5 per cent error in  $\kappa$ ) then the amount of bound water had to be changed from 0.3 to 0.2 g. H<sub>2</sub>O/g. Hb. A more precise knowledge of the protein conductance contribution is needed to improve this technique. Measurements at higher frequencies and somewhat greater precision should improve our knowledge about the distribution function of relaxation time constants and, thereby, enable us to replace Equation 6 by a more appropriate one and thus better define  $\kappa_{\infty}$ .

#### Conclusions

Dielectric constant and conductivity data which pertain to hemoglobin are presented for the frequency range from 1 to 1000 Mc. The interpretation of these data leads to the following conclusions:

1. The effective dielectric constant of the hydrated Hb-molecule undergoes a relaxation process which is centered between 100 and 1000 Mc. Its value above 1000 Mc. is lower than six and below 100 Mc. larger than 20. The magnitude of this dispersion appears to vary but little with the assumed amount of bound water.

2. The electrical conductivity of Hb increases with frequency. For example for the case of a 20 per cent suspension, the conductance contribution caused by the hydrated Hb molecules increases from less than 0.1 to nearly 1 mMho/cm. as the frequency increases from 100 to 1000 Mc. Changes in conductivity and dielectric constant with frequency appear to be related as demanded by relaxation theory.

3. The mechanism responsible for the frequency dependance of dielectric constant and conductivity is likely to be a strong dispersion of the electrical characteristics of bound water. Bound water undergoes its relaxation at frequencies somewhere near 300 Mc. involving a distribution of activation energies. Its structure appears to be intermediate to those of ice and normal water.

4. A new technique to determine protein hydration is outlined which utilizes microwave conductance determinations. Present accuracy is about 0.1 g. H<sub>2</sub>O/g. Hb at best. Further refinements of the technique appear possible and are indicated.

5. A value of  $0.3 \pm 0.1$  g. bound water per gHb is indicated in the case of a 20 per cent in weight Hb-suspension.

#### *References*

- BUCHANAN, T. J., G. H. HARRIS, J. B. HASTED & B. G. ROBINSON. 1952. *Proc. Royal Soc. A*213: 379.  
FRICKE, H. 1925. *Physics Rev.* 26: 678.  
FRICKE, H. & H. J. CURTIS. 1935. *J. Gen. Physiol.* 18: 821.  
HAUROWITZ, F. 1930. *Z. Physiol. Chem.* 186: 141.  
JACOBSON, B. 1955. *J. Am. Chem. Soc.* 77: 2919.  
KIRKWOOD, J. G. & J. B. SHUMAKER. 1952. *Proc. Nat. Acad. Sci.* 38: 855.  
LI, K. 1955. *Electr. Properties and Absorption of Electromag. Energy of Biol. Subst.* Dissertation. University of Pennsylvania. Philadelphia, Pa.  
MAXWELL, J. C., 1873. *A Treatise of Electricity and Magnetism*. Clarendon Press. Oxford and Dover, N. Y. (1954)  
ONCLEY, J. L. 1942. *Chem. Rev.* 30: 433.  
ONCLEY, J. L. 1943. *Proteins, Amino Acids and Peptides*. Chap. 22. Reinhold Publishing Company. New York, N. Y.  
PERRIN, F. 1934. *J. Phys. Radium* 5: 497.  
SCHWAN, H. 1957. *Adv. Biol. Med. Physics.* 5: Academic Press. New York, N. Y.  
SCHWAN, H. 1963. *Physical Techniques in Biological Research*. Chap. 6. 6: Academic Press. New York, N. Y.  
SCHWAN, H. & K. LI. 1955. *Trans. AIEE (Communications and Electronics)*. : 603.

# THE EFFECT OF VARIOUS BIOLOGIC COMPOUNDS ON PROTON CONDUCTIVITY AND ACTIVATION ENERGY IN ICE

F. Heinmets

*Pioneering Research Division,  
U.S. Army Natick Laboratories,  
Natick, Mass.*

Protons participate in numerous biochemical reactions. There are two distinct proton transport mechanisms involved in such processes:

(a) Diffusion, like other ions.

(b) Transfer between adjacent molecules, principally via water. The last process contributes mainly to the high mobility of protons. The details of transfer mechanisms are not entirely clear, but considerable progress has been made by performing experiments in ice where diffusion effects are extremely small. One of the sources of information on proton transfer migration has been electrical conductivity measurements in ice. Since in biological structures water molecules may be oriented, then in such a system proton transfer may have characteristics of ice rather than liquid.

Most conductivity studies involving ice are carried out with pure crystals or impurities are introduced only at concentrations where there are no significant distortions on structure. This subject has been reviewed by Gross in this publication.<sup>1</sup> In order to simulate "biological media," a structure has to be highly complex and essentially noncrystalline. For this purpose, conductivity measurements have been carried out in highly doped ice and the effect of various biological molecules on conductivity and activation energies was investigated. Here only A.C. measurements were made, since in highly doped ice, D.C. and low frequency A.C. yield the same ohmic conductance values. We also made a limited number of D.C. experiments (mostly for control purposes), but bridge-type A.C. conductivity measurements are far simpler and these represent the main work on doped ice.

## *Experimental Methods*

A detailed description of experimental procedures had been given in a previous publication.<sup>2</sup> A.C. conductivity measurements were made in a U-cell by freezing platinum black electrodes into the ice. Exploratory experiments indicated that such a procedure is permissible when the proton concentration is sufficiently high. For temperature measurements, a thermometer was placed in a "tummy" conductivity cell and when the cell temperature was equal to that of the bath temperature, the conductivity was determined. Normal and "tummy" cells had the same dimensions and tests indicated that the same temperatures were reached at the same time. The

A.C. conductivity measurements were usually made with a bridge at 1000 cycles and were carried out in conditions where ice had reached temperature equilibrium (in about 20 min.) with the coolant. There was still a drift in conductance values, but it was small and hours were required to reach constant conductivity value. For carrying out a large number of orientating experiments, it was considered that results from temperature equilibrium conditions are sufficiently accurate and will yield information on factors which influence proton movement in highly doped ice.

### *Experimental Results and Discussion*

*Conductivity during supercooled freezing.* The primary purpose of these experiments was to determine the conductivity values for a solution (.1M HF) and ice at the same temperature. We also wished to study the conductivity as a function of time during supercooled freezing and to determine the minimum time required for reaching near-equilibrium conditions. The solution was cooled to  $-6.0^{\circ}$  and then the cell was tapped with a glass rod; this initiated rapid ice formation. For these measurements, the con-

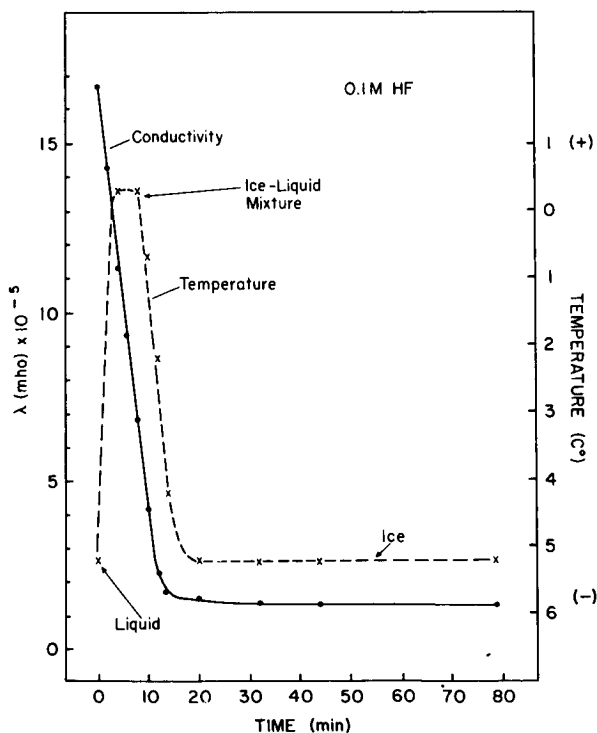


FIGURE 1. Conductivity and temperature measurements of 0.1 M HF solution during supercooled freezing.

ductivity-U cell had an additional central tube which contained a temperature-measuring device. FIGURE 1 shows the conductivity and temperature as a function of time. It is evident that during rapid freezing, enough heat is liberated to raise the temperature of the solution-ice mixture about  $5.5^{\circ}$ . During this time conductance is reduced. In about 20 min., the temperature is again down to  $-6^{\circ}$  and the rapid decrease in conductance has ceased. After that a slow drift of conductance takes place while the temperature is constant.

*Effect of proton concentration.* In FIGURE 2, the log of conductivities of HCl-protonated ice at various concentrations are plotted against inverse absolute temperature. Absolute conductivity values are not directly comparable since different cells had to be used due to frequent breakage of cells by the ice. The primary interest here is to determine the activation energy of proton transport as a function of temperature. It is evident that the slopes of conductivity curves are more uniform at higher HCl concentra-

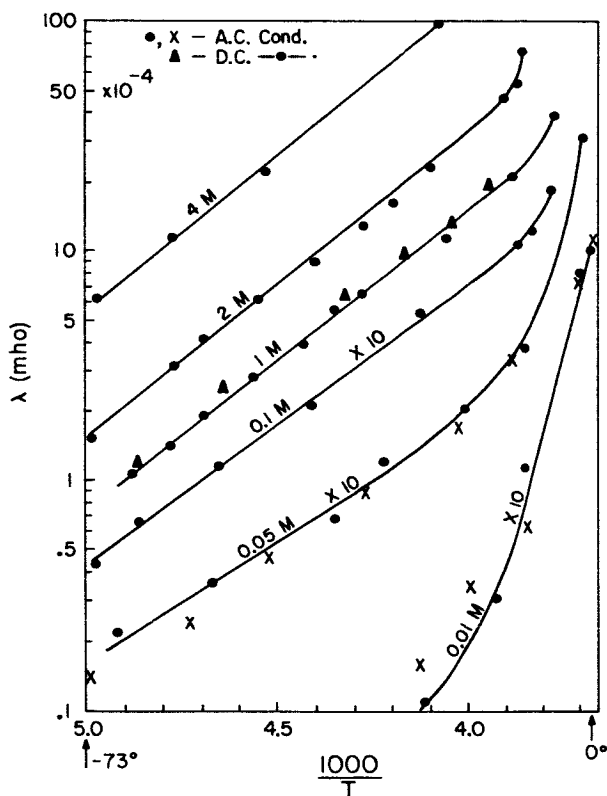


FIGURE 2. Log-conductivity of HCl-ice as a function of  $1/T$ .

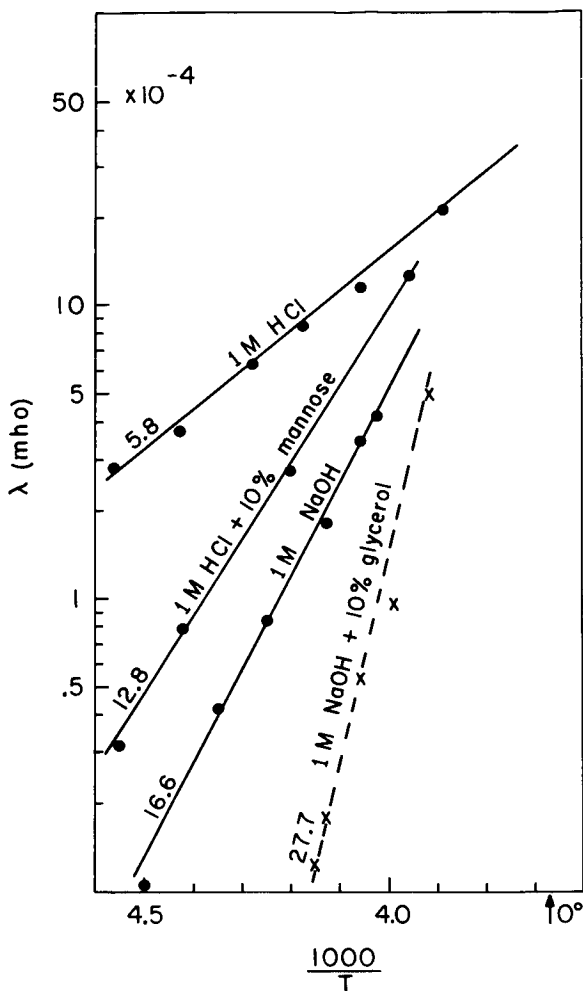


FIGURE 3. Log-conductivity of 1 M HCl-ice and 1 M NaOH-ice as a function of  $1/T$ . Activation energy values in kcal. are indicated on lines.

tions and a drastic change in slopes takes place at lower HCl levels. Reproducible ice conductivity data can be obtained above . 1M HCl concentrations. In the temperature range where log conductivity is a linear function of  $1/T$ , activation energies are in the range of 5-7 kcal.

Conductivities of a few other electrolytes were measured. HBr, HF and MI ice (0.1 M) yielded slope values similar to that for . 1 M HCl. The addition of KCl to HCl-ice had no effect, but adding LiCl increased the conductivity. Tests indicated that the . 1 M LiCl solution was acidic, with a pH

value of 6. Conductivity measurements with hydroxylated ice were of particular interest since OH-ion transport in ice also involves proton transport, but the mechanism is considered to be different from that of protonated ice. This is supported by the conductivity data in FIGURE 3 where the slope of log conductivity of 1 M NaOH-ice is much steeper ( $E$  value is 16.6 kcal.) than that of 1 M HCl-ice.

*Effect of addition of various biologic compounds.* In general there was no significant effect on activation energy when various compounds were present in solutions in the liquid state. The exception was gelatin where at high concentrations (20 per cent gelatin in 0.1 M HCl solution) there was a significant reduction of slope value in the conductivity curve. However, changes were nonlinear and activation energy cannot be represented by a single numerical value. Gelatin solutions during the freezing produced

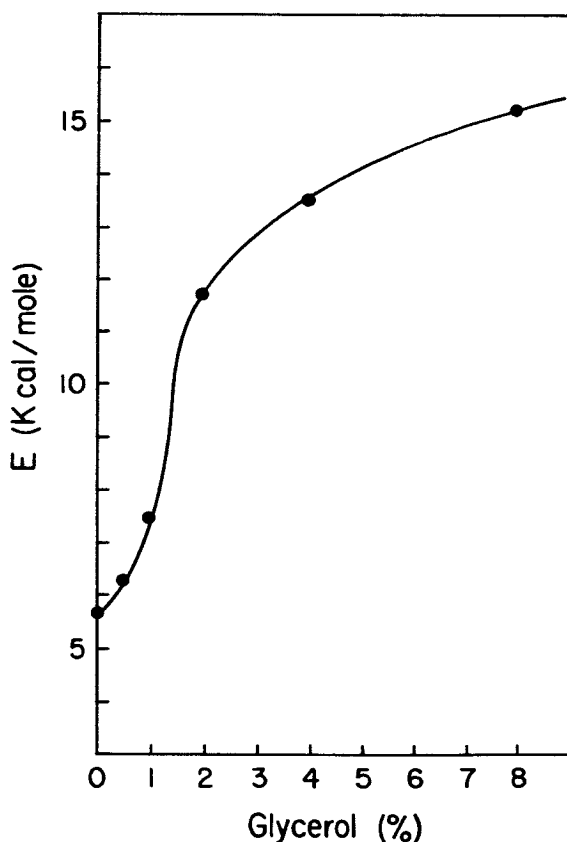


FIGURE 4. The effect of glycerol concentration on the conductivity of 0.2 M HCl-ice in temperature range  $-17^{\circ}$  to  $-44^{\circ}$ .

drastic expansion of ice and cells were broken. Consequently, these studies were discontinued. In contrast, in ice (temperature range  $-10$  to  $-45^{\circ}$ ) the presence of various biological compounds increased activation energy values drastically. In the presence of glycine, diglycine and triglycine (1 gr. per 100 ml. of .1 M HCl) activation energy values were respectively 18.7, 17.3 and 14.2 kcal. It appears that increasing chain length causes reduction in activation energy values. For dl-alanine (0.1 M alanine per .1 M MCl solution) activation energy value was 16.7 kcal. and agar-gel (2 g. agar per 100 ml. 1 M HCl) yielded activation energy value 12.1 kcal.

Further studies were carried out on the effect of various sugars on activation energies. FIGURE 3 shows that there is a significant increase in activation energy value when 1.0 M NaOH-ice also contains glycerin. A similar effect is produced in 1 M HCl-ice in the presence of mannitol. FIGURE 4 shows the effect of glycerol concentration in 0.2 M HCl-ice. There is initially a rapid rise of activation energy values when glycerin concentration

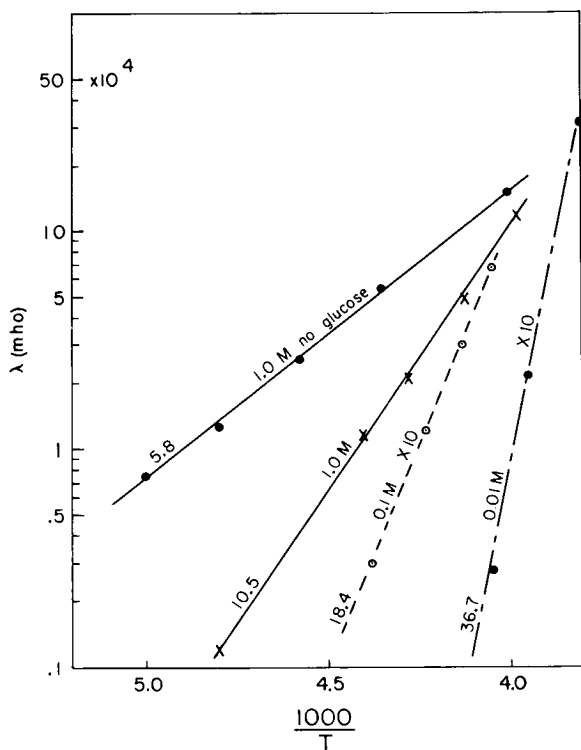


FIGURE 5. The effect of HCl concentration on the conductivity of ice in the presence of 10 per cent glucose. Activation energy values in kcal. are indicated on lines.



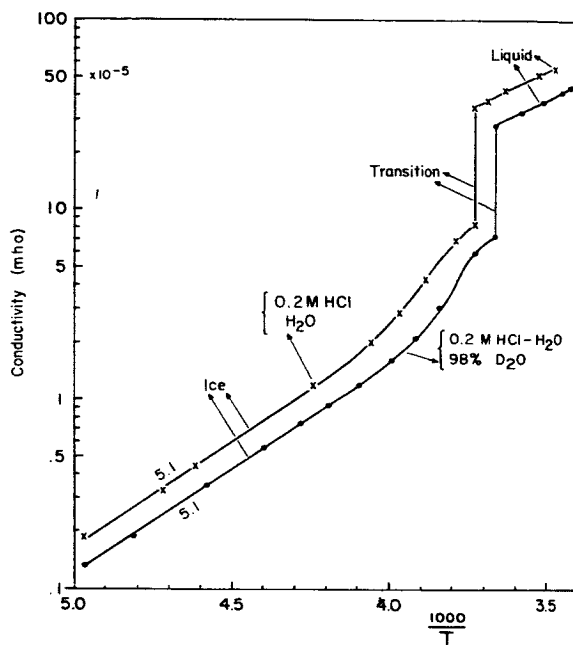


FIGURE 6. Log-conductivity of 0.2 M HCl in  $\text{H}_2\text{O}$  and  $\text{D}_2\text{O}$  during supercooled freezing as a function of  $1/T$ .

is increased but a saturation value is reached at higher glycerin concentrations. In FIGURE 5 conductivity data for various concentrations of HCl-ice in the presence of 10 per cent glucose are presented. It is evident that while activation energy values of 1 M and 0.1 M HCl-ice are practically the same (FIGURE 2), a significant increase takes place when the concentration ratio between glucose and acid is increased.

*The effect of  $\text{D}_2\text{O}$  on conductivity.* Comparative studies were made in  $\text{H}_2\text{O}$  and  $\text{D}_2\text{O}$  by freezing solutions from the supercooled state. FIGURE 6 shows that the absolute value of conductivity is reduced when 0.2 M HCl is in the solution or ice of  $\text{D}_2\text{O}$ . There is no apparent change in activation energy values. However, FIGURE 7 suggests that there may be a small, but significant increase of activation energy in  $\text{D}_2\text{O}$ -ice when doped with NaOH.

*The effect of proton concentration on freezing characteristics.* It is evident from FIGURE 8 that conductivity of 0.1 M HCl solution is drastically reduced during the freezing process. Furthermore, at constant temperature at the freezing point, ice conductivity decreases by a large factor until it finally stabilizes to a constant value. For 0.1 M HCl, for both the liquid and solid states log versus  $1/T$  plot yields straight line (with different slopes),

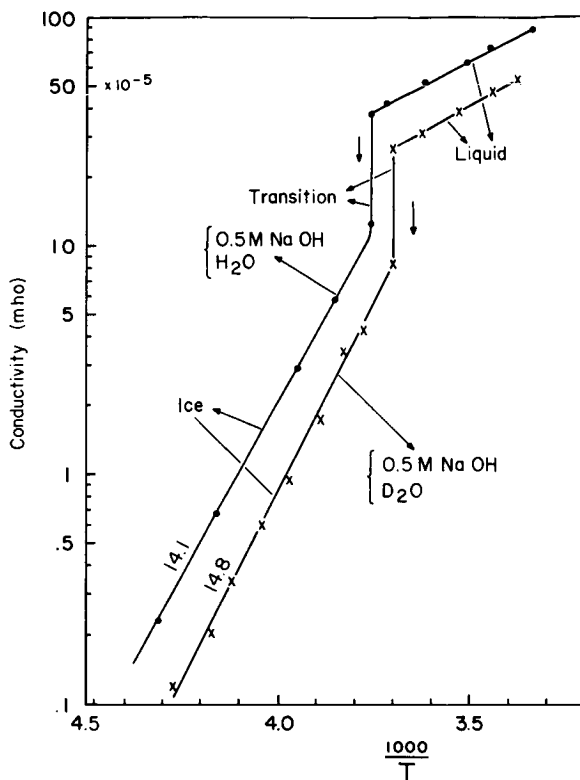


FIGURE 7. Log-conductivity of 0.5 M NaOH in  $\text{H}_2\text{O}$  and  $\text{D}_2\text{O}$  during super-cooled freezing as a function of  $1/T$ .

being separated by nonlinear freezing region. However, the log conductivity of 4 M HCl solution has a nonlinearity in liquid phase in  $-10^\circ$  to  $-30^\circ$  region. It is linear while it passes from liquid to solidly frozen state in region  $-30^\circ$  to  $-70^\circ$  (experimentally measured). It is of interest to note that in this region the log plot versus  $1/T$  slope is the same for both 0.1 M and 4 M MCl. Furthermore, it appears that high proton concentration alters conductivity characteristics of a solution at certain temperature range and activation energies for proton transfer in liquid and frozen state are similar. It suggests perhaps that protons at high concentration at certain temperatures have a strong orientating effect on water molecules.

While the structure of such ice is poorly defined, it nevertheless characterizes biological media better than that of a single crystal. However, activation energy values derived from such systems cannot be used for calculation of various reaction processes involving proton transfer, since experiments show that the other nonionic molecules in the media affect

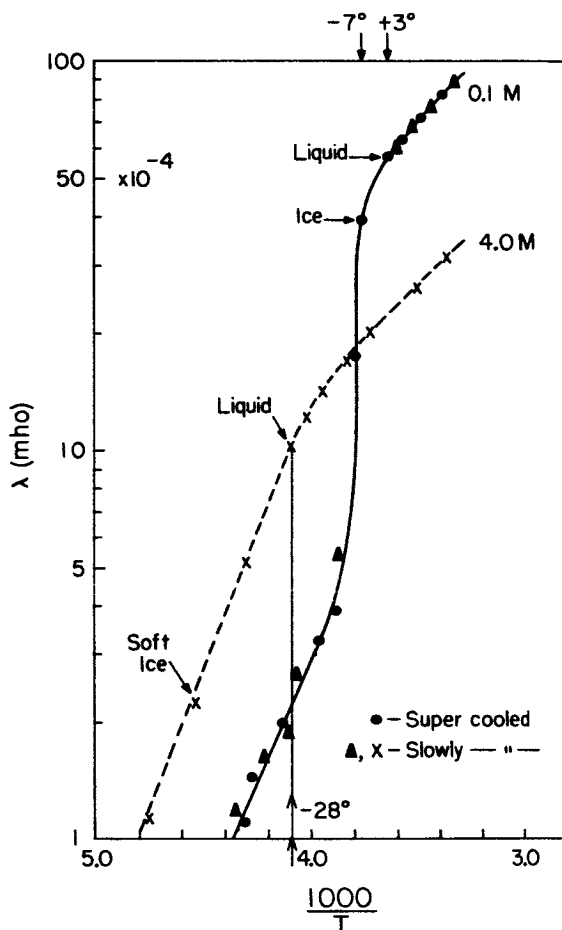


FIGURE 8. The effect of proton concentration on conductivity characteristics in liquid-ice transition region.

the protonic activation energies. Consequently, in complex biological structures where there are high concentration gradients of constituent structural molecules, proton activation energy depends on its local environment. This is of course true only when water is orientated in interphase regions as in "ice-type" structures.

Experiments with supercooled freezing of doped ice show definitely that the absolute conductivity value of doped ice and solution are not the same. The experiment (FIGURE 1) with HF-doped ice shows that there is about 13-fold increase of resistance when solution and ice are at the same tem-

perature. At lower impurity concentration, this difference is more pronounced.

Some exploratory experiments with deuterium show that activation energy is not affected by change of mass, but absolute conductivities are. This observation may have some bearing on the interpretation of the proton transfer mechanism.

#### *References*

1. GROSS, G. W. 1965. Ion incorporation and activation energies of conduction in ice. *This Annal.*
2. HEINMETS, F. & R. BLUM. 1963. Conductivity measurements on pure ice. *Trans. Faraday Soc.* 59: 1141.

## HYDRATION STRUCTURE OF FIBROUS MACROMOLECULES

H. J. C. Berendsen and C. Migchelsen

*Department of Physical Chemistry, The University  
of Groningen, The Netherlands*

It is generally assumed that macromolecular surfaces alter the structure of water in their immediate surroundings. Considering proteins in particular, one might, in analogy with known effects of solutes on the structure of water,<sup>1</sup> venture to predict the following influences:

(a) Polar side chains are expected to hydrate individually, but have a structure-breaking influence beyond the first layer.

(b) Nonpolar side chains will induce order (of the cage-type) similar to the effects of nonpolar solutes.

(c) Backbone structures with no available hydrogen-bond donors or acceptors (as the  $\alpha$ -helix) will act as nonpolar solutes.

(d) Backbone structures able to form H-bonds to water will have structure-breaking or structure-promoting effects, depending on the geometry of hydrogen-bonding sites. If the geometry is such that the sites, to which water may be bound, form an array fitting to an ice-I structure, a structure-promoting influence is to be expected. The same may be true if other regular water structures could be fitted to the hydrogen-bonding sites. With hydrophobic backbones similar effects might occur if short polar side-chains repeat in a pattern fitting to a regular water lattice. The effects will be stronger for rigid backbones or side chains.

It should be kept in mind that effects on the structure of water are not described by the terms hydrophilic and hydrophobic: polar groups and the tendency to form hydrogen-bonds to water make a surface more hydrophilic, while structure-promoting effects make a surface more hydrophobic as a result of unfavorable entropy changes.<sup>2</sup>

There have been few experiments which have yielded clear-cut data on the structure of water near macromolecular surfaces. In the last decade it has been possible to apply nuclear magnetic resonance (NMR) techniques, which have the advantage that the resonance signal produced by the protons of water molecules is generally distinguishable from the signal produced by the protons in the macromolecules, because of the smaller width of the water resonance line due to motion of water molecules. Thus the system studied remains relatively simple in nature. The amount of information gained by NMR measurements is limited, but it is possible to increase the information by using oriented samples, where the orientation introduces an additional variable. Thus we have studied the proton resonance signal of water molecules attached to various fibrous macro-

molecules (collagen, silk fibroin, DNA, keratin), where we could use oriented samples. These experiments are described and discussed in *Part I*. In *Part II* we describe the influence of some neutral salts on the structure of water in hydrated collagen.

*Part I: Fibrous Macromolecular Hydrates*

*Collagen.* The protein collagen has already been studied extensively,<sup>3</sup> and it has been observed that over a wide range of relative humidities (20–90 per cent) the resonance signal of the water protons shows three peaks. The two outer peaks are symmetrically arranged with respect to the central peak and are a result of dipole splitting. This is shown by the angular dependence of the distance between the outer peaks, which is of the order of one gauss. In FIGURE 1 the derivative of the absorption curve from water protons is shown for a sample of collagen (rat-tail tendon) containing 36 g. water per 100 g. dry protein, for various angles between fiber direction and magnetic field. The angular dependence of the splitting follows precisely the dipolar interaction term  $3 \cos^2 \epsilon - 1$  with the angle  $\epsilon$  between fiber direction and magnetic field (FIGURE 2), which indicates that the water molecules rotate anisotropically, the principal axis of anisotropy being in the fiber direction. The magnitude of the splitting is not compatible with any simple rotation about a single axis. A model able to

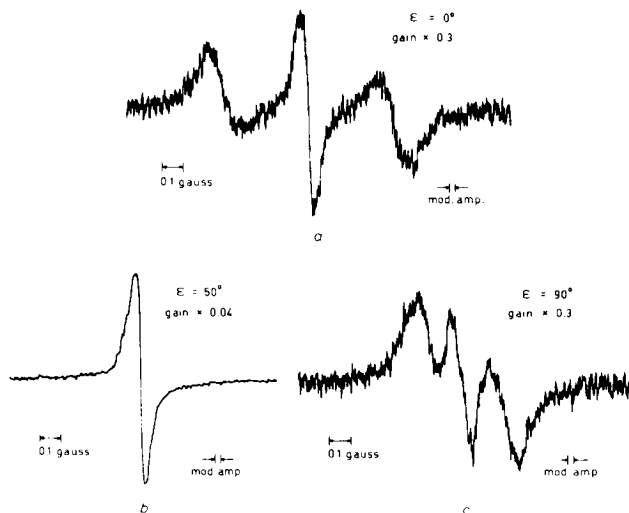


FIGURE 1. Proton magnetic resonance curves from the water in hydrated collagen (oriented rat-tail tendon) containing 36 g. water per 100 g. dry weight (relative humidity 81 per cent). The curves show the derivative of the resonance signal, at fiber-to-field angles  $\epsilon$  of  $0^\circ$  (curve a),  $50^\circ$  (curve b), and  $90^\circ$  (curve c). Scanning rate 200 mgauss/min.

*peak separation*  
(gauss)

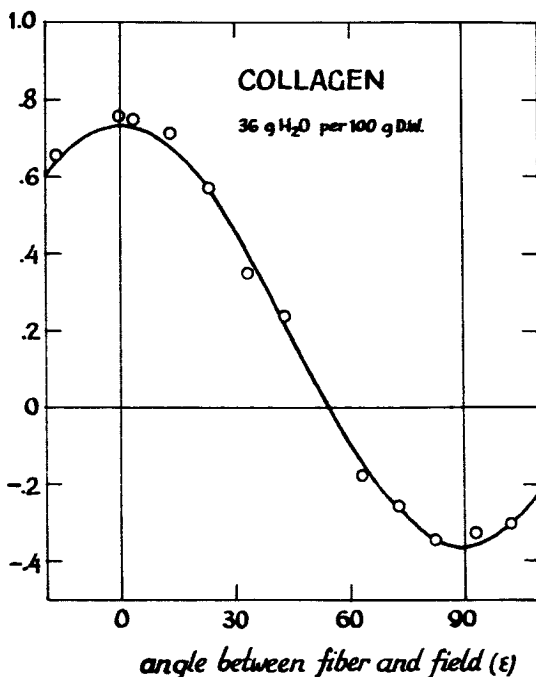


FIGURE 2. Separation between outer peaks as a function of the angle between fiber and field ( $\epsilon$ ), for the sample of FIGURE 1. The separation was obtained by a least-square fit of three Lorentzian curves to the observed resonance curves by a digital computer (Telefunken TR 4). The drawn curve is proportional to  $(3 \cos^2 \epsilon - 1)$ .

explain the experimental data in a quantitative way is that water molecules adhere to each other and to the collagen macromolecules and thus form chains in the fiber direction, as indicated in FIGURE 3. Rotations of water molecules in such chains, which are necessarily anisotropic due to the existence of hydrogen-bonds mainly in the chain direction, yield the observed interaction of proton spins. Assuming that line broadening is a result of intermolecular interactions, the life time of a water molecule in a particular chain was found to be in the microsecond range. Thus such a structure is in a state in between the solid and liquid state, e.g. the molecular life times are five orders of magnitude longer than in the liquid state.

*Silk fibroin, DNA, and keratin.* When studying hydrated silk fibroin (from commercial silk), DNA (salmon sperm), and keratin (unpigmented

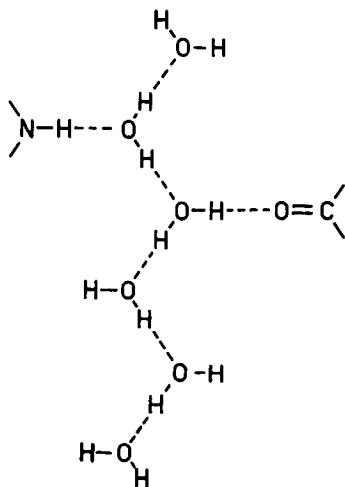


FIGURE 3. Proposed chain-like structure in the water of hydration of collagen at relative humidities below 90 per cent. Two examples of hydrogen-bonds to the collagen backbone are shown. The collagen molecules run in vertical direction in this figure.

horse hair), it was found that none of these exhibit a hydration structure similar to that of collagen. In all cases the water produces a relatively narrow resonance line, even at low humidities, with no particular structure, indicative of a rapid rotation of water molecules. The line widths were generally lower than 200 milligauss, and the observed broadening is very similar to that caused by extreme increase in viscosity. The widths, however, and hence the peak-to-peak amplitudes of the resonance lines, are in some cases dependent on the angle between fiber direction and magnetic field, which indicates that the magnetic interaction between protons is not isotropic, presumably due to nonisotropic rotations of the water molecules. It is possible to analyze the data in such systems by relating the angular dependence of the resonance signal to the direction of anisotropic interaction of protons in a cylindrically symmetric system. Employing the model used for collagen, this amounts to deriving the direction of the chain-like structures (if they occur) with respect to the fiber axis, from the dependence of the width of the resonance signal on the angle between fiber direction and magnetic field.

A theoretical expression was derived<sup>3</sup> for the mean square width  $S$  of absorption curves for a rigid system of protons, as a function of both the angle  $\alpha$  between fiber and direction of proton interaction, and the angle  $\epsilon$  between fiber and field. (FIGURE 4). The same angular dependence will hold for systems in which water molecules exhibit anisotropic rotation. For



$S(\alpha, \epsilon)$   
in units of  $\mu^2/r^6$

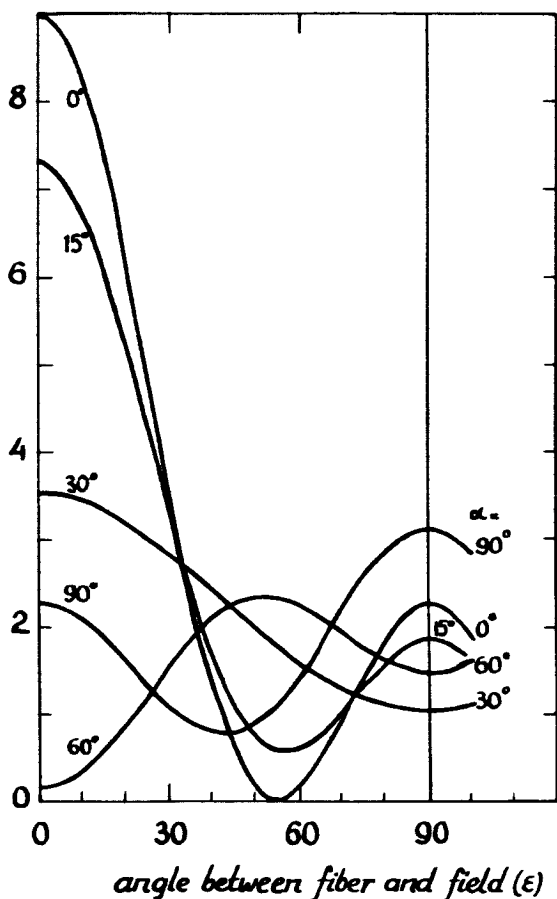


FIGURE 4. Theoretical second moment (mean square width)  $S(\alpha, \epsilon)$  of a cylindrically symmetrical system of protons interacting at an angle  $\alpha$  to the symmetry axis, as a function of the angle  $\epsilon$  between symmetry axis and magnetic field. Ordinate values apply to a system of isolated motionless proton pairs with interproton distance  $r$ .

macromolecules with narrow absorption lines due to water protons, the determination of the mean square widths of the lines is impractical, but it is now possible to compare the inverse peak-to-peak amplitude of the derivative signal  $1/h$  with the calculated curves  $S(\alpha, \epsilon)$ . This is, for qualitative purposes, a reasonable comparison since for two common types of curve shape (lorentzian and gaussian) the square width is inversely pro-

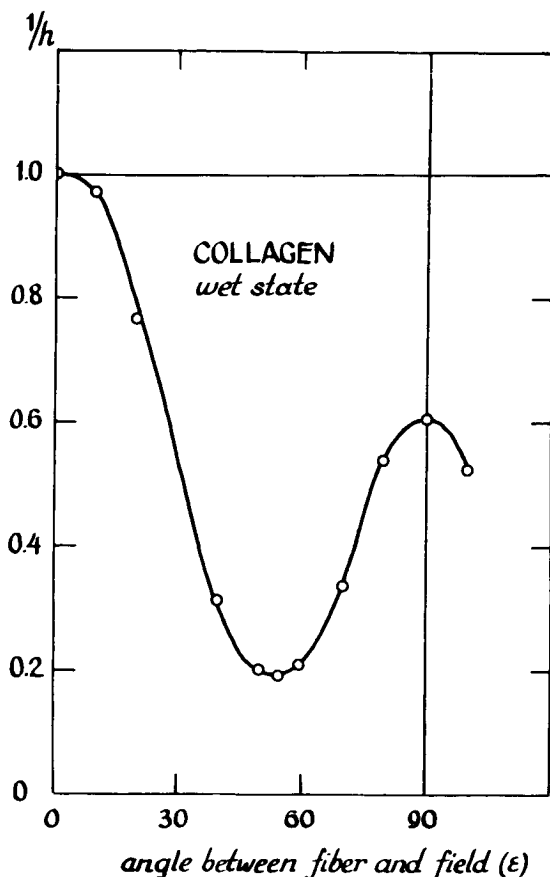


FIGURE 5. Inverse peak-to-peak amplitude of the derivative resonance curves of water in wet collagen (bovine tendon in the native state), showing qualitative agreement with FIGURE 4 for proton interaction close to the fiber direction. Ordinate values are normalized to 1 at  $\epsilon = 0^\circ$  (fibers in direction of magnetic field).

portional to the peak-to-peak amplitude. As a test, this method was applied to wet collagen (FIGURE 5), where it is clear that the  $1/h$  curve is similar to the S-curve for  $\alpha$  close to  $0^\circ$  (FIGURE 4).

For the other macromolecules studied, the shapes of the  $1/h$  curves more closely resemble S-curves in the range  $\alpha = 70-90^\circ$ , indicating an anisotropy of rotations of water molecules almost perpendicular to the fiber direction. For a closer comparison, the S-curves are given in FIGURE 6 for  $\alpha = 65-90^\circ$ , normalized to one at  $\epsilon = 0^\circ$ .

FIGURE 7 gives  $1/h$  curves, plotted in the same way, for silk fibroin at different relative humidities. It is observed that the anisotropy of rotations occurs at an angle of  $70^\circ$  to the fiber axis, and that the magnitude of the

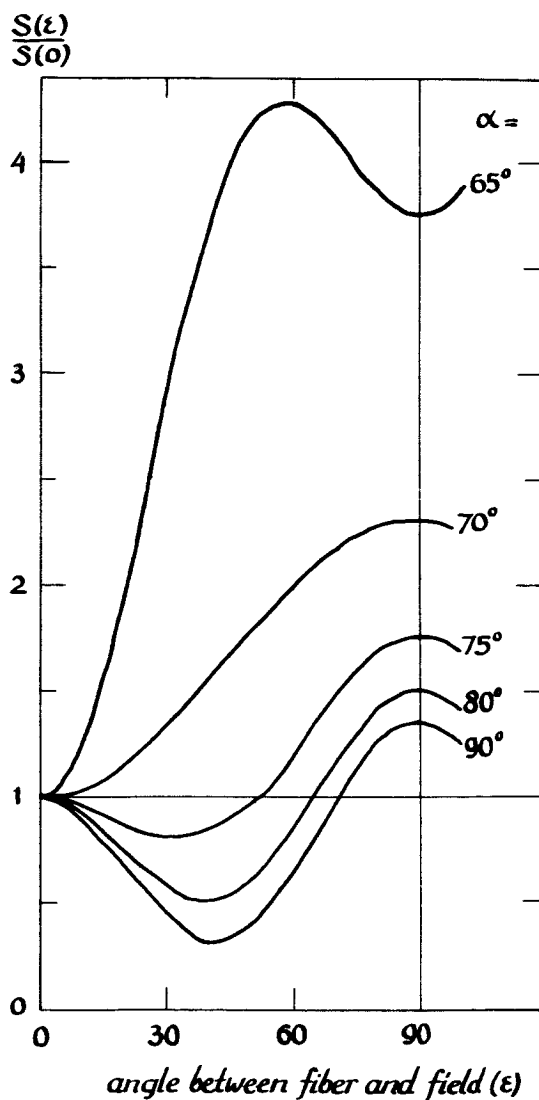


FIGURE 6. Theoretical second moment curves similar to FIGURE 4, but for the range  $\alpha = 65^\circ$  to  $90^\circ$ , and normalized to 1 at  $\epsilon = 0^\circ$ .

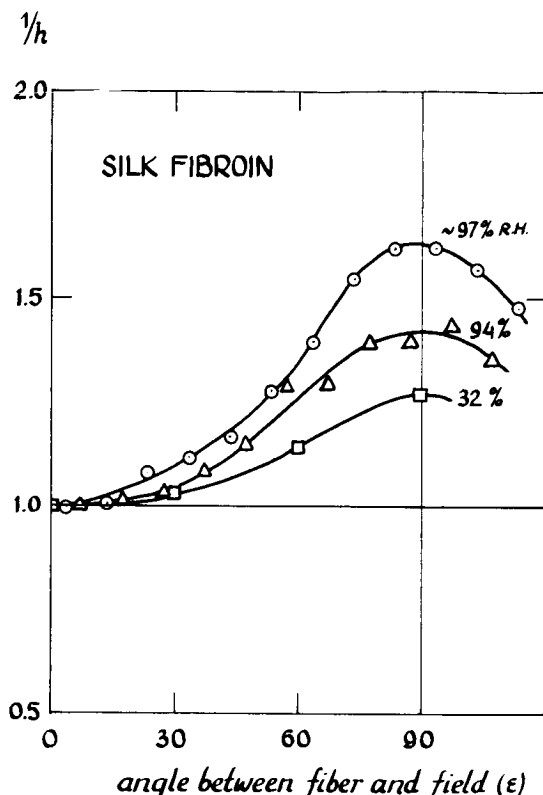


FIGURE 7. Relative inverse peak-to-peak amplitudes of the derivative resonance curves of water in silk fibroin at relative humidities of 32, 94, and 97 per cent. The water contents of these samples were 6.5, 17, and 23 g. water per 100 g. DW.

effect increases with increasing humidity. A possible explanation is that at low humidity mainly isolated side chains hydrate, but at increasing humidity water bridges between these isolated hydrated sites occur, which form preferentially in a direction at an angle of  $70^\circ$  with respect to the fiber axis.

A similar  $1/h$  plot for hydrated DNA (FIGURE 8) yields curves which indicate anisotropy in a direction perpendicular to the fiber axis, also increasing with increasing humidity. The anisotropy is not as strong as in the case of silk fibroin.

Hair keratin in the native state (unstretched) shows only a very slight and probably insignificant angular dependence (FIGURE 9), while in the partly stretched condition the anisotropy has increased slightly, with a direction of anisotropy of about  $75^\circ$  with respect to the fiber axis.

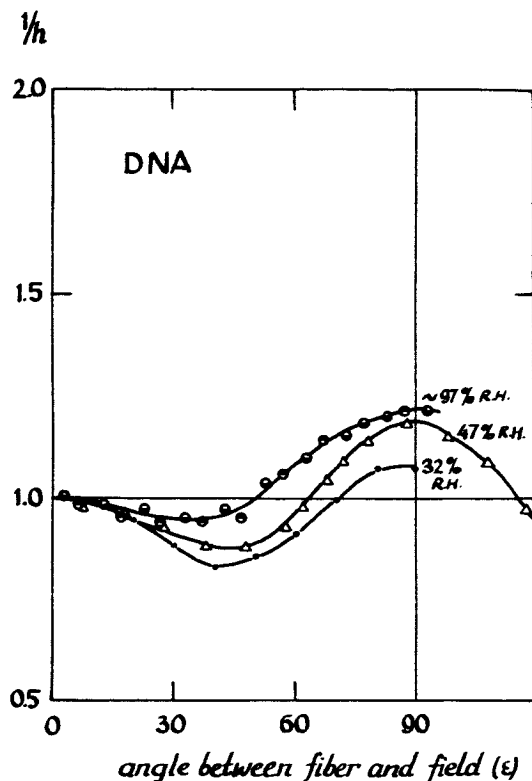


FIGURE 8. Curves similar to FIGURE 7, for DNA (salmon sperm) at relative humidities of 32, 47, and 97 per cent.

*Discussion.* It is an interesting question why collagen behaves so completely different from the other macromolecules studied, in that it induces a much higher degree of structure in its water of hydration and that the direction of anisotropy (the direction of chain-like structures) is in the fiber direction. The main cause for this peculiarity is probably to be attributed to its backbone structure. Collagen distinguishes itself from both the  $\alpha$ -helix and the  $\beta$ -pleated sheet structures in that not all hydrogen-bonding sites on the backbone (N-H and C=O) are occupied within the macromolecular structure, but that a considerable number are available for H-bonds to water molecules outside the threefold collagen helix. Furthermore, the available N-H and C=O groups are directed almost perpendicular to the threefold helix, thus ideally suited to provide H-bonds to longitudinal chains of water molecules in channels between the collagen helices. In the  $\alpha$ -helix (as in  $\alpha$ -keratin), as well as in the  $\beta$ -pleated sheet (as in silk fibroin), all available hydrogen-bonding sites are occupied

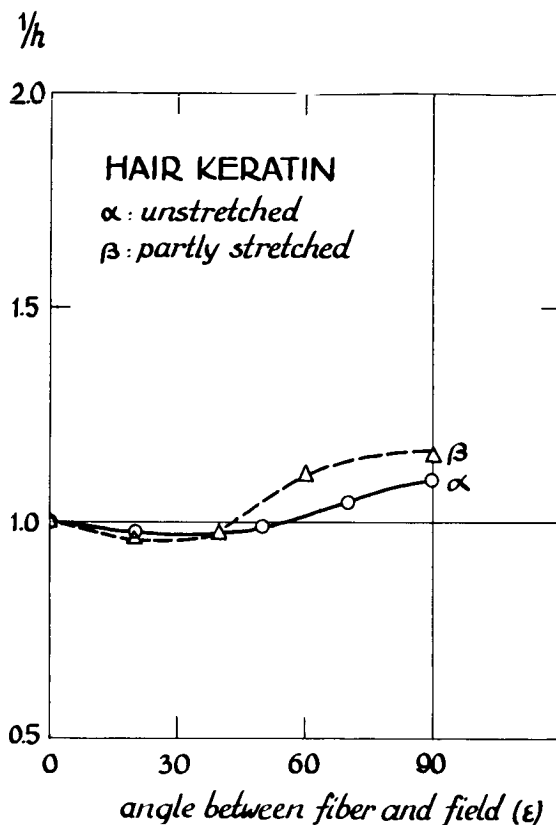


FIGURE 9. Curves similar to FIGURE 7 for hair keratin (horse hair) in native form ( $\alpha$ ), and in partly stretched form ( $\beta$ ). Water content 22 g.  $H_2O$  per 100 g. DW (relative humidity 81 per cent).

internally such that water molecules can only bind to charged or polar side chains. Apparently the hydration of side chains does not show a particular structure observable by NMR. At higher humidities it is likely that isolated hydrated side chains become bridged by water molecules. In the case of silk fibroin it is possible that such bridges run at a direction of  $70^\circ$  to the fiber axis, but it is also possible that most bridges run perpendicular to the fiber, and some parallel, yielding an average effect indistinguishable from  $70^\circ$ .

An interesting feature of collagen is that the axially repeating distance of the threefold helix<sup>1</sup> (28.6 Å as shown in FIGURE 10a) equals exactly six times the repeating distance in chains of water molecules (4.74 Å, based on the hydrogen-bond length in water of 2.9 Å). Thus the collagen structure could possibly stabilize water chains in the fiber direction. In

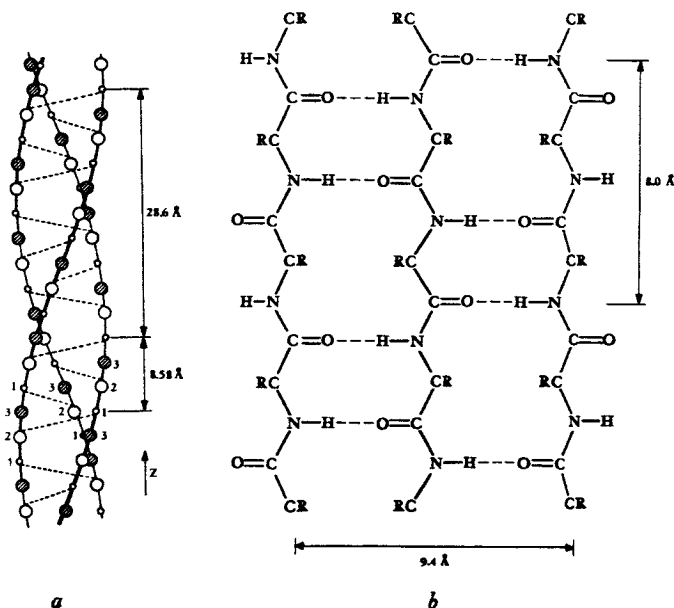


FIGURE 10. Basic structure of (a) collagen and (b) silk fibroin showing the repeat distances in the macromolecules.

silk fibroin, on the other hand, which contains protein chains in antiparallel pleated sheets,<sup>5</sup> there is no such relation in the fiber direction (repeat of 8.0 Å), but perpendicular to the fiber axis the repeating distance is 9.4 Å, equal to two water chain repeats. Thus the structure of silk fibroin might stabilize chains perpendicular to the fiber direction (FIGURE 10b).

The  $\alpha$ -helix, with its axial repeat of 5.4 Å, has no relation to the structure of water, and one would not expect a particular structure to be induced in  $\alpha$ -keratin. In the stretched form, when  $\beta$ -structure is produced, perpendicularly oriented chains might occur. This is confirmed by the experiments, although the anisotropy is not very marked.

In the case of DNA it is not quite clear why a perpendicular type of anisotropy occurs. It may be that horizontal water bridges form between hydrated phosphate and hydrogen-bonding sites of the corresponding base. No indication of anisotropy either in the groove direction or perpendicular to it has been found.

#### *Part II: The Influence of Neutral Salts on Water in Hydrated Collagen*

While investigating the influence of pH and salt content on the water structure in collagen, we found that collagen fibers bathed in a salt-free 10 mM. phosphate buffer at pH 7, and subsequently dried to a humidity

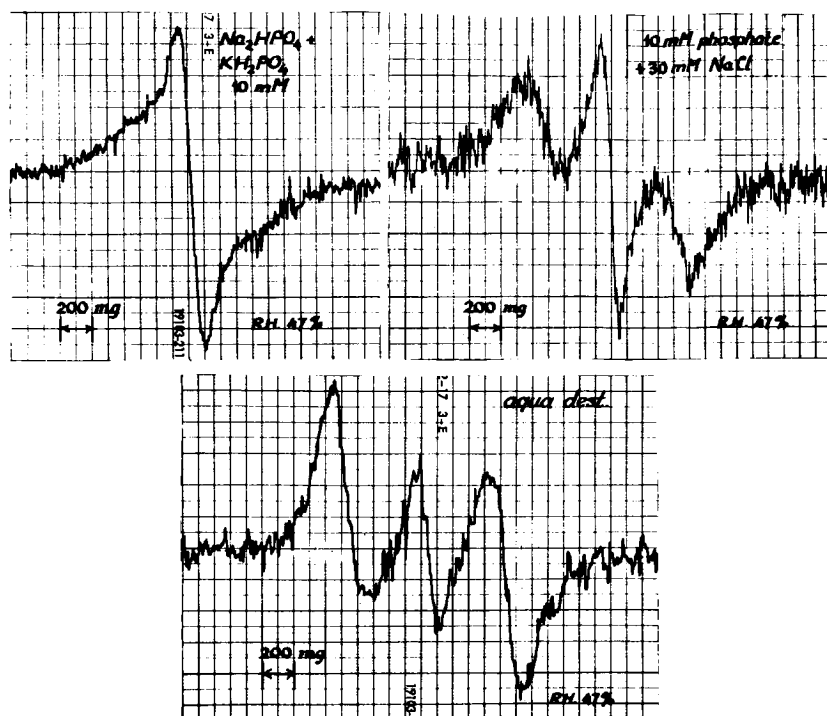


FIGURE 11. Water resonance signal of collagen that had been soaked in 10 mM. phosphate buffer ( $pH$  7), in 10 mM. phosphate buffer containing 30 mM. NaCl, and in distilled water. Relative humidity during measurement was 47 per cent; the water content of each of the samples was 22 g.  $H_2O$  per 100 g. DW.

of 80 per cent or lower, had lost their particular water structure: no splitting of the NMR line of the water protons was observed. In distilled water, however, an excellent splitting is found. When NaCl is present in a concentration three times that of the phosphate buffer, the splitting is again observed (FIGURE 11). At first it seems that the difference between the presence and non-presence of the buffer is due to differences in charge on the collagen, because the charge on histidine, which titrates at  $pH$  6, is known to be important in stabilizing the collagen structure." A series of measurements at several  $pH$ 's between six and eight (adjusted without buffer during several days) showed however that the NMR signal is not  $pH$ -dependent in this range. So the breaking down of the water structure must be due to the phosphate ion.

Recently it was observed by von Hippel and Kwok-Ying Wong<sup>7</sup> that the effect of neutral salts on denaturation of proteins and DNA is very similar for very different macromolecules as collagen, ribonuclease, DNA, and



myosin, and they suggest that the effects on macromolecular conformations are a consequence of very general effects of the various ions on the structure of the solvent, which in turn modifies solvent-macromolecule interactions involved in the stabilization of the native structures. The sequence of a few selected salts according to their stabilizing effects on the native conformation is:

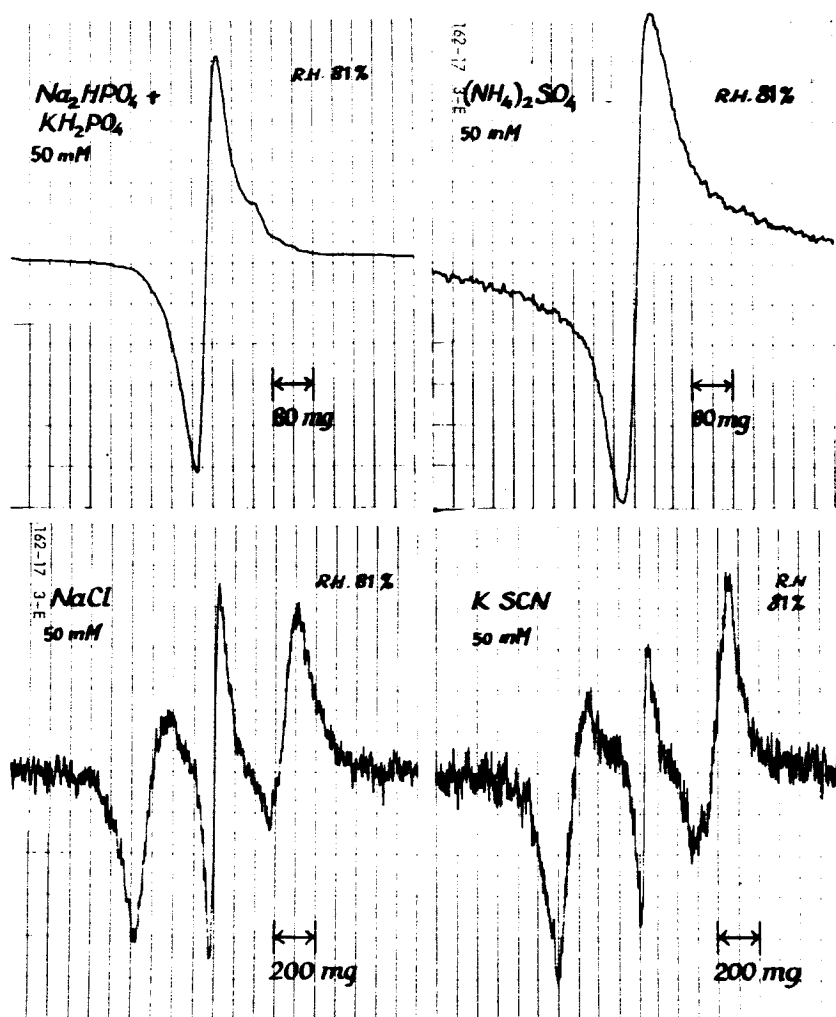
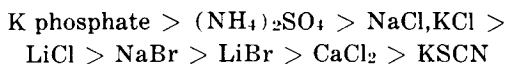


FIGURE 12. Water resonance signal of collagen that had been soaked in 50 mM. solutions of sodium/potassium phosphate, ammonium sulphate, sodium chloride and potassium thiocyanate. Relative humidity during measurement was 81 per cent, water content  $40 \pm 2$  g.  $\text{H}_2\text{O}$  per 100 g. DW for each of the samples.



Salts to the left of NaCl stabilize, those to the right destabilize the native conformation.

Since phosphate occurs at one extreme end of this series and was found to break the organized water structure around collagen, we studied the effect of other salts of this series. FIGURE 12 shows the results for bathing solutions of K-Na-phosphate (pH 7),  $(\text{NH}_4)_2\text{SO}_4$ , NaCl, and KSCN, all at 50 mM. concentration. After bathing in these solutions, the fibers were equilibrated to 81 per cent relative humidity (in the atmosphere of saturated urea solution); the curves shown represent the NMR absorption of the water protons, remaining after this partial dehydration. A splitting of the NMR line indicates a marked anisotropy in the rotation of water molecules, interpreted as the existence of chain-like structures; the absence of such splitting indicates the absence of such structures. It turns out that phosphate and ammonium sulphate break the structure, while NaCl and KSCN have no appreciable influence at this concentration. It was found, however, that NaCl also breaks the structure when a bathing solution of 150 mM. is used. The breaking effect of phosphate is stronger than that of ammonium sulphate, while in KSCN the NMR lines are still better resolved than in NaCl. By lowering the concentration of the bathing solution fivefold the results of FIGURE 13 have been obtained; here it is very clearly shown that phosphate has a stronger breaking effect than ammonium sulphate.

Thus the effect of these electrolytes on the structure of the water of hydration of collagen parallels their effect on the stability of the native

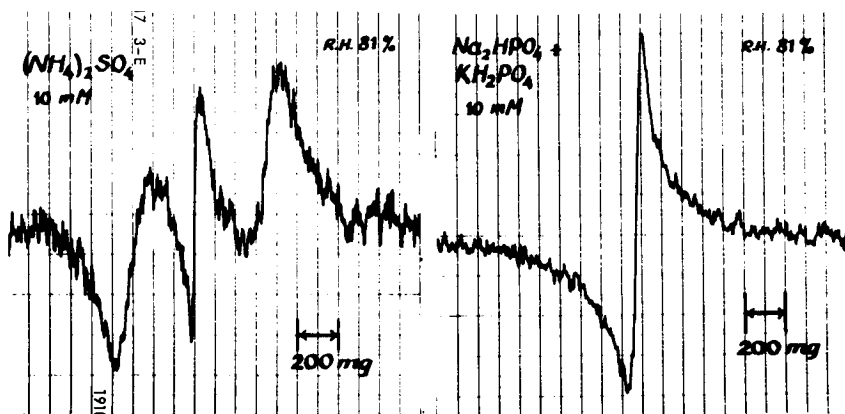


FIGURE 13. Same experiment as shown in FIGURE 12, but for bathing solutions of phosphate and ammonium sulphate at 10 mM. concentrations.

conformation of macromolecules, which supports the suggestion of Von Hippel and Wong that the influence on these ions on water is their primary effect.

It now appears that a structure-breaking effect on 'organized' water, at least on the hydration of collagen, means a *stabilizing* effect on the native macromolecular conformation. One possible explanation of this is that the native conformation induces more order in the surrounding water than the denatured conformation, so that denaturing involves an entropy increase not only due to the macromolecule, but also to the water. The presence of an agent that reduces the order in the water close to the native macromolecule will increase the entropy of the native conformation, while not changing the entropy of the denatured conformation nearly as much. Thus the entropy increase on denaturing will not be as high in the presence of a structure-breaking agent as without it, which thermodynamically favors the native state.

The measurement of NMR absorption in the collagen-water system provides a discriminative and sensitive tool for the experimental study of the effects of various agents on the 'organization' of water in a macromolecular system. It seems to be very promising since practically no other direct methods are available.

#### References

- 1a. FRANK, H. S. & M. W. EVANS. 1945. J. Chem. Phys. 13: 507.
- 1b. FRANK, H. S. & W.-Y. WEN. 1957. Disc. Faraday Soc. 24: 133.
- 1c. FRANK, H. S. 1958. Proc. Roy. Soc. (London) A247: 481.
2. KAUZMANN, W. 1959. Adv. Prot. Chem. 14: 1.
3. BERENDSEN, H. J. C. 1962. J. Chem. Phys. 36: 3297; 1962. Thesis. University of Groningen. Groningen, The Netherlands.
4. RICH, A. & F. H. C. CRICK. 1961. J. Mol. Biol. 3: 483.
5. MARSH, R. E., R. B. COREY & L. PAULING. 1955. Biochim. Biophys. Acta 16: 1.
6. MARTIN, G. R., S. E. MERGENHAGEN & D. B. SCOTT. 1961. Biochim. Biophys. Acta 49: 245.
7. VON HIPPEL, P. H. & KWOK-YING WONG. 1964. Science 145: 577.

# ION INCORPORATION AND ACTIVATION ENERGIES OF CONDUCTION IN ICE\*

Gerardo Wolfgang Gross

*New Mexico Institute of Mining and Technology, Socorro, N. Mex.*

The direct-current conductivity has been measured on a large number of ice samples doped with ionic impurities, as a function of ionic species, concentration, and temperature. Electrolytes studied thus far are hydrofluoric acid, hydrochloric acid, potassium fluoride, and ammonium fluoride.

*Technique.* The preparation of samples, measuring technique, and some preliminary results have been published elsewhere (Gross, 1962). However, an important modification has since been introduced in the method for preparing nonpolarizing electrodes, resulting in a considerable simplification and time savings. Disks of filter paper coated with palladium under high vacuum had been used as nonpolarizing current electrodes. These are now replaced by circular filter disks, 1 mm. thick, composed of sintered platinum or palladium spherules. Pore sizes from 7-40 microns and porosities of up to 25-35 per cent may be achieved according to the manufacturer's specifications. Platinum filters of 7 to 10 microns pore size, 34.5 mm. and 27.5 mm. diameter, are in use at our laboratory; their weight is about 1.3 gm./cm.<sup>2</sup> A comparable palladium disk would weigh only about 0.75 gm./cm.<sup>2</sup> We have found it difficult to locate a supplier for this material. The disks were made by Engelhard Industries, Inc.

They are cleaned by boiling them in concentrated hydrochloric acid, subsequently rinsing them in conductivity water, and again boiling them in conductivity water. They are then soaked in conductivity water, which is checked repeatedly over a period of hours to insure that all electrolytic impurities have been eliminated.

One of the disks is saturated in the solution to be frozen and is then used as the base on which an ice sample is grown. This insures the best possible contact and prevents atmospheric gases from being adsorbed at the electrode. However, the heat flow through a sintered disk is reduced by a factor of one-third to one-half as compared to a solid polished disk. Its surface roughness may act as crystallization centers and thus preclude single-crystal growth. Where this is undesirable, the procedure outlined previously (Gross, 1962) may be used.

A second disk is saturated in dilute hydrofluoric acid (for example,  $5 \times 10^{-3}$  M) and is applied immediately after the sample has been grown.

\*This work was carried out under Office of Naval Research contract NR 082-094.

The disks are manipulated with teflon-tipped forceps. Their performance equals or excels that of palladium-coated filter paper. They can be reused indefinitely.

The samples used for these experiments were polycrystalline with a strongly preferred orientation of the *c*-axis in the direction of growth. The average freezing rate was of the order of one millimeter per minute. Experiments with single crystals have recently been started and thus far seem generally to confirm the results obtained with the polycrystalline samples.

All freezing solutions were prepared with high-grade conductivity water ( $1 \times 10^{-7}$  mhos/cm. or less at  $25^\circ\text{C}.$ ) and the purest reagents commercially available.

Concentrations indicated in this paper as in the ice or in the melt refer to the melted ice phase at room temperature.

### Discussion of Results

Experimental results are tabulated in TABLE 1. Sample curves are shown in FIGURE 1.

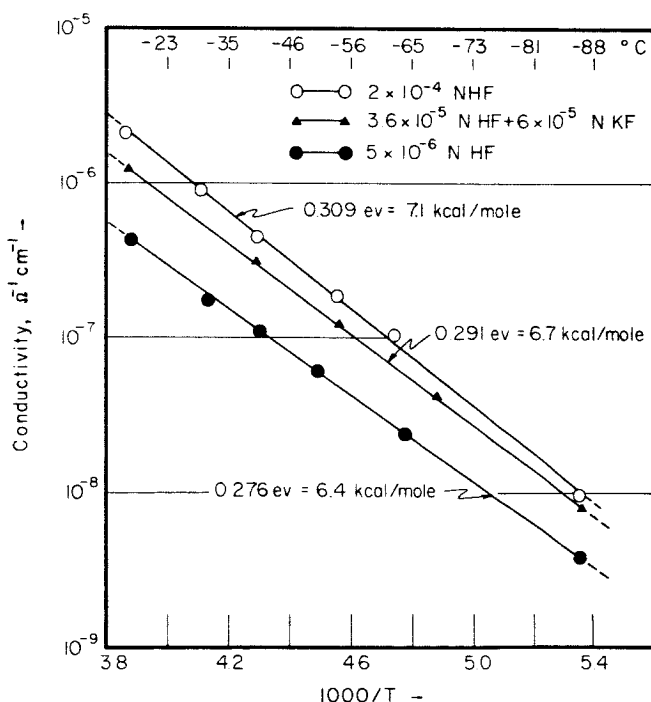


FIGURE 1. Arrhenius plots of ice samples grown from dilute solutions of hydrofluoric acid and of potassium fluoride.

TABLE 1  
SUMMARY OF ACTIVATION ENERGIES; TEMPERATURE RANGE:  $-10^{\circ}\text{C}$  TO  $-86^{\circ}\text{C}$ .

Solute	Molarity in the melt (moles per liter)	Number of samples	E/2 (mean values)	
			ev	Kcal/mole
HF	$10^{-4}$ to $10^{-8}$	33	$0.30 \pm 0.04$	$6.9 \pm 0.92$
HF*	$2.8 \times 10^{-3}$	1	$0.325 \pm 0.005$	$7.5 \pm 0.12$
HF†	Not stated	Not stated	0.338	7.8
HCl	$10^{-5}$ & $1.7 \times 10^{-4}$	5	$0.29 \pm 0.01$	$6.7 \pm 0.23$
KF†	HF: 4 to $10 \times 10^{-6}$	5	$0.31 \pm 0.02$	$7.2 \pm 0.46$
	KF: 3 to $15 \times 10^{-5}$			
KF§	HF: 4 to $6 \times 10^{-5}$	7	$0.31 \pm 0.02$	$7.2 \pm 0.46$
	KF: 4 to $7 \times 10^{-5}$			
CsF†	Not stated	Not stated	0.294	6.8
NH <sub>4</sub> F	$10^{-2}$ to $10^{-5}$	8	0.39 to 0.28	9.0 to 6.5

\*C. Jaccard (1959).

†Computed by A. Steinemann (1957) from low-frequency measurements.

‡Open circuit.

§External shunt, 10 Kiloohms.

The electrical conductivity of ice is largely determined by hydrogen ions associated with ionic impurities built into the lattice. In the case of the halogenic acids, hydrofluoric and hydrochloric, the conductivity at constant temperature is proportional to the square root of the acid concentration in the ice (FIGURE 2). This leads to the following expression for the conductivity as a function of acid concentration and temperature:

$$\sigma \propto [\text{H}_3\text{O}^+] = K(T) [\text{HA}]^{1/2} \quad (1)$$

where  $\sigma$  is the conductivity,  $[\text{HA}]$  is the molarity of the ice of hydrofluoric or hydrochloric acid, and  $T$  is the absolute temperature.

$$K(T) = C \exp (-E/2kT) \quad (2)$$

where  $E$  is the energy of ionization, according to the theory of Jaccard (1959).

The activation energies of TABLE 1 have been computed from the slope of Arrhenius plots such as those of FIGURE 1. They represent the numerical value of  $E/2$  in Equation 2.

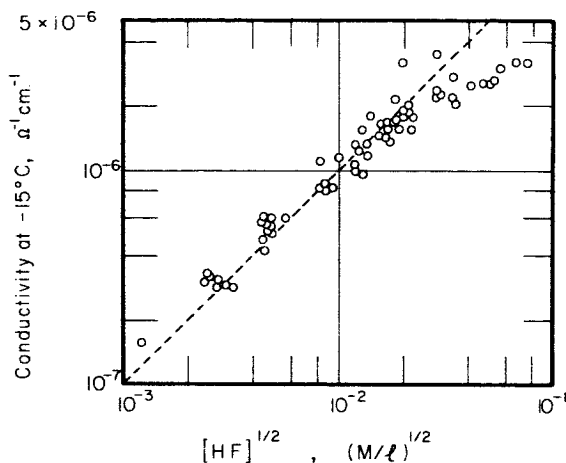


FIGURE 2. Conductivity at  $-15^{\circ}\text{C}$ . vs. the square root of concentration of ice samples grown from dilute solutions of hydrofluoric acid. The deviation from the straight line at the highest concentrations is believed to result from intergranular precipitation of HF. The samples are no longer transparent at these high concentrations.

*Hydrofluoric and hydrochloric acid.* The results obtained for hydrofluoric acid confirm the values given by Steinemann (1957), inferred from low-frequency measurements, and by Jaccard (1959). The present measurements cover a concentration range of about four orders of magnitude. The data indicate that, even at a concentration of as low as  $10^{-7}$  or  $10^{-8}$  moles per liter, the protons associated with the impurity molecules are the dominant current carriers. This appears to be true because the energy for ionization of water molecules in pure ice is at least twice that measured for ice doped with hydrofluoric acid (Jaccard, 1959; Heinmets & Blum, 1962).

Ice prepared from dilute hydrochloric acid solutions shows the same activation energy, within experimental error, as hydrofluoric. At  $-15^{\circ}\text{C}$ . both types of ice show the same conductivity dependence on concentration, given by

$$\sigma = 1 \times 10^{-4} [\text{HA}]^{1/2} \Omega^{-1}\text{cm}^{-1} \quad (3)$$

A plot of the function  $K(T)$  for an activation energy  $E/2 = 0.30$  ev is given in FIGURE 3. It is based on the empirical Equation 3. From this plot the conductivity at any temperature of a sample doped with hydrofluoric or hydrochloric acid may be estimated with the aid of Equation 1 if the average impurity concentration is known or assumed. Generally, the values thus obtained agree with our measurements within a factor of two. This uncertainty is probably due to variations in the activation energy measurements, variable concentration gradients within the samples, and geometrical

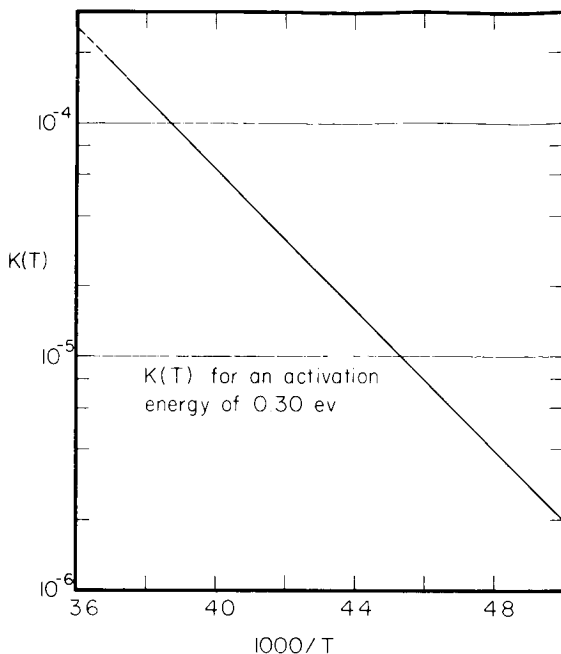


FIGURE 3. The proportionality factor  $K(T)$ , Equation 2, plotted for  $E/2$  0.30 ev and  $C = 71$  in the temperature range  $0^\circ\text{C.}$  to  $73^\circ\text{C.}$

factors. The last two causes likely account for the fact that the constant in Equation 3, as derived from Jaccard's measurements, is only  $0.3 \times 10^{-4}$ . Jaccard's samples were monocrystalline and probably much more uniform in composition.

*Potassium fluoride.* All potassium-fluoride ice samples were prepared from a  $2.5 \times 10^{-4}$  M solution. In TABLE 1, the measurements are given in two groups. In one group, during sample growth, the ice-water interface resistance, which is of the order of 30 megohms per square centimeter (Gross, 1965), was shunted by an external resistor of 10,000 ohms. This arrangement has the effect of expediting the charge neutralization at the growing ice surface (Workman & Reynolds, 1950; Gross, 1963). Potassium ions are rejected into the water and replaced in the ice by hydrogen ions. The ratio of HF : KF in the ice is about 1 : 1. Where no shunt had been used, this ratio for samples grown under otherwise comparable conditions is only about 0.1 : 1.0. Both groups of samples not only show the same activation energy within experimental error, but furthermore, their conductivity-temperature and conductivity-concentration relationships are identical to those for ice grown from dilute hydrofluoric-acid solutions.



The potassium ion, therefore, does not appear appreciably to influence the conduction process. It is possibly not incorporated into the ice structure at all but rather accommodated interstitially. Furthermore, in spite of its considerably smaller radius (1.33 Å), its behavior is similar to that of cesium (1.65 to 1.69 Å). The latter ion was investigated by Steinemann (1957). His results are nearly identical to those for KF here presented (TABLE 1).

If, prior to freezing a  $2.5 \times 10^{-4}$  M solution of potassium fluoride is brought up to a pH of about 7 by means of potassium hydroxide, the activation energy of conduction remains the same or perhaps increases slightly, but the conductivity is reduced by a factor of between 10 and 20, as compared to samples of similar hydrogen-ion content prepared from hydrofluoric acid alone. The additional base shifts the hydrogen-ion concentration equilibrium in the freezing solution. As a result, fewer hydrogen ions are available for neutralization of fluoride ions incorporated into the ice (Cobb, 1964). The rate of fluoride-ion incorporation is, therefore, diminished. But in addition, this preliminary result suggests that the base introduces into the ice a defect structure which affects the conductivity. A further investigation of this question in a controlled, carbon-dioxide-free atmosphere is currently being initiated in our laboratory.

*Ammonium fluoride.* Several investigators have reported that the resistivity of ice doped with ammonium fluoride rises by orders of magnitude as the concentration is increased from  $10^{-5}$  to  $10^{-2}$  M (Workman, 1951; Brill, 1957; Iribarne *et al.*, 1961). The present investigations not only have confirmed this remarkable phenomenon but have shown in addition that the activation energy also increases with concentration in this range, provided the samples have been grown at average rates of one millimeter per minute or more. At concentrations below  $10^{-3}$  M, the activation energy

TABLE 2  
ACTIVATION ENERGIES OF ICE SAMPLES DOPED WITH AMMONIUM FLUORIDE.  
AVERAGE OF TWO SAMPLES AT EACH CONCENTRATION

Concentration in the melt (Moles per liter)	E/2	
	ev	Kcal./mole
$7 \times 10^{-3}$	$0.39 \pm 0.01$	$9.1 \pm 0.2$
$9 \times 10^{-4}$	$0.35 \pm 0.01$	$8.0 \pm 0.2$
$9 \times 10^{-5}$	$0.32 \pm 0.01$	$7.4 \pm 0.2$
$8 \times 10^{-6}$	$0.28 \pm 0.01$	$6.4 \pm 0.2$

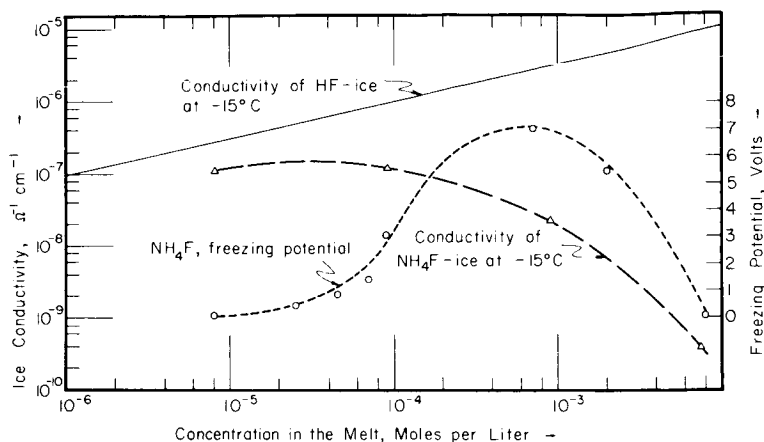


FIGURE 4. Conductivity at  $-15^\circ\text{C}$ . and highest value of the freezing potential, as a function of concentration, for ice grown from dilute ammonium-fluoride solutions. For comparison, the curve of conductivity, also at  $-15^\circ\text{C}$ . vs. concentration of hydrofluoric-acid ice is shown.

approaches the value observed for samples prepared with hydrofluoric acid (TABLE 2).

FIGURE 4 shows measurements, made in our laboratory, of the conductivity and the freezing potential as a function of concentration. These curves suggest a qualitative explanation for the observed phenomena in terms of the different incorporation rates of the two ions,  $\text{NH}_4^+$  and  $\text{F}^-$ . The concentration in the ice of a given ionic species is determined by an "equilibrium constant" which, at least before a steady state has been reached, is a function of freezing rate (Jaccard & Levi, 1961; Gross, 1965). It is different for each ionic species (and combination of species) and, in many instances, is higher for the anion than for the cation. This leads to an ionic separation at the interface and a freezing potential the sign of which is determined by the ion preferentially incorporated into the ice. The freezing potential, too, is a function of freezing rate.

In the case of ammonium fluoride, the fluoride ion is the more readily accepted one. The freezing potential is such that the liquid is positive with respect to the solid. At concentrations of less than about  $5 \times 10^{-5} \text{ M}$   $\text{NH}_4\text{F}$  in the freezing solution, the ionic separation at the interface takes place without an appreciable potential difference because the ion density is too small. The ratio of  $\text{HF}:\text{NH}_4\text{F}$  in the ice is relatively high. The conductivity is high and dominated by the impurity molecule  $\text{HF}$ . Our investigation of ice doped with hydrofluoric acid has shown that a concentration of not more than  $10^{-8}$  to  $10^{-7} \text{ M}$  in the melt is required to reduce the activation energy. A small peak of the hydrogen-ion concentration in the melt (ampli-

tude of about  $5 \times 10^{-6}$  M) appears indeed to exist in the region of highest ice conductivity. However, because of the extremely low value of these concentrations, this result must still be checked by more refined and accurate measurements.

As the ammonium fluoride concentration is increased in the freezing solution, the highest value of the freezing potential (which is reached shortly after the beginning of a freezing run) also rises. Possible cause for the rise is the increased number of unsatisfied charges in the nascent layers adjacent to the interface or the time lag between incorporation and neutralization. As the concentration is increased, the ratio of HF to  $\text{NH}_4\text{F}$  in the ice becomes smaller and the conductivity decreases.

At  $\text{NH}_4\text{F}$  -concentrations in the mother solution of more than  $10^{-4}$  M, the highest value reached by the freezing potential drops, after going through a maximum. This is possibly the result of an increasingly disordered ice structure (Lodge *et al.*, 1956). The conductivity decreases further, as does the ratio HF :  $\text{NH}_4\text{F}$ . The activation energy increases.

At the low concentration end (less than  $10^{-5}$  M), the conductivity vs. concentration curve for ammonium fluoride appears to approach the curve for ice doped with hydrofluoric acid alone.

The curves suggest that the  $\text{NH}_4^+$ -ion introduces into the ice a defect structure which results in a reduction of the mobility and/or the concentration of the current carriers as compared to pure HF-ice. With reference to ice prepared from "pure" water, however, the defect structure introduced by  $\text{NH}_4\text{F}$  would increase the conductivity, at least in an intermediate concentration range (Brill *et al.*, 1957).

An interesting comparison may be made with KF-doped ice. In this case also, the highest freezing potential value goes through a maximum as the concentration in the freezing solution is increased (Cobb, 1964). However, with respect to ammonium fluoride, this maximum is displaced by about two orders of magnitude; it is located at about  $2 \times 10^{-5}$  M. Thus, it would appear that the ammonium ion can reach much higher concentrations in the ice than the potassium ion before seriously affecting the ice structure.

### Conclusions

Samples of ice doped with hydrofluoric or hydrochloric acid show substantially the same conductivities and activation energies. At concentrations of hydrofluoric acid as low as  $10^{-7}$  to  $10^{-8}$  moles per liter, the conductivity characteristics are those of the acid. At constant temperature, the conductivity is proportional to the square root of the acid concentration in the melt. The proportionality factor has been plotted for the temperature range  $0^\circ\text{C.}$  to  $-73^\circ\text{C.}$  and an activation energy of 0.30 ev.

Samples doped with cesium fluoride and potassium fluoride show the same temperature and concentration dependence of the conductivity as those doped with hydrofluoric acid alone. This is due to the ionic separation taking place at the interface by which a fraction of the cations is rejected into the water and replaced by hydrogen ions. The number of hydrogen ions available for incorporation, and hence the ice conductivity, depends on the difference in incorporation rate of the cations and anions present in the water, the hydrogen-ion concentration of the freezing solution, the freezing rate, and the ice-water interface resistance, which in the case of the fluorides may be greatly reduced by a low-resistance external shunt. The freezing potential also depends on all of these factors plus the gases dissolved in the solution.

In ice frozen from dilute ammonium-fluoride solutions ( $10^{-5}$  to  $10^{-2}$  M), the conductivity and activation energy appear to be largely a function of the ratio  $\text{HF} : \text{NH}_4\text{F}$ . The effect of the impurity  $\text{NH}_4\text{F}$  alone is difficult to investigate because, except at the highest freezing rates, a relatively high degree of ionic separation and the resultant incorporation of an appreciable fraction of HF modify the results. The possibility that hydrolysis of the freezing solution influences the conductivity of the ice should be considered in future investigations.

#### *Acknowledgement*

Professor Roland List made valuable suggestions during the course of these investigations.

#### *References*

- BRILL, R. 1957. Structure of Ice. SIPRE Report. **33**: 37-38.
- BRILL, R., H. ENDER & A. FEUERSANGER. 1957. Dielektrisches Verhalten von Eis-Ammoniumfluorid-Mischkristallen. *Z. Elektrochemie* **61**: 1071-1075.
- COBB, A. W. 1964. Interfacial electrical effects observed during the freezing of water. Unpublished report. New Mexico Institute of Mining and Technology, Socorro, N. M.
- GROSS, G. W. 1962. Four-electrode method for measuring the direct-current resistivity of ice. *Science* **138**: 520-521.
- GROSS, G. W. 1963. The direct-current conductivity of ice doped with ionic impurities. Paper presented at the 13th Gen. Assembly I.U.G.G., Abstracts of Papers 5: 197. Berkeley, Calif.
- GROSS, G. W. 1965. The Workman-Reynolds effect and ionic transfer processes at the ice-solution interface. *Jour. Geophys. Res.* **70** (in press).
- HEINMETS, F. & R. BLUM. 1962. Conductivity measurements on pure ice. *Trans. Faraday Soc.* **59**: 1141-1146.
- IRIBARNE, J. V., L. LEVI, R. G. DE PENNA & R. NORSCINI. 1961. Conductivité électrique de la glace dotée de divers électrolytes. *J. Chim. Phys.* **58**: 211.
- JACCARD, C. 1959. Etude théorique et expérimentale des propriétés électriques de la glace. *Helv. Phys. Acta* **32**: 89-128.
- JACCARD, C. & L. LEVI. 1961. Ségrégation d'impuretés dans la glace. *Z. Angewandte Mathematik Physik* **12**: 70-76.

- LODGE, J. P., M. L. BAKER & J. M. PIERRARD. 1956. Observations on ion separation in dilute solutions by freezing. *J. Chem. Phys.* **24**: 716-719.
- STEINEMANN, A. 1957. Dielektrische Eigenschaften von Eiskristallen. II. Teil: Dielektrische Untersuchungen an Eiskristallen mit eingelagerten Fremdatomen. *Helv. Phys. Acta* **30**: 581-610.
- WORKMAN, E. J. & S. E. REYNOLDS. 1950. Electrical phenomena occurring during the freezing of dilute aqueous solutions and their possible relationship to thunderstorm electricity. *Phys. Rev.* **78**: 254-259.
- WORKMAN, E. J. 1951. Some electrical properties of the ice of dilute aqueous solutions. Final Report on Thunderstorm Electricity, Appendix H. Signal Corps, U.S. Dept. of the Army.

# MECHANISM OF THE ELECTRICAL CONDUCTIVITY IN ICE

C. Jaccard

*Swiss Federal Institute for Snow and Avalanche Research,  
Weissfluhjoch-Davos, Switzerland*

## *The Electrical Behavior*

As ice belongs to the most common substances, it has aroused the interest of the scientists for a long time, but questions pertaining to certain of its properties could be elucidated only in recent years, thanks to modern techniques (e.g. neutron diffraction) and knowledge (e.g. defect phenomena in crystalline solids). Investigations of its electrical properties have been performed since the beginning of this century in various countries and yield the following picture.

Pure ice is altogether a bad conductor and insulator. Its DC electrical conductivity<sup>1-5</sup> has a value of  $10^{-7}$  ohms<sup>-1</sup>m<sup>-1</sup> at 10°C. (It should be mentioned that all values given in this paper are for -10°C. unless otherwise specified). The response to temperature changes occurs according to an Arrhenius law with an activation energy which was found at first to be 0.54-0.61 eV, but recently a smaller value was found to be  $0.48 \pm 0.07$  eV.<sup>5</sup> It has been shown by electrolysis experiments that the nature of this conductivity is purely ionic, without any noticeable contribution from the electrons, the charge transport occurring by the proton displacement.<sup>6</sup>

The AC behavior is characterized by a Debye relaxation,<sup>7,8</sup> where the dielectric constant has the form

$$\epsilon - \epsilon_{\infty} = \frac{\epsilon_s - \epsilon_{\infty}}{1 + i\omega\tau} \quad (1)$$

where

$\epsilon_{\infty}$  = diel. const. at high frequency (with respect to the relax. time) = 3.2

$\epsilon_s$  = static diel. constant = 112 parallel and 96 perpendicular to the c-axis

$\omega$  = frequency and

$\tau$  = relaxation time =  $5 \times 10^{-5}$  s. (activation energy: 0.575 eV).

Like in every solid, the high frequency diel. constant which is temperature independent and relaxes to smaller value only at frequencies in the gigacycle range, is caused by the displacement of the electronic clouds and the atom nuclei from their equilibrium position. As we consider here only the peculiar behavior of ice up to the megacycle range, we shall in the following admit implicitly the presence of  $\epsilon_{\infty}$  as an additive constant.

Chemical impurities may have a great influence on the electrical properties. For example hydrofluoric acid HF<sup>9</sup> increases the DC conductivity up to  $5 \times 10^{-4}$  ohm<sup>-1</sup>m<sup>-1</sup> at the solubility limit ( $10^{25}$  m<sup>-3</sup> =  $10^{-2}$  mol./liter), the activation energy being reduced to 0.32 eV<sup>4</sup>. The relaxation time is de-

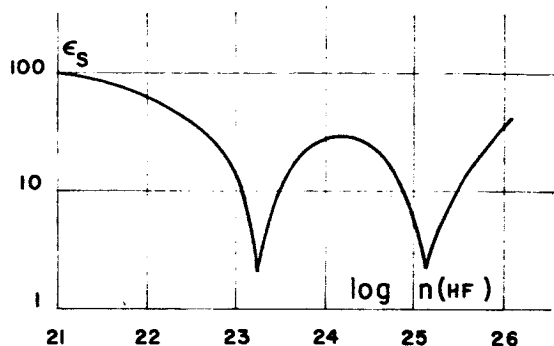


FIGURE 1. Dependence at  $-3^{\circ}\text{C}$ . of the static dielectric constant of ice from the concentration  $n(\text{HF})$  of hydrofluoric acid expressed in  $\text{m}^{-3}$  (Log-log plot, after Steinemann<sup>9</sup>).

creased, but the most interesting effect occurs in the static diel. constant (FIGURE 1). As the HF concentration increases, it goes through two minima, which are very near to  $\epsilon_{\infty}$  in homogenous crystals: for these critical concentrations, the mechanism responsible for the high static diel. constant breaks down.

Although it was obvious that the protons are responsible for the electrical properties, this peculiar behavior could be elucidated only with the help of hypothetic defects produced by thermal fluctuations of the lattice and interacting in a complementary way.

#### *Electrically Active Structural Defects*

The structure of the oxygen lattice has been determined with X-ray diffraction quite early.<sup>10</sup> The oxygen atoms are 2.76 Å apart ( $=r_{\text{OO}}$ ), and disposed in layers of skew hexagons, which are stapled along the  $c$ -axis, giving a  $D_{6h}^4$  space group (FIGURE 2). The position of the protons gave rise to many theoretical considerations, especially with respect to the zero point entropy,<sup>11</sup> until neutron diffraction experiments settled the question.<sup>12,13</sup> The proton configuration is at random, but within the limits of the following rules proposed by Bernal and Fowler (BF-rules):<sup>14</sup> (1) The water molecules preserve their identity in the lattice, and near each oxygen atom are two protons at a distance  $r_{\text{OH}} = 1.0$  Å. (2) The protons lie on the straight lines connecting neighboring oxygen atoms, and there is one and only one proton on each line.

There is also no macroscopic permanent electrical moment, at least at high temperature, because the dipole field of each molecule is canceled by the others.

If one assumes that these BF-rules are strictly valid, one has no explanation for the Debye relaxation with a high static diel. constant and for the

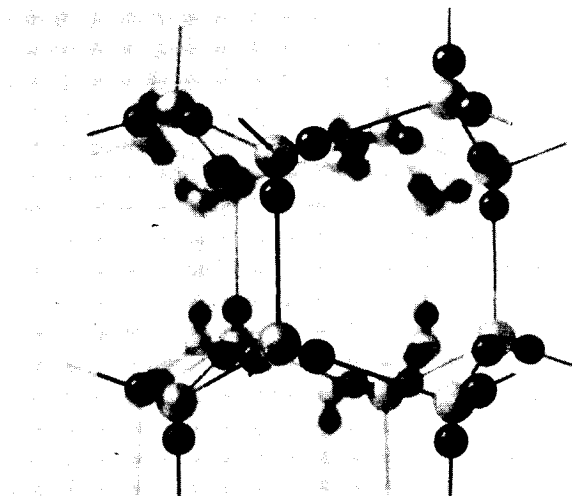


FIGURE 2. Ice lattice, seen perpendicularly to the  $c$ -axis. The light balls represent the oxygen atoms and the dark ones the protons. The layers of skew hexagons are horizontal.

DC conductivity. Therefore, one has to admit that they are locally violated as a result of fluctuations in the thermal equilibrium of the lattice. The first sort of defect is suggested by the water chemistry: *positive* and *negative ions* ( $\text{H}_3\text{O}^+$  and  $\text{OH}^-$  produced in pairs by the shifting of the protons along the O—O bonds. These defects can move in the lattice if a sufficient thermal activation is provided, by the further shifting of the proton along the bonds (FIGURE 3). This would explain the AC but not the DC conductivity because each individual proton is limited to the bond where it sits; and thus, no net charge transfer can be performed through a macroscopical piece of the crystal. A second sort of defect postulated by Bjerrum<sup>15</sup> constitutes a violation of the second BF-rule: certain bonds are occupied by two protons, giving a *doubly occupied bond* or *D defect*, or by no proton at all, leaving an *empty bond* or *L defect* (from the German *leere Bindung*). These defects are produced by the jumping of the protons around the oxygen atoms on an adjacent regular bond, and they can be displaced in the lattice by the continuation of these jumps (FIGURE 4). Now it is possible to explain the DC conductivity by the movement of the protons along the bonds as well as around the oxygen atoms so that they can be transferred from one side of the crystal to the other. As all four defects are characterized by excess or lack of a proton, they respond to an electrical field and charges having a dynamical meaning (because defects only can be noticed when they move) can be attributed to them.



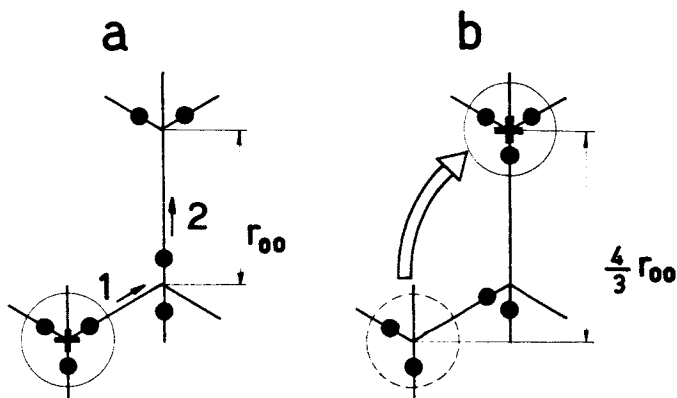


FIGURE 3a. Motion of a positive ion ( $\text{H}_3\text{O}^+$ ) occurring by the shift of the protons according to the arrows 1 and 2. b. The result is a shift of the ionic state on a distance  $\frac{4}{3}r_{00}$  along the c-axis. (The dots represent protons, the oxygen atoms not being shown.)

If a defect state jumps from one lattice point to another along a vector  $\mathbf{r}_s$ , it is accomplished first by the jump of a proton either towards or from the original site, and simultaneously by a displacement of the neighboring nuclei and electronic clouds which go to another equilibrium position. Denoting by  $\rho$ , the charge density (including the protons and nuclei) and by  $\mathbf{r}$ , the distance each charge element is displaced, the defect charge is then

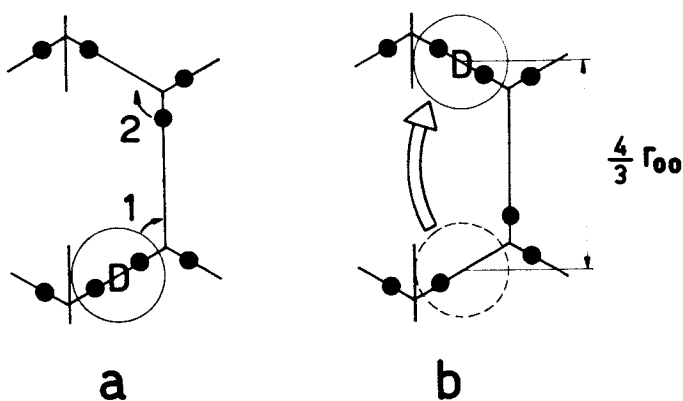


FIGURE 4a. Motion of a positive valence defect (D-defect) occurring by the shift of the protons according to the arrows 1 and 2. b. The result is a shift of the valence defect state on a distance  $\frac{4}{3}r_{00}$  along the c-axis. (The dots represent protons, the oxygen atoms not being drawn.)

defined by the following relation:

$$e_{\text{defect}} \cdot \mathbf{r}_s = \int \rho \cdot \mathbf{r} \cdot dV \quad (2)$$

where the integration occurs on the volume. Thus, it is the mean charge transferred along the distance  $\mathbf{r}_s$ . According to the form of the expression above, it is in the most general case a tensor because it connects two vectors which do not need to be parallel. This dynamical charge accompanies effectively the defect in its travel through the lattice, and at least in principle, it can be measured from outside the crystal. Because of the symmetry, the charges of the ionic defects have the same absolute magnitude but opposite signs ( $e_+ = -e_- = e_{\pm}$ ). The same is valid for the Bjerrum defects ( $e_D = -e_L = e_{DL}$ ), but  $e_{\pm}$  and  $e_{DL}$  are related because a proton, if transported through the lattice in a DC process, must be transferred by *both* sorts of defects in order to shift along the bonds *and* around the oxygen atoms. Consequently, the protonic charge  $e$  is the sum of the defects charges:

$$e = e_{\pm} + e_{DL} \quad (3)$$

#### *Mechanism of the Conductivity*

The quantitative description of the defect activity has been done from different points of view<sup>4,16</sup> practically with the same result. Because of the nonvanishing DC conductivity, we know that both defect sorts are present; one of them may be the major carrier, that is the one for which the product "concentration times mobility" is the largest, and the other one the minor carrier. We know, on the other hand, that their concentration is very low so that the defects are far apart. If a high frequency electrical field is applied, each defect moves to and fro, remaining practically at its place, so that it does not interfere with other ones. The high frequency conductivity is therefore determined by the major carriers because they all act as conductances in parallel, and the contribution to the dielectric constant is zero because the velocities are in phase with the field.

If a static field is applied, the net proton transport, having to be accomplished by both defect sorts, will be governed by the less effective agent, that is by the minor carriers. Both defect sorts act as conductances in series. At the moment when the field is applied, the major carriers rush forward, but while doing so, they modify the proton configuration in such a way that it becomes less and less favorable for their movement: every chain along which a defect has moved is blocked for a defect of the same sort (FIGURE 5). If there were no defects of the other sort, the movement would stop after a certain time (the relaxation time), and would reverse when the field is switched off. This hindered displacement then produces a space polarization, and contributes to the dielectric constant.

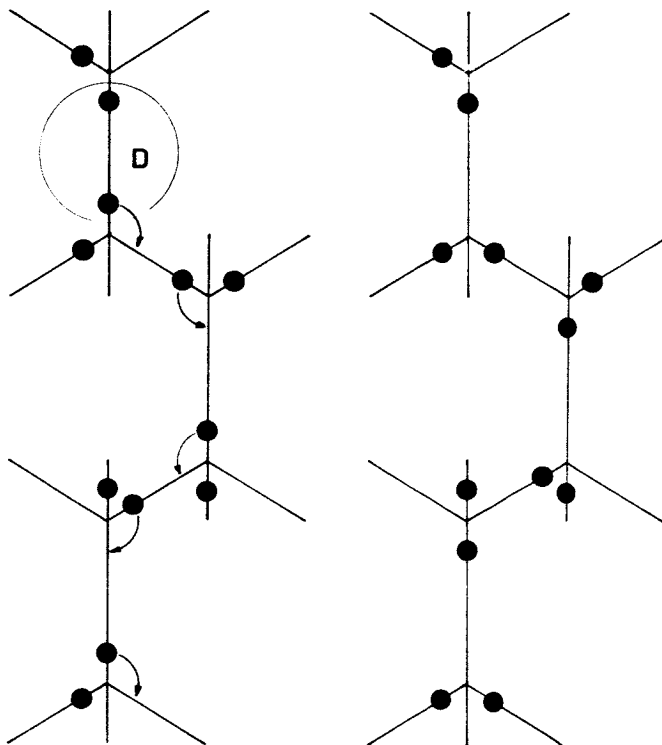


FIGURE 5. Blocking of a chain parallel to the  $c$ -axis by a D-defect (only the protons are shown). While the protons shift according to the arrows, the D-defect moves downward. The chain is then in the state depicted by the FIGURE to the right, offering no possibility of downward motion for another D-defect.

If defects of the other sort are present, they move also and reactivate the chains (FIGURE 6) so that finally the major and the minor currents have the same magnitude. If the concentrations are matched so that no major character can be defined, then no carrier movement is hindered, and the polarization vanishes. In the case of pure ice, the static dielectric constant is large, and this implies that one sort of defect is in a definite majority, but which one? This can be found from the experiments with HF doped crystals." The inclusion of hydrofluoric acid produces positive ions in the lattice, as it does in water; and as the dissociation constant is low, the ion concentration grows with the square root of the acid concentration. But on the other hand, for each HF molecule built in the lattice instead of a  $H_2O$  molecule, a proton is missing. This gives birth to L defects, in a number equal to the acid molecules (at least as long as they are in the oxygen

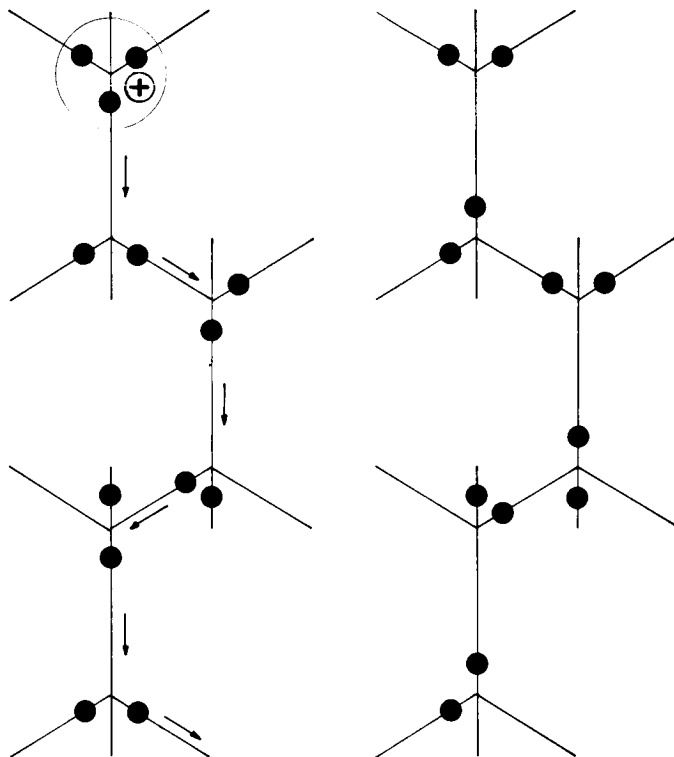


FIGURE 6. Reactivation of a blocked chain by a positive ion (only the protons are shown). The shifting protons move the ion downward, and this brings the chain back in its original state, as it was in the picture to the left of FIGURE 5.

sites). If one examines the static dielectric constant as a function of the acid concentration (FIGURE 1), one knows that the L defects prevail at high concentrations, that is to the right of the second minimum (because the first power grows more than the square root). Just at this minimum, the vanishing  $\epsilon_s$  indicates that the major character changes side, and thus the ions prevail between the two minima. The opposite occurs at the first minimum, and therefore, one has the following situation: In pure ice, both Bjerrum defects, which are in equal number, are the major carriers and responsible for the high frequency conductivity  $\sigma_\infty$ , the relaxation time  $\tau$  and the static dielectric constant  $\epsilon_s$ . The ions, also in equal number, are the minor carriers, and responsible for the DC conductivity  $\sigma_0$ .

In the domain where  $\sigma_\infty$  is proportional to the acid concentration, the DL mobility and the concentration can be determined, which amount to  $2 \times 10^{-8} \text{ m}^2/\text{V}_s$  and  $7 \times 10^{21} \text{ m}^{-3}$  respectively (the concentration of the water molecules is  $3.1 \times 10^{28} \text{ m}^{-3}$ ). The ionic concentration has been deter-

mined by other methods,<sup>5</sup> and amounts to  $8.4 \times 10^{16} \text{m}^{-3}$ , whereas the mobility of the positive ions has a value of about  $8 \times 10^{-6} \text{m}^2/\text{Vs}$ .

### Thermodynamics

The quantitative phenomenological treatment of the mechanism described in *Mechanism of the Conductivity* has been done recently from the point of view of the thermodynamics of irreversible processes.<sup>17</sup> The results are the same as those from the previous theories,<sup>4,16</sup> (except small discrepancies in numerical factors) but allows the direct generalization to the more complicated effects where the electric field interacts also with pressure or temperature gradients. The determining quantity is the contribution to the entropy production from the changes in the proton configuration. In the first approximation it has the form

$$\dot{s}_k = -\frac{8}{\sqrt{3}} k r_{00} \cdot \frac{\partial}{\partial \epsilon} (\Omega^2) \quad (4)$$

where  $\Omega$  is a "configuration vector" related, as we shall see, with the polarization and defined by

$$\Omega = \int_0^t (\mathbf{j}_+ - \mathbf{j}_- - \mathbf{j}_D + \mathbf{j}_2) dt \quad (5)$$

The  $\mathbf{j}$  are the defect currents,  $k$  is the Boltzman constant and  $r_{00}$  is the distance between two neighboring oxygen atoms. The total entropy production is then put in the form of a sum of products between generalized forces  $\mathbf{J}_i$  and the conjugated currents  $\mathbf{X}_i$ :<sup>18</sup>

$$\dot{T}s = \sum_i \mathbf{J}_i \mathbf{X}_i \quad (6)$$

The currents chosen in this case are: the four defect currents conjugated to the forces  $-\text{grad}_{\text{PT}} g_i$  ( $g$  = free enthalpy), the electrical current conjugated to the electric field, the time derivative of the configuration vector  $\dot{\Omega}$  conjugated to  $-16/\sqrt{3} k T r_{00} \Omega$  and reduced mass and heat currents conjugated to the pressure and temperature gradients, respectively. Solving the linear equations relating the currents with the forces yields for the high frequency and for the DC conductivities

$$\begin{aligned} \sigma_{\infty} &= \sigma_{\pm} + \sigma_{DL} \\ \frac{e^2}{\sigma} &\approx \frac{e_{\pm}^2}{\sigma_{\pm}} + \frac{e_{DL}^2}{\sigma_{DL}} \end{aligned} \quad (7)$$

where  $\sigma_{\pm}$  and  $\sigma_{DL}$  are the partial conductivities of the ions and Bjerrum defect respectively. This is in accordance with the considerations of the section on Mechanism of the Conductivity.

The calculation of the dielectric constant lets a quantity  $e_p$  appear with the dimension of a charge which is characteristic for the interaction be-

tween the defects. It is called a "polarization charge" and has the value

$$e_p \approx \frac{\sigma_{\pm}/e_{\pm} - \sigma_{PL}/e_{DL}}{\sigma_{\pm}/e_{\pm}^2 - \sigma_{PL}/e_{DL}^2} \quad (8)$$

It relates the lattice polarization  $\mathbf{P}$  to the configuration vector  $\Omega$ :

$$\mathbf{P} = e_p \Omega \quad (9)$$

In pure ice, where the Bjerrum defects are the major defects ( $\sigma_{DL} \gg \sigma_{\pm}$ ) the "polarization charge" is the same as the charge of the L defects:

$$e_p (\text{pure ice}) = -e_{DL} \quad (10)$$

This charge can be virtually attached to each defect to describe its interaction with the lattice polarization; it acts as a source of the polarization, and the polarization exerts a force on it. The total force acting on a defect is

$$\eta_k = e_k \mathbf{F} - \eta_k e_p \mathbf{P} / \epsilon_0 \epsilon_s \quad (11)$$

$\mathbf{F}$  being the electric field,  $\epsilon_0$  the diel. constant of vacuum, and the factors  $\eta_k$  being  $\pm 1$ . As it was pointed out by Onsager,<sup>19</sup> this charge is a "quantum of polarization," corresponding to the smallest amount of polarization produced as a change in the proton configuration by a single defect. It is related to the static dielectric constant by

$$\epsilon_0 \epsilon_s = e_p^2 \cdot \sqrt{3}/16kT_{00} \quad (12)$$

Thus, the matching of the partial conductivities causes  $e_p$  to disappear according to Equation 8 and also causes the dielectric constant to vanish, which occurs, in fact, with a particular chemical constitution of the ice (FIGURE 1).

On the other hand, the experimental data indicate that the dielectric constant has an anisotropy of about 16 per cent.<sup>7</sup> This implies that the polarization charge and the dynamic charges of both sorts of defects have an anisotropy of about eight per cent. According to Equation 2, this indicates that the molecular movements accompanying a proton jump have no axial symmetry.

The linear equations mentioned above relating the currents with the forces can also be solved if defect concentration, pressure or temperature gradients are present in the crystal. They may induce a static electric field, giving the electrochemical, mechanoelectrical and thermoelectrical effects, respectively. These effects, combined with an adequate HF doping, then yield information on the size, enthalpy and transference numbers of the defects (i.e. the relative amount of charge transported by each one in a DC process). Experimental investigations are now being pursued in this direction.

#### *Proton Transfer*

During the jump of a Bjerrum defect state on a neighboring bond, the proton transfer occurs classically by thermal activation over a potential

step. This is suggested at first by the value of the DL mobility, which has the order of magnitude occurring generally for ionic transport. Moreover, it has been shown experimentally<sup>4</sup> that this mobility has an activation energy of 0.23 eV, giving the height of the step.

The situation is different for the ions. Their mobility has a relatively high value, about 400 times higher than for the Bjerrum defects, and cannot be accounted for by a classical mechanism. According to the picture prevailing now, the protons go through the potential step by a quantum-mechanical tunnel effect. The step height has, at most, the value of the thermal energy  $kT$ , i.e. about 0.02 eV, and the step width is not too large, in the average of 0.76 Å, but certainly less during a part of the time because of the low frequency stretching vibrations of the O-O bonds. This allows a penetration of the protonic wave without too much attenuation through the potential step and, therefore, a shift of the proton without an activation energy. The transfer frequency through the step is about  $2 \times 10^{12} \text{s}^{-1}$  (whereas it is only  $2 \times 10^8 \text{s}^{-1}$  over the step in a Bjerrum defect) and this together with the defect concentration determines the value of the DC conductivity in pure ice.

Although it has not been proven experimentally until now, a difference must be present in the mobility of the positive and negative ions. During the jump of the former, the proton is between two neutral water molecules, whereas in the jump of the latter, it is between two negative  $\text{OH}^-$  ions. This introduces for the negative ions an electrostatic contribution to the potential which reduces the mobility. Therefore, it has been assumed that in pure ice, where the concentrations are equal, only the positive ions are effective for the DC conductivity.

### *Conclusion*

The electrical properties of ice can be explained by the presence of four mobile structural defects of the lattice which are the ions  $\text{H}_3\text{O}^+$  and  $\text{OH}^-$ , and the Bjerrum or valence defects. The opposite action of both sorts on the proton configuration determines the DC conductivity, and the predominance of one of them is necessary for the occurrence of the high dielectric constant and its Debye relaxation. The microscopical charge transfers, accompanying the movement of the defects, allow the definition of dynamical defect charges, which in turn relate the electrical parameters with the defect concentrations and determines their tensorial character. The defects respond also to concentration, pressure and temperature gradients, which induce in the crystal differences of the electrical potential. The defect transport occurs by proton jumps on neighboring lattice sites, either with a thermal activation over a potential step or by a tunnel effect through the step.

This description does not preclude the existence of other defects, which can also have a bearing on certain electrical properties. They might occur, for example, when the ice is doped with other substances, but this more complicated situation is not yet clear.

#### *Acknowledgement*

The author is indebted to Mr. W. C. Mayes for the critical reading of the manuscript, to Dr. M. de Quervain, director of the Institute, for his constant interest in the problems of the ice physics, and to The New York Academy of Sciences for a travel grant to take part in the Conference.

#### *References*

1. JOHNSTONE, J. H. L. 1912. Proc. Trans. Nova Scotian Inst. Sci. **13**: 126.
2. GRÄNICHNER, H., C. JACCARD, P. SCHERRER & A. STEINEMANN. 1957. Faraday Soc. Disc. **23**: 50.
3. BRADLEY, R. S. 1957. Trans. Faraday Soc. **53**: 687.
4. JACCARD, C. 1958. Helv. Phys. Acta **32**: 89.
5. EIGEN, M., L. DE MAEYER & H.-CH. SPATZ. 1964. Ber. Bunsenges. **68**: 19.
6. DECROLY, J. C., H. GRÄNICHNER & C. JACCARD. 1957. Helv. Phys. Acta **30**: 465.
7. HUMBEL, F., F. JONA & P. SCHERRER. 1953. Helv. Phys. Acta **26**: 17.
8. AUTY, R. P. & R. H. COLE. 1952. J. Chem. Phys. **20**: 1309.
9. STEINEMANN, A. 1957. Helv. Phys. Acta **30**: 553.
10. BARNES, W. H. 1929. Proc. Roy. Soc. A. **125**: 670.
11. PAULING, L. 1935. J. Am. Chem. Soc. **57**: 2680.
12. WOLLAN, E. O., W. L. DAVIDSON & C. G. SHULL. 1949. Phys. Rev. **75**: 1348.
13. PETERSON, S. W. & H. A. LEVY. 1957. Acta Cryst. **10**: 70.
14. BERNAL, J. D. & R. H. FOWLER. 1933. J. Chem. Phys. **1**: 515.
15. BJERRUM, N. 1951. K. Danske Vidensk. Selsk. Mat. Fys. Medd. **27**: 56.
16. ONSAGER, L. & M. DUPUIS. 1960. Rendiconti S.I.F. X. Corso: 294; 1962. *In* Electrolytes: 27. Pergamon Press, Oxford, England.
17. JACCARD, C. 1964. Phys. Kond. Materie. To be published.
18. DE GROOT, S. R. 1960. Thermodynamics of Irreversible Processes. North Holland Publishing Company, Amsterdam, Netherlands.
19. ONSAGER, L. 1962. Colloquium on the Physics of Ice Crystals. Erlenbach-Zürich, Zürich, Switzerland.



# THE PHYSICAL STATE OF WATER IN LIVING CELL AND MODEL SYSTEMS\*

Gilbert Ning Ling

*Department of Molecular Biology in the Department of Neurology,  
Division of Medicine, Pennsylvania Hospital, Philadelphia, Pa.*

Living cells, as a rule, contain 15 to 25 per cent proteins and 75 to 85 per cent water. We now know that it is the sequences of amino acid residues in the proteins that underlie biological specificity and that the difference in the nature of one amino acid residue (in a protein containing hundreds) may produce profound differences in the behavior of the entire tissue of which this protein is a part.<sup>1</sup> Yet, important as the proteins are in the living phenomena, there can be no life unless there is also water. Thus, whether in the form of contractile proteins or functioning enzyme, living protoplasm always contains water; the unique behavior it manifests, reflects not the behavior of the proteins per se but that of the protein water systems. The question arises: In what way does water serve this critical role? Does it function merely as a solvent of a suitable dielectric property?

In recent years, considerable evidence has been collected, showing that this is not so. Water molecules in the close vicinity of proteins and other biologically important macromolecules appear to exist in a physical state different from that of normal water. Forslind,<sup>2</sup> for example, suggested that in protein solutions, water molecules close to macromolecules may exist in a state between that of liquid and solid. Jacobsen<sup>3</sup> supported this basic concept with x-ray, dielectric, and nuclear magnetic resonance studies on macromolecular solutions. Szent-Györgyi<sup>4</sup> postulated an ice-like structure of water surrounding proteins; Klotz *et al.*<sup>5</sup> supported and further developed this "iceberg" concept. From x-ray diffraction studies, Beeman *et al.*<sup>6</sup> concluded that serum albumin is surrounded by a layer of water which does not dissolve sucrose as normal water does. Similarly, Hearst and Vinograd<sup>7</sup> by density measurements reached the conclusion that water closely associated with DNA excludes alkali metal ion (see also, Ritland *et al.*)\* The nuclear magnetic resonance studies of Berendsen<sup>8</sup> have shown that in native collagen and partially dried collagen, water molecules are restricted in their rotation and that they form chains in the collagen fiber direction, being oriented by the peptide amide bonds.

\*These studies were aided by Contract Nonr 1-2060-66, (NR 105-327) between the Office of Naval Research, Department of the Navy, and the Pennsylvania Hospital. The investigator was also supported by a Public Health Service Research Development Award (GM K3-19,032) from the National Institute of Health.

The views on the physical state of water in living cells, however, are widely divergent.

According to the classical membrane theory, the intracellular water is permanently and entirely (or almost entirely) in the form of normal water such as is found in a 0.1 M KCl solution. The well-known asymmetry in the distribution of ions and nonelectrolytes between the intracellular and extracellular water is attributed to the critical pore size on the cell membrane or to a continual pumping by "Na pumps" and "permeases" located in this thin structure.

Gortner<sup>10</sup> advocated the view that cell water is bound; his concept, however, was not accepted largely because of a lack of truly convincing evidence.<sup>11,12</sup>

According to Troschin's sorption theory<sup>13</sup> the cell water has different solubility properties for nonelectrolytes, amino acids and ions than normal water; it does not offer molecular interpretations as to the mechanism of this difference in solubility.

The association-induction hypothesis<sup>1,14,15</sup> which deals with a broader topic agrees in essence with Troschin's sorption theory concerning ionic and nonelectrolyte distribution problems, although the two theories were developed independently. The association-induction hypothesis offers, however, specific molecular interpretation of the differences in solubility properties of the cell water in terms of restricted rotation of polyatomic nonelectrolytes and de facto polyatomic hydrated ions<sup>1</sup> and of differences in the H-bond formed in the protoplasmic system.<sup>1</sup> The theory also stresses that the living protoplasm and hence protoplasmic water does not exist in one single physical state but as a rule, exists reversibly in more than one metastable cooperative states in the course of its normal physiological activity. Anticipating the evidence to be presented, we may state that it is our purpose in this paper to demonstrate that all or nearly all water molecules in a living cell can be considered to exist as polarized multilayers oriented on the surfaces of cell proteins. To demonstrate this, however, one cannot apply the direct approach which one uses on water sorption studies of stable inanimate systems because in living cells, the protein water systems are metastable; removal of water may bring about changes that are irreversible. Instead, we shall employ an indirect method which involves the three following steps: (1) establish multilayer adsorption of polarized water in one or more nonliving stable model systems; (2) choose properties exhibited by the water in living cells during its quiescent resting state; these properties must be significantly different from those of ordinary water and yet can be studied in the living cell without producing serious injury; (3) establish that this same property is also exhibited by the water in the nonliving model systems mentioned.<sup>1</sup>

In the following analyses, we have chosen equilibrium distribution of nonelectrolytes and of ions as the properties mentioned<sup>2</sup> and as models, we shall use strong electrolyte solutions,  $\text{Cu}_2\text{Fe}(\text{CN})_6$  gel, and in particular collagen from carp's swim bladder and sheep's wool. The experimental data on ionic distribution is complete and on this the argument rests; those of nonelectrolytes are still in progress. Nevertheless, the nonelectrolyte data are included in this presentation as it brings into focus additional and different facets of the problem.

### *Polarized Water in Proteins*

Association of proteins with water can be demonstrated by analyzing the sorption of water vapor on purified proteins. When the amount of water sorbed is plotted against the relative vapor pressure, the data shows an S-shaped curve typical of sorption of gases in multimolecular layers on solid surfaces. Theories of such gas sorption were presented by de Boer and Zwikker<sup>16</sup> and by Bradley<sup>17</sup>; both suggested electrical polarization (induction) as the cause of the build-up of the multilayers of adsorbed gas. Brunauer, Emmett and Teller<sup>18</sup> severely criticized de Boer and Zwikker's theory (and of Bradley's theory on inert gas adsorption) on the ground that the inductive action on gas molecules such as argon, nitrogen, etc., is quantitatively trivial; they offered instead, what later became known as the BET theory. The BET theory is, in essence, an extension of the Langmuir adsorption isotherm to multilayer adsorption where successive layers are held by London force and such forces operate in a normal liquid. The BET isotherm can be put into a form such a plot of  $p/a(p_0 - p)$  against  $p/p_0$  should yield a straight line; where  $a$  is the amount of gas adsorbed at pressure  $p$ , and  $p_0$  is the gas pressure at full saturation under the same condition. In their criticism of the polarization theories, Brunauer *et al.* were careful in pointing out that: "On the other hand, if the adsorbed gas has a large permanent dipole it is possible that many layers may be successively polarized by the mechanism of De Boer and Zwikker. This case has been treated by Bradley."<sup>19</sup> The Bradley polarization theory for gases with permanent dipole moments is quantitatively represented by the following equation:

$$\log_{10} \frac{p_0}{p} = K_1 + \frac{K_3}{K_2 + K_4} \quad (1)$$

where  $a$ ,  $p$ ,  $p_0$  have the same meanings mentioned above;  $K_1$ ,  $K_3$  and  $K_4$  are constants for a specified system under a specified condition. Since water has a large permanent dipole moment ( $1.834 \times 10^{-18}$  e.s.u.) water sorption on solid surfaces should follow Equation 1.

Bull<sup>20</sup> who studied the water sorption of more than 10 proteins, applied the BET theory to his data and found in many cases, satisfactory fit but

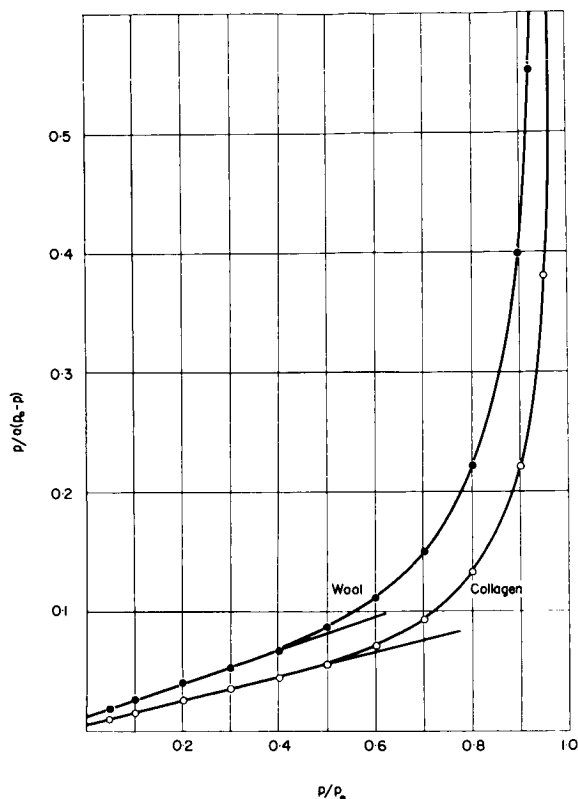


FIGURE 1. Water vapor sorption on collagen and on wool, plotted according to the BET isotherm. Data of Bull.<sup>20</sup>

only up to about 50 per cent vapor saturation. In FIGURE 1, Bull's data on water sorption of collagen (hide) and of wool are plotted according to the BET theory to cover the entire range of vapor pressure studied. The large discrepancy between the theory and experiments for vapor pressure higher than 50 per cent is conspicuous and typical of other data of Bull and others.<sup>21</sup> In 1955, Mellon and Hoover<sup>22</sup> noted a much greater accord between water-sorption on proteins and Bradley's isotherm and commented: "The simplest equation, the two constant equations of Bradley\* fits throughout the whole range of our data from 6 to 93 per cent relative humidity. The description was so accurate. . . ." Particularly relevant for the present discussion is the adherence to Equation 1 of water sorption on polyglycine which Mellon and Hoover demonstrated; in this case the only polar sites on the polymer are the NH and CO groups on the polypeptide chain. The

\*This is Equation 2 with  $K_4 = 0$ .

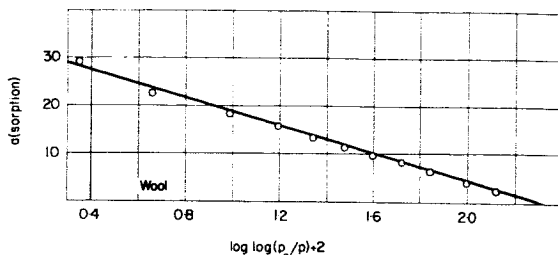


FIGURE 2. Water vapor sorption on sheep's wool, plotted according to the Bradley isotherm. Same data as in FIGURE 1.

agreement suggests that the polypeptide amide groups are inherently capable of orienting and polarizing successive layers of water molecules.

In FIGURE 2 and FIGURE 3, the same data of vapor sorption by collagen and wool that appeared in FIGURE 1 are plotted according to the Bradley equation (Equation 1).† There is good accord up to 95 per cent saturation. Since the data as a whole does not follow the BET theory, it appears probable that in collagen and in wool, water molecules exist in the form of polarized multilayers.

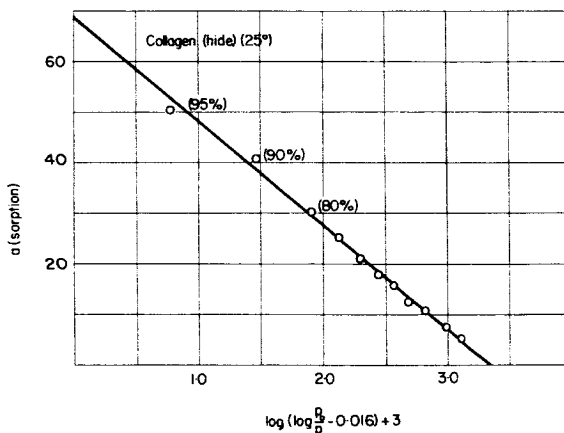


FIGURE 3. Water vapor sorption on collagen plotted according to Bradley's isotherm. Same data as in FIGURE 1.

†A refinement of the Bradley treatment is indicated for multilayer sorption within macromolecular systems such as wool and collagen; in this case the sorption is on two adjacent surfaces and the sorption must oppose forces holding the protein molecules together. Capillary condensation which is bothersome in simple solid surface sorption is reduced since sorption does not greatly alter the surface of the condensed phase.

## SELECTIVE EXCLUSION OF NONELECTROLYTES

*Nonelectrolyte Exclusion in Model Systems*

*Copper ferrocyanide gel.* Sheets of animal tissues had long been known to possess what later van't Hoff named semipermeability, allowing, for example, water but not sucrose to pass through. In the middle of the 19th century, Moritz Traube<sup>23</sup> searched for artificial membranes that have similar attributes; among those he discovered was the copper ferrocyanide ( $\text{Cu}_2\text{Fe}(\text{CN})_6$ ) precipitation membranes which to this day have remained one of the best, if not the best artificial semipermeable membranes. The significant property of the  $\text{Cu}_2\text{Fe}(\text{CN})_6$  gel is that the water it contains accommodates little if any sucrose. Thus, McMahon, Hartung and Walbran<sup>24</sup> studied the equilibrium distribution of sucrose in an aqueous suspension of  $\text{Cu}_2\text{Fe}(\text{CN})_6$  gel; a much higher concentration of sucrose was found in the clear supernatant solution than if all the sucrose was evenly distributed in all the water within the system. Assuming the involved water is 100 per cent inaccessible to sucrose, these authors calculated that each molecule of  $\text{Cu}_2\text{Fe}(\text{CN})_6$  creates 10.6 moles of this type of water, an amount of water so large that it cannot be accommodated in the crystal lattice or on the surface of the salt. McMahon *et al.* suggested most of the water is "imbibed by the gel"; we tend to think that imbibed water, in fact, refers to water adsorbed in multilayers.

*"Coacervate."* The same may apply to the water in the "coacervates" e.g., a colloidal gel composed of gum arabic and gelatin. According to Troschin<sup>13</sup> the equilibrium distribution of sucrose in the water of this coacervate amounts to only 60 per cent of that in the bathing medium.

*Strong electrolyte solutions.* Although  $\text{Cu}_2\text{Fe}(\text{CN})_6$  gel and "coacervates" resemble in their physical consistency the living protoplasm and are therefore its more cogent models; selective exclusion of nonelectrolytes is not restricted to water in colloidal systems. The well-known phenomena of "salting out" of nonelectrolytes in strong electrolyte solutions is another example: the presence of salt diminishes the solubility or the distribution coefficient (against another water-immiscible reference solvent) of many nonelectrolytes including sucrose.<sup>25,26</sup> Although this is a familiar subject, our understanding is far from complete; one aspect, however, is clear: "salting out" owes its origin to the polarization of water molecules around the ions. It is significant that "salting out" is not only caused by strong electrolytes; nonelectrolytes (e.g., sucrose) can salt out other nonelectrolytes (e.g., ethyl acetate).<sup>25</sup> Thus long range electrostatic effect is not an indispensable part of this phenomenon.

*Ion exchange resin.* A variation of the "salting out" effect of strong electrolytes is the similar phenomena observed in ion exchange resins. In this case, one species of the ions is fixed on a three-dimensional matrix; the

TABLE 1  
DISTRIBUTION COEFFICIENTS OF NONELECTROLYTES BETWEEN THE WATER IN  
SULFONATE EXCHANGE RESINS AND ITS SURROUNDING AQUEOUS MEDIUM

	Dowex 50 (H <sup>+</sup> ) (Wheaton and Bauman)	Rexyn RG 50(H <sup>+</sup> ) (25°C)	Amberlite IR-200 (H <sup>+</sup> ) (25°C) (0°)		$\Delta H^\circ$ Kcal/mole	$\Delta S^\circ$ cal/deg/mole
Urea	—	—	22.5	35.0	-2.86	-3.8
Methyl alcohol	0.61	0.94	2.2	—	—	—
Ethylene glycol	0.67	—	0.88	0.87	—	—
Glycerol	0.49	0.56	0.78	0.65	1.18	3.46
Xylose	—	0.23	0.67	0.55	1.28	3.49
Glucose	0.22	0.23	0.61	0.55	0.67	1.27
Sucrose	0.24	0.29	0.63	0.60	0.05	0.15

concentration of the fixed ions is usually high (ca. 5 M); the average number of water molecules associated with each fixed ion-counter ion pair is low, i.e., 5. Wheaton and Bauman<sup>27</sup> reported their findings about equilibrium distribution of various alcohols and sugars between the water in the resin and the external solution. Their data are in general confirmed by our own studies on similar sulfonate-polystyrene exchange resins (TABLE 1).

*The molecular mechanism of sugar exclusion (sugar-ion exchange resin type).* By studying the equilibrium distribution of these alcohols and sugars at two different temperatures (0° to 25°C.) the enthalpy and entropy of the distribution equilibrium can be estimated. Unfortunately, the best grade of ion exchange resin we could obtain was still heterogeneous, containing beads with diverse degrees of sulfonation; this produced considerable scattering of the data. Whereas the data given in TABLE 1 must still be regarded as tentative the trend is obvious: urea, which is selectively accumulated to a concentration 20 times higher than that in the external medium has an average  $\Delta F^\circ = -1.89$  kcal./mole, an enthalpy value of  $-2.9$  kcal./mole and an entropy of  $-3.8$  cal./degree/mole (0°–25°C.). The enthalpy and entropy for the various sugars are all positive; this suggests that their substitution for water is energetically unfavorable. Since the bonds which non-electrolyte molecules form with water and ions are known as H-bonds, the unfavorable enthalpy bespeaks of a restriction in the formation of H-bonds in the resin phase. A diagram of a possible orientation of a sugar molecule in ion exchange resin is shown in FIGURE 4; it illustrates the formation of fewer and/or weaker H-bonds in the resin and hence a higher degree of freedom in motion. This, however, appears not to be the only mechanism of such solute exclusion (see below).

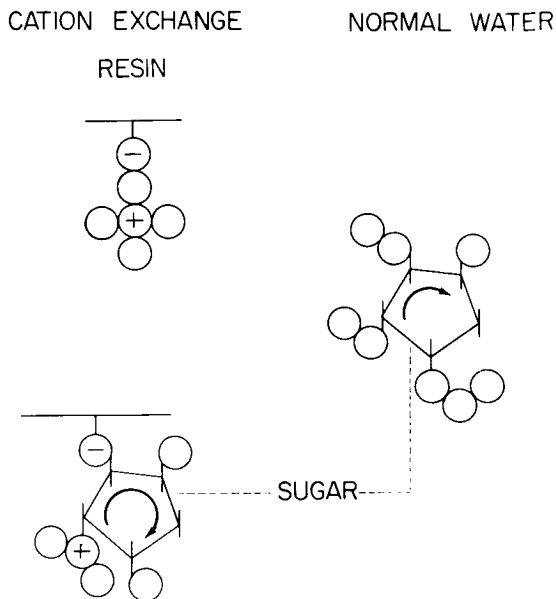


FIGURE 4. Diagram of a possible configuration of a sugar molecule in the ion exchange resin, illustrating the formation of a smaller (and/or weaker) number of H-bonds in the resin and hence a higher degree of rotational freedom. The size of arrows illustrates the relative rotational freedom of the sugar molecules.

#### *Nonelectrolyte Exclusion in Living Cells*

The early cell physiologists attempted to interpret nonelectrolyte distribution in terms of the membrane permeability; permeant nonelectrolytes were assumed to distribute according to thermodynamic equilibrium; impermeant ones remain excluded completely. Advancing years brought in better techniques, which in turn, revealed that many nonassimilated sugars are found in cell water at equilibrium at a concentration considerably lower than that in the external medium.\* A partial list of selected data, largely due to Hechter and Lester,<sup>28†</sup> is given in TABLE 2.

Thus, the exclusion of nonelectrolyte from water found in living cells is also observed in a quantitatively similar manner in various inanimate systems; in the latter cases there can be no question that there are

\*More recently, workers studying selective accumulation of sugars in microorganisms introduced the concept of "permeases" (i.e., sugar "pumps") which were supposed to maintain a high intracellular sugar concentration by a continual pumping mechanism. For a critique of this mechanism, see below.

†Hechter and Lester<sup>28</sup> postulated ordered water lattice in living cells. They invoked Gregor's theory of ionic selectivity in ion exchange resin and attributed ionic and nonelectrolyte exclusion to swelling pressure effect. The critique of this mechanism was given elsewhere.<sup>1</sup>



TABLE 2  
DISTRIBUTION COEFFICIENT OF NONASSIMILATED SUGARS BETWEEN CELL WATER  
AND EXTRACELLULAR WATER

Sugar	Frog muscle	Rat diaphragm muscle	Rat uterus (castrated adrenalectomized)	Rat adrenal gland
D-Xylose	—	0.52 <sup>(41)</sup> 0.341* <sup>(28)</sup>	0.82 <sup>(28)</sup>	0.79 <sup>(28)</sup>
Galactose	0.32 <sup>(13)</sup>	—	—	—
Sucrose	0.29 <sup>(13)</sup>	—	0.36 <sup>(28)</sup>	0.06 <sup>(28)</sup>

Data from references (13) and (41) were derived from *in vitro* studies; those from reference (27) from *in vivo* studies.

\*Concentration of cellular sugar on the basis of fresh tissue weight instead of cell water.

“pumps”; yet, the water molecules differ from normal water only in that they are polarized and oriented in one way or another. Considered together, the data suggest that intracellular water may also be polarized and oriented and in this state, it excludes sugars.

### SELECTIVE IONIC EXCLUSION

#### *Ionic Exclusion in Living Cells*

As in the case of nonelectrolytes, the earlier interpretation of asymmetrical distribution of ions was in terms of permeability or impermeability of the cell membrane. Thus,  $K^+$  ion was recognized as permeant and found in high concentration within the cell;  $Na^+$  ion, which is found at high concentration in the plasma, but low concentration in the tissue, was considered impermeant. As in the case of nonelectrolytes, however, advancing techniques (in particular, radioisotope techniques) soon proved unequivocally that  $Na^+$  ion is in fact also permeant.<sup>29,30</sup> To remedy this failure of the original theory, the Na-pump was proposed. This was a very reasonable assumption at the time it was introduced, since similar “pumps” for  $Na^+$  and for nonelectrolytes undoubtedly operate across such biological “membranes” as intestinal mucosa, frog skin and kidney tubules, etc., at the expense of metabolic energy. Thus, it was thought that  $Na^+$  ion was an exception to the rule; by introducing the Na pump, or original

TABLE 3  
MINIMAL ENERGY REQUIREMENT OF THE Na, Ca AND Mg PUMPS IN  
FROG MUSCLE CELLS IN COMPARISON WITH MAXIMAL  
AVAILABLE METABOLIC ENERGY

	Extracellular concentration (mM./l.)	Theoretical (Donnan equilibrium)		Intracellular concentration (experimental) (mM./l.)	"Permeability constant" (hr <sup>-1</sup> )
		Donnan Ratio	Intracellular concentration (mM./l.)		
K <sup>+</sup>	2.4	53.4	128.0	128.0	0.077 ( (1), p.292)
Na <sup>+</sup>	105	53.4	5600	16.9	1.223 (31)
Ca <sup>++</sup>	4.0	53.4	5704	5.7	2.45 (32)
Mg <sup>++</sup>	2.5	53.4	3565	15.8	4.16 (33)

concept of a sieve-like membrane may still be considered adequate to explain the distribution of all other ions and nonelectrolytes. In reality, this turned out not to be the case.

Extensive tracer studies have long since proven that many ions, hitherto thought to be impermeant, are in fact, also permeant. These include Ca<sup>++</sup>, Mg<sup>++</sup>, orthophosphate, lactate, sulfate ion, free amino acids, and many sugars.<sup>1</sup> The question is: Do they all follow equilibrium distributions predicted on the basis that the intracellular water is entirely the same as in an 0.1 N KCl solution? The answer is no. Thus the anticipated intracellular concentrations (on the basis of an assumption of equilibrium distribution in normal intracellular water) are for Mg<sup>++</sup> 3565 and for Ca<sup>++</sup> 5704 mM. per liter of intracellular water. In reality the intracellular Mg<sup>++</sup> and Ca<sup>++</sup> ion concentrations are 15.8 and 5.7 mM./l. respectively.

The same criteria (permeability and distribution not following that of Donnan equilibrium) that led to the postulation of the Na<sup>+</sup> pump also fully apply to these ions. If the pump theory is not an *ad hoc* but general theory which supplements the pore-size concept whenever needed, there is no choice that there must be Mg<sup>++</sup> pump and Ca<sup>++</sup> pump as well. TABLE 3 summarizes calculations we have presented elsewhere in greater detail.<sup>34</sup> Even if each of the pumps operates at 100 per cent efficiency, the overall

TABLE 3A  
 MINIMAL ENERGY REQUIREMENT OF THE NA, CA AND MG PUMPS IN  
 FROG MUSCLE CELLS IN COMPARISON WITH MAXIMAL  
 AVAILABLE METABOLIC ENERGY

	Fraction of nonenergy consuming efflux according to pump model	Electrochemical work per mole of ion pumped (volt-Farady)	Pump		Maximum available energy (cal./kg./hr.)
			Efficiency assumed	Minimal energy requirement (cal./kg./hr.)	
K <sup>+</sup>	100%	0	—	—	—
Na <sup>+</sup>	0.1%	0.148	100%	51	—
Ca <sup>++</sup>	0.4%	0.142	100%	343	—
Mg <sup>++</sup>	0.15%	0.116	100%	176	—
			Total	570	170

Data of ionic concentrations from (36) Details of calculations given in (34)  
 Calculation of energy requirement for Na pump is essentially that from Levi  
 and Ussing (31)

minimal energy need of the three ions (Na<sup>+</sup>, Ca<sup>++</sup>, Mg<sup>++</sup>) alone would  
 be 335 per cent of the total metabolic energy delivered per unit time.

The critical analysis given above shows that if one assumes the intra-  
 cellular water to be normal and the protein unreactive toward ions and  
 nonelectrolytes neither an equilibrium nor a steady state (pump) inter-  
 pretation is satisfactory because both violate fundamental physical laws.

Since 1951, the theory (the association-induction hypothesis) has been  
 developed<sup>1</sup> that ionic and nonelectrolyte distribution do represent equilib-  
 rium phenomena, that the cell proteins are not inert toward ions and  
 nonelectrolytes and that the cell water is not normal. The entire living  
 cell is considered to constitute a bulk phase fixed-charged system; in this,  
 ionic (and other) sites of the proteins selectively adsorb ions (and non-  
 electrolytes); distribution of these ions and nonelectrolytes within the  
 cell water is, as a rule, lower than in the extracellular water due to re-

striction of rotational (and to some extent translational) motions and hence a lowered entropy of ions and nonelectrolytes found in it. The theory is summarized by the following equation (Troschin arrived at a simpler version of this equation in studying nonelectrolyte distribution):<sup>13</sup>

$$[p_i^+]_{in} = \kappa_i [p_i^+]_{ex} + \sum_{j=1}^N \frac{[f_j^-] \tilde{K}_{ij} [p_i^+]_{ex}}{1 + \sum_{s=1}^m \tilde{K}_{sj} [p_s^+]_{ex}} \quad (2)$$

where  $[p_i^+]_{ex}$  and  $[p_i^+]_{in}$  are the extra- and intracellular concentration of the  $i$ th cation;  $[p_s^+]_{ex}$  is the extracellular concentration of the  $s$ th cation which refers to any one of the  $m$  cations in the external medium including the  $i$ th. Where  $[f_j^-]$  refers to the  $J$ th type of anionic site among a total of  $N$  types of similar sites.  $K_{ij}$  and  $K_{sj}$  are the adsorption constants of the  $i$ th, and  $s$ th monovalent cations on the  $J$ th site. Since  $K_i$  is less than unity (see below) for the  $i$ th ion with a high  $K_{ij}$  value at values of  $[p_i]_{ex} \geq [f^-]$  one may on first approximation assume that there is only one type of site, the  $J$ th, rewrite and simplify Equation 2 as:

$$[p_i^+]_{in} = \frac{[f_j^-] \tilde{K}_{ij} [p_i^+]_{ex}}{1 + \tilde{K}_{ij} [p_i^+]_{ex} + \tilde{K}_{ij} [p_j^+]_{ex} + \sum_{s=1}^{m-2} \tilde{K}_{sj} [p_s^+]_{ex}} \quad (3)$$

where  $p_j$  refers to another multivalent cation in the system. If in one series of experimental studies, concentrations of all cations are kept constant except the  $i$ th and  $j$ th, then,

$$[p_i^+]_{ex} = \frac{[f_j^-] K'_i [p_i^+]_{ex}}{(1 + K'_i [p_i^+]_{ex} + K'_j [p_j^+]_{ex})} \quad (4)$$

where

$$K'_i = \frac{\tilde{K}_{ij}}{1 + \sum_{s=1}^{m-2} \tilde{K}_{sj} [p_s^+]_{ex}} \quad (5)$$

$$K'_j = \frac{\tilde{K}_{ij}}{1 + \sum_{s=1}^{m-2} \tilde{K}_{sj} [p_i^+]_{ex}} \quad (6)$$

Equation 4 can be written reciprocally:

$$\frac{1}{[p_i^+]_{in}} = \frac{1}{K'_i [f_j^-]} (1 + K'_i [p_i^+]_{ex}) \frac{1}{[p_i^+]_{ex}} + \frac{1}{[f_j^-]} \quad (7)$$

If  $1/[p_i^+]_{in}$  is plotted against  $1/[p_i^+]_{ex}$ , a straight line should be obtained at each constant value of  $[p_j^+]_{ex}$ . When the  $i$ th and the  $j$ th apparent adsorption constants are similar (as in the case of  $K^+$ ,  $Rb^+$  and  $Cs^+$  in frog sartorius muscles) this proves to be the case. The complete experimental data were presented elsewhere.<sup>35</sup> Now,

$$\kappa_i = \alpha q_i \quad (8)$$

TABLE 4  
THE DISTRIBUTION COEFFICIENT OF  $\text{Na}^+$  ION IN WATER OF LIVING CELL  
AND OF SHEEP'S WOOL

Frog sartorius muscles (0 - 25°C.)			
$q_{\text{Na}}$	$\Delta F^\circ$ kcal./mole	$\Delta H^\circ$ kcal./mole	$\Delta S^\circ$ cal./deg./mole
0.19 (0°C.)	1.04	-0.94	-6.9
0.13 (25°C.)			

Sheep's wool (25°-37°)			
$q_{\text{Na}}$	$\Delta F^\circ$ kcal./mole	$\Delta H^\circ$ kcal./mole	$\Delta S^\circ$ cal./deg./mole
0.16 (25°C.)	1.247	-3.28	-14.8
0.10 (37°C.)			

where  $\alpha$  is the percentage of water in the living cells and  $K_i$  is the distribution coefficient of the  $i$ th ion between the intracellular water and the extracellular water. The value of  $\kappa_i$ , however, is best studied in the case of an ion which has a very low value of  $K_j$ . This is the case for  $\text{Na}^+$  ion ( $q_{\text{Na}} = 1.0$ ). Since if one chooses a  $j$ th ion which has a much higher adsorption constant as in the case of  $\text{K}^+$  ( $K_j' = 6.67 \times 10^2$ ),  $[p_i^+]_{\text{in}} \sim \kappa_i [p_i^+]_{\text{ex}}$  as  $[p_j^+]_{\text{ex}} \rightarrow \infty$ . The value of  $[p_i^+]_{\text{in}}$  at  $[p_j^+]_{\text{ex}} = \infty$  can be determined by extrapolation based on several values of  $[p_i^+]_{\text{in}}$  obtained at increasing concentrations of  $[p_j^+]_{\text{ex}}$ . From such studies the value of  $q_i$  is obtained. The value of  $q_{\text{Na}}$  so determined are given in TABLE 4.

#### *Ionic Exclusion in Model Systems*

We have made an analogous study on the distribution of  $\text{Na}^+$  ion in two model systems: collagen of carp swim bladder and sheep's wool. Within the concentration range of ions studied (up to 1.0 M) swim bladder collagen does not adsorb an appreciable amount of  $\text{Na}^+$  ion.  $q_{\text{Na}}$  in this case,

is found to be 0.8. However, this estimation was made on the basis of the total water of the swim bladder tissue which contains water outside the collagen tissue in the form of adhering fluid films. Thus, the true value of  $K_{Na}$  between water in collagen and the surrounding fluid must be lower.

The pattern of ion uptake in sheep's wool, on the other hand, is essentially similar to that found in muscle cells and follows both Equation 2 and Equation 7. Wool contains 33 per cent of water; in this  $q_{Na}$  has a value of 0.16 at 25°C. and 0.1 at 37°C.

#### *Molecular Mechanism of Ion Exclusion (Ion-Wool Type)*

From data just given, one can calculate the average  $\Delta F^\circ$  of the equilibrium:

$$[Na]_{in} \rightleftharpoons [Na]_{ex} + \Delta F^\circ$$

to have a value of 1.247 kcal./mole (between 25 and 37°C). The average  $\Delta H^\circ$  is -3.15 kcal./mole and the average  $\Delta S^\circ$  is -14.4 cal./degree/mole. Thus, the  $Na^+$  ion would have accumulated in the cell water to a concentration higher than that in the external medium, had it not been for the large entropy loss which more than offset the favorable enthalpy. As was shown, by Guggenheim and Fowler<sup>36</sup> the hydrated ion is a *de facto* multi-atomic structure; as such by far the largest partition function (and hence entropy) is the rotational partition function. The highly unfavorable entropy of  $Na^+$  ion in the water in sheep's wool must be therefore largely due to the restriction of rotation of the hydrated  $Na^+$  within the protoplasmic water.

If one recalls that we have already demonstrated that the water in sheep's wool and in collagen exist in polarized multilayers (FIGURE 3), a molecular mechanism for this restricted rotation appears readily understandable as shown in FIGURE 5. Water molecules in the "hydrated shell" and in the polarized multilayer merge and become mutually reinforcing, creating a large number of stronger H-bonds for the hydrated ion than in normal water. The hydrated ion also loses in consequence much of its freedom of rotation motion.

It now only remains to be pointed out that our data on studies on frog muscle indicates that the  $q_{Na}$  value also decreases with increasing temperature and hence similar signs in the values of  $\Delta H^\circ$  and  $\Delta S^\circ$ . The overall picture therefore resembles ionic exclusion from wool water rather than the pattern of nonelectrolyte exclusion in ion exchange resin. However, the living cell is a very complicated structure; the detailed mechanisms may very well incorporate in different microscopic regions the sugar-ion exchange resin type but to a minor degree.

We shall conclude this paper by examining an interesting and highly informative experiment reported more than 30 years ago by the late Robert

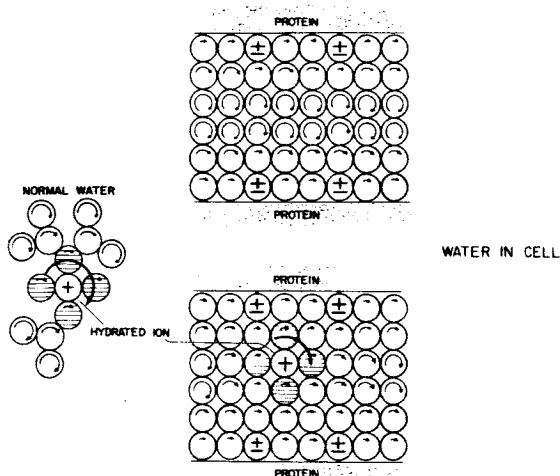


FIGURE 5. Diagram illustrating the physical state of water in the living cell in a region with hydrated ion (*lower right*) and in a region without a hydrated ion (*upper right*). Left figure is a diagram of a hydrated ion in normal water. The length of the curved arrows indicated the degree of rotational freedom of each water molecule; a progressively greater rotational freedom is shown for water molecules further away from the proteins. The merging and mutual reinforcement of the polarization (arising from the ion and from the proteins) and the anchoring effect of the fixed proteins produces a microscopic "droplet" of water molecules. In this "droplet", water molecules have greatly reduced rotational motion.

Chambers and his coworker<sup>38</sup> and later confirmed in more than one laboratory. A single frog muscle cell was supercooled to  $-6^{\circ}\text{C}$ . Formation of one to many ice "spikes" progressed from the cut end of the muscle fiber when it was touched with an ice-tipped micropipette. The orientation of the "spikes" followed the orientation of the muscle fiber, straight when the muscle fiber was straight, twisted when the muscle fiber was twisted. The shape of ice crystal was different in other cells, being feather-like, for example, in sea urchin eggs. When the freezing was very rapid hundreds of such ice "spikes" could form in a single muscle fiber. A comparison of the cross-section of such a frozen cell<sup>39</sup> with a similar cross-section of a frog muscle fiber seen through an electron microscope<sup>40</sup> suggests that the ice formation occurs between the protein filaments which run longitudinally along the length of the muscle fiber. Thus, the frozen portion of the cell water must correspond to the water occupying intracellular space farthest away from the polarizing surfaces of the protein molecules. The fact that (1) water not in the form of ice remains in cell proteins after the completion of the intracellular freezing and that (2) no branching or horizontal propagation of ice "spikes" occurs<sup>39</sup> also suggests that the layer of

water immediately adjacent to the proteins is strongly oriented and that transformation of their structure to ice is energetically unfavorable. All these are in complete accord with the physical state of cellular water which is deduced from the study of ions and nonelectrolyte distribution reported in this paper.

#### SUMMARY

Sorption of water vapor on collagen and on sheep's wool fits the BET theory up to 50 per cent vapor saturation; the same data fits the Bradley multilayer adsorption isotherm of polarized molecules to near saturation, suggesting that water in these systems is polarized and oriented in multilayers. It was shown that  $\text{Na}^+$  ion is excluded from this water in wool so that it reaches an equilibrium concentration of about 0.1 that in the external medium; a quantitatively similar situation exists in living frog muscle cells. In both, the equilibrium distributions have negative enthalpy values and large negative entropy values suggesting that the water in the hydrated shell of  $\text{Na}^+$  ion merge with and reinforce polarized water in the system and form stronger H-bonds, but this advantage favoring distribution in the wool (or cell) is more than offset by the large entropy loss in the restricted rotational freedom.

#### REFERENCES

1. LING, G. 1962. *A Physical Theory of the Living State: The Association-Induction Hypothesis*. Blaisdell. New York, N. Y.
2. FORSLIND, E. 1952. *Proc. Swed. Cement Concrete Res. Inst. No. 16*.
3. JACOBSEN, B. 1955. *Svensk. Kem. Tidskr. 67: 1*.
4. SZENT-GYÖRGYI, A. 1957. *Bioenergetics*. Academic Press. New York, N. Y.
5. KLOTZ, I. M. 1958. *Science 128: 815*.
6. BEEMAN, W. W., P. GEIL, M. SHURMAN & A. G. MALMON. 1957. *Acta. Cryst. 10: 818*.
7. HEARST, J. E. & J. VINOGRAD. 1961. *Proc. Nat. Acad. Sci. 47: 1005*.
8. RITLAND, H. N., P. KAESBERG & W. W. BEEMAN. 1950. *J. Chem. Phys. 18: 1237*.
9. BERENDSEN, H. J. C. 1962. *J. Chem. Phys. 36: 3297*.
10. GORTNER, R. A. 1938. *Outlines of Biochemistry*. 2nd. Ed. New York. Gortner, R. A. 1937. *Selected Topics in Colloid Chemistry*. Chap. 8. Ithaca, New York.
11. BLANCHARD, K. C. 1940. *Cold Spring Harbor Sym. Quant. Biol. 8: 1-8*.
12. WEISMANN, O. 1938. *Protoplasma. 31: 27*.
13. TROSCHEIN, A. S. 1958. *Das Problem der Zellpermeabilität*. Fischer. Jena, Germany.
14. LING, G. N. 1952. *In Phosphorus Metabolism*. W. D. McElroy & B. Glass, Ed. (2): 748. John Hopkins Press. Baltimore. (2): 748.
15. LING, G. N. 1964. *Texas Rep. Biol. Med. 22: 244*.
16. DE BOER, J. H. & C. ZWIKKER. 1929. *Z. Physik. Chem. B3: 407*.
17. BRADLEY, S. 1936. *J. Chem. Soc. : 1467*.
18. BRUNAUER, S., P. H. EMMETT & E. TELLER. 1938. *J. Am. Chem. Soc. 60: 309*.
19. BRADLEY, S. 1936. *J. Chem. Soc. : 1799*.
20. BULL, H. 1944. *J. Am. Chem. Soc. 66: 1499*.
21. HNOJEWYJ, W. S. & L. H. REYERSON. 1959. *J. Am. Chem. Soc. 63: 1653*.



22. MELLON, S. R. & E. F. HOOVER. 1950. *J. Am. Chem. Soc.* **72**: 2562.
23. TRAUBE, M. 1876. *Arch. Anat. Physiol. Wiss. Med.* **87**: 128; 129-165.
24. MCMAHON, B. C., E. J. HARTUNG & W. J. WALBRAN. 1937. *Trans. Farad. Soc.* **33**: 398.
25. EDSALL, J. T. & J. WYMAN. 1958. *Biophysical Chemistry*. 1.: Academic Press. New York, N. Y.
26. LONG, F. A. & W. F. MCDEVIT. 1952. *Chem. Rev.* **51**: 119.
27. WHEATON, R. M. & W. C. BAUMAN. 1951. *Ind. Eng. Chem.* **43**: 1088.
28. HECHTER, O. & G. LESTER. 1960. *Rec. Progr. Hormone Res.* **16**: 139.
29. STEINBACH, H. B. 1952. *Am. J. Physiol.* **166**: 42.
30. HEPPPEL, L. A. & C. L. A. SCHMIDT. 1938. *Univ. Calif. Pub. Physiol.* **8**: 189.
31. LEVI, H. & H. H. USSING. 1948. *Acta. Physiol. Scand.* **16**: 232.
32. TASAKI, I., T. TEORELL & C. S. SPYROPOULOS. 1961. *Am. J. Physiol.* **200**: 11.
33. CONWAY, E. J. & G. CRUESS-CALLAGHAN. 1937. *Biochem. J.* **31**: 828.
34. LING, G. N. 1965. *J. Gen. Physiol.* **24**: S103.
35. LING, G. N. & M. OCHSENFELD. 1965. *J. Gen. Physiol.* **24**: S103. In press.
36. FOWLER, R. H. & E. A. GUGGENHEIM. 1939. *Statistical Thermodynamics*. Cambridge Univ. Press. New York, N. Y.
37. LING, G. N. 1955. *Am. J. Phys. Med.* **34**: 89.
38. CHAMBERS, R. & H. P. HALE. 1932. *Proc. Roy. Soc. B* **110**: 336.
39. LUYET, B. J. 1965. *This Annal.*
40. HUXLEY, H. E. 1957. *J. Biophys. Biochem. Cytol.* **3**: 631.
41. KIPNIS, D. M. & C. F. CORI. 1957. *J. Biol. Chem.* **224**: 681.

# THE STRUCTURE OF WATER NEIGHBORING PROTEINS, PEPTIDES AND AMINO ACIDS AS DEDUCED FROM DIELECTRIC MEASUREMENTS

Edward H. Grant

*Physics Department, Guy's Hospital Medical School, London, England*

With the exception of Schwan's work on hemoglobin (1957) all previous dielectric studies on protein solutions have been carried out in the relaxation regions of the protein molecules or water molecules. Examples of these investigations are found in the work of Oncley (1943) and Buchanan *et al.* (1952) who made measurements on several protein solutions at megacycle and microwave frequencies respectively. Extrapolation of these previous measurements for egg albumen (which was the only protein common to both sets of investigations) suggested that there may be further dispersion occurring between the two main regions, and one of the purposes of the present work was to explore the nature of this possibility. For the sake of comparison it was also decided to study a similar protein over the same frequency and temperature range, bovine serum albumen being chosen for this purpose.

In this paper the results on both proteins are reported and interpreted in terms of the protein molecule structure in its water environment. This procedure is then applied to some recently studied amino acids and peptides (Aaron, 1964; Aaron & Grant, 1964) where the water structure neighboring these smaller molecules is also considered.

## *Experiments and Analysis of Results*

Both albumens were obtained in a pure crystalline form from the Armour Chemical Co. and the solutions prepared in conductivity water. Concentrations were calculated from the ultraviolet absorption at 215  $m\mu$  and 225  $m\mu$ . The solutions were studied over a frequency range of 250 Mc/s — 1200 Mc/s and a temperature range of 0°C — 40°C. The real ( $\epsilon'$ ) and imaginary ( $\epsilon''$ ) parts of the dielectric constant were calculated from measurements of the wave propagation constants made by observation of the standing wave pattern obtained when the specimen was contained in a short-circuited line. The techniques of measurement have been fully described previously (Buchanan & Grant, 1955; Grant, 1955), but the apparatus has been improved by the inclusion of General Radio Co. oscillators and other new circuit components (Aaron & Grant, 1963).

For each frequency and temperature a dielectric decrement ( $\delta$ ) can be obtained from the expression

$$c\delta = \epsilon_s - \epsilon' \quad (1)$$

where  $\epsilon_s$  is the static dielectric constant of water at the temperature in

TABLE 1  
DIELECTRIC DECREMENTS OF THE ALBUMENS

Egg Albumen C = 6.1% pH = 4.75				
Temperature	f = 250 Mc/s	f = 450 Mc/s	f = 780 Mc/s	f = 1200 Mc/s
0	1.05 ± .08	1.02 ± .08	1.12 ± .08	1.10 ± .08
10	0.87 ± .08	0.94 ± .08	1.03 ± .08	1.02 ± .08
20	0.80 ± .07	0.89 ± .07	0.92 ± .07	0.98 ± .07
25*	0.74 ± .07	0.85 ± .07	0.89 ± .07	0.92 ± .07
30	0.69 ± .07	0.80 ± .07	0.85 ± .07	0.87 ± .07
40	0.56 ± .05	—	—	—

Bovine serum albumen C = 6.4% pH = 4.98				
Temperature	f = 250 Mc/s	f = 450 Mc/s	f = 780 Mc/s	f = 1200 Mc/s
0	1.03 ± .08	1.06 ± .08	1.14 ± .08	1.26 ± .08
10	0.89 ± .08	0.92 ± .08	0.97 ± .08	1.14 ± .08
20	0.84 ± .06	0.87 ± .06	0.92 ± .06	1.06 ± .06
30	0.76 ± .06	0.80 ± .06	0.87 ± .06	0.95 ± .06
40	0.61 ± .05	—	—	—

\*  $\delta_s = 0.70$  (Oncley, 1943);  $\delta_\infty = 0.95$  (Buchanan *et al.*, 1952).

question and  $c$  is the concentration of protein in grams per 100 ml. of solution.

The results which are shown in TABLE 1 establish the existence of a small dispersion region, the nature of which will be considered later.

Similarly, an absorption increment ( $\Delta\epsilon''$ ) is obtainable from the expression

$$c\Delta\epsilon'' = \epsilon'' - \epsilon_w'' - \epsilon_p'' - \epsilon_c'' \quad (2)$$

where  $\epsilon_w''$  and  $\epsilon_p''$  are the contributions from the main water and protein relaxation regions respectively, and  $\epsilon_c''$  is the contribution from ionic conductivity. At all frequencies and temperatures for both proteins positive values of  $\Delta\epsilon''$  were observed lying between  $0 \pm 0.03$  and  $0.3 \pm 0.03$ , thereby supporting the conclusions obtained from the decrements that a subsidiary dispersion exists at these wavelengths. It is impossible, however, to draw any conclusions about the specific nature of the disposition from the  $\Delta\epsilon''$  results since  $\epsilon_p''$  cannot be assessed with any degree of accuracy and  $\epsilon_c''$  is calculated from measurements made at 1000 c/s. Although it is commonly assumed that  $\epsilon_c''$  is invariant between 1000 c/s and ultra high frequencies, this assumption could be dangerous when  $\epsilon_c''$  forms an appreciable fraction of the total loss. Finally, even  $\epsilon_w''$  is subject to error since some sort of correction must be made to the dielectric loss of pure

water in order to account for the volume occupied by the protein molecules, and the precise nature of this correction is unknown.

Consequently all deductions about the dispersion parameters have been made from the decrement variation. It is only possible to make a complete analysis for egg albumen at 25°C. since this is the sole case where the decrements at very low ( $\delta_s$ ) and very high ( $\delta_\infty$ ) frequencies are known. For egg albumen at 25°C. the relaxation region is represented by the Cole-Cole equation

$$\hat{\epsilon} = \epsilon_\infty + \frac{\epsilon_s - \epsilon_\infty}{1 + \left(j \frac{\lambda_s}{\lambda}\right)} \quad (3)$$

where the symbols have their usual significance. The value of  $\alpha$  is  $0.15 \pm 0.15$  which indicates the probable existence of a small distribution of relaxation times, but is incompatible with a wide distribution of relaxation times as was reported for hemoglobin by Schwan (1957). The limits of error are necessarily wide in this type of investigation due to the required parameter being deduced from a small difference between two large measured quantities.

The relaxation wavelength ( $\lambda_s$ ) was calculated as 100 cm. (300 Mc/s) at 25°C. and the activation energy ( $\Delta H$ ) was deduced from the variation of  $\lambda_s$  with temperature to give the result  $16 \pm 5$  kcal./mole (TABLE 2).

In the derivation of  $d\lambda_s/dT$  it was assumed that the variation of decrement with temperature at the frequencies of measurement  $d\delta/dT$  was very much greater than  $d\delta_s/dT$  or  $d\delta_\infty/dT$ . This is true when the frequencies of measurement are near the relaxation frequency, and leads to a linear relationship between  $d\lambda_s/dT$  and  $d\delta/dT$ . The assumption is further justified if  $d\delta_s/dT$  and  $d\delta_\infty/dT$  are in opposite directions, which is likely.

Owing to the lack of results at high and low frequencies it is impossible to make analyses of egg albumen at any temperature other than 25°C. Nevertheless, it is clear from TABLE 1 that  $\delta$  varies strongly with frequency at all other temperatures, and strongly with temperature at all frequencies. Similar behavior is exhibited by serum albumen as seen from TABLE 1. These results, taken together with Schwan's observations for hemoglobin, show that this subsidiary dispersion occurs for at least three proteins, and

TABLE 2  
SUBSIDIARY DISPERSION IN EGG ALBUMEN

Cole-Cole Parameter $\alpha$	$\lambda_s$ (cm) at 25° C	$\Delta H$ (kcal./mole)
$0.15 \pm 0.15$	100	$16 \pm 5$

it will be interesting to extend this work to see if similar behavior is shown by other proteins.

*Interpretation of Dielectric Parameters in Terms of Protein Structure*

The preceding sections of this paper have been concerned with establishing the existence of a relaxation region in egg albumen centered around 300 Mc/s with an activation energy of 16 kcal./mole. A very much more difficult task, however, is the interpretation of the dispersion with the same amount of confidence.

Both in this Conference and previously Schwan (1964, 1957) has advanced the idea that bound water may relax in this frequency range, but has not provided activation energies. On the other hand, the water bound to silica gel is reported as having an activation energy of 16 kcal./mole (Hasted, 1961). It therefore seems a reasonable possibility to ascribe the dispersion observed in the present work to bound water, and an approximate mathematical analysis on these lines is now presented.

In a previous communication (Grant, 1957 *a*) it has been pointed out that most known dielectric mixture formulae can be written in the form

$$\epsilon_M = \epsilon_w + kv_p (\epsilon_p - \epsilon_w) \quad (4)$$

where  $\epsilon_M$  refers to the mixture and  $\epsilon_w$ ,  $\epsilon_p$  to the suspending and suspended phases respectively. The volume fraction of the suspended phase is  $v_p$  and  $k$  is a constant equal to or greater than unity when  $\epsilon_p/\epsilon_w < 1$ . The value  $k=1$  refers to a simple proportion mixture formula and  $k=1.5$  to a Fricke type mixture formula as used by Buchanan *et al.* (1952). Since  $k=1$  corresponds to a homogeneous mixture and  $k=1.5$  to a suspension or macroscopic particles, the appropriate value of  $k$  for a protein solution is likely to lie between these limits.

Returning to Equation 4 it is necessary to split up  $\epsilon_p$  into its protein contribution and its bound water contribution. Using the parameters in TABLES 1 and 2 and assuming that  $k=1.25$  it is calculated that the dispersion could be accounted for in terms of bound water of an amount 0.3 gram/gram of protein, if its dielectric constant fell from 78 to 5 through the dispersion. This would be equivalent to passing from the free water value to the value obtained from atomic and electronic polarization only, which is a likely occurrence. The hydration value of 0.3 is reasonable, although no attempt has been made to divide the bound water into irrotationally bound and nonirrotationally bound as was done by Buchanan *et al.* (1952). The protein contribution to  $\epsilon_p$  is taken as 5.0.

A similar result would be obtained for  $k=1.4$ , if the protein contribution to  $\epsilon_p=10$  and  $w=0.18$  which would make some allowance for the fact that  $w$  may be smaller than the total bound water.

The activation energy of 16 kcal./mole is very much higher than that of free water (4 kcal./mole) and therefore accords with any plausible

molecular picture of bound water. It could correspond to the breaking of three hydrogen bonds, that is, indicate that this is necessary before the bound water molecule can rotate in the electric field.

Although the rotation of the bound water molecules appears a likely explanation for the observed dispersion, other possibilities cannot be ruled out. There are many polar groups protruding from the egg albumen molecule bearing both positive and negative charges — for example there are 52 glutamic acid residues and 20 lysine residues. Rotation of such groups in their water environment would presumably be a possibility and would be expected to occur in the same frequency range as the observed dispersion.

A quasimacroscopic explanation of the results would be the undergoing by the albumen molecule of an  $N \rightleftharpoons F$  transition as has been reported by Aoki (1957). The N and F forms of egg albumen travel at different speeds during electrophoresis, and the energy of activation for the change from one form to the other is 15 kcal./mole.

#### *Peptides and Amino Acids*

Some very recent measurements have been made on aqueous solutions of some amino acids and peptides, and the results at 20°C. are summarized in TABLE 3 (Aaron, 1964). This is the first attempt to study the dielectric

TABLE 3  
MOLECULAR PARAMETERS OF SOME AMINO ACIDS AND PEPTIDES AT 20°C.\*

	Dielectric increment $\Delta$	Dipole moment $\mu$ (D)	Charge separation $r$ (Å)	Relaxation wavelength $\lambda_s$ (cm)	$\Delta H_\tau$ (kcal./mole)	$\frac{\Delta H_\eta}{\Delta H_\tau}$
Glycine	$24.3 \pm 1.2$	16.3	3.4	$11.6 \pm 1.2$	$4.4 \pm 0.5$	1.0
Diglycine	$76.8 \pm 3.8$	28.9	6.0	$29.4 \pm 2.9$	$3.4 \pm 0.5$	1.2
Triglycine	$126.8 \pm 6.3$	37.2	7.7	$42.9 \pm 4.3$	$2.3 \pm 0.5$	2.0
$\alpha$ -alanine	$26.3 \pm 1.3$	17.0	3.5	$16.5 \pm 1.0$	$4.2 \pm 0.5$	1
$\beta$ -alanine	$34.6 \pm 1.7$	19.4	4.1	$16.5 \pm 1.0$	$3.7 \pm 0.7$	1
Glycylalanine	$79.9 \pm 3.9$	29.3	6.2	$29.4 \pm 1.5$	$3.3 \pm 0.7$	1.2

\* Very recent measurements have shown the existence of a distribution of relaxation times below room temperature, especially for triglycine. This has the effect of making the value of  $\Delta H_\tau$  equal to within experimental error for all six substances and also necessitates  $\Delta H_\tau = \Delta H_\eta$  in all cases. Further details will be published later.

properties of amino acids and peptides over a temperature and frequency range, the previous measurements having been made over 30 years ago and at 25°C. only (Wyman & McMeekin, 1933). It is very interesting to notice, however, that there is substantial agreement between the dielectric increments obtained by Aaron and Wyman.

The dipole moments were calculated using Kirkwood's theory plus appropriate approximations (Kirkwood, 1943), and the charge separations obtained accordingly.

In the case of the three amino acids studied, the charge separation is in agreement with that expected from structural considerations, and it can be noticed that the larger charge separation in  $\beta$ -alanine gives rise to a much higher dielectric constant than for  $\alpha$ -alanine.

On the other hand, the charge separation ( $\tau$ ) for the peptides is lower than would be expected for a linear ionic polymer. For example, the value of  $\tau$  for diglycine as a linear molecule is calculated as 7.2 Å whereas the observed value is 6.0 Å and the relative difference for triglycine is greater. Even allowing for the approximations involved in using Kirkwood's theory these differences are significant and suggest that the peptide backbone is curved in solution, due no doubt to the electrostatic attraction between the polar groups on the ends of the molecule. That the curvature is not greater could be explained by the screening effects of the charges on the bound water molecules, i.e., the lone pair electrons on the oxygens in the case of the amino groups and the protons in the case of the carboxyl groups. Although the values reported in TABLE 3 are at 20°C. only, measurements were made over the range 0°C. – 50°C. for all six solutions and showed that the increment decreases as the temperature increases. It was also found for glycine, diglycine and triglycine that a straight line relationship exists between the dielectric increment and the number of carbon atoms between the  $\text{NH}_3^+$  and  $\text{COO}^-$  groups.

The activation energies for dielectric relaxation ( $\Delta H_7$ ) shown in TABLE 3 are all compatible with the breaking or distorting of a hydrogen bond between the solute molecule and a neighboring water molecule. The bond energy is smaller for  $\beta$ -alanine than for  $\alpha$ -alanine which is consistent with the observed behavior of the other molecules in TABLE 3 since  $\Delta H_7$  decreases as the charge separation increases. From the structure of the amino acids considered it may be expected that each molecule could form up to a maximum of five hydrogen bonds but the dielectric results show the molecules can rotate upon breaking one bond. This suggests that there must be many molecules which form an average of only two hydrogen bonds to their water environment at any one instant at 20°C.

Turning now to the three peptides, it is seen that the activation energy decreases with the size of the molecule, which is a somewhat unexpected revelation. In contrast, the actual magnitude of the relaxation wavelength increases with molecular size, as is usual. It would therefore appear as

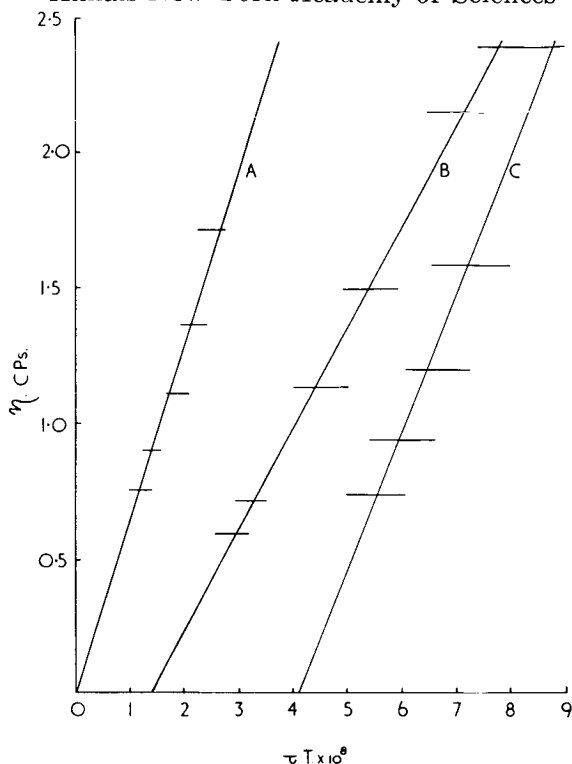


FIGURE 1. Relationship between relaxation time, absolute temperature and viscosity for glycine and its peptides: A—glycine; B—diglycine; C—triglycine.

though the whole molecule turns about a hydrogen bond formed between a water molecule and an N—H group or C—O group on the backbone of the peptide chain. The bond which is broken or distorted, however, would be between a water molecule and an end-charged group. Rotation of part of the molecule as distinct from the whole molecule seems unlikely due to the long relaxation wavelength. These conclusions are further supported by the viscosity measurements where the radius of the rotating unit can be shown by using the Debye equation (see below) to be roughly half the charge separation. The viscosity referred to in TABLE 3 is that of the whole solution which is rarely more than 10 per cent different from the pure water value.

From these viscosity measurements, FIGURES 1 and 2 were plotted in order to examine the validity of the Debye equation

$$\tau = 4\pi a^3 \frac{\eta}{kT} \quad (5)$$

or one of the other relationships (Saxton, 1952; Hill, 1954; Grant, 1957 *b*) that have been suggested to account for a proportionality between  $\tau$  and



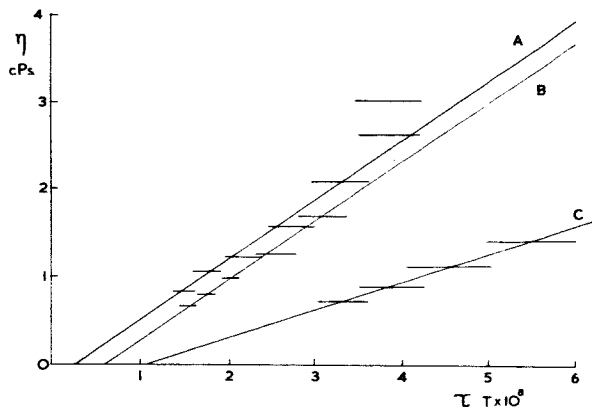


FIGURE 2. Relationship between relaxation time, absolute temperature and viscosity for the alanines and glycylalanine: A —  $\alpha$ -alanine; B —  $\beta$ -alanine; C — glycylalanine.

$\eta/T$ . The macroscopic dielectric relaxation time is indicated by  $\tau$  and "a" is the molecular radius. Although a straight line is obtained in all cases the deviation from the origin increases with molecular size and asymmetry. It is also noticed for the peptides that the activation energy for the viscosity process ( $\Delta H_\eta$ ) is greater than the activation energy for dielectric relaxation. This shows that a significant proportion of the activation energy for viscosity is concerned with translational motion, as distinct from rotational motion, in the case of large nonspherical molecules in a water environment. On the other hand, it is noticed for the amino acids that  $\Delta H_\eta = \Delta H_\tau$  which is consistent with the motion of small fairly symmetrical molecules in aqueous surroundings. Furthermore, a fairly good approximation to Debye behavior is observed for the amino acids (FIGURES 1 and 2).

Glycylalanine and diglycine behave similarly in both the relationship between  $\eta$  and  $\tau T$  and in the ratio  $\Delta H_\eta/\Delta H_\tau$ . The structural difference between these molecules is the replacement of a proton by a methyl group which will only affect the surrounding water molecules through hydrophobic interactions and changes in the steric configuration. This, therefore, confirms that it is mainly the hydrophilic bonds which determine the rates of viscous flow and dielectric relaxation for amino acids and peptides in water.

#### Conclusion

From the measurements presented it would appear that the dielectric constant of protein bound water falls from a free water value to the value due to atomic and electronic polarization only as the frequency changes

from a few megacycles to hundreds of megacycles. The activation energy for this process is such as to suggest that the properties of bound water are "ice-like" rather than akin to liquid water, at least as far as its dielectric properties are concerned.

In the case of the amino acids and peptides studied so far the process of dielectric relaxation is governed by the rupture or distortion of one hydrogen bond linking the solute molecule to its neighboring water molecules. That the energy required to achieve this decreases with the higher peptides seems to suggest that the whole peptide molecule undergoes a partial rotation involving the bending of a hydrogen bond rather than a complete rupture of the bond. There is no evidence that only part of the molecule relaxes. The activation energy for the viscosity process again indicates that one hydrogen bond is involved although this energy is larger than that for dielectric relaxation in the case of the asymmetric molecules, due to the translational motion involved.

This work is being extended to other amino acids, peptides and proteins and, when all the data is available, some of the structural interpretations tentatively advanced in this present paper should become more clear.

#### *Acknowledgments*

Thanks are due to Professor C. B. Allsopp of the Physics Department, Guy's Hospital Medical School, London, for his interest and for providing the necessary facilities to enable the experimental work to be carried out. The author is also grateful to Miss M. W. Aaron of the same department for permission to quote some of the dielectric and viscosity parameters in TABLE 3 prior to publication. It gives pleasure to acknowledge the financial support of the Department of Scientific and Industrial Research of the British Government which has enabled some of the measuring equipment to be purchased.

#### *References*

- AARON, M. W. 1964. Private communication.  
AARON, M. W. & E. H. GRANT. 1963. *Trans. Farad. Soc.* **59**: 85.  
AARON, M. W. & E. H. GRANT. 1964. *Proc. 13th Colloque Ampere*. In press.  
AOKI, K. 1957. *J. Am. Chem. Soc.* **79**: 3385.  
BUCHANAN, T. J. & E. H. GRANT. 1955. *Brit. J. Appl. Phys.* **6**: 64.  
BUCHANAN, T. J., G. H. HAGGIS, J. B. HASTED & B. G. ROBINSON. 1952. *Proc. Roy. Soc. A* **213**: 379.  
GRANT, E. H. 1955. *Brit. J. Appl. Phys.* **6**: 181.  
GRANT, E. H. 1957*a*. *Phys. Med. Biol.* **2**: 17.  
GRANT, E. H. 1957*b*. *J. Chem. Phys.* **26**: 1575.  
HASTED, J. B. 1961. *Progress in Dielectrics*. :138. Heywood & Company Ltd. London, England.  
HILL, N. E. 1954. *Proc. Phys. Soc. (London)*, **B 67**: 149.  
KIRKWOOD, J. G. 1943. *Proteins, Amino-acids and Peptides*. E. J. Cohn & J. T. Edsall, Eds. Reinhold Publ. Corp. New York, N. Y.  
ONCLEY, J. L. 1943. *Proteins, Amino-acids and Peptides*. E. J. Cohn & J. T. Edsall, Eds. Reinhold Publ. Corp. New York, N. Y.

SAXTON, J. A. 1952. Proc. Roy. Soc. A 213: 473.

SCHWAN, H. P. 1957. Advances in Biological and Medical Physics. 5: 191. Academic Press. New York, N. Y.

SCHWAN, H. P. 1964. This Annal.

WYMAN, J., JR. & T. L. McMEEKIN. 1933. J. Am. Chem. Soc. 55: 908.

# SOLUTE BEHAVIOR IN TIGHTLY CROSS-LINKED DEXTRAN GELS

N. V. B. Marsden

*Institute of Physiology,  
University of Uppsala, Sweden*

The selectivity of neutral, or very weakly charged gels has aroused considerable interest in recent years.<sup>1,2</sup> These gels exhibit various kinds of selectivities of which the molecular sieve properties have attracted most attention particularly in the macromolecular domain. As yet there is no general theory regarding the mechanisms responsible for their selectivity, and it is the purpose of this paper to examine the behaviour of some low molecular nonelectrolytes in tightly crosslinked dextran gels.

In general the molecular sieving range is higher the more water the gel contains. The sieving range now available among different gels is enormous, extending from the smallest molecules up into the range of viruses and sub-cellular particles.<sup>3,4</sup>

The distribution of solutes in the tightly crosslinked dextran gels depends on both steric and interactive factors, and the selectivity range makes it possible to study solutes which are sufficiently small for analysis of their behaviour in terms of their chemical structure and interactions with the gel and the solvent water.

The dextran gels are from a biological aspect relatively simple systems, and it seems not unlikely that a study of the distribution of solutes within them may in addition yield information pertinent to solute behaviour in more complicated living systems.

## DEXTRAN GELS

The following highly crosslinked dextran gels were used:

(1) Types G-25 (Sephadex®: water regain (Wr) = 2.5 g water per g dry gel) and G-10 (Wr = 0.97). These were crosslinked with glyceryl bridges (R-O-CH<sub>2</sub>-CH(OH)-CH<sub>2</sub>-O-R).

(2) Type DVS 9 (Wr = 0.93). This was crosslinked with divinyl sulphone (R-O-CH<sub>2</sub>-CH<sub>2</sub>-SO<sub>2</sub>-CH<sub>2</sub>-CH<sub>2</sub>-O-R).

Type G-25 excludes dextran molecules of molecular weight greater than about 4000, while the limit for the other two gels is about 1000.

The glyceryl linked gels are very weak cation exchangers (< 30  $\mu$ Eq carboxyl groups per gram gel). The DVS gel which is crosslinked by a much milder procedure may be regarded as virtually neutral.

\*The gels used in these experiments were generously provided by Dr. B. Gelotte, A. B. Pharmacia, Uppsala.

Dextran, the parent of the dextran gel, is a polymer that can be obtained in an amorphous, non-crystalline state,<sup>5</sup> and provided the relative humidity is high enough the mechanism of water uptake can be regarded as essentially a solution process. Starch<sup>6</sup> and cellulose,<sup>7</sup> for example, are not so simple and possess crystalline areas which do not absorb water. Taylor, Clusky and Senti<sup>8</sup> found that for absorption of water by a dextran which showed little tendency to crystallize the Flory-Huggins theory,<sup>8</sup> which treats the polymer as though it is a randomly coiled molecule in solution, was a good model up to about 65 per cent polymer concentration. Thus as a basic material for gels, dextran seems to have the advantage of a relatively homogeneous structure, though it must be noted that the dextran (B 512) used in the gels studied here has a low degree of branching and some tendency to crystallize.<sup>6</sup>

The introduction of cross-linkages into a dextran would not be expected to promote crystallization since this tendency is lower in branched dextrans. Further, the use of glyceryl bridges means that the chemical structure of the gel is not essentially different from dextran. This is not true of the cross-linkages of the gel DVS 9, but comparison of this gel with the glyceryl linked G-10 of similar water regain indicated a similar pattern of elution behaviour for some sugars and sugar alcohols.

#### *Experimental Details*

Most of the data presented here were obtained by the elution of solutes through columns of the dextran gels (70 cm.  $\times$  0.8 cm.<sup>2</sup>). The solutes were loaded onto the column in a volume of 0.5 ml, i.e.  $< 1$  per cent of the bed volume. Elution was usually performed with a Tris HX (HCl or acetic acid) buffer ( $\mu=0.05$ ), but in some cases deionized water was used. The temperature was controlled to  $\pm 0.1^\circ\text{C}$ .

The elution volume of a test solute was compared with that of two reference solutes, (1) a high molecular weight dextran fraction ( $M_w=500,000$ ), and (2) tritiated water, to define the boundaries of the column. A third solute which eluted in the vicinity of the test solute was also used as a reference. Thus, for aldohexoses, glucose was used as a reference. In this way the uncertainty in determining the  $K_d$  value (see below) could be decreased to  $\pm .002$  units.

All solutes appeared in the effluent as single, quasi-symmetrical peaks and the elution volume was taken to be that after which the maximum concentration appeared in the effluent. The recoveries of all classes of components were measured and were in all cases 100 per cent  $\pm 3$  per cent.

Wheaton and Bauman<sup>9</sup> expressed the dynamic distribution coefficient ( $K_d$ ) of the column as

$$K_d = \frac{V_i - V_o}{V_T - V_o} = \frac{V_i - V_o}{V_I} \quad (1)$$

where  $V_i$  is the effluent volume after which the test solute appears,  $V_o$  is the volume (void) of water outside the gel particles,  $V_T$  is the total volume of water in the column and  $V_I$  is the water volume within the wet particles of gel (= water regain).

It will be assumed that the  $K_d$  value is a true molal distribution coefficient between the phases inside and outside the gel, because (1) the  $K_d$  values (see below) were not affected if the flow rate through the column was considerably increased<sup>10</sup>, (2) the equilibrium distribution coefficient for glucose in a dextran gel (water regain 2.5) was 0.74 while column distribution coefficients measured on other batches with nominally the same water regain values were similar, i.e. 0.78 and 0.80, and (3) Ackers<sup>11</sup> also reported good agreement for equilibrium and column distribution coefficients on a dextran gel type G-75.  $V_I$  may be defined as the total water volume of the system minus the volume of water outside the particles. This latter is usually defined by the space in which a macromolecule such as dextran is distributed.  $H_2^{18}O$  would be a satisfactory indicator of the total water space in a gel system but for ease of measurement tritiated water (THO) has been used instead. Tritium, however, exchanges with hydrogen under certain conditions. It must thus be expected that it exchanges with the three hydroxyl hydrogen atoms of the glucose residue in the dextran chain (and the hydroxyl hydrogen of the glyceryl bridge) since deuterium of  $D_2O$  was found to exchange rapidly with the corresponding hydrogen atoms in the glucose residues of starch and amylose.<sup>12</sup>

The total volume ( $V_{THO}$ ) determined from the distribution of THO is therefore

$$V_{THO} = V_I + V_X + V_o \quad (2)$$

where  $V_X$  corresponds to the tritium which has exchanged with the gel, and we define (in analogy with Equation 1)

$$K_T = \frac{V_i - V_o}{V_I + V_X} \quad (3)$$

and therefore

$$K_d = \frac{V_I + V_X}{V_I} \cdot K_T \quad (4)$$

#### *Evaluation of $(V_I + V_X)/V_I$*

The magnitude of  $V_X$  will vary inversely with the water regain value. Dextran gel (type G-25) is cross-linked with glyceryl bridges which also have one exchangeably hydroxyl hydrogen atom. If each third residue is attached to a cross bridge\*, it may be calculated that the amount of tritium

\*The data on cross-linking density were kindly provided by Mr. B. Söderqvist. activity which can exchange with the gel is 5.9 per cent of the total activity in the wet gel particle, i.e.  $(V_I + V_X)/V_I = 1.06$ .

Samples of gel type G-25 dried for 48 hours at 105°C. (this is probably not sufficient to remove all traces of water) were mixed with known weights of water containing THO. The tritium activity in the gel corresponded to about 106 per cent of that expected if it had been distributed only in the water.

In gel DVS 9 (water regain 0.93) where there is roughly one sulphone cross bridge (with no exchangeable hydrogen) per glucose residue  $(V_I + V_X)/V_I$  will have the value 1.12.

### *Solutes*

The main part of the data concerns non-electrolytes eluted through the gel DVS 9. Four series of solutes were studied: (a) acyclic polyols, (b) aldoses,\* (c) n-alcohols and (d) alkane diols together with urea, formamide and acetone. In addition  $K_d$  values of some mono-substituted benzoates in gel type G-25 are given.

### *Concentration of Solutes*

In most cases solutes were loaded on to the columns in concentrations below 0.1 M and determined in the effluent samples, either as their radioisotopically labelled derivatives, or chemically. Non-electrolyte behavior appears to be largely independent of concentration, thus the  $K_d$  values were unaltered in the following loading concentration ranges: (a) glucose: trace — 0.5 M, (b) ethylene glycol: trace — 1.7 M, (c) urea: 0.02 — 0.6 M and (d) methanol: 0.003 — 1.6 M. The alkaline diols were measured refractometrically and the loading concentration was 10 per cent. In some cases the  $K_d$  values of the glucose reference were abnormal, though the deviations were never more than about 6 per cent (normally S.D. =  $\pm 1$  per cent). It is thus possible that the  $K_d$  is affected at higher concentrations in some cases.

In all cases where a solute was determined both by its radioactivity and chemically, the  $K_d$  values calculated from these two methods did not differ significantly. †

### BEHAVIOR OF NON-ELECTROLYTES IN GEL DVS 9

The selectivity of the gel DVS 9 for small molecules and ions is much greater than that of type G-25 and this gel can be used for the separation of the alkali metals<sup>15</sup> or halides.<sup>16</sup> It must be noted, however, that an ion

\*Dr. H. S. Isbell very kindly provided some of the rarer sugars.

†It has been reported however that D-Lyxose-1-<sup>14</sup>C<sup>13</sup> and L- and D-Arabinose-1-<sup>14</sup>C<sup>14</sup> migrated more slowly in a cyclohexane-ethanol counter current system than their inactive forms. The presence of a <sup>14</sup>C atom at C1 position in ribose and xylose produced no effect, however, and neither did the labelling of arabinose at C5 instead of C1. These results were interpreted as indicating that the lower electronegativity of the <sup>14</sup>C atom as compared with <sup>12</sup>C produced inductive effects which in some cases affected the dipole moment of the aldose.

cannot be characterized by an isothermal  $K_d$  value which is dependent only on the solvent and essentially independent of the other solutes present. In addition to the great effect exerted by the counter ions the elution position of an ion is influenced by the other co-ions present,  $pH$ , concentration and temperature. Studies on electrophoresis of ions through membranes consisting of dextran gel suspensions have also indicated complex interactions.<sup>17</sup>

### *Acyclic polyols*

The general formula for this series is  $CH_2OH - (CHOH)_n - CH_2OH$  with  $0 \leq n \leq 4$  in the present case. The  $K_d$  values are related inversely to molecular weight as is shown in FIGURE 1 and TABLE 1. The  $K_d$  differences between the two hexitols and between the two pentitols are very small compared with the variations among the aldohexoses and aldopentoses (see TABLE 3). Whether the other isomeric alditols also have similar  $K_d$  values is not known, but Isherwood and Jermyn<sup>18</sup> found similar  $R_F$  values for sorbitol and dulcitol in paper chromatography.

As has been mentioned earlier it will be assumed that the  $K_d$  values reported in this paper represent quasi-equilibrium conditions within the gel particles and thus are a measure of the distribution coefficient. It has been

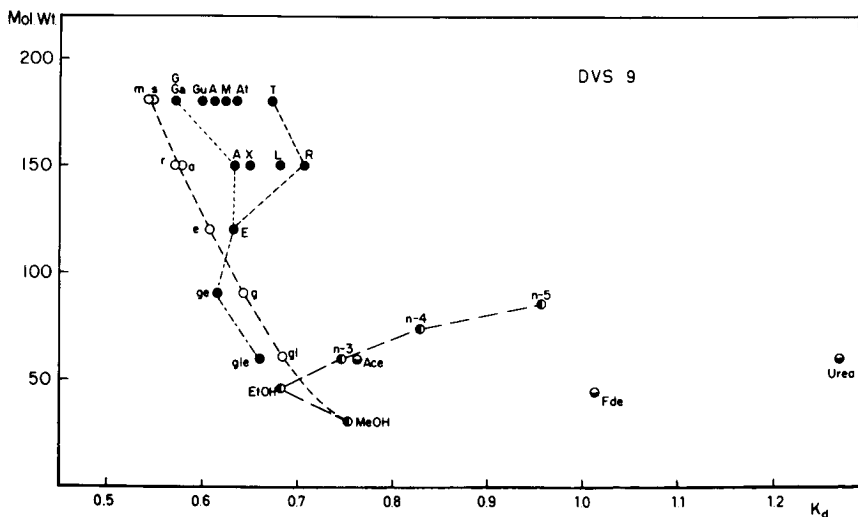


FIGURE 1. Gel DVS 9.  $K_d$  values of some non-electrolytes in relation to molecular weight. *Polyols*: m = mannitol, s = sorbitol, r = ribitol, a = arabitol, e = erythritol, g = glycerol, gl = ethane diol. *D-Aldoses*: C<sub>6</sub>, G = glucose, Ga = galactose, Gu = gulose, A = allose, M = mannose, At = altrose, T = talose; C<sub>5</sub>, A = arabinose, X = xylose, L = lyxose, R = ribose; C<sub>4</sub>, E = erythrose and ge = glyceraldehyde and gle = glyceraldehyde. *Alkanols*: n-5 = n-Pentanol, n-4 = n-Butanol, n-3 = n-Propanol, EtOH = ethanol, MeOH = methanol. Ace = acetone, Fde = formamide.



TABLE 1  
POLYHYDRIC ALCOHOLS: Gel DVS 9, 25°C.

Polyol	Mol Wt	$V_m^*$	$K_d$	$\Delta (\log K_d)$
Ethane diol	62	66.6	0.684	-0.0255
Glycerol	92	96.2	0.645	-0.0250
Erythritol	122	125.8	0.609	-0.0243
Pentitol†	152	155.4	0.576	-0.0226
Hexitol‡	182	185.0	0.547	

\* $V_m$  = molal volume calculated from atomic volumes<sup>20</sup>

†Mean of ribitol and arabitol

‡Mean of mannitol and sorbitol

suggested that hindered diffusion may contribute to the differences between migration rates of solutes through a column, but this seems unlikely for small solutes at least in moderately tightly cross-linked gels. Horowitz and Fenichel<sup>19</sup> studied a series of low molecular weight solutes differing in both size and polarity in a dextran gel containing 83 per cent water (water regain  $\sim 5$ ) and concluded that the diffusional specificity was essentially the same as in free water, i.e. there appeared to be no increasing hindrance with increasing molecular size or change of polarity. The gel DVS 9 from which most of the data reported here is obtained, however, contains considerably less water (45 per cent w/w) and it cannot be excluded that such a dense polysaccharide matrix may affect diffusion coefficients. It is true that the diffusion coefficients of, for example, urea and ethyl acetate in sulphonated polystyrene gels varied differently with different counter ions and hence degree of swelling.<sup>21</sup> This effect, however, may be due to the presence of ions and their effects on the water structure in their vicinity (see below).

In their now classic paper Lathe and Ruthven<sup>22</sup> observed that starch columns exerted a molecular sieve effect on non-electrolytes, and suggested that such a system might be used for molecular weight determinations. Recently dextran gels of high water regain value have been used for this purpose.<sup>23-25</sup>

Various geometrical models of the internal spaces within the gel<sup>1,23,26,27</sup> have been proposed to account for the molecular sieve properties which Pedersen<sup>28</sup> suggested might be called "exclusion chromatography." Common to these models is the assumption that the selectivity lies in some sort of steric hindrance by the gel chains and cross-links creating forbidden domains for solute molecules within the wet gel particles. Calculations based on such models have given reasonably good fits for selected solutes for the relationship between some molecular size parameter such as the Einstein-Stokes radius and the elution volume. Laurent and Killander<sup>27</sup> treated the wet gel as a random suspension of fibres<sup>29</sup> and solutes as spherical particles. In this model the volume within the gel which is available for the solute depends on the distance of the center of the solute molecule from that of the polyglucose chain of the gel at the position of closest approach; the greater the center-to-center distance, the greater the exclusion of the solute. This model thus has the important characteristic, in contradistinction to other models, that it does not postulate any locality within the gel where a solute molecule may not approach the gel chains. All the gel matrices would therefore be able to partake in possible interactions with solutes. This difference would have important consequences, as will be discussed below.

The success of these models in predicting the relationship of the slope between the elution volume and a molecular size parameter is presumably limited to solutes whose interactions with the gel are either negligible or similar and for which size is the overriding difference. Thus the geometric model cannot alone predict the absolute value of the  $K_d$  since this may depend also on other interactive factors, but the model is very useful for solutes where the latter are similar. The subtractive effect on the  $K_d$  of increasing molecular size is perhaps analogous to the situation discussed by Martin<sup>30</sup> for partition chromatography between two phases. Martin inferred that as a first approximation the free energy ( $\Delta G^\circ$ ) required to transport a molecule from one solvent phase to another is the sum of the free energies required for transport of the individual constituent groups of the molecule. Thus since

$$\Delta G^\circ = -RT \ln K_d \quad (5)$$

the logarithm of the distribution coefficient is also the sum of the contributions of the individual groups. For a series such as the polyols where the same group is added repeatedly in ascending the series the difference between any two members of the series ( $\Delta \log K_d$ ) should be constant. As can be seen in TABLE 1 this was approximately true for the polyols.

A swollen cross-linked gel network may be regarded as a solution of an elastic rather than viscous type.<sup>31</sup> The swelling equilibrium is a balance of two opposing forces, the tendency for dissolution being resisted by the

elasticity of the gel matrix, creating a pressure which increases the chemical potential of the solvent in the swollen gel to equal that in the solvent outside the particles. To quote Flory<sup>31</sup> the "network structure performs the multiple role of solute, osmotic membrane and pressure generating device." The internal pressure will affect the activities of components within the wet gel. Thus

$$\pi V_i = -RT \ln \frac{a_i^g}{a_i^o} \quad (6)$$

where  $\pi$  is the internal pressure of the gel closely analogous to osmotic pressure  $V_i$  = partial molal volume of the solute and  $a_i^g$  and  $a_i^o$  are its activities in gel and external solution respectively. From equation (6) it can be seen that for a given internal pressure the reduction in activity of a species within the gel will be proportional to its partial molal volume, and since the distribution coefficient is the ratio of the activities in the two phases, this will also vary inversely with the partial molal volume of the solute.

The difficulty in assessing the magnitude of this effect is that if two dextran gels with different internal pressures are compared, they have different water regain values and hence different degrees of cross-linking. From a structural point of view, however, the glyceryl cross bridges are very similar to the glucose residues of the dextran chains, and variation in the degree of cross-linking should not alter the gel very much apart from its ability to swell. Ginzburg & Cohen<sup>32</sup> attempted to overcome this difficulty by studying the partition of some polyhydric alcohols and sugars in a more swollen ( $\text{Li}^+$ ) and a less swollen ( $\text{NH}_4^+$ ) form of the sulphonated polystyrene Dowex 50, thus using the same gel with different degrees of swelling and hence different internal pressures. There appeared to be a general trend for the  $K_d$  value to be lower in the more highly swollen  $\text{Li}^+$  form, a result apparently at variance with a steric exclusion mechanism but predicted by equation (6) providing that a pressure difference was the only significant factor. Wheaton and Bauman,<sup>33</sup> however, found that while the  $K_d$  value of glycerol was lower in the  $\text{H}^+$  form than in the less swollen  $\text{Na}^+$  form of Dowex 50, the reverse was true for triethylene glycol and ethylene glycol (for the latter solute Ginzburg & Cohen found no significant difference between the  $\text{Li}^+$  and  $\text{NH}_4^+$  forms).

It is questionable, however, whether the states of water are the same in the different ionic forms of the resin and the lower  $K_d$  values found in the more swollen  $\text{Li}^+$  form may possibly be a salting out effect.

All the water in a sulphonated polystyrene resin is closely associated with ions and the molal water:ion ratio is low. In solution  $\text{Li}^+$  has a structure ordering effect on the water molecules in its immediate vicinity,<sup>34</sup> while  $\text{NH}_4^+$  which has a similar entropy of hydration to  $\text{K}^+$ <sup>35</sup> may be expected

to have a small disordering effect.\* Although the terms "free" and "hydration" water are thermodynamically unsatisfactory, they serve to indicate that some of the water may be associated more closely with an ion.<sup>32</sup> Glueckauf & Kitt<sup>36</sup> give the hydration numbers of  $\text{Li}^+$  as 3.3 and  $\text{NH}_4^+$  as  $\sim 0.7$  in a sulphonated polystyrene. Thus although the total water content of the more swollen  $\text{Li}^+$  form is higher than that of the  $\text{NH}_4^+$  form, the "solvent" water available for the nonelectrolytes may be actually less.

More work is required to elucidate the importance of the pressure factor. Laurent<sup>37</sup> compared the behaviour of some macromolecules in both hyaluronic acid gels and solutions. There was some exclusion from the solutions where the internal pressure should be zero.

It is however of interest that the exclusion from hyaluronic acid solution was somewhat lower than that calculated for a gel of similar hyaluronic acid concentration.<sup>37</sup> It would be interesting to know whether a pressure factor contributed to the apparent greater exclusion ability of the gel.

### *Aldoses*

The relationship between  $K_d$  and molecular weight is not monotonic as with the polyols, and the isomeric aldoses exhibit considerable variation in  $K_d$  values (FIGURE 1, TABLE 3). These variations do not, however, necessarily indicate the effect of other interactions in addition to steric factors. Substitution of molecular weight by a more precise parameter such as the partial molal volume in solution is unlikely to remove the apparent  $K_d$  variation among, for example, the aldohexoses. Closer examination of the probable structure of the aldoses suggests that variations in conformation may be the cause of the  $K_d$  differences.

The lower members of the aldose series glyceraldehyde and glyceraldehyde had a roughly similar "slope" to the polyols but their  $K_d$  values may be somewhat low due to dimerization<sup>38</sup> as their mean concentration in the column was about 0.02 M. Thus the apparent reversal in the direction of the aldose line between the  $\text{C}_3$  and  $\text{C}_4$  stages may not be real. On the other hand there is a real positive slope for the  $K_d$ —molecular weight line between erythrose and the pentoses. This coincides with the transition from the rigid furanose to the flexible pyranose ring and the wide variation in  $K_d$  values is presumably associated with the different spatial arrangement of the hydroxyl groups which will have steric and possibly interactive consequences. Subsequently in the pentoses and hexoses the variation is great but the  $K_d$  changes within a homomorphous series<sup>38</sup> (see TABLE 4) all go in the same direction, i.e. a hexose has a lower  $K_d$  than its homomorphous pentose.

\*In view of the similarity in size between  $\text{NH}_4^+$  and water, the disordering effect may be very small.

TABLE 2  
 $K_d$  VALUES OF FOUR ENANTIOMORPHIC ALDOSE PAIRS: Gel DVS 9,  $T = 25^\circ\text{C}$ .

Sugar	L-	D-	L - D
Arabinose	0.647	0.646	.001
Xylose	0.659	0.657	.002
Glucose	0.576	0.573	.003
Mannose	0.627	0.626	.001

TABLE 2 shows that there was no significant difference between the  $K_d$  values of the D and L forms of arabinose, xylose, glucose, or mannose. This suggests that specific adsorption to the gel is not important for these sugars since the asymmetric glucose residues might be expected to exhibit some selectivity towards enantiomorphs.

The point at which the  $K_d$  behaviour diverges from the simple sort of relationship of the polyols coincides with the appearance of cyclic forms and marked conformational variations, and the following discussion applies to the aldopentoses and aldohexoses.

Free forms of these sugars in aqueous solution probably exist in both acyclic forms (polyhydroxyaldehydes) and cycle forms (polyhydroxyhemiacetals). Ring closure of the open chain transfers the carbonyl oxygen ( $\text{C}=\text{O}$ ) to the ring and creates a new asymmetric carbon atom ( $\text{C}_1$ ) with two possible configurations of the hydroxyl group and the sugar in aqueous solution mutarotates to yield an equilibrium mixture of these  $\alpha$  and  $\beta$  anomers. Mutarotation from one cyclic anomer to the other is thought to require the intermediate formation of the acyclic aldehyde form.<sup>38</sup> The  $\alpha/\beta$  anomeric ratios for some of the hexoses are given in TABLE 3.

Although each sugar is a mixture of two anomers the elution profiles were always single and not skewed. This is presumably because mutarotation is a much faster process than elution and the  $K_d$  value obtained is a mean of those of the  $\alpha$  and  $\beta$  anomers.<sup>39</sup> The dextran gel might in fact accelerate mutarotation were a component not in anomeric equilibrium, but it is also possible (as suggested by Dr. H. S. Isbell) that the gel alters the anomeric equilibrium ratio.

The tetroses can form the rigid five-membered furanose ring in which form they probably exist in solution, as there is no evidence of dimerization as in the linear homologues.<sup>38</sup> The most usual cyclic form of the aldopentoses and aldohexoses is the more flexible six membered pyranose ring. The pyranose ring, which contains 5 carbon and 1 oxygen atom, differs geometrically very little from the cyclohexane ring, which theoretically, it was shown, can exist in an infinite number of strain free conformations.<sup>40</sup>

TABLE 3

INSTABILITY FACTORS AND  $K_d$  VALUES OF ALDOPYRANOSSES: \* DVS 9,  $T=25^\circ\text{C}$ .[A anomer; AE composition of the and anomers after mutarotation; C1, 1C instability ratings in these two conformations; (C1), (1C) weighted sum (Kelly) of instability ratings;  $R_F$  values are those of Ref. 18.]

	A	AE	Instability Rating				$K_d$	$R_F$
			C1	$\Sigma(\text{C1})$	1C	$\Sigma(1\text{C})$		
D-Arabinose	$\alpha$		(1,2,3)	(3)	4	1	0.646	0.23
	$\beta$		( $\Delta$ 2,3)	(3.5)	1,4	2		
D-Xylose	$\alpha$		1	1	( $\Delta$ 2,3,4)	(4.5)	0.657	0.28
	$\beta$		-	0	(1,2,3,4)	(4)		
D-Lyxose	$\alpha$	76.0 —	1,2	2	3,4	2	0.683	0.30
	$\beta$	24.0	$\Delta$ 2	2.5	1,3,4	3		
D-Ribose	$\alpha$		1,3	2	( $\Delta$ 2,4)	(3.5)	0.710	0.33
	$\beta$		3	1	(1,2,4)	(3)		
D-Galactose	$\alpha$	29.6 —	1,4	2	(H, $\Delta$ 2,3,5)	(6)	0.573	0.175
	$\beta$	70.4	4	1	(H,1,2,3,5)	(5.5)		
D-Glucose	$\alpha$	36.2 —	1	1	(H, $\Delta$ 2,3,4,5)	(7)	0.573	0.195
	$\beta$	63.8	-	0	(H,1,2,3,4,5)	(6.5)		
D-Gulose	$\alpha$	18.5 —	1,3,4	3	( $\Delta$ 2,5)	(4.5)	0.605	0.23
	$\beta$	81.5	3,4	2	H,1,2,5	(4.5)		
D-Allose	$\alpha$		1,3	2	( $\Delta$ 2,4,5)	(5.5)	0.614	0.22
	$\beta$		3	1	(H,1,2,4,5)	(5.5)		
D-Mannose	$\alpha$	68.8 —	1,2	2	(H,3,4,5)	(4.5)	0.626	0.24
	$\beta$	32.2	$\Delta$ 2	2.5	(H,1,3,4,5)	(5.5)		
D-Altrose	$\alpha$		1,2,3	3	H,4,5	3.5	0.638	0.27
	$\beta$		$\Delta$ 2,3	3.5	H,1,4,5	4.5		
D-Talose	$\alpha$	55.9 —	1,2,4	3	H,3,5	3.5	0.676	0.285
	$\beta$	44.1	$\Delta$ 2,4	3.5	H,1,3,5	4.5		
D-Idose	$\alpha$		(1,2,3,4)	4	5	2	—	0.31
	$\beta$		$\Delta$ 2,3,4	4.5	H,1,5	3.5		

\*The figures in parentheses refer to conformations which are unlikely to be present in significant amounts.

Applying this to the pyranose ring where, because of the asymmetry, each conformation produces a unique structure, Reeves<sup>41</sup> postulated that there will be two rigid "chair" forms (designated C1 and 1C) and an infinite number of flexible "boat" forms, which may be described in terms of six specific forms whose interconversion involves little ring strain. Interconversion of the rigid chair forms, on the other hand, involves considerable deformation and rotation of the ring valences.

The sugar in solution is thus an equilibrium of a number of conformations of the pyranose ring in addition to possible acyclic and furanose forms. The evidence seems to favour the predominance of chair forms of most of the aldopentoses and aldohexoses and an apparent correlation between the so called instability rating and the order of  $K_a$  values will be discussed below. The most stable form<sup>42</sup> will be that in which the substituents are staggered (chair form) with respect to each other; if viewed down the axis of a C-C bond the substituent group of the further atom would not be eclipsed, i.e. in line with the substituents of the nearer atom. This will occur in the boat forms and the substituents on adjacent carbon atoms will approach each other so closely that van der Waal's repulsion (destabilizing) forces will oppose this conformation. Thus energetically the "staggered" chair conformation will be preferred to the boat form unless other considerations make the chair form energetically unfavourable.

In the aldopyranoses the assumption of a chair form in solution means that in all cases except  $\beta$ -D-Xylose and  $\beta$ -D glucose some of the substituents (other than hydrogen) will lie axially.

FIGURE 2 illustrates the structure of the chair forms and shows (III) that equatorial groups ( $e_1, e_2$ ) on adjacent carbon atoms are directed within  $30^\circ$  of the plane of the ring but do not eclipse each other, while axial groups ( $a_1, a_2$ ) are nearly perpendicular to the plane of the ring. The staggering of the substituents means that if hydroxyls on adjacent carbon atoms are *cis* they will have different directions (i.e.  $ea$  or  $ae$ ) while if they are *trans* they will be either both equatorial or both axial [FIGURE 2 (II)].

The positions of the hydroxyl groups at carbon atoms 1, 2, 3 and 4 ( $C_{1-4}$ ) and the exocyclic carbinol group at  $C_5$  affect the conformational stability and chemical reactions of the ring.<sup>43</sup> An axial position creates instability, and in general the chair conformation most preferred will be that with most bulky or polar substituents equatorial. Most sugars could theoretically be arranged with all their hydroxyl groups equatorial in a boat form, and although a pure boat form is improbable on energetic grounds, it is possible that distorted boat forms exist because of this tendency of axial groups to become equatorial.<sup>44</sup>

The instability rating depends on the presence of axial groups and the weights attached to them. Two axial arrangements appear to be particu-

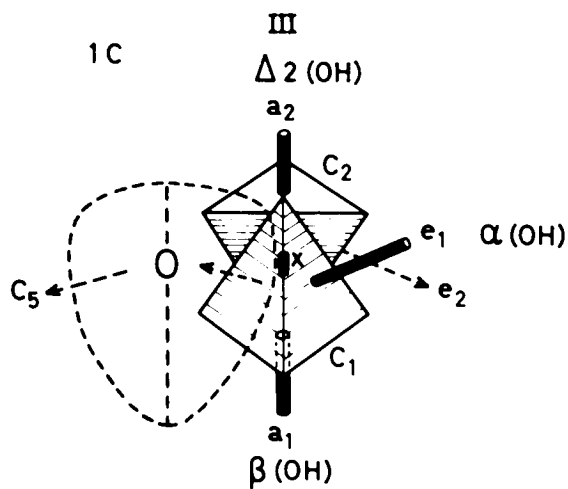
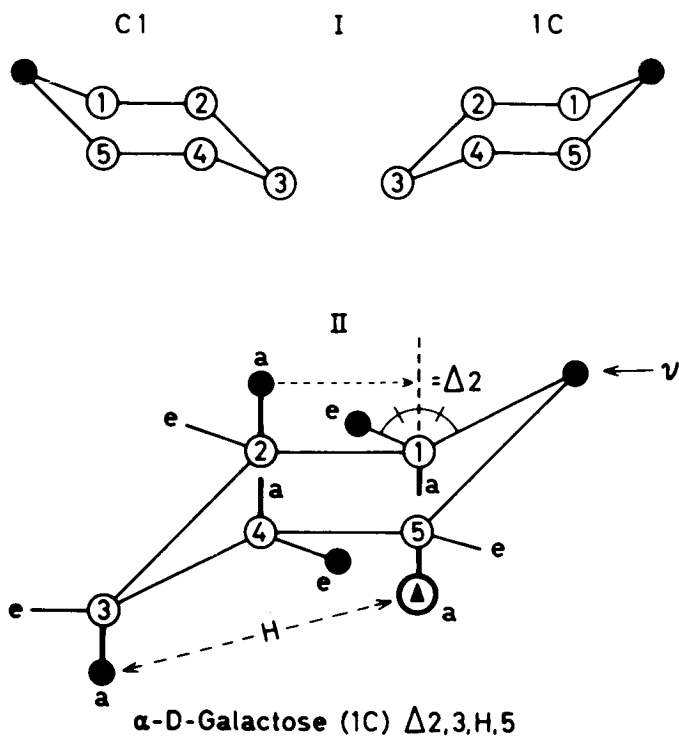


FIGURE 2.



larly important.<sup>43</sup> The  $\Delta 2$  factor occurs when the C-O bond at C<sub>2</sub> bisects the two C-O valences of C<sub>1</sub>; this can only occur if the hydroxyls at C<sub>1</sub> and C<sub>2</sub> are *cis* and in the  $\alpha$  anomer in the 1C form (FIGURE 2, III) and in the  $\beta$  anomer in the C1 form. The Hassel-Ottar (H) effect<sup>45</sup> occurs when the carbinol at C<sub>5</sub> is axial on the same side of the ring as another axial hydroxyl (FIGURE 2, II).

Kelly<sup>46</sup> weighted the instability factors as follows: axial OH = 1 unit,  $\Delta 2$  = 2.5 units, C<sub>5</sub>-CH<sub>2</sub>OH axial, without H effect = 2.0 units, with H effect = 2.5 units.

If the instability rating (sum of the weighted instability factors) of the two chair conformations differ by one unit, or less, then the presence of both C1 and 1C forms is presumed. If the difference is more than one unit, it is assumed that the sugar is entirely in the conformation with the lower instability rating.<sup>43,46</sup> Reeves<sup>43</sup> also proposed that whatever the difference a rating of 2.5 units or more would produce instability; this would mean that the  $\Delta 2$  factor alone could induce conformational instability.

When attempting to correlate these instability factors with other data, due weight should be given to the anomeric equilibrium, and it should also be borne in mind that, in addition to possible boat or distorted boat forms, furanose rings or acyclic forms may also be present in significant proportions in some cases.

TABLE 3 gives K<sub>a</sub> values and instability data for the C1 and 1C forms of the aldopentoses and aldohexoses. Of the aldopentoses arabinose and xylose have low instability ratings and the lowest K<sub>a</sub> values of the pentoses, while glucose and galactose have the lowest instability ratings and K<sub>a</sub> values of the hexoses. Lyxose has a higher K<sub>a</sub> value than xylose or arabinose and has a high instability rating, complex mutarotation and calculations of its molecular optical rotation suggest the presence of both C1 and 1C forms.<sup>47</sup>

FIGURE 2. Chair conformations of the pyranose ring. I, the two conformations C1 and 1C; the terminal black circle is the ring oxygen atom. II,  $\alpha$ -D-Galactose(1C) showing the relative positions of the hydroxyl groups (black circles). e and a refer to the equatorially and axially directed valences respectively. v is the ring oxygen atom and the carbinol group is axial at C<sub>5</sub>. Note (a) that the carbon-oxygen (hydroxyl) bond at C<sub>2</sub> bisects the angle between the two C-O bonds at C<sub>1</sub> ( $\Delta 2$  effect) and (b) the Hassel-Ottar effect when there is another hydroxyl axial on the same side of the ring as the carbinol group at C<sub>5</sub>. The instability rating is given below. III, A Courtauld model of the right hand end of the 1C form (viewed in the direction 'v' indicated in II). The ring oxygen atom is in dotted outline (O) with the bond to C<sub>5</sub> also dotted. The tetrahedra of C<sub>1</sub> and C<sub>2</sub> are shown (X is the C<sub>1</sub>-C<sub>2</sub> bond) and the dotted arrow is the C<sub>1</sub>-O bond.  $\alpha$  (OH) and  $\beta$  (OH) refer to the anomeric hydroxyl group. The model shows (1) the bond angles and (2) the  $\Delta 2$  effect with a<sub>2</sub> bisecting the angle between e<sub>1</sub> and the C<sub>5</sub>-O bond. This can only occur with a non-erected (equatorial) hydroxyl at C<sub>1</sub>, i.e. in the  $\alpha$  anomer in the 1C form and in the  $\beta$  anomer in the C1 form.

Ribose is apparently anomalous, it has the highest  $K_d$  value of the pentoses and has a low instability rating. However, it has a complex mutarotation and contains at least 8.5 per cent of a reducible form<sup>48</sup> which may represent the acyclic aldehyde (the reducible contents of the other pentoses at pH 7.6 do not exceed 0.4 per cent). The presence of an open chain form would be expected, however, by analogy with ribitol (interactions being equal) to reduce the  $K_d$  value.

The three aldohexoses with the highest  $K_d$  values also have the  $\Delta 2$  factor in their probably preferred forms while the two highest also exhibit the H factor in their 1C forms.

Erection of a hydroxyl group (i.e. transfer from an equatorial to an axial position) at  $C_2$  or  $C_3$  is associated with an increase of  $K_d$ , the effect being greater at  $C_2$  (this involves the  $\Delta 2$  factor in the C1 form of the  $\beta$  anomer). Erection at  $C_4$  appears to have little effect (as evidenced by the closeness of xylose-arabinose, glucose-galactose and allose-gulose) except when the  $C_2$  hydroxyl is also erected (talose).

The effects of erection at  $C_1$  are difficult to assess because each sugar is an anomeric mixture in solution. More data on the anomeric equilibrium values might be of help both in this respect and as regards the weighting of the contributions of the  $\alpha$  and  $\beta$  anomers to the instability rating.

The right hand column of TABLE 3 shows the  $R_F$  values obtained in paper chromatography<sup>49</sup> with an ethyl-acetate-pyridine-water mixture as the solvent. The order is generally similar (in reverse) to that found for the dextran gel.

Though there is a large variation among the pentoses and hexoses, TABLE 4 shows that  $K_d$  always decreases with increase of molecular weight among the members of a homomorphous series. Here it is evident that if addition of the carbinol group at  $C_5$  of the pentose induces greater conformational instability the  $K_d$  is changed less than when the hexose has a conformational stability similar to the parent pentose.

Finally the  $K_d$  differences between mannose and glucose and their  $\alpha$ -methylpyranosides are not significantly different (TABLE 4). Thus methylation, which does not alter the conformations of two hexoses (with different  $K_d$  values), has the same effect on  $K_d$  in both cases. This effect is then due to the bulk and/or effect on interactions of the methyl group.

In addition to any steric effects, conformational variations or instabilities may affect the interactions of the sugar with the gel or water. Changes in distribution of the hydroxyl groups of the sugars alter both the geometry of the molecule and its interactions with neighbouring species.

Kuhn<sup>19</sup> found no evidence of intermolecular hydrogen bonding for a series of diols below a concentration of 0.005 M. Thus this can be neglected for the sugars since the  $K_d$  was concentration independent. It is also highly probable that the presence of water obliterates all intramolecular hydrogen

TABLE 4  
 $K_d$  VALUES AND INSTABILITY RATINGS OF HOMOMORPHOUS SERIES  
 $(\Delta K_d^1 = \text{difference between pentose and hexose}; \Delta K_d^2 = \text{difference between hexose and methyl-pyranoside.})$   
 Other notations are same as in TABLE 3.)

	pentoses				hexoses						-methyl hexapyranoside		
	$K_d$	A	$\Sigma(C1)$	$\Sigma(1C)$	$K_d$	A	$\Sigma(C1)$	$\Sigma(1C)$	$\Delta K_d^1$	$K_d$		$K_d$	$\Delta K_d^2$
D-Ribose	0.710	$\alpha$ $\beta$	2 1	0 0	D-Allose	$\alpha$ $\beta$	2 1	0 0	0.093				
L-Ribose	(0.710)	$\alpha$ $\beta$	0 0	1 2	D-Talose	$\alpha$ $\beta$	3 3.5	3.5 4.5	0.034				
D-Arabinose	0.646	$\alpha$ $\beta$	0 0	1 2	D-Altrose	$\alpha$ $\beta$	3 3.5	3.5 4.5	0.008				
L-Arabinose	0.647	$\alpha$ $\beta$	1 2	0 0	D-Galactose	$\alpha$ $\beta$	2 1	0 0	0.074				
D-Xylose	0.657	$\alpha$ $\beta$	1 0	0 0	D-Glucose	$\alpha$ $\beta$	1 0	0 0	0.084	gluco-	0.496	0.077	
L-Xylose	0.659	$\alpha$ $\beta$	0 0	1 0	D-Gulose	$\alpha$ $\beta$	3 2	0 0	0.059				
D-Lyxose	0.683	$\alpha$ $\beta$	2 2.5	2 3	D-Idose	$\alpha$ $\beta$	0 4.5	2 3.5					
L-Lyxose	(0.683)	$\alpha$ $\beta$	2 3	2 2.5	D-Mannose	$\alpha$ $\beta$	2 2.5	0 0	0.061	manno-	0.551	+0.075	

\*The instability ratings do not include the non-probable conformations.

bonding.<sup>50</sup> Thus the only interactions to be considered are solute-solvent, solute-gel and gel-solvent, but their reciprocity must be borne in mind.

Equatorial hydroxyl groups in alicyclic compounds are, in general, more strongly adsorbed than axial groups.<sup>42</sup> Specific adsorption seems unlikely in view of the lack of any differences between the enantiomorphs, though the temperature dependence of the  $K_d$  value of glucose indicates the probability of some interaction.

Kabayama and Patterson<sup>50</sup> suggest that  $\beta$ -D-Glucose (and  $\beta$ -D-Xylose) with all their hydroxyl groups equatorial (instability rating of zero) can fit into a water lattice with all hydrogen bonds unbent. Axial hydroxyl groups will, on the other hand, involve considerable hydrogen bond bending if the sugar is to be fitted into a water lattice.

Glucose and xylose have lower  $K_d$  values than most of their isomers and from an interactive view point this suggests that they may have either a relatively low affinity for the gel or a high affinity for water. It is only their isomers with a hydroxyl group erected at  $C_1$  (galactose and arabinose) that have similar or slightly lower  $K_d$  values. It would be interesting to have more information about the hydrogen bond deformations expected from incorporation of an axial  $C_1$  hydroxyl into the water lattice compared with the situation with other axial hydroxyls ( $C_2$ ,  $C_3$ ) which affect the  $K_d$  value much more.

*N-Alkanols, Alkane Diols, Acetone, Formamide, Urea and Thiourea*

The  $K_d$  value of ethanol is lower than that of methanol but subsequently there is a reverse trend (FIGURE 1). As this series is ascended, there is a progressive increase in the length of the non-polar chain with a constant increment of  $C - CH_2 -$ . The change in molecular properties, however, outweighs completely any  $K_d$  reducing steric effect of this group; instead there is a net increase. This phenomenon was first observed in the presence of 0.05 M Tris-HCl ( $pH$  7.6) but cannot be attributed to a "salting in" effect that increases with ascent of the series because the  $K_d$  values remained the same when deionized water was the eluant. A similar ascending order was found for the molal distribution coefficients of ethanol, n-propanol and n-butanol in a sulphonated polystyrene resin (Dowex 50) in the  $H^+$  form.<sup>51</sup>

The  $K_d$  values of the diols decrease with increase of molecular size from ethylene glycol through to the butane diols (TABLE 5). Thereafter there is an increase in  $K_d$  to 1.5 pentane diol. Thus reversal occurred when the hydroxyl bearing carbon atoms were separated by a three carbon chain.

This may be analogous to the n-alcohols where it is not until the three carbon stage (n-propanol) that  $K_d$  reversal occurs. The relationship cannot be as simple as in the n-alcohols, however, since 1.6 hexane diol has a

TABLE 5  
ALKANE DIOLS: Gel DVS 9; T = 25°C.  
[Concentration of diol loaded onto column was 10 per cent (W/W)]

Diol	Mol. Wt.	K <sub>d</sub>
Ethylene glycol	62	0.68
1.2 Propane	76	0.65
1.3 Propane	76	0.66
1.3 Butane	90	0.60
1.4 Butane	90	0.64
2.3 Butane	90	0.62
1.5 Pentane	104	0.72
1.6 Hexane	118	0.68

K<sub>d</sub> value a little less than that of 1.5 pentane diol, and not unexpectedly there is some variation among the different butane diols.

Acetone, which is weakly polar, has a K<sub>d</sub> value near to n-propanol (FIGURE 1).

The effect of non-polar groups is illustrated in TABLE 6, which gives the changes in K<sub>d</sub> produced by hydroxyl substitution in the pentane and hex-

TABLE 6  
EFFECT OF HYDROXYL SUBSTITUTION ON N-ALKANES: DVS 9, T = 25°C.  
(C<sub>n</sub>/(OH)<sub>m</sub> = number of carbon atoms divided by number of hydroxyl groups; V<sub>m</sub> = molal volumes as calculated from Ref. 20.)

Derivative	C <sub>n</sub> /(OH) <sub>m</sub>	K <sub>d</sub>	Δ (log K <sub>d</sub> )	Δ V <sub>m</sub>	$\frac{\Delta (\log K_d)}{\Delta (V_m)}$
n-Pentanol	5	0.96	-0.1257 -0.1014	7.4	-0.017
1,5 Pentane diol	2.5	0.72		22.2	-0.0046
Pentitol*	1	0.57			
1,6 Hexane diol	3	0.68	-0.0766 -0.0155	7.4	-0.010
1,2,6 Hexane triol	2	0.57		22.2	-0.00070
Hexitol†	1	0.55			

\*Mean of ribitol and arabitol.

†Mean of mannitol and sorbitol.

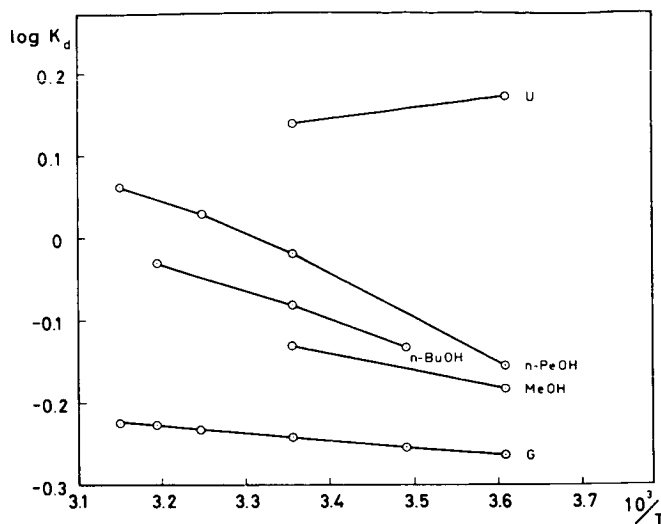


FIGURE 3. Gel DVS 9. The variation of  $\log K_d$  with  $1/T$  for some non-electrolytes eluted with deionized water. u = urea, G = glucose, MeOH = methanol, n-BuOH = n-butanol and n-PeOH = n-pentanol. The four glucose points correspond to 4.2°, 12.5°, 25°, 35°, 40° and 45°.

ane series. The fewer the hydroxyl groups already present the greater is the decrease in  $K_d$ . Thus adding one hydroxyl group to either n-pentanol or 1.6 hexane diol produced a greater change than subsequent addition of three more hydroxyls to form the polyols. The last column of TABLE 6 gives the changes ( $\Delta \log K_d$ ) expressed per unit change of molal volume.

The  $K_d$  values of both formamide and urea were greater than unity (TABLE 7). This was also the case for urea in gels G-25 and G-10. The high value of urea seems to be of wide occurrence. The  $K_d$  calculated for starch gels was 1.5, while sulphonated polystyrene<sup>21</sup> and amberlite<sup>22</sup> also gave high values.

Thiourea had a  $K_d$  value (1.41) in gel G-25 much higher than that of urea.

Since in a sterically determined partition the  $K_d$  value cannot exceed unity, some interactive process is indicated. The temperature data (FIGURE 3 and TABLE 7) obtained between 4°C and 45°C throw some light on this matter. These data are calculated on the assumption that the gel volume is unaffected by temperature. This is not quite true and there were small changes in the internal volume as estimated from the difference in elution volume of tritiated water and a higher molecular weight dextran. For gel DVS 9,  $V_1$  was slightly lower at 4.2°C than at 25°C but the difference (< 1 per cent) may not be significant. In Gel G-25,  $V_1$  increased a little

TABLE 7  
 ENTHALPY, FREE ENERGY AND ENTROPY OF SOME SOLUTES  
 (P-fluorobenzoate was only measured at one temperature and is assumed to behave as the meta derivative.)

	Gel	$K_d$	$\Delta H^\circ$ cal. mole <sup>-1</sup>	$\Delta G^\circ$ cal. mole <sup>-1</sup>	$\Delta S^\circ$ cal. mole <sup>-1</sup> deg <sup>-1</sup>
Methanol	DVS-9	0.74	+ 960	+180	+2.6
n-Butanol	DVS-9	0.83	+1540	+110	+4.8
n-Pentanol	DVS-9	0.96	+2500	+ 25	+8.3
Glucose	DVS-9	0.57	+ 410	+330	+0.3
Urea	DVS-9	1.30	-1020	-160	-2.9
Thiourea	G-25	1.49	-1600	-240	-4.6
o-hydroxybenzoate	G-25	1.69	-1050	-310	-2.5
m-hydroxybenzoate	G-25	1.34	- 880	-170	-2.4
p-hydroxybenzoate	G-25	1.34	- 880	-170	-2.4
o-fluorobenzoate	G-25	1.02	0	- 12	+0.04
m-fluorobenzoate	G-25	1.21	0	-110	+0.4
p-fluorobenzoate	G-25	1.21	(0)	(-110)	(+0.4)

$\Delta H^\circ$  is calculated between either 42°C or 12.5°C and 25°C assuming linearity. The values of  $\Delta G^\circ$  and  $\Delta S^\circ$  are for 25°C.

with temperature, there being a difference of about 5 per cent in  $V_1$  between 10°C and 45°C. The slopes of the lines in FIGURES 3 and 4 and hence the calculated enthalpy values may not be quite correct but should reflect the difference between solutes faithfully.  $\Delta H^\circ$  is calculated from  $d \ln K_d/dT - \Delta H^\circ/RT^2$ ,  $\Delta G^\circ$  by equation (5), and  $\Delta S^\circ = (\Delta H^\circ - \Delta G^\circ)/T$ .

The effect of interactions on the  $K_d$  value may depend also to some extent on the mechanism by which the gel achieves steric exclusion. As discussed above, two types of steric models have been postulated; (a) where the exclusion depends on localities inaccessible to the solute and where the latter cannot approach the gel chains closely and (b) where the exclusion depends on the distance of the molecular centers at the position of closest approach, there being no region of the chains that is not accessible to the solute. The second model raises no difficulty about the contribution of interactions to the  $K_d$  value as far as comparing two solutes is concerned; both have equal masses of gel chain available for interactions. A consequence of the first model is, however, that two solutes which are sterically excluded to different extents will also have different amounts of gel available for interactions. In this case it would therefore be necessary to introduce a correction factor to compare  $K_d$  values. This uncertainty makes the interpretation of the observed  $K_d$  values more difficult and the thermodynamic functions calculated from  $K_d$ , i.e.  $\Delta G^\circ$  and  $\Delta S^\circ$  will require some adjustment if the first type of model is correct.

Adsorption will only occur spontaneously if the free energy of the system decreases<sup>53</sup> ( $\Delta G < 0$ ). This may be associated either with an exothermic reaction ( $\Delta H < 0$ ) or an increase in entropy ( $\Delta S > 0$ ) or both. For both urea and thiourea there is a negative enthalpy and entropy change which is what would be expected from a solute-gel association.

The *n*-alcohols, on the other hand, exhibit positive enthalpy and entropy changes. Adsorption may occur with a positive enthalpy change if the increase in entropy is sufficient to give  $\Delta G < 0$ . Ideally solute molecules adsorbed from a solution on to a surface will lose entropy (analogous to the transfer from a three-dimensional to a two-dimensional gas phase on the surface). If, however, solute-solvent interactions occur which decrease the entropy in the solution, the entropy may in fact be increased if the solute can move to a position where it is either wholly, or partly, not surrounded by the solvent, e.g. in the vicinity of the gel matrix.

Non-polar solutes such as the noble gases and alkanes have remarkably high negative entropies of solution and partial molal heat capacities in solution. Frank and Evans<sup>54</sup> suggested that these phenomena could be explained by increased organization of the water structure around the non-polar, non-hydrogen bonding molecule. This so-called "iceberg" formation would thus account for their excess entropy loss in aqueous solution and their high positive entropy of vaporization ( $\Delta S_v$ ) and also for the high heat capacity, since on raising the temperature heat is required for melting of the icebergs. This concept has been extended by Némethy and Scheraga<sup>55</sup> who have proposed a detailed model in which the non-polar species is surrounded by a partial rather than complete cage. These cages may contain from 15-20 water molecules and a large non-polar solute may be in contact with more than one such cage. Hydrogen bonds will also form between the water molecules and the terminal hydroxyl groups of the *n*-alcohols. This will, apart from a disordering effect on the water structure, cause restriction of the rotational movements of the alcohol. The resulting entropy loss will depend on the size of the solute (i.e. the contribution to  $\Delta S_v$  of this component will be greatest in *n*-pentanol.

The length of the non-polar part of the molecule increases with ascent of the series as do the  $\Delta S_v$  values. From FIGURE 3 and TABLE 7 it can be seen that the  $\Delta H^0$  and  $\Delta S^0$  values for methanol, *n*-butanol, and *n*-pentanol also constitute an ascending series, and it thus seems valid to ascribe this to the influence of the increasing length of the hydrocarbon part of the molecule. The fact that the lowest  $K_{ii}$  value was found for ethanol not methanol is not necessarily evidence against such a view. If we suppose that the distribution of a solute arises from the influence of more than one factor, e.g. steric and adsorptive, the resultant  $K_{ii}$  value need not be a monotonic function of molecular size. In this case the steric effect of a  $-\text{CH}_2$  group would outweigh the effect of the additional entropy gained between



methanol and ethanol, but between ethanol and propanol the entropic gain would predominate.

Similar considerations would also apply to the  $\alpha\omega$ -diols where the  $K_d$   $\alpha\omega$ -diols reverse their trend when the intervening hydrocarbon chain is long enough (3 atoms).

If the peculiar structure of water is responsible for increasing the  $K_d$  values of weakly polar solutes, it should be possible to reduce this effect in two ways. The ability of water to form organized domains is reduced with rising temperature. The excess  $\Delta S_v$  values of the noble gases, for example, fall with temperature, the higher the atomic weight the sharper being the fall.<sup>54</sup>

More experimental points are required to investigate this point, but in FIGURE 3 it can be seen that at the highest temperature (45°C) the  $K_d$  slope of n-pentanol has apparently fallen off slightly. At 40°C about half the maximum possible number of hydrogen bonds in water are broken, while on melting about 15 per cent of the hydrogen bonds present in ice are broken.<sup>55</sup> If sufficiently high temperatures could be reached, reversal of the  $K_d$  values might be achieved and the n-alcohols might exhibit a monotonic relationship similar to that of the acyclic polyols.

Use of a hydrogen bonding solute which cannot form organized domains, e.g. formamide, should, other things being equal, also tend to reduce the high alcohol  $K_d$  value.

If the n-alcohols or other weakly polar solutes tend to accumulate at the gel surface there are various possibilities as to their orientations. They might be arranged either randomly, parallel or normal to the gel surface. The hydroxyl groups might be hydrogen bonded either to the gel hydroxyl and/or to water. In the event of a normal orientation hydrophobic bonding between the non-polar chains might occur. Such interactions will, of course, also contribute to the energy changes.

High  $K_d$  values may occur with more polar solutes e.g. formamide, urea and thiourea. At present there is insufficient data to say much about these except that for the two latter gel-solute association seems energetically favourable. The reason for the  $K_d$  higher value of thiourea is not clear.

Finally the question of the state of water within the gel must be discussed. The finding that the diffusional specificity was essentially the same in a gel of water regain 5 as in free water<sup>19</sup> may not be applicable to a very highly cross-linked gel such as DVS 9. It is possible that the high density of glucose residues exerts either an ordering or structure breaking influence on the internal gel water,<sup>56</sup> since although glucose appears to be a structure promoter sucrose (glucose-fructose) appears to be a structure breaker.<sup>57</sup>

The structure of a dextran gel is rather homogeneous in that the parent dextran is rather free from crystallization, which creates regions deficient

in water. The cross-linkages almost certainly introduce microheterogeneities, the density of glucose residues being presumably higher in some localities. In view of the high amount of gel substance ( $\sim 55$  per cent present in the gel DVS 9) it might be expected that "interface effects" might be more in evidence. Up to now, however, the behavioural pattern of gel DVS 9 has not been shown to be different from the gel type G-25 which contains about 70 per cent of water. This, together with the finding of similar diffusional specificity as in free water,<sup>10</sup> indicates that so far the evidence does not suggest that solute behaviour in the dextran gel is due to any particular influence of the gel matrix on its internal water. This problem awaits further study.

#### BENZOIC ACID DERIVATIVES IN GEL G-25

##### *K<sub>a</sub> Differences Induced by Hydrogen Bonding Differences*

Although at pH 7.6 the hydroxy and fluoro\* benzoic acid derivatives are virtually completely ionized, their behaviour is instructive.

FIGURE 4 shows that for each group of isomers, the meta and para compounds have similar  $K_a$  values while *o*-hydroxybenzoate has a much higher and *o*-fluorobenzoate a much lower value than the corresponding *m* and *p* isomers. In addition all calculated  $K_a$  values exceed unity.

An intramolecular hydrogen bond is possible between the oxygen of the carbonyl group and the hydrogen atom of the ortho-hydroxyl group and between the hydrogen atom of the carboxylic group and the ortho-fluorine atom. This internal chelation is only possible in the ortho substituted benzoic acids because in the *m* and *p* positions the substituent groups are too far apart.<sup>58</sup> This phenomenon, which is illustrated diagrammatically in FIGURE 5, reduces the intermolecular attractive forces of the ortho compounds as is reflected, for example, in their lower melting points. The dependence of physical properties on whether or not intramolecular hydrogen bonding is possible, may not however be so simple in more complicated processes such as dissolution in a polar solvent. In the latter case various interactions are involved<sup>58</sup> and the ortho compound may be more soluble than the meta or para isomers. In fact, while the ortho derivative is the least soluble of the hydroxybenzoates, it is the most soluble of the fluorobenzoates.

Many ortho compounds including *o*-hydroxybenzoic acid have higher  $R_F$  values, i.e. a lower affinity for the water phase, in paper chromatography,<sup>60</sup> and this "ortho" effect has been used to detect internal chelation, for example, in flavones.<sup>61,62</sup> The masking of hydroxyl groups by an internal bond makes the molecule more hydrophobic and generally increases the  $R_F$  value.

\*These were kindly provided by Professor A. Fredga and Dr. G. Claeson<sup>59</sup>.

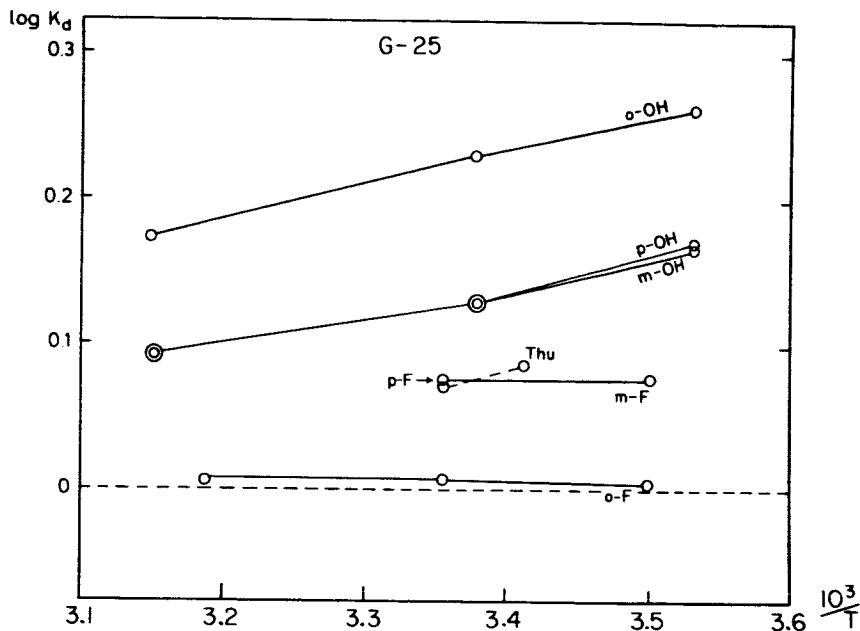


FIGURE 4. Gel G-25. The variation in  $\log K_d$  with  $1/T$  for ortho, meta and para hydroxyl and fluorobenzoates and thiourea (Thu). p.F. is a single point for para-fluorobenzoate which coincides with the position of the meta derivative (TABLE 7).

The high  $K_d$  values together with the exothermic type of temperature dependence (FIGURE 4) suggest that sorption to the gel matrix occurs. In the gel therefore both the interactions of the hydroxybenzoates with the aqueous phase and gel must be considered. (Intermolecular solute-solute interactions can be neglected because the concentrations were  $< 10^{-4}M$ ).

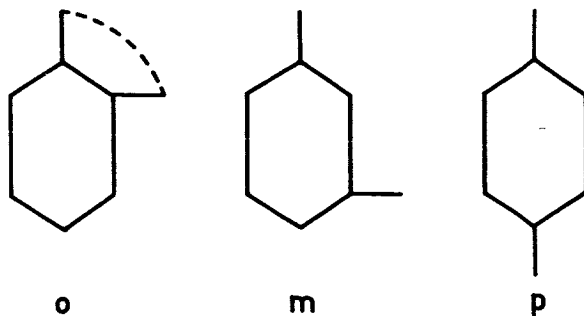


FIGURE 5. Intramolecular H bonding in ortho derivative.

The *o*-hydroxybenzoate appears to have more affinity for the dextran gel than its isomers and the fact that their  $K_d$  values are similar suggests that internal hydrogen bonding is responsible for the difference.

It is difficult, however, to speculate as to the reason for the order because all isomers showed a strong *pH* dependence and the order became reversed at about *pH* 5.

The same explanation, however, at first sight, cannot be applied to *o*-fluorobenzoate since in the ionic form this cannot form an internal hydrogen bond because the only proton utilizable for this purpose was lost in the ionization process.

The *pH* value used here refers, of course, strictly only to the solution outside the gel particles. Even if the water within the particles can be regarded as essentially similar to that in free solution,<sup>19</sup> the buffer composition and hence internal *pH* may not be homogeneous within the internal water space since the  $K_d$  values of the buffer constituents probably differ. It may therefore not be valid to assume that internal hydrogen bonding is not responsible for the divergent  $K_d$  value of the *o*-fluorobenzoate merely because at the value of the external *pH* this is not possible. There is some evidence from experiments with ions that internal *pH* may not follow that of the external solution (Marsden, unpublished observations). It is of interest to note that in paper chromatography ortho compounds may also exhibit deviations of  $R_F$  value in opposite directions. The ortho compounds usually have higher values than the *m* and *p* isomers but in some cases, e.g. *o*-diphenyls<sup>63</sup> a lower  $R_F$  value is obtained.

The ortho hydroxybenzoates exhibited the same type of temperature dependence (negative enthalpy) as for urea and thiourea, while the fluoro derivatives were essentially temperature independent. The behaviour of the fluoro derivatives may indicate the absence of interactions, but this is unlikely in view of the difference between  $K_d$  values of the ortho and the *m* and *p* compounds. The other alternative is that there is more than one temperature dependent parameter and these balance each other in the fluoro derivatives. The behaviour of these hydroxy and fluoro compounds thus perhaps provides a warning against interpreting temperature data in too simple a manner.

#### THE DEXTRAN GELS AND OTHER SYSTEMS

The behaviour of the tightly cross-linked gel DVS 9 appears to be essentially similar to that of gels of higher water regain. It is only to be expected that interactions may appear to play a larger role in the more densely cross-linked gels since the chemical differences among the small solutes are much greater than among the macromolecules usually studied in the gels of high water regain. In view of the high reproducibility of

behaviour of these gels and in particular the relatively high selectivity they should be useful adjuncts for structural and chemical analysis.

It seems that the dextran gels share properties in common with other neutral gels, in exchange resins and also living systems. In this respect it is perhaps pertinent to point out that the parent polymer is a natural product. There was similarity, for example, between the behaviour of the sugars in dextran gels and in starch<sup>22</sup> and paper chromatography.<sup>18</sup> As regards such nonelectrolytes as the *n*-alcohols and thiourea the pattern is also similar in some ion-exchange resins.<sup>51,52</sup>

Perhaps more interesting is the comparison of the behaviour in the gel with that in living systems. LeFevre<sup>64</sup> found some correlation between the instability classification of the pentoses and aldoses and their transport into red blood cells.

For the distribution between the cellular and extracellular spaces in frog sartorius muscle<sup>65</sup> the order of the  $K_d$  values at 1.6°C was ethanol, < methanol  $\sim$  propanol < *n*-butanol < formamide < thiourea, which is precisely the same order as with the gel DVS 9.

While the equilibrium behaviour of the gel and the muscle were similar, this was not true for the diffusional properties. In a dextran gel containing 86 per cent water the order of diffusion coefficients was as in water<sup>19</sup> (alcohol < amides < thioureas) but was reversed in the frog muscle.<sup>64</sup>

Teorell<sup>17</sup> has studied the behaviour of membranes consisting of suspensions of neutral and charged dextran gels. The extension of such studies to membranes containing only neutral dextran gel would be interesting. Such a neutral membrane could, for example, act at least in the presence of a transient water flow as a filter or "pump" for solutes of low  $K_d$  value. Thus sodium has a lower  $K_d$  value than potassium and elution (flow) of mixture of these two ions through such a membrane would result initially in the appearance of sodium alone on the other side of the membrane.

#### SUMMARY

1. The behaviour of some non-electrolytes and hydroxy and fluorobenzoates on elution through columns of tightly cross-linked dextran gels is described. The non-electrolytes studied were (a) acyclic polyols, (b) aldose sugars, (c) *n*-alcohols, (d) alkane-diols and some miscellaneous solutes including urea and thiourea.

2. The acyclic polyols showed a simple inverse relationship between the distribution coefficient  $K_d$  (calculated from the elution volume) and molecular size.

3. The aldoses although exhibiting considerable irregularity in their  $K_d$  values also appeared to have basically the same relationship as the polyols. It was shown that there is some degree of correlation between the conformational variations of the aldoses and the apparent  $K_d$  anomalies.

4. The  $K_d$  of the n-alcohols increased (except between methanol and ethanol) with molecular size. This was interpreted as due to adsorption which increases with decreasing polarity of the alcohols. The  $K_d$  value increased with temperature (endothermic) and the possibility of adsorption due to gain in entropy was discussed in the light of the Frank-Evans iceberg model.

5. The pattern among the alkane diols resembled that of the n-alcohols.

6. Urea and thiourea have high  $K_d$  values and the  $K_d$  decreases with temperature (exothermic). It is suggested that solute-gel association occurs in these energetically favourable circumstances.

7. The monosubstituted benzoates show  $K_d$  differences which appear to arise from the internal hydrogen bond in the ortho derivatives.

8. The similarity of the properties of the dextran gels to other non-living and living systems is briefly discussed.

#### ACKNOWLEDGEMENTS

I am very grateful to Professor T. Teorell, Dr. R. I. Fenichel, Dr. B. Gelotte, Dr. K. Granath, Dr. S. B. Horowitz, Dr. H. S. Isbell, Dr. S. G. Östling and Dr. M. Zade-Oppen for much very useful advice and discussion. I would also like to thank Mrs. A. Grönqvist, Mrs. K. Broén and Miss Å. Andersson for valuable technical help. Financial support has been received from U. S. Air Force Grant No. AF EOAR 64-33 and from the Swedish Medical Research Council.

#### REFERENCES

1. FLODIN, P. 1962. Dextran Gels and Their Applications. Halmstad, Sweden.
2. GELOTTE, B. 1960. Studies on gel filtration: sorption properties of the bed material Sephadex. *J. Chromatogr.* 3: 330-342.
3. HJERTÉN, S. 1962. Chromatographic separation according to size of macromolecules and cell particles on columns of agarose suspensions. *Arch. Biochem. Biophys.* 99: 466-475.
4. POLSON, A. 1961. Fractionation of protein mixtures on columns of granulated agar. *Biochim. Biophys. Acta* 53: 518.
5. TAYLOR, N. W., H. F. ZOBEL, N. N. HELLMAN & F. R. SENTI. 1959. Effect of structure and crystallinity on water sorption of dextrans. *J. Phys. Chem.* 63: 599-603.
6. TAYLOR, N. W., J. E. CLUSKEY & F. R. SENTI. 1961. Water sorption by dextrans and wheat starch at high humidities. *J. Phys. Chem.* 65: 1810-1816.
7. HERMANS, P. H. 1949. *Physics and Chemistry of Cellulose Fibres*. Elsevier Publishing Co. New York. Chapter 2.
8. FLORY, P. J. 1953. *Principles of Polymer Chemistry*. Cornell University Press. New York. 495-540.
9. WHEATON, R. M. & W. C. BAUMAN. 1953. Non-ionic separations with ion-exchange resins. *Ann. N. Y. Acad. Sci.* 57: 159-176.
10. TISELIUS, A., J. PORATH & P. Å. ALBERTSSON. 1963. Separation and fractionation of macromolecules and particles. *Science*. 141: 13-20.
11. ACKERS, G. K. 1964. Molecular exclusion and restricted diffusion processes in molecular-sieve chromatography. *Biochemistry*. 3: 723-730.

12. TAYLOR, N. W., H. F. ZOBEL, M. WHITE & F. R. SENTI. 1961. Deuterium exchange in starches and amylose. *J. Phys. Chem.* **65**: 1816-1820.
13. MARSHALL, L. M. & D. MAGEE. 1964. Countercurrent distribution of D-lyxose-1-<sup>14</sup>C. *J. Chromatog.* **15**: 97-99.
14. MARSHALL, L. M. & R. E. COOK. 1962. An isotope effect during the countercurrent distribution of arabinose-1<sup>14</sup>C. *J. Am. Chem. Soc.* **84**: 2647-2648.
15. MARSDEN, N. V. B. 1965. Cation selectivity of dextran gel systems. To be published.
16. MARSDEN, N. V. B. & H. R. ULFENDAHL. 1963. Halide and protein separation by gel filtration. *Acta Physiol. Scand.* **59**: Supp. 213. 99.
17. TEORELL, T. 1961. Oscillatory electrophoresis in ion exchange membranes. *Arkiv f. Kemi.* **18**: 401-408.
18. ISHERWOOD, F. A. & M. A. JERMYN. 1951. Relationship between the structure of the simple sugars and their behaviour on the paper chromatogram. *Biochem. J.* **48**: 515-524.
19. HOROWITZ, S. B. & I. R. FENICHEL. 1964. Solute diffusional specificity in hydrogen-bonding systems. *J. Phys. Chem.* **68**: 3378-3385.
20. WILKE, C. R. 1949. Estimation of liquid diffusion coefficients. *Chem. Eng. Prog.* **45**: 218-225.
21. GREGOR, H. P., F. C. COLLINS & M. POPE. 1951. Studies on ion exchange resins III. Diffusion of neutral molecules in a sulfonic acid cation-exchange resin. *J. Coll. Sci.* **6**: 304-322.
22. LATHE, G. H. & C. R. J. RUTHVEN. 1956. The separation of substances and estimation of their relative molecular sizes by the use of columns of starch in water. *Biochem. J.* **62**: 665-674.
23. SQUIRE, P. G. 1964. A relationship between the molecular weights of macromolecules and their elution volumes based on a model for Sephadex gel filtration. *Arch. Biochem. Biophys.* **107**: 471-478.
24. ANDREWS, P. 1964. Estimation of the molecular weights of proteins by Sephadex gel filtration. *Biochem. J.* **91**: 222-233.
25. WHITTAKER. 1963. Determination of molecular weights of proteins by gel filtration on Sephadex. *Anal. Chem.* **35**: 1950-1953.
26. PORATH, J. 1963. Some recently developed fractionation procedures and their application to peptide and protein hormones. *Pure App. Chem.* **6**: 233-244.
27. LAURENT, T. P. & J. KILLANDER. 1964. A theory of gel filtration and its experimental verification. *J. Chromatogr.* **14**: 317-330.
28. PEDERSEN, K. P. 1962. Exclusion chromatography. *Arch. Biochem. Biophys.* Supp. **1**: 157-168.
29. OGSTON, A. G. 1958. The spaces in a uniform random suspension of fibres. *Trans. Farad. Soc.* **54**: 1-4.
30. MARTIN, A. J. P. 1951. Some theoretical aspects of partition chromatography. *Biochem. Soc. Symp.* **3**: 4-20.
31. FLORY, P. J. 1953. Principles of Polymer Chemistry. Cornell University Press. New York. p. 577.
32. HELFFERICH, F. 1962. Ion exchange. McGraw Hill Book Co. New York. Chapter 4.
33. GINZBURG, B. Z. & D. COHEN. 1964. Calculation of internal hydrostatic pressure in gels from the distribution coefficients of non-electrolytes between the gels and solutions. *Trans. Farad. Soc.* **60**: 185-189.
34. FRANK, H. S. & W. I. WEN. 1957. Ion Solvent Interaction. Structural aspects of ion solvent interaction in aqueous solutions: a suggested picture of water structure. *Trans. Farad. Soc.* **24**: 133-140.
35. EIGEN, M. & L. DE MAEYER. 1958. Self-dissociation and protonic charge transport in water and ice. *Proc. Roy. Soc. Lond. A* **247**: 505-533.

36. GLUECKAUF, E. & G. P. KITT. 1955. A theoretical treatment of cation exchangers. III The hydration of cations in polystyrene-sulphonate. *Proc. Roy. Soc. Lond. A* **228**: 322-341.
37. LAURENT, T. C. 1964. The interaction between polysaccharides and macromolecules. 9. The exclusion of molecules from hyaluronic acid gels and solutions. *Biochem. J.* **93**: 106-112.
38. PIGMAN, W. 1957. *The Carbohydrates*. Academic Press, New York. Chapter I.
39. JÄGER, H., A. RAMEL & O. SCHINDLER. 1957. Versuch zur Erklärung des papierchromatographischen Verhaltens von Zuckern. *Helv. Chim. Acta* **40**: 1310-1319.
40. HAZEBOOK, P. & L. J. OOSTERHOFF. 1951. The isomers of cyclohexane. *Disc. Farad. Soc.* **10**: 87-93.
41. REEVES, R. 1958. Chemistry of the carbohydrates. *Ann. Rev. Biochem.* **27**: 15-34.
42. BARTON, D. H. R. & R. C. COOKSON. 1956. The principles of conformational analysis. *Quart. Rev.* **10**: 44-82.
43. REEVES, R. E. 1951. Cuprammonium-glycoside complexes. *Adv. Carb. Chem.* **6**: 107-134.
44. REEVES, R. A. & F. A. BLOUIN. 1957. The shape of pyranoside rings. II. The effect of sodium hydroxide upon the optical rotation of glycosides. *J. Amer. Chem. Soc.* **79**: 2261-2264.
45. HASSEL, O. & B. OTTAR. 1947. The Structure of molecules containing cyclohexane or pyranose rings. *Acta Chem. Scand.* **1**: 927-942.
46. KELLY, R. B. 1957. A relationship between the conformation of cyclohexane derivatives and their physical properties. *Canad. J. Chem.* **35**: 149-155.
47. WHIFFEN, D. H. 1956. Optical rotation and geometrical structure. *Chem. Ind.* 964-968.
48. CANTOR, S. M. & Q. P. PENISTON. 1940. The reduction of aldoses at the dropping mercury electrode: estimation of the aldehyde structure in aqueous solutions. *J. Amer. Chem. Soc.* **62**: 2113-2121.
49. KUHN, L. P. 1952. The hydrogen bond. I. Intra and intermolecular bonds in alcohols. *J. Amer. Chem. Soc.* **74**: 2492-2499.
50. KABAYAMA, M. A. & D. PATTERSON. 1958. The thermodynamics of mutarotation of some sugars. II. Theoretical considerations. *Canad. J. Chem.* **36**: 563-573.
51. REICHENBERG, D. & W. F. WALL. 1956. The absorption of uncharged molecules by ion exchange resins. *J. Chem. Soc.* 3364-3373.
52. LING, G. N. 1965. The physical state of water in living cell and model systems. *Ann. N. Y. Acad. Science* (this Symposium).
53. DE BOER, J. H. 1953. *The Dynamical Character of Adsorption*. Oxford University Press, Oxford. p. 90.
54. FRANK, H. S. & M. W. EVANS. 1945. III. Entropy in binary liquid mixtures; partial molal entropy in dilute solutions; structure and thermodynamics in aqueous electrolytes. *J. Chem. Phys.* **13**: 507-532.
55. NEMETHY, G. & H. A. SCHERAGA. 1962. Structure of water and hydrophobic bonding in proteins. II. Model for the thermodynamic properties of aqueous solutions of hydrocarbons. *J. Chem. Phys.* **16**: 3401-3417.
56. PAULING, L. 1948. *The Nature of the Chemical Bond*. Cornell University Press, New York. p. 304.
57. GOOD, W. 1962. The haemolysis of human erythrocytes in relation to the lattice structure of water. VI. Osmotic haemolysis in solution of non-electrolytes. *Biochim. Biophys. Acta* **57**: 104-110.
58. PIMENTEL, G. C. & A. L. McLELLAN. 1960. *The Hydrogen Bond*. San Francisco.
59. PORATH, J. & G. CLAESON. 1950. The phase systems fluorobenzoic-chlorobenzoic acids and fluorobenzoic-hydroxybenzoic acids. *Arkiv. f. Kemi* **2**: 389-396.



60. DVORÁK, J., I. M. HAIS & A. TOCKSTEIN. 1963. Principles and Theory of Paper Chromatography. p. 73 in Hais, I. M. and Maček, P. Paper Chromatography, Prague and New York. Academic Press.
61. SIMPSON, T. H. & L. GARDEN. 1952. Chelate systems I. J. Chem. Soc. 4638-4644.
62. SHAW, B. L. & T. H. SIMPSON. 1952. Chelate systems II. J. Chem. Soc. 5027-5032.
63. ROUX, D. G. & S. R. EVELYN. 1958. The correlation between structure and paper chromatographic behaviour of some flavonoid compounds and tannins. J. Chromatogr. 1: 537-546.
64. LEFEVRE, P. G. 1961. Sugar transport in the red blood cell: Structure-activity relationships in substrates and antagonists. Pharmacol. Rev. 13: 39-70.
65. FENICHEL, I. R. & S. B. HOROWITZ. 1963. The transport of nonelectrolytes in muscle as a diffusional process in cytoplasm. Acta Physiol. Scand. 60, Supp. 221: 1-63.

# N.M.R. AND RAMAN PROPERTIES OF WATER IN COLLOIDAL SYSTEMS

J. Clifford, B. A. Pethica, W. A. Senior

*Unilever Research Laboratory, Port Sunlight,  
Cheshire, England*

## INTRODUCTION

There have been a number of investigations of water in biological systems by nuclear magnetic resonance methods. The line width or relaxation time of water protons have been measured. Much interesting information has been obtained which, in general, indicates that the rate of molecular motion of water protons in biological systems is less than in pure water. However, with few exceptions the systems investigated have been much too complex to allow detailed interpretation of the results.

Solutions of surface active agents serve as a convenient and simple model for the investigation of the interaction with water of part of biological systems. Below the critical micelle concentration (CMC) the surface active agents exist as single ions containing long hydrocarbon chains in contact with the water, and the results of investigations of the interaction between chains and the water are relevant to the interaction of hydrophobic parts of biological molecules with water. Above the critical micelle concentration the surface active agent form micelles, colloidal particles with highly charged surfaces, and the interaction of these surfaces with water will also be relevant to many biological situations.

We have measured the N.M.R. chemical shift of water protons, the N.M.R. spin lattice relaxation time of water protons, and the change in frequency and intensity of the Raman bands of water, in aqueous solutions of a series of sodium alkyl sulphates from  $C_2$  to  $C_{12}$ . The chemical shift and Raman measurements provide information about hydrogen bonding in the water in these solutions, and the spin lattice relaxation time results provide information about the mobility of water protons.

## EXPERIMENTAL

*Materials.* Sodium salts of the higher alkyl sulphates ( $C_4$ - $C_{12}$ ) were prepared by the method of Dreger<sup>1</sup> and purified by prolonged extraction with ether; commercial sodium ethyl sulphate was purified by recrystallization. For the measurements on solutions of alcohols, 'Analar' n-butanol and spectroscopic-grade ethanol were used without further purification. Laboratory-distilled water which had been deionized by means of an ion-exchange column was used as a solvent.

*N.M.R. chemical shift measurements.* The method used to obtain the chemical shifts of water protons in solutions of sodium alkyl sulphate has already been described.<sup>2</sup> A Perkin Elmer 40 MCS N.M.R. spectrometer was used. The shift between the water peak and an internal standard was measured and the position of the water peak at zero concentration of solute was obtained by extrapolation. The precision of the measurements of the separation between the water peak and the  $\text{CH}_3$  peak was about  $\pm 0.2$  cycles per second, i.e., the results given below for the chemical shifts of the water protons are accurate to  $\pm 0.005$  p.p.m.

*N.M.R. relaxation time measurements.* The experimental method used will be described elsewhere.<sup>3</sup> The spin lattice relaxation times of water protons in these solutions were measured by means of an adiabatic rapid passage technique. As signal recovery of the water proton resonance in each solution was exponential within experimental error it could be characterized by a single  $T_1$ . The overall precision of the measurements was  $\pm 2$  per cent.

*Raman Measurements.* All Raman measurements were made on a Cary Model 81 recording Raman spectrophotometer. The normal filter solution was employed together with the standard Toronto arc source unit.

The solutions of long chain sulphates were made up on weight/weight basis. All the intensity values have been corrected for the effect of volume dilution.

The frequency measurements must be considered circumspectly, as the band under observation ( $\sim 3450 \text{ cm}^{-1}$  is  $\sim 420 \text{ cm}^{-1}$  wide at half-maximum intensity and is rather asymmetric in shape, due to overlap from another band at  $3225 \text{ cm}^{-1}$  ( $2\nu_2$ ). This difficulty in measurement is increased in the more concentrated sulphate solutions when the intensity of the C-H stretching vibrations  $\sim 3000 \text{ cm}^{-1}$  becomes appreciable. These factors make it difficult to locate the band center exactly.

The intensity measurements refer to integrated band areas and are given relative to the band intensity in pure distilled water. Because of the band asymmetry and the contribution from the  $3000 \text{ cm}^{-1}$  C-H stretching vibration integrated areas were measured between fixed frequency limits ( $3000 \rightarrow 3700 \text{ cm}^{-1}$ ). This procedure minimizes errors arising from the  $3000 \text{ cm}^{-1}$  C-H- band.

Because of the low intensity of the Raman bands of water a spectral slit width of  $20 \text{ cm}^{-1}$  was employed for all measurements. However, this value is small compared to the overall band width ( $\sim 400 \text{ cm}^{-1}$ ) so that there is no resolution error.

For reasons of instrumental convenience the chemical shift measurements were made at  $34^\circ\text{C}$ ., relaxation times at  $34^\circ\text{C}$ . and Raman results at  $28^\circ\text{C}$ .

## RESULTS

The variation of the N.M.R. chemical shift of the water peak in solutions of butanol and ethanol, and in solutions of the  $C_2$ ,  $C_4$ ,  $C_6$ ,  $C_8$  and  $C_{12}$  sodium sulphates with concentration is shown in FIGURES 1 and 2.<sup>2</sup> Shifts to higher applied fields are regarded as positive. The shift for pure water is defined as zero. Integration of the water and alkyl protons signals indicate that within the accuracy of the measurements ( $\pm 1$  per cent) no water is removed from the liquid state by being permanently bound as 'ice' on the

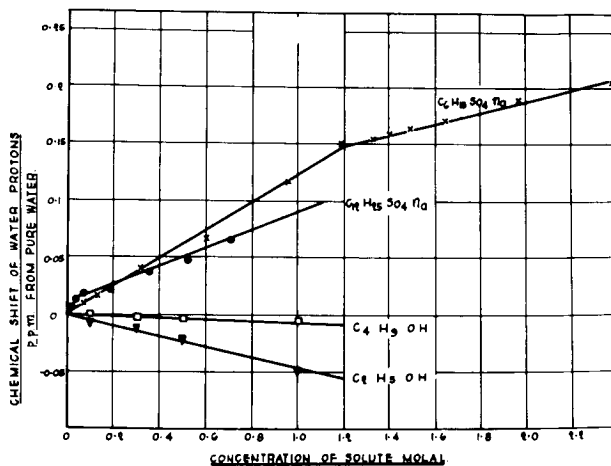


FIGURE 1. The chemical shifts of water protons in solutions of  $C_2H_5OH$   $\blacktriangledown$ ;  $C_4H_9OH$   $\square$ ;  $C_{12}H_{25}SO_4Na$   $\bullet$ ;  $C_6H_{13}SO_4Na$   $\times$ ; all relative to pure water. Reproduced by permission of the Faraday Society.

micelles or single molecules. Because of this and because there is no broadening of the NMR bands it can be assumed that water protons near the solute molecules exchange rapidly with those remote from the solute molecules and that an average chemical shift is observed.

For all the sulphates investigated the addition of sodium alkyl-sulphate to water results in a positive shift. For ethanol and butanol and for the  $C_2$  and  $C_4$  sulphates, which do not form micelles, the chemical shift-concentration curves are linear over the concentration ranges shown. For the  $C_6$  and  $C_8$  sulphates the chemical shift concentration curves have two linear parts which meet at a concentration corresponding approximately to the critical micelle concentration (CMC) of the compounds. For the  $C_{12}$  sulphate the CMC is so low that only the part of the curve above the CMC can be measured with any accuracy.

It is assumed that below the CMC only single ions exist and that the slope of the chemical shift-concentration curve is a measure of the effect

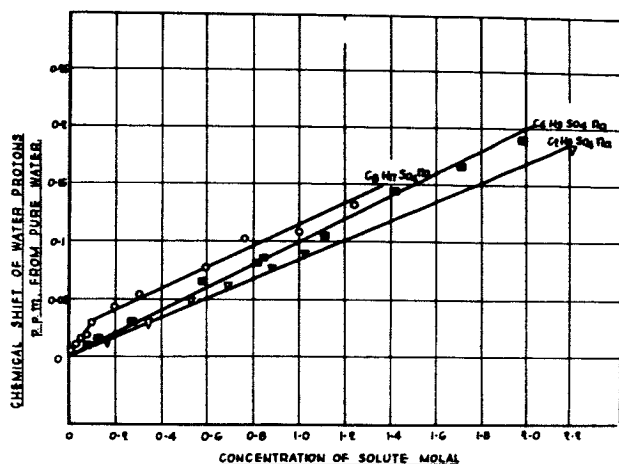


FIGURE 2. The chemical shifts of water protons in solutions of  $\text{C}_2\text{H}_5\text{SO}_4\text{Na}$   $\nabla$ ;  $\text{C}_4\text{H}_9\text{SO}_4\text{Na}$   $\blacksquare$ ;  $\text{C}_8\text{H}_{17}\text{SO}_4\text{Na}$   $\circ$ ; all relative to pure water. Reproduced by permission of the Faraday Society.

of the nonmicellised alkyl sulphate and sodium ions on the water. Above the CMC the concentration of single ions is assumed to be that at the CMC so that all the excess concentration of alkyl sulphate above the CMC is in the form of micelles. Consequently the slope of the chemical shift-concentration curve above the CMC is a measure of the effect of the micelles on the water. Thus TABLE 1 is obtained (see FIGURE 3 also).

Similarly, from the curves in FIGURE 1 the molal shifts for ethyl and *n*-butyl are  $-0.047$  and  $-0.005$  p.p.m. It is clear that both for the longer sodium alkyl sulphates and for the alcohols, the addition of  $\text{CH}_2$  groups to the chain results in an increased positive shift.

TABLE 1  
EFFECT OF ALKYL SULPHATES ON THE CHEMICAL  
SHIFT OF WATER PROTONS

Form of alkyl sulphate in solution	Molal chemical shift (ppm/mol/1000 g. water) for the alkyl sulphate				
	$\text{C}_2$	$\text{C}_4$	$\text{C}_6$	$\text{C}_8$	$\text{C}_{12}$
Single ions	0.09	0.10	0.13	0.20	0.34 (approx.)
Micelles	—	—	0.05	0.09	0.09

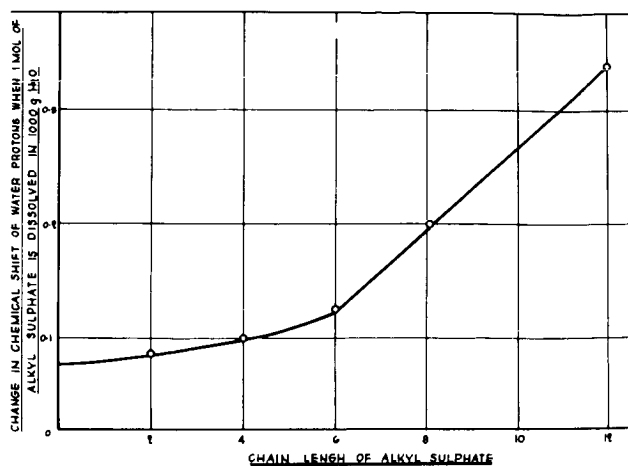


FIGURE 3. The effect of chain length on the chemical shifts of water protons in solutions of sodium alkyl sulphates. Reproduced by permission of the Faraday Society.

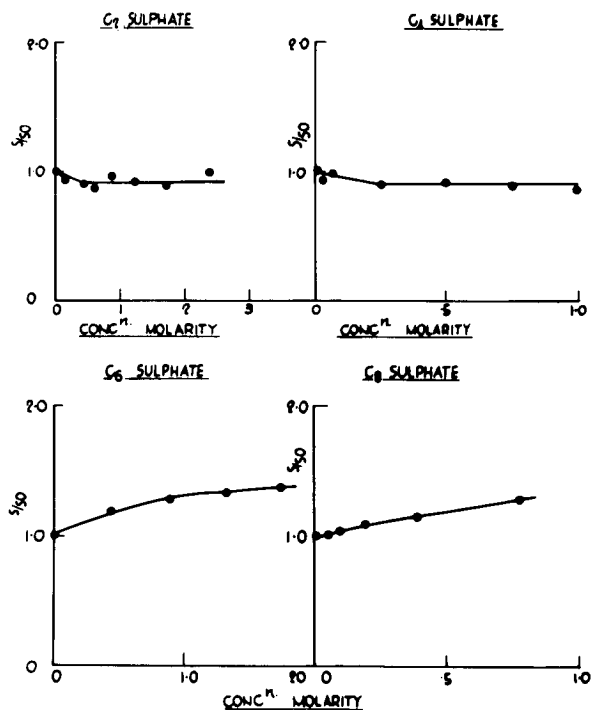


FIGURE 4. The changes in intensity of the  $3450\text{ cm}^{-1}$  Raman band of water in solutions of sodium alkyl sulphates, relative to pure water.

The Raman measurements can be divided into two distinct classes:—those related to intensity measurement and those derived from frequency measurements.

Raman intensities are related to the changes in polarizability of a molecule when it undergoes a vibrational motion. The components of the polarizability are very susceptible to changes in the environment of the molecule, and can thus be used to study the influence of environment upon the molecule.

The results (FIGURE 4) show that for the  $C_2$  and  $C_4$  sulphates a slight reduction in intensity occurs whereas for the  $C_6$  and  $C_8$  sulphates an increase (up to  $\sim 40$  per cent) is found.

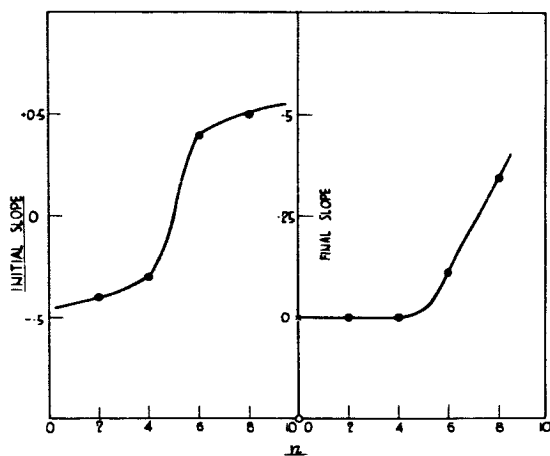


FIGURE 5. The effect of chain length on the relative intensity of the  $3450\text{ cm}^{-1}$  Raman band of water in sodium alkyl sulphate solutions.

In order to see the effects more clearly we have measured both the initial slopes of the intensity vs. concentration curves and the final slopes (above the CMC's where this occurs). These modified results are shown in FIGURE 5. In both cases it is noticeable that a change in the trend of these slopes with chain length occurs at about five carbon atoms. The same type of behaviour can be seen from the N.M.R. data on chemical shifts.

Turning to the frequency measurements (FIGURE 6), as the sulphate concentration is increased the  $H_2O$  band frequency falls to a minimum and then slowly increases to an approximately constant value. However, it never increases to the value observed in pure water.

These results are conveniently summarized in FIGURE 7 which shows the initial slope  $\Delta\nu/c$  vs. chain length,  $\Delta\nu$  (at the minimum) and  $\Delta\nu$  at high

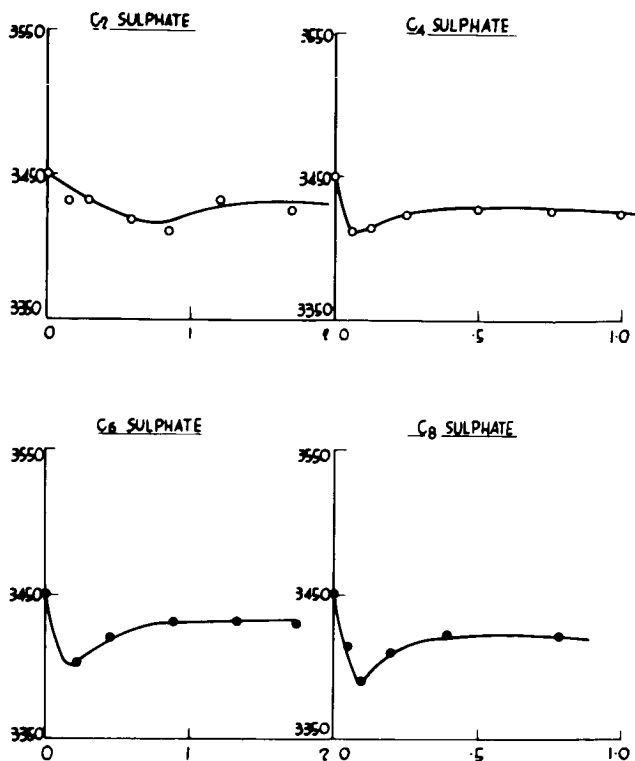


FIGURE 6. The variation in frequency of the 3450  $\text{cm}^{-1}$  Raman band of water in solutions of sodium alkyl sulphates. (The abscissae scales are identical to those of FIGURE 4.)

concentrations) vs. chain length. All these results show evidence of a discontinuity in trend of these properties at a change length of about  $\text{C}_5$ .

FIGURES 8 and 9 show the relaxation rates ( $1/T_1$ ) of water protons in solutions plotted against the molal concentrations of the  $\text{C}_2$ ,  $\text{C}_4$ ,  $\text{C}_6$ ,  $\text{C}_8$  and  $\text{C}_{12}$  sodium alkyl sulphates and of ethanol and n-butanol at  $32^\circ\text{C}$ .<sup>3</sup>

For the alcohol solutions and for the solution of the  $\text{C}_2$  and  $\text{C}_4$  alkyl sulphate  $1/T_1$  for water protons varies linearly with concentration. For solutions of the higher alkyl sulphates change of slope is observed near the critical micelle concentration (CMC).

As before the slope of the relaxation rate — concentration curve below the CMC is a measure of the effect of single ions on the water, and the slope above the CMC is a measure of the effect of micelles on the water. From the slopes of the curves the effect on the relaxation rate of the water



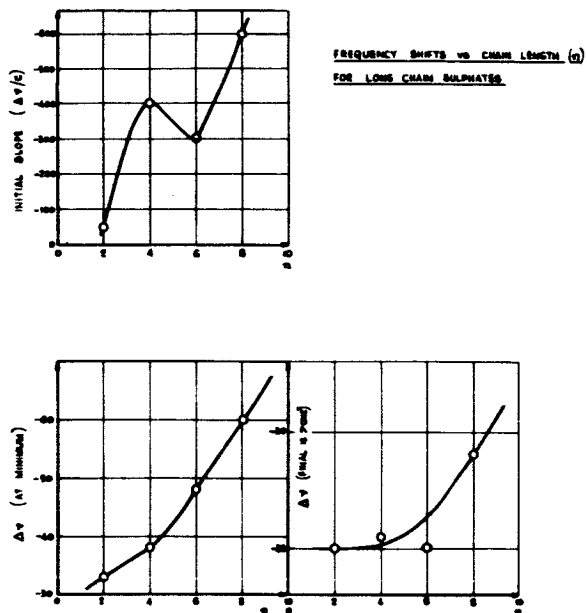


FIGURE 7. The effect of chain length on the Raman frequency shifts in alkyl sulphate solutions.

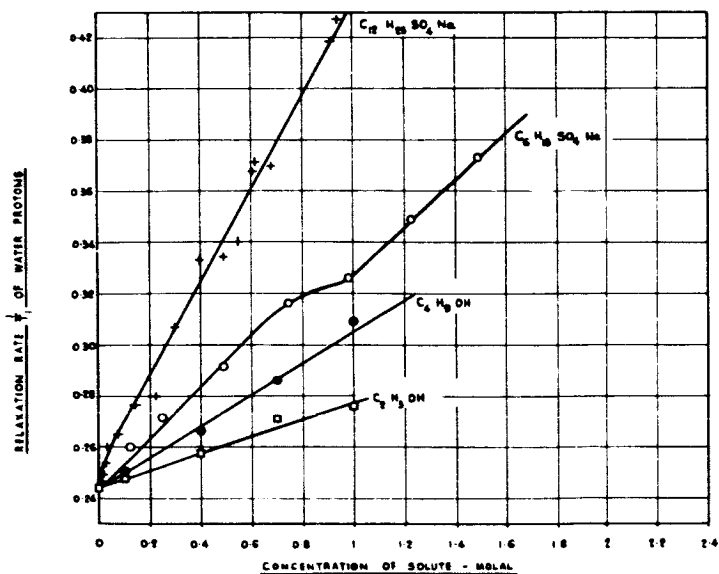


FIGURE 8. The relaxation rates of water protons in solutions of  $C_2H_5OH$  □ ;  $C_4H_9OH$  ● ;  $C_6H_{13}SO_4Na$  ○ ; and  $C_{12}H_{25}SO_4Na$  +. Reproduced by permission of the Faraday Society.

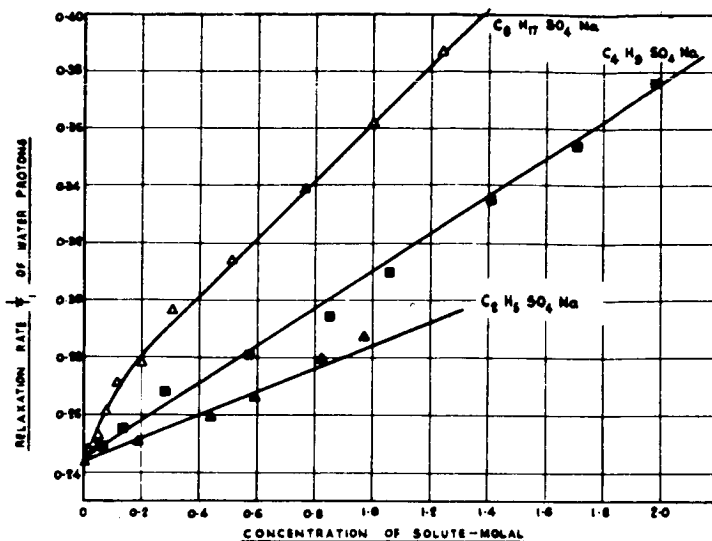


FIGURE 9. The relaxation rates of water protons in solutions of  $C_2H_5SO_4Na$  ▲;  $C_4H_9SO_4Na$  ■; and  $C_8H_{17}SO_4Na$  △. Reproduced by permission of the Faraday Society.

protons of one mole of solute per 1000 grams of water is calculated and given in TABLE 2.

In FIGURE 10 the increase in relaxation rate caused by the solution of one mol of alkyl sulphate as single ions in 1000 gm. of water is plotted against the length of the alkyl chain. The CMC for the  $C_{12}$  salt is too low for an

TABLE 2  
EFFECT OF ALKYL SULPHATES ON THE SPIN LATTICE  
RELAXATION TIME OF WATER PROTONS

Sodium alkyl sulphate Chain Length	Effect on the relaxation rate of water protons at 32° C. sec. <sup>-1</sup> per mol. per 1000 gm. of water	
	As single ions	As micelles
$C_2$	0.04	—
$C_4$	0.07	—
$C_6$	0.10	0.09
$C_8$	0.14	0.11
$C_{10}$	—	0.16

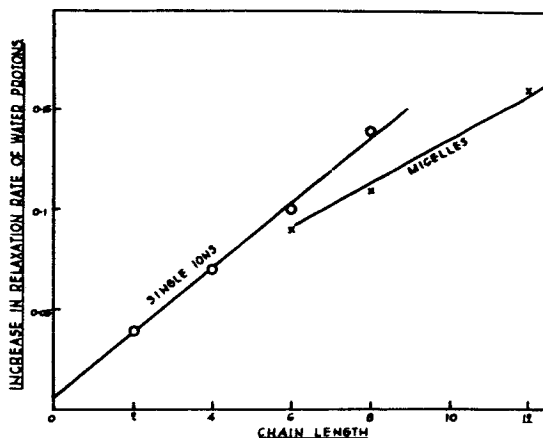


FIGURE 10. The effect of chain length on the relaxation rate of water protons in solutions of sodium alkyl sulphates, in the forms of both single ions and micelles. Reproduced by permission of the Faraday Society.

accurate evaluation of the effect of single ions. Close to the CMC the slopes of the  $1/T_1$  concentration curves for single ions are reduced. The slopes given in TABLE 1 are estimated from solutions below the concentration at which this reduction of slope appears. The slope of the  $1/T_1$  concentration curve for the alcohols give  $0.03 \text{ sec.}^{-1}$  for ethanol and  $0.6 \text{ sec.}^{-1}$  for butanol as the molal increase.

#### DISCUSSION

The N.M.R. chemical shift measurements and the Raman results provide information about the nature of the hydrogen bonding in water. The N.M.R. signal in water vapor occurs at a relatively high field, whereas that in liquid water occurs at a much lower field.

If the hydrogen bond is treated as being electrostatic in nature this shift to lower field can be readily explained. In an isolated water molecule, the oxygen atom carries a net negative charge and each of the hydrogen atoms a net positive charge.

As the oxygen of one  $\text{H}_2\text{O}$  molecule approaches the hydrogen of a second molecule the electron clouds tend to repel one another, the result being that the density of electrons in the vicinity of the hydrogen atom is reduced. This leads to a reduction in screening and the proton resonance now appears at a lower field. Pople and Marshall<sup>4</sup> have calculated the magnitude of this effect and shown that it is of the same order of magnitude as the observed shift. However, their calculation does not exclude the possibility of electron donation from the oxygen to the hydrogen, which should give a small shift to higher field. This process gives a certain amount of covalent character to the hydrogen bond. Since this effect, if it exists, is much

smaller than the electrostatic effect, the net result of liquefaction is a shift to lower field.

The experimental N.M.R. results, both below and above the CMC show positive chemical shifts on adding long chains to water and the chemical shift becomes more positive as the chain length increases, i.e., the resonance moves to higher applied field. In the light of the above discussion this result can be interpreted in two ways: a reduction in the electrostatic repulsion or an increase in the covalent character of the hydrogen bond. From chemical shift evidence alone it is not possible to distinguish between the two mechanisms, but when the Raman results and the relaxation time measurements are considered, it appears likely that the second effect is the more important.

The Raman intensity measurements show two distinct types of behavior. For the C<sub>2</sub> and C<sub>4</sub> sulphates a slight decrease in intensity is observed, whereas for the C<sub>6</sub> and C<sub>8</sub> compounds a substantial increase is found. Measurements on the simple systems of Na and K sulphates show slight decreases which can be attributed to the SO<sub>4</sub><sup>2-</sup> ion. It seems therefore that for the C<sub>2</sub> and C<sub>4</sub> sulphates the dominant effect is that due to the polar head group. For the C<sub>6</sub> and C<sub>8</sub> sulphates the alkyl chain is the important factor, and by comparison with the systems water/dioxan and water/acetone (to be reported later) the conclusion is that the hydrogen bonding of the water is increased.

In the system water/dioxan as the concentration of water is increased a very large intensity increase accompanied by a significant lowering of the frequency, is observed. In this case it is reasonable to assume that as the concentration of water becomes greater the degree of hydrogen bonding between water molecules increases. We may therefore conclude that the C<sub>6</sub> and C<sub>8</sub> sulphates create a more powerfully hydrogen bonded solution than water alone.

This conclusion is confirmed by the Raman frequency measurements. For all the sulphates studied a drop in frequency is found which is consistent with an increase in hydrogen bonding. (cf. Water vap. to liquid water or water/dioxan mixtures).

The Raman results are thus consistent with the N.M.R. chemical shift measurements only if an increase in covalent hydrogen bonding is postulated. If we attempt to explain the N.M.R. chemical shift data by a reduction of the electrostatic effect the Raman results would be expected to show a decrease in intensity and an increase in frequency. The two sets of data can only be reconciled if the second mechanism of hydrogen bonding is adopted, i.e., the hydrogen bond in water is given some covalent character which is increased by the presence of alkyl chains.

This conclusion is further supported by the N.M.R. relaxation time measurements. In the systems we are considering the spin lattice relaxation of

water protons will be caused largely by dipole-dipole interaction between protons and the relaxation rate  $1/T_1$  will be proportional to the correlation time  $\tau$  describing the motion of the water molecules. Our results show that  $1/T_1$  for water protons is increased by the presence of alkyl chains.

Part of this effect, can be explained by magnetic dipole-dipole interactions between water protons and alkyl chain protons. If liquid water has a tetrahedrally coordinated structure this effect may be quite large, since the nearest H . . . . H distance between H-atoms in different water molecules is  $\sim 2.8$  Å, whereas the H . . . . H-C distance could be as low as 1 Å.

However, more evidence to clear up this point is available. We have investigated the variation of  $T_1$  with temperature for both  $H_2O$  and a 0.5 Molal solution of  $C_6$  sulphate over the range  $20^\circ \rightarrow 40^\circ C.$  and obtained activation energies for the relaxation processes in the two systems of 4.45 and 4.65 K cal./mole respectively. This result indicates that in the presence of a hydrocarbon chain the forces restricting the mobility of the water protons are increased in agreement with the conclusions drawn from the chemical shift and Raman data.

It is particularly interesting that many of the properties investigated here show discontinuities at a chain length of  $C_4 \rightarrow C_6$ , the point at which the alkyl sulphates first form micelles. From our results it appears evident that for chain lengths less than  $C_5$  the sulphate ion dominates the effect of the solute on water. However, when the chain is longer than six carbon atoms the influence of the chain on the water becomes important. The sulphate ion thus seems to affect the water structure over a range corresponding to  $\sim$  five carbon atoms, i.e., approximately 4 Å.

When micelles are formed alkyl chains are removed from contact with the water. The chemical shift and Raman spectra results indicate that the effect of the micelles on hydrogen bonding in the water is much the same as the effect of an equivalent number of nonmicellised head groups and counter-ions.

On the other hand, the relaxation time measurements indicate that micelles increase the spin lattice relaxation rate of water protons more than nonmicellised  $SO_4^- Na^+$  groups. This can be ascribed to electrostriction of water molecules on the electrical double layer of the micelles with a consequent reduction of the rate of molecular motion.

By assuming that micelles are spherical and that the hydrocarbon part of the micelle has a radius equal to the length of the  $CH_2$  chains of which it is composed and a density equal to a liquid hydrocarbon — say 0.8 gm./ml., values for the radius and for the aggregation number of micelles can be calculated.<sup>5</sup> On this basis the micelle of the  $C_{12}$  sodium sulphate has a radius of 20 Å and contains 55 molecules, the micelle of the  $C_8$  sulphate has a radius of 15 Å and contains 27 molecules, and the micelle of the  $C_6$  sulphate has a radius of 12.5 Å and contains 20 molecules. The surface

areas of the  $C_{12}$ ,  $C_8$  and  $C_6$  micelles will be  $56\text{\AA}^2$ ,  $62\text{\AA}^2$  and  $57\text{\AA}^2$  per molecule of micellised sulphate. If one assumes that there is a monomolecular layer of water around each micelle whose proton relaxation time is affected by the micelle then about 13 moles of water per mol of alkyl sulphate are required and the relaxation rate for this affected water is about  $1.0\text{ sec}^{-1}$  for solutions of all the alkyl sulphates. A model in which water molecules are bound for long periods in a rigid ice-like structure around the micelle can be rejected. In such a model the intramolecular rate of the water protons would be determined by the correlation time for rotational Brownian motion of the micelle. Assuming that the micelle is a sphere rotating in a medium with a viscosity of 0.01 poise this correlation time can be calculated and from it an intramolecular relaxation rate. This is two orders of magnitude greater than the observed relaxation rate. Consequently, it can be said that the water on the micelle is not rigidly bound and the lifetime of any molecule on the micelle is much less than  $10^{-7}$  sec. and is probably not more than one or two order of magnitude greater than its rest time between jumps in any one position in ordinary water.

## REFERENCES

1. DREGER, E. E. 1944. *Ind. Eng. Chem.* **36**: 610.
2. CLIFFORD, J. & B. A. PETHICA. 1964. *Trans. Faraday. Soc.* **60**: 1483.
3. CLIFFORD, J. & B. A. PETHICA. *Trans. Faraday. Soc.* In press.
4. MARSHALL, J. & J. A. POPE. 1958. *Mol. Physics.* **1**: 199.
5. TARTAR, H. V. 1959. *J. Coll. Sci.* **19**: 115.

# THE EFFECTS ON BIOLOGIC SYSTEMS OF HIGHER-ORDER PHASE TRANSITIONS IN WATER\*

Walter Drost-Hansen

*Institute of Marine Science, University of Miami, Miami, Fla.*

The purpose of this conference is to discuss "Forms of Water in Biologic Systems." This undertaking is very ambitious and most likely our achievements at the present time will be limited. The principal difficulty before us is simply that we do not as yet possess a picture of the structure of water or aqueous solutions that has any degree of finality about it. Hence, it is indeed somewhat presumptuous for us to try to discuss various forms of water in biologic systems as long as we are without any appreciable understanding or agreement about the structure of bulk water or aqueous solutions. We might well add to this regrettable state of affairs our lack of knowledge of the structure of water near such simple interfaces as the air-water interface, water-immiscible liquid interface, or the structure of water near any simple solid-water interface, such as may exist near the surface of a mineral grain.

## *Theories of Water Structure*

A few years ago, Henry Frank (1963) gave a brief but eloquent survey of the current status with respect to theories of liquid water and more recently Kavanau (1964) has reviewed the current theories of water structure in some detail. From these reviews, one sees the great range of physical models that have been invoked over the past 30 years to account for the properties of water. These theories range from the "purists'", "average" models of liquids — due primarily to physicists and other strictly "theoretical" liquid structure researchers — to the models that Henry Frank has termed the "mixture models." The mixture models embrace a variety of models from simple water-ice mixtures to water polymers and water clusters. These include Euckens polymer model (consisting of small polymeric species of water), the more recent cluster and cage models, and the "super clusters" (the older cybotactic groups of Stewart, Frenkel and Nomoto). The current status of water structure research certainly lacks finality. Because of the present state of knowledge, any discussion of water in biologic systems must definitely be limited. Without knowing the structure of water, how can we predict or understand the influence that the multitude of solutes in biologic systems have on the structure of water, or

\*Contribution No. 601 from The Marine Laboratory, Institute of Marine Science, University of Miami, Miami, Fla. Acknowledgment is given the Office of Saline Water, U. S. Department of the Interior, for support of the author's research at the Institute of Marine Science.

how can we describe the water near the all-dominating interfaces of biologic systems? The unsettled question of the existence or nonexistence of long-range ordering in water adjacent to a solid surface, for instance, must surely be decided before we can hope to understand in detail the behavior of water in membrane systems.

### *Thermal Anomalies*

The present paper is a summary of 10 years' thinking by the author and his coworkers with regard to water in biologic systems. The major shortcoming — and at the same time perhaps the major advantage — of our approach is that we do not build on any specific model for the structure of water. Rather, our speculations are based on the observation, sporadically reported in the literature, of the existence of thermal anomalies in the properties of water and aqueous solutions. Over the past decade, we have studied the properties of water and a large number of aqueous solutions and have become convinced that the properties of liquid water do exhibit anomalies at a number of different temperatures and that these anomalies reflect more or less abrupt structural changes in the water. Such anomalies, which for want of a better name have become known as "kinks," have been suggested previously by several other authors. For instance, Dorsey (1940) in his monograph points out that the measurements of magnetic susceptibility by Wills and Boecker and by Seely seem to indicate anomalies in the vicinity of 35 to 55°C., and Dorsey also points out that Tammann expected the existence of an anomaly near 50°C. Likewise, in 1935 Magat (1935) proposed that anomalies exist in the properties of water near 40 to 45°C. based on measurements of solubility, viscosity, compressibility, and specific heat. Antonoff (1950) and Forslind (1952) have also studied in some detail the more or less abrupt transitions in the properties of water, and other authors have, over the years, sporadically mentioned the existence of kinks. Forslind has specifically suggested that anomalies exist at 12, 35 and 55°C.; however, the evidence presented by Forslind was not very extensive. Ives and coworkers (1963) have discussed the existence of anomalies in the properties of water and aqueous solutions and postulated an anomaly near 30-35°C. Attention is called in particular to Feates and Ives' (1956) study of the dissociation of cyanoacetic acid, and Franks and Ives' (1960) study of interfacial phenomena.

The kinks are evident in the data from many different types of aqueous systems, and the present author has come to believe that at least four kinks occur between the freezing and the boiling point of water, namely near 15, 30, 45 and 60°C.

### *Evidence*

It is not possible to detail here all the evidence available to show the reality of the anomalies in the properties of water and aqueous solutions;



a general review of the evidence will be presented elsewhere (Drost-Hansen, 1965). In this section we show only a small group of examples to indicate the diversity of conditions and phenomena in which the anomalies are observed in both pure water and aqueous solutions. In *General Observations* is a brief summary of the major generalizations and conclusions that can be drawn from an examination of all the available data. Finally, in sections *Biologic Implications* and *Discussion* the evidence for the role played in biologic systems by the anomalies observed in water and aqueous solutions is discussed.

The kinks are manifested in both the properties of pure water and of aqueous solutions. It is instructive first to consider the evidence available from measurements on pure water. One difficulty frequently encountered in searching for the anomalies is the lack of measurements of any one parameter at sufficiently closely spaced temperature intervals. There are, however, a few cases in which parameters have been measured at enough temperatures (over a relatively narrow temperature range) to permit a statistical analysis of the resulting data. One such example is the density of water as determined by Chappuis at the International Bureau of Weights and Measures (1907). We have previously analyzed and published these data (Lavergne & Drost-Hansen, 1956) and we shall only briefly summarize the results here. The data obtained by Chappuis extend from near zero to 41°C. Rather than work with the density itself, the reciprocal of the square root of the density was used, in other words, the square root of specific volume. Plotted against temperature this has, to a rough approximation, the form of two intersecting, straight lines, the intercept being near 4°C. Considering only the data from about 5 to 41°C., it appears as if there are three distinct, separate curve segments, namely, one from 5 to 15°C., one from 15 to 30°C., and one from 30 to 41°C. By the method of least-squares best-fit, second order polynomials were fitted to each of the three curve segments and separate curves were fitted for the two combined intervals from 5 to 30°C. and from 15 to 41°C. By an F-analysis, it was possible to show, taking properly into account the added degrees of freedom when using separate curve segments for each interval, that the fitting of two curves over two intervals gave significantly better fit than one curve through any combined interval. Hence, it was concluded that there appears to be anomalies near 15 to 30°C.

We have analyzed in a similar fashion the dielectric constant data obtained by Devoto (as quoted by Dorsey, 1940). In this case, the data extend to slightly above 30°; hence, the analysis was made to test only for an anomaly in the vicinity of 15°C. and it was again found highly significant statistically that two separate curve segments give a better fit than one curve through the combined interval from zero to 30°C. An examination of the more recent dielectric data on water by Malmberg and Maryott

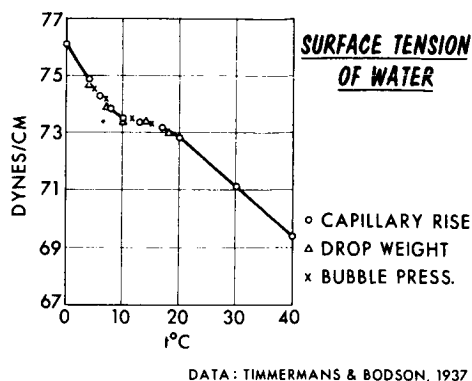


FIGURE 1. Surface tension of water determined by Timmermans & Bodson (1937).

(1956) shows a minimum in the relative temperature coefficient ( $1/\epsilon$ ) ( $d\epsilon/dt$ ) near 60-65°C. and very possibly an inflection point in this quantity near 30-35°C. An anomaly in the specific heat of water has been proposed earlier by Magat, Dorsey and Feates and Ives (1956). Further evidence for anomalies in the properties of pure water is found in particular in the temperature dependence of many surface and interfacial phenomena. Thus, Franks and Ives (1960) have noted an inflection point near 34°C. in the interfacial tension between water and n-hexane. The present author (1964) has recently examined some other surface and interfacial properties of water and aqueous solutions and found considerable evidence for the existence of the kinks in such systems as well as evidence for structural discreteness near interfaces. As an example, FIGURE 1 shows the surface tension of

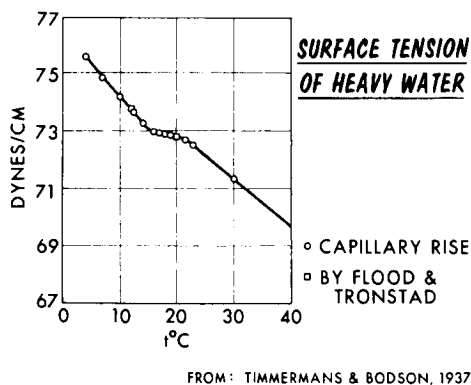


FIGURE 2. Surface tension of heavy water. Timmermans & Bodson (1937).

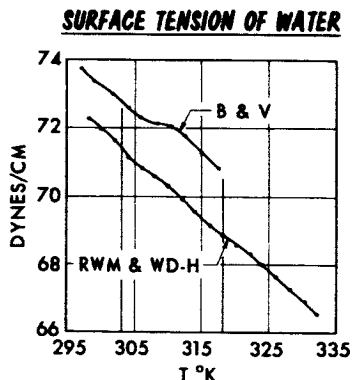


FIGURE 3. Surface tension of water. Data by Bordi & Vannel and by Drost-Hansen and Myers.

water as determined by Timmermans and Bodson (1937) in the middle thirties. FIGURE 2 shows the data for heavy water obtained by the same authors. It is remarkable that such a pronounced inflection point should have been observed by these authors but gone unrecognized by other investigators of the surface tension of water. A careful inspection shows, however, that inflection points are indeed apparent in practically all other measurements of the surface tension of water where sufficiently closely spaced data have been obtained. Thus, in data as old as those obtained by Brunner (1847) and Wolf (1857) one can recognize the presence of an inflection point near 15°C. Other authors have suggested anomalies in the surface tension of water at other temperatures and FIGURE 3 shows the surface tension of water as obtained respectively by Bordi and Vannel (1962)

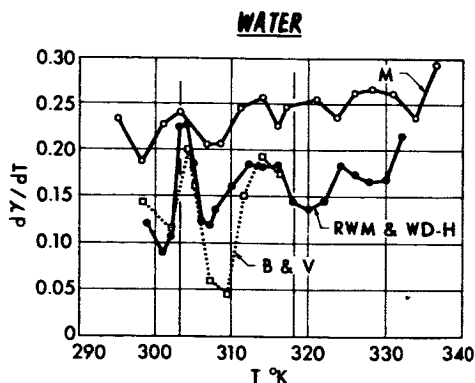


FIGURE 4. Derivative of surface tension with respect to temperature. Based on data by Moser, Bordi & Vannel, and Drost-Hansen and Myers.

in Italy and by the present author and Myers (1963). Again, inflection points are observed near 30 to 33°C. and 45°C. (present author's data). Finally, FIGURE 4 shows the "entropy of surface formation" as reported by Drost-Hansen (1965). The three curves depict the numerically differentiated surface tension data obtained respectively by Moser (in 1927), Bordini and Vannel, and Drost-Hansen and Myers. It is interesting that agreement exists to the extent shown in FIGURE 4 with regard to the temperature derivative of the surface tension. Although it is not permissible to identify directly this quantity with the entropy of surface formation, the data do indicate an abrupt change of ordering near 30°C. For a more detailed discussion, the reader is referred to the article by the present author.

Anomalies in the viscosity of water and aqueous solutions as a function of temperature have been noted by several authors, for instance, Forslind (1952), Magat (1935), Neill and Drost-Hansen (1955), de Carvalho (1944), Qurashi and Ahsanullah (1961) and Othmer and Thakar (1953). In a study of the viscosity and diffusion in solutions, Othmer and Thakar state that "where water is the solvent, the lines show a definite break at about 30°C. An exactly similar break was found to occur near the same temperature when viscosity of water was plotted in a similar way against a vapor pressure of water."<sup>10</sup> They also state with respect to aqueous solutions: "The temperature at which the changes in internal structure of water occur may vary somewhat with the dissolution therein of the solute; hence, the breaks in the line may be at somewhat different temperatures in the general range of 30°C."

Nuclear magnetic resonance studies have also suggested the existence of changes in the structure of water according to several authors. Brown (1958) has suggested that anomalies exist in the transverse relaxation times for water in the vicinity of 18, 42, and 60°C. FIGURE 5 shows a plot

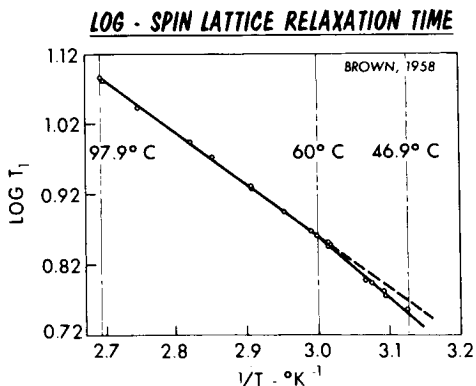


FIGURE 5. Transverse relaxation time for protons in water. Data by Brown.

of some of Brown's data: the ordinate is log transverse relaxation time while the abscissa is the reciprocal absolute temperature. The kink near 60°C. is fairly pronounced. An anomaly in the NMR data is also suggested by Simpson and Carr (1958) in the vicinity of 40-45°C. on basis of their NMR studies.

Spectroscopic evidence for anomalies in water has been suggested by Magat (1937) near 40°C. Other evidence for the existence of anomalies in the properties of pure water may be obtained from the data by Pinkerton on the ultrasonic amplitude absorption coefficient (1947). FIGURE 6 shows

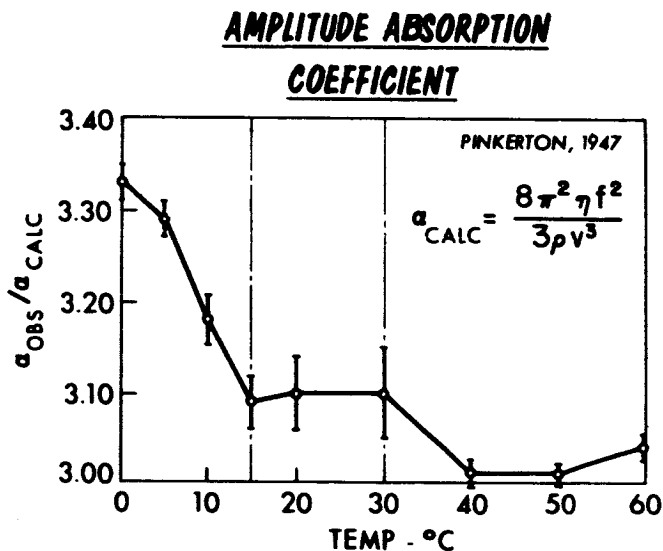


FIGURE 6. Excess ultrasonic sound absorption coefficient. Based on data by Pinkerton.

Pinkerton's data point and his estimated errors on the determinations. It should be noted that the limits of error suggested by Pinkerton appear to be unnecessarily large for the data points near 20 and 30°C., thus the apparent anomalies at 15 and near 30°C. seem very likely to be real. The thermal conductivity data obtained by Frontas'ev (1956) are also suggestive of an anomaly and Frontas'ev states: "It can be assumed that a fundamental modification in the structure of water takes place in the range of 30 to 40°C. which is reflected in the indicated anomaly in the thermal conductivity polytherm."

Much skepticism has been voiced with regard to the reality of the anomalies discussed above. One frequent criticism has been that it often appears that each investigator has his "choice" temperature or temperatures

for the anomaly (or anomalies). While unfortunate, this in itself can hardly condemn the notion that anomalies may indeed exist in water and considering the present author's contention that at least four anomalies exist, it is obvious that a considerable choice exists for anyone concentrating on a particular range of temperatures. While the temperatures of approximately 15, 30, 45, and 60°C. may appear unnecessarily "generalized" and "symmetrical," evidence will be presented elsewhere in favor of the transitions being at least in the vicinity of these temperatures.

*"Kinks" in Properties of Aqueous Solutions*

We shall briefly show a number of examples of anomalies in the properties of aqueous solutions. While the existence of the kinks is often difficult

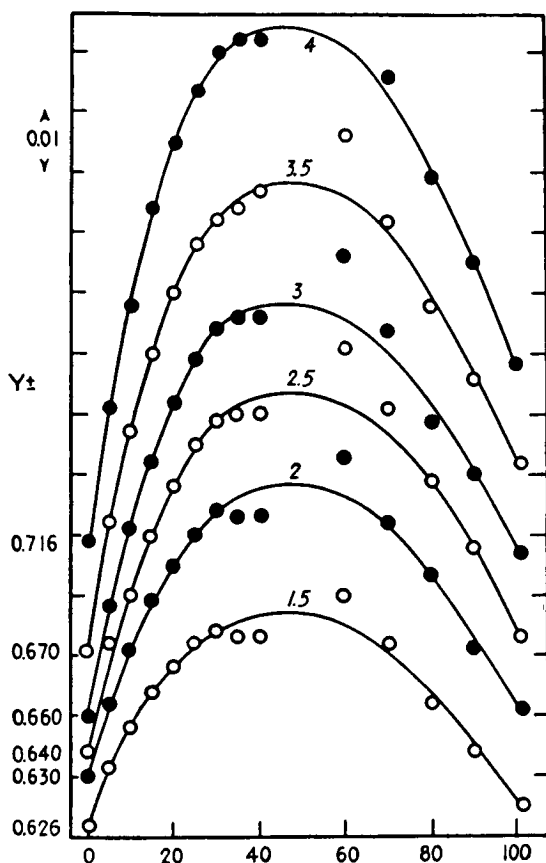


FIGURE 7. Mean activity coefficients for sodium chloride in water as a function of temperature. This illustration is taken directly from Harned & Owen's Monograph: "The physical chemistry of electrolytic solutions". (By permission).

to demonstrate unambiguously on any one particular set of data obtained on pure water, it is often easier to find more unique evidence for the anomalies in the properties of aqueous solutions. In particular, such areas as solubility, kinetic data for hydrolysis, and optical rotation of aqueous solutions seem frequently to exhibit the kinks particularly clearly.

FIGURE 7 shows the activity coefficients for sodium chloride in water as a function of temperature. This illustration is taken directly from Harned and Owen's monograph (1958); it shows the experimental values of the activity coefficient for sodium chloride in water and smoothed curves to fit the data. In FIGURE 8 we have shown the same points but omitted the smoothed curves; instead, we have drawn a series of curves which we be-

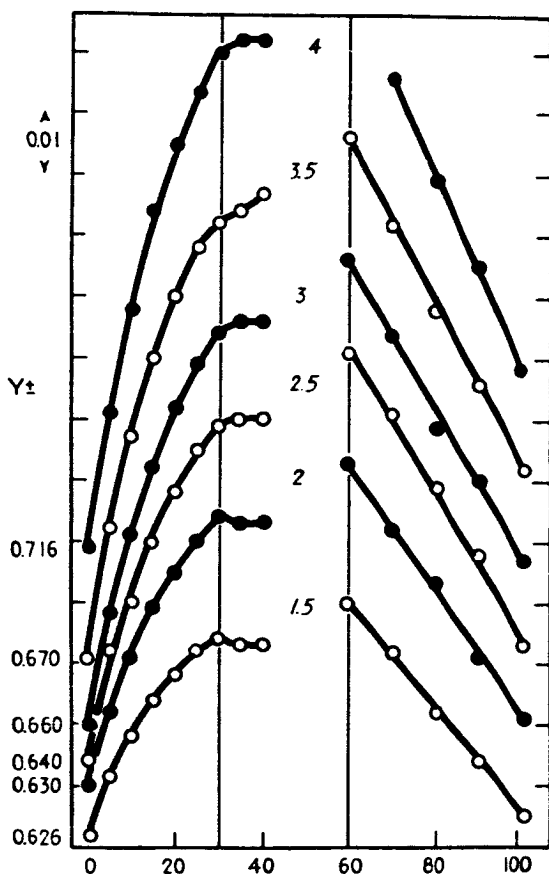


Figure 8. Mean activity coefficients for sodium chloride in water as a function of temperature. Same data point as in FIGURE 7 but curves redrawn by present author.

lieve represent far more realistically the temperature dependence of the activity coefficient. Unfortunately, there are no data between 40 and 60°C., also, the data below 40°C. were obtained from electromotive force measurements while the measurements from 60 to 100°C. were obtained from boiling point elevations. While it is unfortunate that different methods of observation were used for the different ranges studied, it seems significant that there are pronounced trends in the data. Thus, it is difficult to see how one can escape the conclusion that the activity coefficient to a first approximation decreases linearly with temperature in the region above 60°C. Secondly, in all cases there is a notable "gap" between the data at 40°C. and the data at 60°C. Furthermore, it seems that an actual reversal in curvatures may exist for the 1.5 and 2 molar solutions near 30°C. The diameter of the circles representing the measured values is 0.002 in  $\gamma_{\pm}$ , corresponding to, respectively, 0.15 mV or 0.003° in the boiling point elevation. Considering the accuracy and in particular the precision with which EMF's may ordinarily be measured, the deviations — even from the very optimistic, smooth curve of FIGURE 7 — seem highly significant. As pointed out above, the *trend* in the data is exceedingly difficult to ignore. Note also the amazingly high concentrations for which the anomalies seem to exist — up to three to four molar.

FIGURES 9 and 10 show the concentration independent term for the partial molal volume for potassium chloride and potassium iodide; the data

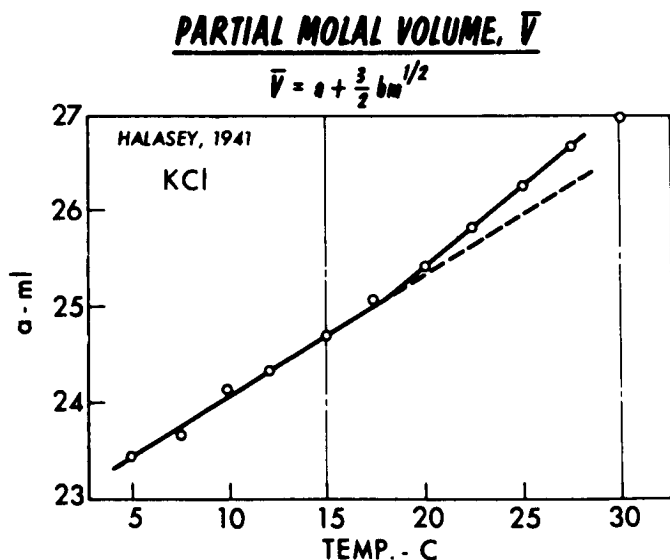


FIGURE 9. Concentration-independent term,  $a$ , in the equation for the partial molal volume of potassium chloride  $\bar{v}_1 = a + (3/2) \cdot bm^{1/2}$ .



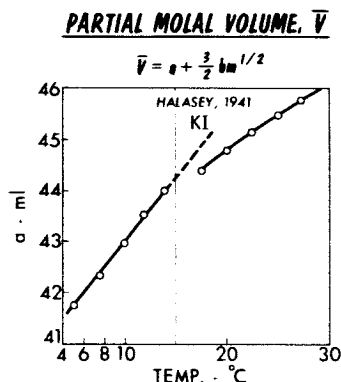


FIGURE 10. Concentration-independent term,  $a$ , in the equation for the partial molal volume of potassium iodide.

were obtained by Sister Halasey (1941). In the two systems shown, the kinks do not occur exactly at the temperature mentioned earlier, namely 15°C., but certainly in the vicinity of that temperature. It is of interest also to notice the opposite trends in changes of slope for the two salts in the vicinity of 15°C.

Solubility data often reflect the kinks particularly clearly, and Magat (1935), for instance, used the minimum in solubility of bromine in water near 30°C. as a suggestion of an anomaly in the vicinity of that temperature.

FIGURE 11 shows a recent example of solubility as determined by Klots and Benson (1963). These authors determined the solubility ratio between argon and nitrogen. The left side of FIGURE 11 shows the data and the

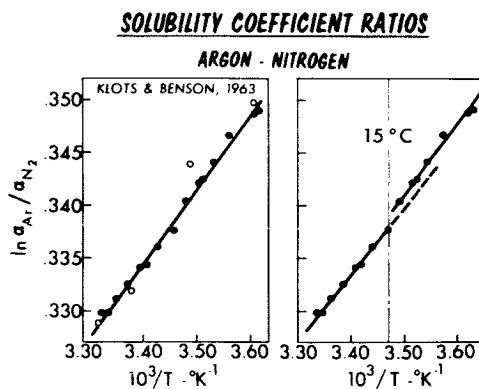


FIGURE 11. Solubility ratio between argon and nitrogen as determined by Klots and Benson.

smoothed curve originally suggested by Klots and Benson, obtained by a manometric method. The right side shows the same data but instead of one curve, two separate curve segments have been fitted to the data. As previously done for the density and dielectric constant data, we have made a statistical analysis of the solubility data. Again it was found highly significant that two separate curve segments give a better fit than one curve through the combined intervals. It is indeed interesting that the kinks show up so markedly in the present case where we are dealing with *ratio* of solubility of two quite similar gases, especially if one attempts to relate the solubility of these gases to their clathrate-forming tendencies. Both gases form Type I hydrates and both have almost the same Parachor (van der Heem, 1964), hence, it is particularly hard to find any reason here for specificity; it should be noted, however, that the dissociation pressure of the hydrates at 0°C. is only 95 atm. for argon but 160 atm. for nitrogen.

Many other solubility studies suggest the existence of the kinks. It is unfortunately quite rare to find the solubility of any particular solute in water studied at sufficiently closely spaced temperature intervals to permit one to look for all four kinks. However, the kinks are quite noticeable, for instance, in the solubility of lanthanum chloride (data from Seidell, 1940) as shown in FIGURE 12 where the kinks near 45 and 60°C. are quite distinct although apparently displaced a few degrees from the values for the temperatures for the kinks in pure water and dilute solutions. Note the high concentration for which the kinks seem to persist (the solid phase in equilibrium with the solution is the heptahydrate throughout the temperature range investigated). Anomalies are indeed often found for very high concentrations. Thus, when the usual plot of logarithm of the solubility versus  $1/T$  is made, the data for the solubility of silver nitrate obtained by Campbell and Boyd (1943) also show quite distinct anomalies near 10 to

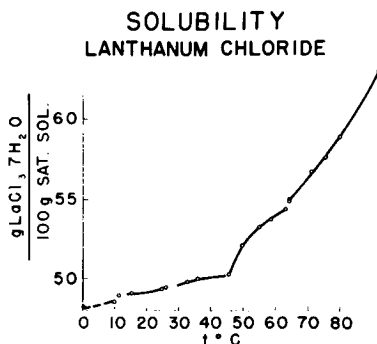


FIGURE 12. Solubility of lanthanum chloride heptahydrate versus temperature.

15°, 25 to 30° and in the vicinity of 60°C. Here the molar ratio of solute to solvent is approximately 1:4. Similarly, the solubility of substances like *r*- and *l*- mandelic acid also shows the kinks, again for extremely high molar ratios of solute to solvent. Among many other examples, we might mention the solubility of thiourea (Jänecke & Hoffman, 1932), thallium nitrate, thallium hydroxide, silver iodate, silver nitrite, barium sulfamate, ether and benzoic acid (Seidell, 1940).

#### *General Observations*

A large number of other examples could be cited as evidence for the reality of the anomalies in water and aqueous solutions; however, because of the limited time we refer to the forthcoming monograph which will present in greater detail the total evidence available. Before proceeding we summarize the main conclusions which we have drawn with respect to the thermal anomalies in water based on all the available evidence (see Drost-Hansen, Sept. 1963).

- A. The temperatures of the kinks are approximately 15, 30, 45 and 60°C. within  $\pm 1^\circ - 2^\circ$  of these temperatures; this is to say that kinks may be centered, for instance, near 13° and 31°C. while the next kink may occur at 44°C. Hence, the glaring symmetry that would otherwise be implied is not necessarily real, and the enumeration of the 15°C. multiples may serve conveniently and only as a mnemotechnic device for remembering the temperatures of the transitions. The changes occur, as best as one can tell, over a fairly narrow temperature interval, about one to two degrees on either side of the "center" of the transition temperature. It is possible, and in fact likely, that more than four kinks exist. I believe the next kink would be found for temperatures in excess of 80°; however, we do not yet have enough data to propose any specific temperature. Very likely there is also a kink in the vicinity of 140-160°.
- B. The kinks occur in the properties of both pure water and aqueous solutions. For this reason, we believe that the kinks owe their existence to some phenomena associated with the structure of water and that the existence of the kinks in aqueous solutions is due to the persistence of particular structural features of pure water in the presence of solutes.
- C. The temperatures at which the kinks occur in aqueous solutions are rather insensitive to both the nature and the concentration of solutes. We have not yet sufficient material on hand to state the excursions to be expected from the pure water values for the temperatures of the kinks as a function of concentration or nature of the solute. However, generally the changes are probably within a few degrees for most solutes up to concentrations of the order of, say, two-five molar.

Only strong acids in moderate to high concentrations seem to change the temperatures of the kinks to any appreciable extent. The kinks, how-

ever, remain but the temperatures are noticeably changed from the values for pure water and dilute solutions.

D. The kinks are present in both equilibrium properties and in transport phenomena.

E. The kinks show up in surface and interfacial phenomena as well as in bulk properties. For surface phenomena the kinks may occur at slightly different temperatures than observed for bulk phenomena.

*Biologic Implications: "Simple" Kinetic Phenomena*

It has been claimed that there exist in water structural transitions that are manifested in the temperature dependence of many properties. We have also claimed that these transitions occur even in very concentrated aqueous solutions and have inferred that the occurrence of the transitions in such solutions must reflect the persistence of elements of structure that are unaffected by the presence of the solute. Hence, it is reasonable to propose that the water in biologic systems may undergo similar transitions.

Over the years, many authors have discussed the possible existence of more or less abrupt anomalous changes in biologic phenomena as a function of temperature. FIGURE 13 shows an example of such an alleged, abrupt

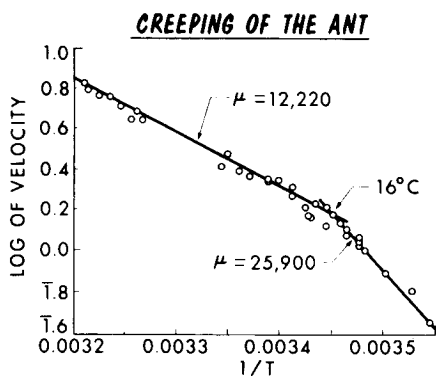


FIGURE 13. Rate of creeping of ant as a function of temperature.

change with temperature. This illustration shows the logarithm of the rate of creeping of the ant as a function of the reciprocal, absolute temperature. This illustration is redrawn from Johnson, Eyring and Polissar's book, *The Kinetic Basis of Molecular Biology* (1954); the data were obtained by Shapley and have been discussed by Crozier. Please note that the previous authors have kindly provided their estimate of the temperatures at which the two straight lines intersect. FIGURE 14, also redrawn from the book by Johnson, Eyring and Polissar, shows the temperature dependence

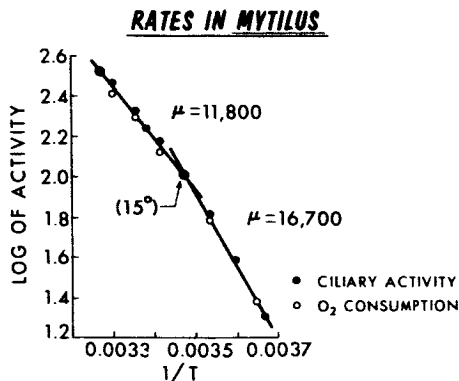


FIGURE 14. Rate of ciliary activity and oxygen consumption of the gill epithelium in the clam, *Mytilus*.

of two other phenomena, namely, ciliary activity of the clam *Mytilus*, which is shown as solid circles, and the oxygen consumption of the gill epithelium of the same clam, shown as open circles. These data are by Gray, worked up by Crozier in the middle twenties. The two curves both show a kink; again the previous authors have indicated the temperature at which they believed the kink occurs, and again this coincides nicely with the 15°C. anomaly in water.

It may be argued that perhaps it takes some "degree of faith" to draw lines of the type indicated and that the kinks may just be the result of a rather subjective curve fitting on the part of those who have analyzed the data. I would like to show another graph which I think will indicate that at least in some cases the kinks are not a matter of "sighting down the line to make it break at the right place." FIGURE 15 shows the protoplasmic

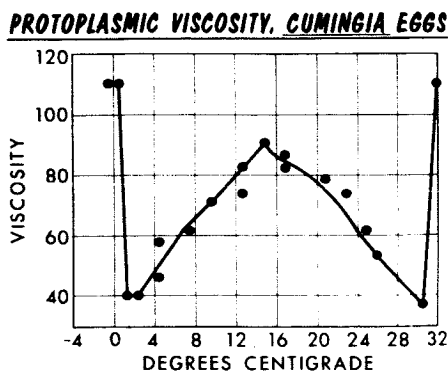


FIGURE 15. Viscosity of protoplasm for *Cumingia* eggs.

viscosity in *Cumingia* eggs as determined by Heilbrunn (1924). One sees that marked changes occur in the viscosity of the protoplasm in the vicinity of 2, 15 or 16°C., and again near 30 or 31°C. I do not pretend to understand in detail the significance of these marked changes, but they seem well above any criticism concerning "forced" curve drawing to give straight line segments deviating only slightly from each other. I am somewhat puzzled by the anomaly near 2°C.; however, the anomalies at 15 and 30°C. coincide very nicely with the anomalies in water and aqueous solutions. Not all examples are as dramatic as FIGURE 15; yet a very large amount of evidence indicates that the temperatures of the kinks in water are coincident with the marked changes in biological systems.

FIGURE 16 shows the relation between temperature and the frequency of division in *Chilomonas paramecium* (data by Smith, 1940). Again one

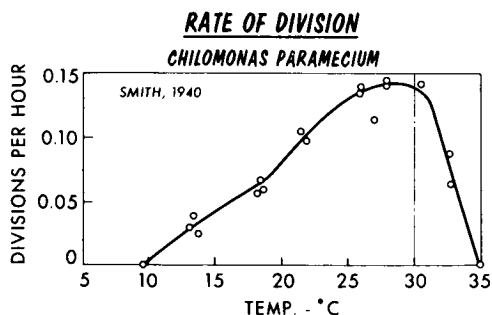


FIGURE 16. Frequency of cell division in the *Chilomonas paramecium* as a function of temperature.

notices a marked drop in the rate of cell division starting at 30 and vanishing at 35°C. Whether the anomaly indicated on the graph near 18°C. is a reflection of the 15°C. anomaly cannot be decided.

FIGURE 17 shows the time required for breakdown of the germinal vesicle of *Chaetopterus* eggs at various temperatures. These data are from a paper by Heilbrunn and Wilson (1955); the ordinate here is log of the time (in minutes) for breakdown of the vesicle, the abscissa is the temperature. Pronounced changes occur at both 12 and 30°C. It seems very reasonable to assume that the change at 30°C. reflects the kink at 30°C. in water; it is also likely that the anomaly at 12°C. reflects the 15°C. kink.

FIGURE 18 shows a study by Brown and Taylor (1938) of the excystment process for the ciliate *Colpoda duodenaria*. The abscissa is the reciprocal absolute temperature and the ordinate is the logarithm of the time for the excystment process. In this figure are shown the experimental points obtained by the author; the curve drawn, however, is what the present author

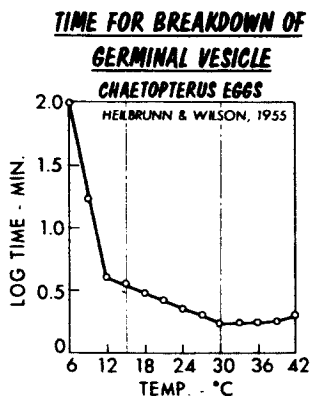


FIGURE 17. Time for breakdown of germinal vesicle of *Chaetopterus* eggs as a function of temperature.

considers a reasonably good fit to the data. Again one observes an anomaly near 15 and 30°C.

*Complex Physiological Processes: Temperature Optima and Minima*

As shown above, a number of "simple" kinetic phenomena in biologic systems show the occurrence of more or less abrupt changes at the temperatures of the kinks. We have now postulated (Drost-Hansen, 1956) that for a number of complicated biologic phenomena the existence of the structural transitions makes the biological system "prefer" to operate as far as possible from the temperatures of the kinks. Hence, we propose that in the process of evolution, biologic systems were selectively favored that operated in the middle of the interval between two consecutive transition

**LOG TIME FOR THE EXCYSTMENT PROCESSES**

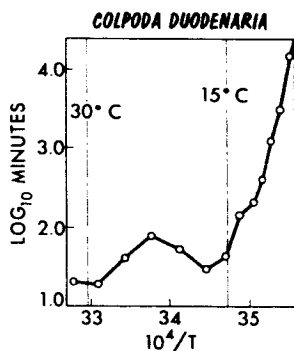


FIGURE 18. Rate of excystment for *Colpoda duodenaria*.

temperatures. Consider, for instance, the kinks at 30 and 45°C.: at either temperature the properties and behavior of a large number of individual processes may undergo rapid and "unpredictable" changes and hence it seems "safer" to operate the biological system near 37–38°C., in other words, as far removed as possible from either of the two kinks. Thus, we propose that in the course of evolution, temperatures near 37 and 38°C. have been favored by mammals as the optimum temperature for existence. FIGURE 19 shows a graph of body temperatures of approximately 160 mam-

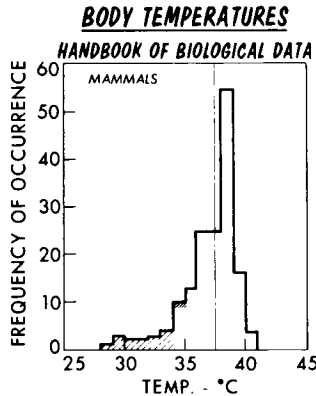


FIGURE 19. Distribution of body temperatures of mammals.

mals. From this graph it is seen that there is a strong predilection for body temperatures in the mammals between 37 and 39°C. The shaded area under the curve at the low temperature end indicates the body temperatures of such mammals as the anteater, the sloth, the echidna, the armadillo and a few other species of the type which, to a large extent, owe their existence only to freaks of nature, such as, isolation in unusual environments. Indeed, an animal like the duckbill platypus (body temperature around 30°C.) is a strange kind of a mammal in that it lays eggs, nests, feeds under the water as much as above the water, and in general does not seem to exhibit very predominantly mammalian behavior.

Further evidence of the importance of the kinks is the upper lethal temperatures. For all the mammals for which upper lethal temperatures have been established, it seems certain that 45°C. is an absolute upper lethal limit.

We have studied also the body temperatures of the birds. In this case, the agreement is not quite as impressive: the mean body temperature is around 41.5°C. However, it seems established that for the birds also, 45°C. constitutes an absolute, upper thermal limit. We may speculate as to the



cause for the displacement from 37 or 38°C. to near 41°C.; I should like to venture the guess that this is a compromise to the requirement of the highest possible energy production (such as we might predict from an Arrhenius type of activation mechanism) and the conformance to the structure and properties of water. In other words, the increased temperature may facilitate the production of energy necessary for flight while at the same time sacrificing "thermal latitude" such as resistance to infectious diseases (by minimizing the temperature range available for the bird in hyperthermia). It is interesting in this connection to note that most of the birds that do not fly, such as the ostrich, kiwi or penguin seem to have "normal" body temperatures namely between 38 and 39°C.

It is well known that in both man and many other mammals, 30°C. is a temperature of considerable physiological importance. For example, in man there is loss of consciousness below 30°C., together with a loss of the ability to regulate body temperature. Moreover, below 30°C., marked changes occur in the oxygen consumption of various tissues (this being one of the reasons why cardiovascular surgery is sometimes performed under hypothermia, often at temperatures around 27 or 28°C.). FIGURE 20

#### OXYGEN UPTAKE IN RABBITS

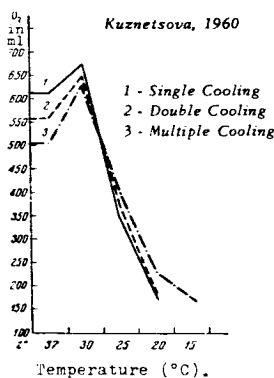


FIGURE 20. Rate of oxygen consumption of rabbits; (By permission — Pergamon Press).

shows an example of change in oxygen consumption. The ordinate is the oxygen uptake of rabbits, the abscissa is the temperature (Kuznetsova, 1960); the rate of O<sub>2</sub>-uptake drops abruptly below 30°C.

By analogy with the systems enumerated above, we suggest that optima between 45 and 60°C. should exist for other types of living organisms. Indeed, many thermophilic bacteria are known to possess optima around

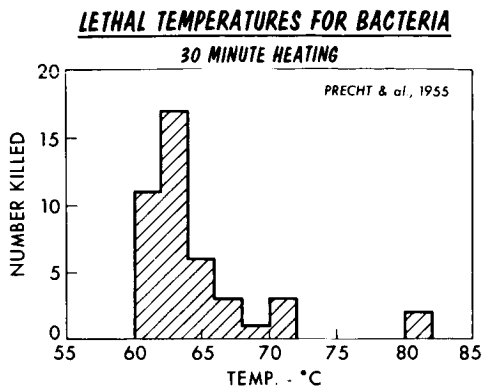


FIGURE 21. Lethal temperatures for a number of bacteria under various conditions (heating time: 30 minutes).

53–55°C., pasteurization temperatures usually tend to be approximately 60 to 62°C. FIGURE 21 shows the lethal effects of heating above 60°C. for a compilation of 20 different bacteria under a variety of different conditions, mostly different media. The data shown are all those cases for which heating times of 30 minutes have been used; this histogram has been drawn from data compiled by Precht, Christophersen and Hensel (1955).

The same type of argument as presented above can be applied to the interval between 15 and 30°C. Here we find optimum activity near 22 to 25°C. for a large number of vastly different types of animals: many insects (though not all), many fishes, and many soil bacteria seem to have optima in the vicinity of 23 to 25°C. Also, 30°C. is known to be an important temperature physiologically for both fishes and insects. We shall illustrate this shortly with a number of specific examples. Furthermore, it is known that 15°C. often is a controlling factor in ecology: for example, in the distribution of fishes in the South Pacific (Jones, 1947) where the density of fishes of commercial interest drops precipitously at temperatures below 15°C. Another example of ecologic interest is shown in FIGURE 22 where the ordinate is the rate of egg deposition of the gastropod *Urosalpinx cinerea* and the abscissa is the temperature. This illustration, which is redrawn from the data by Moore (1958) shows that 15°C. is indeed a critical temperature below which no deposition of eggs take place.

#### *Some Kinetic Aspects and Examples*

As outlined above, there exist in water more or less abrupt structural changes that give rise to changes in the properties of pure water and in aqueous solutions. I believe that these changes significantly influence the behavior of biologic systems. Obviously, it is not claimed that these changes

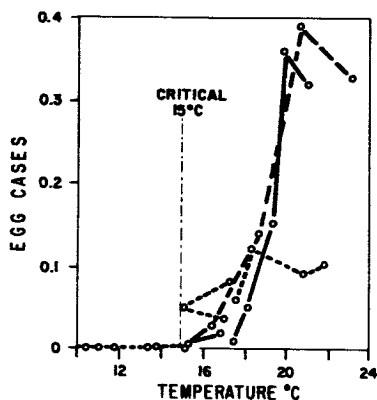
EGG DEPOSITION OF GASTROPOD (*UROSALPINX CINEREA*)

FIGURE 22. Rate of egg deposition of gastropod.

determine all the thermal properties of biological systems but the structural changes in water can certainly account for at least some of the anomalous and often abrupt changes encountered in biologic systems.\* Thus, these changes may suggest reasons for tendencies in optimum temperature selections in biological systems. While I do not in general take issue with the formulations of the kinetics of biologic systems, as developed, for instance, by Johnson, Eyring and Polissar (1954), I believe that the structural changes in water must also be considered as important constraints on the biologic systems and that these constraints superimpose on other mechanisms so as to greatly affect the systems' over-all temperature-dependence. The notion of the kinks can assist us significantly in understanding the behavior of many biologic systems where, for instance,

\*One might inquire as to how often the anomalies show up at the "right temperatures" in the biological systems; — "right temperatures" meaning, say, within 2 to 3°C. of the temperature of the kinks in water and aqueous solutions. Based on all available data, the author is of the opinion that the "agreement" at least holds for something like 75 out of 100 cases (this does not include the problem of body temperatures of mammals and birds covered in the preceding section). The general validity of this estimate, however, depends on the reliability of the sampling of examples and it may be argued that perhaps the author and his associates have chosen only those examples which "fit" the notions expressed above at the expense of examples which do not support the theory (either by showing no inflection points, maxima or minima, or by having the kinks at the "wrong" temperatures). Initially, we were indeed looking for specific examples which could be used to support our original hypothesis — this is the way one goes about constructing empirical theories. Over the years, however, we have tried to exercise appropriate objectivity although the possibility remains that we may be "subconsciously" prejudiced. At least, we are aware of the problem.

Johnson, Eyring and Polissar's theory alone is not likely to provide all the answers. One example is the observation made by Andrewartha and Birch (1954), based on an analysis by Moore, that for 41 aquatic animals (*Crustacea*, *Echinodermata*, *Mollusca*, *Tunicata* and *Pisces*), 91 per cent of them were restricted to a range of 16°C. or less (for 42 per cent of them, the range was 14°C. or less). It is interesting that this activity interval of 16° coincides very closely with the interval between consecutive kinks, optima for the activity of fishes often being approximately midway between 15 and 30°C. As an example, FIGURE 23 shows the distribution of

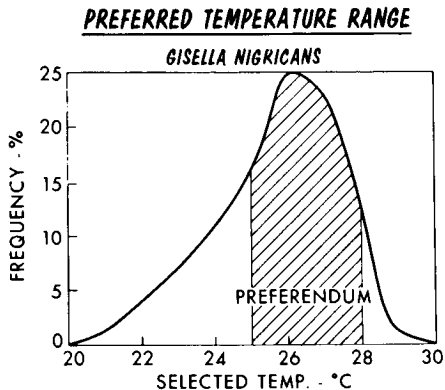


FIGURE 23. Preferred temperature ranges for the fish, *Gisella nigricans*.

preferred temperatures for the fish *Gisella nigricans* as a function of temperature (See Andrewartha and Birch, 1954). About 75 per cent of the fish congregate between 25 and 28°C., with no fishes preferring temperatures above 30 or below 20°C.

FIGURE 24 shows the temperature ranges for normal development of eggs of the meadow frog, *Rana pipiens*, from different localities in North America (see Andrewartha & Birch, 1954). Again one observes that 30°C. is, with a few exceptions, as high as the normal development is encountered. Note also that 15°C. does not seem to be nearly as important a temperature for the frog as 30°C.

FIGURE 25 shows the logistics curve for development per hour in per cent of the egg stage of *Calandra oryzae* (Andrewartha & Birch, 1954) again the abscissa is the temperature. The logistics curve is very accurately followed in the range from 15.5 to 30°C., but for temperatures of 30 to 34°C., very marked deviations occur.

FIGURE 26 shows the "calculated" and observed development curves for *Drosophila melanogaster* in the pupa state (see Davidson, 1944). Again,

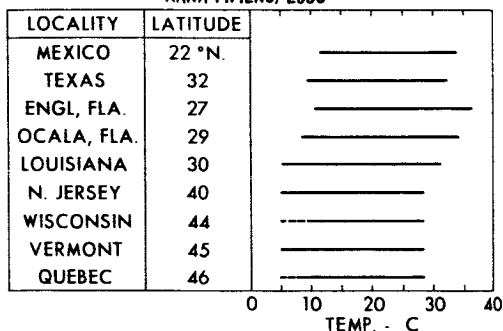
**RANGES FOR NORMAL DEVELOPMENT****RANA PAPIENS, EGGS**

FIGURE 24. Ranges of temperature for normal development of eggs of the meadow frog, *Rana pipiens*.

the behavior follows closely the logistics curve between 15 and 30°C., but deviations occur above 30°C. The logistics curve for the egg state is almost identical in shape. This points to an observation that we have often made. The properties of water are alleged to be very anomalous and indeed this is so. However, in studying the behavior of solutions we often find that "normal" behavior is encountered as long as attention is restricted to the properties between consecutive kinks. For instance, plotting logarithm of solubility or logarithm of reaction rates versus the reciprocal, absolute temperature often gives to a very good approximation "perfectly straight lines" between say 15 and 30°C. or between 30 and 45°C. Within these intervals the behavior is indeed "normal." Hence, we should perhaps not

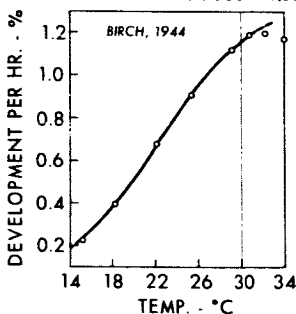
**RATE OF DEVELOPMENT****CALANDRA ORYZAE, EGG STAGE**

FIGURE 25. Logistics curve for development of the egg of *Calandra oryzae*.

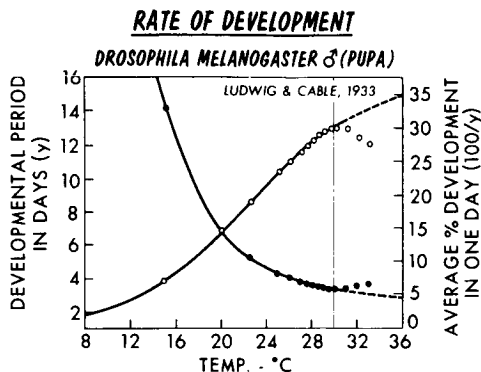


FIGURE 26. Logistics curve for development of the pupa of *Drosophila melanogaster*.

be too surprised to find, as we did, that the development of the egg stage of the insect follows very nicely a moderately simple logistics curve. On the other hand, we should expect the marked anomalies that, in fact, occur near the kink at 30°C.

#### *Multiple Temperature Optima*

If we are correct in assessing the importance of the structural changes in water for the behavior of biologic systems, it may be possible to delineate ranges of environmental temperatures that are conducive to life. Life generally cannot be maintained for any organism over a wide range of temperatures. Andrewartha and Birch, state, for instance: "...no individual species is known which can thrive over such a wide range as from 0 to 50°C." This statement is probably generally quite true, however, in our own studies we have come upon bacteria that have multiple ranges for optimal growth.

We have studied a sulfate-reducing bacteria, probably a *clostridium*, that was able to grow over a temperature range of from 7 to 45°C., with three separate ranges of optimum activity (Oppenheimer & Drost-Hansen, 1960). FIGURE 27 shows the initial results obtained in this study; growth optima are seen to occur near 12, 26 and 39°C. Because the initial study was performed using only visual estimation of the turbidity as a means of estimating the growth, we have since repeated this experiment and checked the amount of growth with the spectrophotometer (Schmidt & Drost-Hansen, 1960); FIGURE 28 shows the results. Again, optimum activity occurs near 24 and 40°C., with growth minima near 15, 30 and above 45°C. In this particular experiment the activity did not drop to zero at the 30°C. kink, but the optical density does go through a minimum near this temperature. Unfortunately, the experiment was not conducted at sufficiently

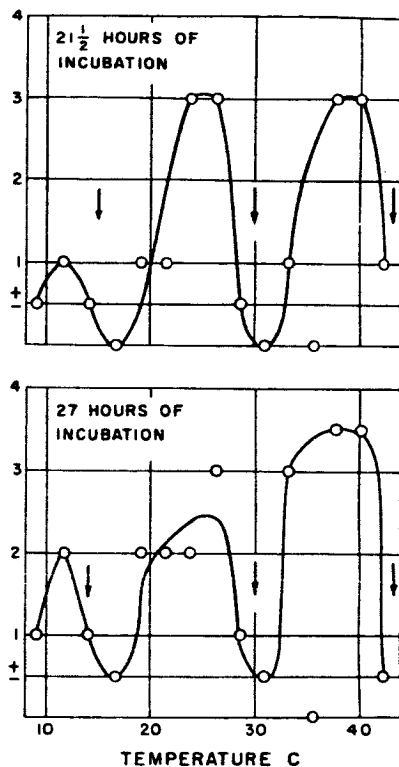


FIGURE 27. Growth of a sulphate-reducing bacterium, probably a *clostridium*.

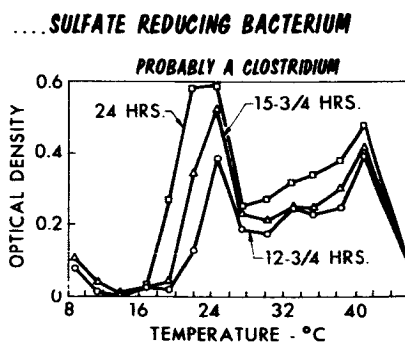


FIGURE 28. Growth of a sulphate-reducing bacterium, probably a *clostridium*, as determined by optical density measurements with spectrophotometer.

GROWTH OF NEUROSPORA - MUTANT

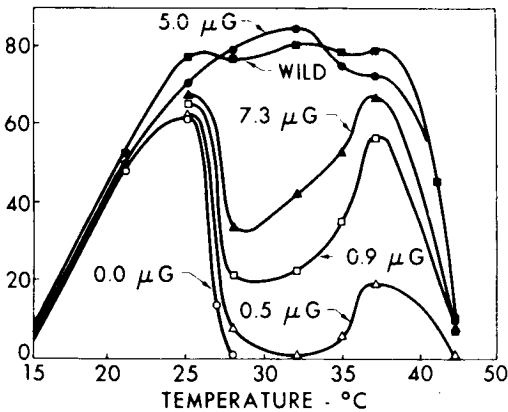


FIGURE 29. Growth of mold; a mutant of *Neurospora crassa*.

low temperatures to determine if a third optimum existed below the 15°C. minimum.

A similar type of growth curve was reported earlier by Mitchell and Houlahan (1946), who studied the growth of a *Neurospora crassa* mutant that was made to require lactoflavin for growth. The amount of growth (determined as dried weight of the cells) is shown in FIGURE 29 as a function of temperature in the presence of the amounts of lactoflavin indicated on the curves. We are here dealing with an organism that for small concentrations of lactoflavin has distinct growth minima near 15, 30 and 45°C., with optima near 23 and 37°C. These are exactly the type of results we

..... UNBUFFERED MEDIUM, NO DEXTROSE

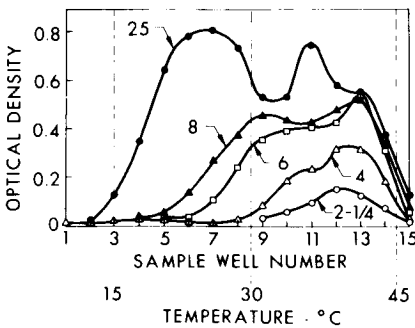


FIGURE 30. Growth of *E. coli* as a function of temperature for five different times of growth.



would predict from our considerations of the influence of the kinks on the biological systems.

Further corroboration of these predictions is given by a more recent study of the growth of *E. coli* (Schmidt & Drost-Hansen, 1961). FIGURE 30 shows the amount of growth, measured as optical density, at five different times of growth as a function of temperature. In the older cultures there are again two optima for growth, namely near 26 and 35°C. FIGURE 31

.....UNBUFFERED MEDIUM, NO DEXTROSE

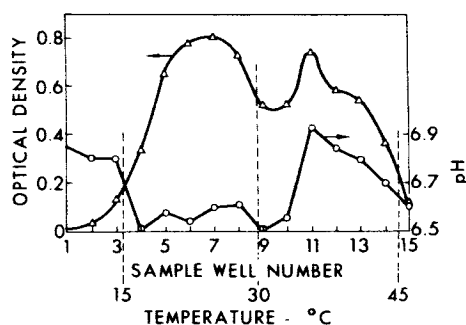


FIGURE 31. pH of system shown in FIGURE 30 at the end of 25 hours of growth.

shows the measured pH of the system at the end of 25 hours of growth: between 15 and 30°C., the pH dropped to 6.6, while below 15°C. and above 32°C., pH was increased over the initial value. We have observed this type of behavior on several occasions. In FIGURES 28 and 30, the two peaks and the minimum between them suggest the superposition of two growth peaks that overlap to some extent. We offer the accompanying pH changes as evidence for a hypothesis formulated earlier (Oppenheimer & Drost-Hansen, 1960): that some organisms are able to grow optimally in different temperature intervals by utilizing different metabolic pathways. We have also obtained evidence from a study of *Serratia marcescens* (Schmidt & Drost-Hansen, 1960) that the well known difference in red pigment formation changes near 30°C. This, perhaps, is another manifestation of different metabolic pathways utilized by the organism for growth above and below 30°C.

### Discussion

Evidence has been presented for the existence of thermal anomalies in the properties of water. The anomalies probably reflect higher order phase-transitions or some other order-disorder phenomenon involving cooperative action on the part of the water molecules. On this basis, one may then

suggest that the structure of water must be characterized by cooperating units whether they be cages or clusters. Very likely, the sizes of the cooperating units are between 10 to 200 molecules; the lower limit is determined very roughly by the number of particles necessary to obtain cooperativeness, and the upper limit seems reasonable, since, were the clusters much larger, they would have manifested themselves quite readily in optical scattering, X-ray and neutron diffraction measurements and presumably in several other types of measurements. Recently some direct evidence has been reported of "clusters" in water in the size range mentioned (Egelstaff, 1962). It has also been argued that the kinks remain unchanged in the presence of most any solute and that this must imply the persistence of structural features characteristic of pure water in the presence of solutes. Hence, it was a simple matter to extend the notion of the existence of the kinks to biologic systems that are indeed aqueous solutions with, albeit, large surface-to-volume ratios.

It remains to be explained how the kinks may play such a prominent role in biologic systems when they are oftentimes quite difficult to determine, for instance, from data on the properties of pure water. The explanation may possibly be related to the fact that the biologic phenomena of interest to us take place over a considerably narrower temperature range than that over which we are able to study ordinary physicochemical systems. Hence, with equal diligence on the part of the physical chemist and the biologist, the biologist may "squeeze in", say, 10 measurements over a range of 20 to 30°C. — the total range of interest in nondestructive studies of an organism or a protein solution — while the physical chemist may well be interested in the properties extending from far below 0°C. to considerably above the boiling point. Hence, we simply have more data available at more closely spaced temperature intervals for biologic systems than are available for most physico-chemical parameters.

In addition to the "numerical" advantage of the biologic examples, we may perhaps speculate that such phenomena as hydrophobic bonding of water around a protein molecule or ordering of water molecules adjacent to a biologic membrane may constitute far more sensitive probes of the aqueous environment than the behavior of, say, an alkali ion or any other "single", "small" solute species in water. The cooperative action between many water molecules in the water clusters of the solvent water may well be expected to influence drastically the rather larger amount of water associated with the proteins or membrane material. In other words, the structural transitions in water may exert a direct and profound influence on the immediate environment of the macromolecules of the biologic systems; the effects of the transitions are not merely "solvent effects" manifested by minute changes in the solvent viscosity, dielectric properties or activity. Except for vaguely defining some cooperating units such as

clusters or cages we are able to appreciate structural peculiarities of water in biologic systems without a more specific model.

In a recent paper, Davey and Miller (1965) at North Carolina State University have provided important experimental evidence for the reality of growth minima for microorganisms in the vicinities of the temperatures of the kinks in pure water. We quote their abstract: "Water in the liquid phase has been shown, by others, to undergo subtle changes in physical structure near 15, 30, 45 and 60°C. Four bacteria were used to cover the range in temperature from 5 to 70°C. in order to determine whether these temperature-dependent anomalies in the structure of water may have biological implications. In all cases growth was suppressed at the predicted temperatures. This suggests a strong interaction between the structure of water and biological activity." Davey and Miller also noted that anomalies at temperatures other than the four predicted ones were not observed (between 5 and 70°C.) and that the observed temperature-related anomalies in the growth of the four bacteria seemed to be greater in magnitude than in most, if not all, of the published physical data, indicating the highly sensitive nature of biologic systems to subtle alterations in their micro-environment.

### *Conclusions*

There appear to exist in water and aqueous solutions thermal anomalies reflecting cooperative order-disorder phenomena in the water structure. It is suggested that these structural anomalies significantly influence the behavior of biologic systems, specifically that they may account for the existence of more or less abrupt changes with temperature in many biologic phenomena and that they delineate optimum and minimum temperatures for biologic activity.

### *References*

- ANDREWARTHA, H. G. & L. C. BIRCH. 1954. The Distribution And Abundance Of Animals. Univ. of Chicago Press. Chicago, Ill.
- ANTONOFF, G. 1950. Colloid Chemistry. A. E. Alexander, Ed. 8: 83. Oxford Press. London, England.
- BORDI, S. & F. VANNEL. 1962. Proprieta superficiali e variazioni strutturali dell'acqua. *Ann. Chim.* 52: 80.
- BROWN, M. G. & C. V. TAYLOR. 1938. The kinetics of excystment in Colpoda Duodenaria. *J. Gen. Physiol.* 21: 475.
- BROWN, R. J. S. 1958. Private communication. See also *Bull. Am. Phys. Soc.* 2(3): 166.
- BRUNNER, C. 1847. Untersuchung über die cohäsion der flüssigkeiten. *Ann. der Physik und Chemie (Poggendorff's Ann.)* 70: 481.
- CAMPBELL, A. N. & M. L. BOYD. 1943. The system: Silver-nitrate-water. *Can. J. Res.* B21: 163.
- CHAPPUIS, M. P. 1907. Dilation de l'eau. *Trav. Mem. Internat. Poids et Mesures.* 13: D1-D40.
- DAVIDSON, J. 1944. On relationship between temperature and rate of development of insects at constant temperatures. *J. Anim. Ecol.* 13: 26-38.

- DAVEY, C. B. & RAYMOND J. MILLER. 1965. Temperature-Dependent Anomalies in the Growth of Microorganisms; paper submitted to Soil Science Society of America, Proceedings.
- DECARVALHO, H. G. 1944. Contribution to the physicochemical study of water (transl). *Anais. Assoc. Brasil. Quim.* 3: 152-158.
- DORSEY, N. E. 1940. Properties of Ordinary Water-Substance. ACS Monograph #81 Reinhold Publishing Corp. New York, N. Y.
- DROST-HANSEN, W. 1956. Temperature anomalies and biological temperature optima in the process of evolution. *Naturwissenschaften*. 43: 512.
- DROST-HANSEN, W. 1963. The evidence for higher order phase transitions in liquid water and some structural implications. Abstract of paper 21. 145th ACS Meeting (Sept.) New York, N. Y.
- DROST-HANSEN, W. 1964. Aqueous interfaces — methods of study and some structural properties. Paper presented at symposium on physics and chemistry of interfaces. *Indust. & Eng. Chem.* 57(3), 38, 1965, 57(4), 18, 1965.
- DROST-HANSEN, W. 1965. Monograph on the structure of water. In preparation.
- DROST-HANSEN, W. & R. W. MYERS. 1963. Temperature dependence of interfacial tension between water and n-decane. Abstract Paper 5F. 144th National ACS Meeting in Los Angeles, Calif.
- EGELSTAFF, P. A. 1962. Neutron scattering studies of liquid diffusion. *Adv. Phys.* 11: 203.
- FEATES, F. S. & D. J. G. IVES. 1956. The ionisation functions of cyanoacetic acid in relation to the structure of water and the hydration of ions and molecules. *J. Chem. Soc. (London)* : 2798.
- FORSLIND, E. 1952. A Theory Of Water. Handlingar, Svenska Forskningsinstitutet för Cement och Betong vid Kungl. Tekniska Högskolan Stockholm, p. 16.
- FRANKS, F. & D. J. G. IVES. 1960. The adsorption of alcohols at hydrocarbon-water interfaces. *J. Chem. Soc. (London)* : 741.
- FRANK, HENRY S.: 1963. Some questions about water structure. Desalination Research Conference. National Academy of Sciences — National Research Council. Publication. 942: 141-55.
- FRONTAS'EV, V. P. 1956. The nature of the thermal conductivity polytherm of water in the range of 10 to 60°C. *Dokl. Akad. Nauk. SSSR* 111: 1014-16.
- HALASEY, SISTER M. EVA. 1941. Partial molal volumes of potassium salts of the Hofmeister series. *J. Phys. Chem.* 45: 1252.
- HARNED, H. S. & B. B. OWEN. 1958. The physical chemistry of electrolytic solutions. ACS Monograph #137. Reinhold Publishing Corp., New York, N. Y.
- HEILBRUNN, L. V. 1924. The viscosity of protoplasm at various temperatures. *Am. J. Physiol.* 68: 645.
- HEILBRUNN, L. V. & W. L. WILSON. 1955. Changes in the protoplasm during maturation. *Biol. Bull.* 108: 271.
- IVES, D. J. G. 1963. Some reflections on water. Inaugural Lecture at Birkbeck College.
- JÄNECKE, M. K. & HOFFMAN. 1932. The system  $\text{CS}(\text{NH}_2)_2\text{-NH}_3\text{-H}_2\text{O}$ . *Z. Elektrochemie* 38: 880.
- JOHNSON, F. H., H. EYRING & M. J. POLISSAR. 1954. The Kinetic Basis Of Molecular Biology. John Wiley & Sons. New York, N. Y.
- JONES, EVERETT C. 1957. Personal Communication.
- KAVANAU, LEE. 1964. Water and Solute-Water Interaction. Holden-Day, Los Angeles, Calif.
- KLOTS, C. E. & B. B. BENSON. 1963. Thermodynamic properties of the atmospheric gases in aqueous solutions. *J. Phys. Chem.* 67: 933.
- KUZNETSOVA, Z. P. 1960. The Problem of Acute Hypothermia. P. M. Starkov, Ed. Pergamon Press. New York, N. Y.
- LAVERGNE, M. & W. DROST-HANSEN. 1956. Discontinuities in slope of the temperature dependence of the thermal expansion of water. *Naturwissenschaften* 43: 511.

- MAGAT, M. 1935. Sur un changement des propriétés de l'eau aux environs de 40°C. *J. Physique* 6: 179.
- MAGAT, MICHEL. 1937. Raman spectra and the constitution of liquids. Discussion — *Faraday Society* 33: 114–120.
- MALMBERG, C. G. & A. A. MARYOTT. 1956. Dielectric constant of water from 0° to 100°C. *J. Res. Nat. Bur. Std.* 56: 1.
- MITCHELL, H. K. & M. B. HOULAHAN. 1946. *Neurospora*. IV., A temperature-sensitive riboflavinless mutant. *Am. J. Botany* 33: 31.
- MOORE, H. B. 1958. *Marine Ecology*. John Wiley & Sons. New York, N. Y.
- MOSER, H. 1927. Der absolutwert der oberflächenspannung des reinen wassers nach der bügelmethode und seine abhängigkeit von der temperatur. *Ann. Physik*. 82: 993.
- NEILL, H. W. & W. DROST-HANSEN. 1955. Activation energy for viscous flow of water. Unpublished.
- OPPENHEIMER, C. H. & W. DROST-HANSEN. 1960. A relationship between multiple temperature optima for biological systems and the properties of water. *J. Bacteriol.* 80: 21.
- OTHMER, D. F. & M. S. THAKAR. 1953. Correlating diffusion coefficients in liquids. *J. Indust. Eng. Chem.* 45: 589.
- PINKERTON, J. M. 1947. A pulse method for the measurement ultrasonic absorption in liquids: results for water. *Nature*. 160: 128–9.
- PRECHT, H., J. CHRISTOPHERSEN & H. HENSEL. 1955. *Temperatur und Leben*. Springer Verlag. Berlin, Germany.
- QURASHI, M. M. & A. K. M. AHSANULLAH. 1961. Investigation of periodic discontinuities in the mutual potential energy of molecules of water and some polyhydric alcohols. *Brit. J. Appl. Phys.* 12: 65.
- SCHMIDT, M. G. & W. DROST-HANSEN. 1960. unpublished.
- SCHMIDT, M. G. & W. DROST-HANSEN. 1961. (Sept.) Multiple temperature optima for the growth of *E. coli*. Abstract of paper P-9. 140th National ACS Meeting in Chicago, Ill.
- SEIDELL, A. 1940. *Solubilities of Inorganic and Metal Organic Compounds*. Von Nostrand. Vol. I, Third Ed. (see also:) SEIDELL, A. 1941. *Solubilities of Organic Compounds*. Von Nostrand. Vol. II, Third ed. (see also:) SEIDELL, A. & W. F. LINKE. 1952. *Solubilities of Inorganic and Organic Compounds*. Von Nostrand. Supplement to Thir dEd. (see also:) LINKE, W. F. 1958. *Solubilities; Inorganic and Metal-Organic Compounds*. Von Nostrand. Vol. I, A-Ir Fourth Ed.
- SIMPSON, J. H. & H. Y. CARR. 1958. Diffusion and nuclear spin relaxation in water. *Phys. Rev.* 111: 1201.
- SMITH, J. A. 1940. Data by Smith. *Biol. Bull. Woods Hole*. 79: 379 Ref. Kitching's VII Symposium Soc. Gen. Microbiology. Cambridge Univ. Press. 1957. : 271.
- TIMMERMANS, J. & H. BODSON. 1937. La tension superficielle de l'eau et celle de l'eau lourde. *Compt. Rend.* 204: 1804–07.
- VAN DER HEEM, P. 1964. Personal communication.
- WOLF, C. 1857. Vom einfluß der temperatur auf die erscheinungen im haar-röhrchen. *Poggendorf Ann.* 102: 571. *Ann. Physik Chem.* : 178.

# PHASE TRANSITIONS ENCOUNTERED IN THE RAPID FREEZING OF AQUEOUS SOLUTIONS\*

B. J. Luyet

*American Foundation for Biological Research, Madison, Wisc.*

The findings of the last few years have resulted in a new outlook on the problem of the phase transitions which take place during the rapid freezing and the rewarming of aqueous solutions. In the present review of that problem, I shall, after a short historical survey of the principal events in the development of our knowledge in the field, examine in some detail the newly established facts and some of the proposed interpretations.

## HISTORICAL SURVEY

### *Early Developments: The Vitrification-Devitrification Theory*

The German physicist Tammann (1898) pointed out that, when a liquid is cooled very rapidly, the transition to the crystalline state may be suppressed, and the liquid may solidify in the amorphous or "vitreous" state. He reported experiments in which the passage into the vitreous state, "vitrification," was verified in some 50 organic liquids. Tammann described also how his vitrified material would "devitrify," that is, crystallize, upon being rewarmed. The answer to our question about the phase transitions encountered in rapid freezing would then be that, when a liquid is cooled very rapidly, it undergoes *no phase transition*, and when it is rewarmed it *crystallizes*.

Moran (1926), experimenting with gelatin gels, observed that, when the water content is less than about 35 per cent, none of the water crystallizes, even upon slow cooling. We would then have a case of an *aqueous solution* containing amorphous ice at low temperature without having been subjected to rapid cooling. (Although this process is not classified in the category vitrification, it should be mentioned here as a related phenomenon.)

According to Burton and Oliver (1935), when water vapor is deposited on a cold metal plate *in vacuo* (a form of very rapid cooling), it solidifies in the amorphous state. This experiment has been repeated by several investigators who checked the resulting structure by x-ray diffraction (for references on the earlier work on this subject see Blackman & Lisgarten, 1958, and, for later work, Dowell & Rinfret, 1960).

Luyet and collaborators (1937), applying the methods of Tammann to aqueous solutions of colloids and crystalloids, reported to have obtained

\*Work supported principally by Grant GP-3630 (formerly G-20900) from the National Science Foundation.

vitricification and devitrification by combining the effects of the two factors; solute concentration and high cooling rate, for example, by cooling 50 per cent gelatin at rates of several hundred degrees per second.

Barnes (1939), studying by x-ray diffraction the gelatin gels frozen by Luyet's method, found them to be amorphous.

Thus, according to the findings reported so far, aqueous solutions, and even pure water, like the organic liquids studied by Tammann, would vitrify upon being rapidly frozen and devitrify upon being rewarmed. From the point of view of the phase transitions encountered, the situation would be as outlined above: no transition upon rapid cooling and a crystallization upon rewarming.

*Later Developments: Actual Structure  
of Rapidly Cooled Aqueous Solutions*

Zachariasen (1932), Randall (1934), and others, on the basis of x-ray analysis, came to the conclusion that several of the substances reported to be vitreous contain crystallites and consist of poorly ordered, or of partly ordered and partly disordered, material; in other words, the "vitreous" substances in question had undergone incomplete and/or imperfect crystallization. (For more detailed information, see Luyet. 1957. : 440.)

Then Luyet and Rapatz (1957 & 1958) found that most of the *aqueous solutions* thought to be amorphous after having been cooled rapidly were really crystalline. In polarized light, between crossed polarizer and analyzer, the thin preparations generally used in the freezing experiments showed conspicuous Maltese crosses (see FIGURE 2). Thus rapid freezing, under certain conditions, would cause aqueous material to *crystallize into spherulites* in which the ice forms thin radial fibers not visible with ordinary light.

Meryman (1958), making a cursory x-ray-diffraction study of the spherulitic structures obtained in gelatin gels, observed an incomplete x-ray diagram which suggested some form of hindrance to crystallization.

Further x-ray analysis by Dowell, Moline and Rinfret (1961) led these authors to apply to gelatin gels the interpretation previously accepted in the case of pure water and to conclude that the frozen gels contain vitreous, cubic or hexagonal ice, or a mixture, in various proportions, of these different kinds of ice, depending on the cooling rate and the solute concentration. With a 50 per cent gelatin gel, frozen at  $-85^{\circ}$ , for example, they reported vitreous ice (cf. their FIGURE 1).— Upon rewarming, vitreous ice would be transformed into cubic and, finally, cubic ice would be transformed into hexagonal.

Luyet, Tanner and Rapatz (1962), in a systematic study of gelatin gels of various concentrations cooled at various rates, obtained x-ray diagrams

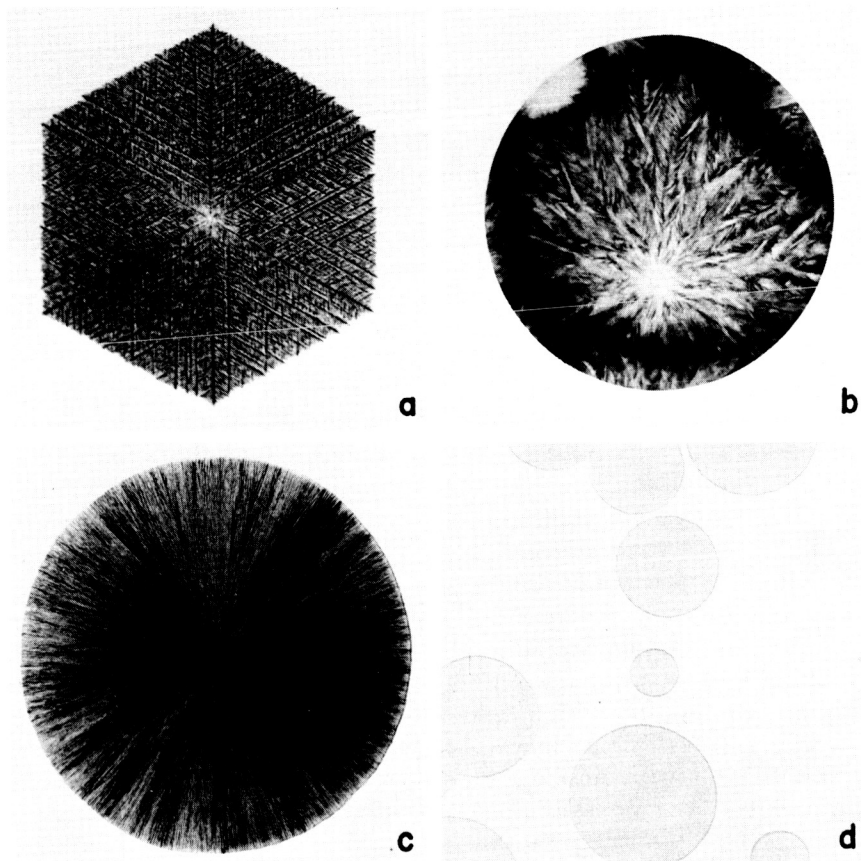


FIGURE 1. The three principal types of ice formations encountered in aqueous solutions. (a) Regular dendrite (hexagonal crystal); (b) irregular dendrite; (c and d) spherulites; (c) coarse spherulite; (d) "evanescent" spherulite.  $\times 86$ . (Reproduced from Luyet & Rapatz, 1958, by permission of *Biodynamica*.)

which indicated a gradual hindrance to crystallization at increasing rates, but which did not furnish evidence of complete inhibition.

According to the latter authors, the situation, in regard to the phase transitions encountered in the rapid freezing of aqueous solutions, would then be that the highest cooling rates obtainable with the method of immersion of specimens in liquid baths are still insufficient to prevent the transition of water into the crystalline state; rapid cooling would only *hinder* and *limit* that transition. Rewarming would merely permit a *re-sumption* and *completion* of the hindered, interrupted crystallization.



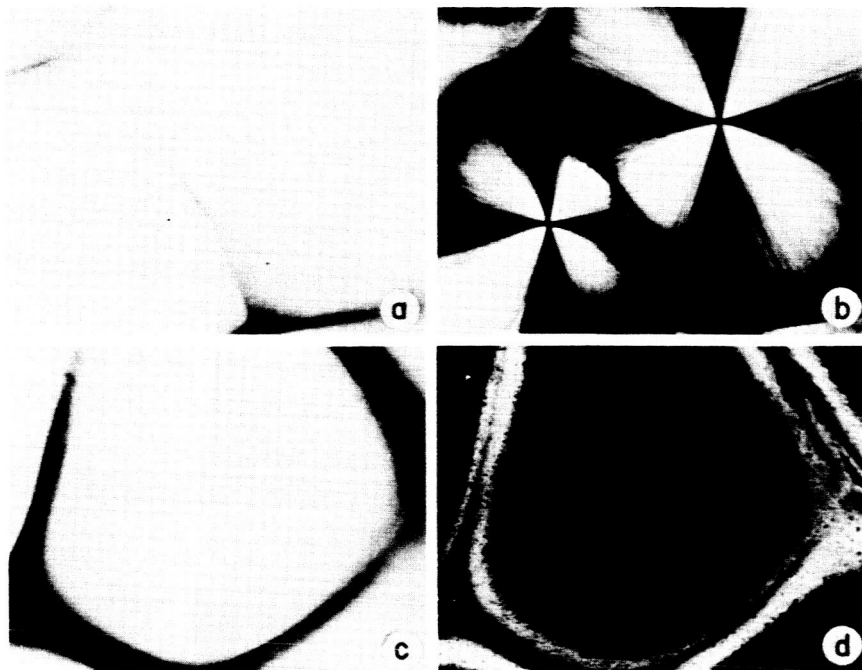


FIGURE 2. "Evanescent spherulites" formed in thin layers of 30% gelatin solutions rapidly frozen. (a and c) Spherulites seen in ordinary light; they are optically empty, except for their borderlines. (b) Same field as in a, in polarized light; the spherulitic structure is evidenced by the Maltese crosses. (d) Same field as in c, after the temperature had been raised to  $-10^{\circ}$ ; the spherulite has become opaque, as a result of recrystallization.  $\times 62$ . (Reproduced from Luyet & Rapatz, 1958; Rapatz & Luyet, 1959, by permission of *Biodynamica*.)

The second part of this paper will consist in a presentation and a discussion of the factual evidence about this situation.

#### THE PRESENT STATUS OF OUR KNOWLEDGE FACTUAL DATA AND PROPOSED INTERPRETATIONS

The material to be discussed will be presented under three headings: Crystallization, Recrystallization, Overall Picture of the Phase-Transitions Complex.

##### (A) Crystallization

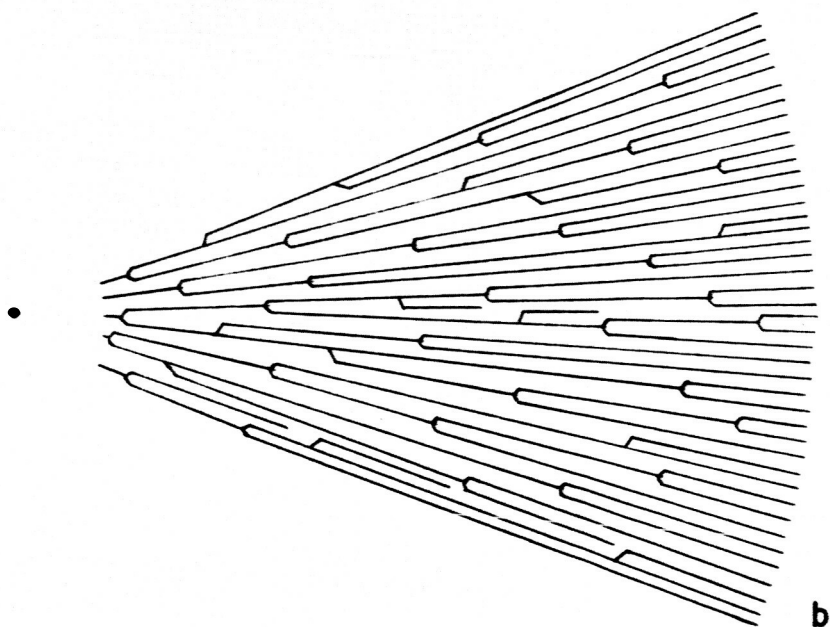
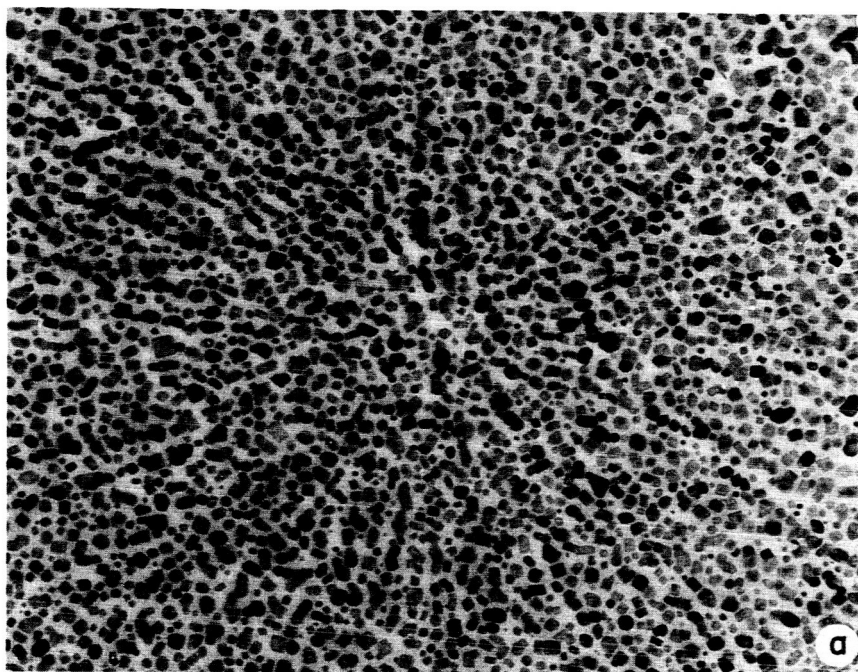
*Effect of rapid cooling on the pattern of ice formation.* (a) Types of crystalline structures encountered. In a systematic study of the patterns of ice formation obtained with solutions of some 15 solutes, crystalloids and colloids, of various concentrations, frozen at various cooling velocities, Luyet and Rapatz (1958) described three basic types: (1) regular den-

drites, which are well formed structures with hexagonal symmetry (FIGURE 1, Photo. 1), (2) irregular dendrites in which the regularity in the number and arrangement of branches is lost or disturbed (Photo. 2), and (3) spherulites, which appear to consist of unbranched fibers radially arranged around the center of crystallization (Photos. 3 and 4). — The spherulites can conveniently be divided into two varieties according to the apparent dimensions of the radial fibers: coarse and “evanescent” spherulites (Photos. 3 and 4, respectively). (The term evanescent has been applied to those units of which the radial fibers are so thin that they are invisible in ordinary light; polarized light brings out their presence.) Within each of the two types, the radii become gradually finer at gradually higher cooling rates.

The evanescent spherulites are of such importance in the study of the effects of rapid freezing that they deserve a closer look.

(b) The type “evanescent spherulites.” Examination of the spherulites under the electron microscope reveals that what appear to be unbranched fibers growing radially around crystallization centers are really arborescent structures, the branches of which have a gradually decreasing diameter at increasing cooling rates. In electron micrographs of gelatin gels and of blood plasma, MacKenzie and Luyet (1960) observed arborescent formations of solid material (left after the sublimation of the ice) which had branches of diameters of the order of 1000 to 500 Å. Branches of smaller diameter were poorly resolved, indicating that either the ice did not separate entirely from the solute, or the delicate structures did not survive the treatment preparatory to electron microscopy. In the case of solutions of potassium chloride (FIGURE 3, electron micrograph 1), well-resolved salt crystals appear in radially arranged rows separated from each other by spaces (previously occupied by ice) which measure a few hundred angstroms.

In well-formed regular dendrites (that is, in hexagonal crystals, such as that shown in FIGURE 1, Photo 1), all the branches and subbranches are parallel to one or other of the six axial columns growing from the center of crystallization; the prolongation lines of these branches, therefore, do not meet at the center, as the six axial columns do. On the other hand, the “radial” fibers of the spherulites are truly radial, that is, their prolongation lines meet in the center. It is, therefore, necessary that the ramifications which develop, in the course of the growth of the spherulites, from the original radial fibers readjust their directions, if they are to become truly radial. We may picture that readjustment in the following manner: when the original fibers arising from the center (FIGURE 3, Diagram 2) have grown a certain distance, they branch out; but the newly formed lateral branches cannot grow to any appreciable length before meeting a radially growing fiber; they then form subbranches which would normally grow at 60°



angles to the parent branch, but have to grow radially, in the centrifugal direction, for the simple reason that they cannot grow in any other direction, due to the crowded condition everywhere. (The diagram of FIGURE 3 is, of course, an idealized representation; the branching and subbranching of the spherulitic structures, as seen in some cases of semi-evanescent spherulites, have nothing of the regularity shown in the diagram.)

These observations and considerations lead one to the conclusion that the three forms of crystalline structures mentioned: regular dendrites, irregular dendrites and spherulites, belong to one basic type: they are all dendrites. The main distinctive characteristics between them are the diameters of the branches and the frequency of branching, which result from differences in cooling rates.

*Effect of rapid cooling on nucleation and growth rate.* It is a well established fact that, when a preparation, such as a thin layer of aqueous solution, is immersed abruptly into a cooling bath, the *number* of crystallization units that reach observable size increases with decreasing temperatures, within a certain range. Conversely, the *dimensions* of the units reaching observable size decrease proportionately (FIGURE 4, Photos. 1 to 4). Curves representing the number of such units per given volume or area, in terms of decreasing temperatures, reach a maximum and then drop. But such a drop is apparently due, at least in part, to the slower *growth* of the units at lower temperatures. A better approach to the fundamental problem would be to determine the actual size of the nuclei and the number formed under given conditions of temperature, cooling rate and solute concentration (instead of the number of those which reach visible size).

For our purpose here, it will suffice to point out that the cooling rate plays an important role in the number and size of crystallization units developed in a preparation.

*Effect of rapid cooling on crystallographic structure.* Let us now examine the basis for the claim that rapid cooling permits the formation of cubic, instead of hexagonal ice, and that still more rapid cooling prevents any crystallization. (The cooling rates under discussion are those obtained by the method of immersion of the specimen in a cooling bath, which are far from comparable with those obtained in the deposition of vapors on a cold plate.)

---

FIGURE 3. Structure of evanescent spherulites. (a) Electron micrograph of a spherulite formed in a very thin layer of a 20% KCl solution, sandwiched between two collodion films, frozen rapidly and freeze-dried.  $\times 19,800$ . (b) Diagrammatic representation of growth and branching of the radial fibers arising from a center of crystallization in an evanescent spherulite. (Selected from the files of MacKenzie & Luyet. Reproduced by permission of the authors.)

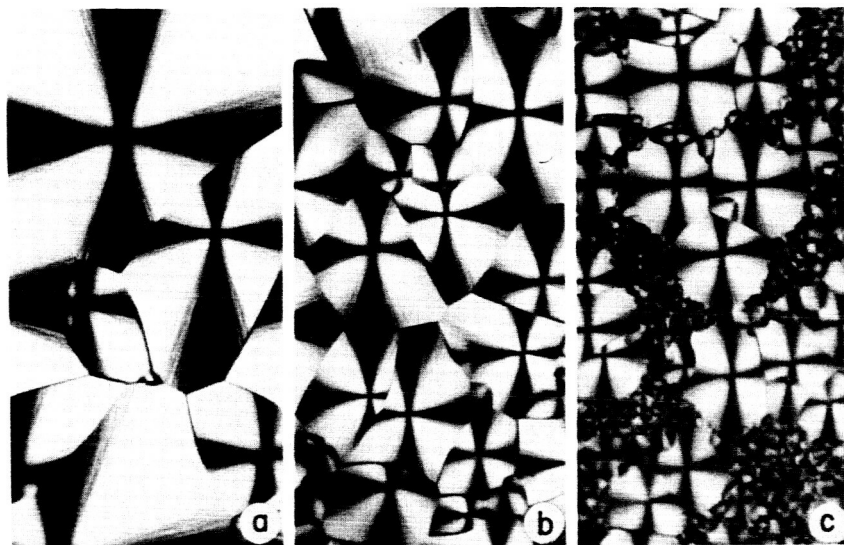


FIGURE 4. Photographs, in polarized light, of spherulites formed in thin layers of a 5M glycerol solution, illustrating the increasing number and decreasing size of the crystallization units at increasing cooling rates and decreasing temperatures. — Temp. of freezing bath: (a)  $-60^{\circ}$ ; (b)  $-70^{\circ}$ ; (c)  $-75^{\circ}$ .  $\times 83$ .

When a layer  $75\mu$  thick of a 50 per cent gelatin gel is cooled at a rate of a few thousand degrees per second by immersion in an isopentane bath at  $-150^{\circ}$ , the x-ray diffraction diagram shows no reflection peak (FIGURE 5, Tracing 1). When a similar preparation is immersed in a bath at  $-60^{\circ}$  or  $-30^{\circ}$ , the cooling rate being of the order of hundreds of degrees per second, three peaks emerge in succession: first, Peak No. 2, which one would normally expect to be produced by the basal planes 002 of hexagonal crystals, then Peaks 5 and 7, from Planes 110 and 112 (Tracings 2 and 3). Peak No. 1 (from Planes 100) also begins to emerge. When the temperature of the coolant bath is  $-20^{\circ}$ ,  $-15^{\circ}$  or  $-10^{\circ}$ , which reduces the cooling rates to tens of degrees per second, Peak No. 1 completes its rise, and is followed by Peak No. 3, from Planes 101, and finally by Peaks 4 and 6, from Planes 102 and 103 (Tracings 4 to 6).

The facts that: (a) the most rapidly cooled specimens have no peaks (Tracing 1), (b) the specimens cooled at intermediate rates show three peaks which occupy the same position in the diagram as the three principal peaks of cubic ice (Tracings 2 and 3), and (c) the most slowly cooled specimens exhibit the full set of peaks of hexagonal ice (Tracings 4, 5 and 6) gave rise to the idea that the three cooling rates result in the formation of, respectively, amorphous, cubic and hexagonal ice.

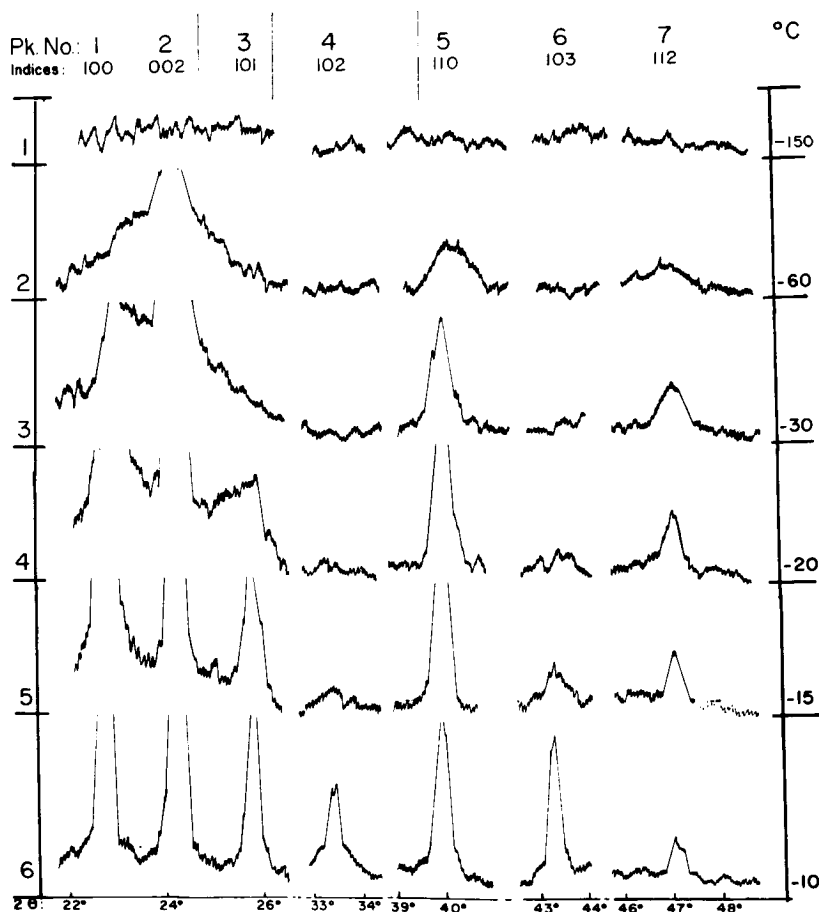


FIGURE 5. X-ray diffraction diagrams of ice in gelatin gels of 50% concentration frozen in thin layers by immersion in baths at the temperatures indicated on the right side of each diagram. — The order numbers of the angles, or peaks, are given in the top line, the indices on the second line, the order numbers of the tracings in the column at left, the freezing temperatures in the column at right, and the scale of two-theta angles underneath the tracings. — Tracing 1: No evidence of any rise. Tracing 2: Inverted V at Angle 2 and humps at Angles 5 and 7. Tracing 3: Inverted V at Angle 1, spikes at 2 and 5, inverted V at 7. Tracing 4: High spikes at Angles 2, 5 and 1, and inverted V at 3. Tracing 5: Peak at Angle 3, and elevation or inverted V at 4 and 6. Tracing 6: Tall peaks at Angles 2, 5, 1, 3 and 6. (Reproduced from Luyet, Tanner & Rapatz. 1962, with permission of *Biodynamica*.)

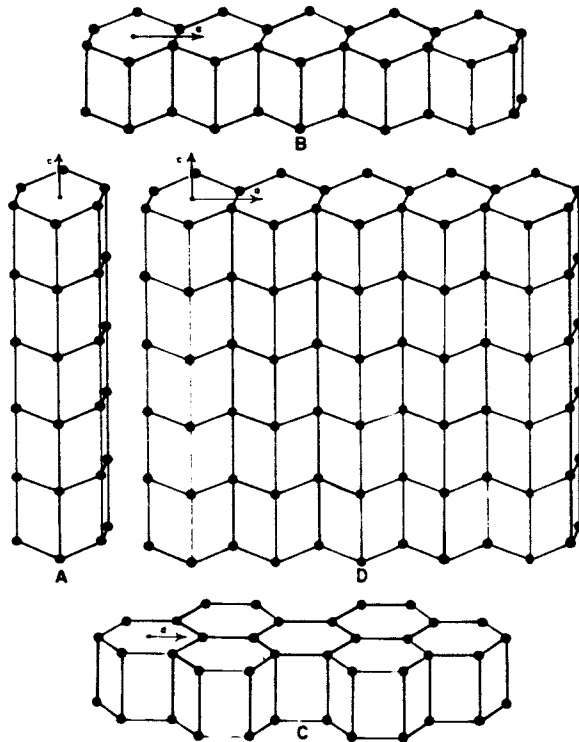


FIGURE 6. Diagrams illustrating the structure of the needles and of the slabs which one would obtain if hexagonal ice crystals would grow preferentially in some directions. The molecules of water are represented by dots; the molecules which form hexagonal rings are connected by lines, and so are the rings when piled up vertically. — Diagram A: Needle formed when preferential growth is along the  $c$  axis; Diagram B, when growth is along the  $a$  axis; Diagram C, when growth is along a direction  $d$  at  $30^\circ$  from  $a$ . Diagram D: Slab formed when preferential growth is along the  $c$  and the  $a$  axes. (Reproduced from Luyet, Tanner & Rapatz, 1962, with permission of *Biodynamica*.)

But Luyet and associates pointed out that the x-ray diagrams recorded can be accounted for on the basis of different degrees of hindrance to the growth of hexagonal crystals. (a) When the gels are cooled at the highest rates, the crystals would be too small to reflect the x-rays; (b) when the rates are intermediate, crystal growth would take place in preferred directions so as to produce needles along the  $c$  axis (Diagram A of FIGURE 6) responsible for Peak 2, and slabs along the  $c$  and  $a$  axes (Diagram D) responsible for Peaks 2, 5 and 7; (c) when the rates are low, the crystals would grow freely in all directions and would have enough planes in any direction to produce all the peaks.

The authors note that the *gradual* rise of the peaks and the *early emergence of Peak 1*, which does not belong to the cubic series, do not speak in favor of the theory of cubic ice. (For details we refer the reader to the original paper.)

On the whole, if the interpretation proposed by Luyet and collaborators is correct, rapid cooling would hinder crystal growth and favor development in some preferred directions.

*Effect of rapid cooling in limiting the amount of ice formed.* The quantitative determination of the degree of hindrance to crystallization exerted by rapid cooling has been attempted, in various ways, in our laboratory. A microdilatometer method (in which capillary tubes were used as dilatometers) gave the amounts of ice formed in solutions of the polymer polyvinyl pyrrolidone (PVP) and, by difference, the amount of water not permitted to freeze, when the cooling rate (measured at  $0^\circ$ ) was some 100 to 200 degrees per second.

The results, plotted in the curves of FIGURE 7, show that the per cent of the freezable water which remains unfrozen (ratio of  $I_R$  to  $I_C + I_R$ ) increases from small values at PVP concentration of 20 per cent, to about 50 at a concentration of 35 per cent, at which the prevention of freezing is maximum, and decreases to small values again, when the concentration increases to 45 per cent.

The question arises then of the chances that one may have of completely preventing crystallization by increasing further the cooling rates. MacKenzie and Luyet (1962), using the "collodion sandwich" technique, reached cooling rates which they estimate to be of the order of 100,000 to 500,000 degrees per second, but did not succeed, even at those rates, in preventing crystallization in gelatin solutions of about 20 per cent concentration. The general relationship between (a) the factors: cooling rate and concentration of solute (for various solutes), and (b) the effects: rate of nucleation, rate of crystal growth, and overall limitation in the amounts of ice formed still remains to be investigated.

#### (B) Recrystallization

*Notion of recrystallization.* (a) Irruptive recrystallization. At the macroscopic level, aqueous solutions frozen rapidly enough to reach the state of evanescent spherulites and to be transparent in ordinary light become intensely opaque upon being rewarmed to sufficiently high temperatures (FIGURE 2, Photos. 3 and 4). Examination under the light microscope reveals that the opacity is due to the formation of a cloud of ice particles which have become large enough to render the cloud visible. Since we know now that the transparent material was not amorphous but contained ice spherulites, we cannot call the change a devitrification in the sense originally given to that word; we are dealing, rather, with a resumption of the



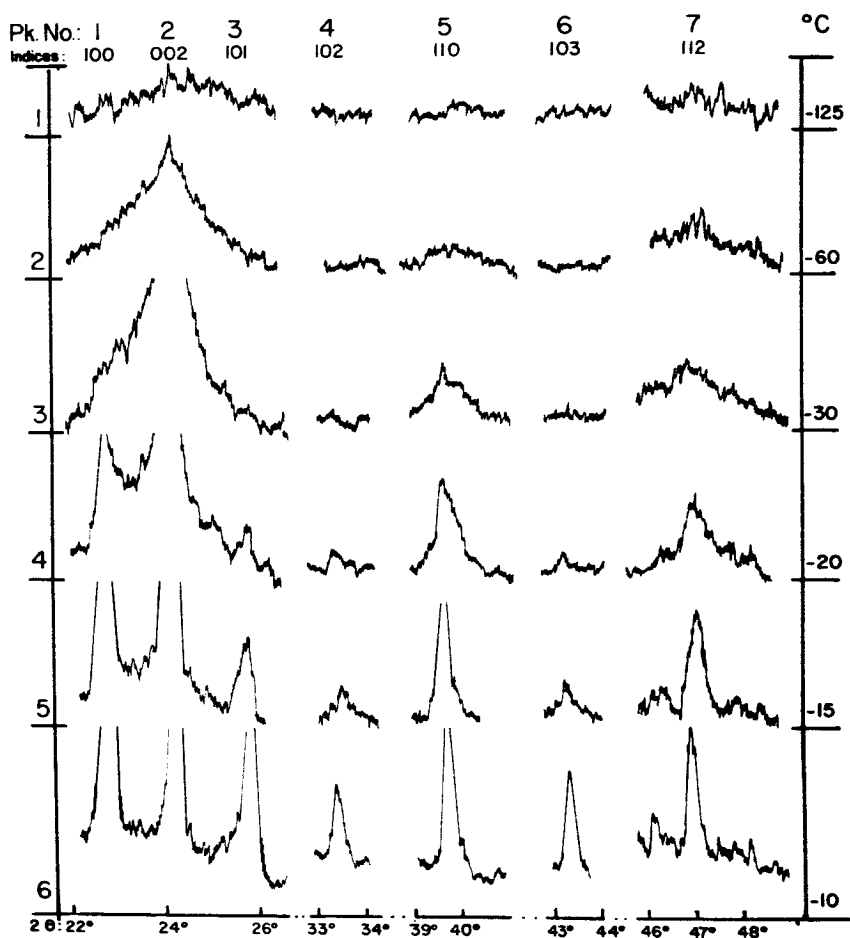


FIGURE 7. X-ray diffraction diagrams of ice in gelatin gels of 50% concentration, frozen in thin layers by immersion in a bath at  $-150^{\circ}$ , and rewarmed successively to the temperatures indicated on the right side of each diagram. — The order numbers of the angles, or peaks, are given in the top line, the indices in the second line, the order numbers of the tracings in the column at left, the rewarming temperatures in the column at right, and the scale of two-theta angles underneath the tracings. — A comparison of each tracing with the corresponding one in Fig. 5 shows that the diagrams obtained upon rewarming to a given temperature are about the same as those obtained upon freezing in a bath at the same temperature. (Reproduced from paper in press by Luyet, Tanner & Rapatz, with permission of *Biodynamica*.)

interrupted or inhibited crystalline growth, a process which belongs to the category designated by the physicists as recrystallization. Since the onset of opacity is rather abrupt, when the temperature is raised to a certain range, we called the phenomenon "irruptive recrystallization."

This type of recrystallization is described first in this survey because it illustrates well the process; but one should not infer that it differs in nature from other forms of recrystallization.

(b) General form of recrystallization. The form which has received wider attention from the physicists consists in the growth of the large crystals in a population at the expense of smaller ones. It has been designated by them as "migratory recrystallization" because it involves a migration of molecules from the small to the large crystals, as a result of a disequilibrium caused by the difference in surface-to-volume ratio in small and in large particles. The rate of the migration increases at rising temperatures and the process is particularly noticeable when one approaches the melting point, where one can actually see, under the microscope, the large ice masses grow larger.

The same principle controls the "critical size" of crystallites, that is, the size below which crystals are not stable because they sublime at a higher rate than that at which they would grow.

The principal characteristic of *irruptive* recrystallization is that the rate of crystalline growth increases rather suddenly in a given temperature range and that this sudden growth renders the system opaque. Thus, irruptive recrystallization may differ only by its suddenness and by the relative size of the particles from other forms of recrystallization.

*Temperatures of recrystallization.* A point which did not receive from the physicists the attention that it deserves is that of the abrupt resumption of crystal growth in a certain temperature range, during rewarming.

One of the characteristic properties of that range, which is also hardly known, is that, in aqueous solutions, it is determined mostly by the nature (apparently the molecular weight) of the solute, and is little affected by the concentration. These features are illustrated in TABLE 1.

Since, in the last analysis, temperature is the rate of motion of the molecules, these properties mean that the molecules of water, in a solution, break loose from their former rigid state and acquire motility rather suddenly. This phenomenon may play an important role in the physical stability of solutions in the frozen state (cf. Luyet, 1962).

*Release of heat during recrystallization.* When one attempts to raise at a constant rate the temperature of a specimen which has crystallized into spherulites, one observes a spontaneous, rather sudden, rise when the recrystallization range is reached; the rise is clearly due to the release of

TABLE 1  
TEMPERATURES OF "IRRUPTIVE RECRYSTALLIZATION" OF VARIOUS  
AQUEOUS SOLUTIONS

Solute:	Temp. °C.	Solute:	Temp. °C.
Hemoglobin	- 3.5	Raffinose	-25.4
Soluble starch	- 5.0	Sucrose	-30.5
Bovine albumin	- 5.3	Dextrose	-38.0
Dextrin	- 9.9	Glycerol	-58
Gelatin	-11.5	Acetamide	-65
Polyvinyl pyrrolidone	-14.5	Formaldehyde	-72

The temperatures recorded are those at which thin layers of solution become intensely opaque in one minute. With high-molecular-weight solutes the temperature-time curve is practically asymptotic after one minute, with low-molecular-weight solutes it is not. (With glycerol, for example, the recrystallization temperature is about  $-64^{\circ}$  if five minutes are allowed for the preparation to become opaque.)

The concentration of the solute has little effect on the recrystallization temperature; the values tabulated are for concentrations between 30 and 50 per cent.

The data are excerpted from various papers and from the files of unpublished observations of Luyet and collaborators.

heat in the recrystallization process (see the curves reported by Luyet, Kroener & Rapatz, 1958). We are at present determining the amounts of heat released.

*Quantity of ice formed during recrystallization.* As was mentioned above, we measured, by means of microdilatometers, the amount of ice formed during rapid freezing, and calculated the degree of hindrance produced under some particular conditions. Next, in that project, we measured the amount of ice formed during recrystallization upon rewarming; the results are presented in FIGURE 7. The sum of the amount  $I_R$  of ice formed on the resumption of crystallization, when the temperature reaches the recrystallization range, and of the amount  $I_c$  formed during cooling is apparently equal to the total amount of crystalline ice that one would obtain in slow freezing.

*Nature of the phase transitions occurring during rewarming.* According to the older concept, as was already said, the transition was thought to be a devitrification. I mentioned observations leading to the conclusion that it is a recrystallization. But the two processes are not necessarily self exclusive. There is the possibility that the transition involves two steps: a devitrification, followed by a change from one crystalline form to another. This is what would happen according to the interpretation given by Dowell, Moline and Rinfret (1960) of the x-ray diffraction diagrams that they obtained during the *rewarming* of rapidly frozen gelatin gels. The diagrams, which are quite similar to those produced in the rewarming of very rapidly frozen water, were interpreted as indicating a first transition, during rewarming, from vitreous to cubic ice, followed by a second, from cubic to hexagonal ice.

The x-ray diagrams that we obtained when a rapidly frozen 50 per cent gelatin gel was rewarmed gradually (FIGURE 8) are essentially the same as those obtained by Dowell, Moline and Rinfret, though we have again evidence for a *gradual* rise in the reflection peaks at gradually rising temperatures and for the *intrusion of Peaks 1 and 3* in the cubic series in which they do not belong. The striking similarity of the diagrams obtained

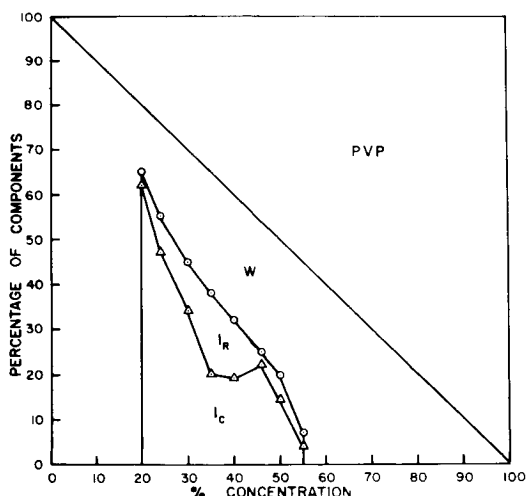


FIGURE 8. Diagram representing the percent by weight (in ordinate) of ice formed during rapid cooling  $I_c$ , of ice formed during rewarming  $I_R$ , of non-frozen water W, and of the solute PVP, at initial solute concentrations (in abscissa), varying from 20 to 55%. (Reproduced from paper in press by Luyet, Vehse & Gehenio, with permission of *Biodynamica*.)

upon rewarming and of those obtained upon rapid freezing to the same temperatures suggests that they result from the same process. So, it appears that here again, rewarming merely permits the completion of the crystallization which has been hindered and interrupted in the course of rapid freezing. One should note that the greatest change takes place in the recrystallization range, at  $-10^{\circ}$  in the case of a gelatin solution.

*Recrystallization during rapid freezing (spontaneous recrystallization).* Since rapid cooling results in the formation of spherulites, that is, in a crystallization, it involves a release of latent heat during the course of cooling. The heat released is sufficient, in some places, to raise the temperature locally, and so, to bring about recrystallization. This we call *spontaneous* recrystallization during cooling, and distinguish it from recrystallization *induced* by rewarming. The phenomenon is illustrated in FIGURE 9, in which one sees (Photo. 1) areas that became opaque as a result of a recrystallization brought about by the heat released at the meeting points of several neighbor spherulites. When the freezing temperature is closer to the recrystallization temperature, the opaque borderlines between spherulites are broader (Photo. 2). Electron micrographs of specimens cooled very rapidly and freeze-dried show clouds of spontaneous recrystallization along the border lines of the evanescent spherulites (white specks

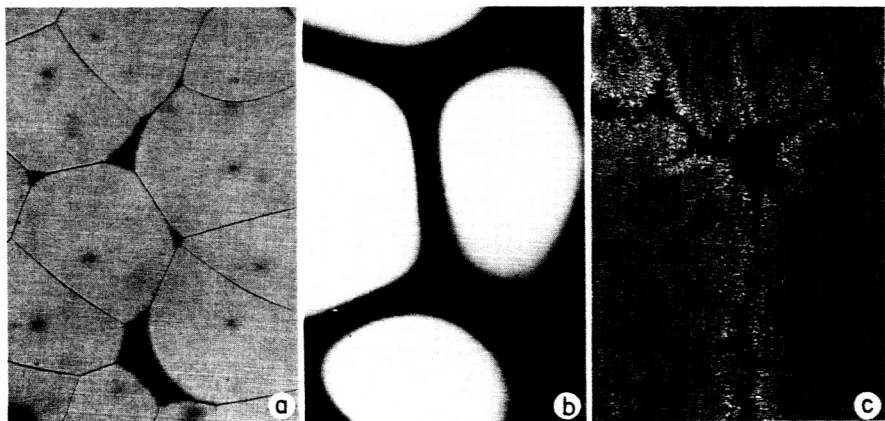


FIGURE 9. Spontaneous recrystallization. (a) Recrystallization clouds (dark areas) formed at the meeting of several adjacent spherulites.  $\times 51$ . (b) Recrystallization clouds covering larger areas when the temperature of freezing is closer to the recrystallization temperature. (The white areas are evanescent spherulites.)  $\times 51$ . (c) Electron micrograph showing recrystallization clouds (white specks) formed on the borderlines between adjacent spherulites.  $\times 4,860$ . a: reproduced from Luyet & Rapatz, 1958, with permission of *Biodynamica*; c: reproduced from paper in press by MacKenzie & Luyet, with permission of *Biodynamica*.)

in electron micrograph 3 of FIGURE 9). — (See below the note about the probable universality of spontaneous recrystallization.)

(C) *Overall Picture of the Phase-Transition Complex*

*General considerations.* The preceding observations lead to the view that the phase transitions encountered during rapid freezing and during subsequent rewarming are fundamentally the same transitions which take place in slow freezing and rewarming, the effect of the high cooling rate being merely to hinder some of the stages of the process, and the effect of rewarming being to permit the resumption and completion of the hindered stages.

The transitions involve three main steps: (1) the formation of nuclei, (2) the growth of nuclei to a certain size, and (3) the continued growth to larger sizes and, if that growth has been interrupted, its resumption. The first two steps constitute crystallization, the third is recrystallization. In principle, one or two of the three steps and, in the case of spontaneous recrystallization, all three steps may be hindered by rapid cooling.

Variations in cooling rates involve, by definition, the factor *time*. The factor *time*, in turn, controls the *equilibrium* conditions. I shall now examine briefly some of the problems encountered in the study of phase transitions in which these two notions intervene. Then I will evaluate the overall relationships.

*The factor time.* (a) Balance of rate of crystal growth and of rate of heat removal. It seems that the sequence of events described is controlled primarily by a balance between the rate of growth of the evanescent spherulites and the rate of heat removal. Whenever a group of molecules come together to form a nucleus, or to join a nucleus already formed, they will release heat. That heat will raise the local temperature and delay or interrupt further growth until it is dissipated. A repeated occurrence of unbalance between the rate of heat production and the rate of heat dissipation will result in a periodical succession of advances and interruptions of crystallization.

The phenomenon described as "spontaneous recrystallization" could then well be a universal process occurring in any freezing. In some cases the volume involved may be only a few cubic angstroms, in others it may be several cubic millimeters. We would observe it only when the amount of heat released is sufficient to raise the temperature and to bring about opacity within an appreciable volume.

(b) Delay in molecular motion caused by obstacles. The effect of the factor *time* may be looked upon from another point of view. The molecules of water need time to take their position in the crystal and, if one does not allow them the time necessary, crystallization is hindered; a part only of the water in the solution will then crystallize, the rest remaining in the

amorphous or semicrystalline state. The main factors responsible for delaying the motion of the water molecules are low temperature and the presence of molecules of solutes which act as obstacles.

One of the manifestations of the combined action of these two factors is the delay in the appearance of crystallization units when some highly concentrated solutions are cooled to very low temperatures, and the shortening of that delay when the temperature is raised. Thus, when gelatin gels of concentration higher than 50 per cent are cooled rapidly in a bath at  $-100^{\circ}$ , crystalline structures may not appear in them for a long time (up to several days) unless the temperature is raised. A rise to  $-37^{\circ}$  (Gehenio & Luyet, 1959) causes the crystallization units, which are tiny balls of ice that do not seem to have the properties of typical spherulites, to grow, in a matter of minutes, to visible size (Persidsky & Luyet, 1959). Upon a further rise in temperature to  $-10^{\circ}$ , the balls, like the evanescent spherulites, undergo irruptive recrystallization (Rapatz & Luyet, 1958). Apparently rapid cooling to  $-100^{\circ}$  brought about *nucleation*, but the nuclei could not *grow* until the temperature was raised.

*Equilibrium versus nonequilibrium conditions.* The problem of the phase transitions encountered in the rapid freezing of aqueous solutions may be considered as a particular case in the classical study, by "phase diagrams," of the relationships between the two factors temperature and solute concentration and the occurrence of phase transitions. But, whereas the classical phase diagrams include only cases of slow freezing, in which phase equilibrium has time to be established, we are concerned here with cases in which *equilibrium is not attained*, partly because of a too high freezing rate.

Another major difference between the cases in which equilibrium is reached and those in which it is not is that, in the former, the processes are immediately reversible: at a given temperature, a liquid crystallizes upon being cooled and the crystals melt upon being warmed, whereas, in the latter, the processes leading to nonequilibrium conditions during cooling tend to reach equilibrium upon rewarming, before they are ready for reversibility: a rapidly cooled solution, incompletely crystallized, will complete its crystallization, when slowly rewarmed, before it melts. Thus, the effects of temperature are to be explored in two directions, that is, *during cooling and during rewarming*; and the effects of both the cooling and rewarming rates should be investigated. One may thus expect rather complex phase diagrams.

*Overall relationships.* Since the effects of rapid cooling depend, to a great extent, on the factor solute concentration, I shall, in this overall survey, consider that factor first and divide the material of the survey according to the concentrations used. Most of the information available having been obtained with gelatin as solute, I will limit my survey to solutions of that

substance. (Studies of such overall relationships are now in progress with solutions of three other substances.)

From the point of view of the effects of rapid cooling on phase transitions in gelatin gels, there are four principal ranges of solute concentration to consider:  $C_1$ : up to 20 per cent;  $C_2$ : from 20 to 50 per cent;  $C_3$ : from 50 to 65 per cent;  $C_4$ : above 65 per cent.

Most of what has been said in this paper about phase transitions encountered during rapid cooling or during rewarming applies to Range  $C_2$ , in which one obtains evanescent spherulites that recrystallize upon rewarming to  $-10^\circ$ . What has been said about hindrance to crystallization, including, in particular, the limitation in the amounts of ice formed, also applies typically to this range.

In Range  $C_3$ , the same general principles seem to hold, but, as was reported above, instead of rapidly growing evanescent spherulites, one obtains slowly growing crystalline balls which remain at the submicroscopic stage until the temperature is raised to a range which permits their *growth* to microscopic or macroscopic dimensions (above  $-40^\circ$ ). Finally the crystalline balls undergo recrystallization (becoming intensely opaque) at  $-10^\circ$ .

In Range  $C_4$ , there is no evidence for any crystallization upon cooling, no matter what the cooling rate is, or for any recrystallization upon rewarming. Apparently the material is not nucleated.

In Range  $C_1$  (dilute solutions), cooling at rates of the order of hundreds of degrees per second leads to changes in the pattern of ice formation from regular to irregular dendrites, but not to an appreciable reduction in the amount of ice formed. Some irruptive recrystallization at  $-10^\circ$  is still observed under certain conditions.

#### REFERENCES

- BARNES, W. H. & F. W. MATTHEWS. 1939. A note on the diffraction of x-rays by vitrified and by frozen gelatin gels. *Biodynamica* 2(49): 1-7.
- BLACKMAN, M. & N. D. LISGARTEN. 1958. Electron diffraction investigations into the cubic and other structural forms of ice. *Adv. Phys., Suppl. Phil. Mag.* 7: 189-198.
- BURTON, E. F. & W. F. OLIVER. 1935. The crystal structure of ice at low temperature. *Proc. Roy. Soc. A* 153: 166-172.
- DOWELL, L. G. & A. P. RINFRET. 1960. Low-temperature forms of ice as studied by x-ray diffraction. *Nature* 188: 1144-1148.
- DOWELL, L. G., S. W. MOLINE & A. P. RINFRET. 1962. A low-temperature x-ray diffraction study of ice structures formed in aqueous gelatin gels. *Biochim. Biophys. Acta* 59: 158-167.
- GEHENIO, P. M. & B. J. LUYET. 1959. On the existence of two ranges of recrystallization temperatures in gelatin gels. *Biodynamica* 8: 81-84.
- LUYET, B. J. 1937. The vitrification of organic colloids and of protoplasm. *Biodynamica* 1: 1-14.
- LUYET, B. J. 1957. On the growth of the ice phase in aqueous colloids. *Proc. Roy. Soc. B* 147: 434-451.
- LUYET, B. 1962. Principles governing the stability of the ice phase in frozen aqueous substances. *Suppl. Bull. Intern. Inst. Refrig. Commission 4, Annex 1962-1*: 1-12.



- LUYET, B. & G. RAPATZ. 1957. Devitrification of aqueous solutions. *Bull. Am. Phys. Soc. Ser. II* 2: 342.
- LUYET, B. & G. RAPATZ. 1958. Patterns of ice formation in some aqueous solutions. *Biodynamica* 8: 1-68.
- LUYET, B., C. KROENER & G. RAPATZ. 1958. Detection of heat of recrystallization in glycerol-water mixtures. *Biodynamica* 8: 73-80.
- LUYET, B., J. TANNER & G. RAPATZ. 1962. X-ray diffraction study of the structure of rapidly frozen gelatin solutions. *Biodynamica* 9: 21-46.
- MACKENZIE, A. P. & B. J. LUYET. 1962. Electron microscope study of very rapidly frozen gelatin solutions. *Biodynamica* 9: 47-69.
- MERYMAN, H. T. 1958. X-ray analysis of rapidly frozen gelatin gels. *Biodynamica* 8: 69-72.
- MORAN, T. 1926. The freezing of gelatine gel. *Proc. Roy. Soc. A* 112: 30-46.
- PERSIDSKY, M. & B. LUYET. 1959. Low-temperature recrystallization in gelatin gels and its relationship to concentration. *Biodynamica* 8: 107-120.
- RANDALL, J. T. 1934. *The Diffraction of X-rays and Electrons by Amorphous Solids, Liquids and Gases*. Chapman and Hall, London, England.
- RAPATZ, G. & B. LUYET. 1959. Recrystallization at high subzero temperatures in gelatin gels subjected to various cooling treatments. *Biodynamica* 8: 85-106.
- TAMMANN, G. 1898. Ueber die Abhaengigkeit der Zahl der Kerne, welche sich in verschiedenen unterkuehlten Fluessigkeiten bilden, von der Temperatur. *Z. phys. Chem.* 25: 441-479.
- ZACHARIASEN, W. H. 1932. The atomic arrangement in glass. *J. Am. Chem. Soc.* 54: 3841-3851.

# FACTORS AFFECTING THE MECHANISM OF TRANSFORMATION OF ICE INTO WATER VAPOR IN THE FREEZE-DRYING PROCESS\*

Alan P. MacKenzie

*American Foundation for Biological Research, Madison, Wis.*

## INTRODUCTION

During the past 25 years, freeze-drying processes have assumed ever-increasing importance as means for the removal of water from biological systems. Early developments, summarized by Flosdorf<sup>1</sup> were followed by steady progress reported and discussed at a succession of international meetings<sup>2-5</sup> and in several texts.<sup>6,7</sup> From such accounts, one may trace the increase in the number of successful applications and the development of the theoretical aspects of the process. Furthermore, one may seek to relate advances in practical procedure to those made in theory of the mechanism.

It is at once apparent, however, that, while extensive improvements in the design of apparatus have resulted from thorough analysis of the patterns of vapor flow from specimen to condenser and of heat transfer within the system,<sup>7-9</sup> analysis has not been extended to include a detailed examination of the processes taking place within the sample (though it can be argued that it is the latter processes which actually constitute the mechanism of freeze-drying). To the contrary, the preservation of a desired property seems almost always to have been the result of an empirical selection of conditions — sample pretreatment, chemical and physical, and freeze-drying temperature — and only in the occasional instance, for example, studies reported by Rey,<sup>4</sup> to have been determined on the basis of preliminary experiments conducted on model systems yielding basic information.

What then does one wish to know? What remains to be studied? The answer would appear to be determined by the need to understand the various processes occurring *within* a specimen undergoing freeze-drying, to seek a relationship between freeze-drying mechanism and specimen composition, treatment prior to, and temperature during freeze-drying, and to study the effects of changes brought about by freeze-drying on the properties of materials after rehydration. Now it seems that it has, in general, been assumed that freezing converts a specimen, regardless of type, into a rather rigid structure in which ice crystals extend, without interruption, from free surfaces, branching and rebranching in their inward progression. Changes occurring during freeze-drying, as water molecules are removed

\*The work reported in this paper was supported in large part by grants-in-aid from the National Institutes of Health, Public Health Service, Bethesda, Md., and from the National Science Foundation, Washington, D.C.

from the specimen, have thus supposedly been limited to (a) direct sublimation of ice, followed by passage of water vapor through channels connecting directly with the sample surface<sup>3-6</sup> and (b) direct evaporation of unfrozen water into channels left empty by sublimation of ice — a phenomenon discussed in considerable detail by Robson and Rowe.<sup>4</sup>

The inadequacy, *in certain cases*, of the foregoing description of freeze-drying was first apparent in results reported by Kramers<sup>10</sup> and became even more strongly apparent to the present author from the results of various experiments which are best summarized, perhaps, in the following order. *Firstly*, it was observed, with the aid of an automatically recording microbalance,<sup>11</sup> that the rate at which a solution containing ice crystals of a given size freeze-dries, at a given temperature, depended on the nature of the solute present. This point is, perhaps, almost common knowledge but its significance appears often to have been missed. *Secondly*, it was found, again with the aid of the microbalance, that freeze-drying rates are frequently not determined by the resistance to vapor flow occasioned by the narrowness of channels vacated by the subliming ice; that is, freeze-drying velocity is not always primarily determined by the size of ice crystals. For example, 30 per cent polyvinyl pyrrolidone solutions containing ice crystals and thus, presumably, channels with diameters of a micron or less and of about 100 microns, respectively, freeze-dried at  $-45^{\circ}\text{C}$ . at velocities in the ratio of 1:4 and not of 1:100, or thereabouts, as might be predicted on the basis of resistance to free molecular *vapor* flow within the samples. (One may note here that these experiments were carried out in such a way that the temperature within the undried part of each specimen was kept constant within  $\pm 0.5$  deg. C. by automatic means<sup>11</sup>; thus the true differences in freeze-drying rates at given sample temperatures were obtained directly.)

*Thirdly*, freeze-drying was found to occur to completion in systems in which countless small ice masses were each entirely surrounded by the concentrated solute phase. In particular, thin layers of 20 per cent and 30 per cent gelatin gel, frozen very rapidly and rewarmed to an extent sufficient to convert all submicroscopic ice into discrete globular particles, were freeze-dried at various temperatures, as low as  $-78^{\circ}\text{C}$ ., and examined by light and electron microscopy. The electron micrographs served to confirm the observations made with the light microscope, that the ice crystals and the resultant cavities were truly isolated from one another and that freeze-drying had occurred in the absence of a continuous system of channels (FIGURES 1 and 2).

*Fourth*, the appearance of fissures in the dry solute matrix was repeatedly encountered, depending upon freeze-drying conditions, in a wide variety of solutions of compounds ranging in molecular weight from sucrose to bovine albumin. Similar phenomena have been reported by others,<sup>12,13</sup>

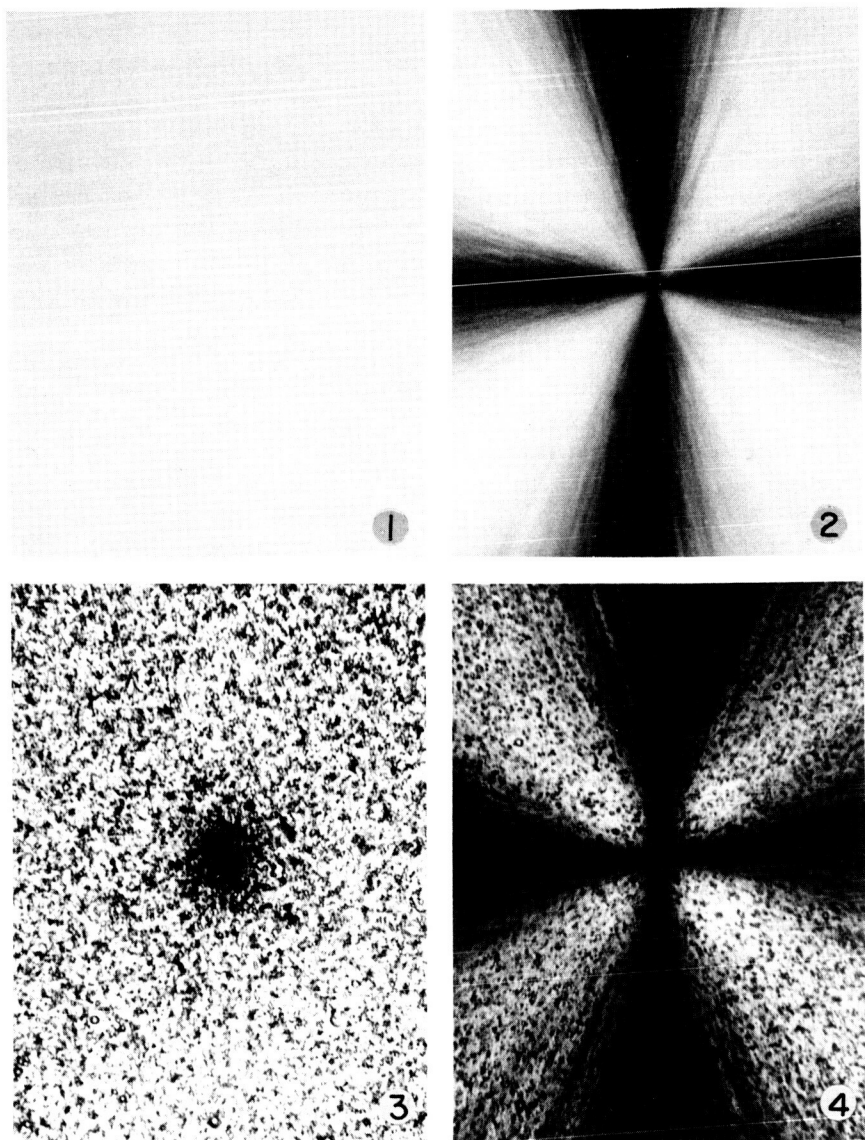


FIGURE 1. Effect of rewarming on a gelatin solution frozen very rapidly by abrupt immersion in a cooling bath at  $-50^{\circ}\text{C}$ . Concentration: 30%. Sample thickness: ca. 20 microns. Photos. 1 and 2: before rewarming (sample transparent to naked eye); photos 3 and 4: after rewarming to  $-10^{\circ}\text{C}$ . for 10 minutes (sample white and almost opaque to naked eye). Photos 1 and 3: ordinary light; photos 2 and 4: polarized light.  $\times 75$ .

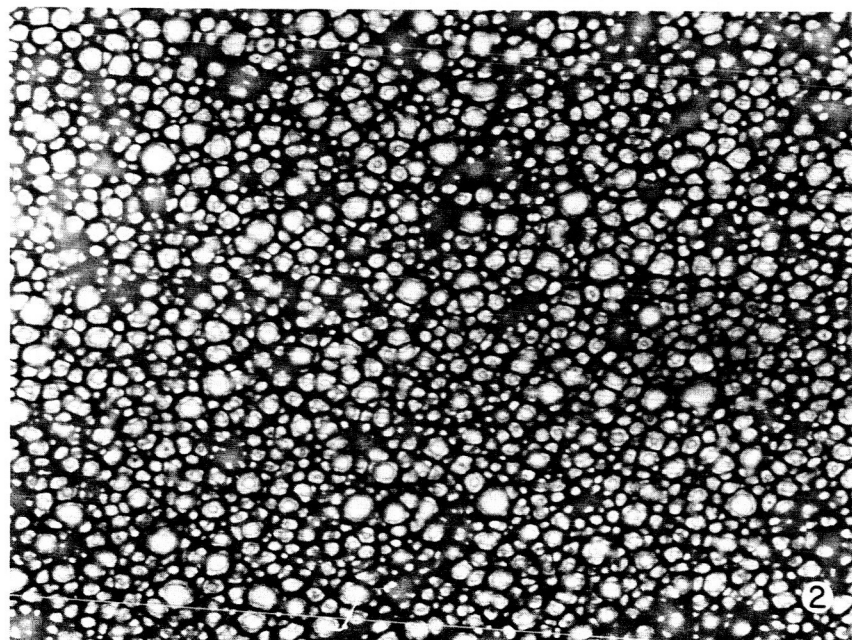


FIGURE 2. Electron micrographs illustrating effect of rewarming on very thin layers of gelatin solution frozen by sudden immersion in isopentane at  $-78^{\circ}\text{C}$ . Concentration: ca. 25%. Sample thickness: ca.  $1/4$  micron (collodion sandwich film technique). Photo. 1: before rewarming; photo 2: after rewarming to  $-6^{\circ}\text{C}$ . for 30 minutes. Note that recrystallization upon rewarming has occurred to an extent sufficient to eliminate all evidence of initial freezing pattern. Approx.  $\times 3,300$ .

are commonly encountered in many freeze-drying applications, and are distinguished from cracks formed in the frozen material due to freezing. The variation in the extent of secondary drying necessary to initiate formation of cracks does not appear, however, to have been noted and has considerable bearing on a discussion of the mode of water transport within a freeze-drying material.

Lastly, several sugar solutions were found to "freeze-dry," with complete loss of structure, at  $-30^{\circ}\text{C}$ . (more than 20 degrees lower than the temperatures at which ice crystals dissolved completely upon gradual re-warming). That is, freeze-drying, in these conditions, led to a collapse of the solute framework and the formation of a uniformly clear glassy product devoid of cavities. Such results were in dramatic contrast to those of other experiments in which sugar solutions were freeze-dried at  $-40^{\circ}$ , and at lower temperatures, when the original freezing pattern was well preserved by freeze-drying.

These results, diverse in nature, were interpreted to indicate the existence of variations of the accepted mechanism of freeze-drying and, in particular, to demonstrate in some cases the existence of condensed homogeneous barriers to movement of water molecules — barriers in which the narrowest real channels were most likely absent. The need for further factual evidence was most apparent and several promising approaches are now under way. A versatile form of freeze-drying microscope has been designed and built and is described in the next section. An automatically recording microbalance in which specimen temperatures can be continuously controlled to within  $\pm 0.5^{\circ}\text{C}$ . is also in use but detailed analysis of the results of weight/time curves must await the gathering of a greater quantity of data. Lastly, methods of direct observation of freeze-drying in the electron microscope are still being explored and are not yet in use in the author's laboratory — several preliminary reports have, however, appeared from other workers.<sup>14-16</sup>

The remaining part of this paper will thus comprise (1) a brief description of the freeze-drying microscope, (2) the presentation of some selected observations made with low and medium power objective lenses, (3) a discussion of mechanisms, and (4) some appended comments in which useful directions for further basic study will be mentioned.

#### EXPERIMENTAL METHOD

##### *The Freeze-drying Microscope*

The apparatus,<sup>17</sup> shown in FIGURES 3 and 4 comprises a microscope, set in a horizontal position, and a flexible vacuum system, part of which can be moved in two directions. The microscope stage has been replaced with an automatically controlled low-temperature bath into which the freeze-drying chamber is suspended and through the windows of which the course

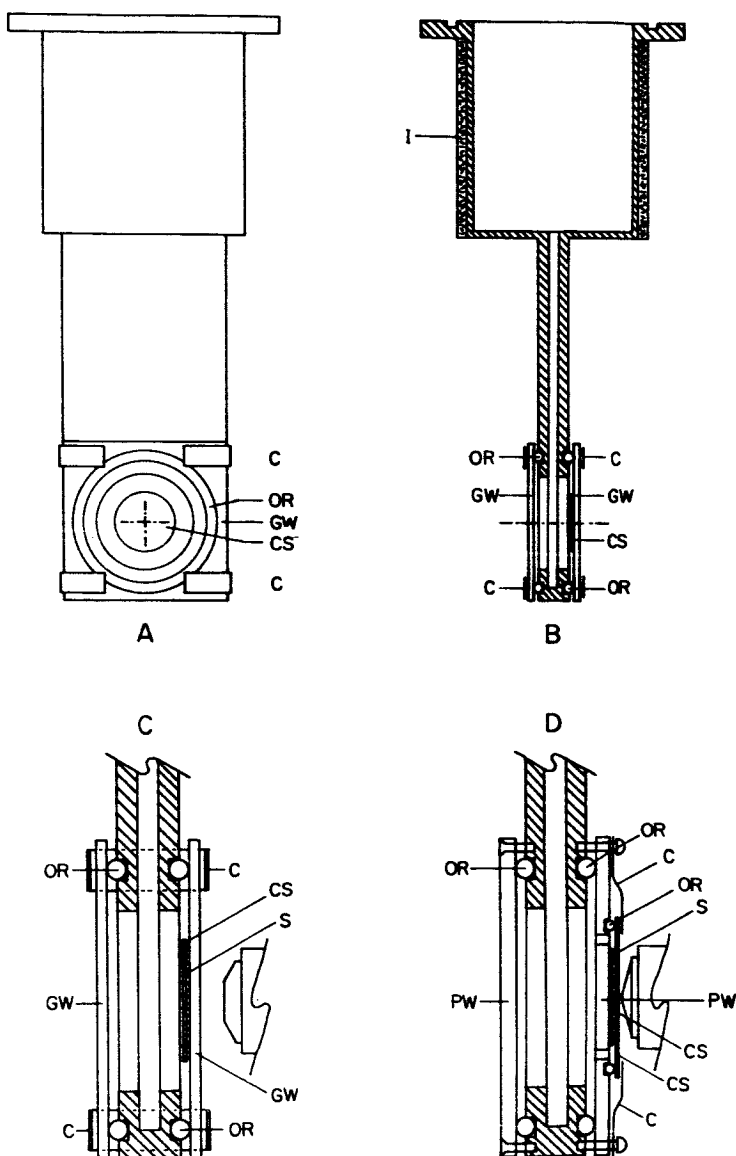


FIGURE 3. Freeze-drying chamber for an apparatus for microscopic observations during freeze-drying. Drawing A: front elevation; drawing B: side view, seen in cross-section; drawing C: side view in detail showing sample location; drawing D: side view, seen in cross-section, showing modified system for use with oil-immersion objective lenses. C: clip; CS: cover slip; GW: glass window; I: insulation; OR: O-ring; PW: Plexiglass window; S: Sample.

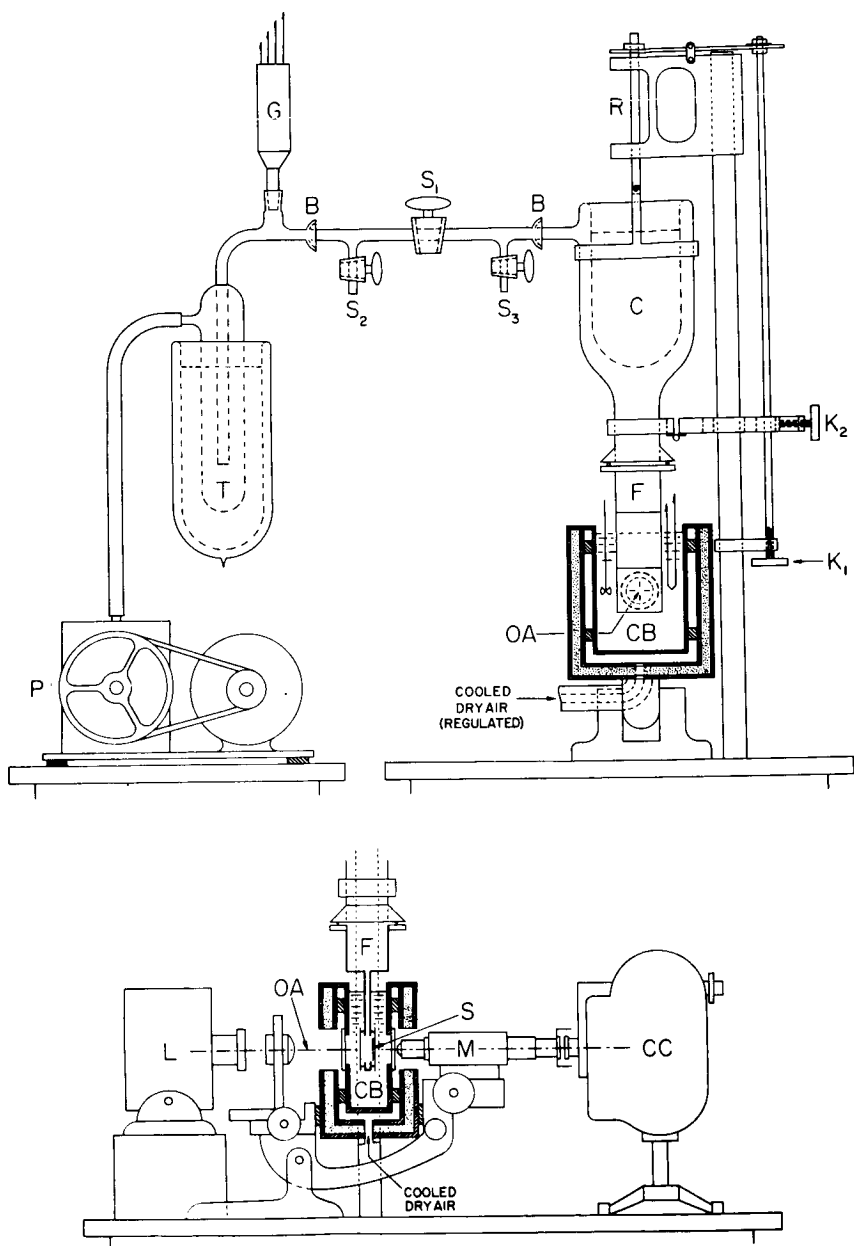


FIGURE 4. Diagrammatic views of freeze-drying microscope. Upper drawing: front elevation of the apparatus, showing the cooling bath in cross-section. Lower drawing: side elevation of part of the apparatus, showing both freeze-drying chamber and its cooling bath in cross-section. B,B: ball joints; C: condenser; CB: cooling bath; CC: cine camera; F: freeze-drying chamber; G: pirani gauge; K<sub>1</sub>, K<sub>2</sub>: stage control knobs; L: lamp; M: microscope tube; OA: optical axis of the system; P: two-stage mechanical pump; R: movable rod; S: sample; S<sub>1</sub>, S<sub>2</sub>, S<sub>3</sub>: stopcocks; T: refrigerated trap.



of freeze-drying of the specimen can be observed. The freeze-drying chamber (FIGURE 3) takes the form of a hollow metal blade with glass windows on its two main faces and a flange at one end (the upper end, when in position in the apparatus) for connections to the vacuum system. Thermal contact between the specimen and the cooling bath, the temperature of which is regulated to  $\pm 0.1^{\circ}\text{C}$ ., or better, is achieved through one of the glass windows.

Samples may be mounted between two glass coverslips or between a coverslip and one of the chamber windows — the choice is governed largely by the rate at which the specimen is to be frozen and the magnification required — and the method of assembly is varied accordingly. In cases where slow freezing is to be employed, the entire apparatus is conveniently assembled at room temperature. The cooling bath temperature is then lowered and freezing is initiated, if necessary, by seeding with a cold metal rod. Specimens may be further cooled or rewarmed, as desired, and freeze-drying commenced by opening the stopcock situated between the freeze-drying chamber/condenser assembly and the vacuum pumps and by filling the condenser with dry ice or liquid nitrogen.

Freeze-drying takes place in directions at right angles to the optic axis of the microscope and is most conveniently recorded by single-frame photography or by cinematography. One can raise or lower the sample temperature during the course of freeze-drying and, due to the design of the apparatus, and the consequent patterns of heat and vapor flow, the temperature of the ice at the freeze-drying interface will remain within a fraction of a degree of the surrounding bath temperature. Some of the results obtained with the instrument are described in the following section and comprise the main part of this paper.

## RESULTS

### *Direct Microscopic Observations of the Freeze-drying Processes*

The results obtained to date can be presented in the following six categories, depending on (a) the water form or sequence of forms through which the water molecules have to pass in order to escape from the sample and (b) the nature of the accompanying changes occurring in the solute phase. The factors determining the mechanism in each case will, to some extent at least, become apparent as the processes are described and will be treated systematically in the Discussion.

1. *Water vapor escaping via open channels.* The freeze-drying of salt solutions at low temperatures exemplifies the case of direct sublimation of ice, followed by the passage of water vapor, via channels vacated by ice, unaltered in size, to the sample surface. FIGURE 5 shows selected frames from a cinematographic record of the freeze-drying of 10 per cent KCl solutions at  $-30^{\circ}\text{C}$ . The recession of the ice interface leaves the solute,

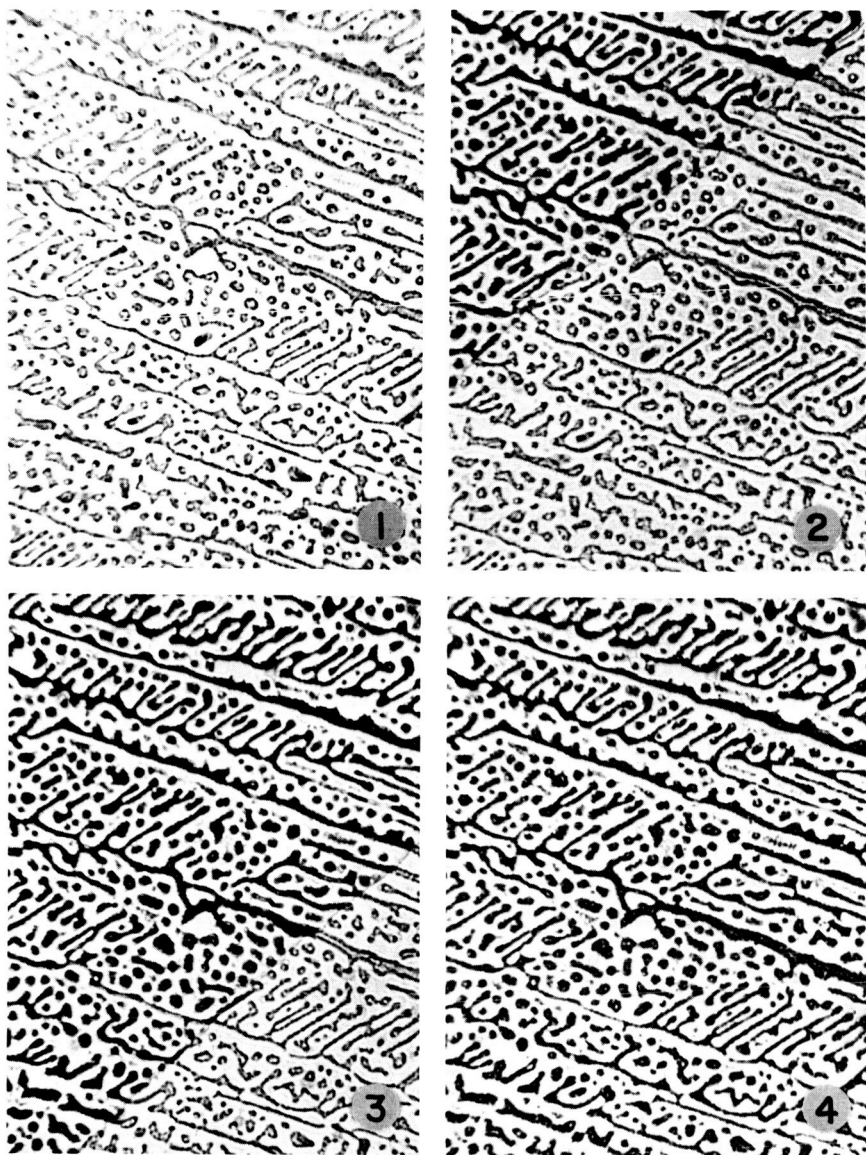


FIGURE 5. Sequence showing freeze-drying by direct sublimation of ice from a slowly frozen KCl solution. Water vapor travels via spaces between salt crystals. Concentration: 10%. Sample thickness: ca. 10 microns. Freeze-drying temperature:  $-30^{\circ}\text{C}$ . Photo. 1: before freeze-drying; photos. 2 and 3: during freeze-drying; photo. 4: after completion of freeze-drying. Magnification: approx.  $\times 300$ .

apparently unchanged, in the pattern in which it was deposited during freezing. There is no contraction of solute upon freeze-drying and no cracking — frozen solutions of hydrate-forming salts (for example, NaCl) freeze-dried, however, by sublimation of ice followed by the expected efflorescence of the hydrated crystals.

Dilute solutions (up to several per cent solids) of a number of non-ionizing solutes, of low and of high molecular weight, were also found to freeze-dry by this mechanism but only in cases where freezing was such that ice crystals all grew inward from the external surface of the sample (conditions of very little or no supercooling and surface-nucleated freezing). It is noteworthy that such conditions of solute concentration, freezing and freeze-drying are very frequently encountered in commercial application of the process. However, another mechanism by which dilute solutions freeze-dry is described in the third category.

2. *Water vapor escaping through the walls of totally enclosed cavities.* The physical structure of many frozen solutions, particularly those of solute concentration greater than about 20 per cent, may be modified by rewarming treatments in such a way that finely branched crystal structures undergo complete disintegration, large numbers of rounded ice particles, each distinctly separate from the rest, being formed in the process<sup>18,19</sup> (see FIGURES 1 and 2). Solutions of polyvinyl pyrrolidone and of gelatin, so treated, subjected to freeze-drying, are seen to undergo the following changes (FIGURE 6). Ice disappears from one particle at a time, beginning at the edge of the preparation, and leaves a sample full of empty, isolated cavities. Ice/void interfaces form, in turn, within each cavity, moving from one side to the other, and are usually flat or formed by intersection of two or three flat planes inclined to each other at angles of about 120°. Such behavior indicates the recession of the surface of a separate monocrystalline mass in each cavity.

A somewhat different behavior is observed in the case of 50 per cent gelatin gel, supercooled to -40°, and allowed to freeze spontaneously. Numerous separate particles form upon freezing but do not appear to consist of monocrystalline material. While freeze-drying causes removal of ice from these particles, as in the cases just described, though each is totally surrounded by concentrated solute, a certain residual solute network is seen to be preserved within each isolated structure.

In both cases, the removal of water by sublimation of ice, passage of water vapor through short distances and diffusion of redissolved water molecules through the solute phase is demonstrated.

3. *Water vapor escaping via cracks in addition to channels.* Certain solutes retain large amounts of unfrozen water and shrink considerably upon secondary or pseudo freeze-drying, generating stresses which find release in the formation of cracks or fissures, depending upon the geome-



FIGURE 6. Successive stages in freeze-drying by transport of water molecules through the concentrated solute phase present in a frozen polyvinylpyrrolidone solution. The sample was frozen at  $-40^{\circ}$  and recrystallized by rewarming to  $-10^{\circ}\text{C}$ , for 4 hours prior to freeze-drying. Concentration: 50%. Sample thickness: ca. 20 microns. Freeze-drying temperature:  $-30^{\circ}\text{C}$ . Freeze-drying occurs from upper left to lower right in each case. Note the progression of the ice/void interface through the cavities marked by arrows. Approx.  $\times 300$ .

try of the sample. With the flat samples of the type necessary in the freeze-drying microscope, cracking during freeze-drying has been recorded in the cases of several different solutes, the most marked fissures being seen in materials of high molecular weight. FIGURE 7 shows a sequence representing development of cracks in the freeze-drying at  $-30^{\circ}\text{C}$ . of a salt-free solution of recrystallized ovalbumin, 30 per cent w/w, rapidly frozen (note how cracks are formed close behind the freeze-drying front). Similar cracking is observed in freeze-drying of this solution at  $-40^{\circ}$  and at  $-20^{\circ}\text{C}$ . Dextran solutions behave in some cases in a similar way and one deduces that very little secondary drying is necessary in those cases to cause crack formation. Solutions of sucrose and of polyvinyl pyrrolidone, on the other hand, were observed to crack upon prolonged freeze-drying at low temperatures but cracks extended only a small fraction of the way from the edge of the preparation to the interface where sublimation of ice was occurring.

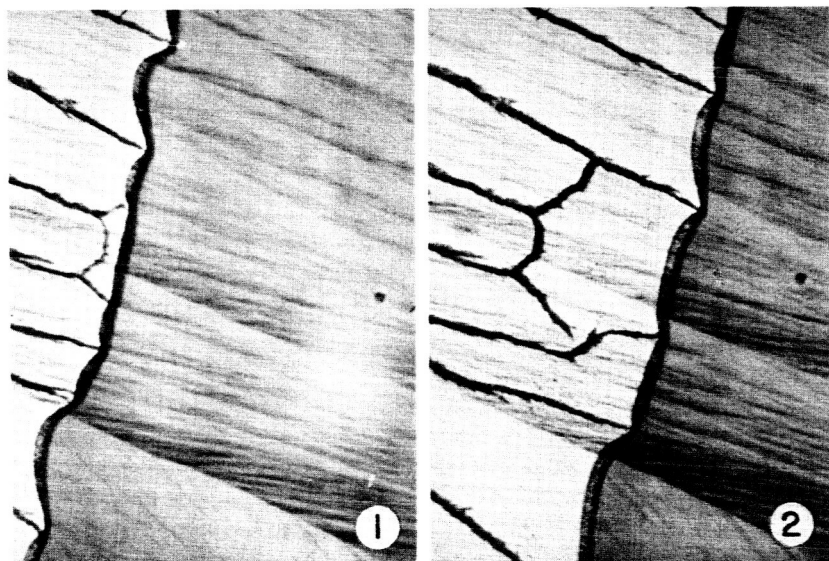


FIGURE 7. Photographs illustrating the formation of cracks in the freeze-dried portion of a rapidly frozen salt-free albumin solution. Concentration: 30%. Sample thickness: ca. 20 microns. Freeze-drying temperature:  $-30^{\circ}\text{C}$ . Note the deeper penetration of the front at points ahead of the fissures. Note also the increase in crack width at any point with progression of secondary drying. Magnification: approx.  $\times 270$ .

It is evident from the distribution of the cracks that vapor flow occurs both via channels left by subliming ice (these channels are too small to be resolved in FIGURE 7) and by fissures formed subsequently. From the shape of the freeze-drying front it is apparent that the fissures offer less resistance to vapor flow than do the channels emptied of ice.

One may also note, in passing, the likelihood that rapid freezing will crack a specimen; Stephenson has, in fact, expressed the observation in diagrammatic form in his well known studies on the freeze-drying process.<sup>20</sup> The further possibility exists, however, that secondary drying of the first parts to freeze-dry, that is, of all the surfaces, will cause the cracks formed by freezing greatly to enlarge and to serve as even better conduits as drying proceeds.

4. *Water vapor escaping via cracks.* In some instances, samples in which ice is present only as distinct and separate particles freeze-dry by yet another process. FIGURE 8 shows a sequence in the freeze-drying at  $-30^{\circ}\text{C}$ . of 50 per cent salt-free, crystalline ovalbumin frozen rapidly and recrystallized by rewarming. In this case, secondary drying, which evidently occurs extremely readily, causes cracks to form in the walls which separate one ice containing cavity from another. As soon as ice is sublimed from one cavity, secondary drying of the wall next to adjacent ice cavities takes place; cracks form in the wall, ice sublimes from the neighboring particles, and water vapor passes through a succession of cavities and interconnecting fissures. Freeze-drying occurs much more readily by such a mechanism than it does when the walls separating discrete cavities resist the formation of cracks (see second of these six mechanisms.)

5. *Freeze-drying resulting in a total collapse of the solute matrix.* Solutions of several substances examined to date have been found to freeze-dry according to some of the four mechanisms, just listed, at all temperatures below certain values, but to "freeze-dry" in a very different way at all higher temperatures: The case of PVP solutions may be taken as an example. At  $-40^{\circ}$ ,  $-30^{\circ}$  and  $-25^{\circ}\text{C}$ ., PVP solutions from 10 to 50 per cent w/w., frozen rapidly and recrystallized, or frozen slowly, freeze-dry by mechanisms *two* or *three* or by a combination of the two. At  $-20^{\circ}\text{C}$ ., however, and at higher temperatures, no channels or cavities remain after the ice is gone, though the cavities produced in the same sample by prior partial freeze-drying at lower temperatures are preserved unaltered. Thus, "freeze-drying" leads, at a temperature 15 degrees lower than the m.p. of the solution, to a dissolution of ice and a cooperative flow of solute sufficient to prevent sublimation from taking any part in the process of dessication. The phenomenon is illustrated by the sequence reproduced in FIGURE 9.

The temperature range within which such a change in mechanism occurs seems always to be limited to one or two degrees and to depend strongly

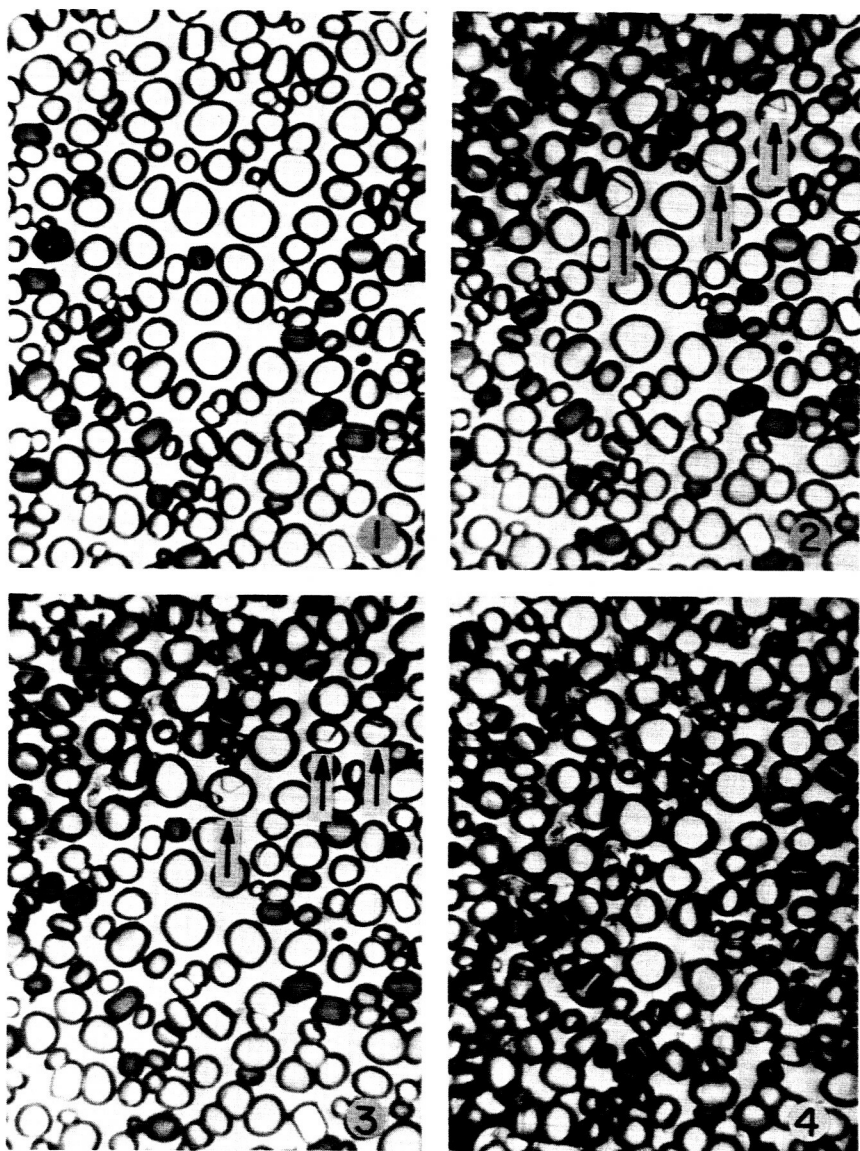


FIGURE 8. Sequence showing how crack formation may facilitate freeze-drying of a system containing many discrete ice particles isolated one from another by concentrated solute. Sample: salt-free ovalbumin frozen rapidly, rewarmed to  $-1^{\circ}\text{C}$ . for 1 hour, and cooled slowly thereafter to  $-30^{\circ}\text{C}$ . Concentration: 50%. Sample thickness: ca. 20 microns. Freeze-drying temperature:  $-30^{\circ}\text{C}$ . Photo. 1: before freeze-drying; photos. 2 and 3: during freeze-drying; photo. 4: after completion of freeze-drying. Photographed in polarized light. Note the cracks (dark lines) which interconnect cavities in the freeze-dried material. Note also the ice/void interface on each subliming ice crystal (see arrows). Approx.  $\times 210$ .

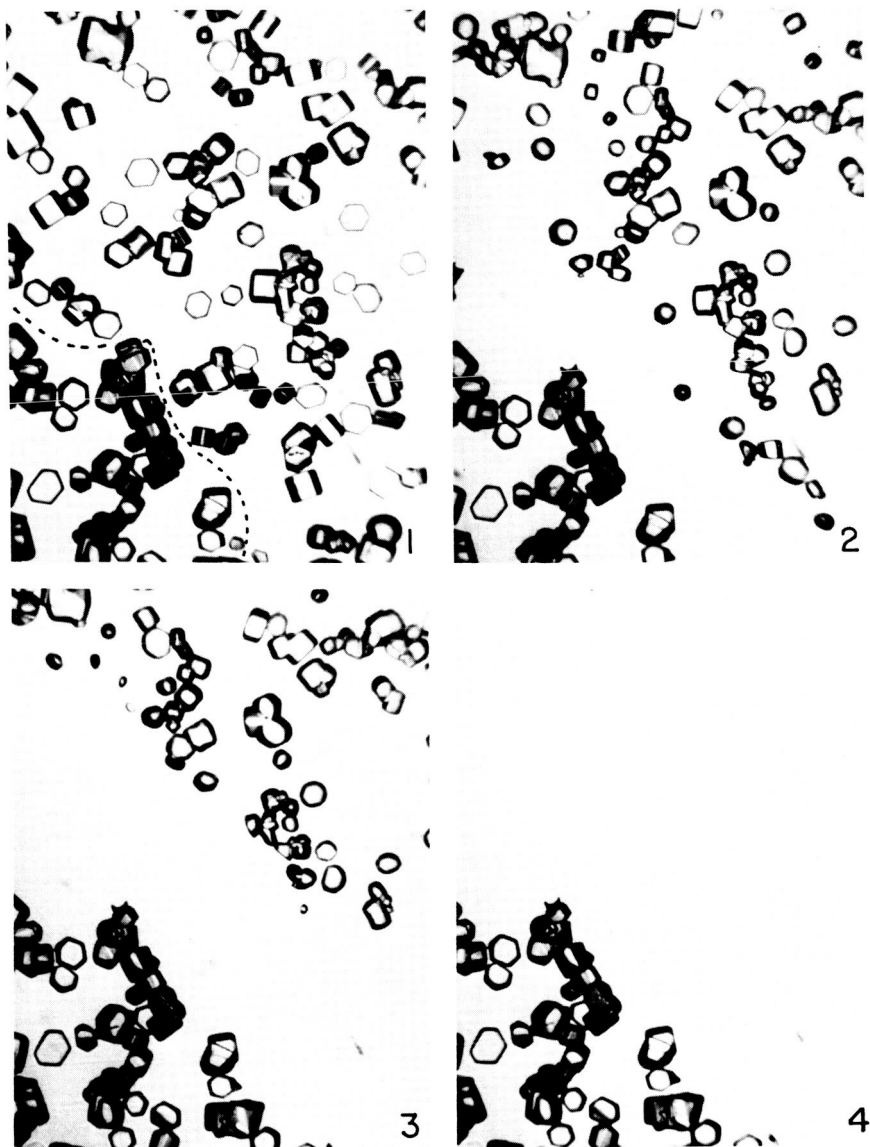


FIGURE 9. Micrographs illustrating "freeze-drying" resulting in total collapse of the solute matrix. Sample: polyvinylpyrrolidone solution, frozen at  $-40^{\circ}$  and recrystallized by rewarming to  $-10^{\circ}\text{C}$ . for 4 hours. Concentration: 50%. Sample thickness: ca. 20 microns. Freeze-drying temperature:  $-25^{\circ}$  (photo. 1),  $-20^{\circ}\text{C}$ . (photos. 2, 3, and 4). Freeze-drying progresses in each photograph from lower left to upper right. The area under the dotted line in photo 1 represents the portion freeze-dried at  $-25^{\circ}$ . Note how freeze-drying at  $-25^{\circ}$  leads to preservation of frozen structure while freeze-drying at  $-20^{\circ}$  causes its total disappearance. Note also that warming to  $-20^{\circ}$  following a period of freeze-drying at  $-25^{\circ}$  does not result in disappearance of structure in the portion freeze-dried prior to warming. Approx.  $\times 183$ .



on the nature of the solute but not on its concentration (within the range 10 to 50 per cent w/w) and only to vary with freezing rates when the latter are extremely high. Similar changes in mechanism have been observed at about  $-30^{\circ}$  and  $-40^{\circ}\text{C.}$ , more than 20 and 30 degrees lower than the freezing points of the solutions, in the cases of sucrose and glucose respectively. Note also that in every case salts were absent.

6. *Behavior of salts close to eutectic temperature.* FIGURE 10 shows the freeze-drying of a 15 per cent KCl solution maintained at  $-30^{\circ}$ ,  $-20^{\circ}$ ,  $-15^{\circ}$ ,  $-13^{\circ}$  and  $-20^{\circ}\text{C.}$  in succession, the bands in the freeze-dried portion denoting freeze-drying at the temperatures recorded and reproduced in FIGURE 11. One sees that sublimation of ice from a mixture of ice and salt crystals takes place at  $-30^{\circ}$  and at  $-20^{\circ}\text{C.}$  according to the first of the mechanisms just described. At higher temperatures, however ( $-15^{\circ}$  and  $-13^{\circ}$ ), a growth of salt crystals accompanies the sublimation of ice (despite the slight and very localized evaporative cooling which must occur in the interface). That it is freeze-drying, and not rewarming of the frozen material, which brings about the growth of salt crystals is seen by reference to the appearance of the portion remaining to be freeze-dried in FIGURE 10, which resembles very closely the structure of the portions freeze-dried at  $-30^{\circ}$  and  $-20^{\circ}\text{C.}$  Further evidence for this conclusion is provided by the appearance of the band freeze-dried at  $-20^{\circ}$  following exposure to  $-13^{\circ}$ . One may also note that an increase in temperature of the entire preparation from  $-11.5^{\circ}$  to  $-11^{\circ}\text{C.}$  caused eutectic melting of the frozen portions. The matter of the behavior of salts at temperatures close to their respective eutectic temperatures is perhaps of some importance in relation to their probable sub-microscopic behavior upon freeze-drying at considerably lower temperatures.

## DISCUSSION

This section will consist of the following parts: (1) An examination, in terms of water forms and the properties of solute molecules, of the basic processes likely to occur in freeze-drying, depending on conditions. (2) An evaluation of the effect of experimental factors in determining the observed mechanisms. Some points of practical significance arising from the findings will then be discussed separately in an Appendix.

### 1. Basic Processes

*The following list* is based on the fact that water must exist in one of two forms in frozen biological materials, that is, as ice or as water which, for one reason or another, does not freeze (water in the latter form is often described as "bound water" but it is most important to remember that the freezing and post-freezing treatments frequently determine the quantity of water which does not freeze and that a distribution or "spectrum" of

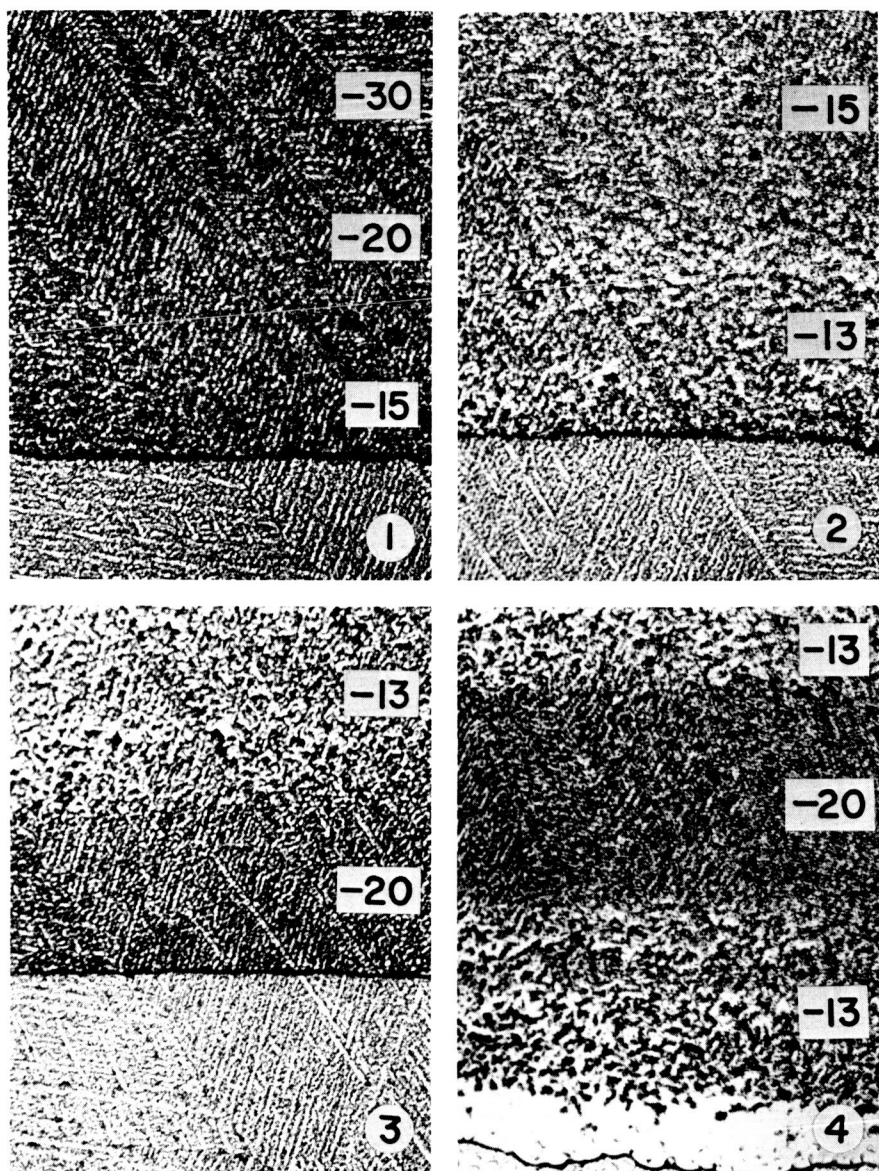


FIGURE 10. Sequence illustrating behavior of a KCl solution freeze-dried at temperatures close to the eutectic melting point. Concentration: 15%. Sample thickness: ca. 20 microns. Freeze-drying temperature:  $-30$ ,  $-20$ ,  $-15$ ,  $-13$ ,  $-20$ , and  $-13$ , in succession (see FIGURE 11). Photo. 1: freeze-drying at  $-30$ ,  $-20$ , and  $-15$ ; photo. 2: freeze-drying at  $-15$  and  $-13$ ; photo. 3: freeze-drying at  $-13$  and  $-20$ ; photo. 4: freeze-drying at  $-13$ ,  $-20$ , and  $-13$ , followed by warming to  $-9^{\circ}\text{C}$ . The portion not freeze-dried underwent eutectic melting at  $-11^{\circ}\text{C}$ . Approx.  $\times 200$ .

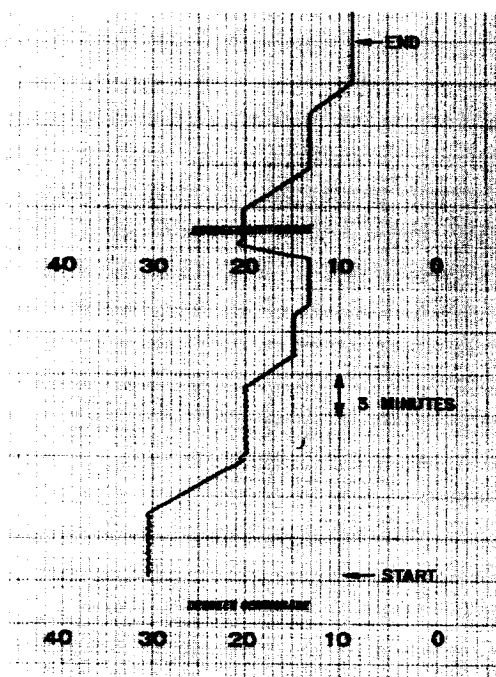


FIGURE 11. Temperature/time record illustrating temperature control during freeze-drying experiments conducted to determine effect of freeze-drying temperature on freeze-drying mechanism in KCl solutions (see FIGURE 10 and text).

binding energies for water must always exist within a frozen biological sample). The list is also based on the behaviour of the solute components and is divided as follows: *basic processes describing the movement of water molecules*, (a) gaseous flow of water vapour, free molecular or otherwise, (b) sublimation of ice, (c) diffusion of water molecules *within* the concentrated solute phase or phases (this water is sometimes described as “internally bound” water and diffusion presumably occurs from one binding site to another, in steps), (d) conversion of internally bound to “externally bound” (or surface adsorbed) water and vice versa, accompanied by local molecular rearrangement of the solutes, (e) desorption, and readsorption of externally bound water; *basic processes describing the behaviour of non-crystallized solutes*, (f) formation of various solute-solute bonds (by ionic interaction, hydrogen bonding and van der Waals’ forces), (g) fragmentation of the solute phase (initiation and propagation of cracks or fissures), (h) viscous flow of concentrated solute phase; *processes involving crystallized solutes*, (i) dissolution and crystallization of salts and other non-volatile substances. Each one of these processes constitutes a well-known physical or physicochemical phenomenon; moreover, the foregoing list would seem to be complete in as much as it appears to explain both previous

observations and those reported earlier in this paper.\* A brief review of the facts will suffice to show the way in which the basic processes enumerated may interact to produce a given behavior upon freeze-drying.

*First among the six mechanisms* reported in the RESULTS is the one by which, according to the conventional view, freeze-drying always proceeds, the one in which the sublimation of ice is followed by "secondary drying." Observations of various solutions indicate that water vapour flows, in the first place through channels vacated by ice (e.g. FIGURE 5), to the outer surface and, in the later stages, also from the cracks, if any, in the solute. Such a description will be but slightly modified or, rather, amplified, by recourse to the list of basic processes just given. Secondary drying is seen to consist of the three simultaneous processes: diffusion of internally bound water, conversion of internally to externally bound water, and desorption of the latter; formation of cracks will result from stresses caused by shrinkage of the solute and will involve the same three basic processes, also the formation of extra solute-solute bonds, and will depend upon the mechanism of initiation of the cracks. While the recognition of the role of each basic process is essential to further understanding of this particular form of freeze-drying, the most important point about the mechanism is, perhaps, that sublimation of ice can take place *before* secondary drying begins.

*The second mechanism.* By contrast, the freeze-drying of a system in which ice exists in the form of separate particles, each surrounded by solute, requires the diffusion of bound water to an extent sufficient to set up a water concentration gradient within the solute separating the ice particles from the exterior surface of the sample; sublimation of ice is thus *dependent* on secondary drying. Further dehydration then leads to transfer of water molecules from the ice crystal to the solute at one or two points with the formation of minute empty spaces, subsequently seen to grow (FIGURE 6). The water molecules evidently sublime over very short distances, undergo adsorption on the solute surface enclosing the disappearing ice crystal and are, in turn transferred into, through and out of the solute phase. The result may be the ultimate production of empty isolated cavities observed, e.g., in PVP and in gelatin. That these cavities are truly isolated is shown by the impossibility of infiltrating such specimens with paraffin or other embedding agent.

*The third group* of observations indicates a freeze-drying mechanism, not unlike the "conventional mechanism" in some ways, but different in that the early cracking of the solute phase plays a significant part. There

\*The present treatment has not been extended to include those cases where volatile components other than water are involved; furthermore, the question of the behavior of very small entrapped volumes of liquid water, the freezing points of which are well below 0°C., is admitted but will not be discussed.

is, on the one hand, the direct transport to the surface of water vapor through spaces from which ice has just sublimed. On the other hand, the desorption of externally bound water and the reduction in the quantity of internally bound water lead, via molecular rearrangement, to such solute-solute bonding and shrinkage that gross stresses evidently develop in the solute phase. Cracks are then initiated and grow with further dehydration of the system. In rapidly frozen ovalbumin solution, which upon freeze-drying, cracks easily and shrinks considerably thereafter, the fissures formed may be much wider than the ice crystals (FIGURE 7). Water vapor will thus flow much more easily through the cracks than through the channels vacated by ice and freeze-drying will be considerably accelerated by the presence of the cracks, a fact which is readily verified by observations of the shape of the freeze-drying front in an area in which a crack extends inwards into the sample. Freeze-drying by this mechanism is thus dependent, but only for its increased velocity, upon the progress and results of secondary drying.

*The fourth of the reported mechanisms* involves the formation of cracks before the sublimation of ice can take place. If the cracks did not form at all, freeze-drying would have to proceed by the transport, discussed earlier, of all the water molecules through the concentrated solute phase. The ready formation of cracks in some solutes, however, opens up routes for vapor flow where none existed prior to freeze-drying and dehydration by this mechanism is, in fact, observed (FIGURE 8) to occur many times faster than in solutions less susceptible to cracking, e.g., those of gelatin treated, prior to freeze-drying, to yield a similar distribution of ice crystals.

*The fifth of the modes of behavior* described appears to raise different questions. To answer them, it has been necessary to postulate a massive shear flow, rather than a series of limited local rearrangements at the molecular level, upon dehydration of the system. As noted earlier, this flow only appears to occur at temperatures higher than a certain value for each solute, for example, at about  $-40^{\circ}$  for glucose,  $-30^{\circ}$  for sucrose and  $-22^{\circ}$  for PVP. While the fundamental basis for these threshold temperatures is still obscure, as it remains in the case of recrystallization of frozen solutions by rewarming,<sup>21,22</sup> it is clear that the viscosity of a concentrated solute phase may decrease very considerably with a small increase in temperature and that, above this temperature, sublimation of ice does not yield an empty space in place of each ice crystal.

This failure to retain the solute framework from the frozen structure, combined with the absence of cracking, appears to require the direct transfer of water molecules, by very limited translational and rotational movements, from sites in the surfaces of the ice crystals to binding sites in the surfaces of the enclosing solute phase. The further movement of water must then occur, as in certain of the other cases discussed, by transfer of surface bound water to the interior of the solute, diffusion

through the latter, etc. Since ice crystals connecting with the sample surface before freeze-drying are quickly surrounded, by the flow of solute, as they diminish in size, direct sublimation, even near the surface of the sample, is eliminated. In such conditions, it appears to be more appropriate to speak of the "dissolution" of ice upon exposure to vacuum, rather than of its sublimation and it may even be doubted that such a process should be called "freeze-drying." Alternative terms are, however, lacking.

*Sixth, and last, of the reported mechanisms* is the surprising behavior of salt solutions freeze-dried at temperatures ten degrees, or less, below their eutectic points (electron microscopic observations suggest the same phenomenon may occur at temperatures fifty degrees lower<sup>23</sup>). The direct sublimation of ice is undoubtedly still involved and the growth of salt crystals upon freeze-drying (FIGURE 10) must therefore be explained by the tendency towards a reduction in the surface energy of the system. While the most likely mechanism would seem to lie in a transport of salt solution via a thin surface film on each crystal, the presence of such a film below the eutectic temperature remains to be demonstrated.

## *2. Dependence of Mechanism on Experimental Variables*

It is now logical to ask what determines the state of subdivision and geometric distribution of ice crystals, the capacity of the solute matrix to crack upon dehydration, and the rigidity or, conversely, the fluidity of the solute phase since it is evident that the freeze-drying mechanism, in any given case, is determined by these factors. The answer, furnished by experimental observation, may be summarized as follows: (1) The subdivision of the ice phase, discussed in particular by Luyet<sup>3,4,22</sup> and by Luyet and Rapatz<sup>24</sup> is found to be a function of water content, chemical and physical nature of other components, size and shape of sample, method of freezing, and subsequent thermal history. As might be expected, the ice crystal pattern depends much more upon the nature of the solute at high concentrations of the latter than at low ones; for example, elongated polymer molecules tend to cause much greater subdivision of ice than globular ones except in dilute solutions. The temperature at which changes in the ice pattern occur upon rewarming depend much more, however, upon the nature of the solute than upon its concentration though the latter, and also the method of freezing are not without effect.<sup>25</sup> (2) The tendency of the solute framework to crack is determined almost exclusively by the chemical nature of solute or solute mixture and seems to be related to the shape of the molecules and the ability of one molecule to disentangle from another. Thus salt-free recrystallized ovalbumin, redissolved and freeze-dried, cracks very readily while gelatin and PVP do not, in general, do so. Occasional cracking of PVP and dextran is, however, observed and raises the possibility that rupture of covalent bonds may occur with the formation, as Karel,<sup>26</sup> has suggested, of reactive free radicals. (3) The tendency

of the solute to flow is determined principally by the nature of the solute and the freeze-drying temperature though it now appears that each of the factors controlling the distribution of ice in the sample has at least a minor effect. In particular, a recrystallization of the ice by brief rewarming seems to raise the threshold temperature, probably by further dehydration of the solute. (4) Recrystallization of salts, like solute flow, also depends upon freeze-drying temperature but the effect of other factors is, as yet, almost uninvestigated. It is only possible to add the observation that the simultaneous presence of non-crystallizing solutes, even in relatively small amounts tends to inhibit the phenomenon.

Much further fundamental research is needed in order more fully to catalogue the behavior of solutions. In particular, simple mixtures of solutes, some of which have already been studied by differential thermal analysis and by conductivity measurements,<sup>3,4</sup> must be examined further by these methods and also from the morphological viewpoint, by microscopic, electron microscopic and X-ray diffraction methods. It is not, however, suggested that studies of simplified model systems will eliminate the need to study the more elaborate cellular structures prior to successes in freeze-drying of the latter for various purposes. In particular, the freeze-drying of organized structures will be duplicated only with very great difficulty through *in vitro* experiments.

### CONCLUSIONS

The results suggest that the water molecules liberated by the sublimation of ice may travel from the interior to the surface of a specimen in several ways; (a) via open-ended channels, previously occupied by ice; (b) through the walls of totally enclosed cavities, previously filled with ice; (c) partly through cavities and/or channels, previously occupied by ice, and partly through cracks or fissures formed in the course of the removal of unfrozen water; sublimation may also be replaced, in certain cases, by a dissolution of ice crystals at temperatures considerably below their melting point in the system in question.

Solute concentrations, sample size and shape, manner of freezing, subsequent thermal history in storage, freeze-drying temperatures and most especially, the chemical nature of the solute molecules, combine to determine which of the freeze-drying mechanisms obtain in any given instance.

### APPENDIX

The following two topics are briefly discussed by reference to actual problematical examples. 1. An assessment, in terms of basic processes, occurring in operating conditions, of the likelihood of experimental success. 2. Some technical innovations seemingly necessary if the freeze-drying process is to be used with greater effectiveness.

1. *Chances of attaining specific experimental objectives by freeze-drying.* It is apparent from the foregoing section that, given, for example, certain solutes, certain ranges of water content, freezing velocity and freeze-drying temperatures, the number of possible freeze-drying mechanisms may be limited. It is therefore of interest to consider, by taking an example, the likelihood that experimental objectives will be attained in a given case.

For instance, the freeze-drying of small pieces of tissue with a view to preservation of ultrastructural and histochemical properties requires, first, an extremely rapid initial freezing. This, however, is most likely to produce many very small isolated ice crystals since the ratio of the rate of nucleation to the rate of crystal growth and the probability of spontaneous recrystallization upon cooling will both be high in these conditions.<sup>19,27</sup> Such a system, freeze-dried at the very low temperatures (e.g.  $-78^{\circ}\text{C}.$ ) believed necessary for preventing recrystallization by rewarming will thus have to proceed either by transport of water through the concentrated solute matrix, which will be a very slow process, or by transport of vapor through fissures, if they are formed. The latter process will be faster but a second series of artifacts will have been introduced. Freeze-drying at higher temperatures where solute flow occurs in place of the development of cracks must obviously be avoided on account of the distortions introduced.

2. *Some seemingly desirable features of freeze-drying techniques.* One further and most important question arises from the points just examined. In what ways must freeze-drying techniques be changed before objectives not yet realized are attained? While one can, of course, only guess at the answer, the following suggestions are now offered, tentatively, as indications of directions for future research. Since, however, space will not permit reference to all the applications of the process, the following comments will be restricted to the preservation of viability of cells and tissues, perhaps the most challenging of present problems.

First it will be necessary to prevent the formation of cracks which run through cells and which may cause rupture of covalent bonds, of membranes and other molecular complexes.\* Secondly, flow of component solutes must not occur to extents sufficient to entrain and distort structural elements beyond the elastic limits of the latter. Thirdly, chemical reactions accelerated at constant temperature during the earlier stages of secondary drying, must be restricted to a level which is not intolerable to the cells upon rehydration. To these three requirements, it is of course necessary to add those of suitable freezing procedures, storage for freeze-drying, and rehydration.

The proposed suggestions fall into two categories: (A) those related to freeze-drying in which secondary drying is deliberately limited, and (B)

\*It is interesting in this connection to note that frozen yeast cells, cleaved at very low temperatures, crack across some subcellular structures and over the surfaces of others.<sup>28</sup>



those in which one aims for exhaustive dehydration.

(A) Greaves<sup>1</sup> has attributed the successful freeze-drying of certain bacteria to the ability of the suspending medium to resist dehydration; experimental conditions were supposed, by chance, to have led to sufficient secondary drying to preserve the system but insufficient drying to result in loss of essential water. Nei,<sup>20</sup> more recently, reported the freeze-drying of a suspension of *E. coli* in distilled water in which a different experimental approach led to a limitation of secondary drying, again with marked success. The notion of limited drying may be further developed, both from theoretical and technical viewpoints. It may be supposed that certain dehydration is essential to prevent enzymatic and some non-enzymatic reactions upon rewarming freeze-dried preparations prior to storage and, further, that over-drying may lead (a) to other nonenzymatic reactions, oxidative in particular, which may, for example, cause lethal cross-linking reactions, and (b) to irreversible destruction of emulsions and, especially, of membrane systems.<sup>30,31</sup>

Different cell systems, however, depending on their nature and on the protective agent, if any, used for freezing, cannot be warmed above certain different temperatures without loss of viability and should not, presumably, be freeze-dried above these temperatures. A means is thus required for maintaining the sample at a given low temperature, most usually lower than  $-30^{\circ}\text{C}.$ , and for removing all the ice together with a predetermined portion of the unfrozen water. Samples thus dehydrated, uniformly and to a limited extent, will need to be sealed so as to prevent further dehydration and to exclude oxygen (a freeze-drying apparatus designed with these objectives in mind has recently been set up in the author's laboratory and is at present undergoing preliminary tests).

Such a technique of limited dehydration at low controlled temperatures must, of course, avoid over-drying the cells nearer the outside of the sample while cells at the center remain underdried. When properly conducted, it should, therefore, be possible to avoid the cracking of the specimen, if necessary with the aid of additional protective substances included for this purpose. At the same time, it should also be possible to avoid damage due to flow of solutes and to chemical reaction by the use of low freeze-drying temperatures and, again, by use of additional protective agents.

(B) On the other hand, the most complete freeze-drying possible, conducted in certain ways, appears to hold considerable promise. It is suggested that a search be made for new protective substances capable of preventing cells and tissues from cracking upon extreme dehydration either by increasing the tensile strength of the frozen system or by "annealing" surfaces in contact with ice. Again, flow of solutes must be prevented by use of low freeze-drying temperatures. The latter will also serve to inhibit chemical reactions but further use of protective compounds should be con-

sidered as a means for reducing the effective concentrations of reacting species, even up to complete dryness. The clear demonstration by Greaves<sup>12</sup> that substances which protect against freezing and thawing damage are of little use in protecting cell suspensions against freeze-drying underlines the need for a new search for effective additives.

The further possibility arises that deleterious chemical reactions may, in the absence of protective agents, be equally well prevented by *lowering* the freeze-drying temperature when ice has been sublimed and by conducting secondary drying at extra low temperatures while the water content is such that solutes are most reactive (the suggestions are in marked contrast to present practice where the temperature is usually *raised* during secondary drying). Such an approach will, however, require an apparatus capable of controlled, limited dehydration during the first stage of the process and the doubt remains that, in the absence of additives, complete dehydration will not disrupt membrane complexes, regardless of freeze-drying temperature. Experiments to answer this last question are now in progress and it is hoped to report them shortly.

In summary, two freeze-drying techniques are thought to be worthy of careful examination.

1. Limited dehydration, based on rational design of apparatus.
2. Complete dehydration at low or very low temperatures with secondary drying at very low temperatures.

The need for the development of new types of additives, protective agents expressly chosen for their effectiveness in freeze-drying rather than in freezing, is also indicated.

#### REFERENCES

1. FLOSDORF, E. W. 1949. Freeze-Drying. Reinhold Publishing Corporation. New York, N. Y.
2. HARRIS, R. J. C. Ed. 1954. Biological Applications of Freezing and Drying. Academic Press. New York, N. Y.
3. PARKES, A. S. & A. U. SMITH. Eds. 1960. Recent Research in Freezing and Drying. Blackwell. Oxford, England.
4. WHITELOCK, O. V. St. Ed. 1960. Freezing and drying of biological materials. Ann. N. Y. Acad. Sci. 85(2): 501-734.
5. FISHER, F. R. Ed. 1962. Freeze-Drying of Foods. National Academy of Sciences — National Research Council. Washington, D. C.
6. REY, L. *et al.* 1960. Traité de Lyophilisation. Hermann. Paris, France.
7. ROWE, T. W. G. The Freeze-Drying of Food. A Review of the Principles. Edwards High Vacuum. Crawley. Sussex, England.
8. STEPHENSON, J. L. 1954. Theory for the design of apparatus for drying frozen tissues. Bull. Math. Biophys. 16: 23-43.
9. HARPER, J. C. & A. L. TAPPEL. 1957. Freeze-drying of food products. Advances in Food Research. 7: Academic Press. New York, N. Y.
10. KRAMERS, H. 1959. Rate controlling factors in freeze-drying. Fundamental aspects of the dehydration of foodstuffs. Soc. Chem. Ind. (London) Conference.
11. MACKENZIE, A. P. & B. J. LUYET. 1964. Apparatus for the automatic recording of freeze-drying rates at controlled specimen temperatures. Biodynamica 9: 193-206.

12. MENZ, L. J. & B. J. LUYET, 1965. Stresses and fissures observed in the freeze-drying of aqueous solutions crystallized into spherulites. *Biodynamica*. In press.
13. NEI, T. 1964. Formation of cracks in the freezing and freeze-drying of some biological preparations. *Biodynamica* 9: 247-255.
14. FERNANDEZ-MORAN, H. 1960. Low-temperature preparation techniques for electron microscopy of biological specimens based on rapid freezing with liquid helium II. *Ann. N. Y. Acad. Sci.* 85(2): 689-713.
15. NEI, T. 1962. Electron microscopic study of microorganisms subjected to freezing and drying: cinematographic observations of yeast and coli cells. *Exptl. Cell Res.* 28: 560-575.
16. COLEMAN, J. W. 1962. A freezing technique in the (electron) microscope giving self supporting specimens. *Electron Microscopy*: 1. Paper EE-5. S. S. Breese Jr., Ed. Academic Press. New York, N.Y.
17. MACKENZIE, A. P. 1964. Apparatus for microscopic observations during freeze-drying. *Biodynamica* 9: 214-222.
18. LUYET, B. J. & G. L. RAPATZ. 1957. Unpublished data.
19. MACKENZIE, A. P. & B. J. LUYET. 1965. An electron microscope study of the recrystallization of ice in rapidly frozen gelatin gels. *Biodynamica*. In press.
20. STEPHENSON, J. L. 1953. Theory of the vacuum drying of frozen tissues. *Bull. Math. Biophys.* 15: 411-429.
21. LUYET, B. J. 1939. The devitrification temperatures of solutions of a carbohydrate series. *J. Phys. Chem.* 43: 881-885.
22. LUYET, B. J. 1957. On the growth of the ice phase in aqueous colloids. *Proc. Roy. Soc. B.* 147: 434-451.
23. MACKENZIE, A. P. & B. J. LUYET. 1961. Unpublished observations.
24. LUYET, B. J. & G. L. RAPATZ. 1958. Patterns of ice formation in some aqueous solutions. *Biodynamica* 8: 1-68.
25. RAPATZ, G. L. & B. J. LUYET, 1959. Recrystallization at high sub-zero temperatures in gelatin gels subjected to various cooling treatments. *Biodynamica* 8: 85-105.
26. KAREL, M. October 1964. Private Communication.
27. MACKENZIE, A. P. & B. J. LUYET. 1963. An electron microscope study of the fine structure of very rapidly frozen blood plasma. *Biodynamica* 9: 147-164.
28. MOOR, H. & K. MÜHLETHALER. 1963. Fine structure in frozen-etched yeast cells. *J. Cell Biol.* 17: 609-628.
29. NEI, T., H. SOUZU & T. ARAKI. 1964. Studies of dehydration of cellular water in the freeze-drying of microorganisms, with special reference to changes in cell viability. *Contributions from the Inst. of Low Temp. Sci. Ser. B* No. 13: 14-26.
30. BANGHAM, A. D. & R. W. HORNE 1964. Negative staining of phospholipids and their structural modification by surface active agents as observed in the electron microscope. *J. Mol. Biol.* 8: 660-668.
31. LUCY, J. A. & A. M. GLAUERT. 1964. Structure and assembly of macromolecular lipid complexes composed of globular micelles. *J. Mol. Biol.* 8: 727-48.
32. GREAVES, R. I. N. 1965. *This Annal.*

# SEPARATE EFFECTS OF FREEZING, THAWING AND DRYING LIVING CELLS

R. I. N. Greaves and J. D. Davies

*The University Department of Pathology, Cambridge, England*

## Introduction

Freezing, thawing and drying are all potentially lethal processes to living cells. Yet, if water is immobilized by freezing or removed by drying, the cell metabolism ceases and, if it is not destroyed by the process, it may be preserved indefinitely.

Organisms vary considerably in their frost resistance and also in their resistance to drying, but even with frost resistant organisms their resistance to freeze drying is considerably influenced by the medium in which they are dried.

The discovery that glycerol and later that dimethylsulphoxide (DMSO) protected cells against injury by freezing has enabled many delicate cells to be preserved by freezing. Unfortunately, neither additive has been used successfully for freeze-drying. However, it has been shown, particularly with red blood cells, that other additives will protect against injury by freezing and thawing, and in this group we find several sugars such as glucose, lactose and sucrose and polymers such as polyvinylpyrrolidone (PVP). The protection afforded by this latter group of additives is not as good as the protection afforded by glycerol or DMSO so that the conditions for freezing and thawing are more critical.

Since sugars and polymers are also used as protective additives in freeze-drying media, it is of considerable interest to try to discover whether they are acting primarily against frost injury or against drying injury.

This paper describes an experimental approach to this problem, first by observing the effect of these additives on salt concentration and crystallization, using the methods of thermal analysis, and second by comparing these observations with the protection afforded when using each additive for freeze-drying.

## EXPERIMENTAL APPROACH

*Thermal analysis.* The apparatus used was similar to that described by Rey (1960). The stainless steel block with its four holes, two for the reference fluid which was distilled water and two for the test fluid, was placed in the gas space of a Linde LNR25 refrigerator. This results in a cooling rate of approximately 1°C. per minute. A warming rate of 1°C. per minute was achieved by placing the stainless steel block in an aluminum block which was electrically heated precisely as described by Rey.

A Kipp Micrograph Recorder was used to give a simultaneous recording of temperature, resistance and differential temperature.

### Results

FIGURE 1 records the analysis of a 0.9 per cent solution of NaCl. The arrows indicate the direction of change.

On cooling an exothermic reaction starts at  $-27.5^{\circ}\text{C}$ . due to the crystallization of the eutectic mixture. This is completed at about  $-33^{\circ}\text{C}$ . when the resistance rapidly rises to over  $1\text{ M}\omega$ .

On warming, this resistance does not change much until  $-22^{\circ}\text{C}$ . is reached when it suddenly falls to a very low value. The differential tem-

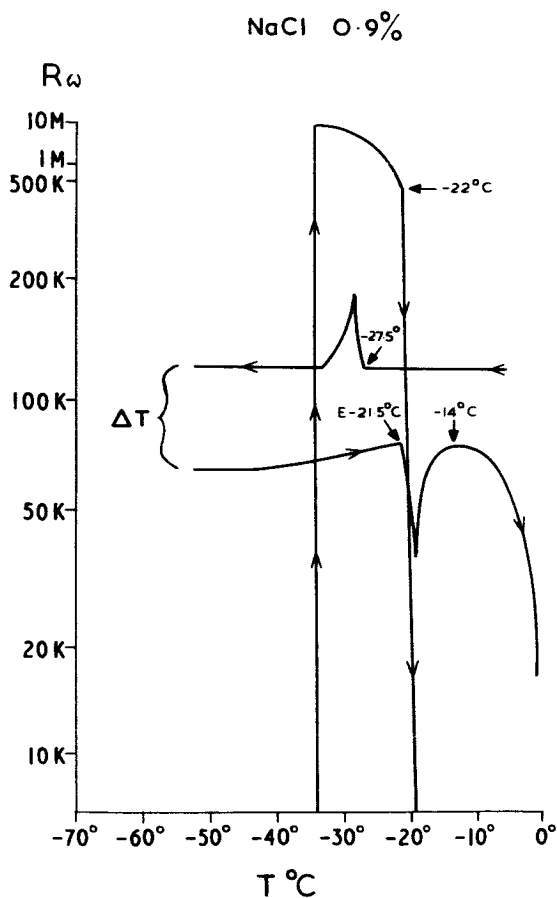


FIGURE 1. Thermal analysis of a 0.9% solution of NaCl. The arrows indicate the direction of change

perature shows an endothermic reaction at  $-21.5^{\circ}\text{C}$ . due to the thawing of the eutectic mixture.

The main points to observe from these measurements are first the marked degree of supercooling that occurs, which prevents the measurement of the eutectic temperature on freezing, and secondly that the freezing and thawing of the eutectic mixture can readily be detected by differential thermal measurement.

FIGURE 2 shows a similar experiment with 20 per cent glycerol in 0.9 per cent NaCl. On cooling, the resistance starts to rise at  $-25^{\circ}\text{C}$ . and continues to rise slowly not reaching a value higher than  $1\text{ M}\omega$  until the temperature is below  $-60^{\circ}\text{C}$ . On warming, the resistance curve closely approximates the cooling curve, indicating that there is little or no supercooling. Differential thermal analysis shows no evidence of the crystallization or melting of a eutectic mixture.

Ten per cent DMSO in 0.9 per cent NaCl gave a very similar picture, except that the resistance did not start to rise until  $-50^{\circ}\text{C}$ . was reached and did not reach  $1\text{ M}\omega$  until the temperature was  $-80^{\circ}\text{C}$ . Supercooling and the NaCl eutectic were also abolished.

FIGURE 3 records an unique experiment using one per cent DMSO in 0.9 per cent NaCl. On cooling the resistance started to rise at  $-40^{\circ}\text{C}$ .

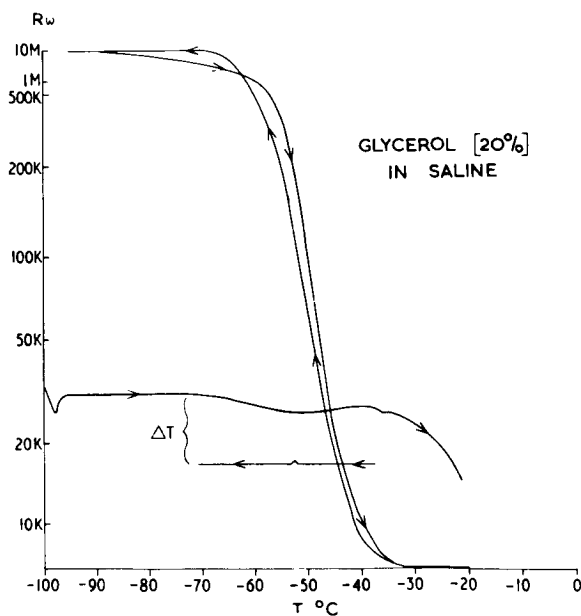


FIGURE 2. Thermal analysis of 20% glycerol in 0.9% NaCl. The arrows indicate the direction of change.

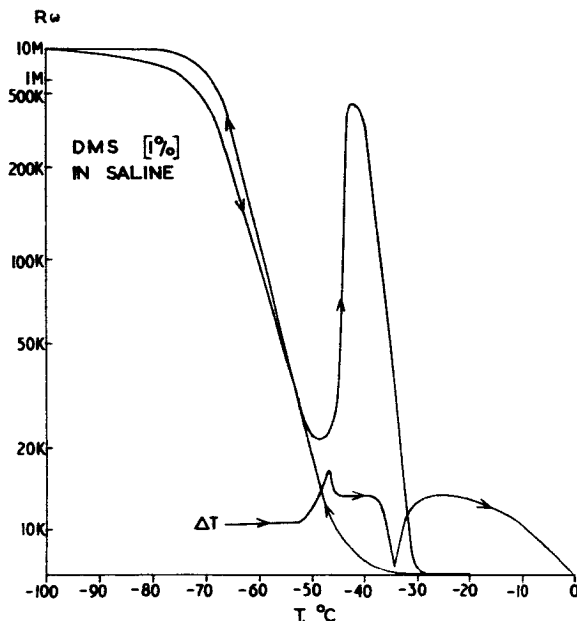


FIGURE 3. Thermal analysis of 1% D.M.S.O. in 0.9% NaCl. Note the sudden increase in resistance on thawing which occurs immediately after an exothermic reaction which suggests crystallization of a metastable glass.

reaching 1  $M_{\omega}$  at  $-75^{\circ}\text{C}$ . On warming the resistance curve started by following the freezing curve. At  $-50^{\circ}\text{C}$ ., however, the differential temperature showed the start of an exothermic reaction which was complete at  $-47^{\circ}\text{C}$ . The moment crystallization was complete the resistance rose suddenly to a high value and then fell rapidly when an endothermic reaction, indicating melting of the crystals started at  $-38^{\circ}\text{C}$ .

These experiments would indicate that both glycerol and DMSO prevent the formation of a eutectic concentration when NaCl solutions are frozen. They would appear to do this by forming a glass which slowly hardens as indicated by the slow change in conductivity. These glasses formed on slow freezing are very stable; only on one occasion (FIGURE 3) was metastability observed. These results are consistent with those of Rey (1960) who showed that with rapid freezing and slow thawing of glycerol in Earle's solution, a metastable glass was formed.

FIGURE 4 shows a similar experiment with 10 per cent sucrose in 0.9 per cent NaCl. The resistance change starts sooner at  $-20^{\circ}\text{C}$ . and rises more rapidly, reaching 1  $M_{\omega}$  at  $-30^{\circ}\text{C}$ ., than with glycerol or D.M.S.O. but both supercooling and eutectic melting are abolished, which suggests glass formation.

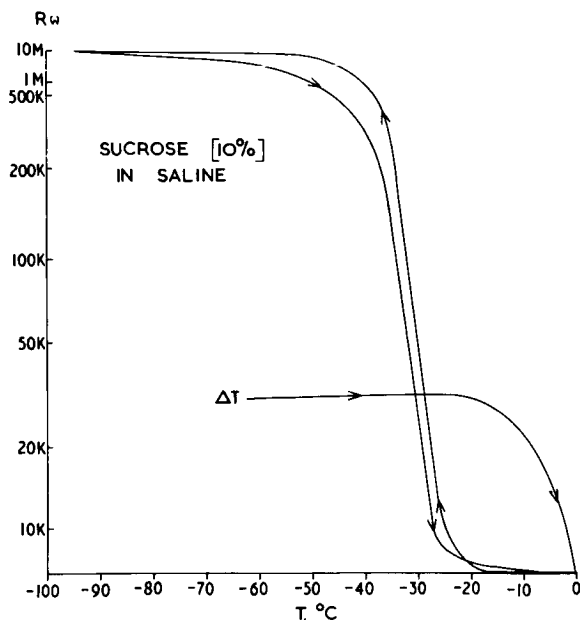


FIGURE 4. Thermal analysis of 10% sucrose in 0.9% NaCl. The arrows indicate the direction of change.

Ten per cent glucose in 0.9 per cent NaCl gave a more gentle resistance change than sucrose, but differential thermal analysis showed that there was melting of an eutectic mixture. Glucose at 10 per cent had not completely suppressed eutectic concentrates. Ten per cent PVP in 0.9 per cent NaCl gave a more gradual change in resistance and greater though not complete suppression of eutectic concentration than did 10 per cent glucose.

Mazur (1960) has shown that the yeast *Saccharomyces cerevisiae* is very sensitive to rapid freezing and slow warming but is fairly resistant to slow freezing and fast thawing. He suggests that death is due to intracellular ice formation which occurs when external ice crystals grow through aqueous channels in the cell wall and seed supercooled water in the cell interior. An extract of this yeast was made by disintegrating it in a freeze-press. To this extract was added NaCl to a final concentration of 0.9 per cent. On freezing, once again we observed a slow rise of resistance starting at  $-20^{\circ}\text{C}$ . and reaching  $1\text{ M}_{\omega}$  at  $-50^{\circ}\text{C}$ ., and this was coupled with suppression of the NaCl eutectic.

This yeast has its own built-in, protective additive and we wondered if its stability to slow freezing and fast thawing and susceptibility to fast freezing and slow thawing might be due to the glass being stable in the



first instance and metastable in the second. Rapid freezing and slow thawing of the extract, however, failed to show metastability.

### Conclusions

All the additives tested which are used for protecting cells against freezing injury prevent the formation of eutectic concentrations of salts. They appear to do this by producing a glass-like material which progressively hardens as the temperature falls.

Glasses formed on slow freezing tend to be stable, only one instance of metastability being recorded.

The additives tested could be placed in order of their effectiveness to form glasses and prevent eutectic concentrations of salts. DMSO was the most efficient, followed by glycerol, sucrose, PVP and glucose in that order.

### FREEZE-DRYING

Preliminary experiments were carried out by drying the yeast *S. cerevisiae* on nylon gauze in an apparatus similar to that described by Meryman (1959). This apparatus relies on the direct pumping of the water vapor by a large air-ballasted pump. A calibrated vacuum valve in the pumping line enables various freezing rates and drying rates to be achieved.

FIGURE 5 presents the results of drying the yeast *S. cerevisiae*, suspended in one per cent bovine albumin at temperatures from 0°C. to -40°C. Superimposed on this FIGURE in a dotted line are the results obtained by Mazur (1960) on fast freezing and slow thawing of the same yeast. These results show that drying from the liquid phase is a fairly lethal process, that as the temperature of drying falls the immediate survival improves until Mazur's curve is reached when the two curves follow approximately the same line. If drying took place between -5 and -10°C. sometimes a phase-change occurred; sometimes drying took place from the liquid phase. In either case the percentage survival was the same, showing that extracellular ice did not affect survival. This is in direct contrast to the drying of *Strigomonas oncopelti* in which an extracellular phase change led to total death of the organisms.

If 7½ per cent glucose or, better still, 7½ per cent glucose and 10 per cent PVP were used as the suspending medium for the yeast, the survival curve continued to rise as the temperature of drying fell reaching a maximum of 60 per cent survival at -25°C. This might be interpreted as indicating that the additive was giving protection against freezing injury if it were not appreciated that the freezing rate was faster on this particular apparatus the lower the drying temperature. When it was found that if the yeast was frozen at a rate of 1°C. per minute and thawed rapidly about 80 per cent survived freezing to -35°C. even when suspended in dis-

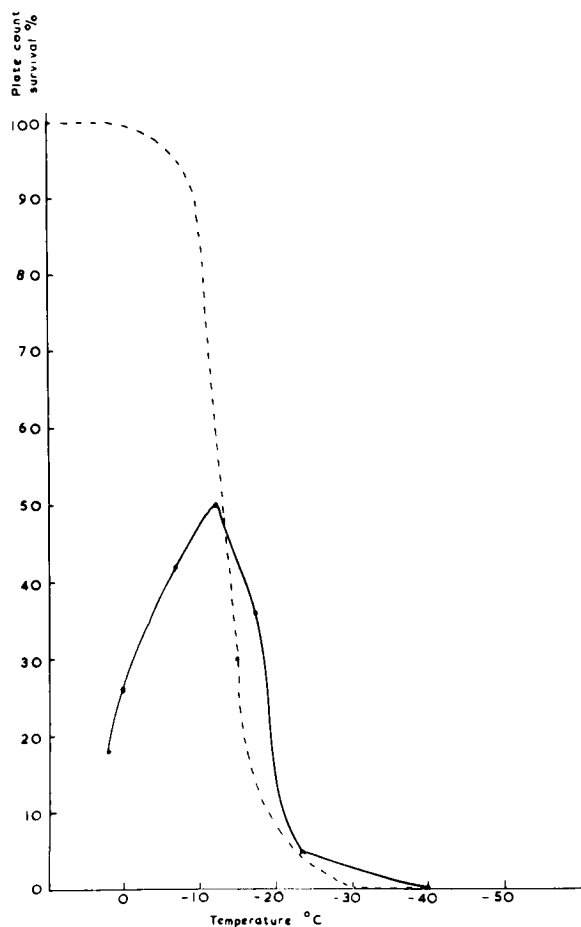


FIGURE 5. Percentage survival of *Saccharomyces cerevisiae* when dried at temperatures ranging from  $+2^{\circ}\text{C}.$  to  $-40^{\circ}\text{C}.$  Dotted line — percentage survival of same yeast on fast freezing and slow thawing at different temperatures as observed by Mazur (1960).

tilled water, it became obvious that this apparatus was not suitable for this type of experiment.

What was required was an apparatus giving a constant rate of freezing of  $1^{\circ}\text{C}.$  per minute to a temperature of at least  $-40^{\circ}\text{C}.$ , and an adjustable and exact drying temperature which should be maintained until the culture was dry so that it was only brought up to ambient temperature when dry.

*Description of Apparatus*

Thermoelectric refrigeration seemed to be the ideal solution to these problems and a two-stage 'Frigistor' refrigerator was obtained. This was mounted on a thick brass base plate which was water cooled on the opposite side. A recessed "O" ring in this plate gave a vacuum seal for the "bell jar" top of the desiccator (FIGURE 6).

The desiccator chamber was connected to a 'Megavac' pump, via a vacuum valve and a phosphorus pentoxide trap.

At maximum current the first stage reaches  $-25$  to  $-30^{\circ}\text{C}$ . and the second stage  $-55$  to  $-60^{\circ}\text{C}$ . Ampules or tubes may be placed in aluminum blocks on either stage.

There are several ways in which the apparatus may be used. For experimental purposes the ampules are placed on the second stage and  $\text{P}_2\text{O}_5$  in the trap is used as the drying agent. As the vacuum valve is between the drying chamber and the trap, it can be used to give a very fine control of the drying rate and consequently the drying temperature. For routine drying the ampules are placed on the first stage, the second stage being used as a refrigerated condenser at  $-60^{\circ}\text{C}$ .

The temperature can be held constant until drying is complete when the current in the refrigerator is reversed so that the ampules are rapidly heated to ambient temperature. In this way a gradual rise in temperature during the period of desorption is avoided.

*Results*

The results of drying *S. cerevisiae* in different support media and at three different temperatures are shown in TABLE 1. The percentage survival was estimated immediately after drying, no long-term storage test or accelerated tests were performed. Previous experience would suggest that a good immediate survival need not necessarily correspond with good long-term survival. For instance the fact that 100 per cent survival was obtained using a drying mixture of  $7\frac{1}{2}$  per cent glucose, 5 per cent peptone and 10 per cent PVP at a drying temperature of  $-25^{\circ}\text{C}$ . while only 93.5 per cent survival was obtained when  $12\frac{1}{2}$  per cent sucrose and 10 per cent PVP was the drying medium, does not necessarily mean that the first medium is the better and on an accelerated degradation test the sucrose PVP medium would probably be superior.

In all these experiments prefreezing was at the same rate of approximately  $1^{\circ}\text{C}$ . per minute. There is no evidence that frost damage was significant as a cause of death even at  $-35^{\circ}\text{C}$ .

These results confirm the original experiments in that the lower the drying temperature the better the survival. They differ from the original experiments in that by preventing frost damage by slow freezing, the sur-



FIGURE 6. Experimental drying apparatus. The two stage thermoelectric Frigistor refrigerator can be seen mounted on a solid brass base plate. The DC power supply is mounted below the desiccator chamber. The different types of aluminum blocks for holding tubes and ampules can also be seen.

TABLE 1  
PERCENTAGE SURVIVAL IMMEDIATELY AFTER DRYING *S. CERVISIAE* IN  
DIFFERENT DRYING MEDIA

Suspending medium	Percentage survival immediately after drying at:		
	-12.5°C.	-25°C.	-35°C.
Distilled water	1	19	18
Glucose 7-1/2 %	71	70	85
Sucrose 12-1/2 %	63	72	75
Peptone 10 %	59	63	83
Na glutamate 5 %	31	16	52
PVP 10 %	4	50	49
Glucose 7-1/2 % } Peptone 5 % } PVP 10 % }	70	100	85
Sucrose 10 % } Na glutamate 2 % } PVP 10 % }	71	85	74
Sucrose 12-1/2 % } PVP 10 % }	80	94	84
Na glutamate 5 % } PVP 10 % }	26	10	18

vival curve continues to rise even down to a temperature of  $-35^{\circ}\text{C}.$ , the lowest temperature used in these experiments.

One cannot help being surprised that the additive mixtures were so little better than the single additive substance, and in fact the mixture of Na glutamate and PVP was inferior to either used separately.

#### *Conclusions*

These experiments were an attempt to eliminate as many variables as possible from the freeze-drying technique. Only one organism has been used and quite different results might have resulted with some other

organism. The prefreezing rate and drying temperature was kept constant and the temperature was not allowed to rise during desorption.

These experiments would suggest that provided frost injury can be avoided the lower the drying temperature the better. They would also suggest that the effectiveness of a drying additive is not related to any protective effect it might have against frost injury.

#### *References*

1. MAZUR, P. 1960. Physical factors implicated in the death of microorganisms at subzero temperatures. *Ann. N. Y. Acad. Sci.* 85: 610-629.
2. MERYMAN, H. T. 1959. Survival of spermatozoa following drying. *Nature* 184: 470.
3. REY, L. R. 1960. Thermal analysis of eutectics in freezing solutions. *Ann. N. Y. Acad. Sci.* 85: 510-534.

## TRANSPORT PROPERTIES OF WATER\*

Alexander Leaf

*Department of Medicine, Harvard Medical School and  
Massachusetts General Hospital, Boston, Mass.*

The introduction of isotopes in the measurement of membrane permeability has afforded information unobtainable by prior methods of measurement. At the same time the interpretation of permeability measurements was made more complicated. This complexity is nowhere more evident than in the case of water. Without isotopes only net transfers of matter were measureable. In the case of water movement through a membrane or other permeability barrier, one could measure a mobility either from filtration experiments in which a hydrostatic pressure provided the driving force for net transfers of water or from osmotic experiments in which the gradient of a nonpenetrating or poorly penetration solute across the permeability barrier provided an equivalent driving force.

For a simple binary aqueous solution divided by a barrier totally impermeable to the solute, these relations are simply expressed as

$$\frac{J_v}{\Delta p - \Delta \pi} \approx L_p$$

with  $J_v$  the volume flow, essentially equal in the case of dilute aqueous solutions to the flow of water;  $\Delta p$  and  $\Delta \pi$  are the gradients of hydrostatic and osmotic activity, respectively;  $L_p$  is the ordinary mechanical filtration coefficient of Staverman.<sup>1</sup> The inverse of the above relation gives us the resistance of the barrier to the filtration or osmotic flow of water.

When a steady state of filtration or osmotic flow is achieved across the barrier in our simple system, the driving force for the movement of water will be dissipated in overcoming the frictional resistance between the water and the membrane,<sup>2</sup>  $f_{wm}$ , and the internal friction of the water,  $f_{ww}$ . To express these relationships quantitatively, however, one needs a precise description of the chemical and physical nature of the barrier as well as a model to describe how the water moves. The term,  $f_{wm}$ , is determined both by the chemical nature of the barrier which determines its interaction with water molecules and the geometry of the membrane, as the frictional terms are defined per mole of water and the size and shape of the channels in the membrane will determine the amount of interaction with the membrane that a mole of water encounters on its passage through the barrier. Even

\*This investigation was supported by a grant from the John A. Hartford Foundation, Inc. and by United States Public Health Service Research Grants No. HE 06664 from the National Heart Institute and AM 04501 from the National Institute of Arthritis and Metabolic Diseases.

in a membrane in which the interaction with the channel walls per molecule of water is great, the presence of large channels will so reduce the contacts between water and membrane that  $f_{wm}$  will be small and most of the resistance in the barrier will be that arising from the internal friction of water with water in such large channels.

The friction term,  $f_{wm}$ , is dependent upon the model of how the water moves. Since it also is defined per mole of water passing through unit area and unit thickness of the membrane it can vary greatly from a maximal value if individual molecules move alone through the barrier, as in the process of diffusion — *vide infra*, or approach minimal values during bulk flow through large channels when movement together of large molecular groups occurs. Within these limits each water molecule may encounter frictional interactions in the direction of net movement from theoretically zero to the maximal value which is obtained in free diffusion. Generally, it is assumed that laminar flow is the model which applies if the channels through which the water moves are large relative to the size of water molecules and the known viscosity of bulk water is used for  $f_{ww}$ . If the channels are very small then the free diffusion coefficient is used to characterize the frictional interactions of water with water. Between these limiting models, however, it seems likely that other possibilities exist.

It seems probable that if aqueous channels perforate biological membranes, hydrophilic groups within the membrane will orient so as to form the lining of such channels. Where this occurs the interaction of water molecules with the surface of the channel, largely through hydrogen bonding, may not be very dissimilar to the interactions between water molecules in free solution. In this case the molecular friction between water and membrane and water and water may not differ significantly and a single frictional term will be applicable. As mentioned, even if the molecular interaction between water and membrane is quite different from that between water and water in bulk, where the channels are sufficiently large so that water-membrane contacts are infrequent relative to water-water interactions, the frictional term of the latter may suffice to describe the system.

We appreciate now, as we have heard at this Conference, that water may have quite different properties at interfaces and surfaces from those usually associated with it in bulk. Either a net decrease in the ice-like structure or a net increase in the ordering of water within biological membranes may occur; both situations will affect the frictional resistance of the barrier to the passage of water. A decrease in the ice-like structure of water occurring within sizeable channels would increase the fluidity of water and decrease the resistance of the barrier to its passage. On the other hand, a barrier with channels of dimensions which will admit only single water molecules will simulate the situation of water dissolved in



the barrier if interactions of individual water molecules with the membrane approximate those in bulk water. If the attractive forces between water and membrane are either much greater or, in the case of hydrophobic materials, much less, the barrier in all likelihood will be largely impermeable to water. If water becomes organized either about ionic and polar groups at the surface of the channel or at nonpolar, hydrophobic surfaces, the increased ice-like structure of the water within the channels may profoundly affect the penetrability of the barrier to water. Common experience indicates the marked difference in the viscosity of ice and water. Either cause of an increased structure of water within small aqueous channels may obstruct the passage of water but possibilities for different effects may exist. The increased organization of water molecules that surround ionic groups arises as a result of the interaction of the dipoles of water molecules with charged groups. An attractive force between membrane and neighboring water molecules would be responsible for the ice-like state of water in the membrane in this situation. At nonpolar surfaces the increased structure of water results, on the other hand, from the lack of interaction of water with the nonpolar surface or group.<sup>3</sup> Thus both conditions may result in a more ice-like water in the membrane but the frictional resistance between water and membrane will be high in the former situation and may be low in the latter. The latter situation may give rise to molecular slippage at the interface between liquid and membrane.<sup>4</sup>

Thus far we have considered those factors which may influence net transfers of water through the membrane, the mechanical filtration or permeability coefficient, describing the penetration of the membrane in response to hydrostatic or osmotic pressure gradients. The diffusion permeability, as measured by the penetration rate of isotopically labeled water molecules through the membrane, will be affected by the same factors. Labeled water added to the medium bathing one membrane surface may appear in the medium bathing the opposite surface, however, even under conditions in which no net water transfer across the membrane is occurring. In fact, it is generally under such conditions that isotopic permeability measurements are made to obtain the diffusion permeability of a barrier unaffected by solvent or solute drag. The individual tagged water molecule penetrates the barrier by diffusion, a process of isotopic exchange, in which the gradient of chemical potential of the isotopic species or a gradient of specific activity is the driving force and is equal to the entropy of mixing. As the isotopic water molecule penetrates the barrier it will be subject to the frictional forces described as it randomly jumps from one position to the next. It may at one moment be associated with one cluster of water molecules and the next moment be part of another. In the absence of net transfers of water across the barrier the clusters will have no statistical direction and the progress of the labeled water molecule will depend upon

the molecular friction between it and its neighboring water or membrane molecules.

In general<sup>2</sup>

$$\omega = \frac{\alpha_w}{\Delta x (f_{ww} + f_{wm})}$$

the permeability coefficient,  $\omega$ , is inversely proportional to the sum of the frictional coefficients of water and water,  $f_{ww}$ , and of water and membrane,  $f_{wm}$ , and directly proportional to the volume fraction of water in the membrane,  $\alpha_w$ . In a very finely porous membrane  $f_{wm} > f_{ww}$  but in coarse, porous membranes the importance of  $f_{wm}$  diminishes and  $f_{ww}$  becomes the determining factor, as in free diffusion. The familiar Fick equation may be used to describe the diffusion process of labeled water, e.g. tritiated water, THO, penetrating the membrane

$$J_{\text{THO}} = -DA \frac{\Delta c}{\Delta x}$$

with  $J_{\text{THO}}$  the quantity of labeled water penetrating unit area of membrane per unit time;  $\Delta c/\Delta x$  the gradient of isotope concentrations across the barrier,  $A$  is the fraction of membrane unit area available for penetration by the isotopic water, and  $D$  is the diffusion permeability constant.\* When the frictional forces that the isotopic water encounters in the membrane are largely those of water-water interactions as in bulk water, then  $D$  will be the familiar free diffusion constant,

$$D^0 = \frac{RT}{f_{ww}}$$

If it is known, or assumed, that the free diffusion coefficient of water does in fact apply in a given situation and, as  $\Delta c/\Delta x$  and  $J_{\text{THO}}$  may be determined, a value for  $A$  can be obtained. The dimensions of the individual channels which contribute to  $A$  cannot, however, be assessed by measurements with labeled water. Either independent permeability measurements of the barrier to a series of solute molecules of known dimensions<sup>5,7,8</sup> or, alternatively, measurements of net transfers of water across the membrane in response to known hydrostatic or osmotic gradients may be made to estimate the size of the individual channels which comprise  $A$ . According to the latter method a number of assumptions are made about the barrier which must be very unrealistic for biological membranes. It is assumed that the volume flow of water,  $J_v$ , occurs through the right circular cylinders arranged perpendicular to the membrane and, from the Poiseuille equation

$$J_v = \frac{\pi r^4}{8\eta} \frac{\Delta p}{\Delta x}$$

\*The dimensions of  $D$  and of  $\omega$ , referred to above, are related by  $D = \omega RT$ .

in which  $r$  is the mean radius of the individual pores,  $\eta$  is the viscosity of water and  $\Delta p/\Delta x$  is the gradient of hydrostatic or osmotic pressure which provides the driving force for the flow of water. The ratio of bulk flow,  $J_v$ , to the diffusional flow,  $J_D$ , measured with isotopic water in the absence of bulk flow, is

$$\frac{J_v}{J_D \bar{V}_w} = \frac{RT r^2}{8\eta D \bar{V}_w}$$

From this relationship the equivalent mean pore radius,  $r$ , may be calculated.<sup>5-8</sup> As emphasized by several workers<sup>2,6</sup> if the mean pore radius is even as large as 10 Å, net transfer of water by bulk flow will greatly exceed that by diffusion.

For a diffusional process the flux ratio across a barrier is equal to the activity ratio of the diffusing species on the two sides of the barrier.<sup>6</sup> Thus if  $J_{12}$  is the flux of the diffusing species from side 1 to side 2 of the barrier and  $J_{21}$  is the flux in the reverse direction then,

$$\frac{J_{12}}{J_{21}} = \frac{a_1}{a_2}$$

with  $a_1$  and  $a_2$  the activity of the uncharged diffusing species on the sides 1 and 2, respectively. If however, the transfer of water in bulk occurs across a homogeneous semipermeable membrane, then

$$\frac{J_{12}}{J_{21}} = \left( \frac{a_1}{a_2} \right)^n$$

with  $n = f_{wv}/f_{wm}$ ; "n" may be  $> 100$  in the biological system to be discussed below.

"n" only approaches unity when the dimensions of the channels through which water moves approximate the dimensions of individual water molecules.<sup>6</sup> This calculation confirms the view that water diffusion is a process in which the moving unit is a single water molecule and for this process the frictional term per molecule is maximal. Through all pores of larger dimensions the associated nature of water will result in the movement of clusters or bulk water which thereby reduces the friction per molecule and allows larger net water transfers for a given pressure difference than could occur by diffusion alone.

Although a value of  $n > 1$  indicates movement of associated water molecules through the barrier it should not be construed necessarily to mean the presence of continuous aqueous channels through the barrier. This has been shown by the studies of Sidel and Hoffman<sup>9</sup> using a synthetic liquid "membrane" of well stirred mesityl oxide separating two aqueous solutions. In such a system it is likely that small water droplets move together through the barrier rather than individual molecules moving separately. Such aggregates of water in the mesityl oxide barrier may even entrap solute molecules such as urea to give the appearance of solvent drag.

To summarize, we may state that the frictions that water molecules may encounter during either diffusional movement (individual molecules moving singly) or bulk transfer (associated molecules moving together) across a permeability barrier are the same. However quantitatively the total friction per molecule may be markedly reduced by bulk flow and the prevalence and dominance of this type of movement is dependent upon the strong tendency of water to associate through hydrogen bonding.

Next, this author would like to consider some of the speculations made above in regard to water movement across a biological membrane which we have been studying because of our interest in the similarities in its activities to those of the portions of the human nephron. This refers to the urinary bladder of the toad, *Bufo marinus*. It has been observed by Ewer<sup>10</sup> that in the toad the urinary bladder serves as a reservoir for water which may be reabsorbed during periods of water deprivation or rapidly in response to neurohypophyseal hormone injections.

The toad urinary bladder is a bilobed organ which may fill one-third or more of the entire abdominal cavity in the hydrated animal. It may easily be removed and used as either a sheet or a bag of tissue. The bladder wall is transparently thin consisting of a single mucosal cell layer supported on a thin connecting tissue layer containing bundles of smooth muscle and capillaries. A serosa lines the contramucosal surface.

As very dilute urine may remain in the bladder for hours with no apparent diminution in volume or rise in concentration; one's first expectation might be that the bladder mucosa is very impermeable to water. However, when water labeled with either deuterium or tritium is added to the medium bathing the mucosal surface and the appearance rate of labeled water in the medium bathing the serosal surface determined, quite rapid rates of water permeation are observed, as shown in TABLE 1.<sup>11</sup> The values are quite constant over the successive periods and note that vasopressin induces an increase of some 70 per cent in this diffusion permeability.

On the other hand, we obtain an entirely different view of the permeability of this tissue if we examine the net transfers of water that occur across it in response to an osmotic gradient. FIGURE 1<sup>11</sup> indicates the large effect of the hormone on net transfer of water in the presence of an osmotic gradient. In these experiments an osmotic gradient was established by bathing the mucosal surface with a Ringer's solution diluted to attain the desired transmembrane concentration gradient which is plotted on the abscissa. The ordinate is the net water movement. The broken line indicates the very small net transfers of water across the bladder which occur in the absence of vasopressin despite large osmotic gradients, a finding consistent with the observation that dilute urine may remain for long periods of time in the bladder with little or no detectable changes in concentration. The

TABLE 1  
EFFECT OF VASOPRESSIN ON DIFFUSION PERMEABILITY (UNIDIRECTIONAL  
WATER FLUX) OF ISOLATED TOAD BLADDER TO WATER MEASURED WITH  
D<sub>2</sub>O OR T<sub>2</sub>O IN ABSENCE OF OSMOTIC GRADIENT

Preparation*	Periods (30 minutes) ( $\mu\text{l}/\text{cm}^2/\text{hr.}$ )			Mean difference (period 2-1)	S. E. mean difference	P
	1	2	3			
Control	343	338	339	- 5	$\pm 9$	> 0.5
With hormone	338	543	599	+205	$\pm 35$	< 0.001

\*Control includes 10 experiments; seven measured from mucosal to serosal surface and three in opposite direction. Hormone-treated group includes 13 experiments; nine were mucosal to serosal fluxes and four were measured in reverse direction. Hormone added at end of first period (two units commercial Vasopressin to medium bathing serosal surface). Fifteen milliliters frog Ringer solution bathing each surface; 3.14 cm.<sup>2</sup> area of chambers. (From Hays, R. M. & A. Leaf. 1962. Studies on the movement of water through the isolated toad bladder and its modification by vasopressin. J. Gen. Physiol. 45: 905.)

upper line shows the large net transfers of water which may occur in the presence of vasopressin.

The finding that net water movement is proportional to the trans-epithelial osmotic gradient and that no water movement occurs in the absence of such an external driving force indicates that water moves

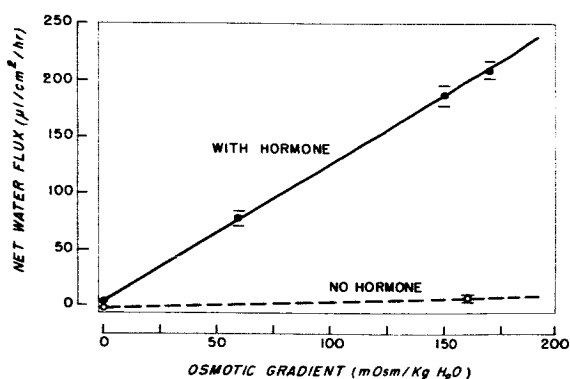


FIGURE 1. Dependence of net water flux on the transmembrane osmotic gradient in the presence and absence of vasopressin. (From Hays, R. M. & A. Leaf. 1962. Studies on the movement of water through the isolated toad bladder and its modification by vasopressin. J. Gen. Physiol. 45: 905).

passively across the bladder. The osmotic gradient *in vivo* arises from the active reabsorption of sodium and this is the step in the process of water reabsorption which requires energy.

Thus water moves passively across the toad bladder and in spite of a high unidirectional diffusion permeability to water, very little net movement occurs in the absence of the hormone. Vasopressin possesses the ability to induce large net transfers of water with only a moderate further increase in unidirectional diffusion permeability. How does the hormone modify the bladder to produce these effects on the transport of water? Koefoed-Johnsen and Ussing<sup>10</sup> have proposed the most satisfactory explanation at the present time on the basis of the "pore hypothesis." According to their hypothesis, net water movement occurs predominantly by bulk flow in aqueous pores through the membrane rather than by diffusion, and vasopressin increases the net transfer of water by enlarging the radius of individual pores. As discussed earlier, diffusion depends upon the area (or pore radius squared) available for penetration by the diffusing species while laminar flow, according to the Poiseuille equation, is a function of the fourth power of the radius of the individual pores, an increase in the radius,  $\Delta r$ , will affect diffusion only by  $(r + \Delta r)^2 - r^2$  while bulk flow will be increased by  $(r + \Delta r)^4 - r^4$ . They conceive of neurohypophyseal hormones as altering the responsive membrane from one containing many small pores to one containing fewer large pores. Little change in area or diffusion permeability would be consistent with large increases in the bulk transfer of water with vasopressin according to this hypothesis of hormonal action.

By combining the equations for diffusion and for bulk flow, as noted above, one can calculate the mean pore radius making the highly artificial assumptions that the water moves through pores which are right circular cylinders aligned perpendicularly to the mucosal surface. This is a formal and probably meaningless exercise but serves to emphasize the porosity of the bladder to water. Such calculations suggest that some four per cent of the surface is made up of right circular cylinders having a mean radius of 40 Å.<sup>11</sup> This seems to be the size of channel necessary to accommodate the large bulk transfers of water observed. Although channels of such size might be expected to be visible by electronmicroscopy, none have been seen. Before turning to the evidence from the penetration of this tissue by small solutes, which quite convincingly demonstrates that no naked pores of such dimensions can in fact perforate the rate limiting barrier in the bladder, the author would like to mention some observations relating to the state of water in the bladder.

In an attempt to learn whether one may justifiably apply the known properties of bulk water to water in a living tissue in proximity to complex surfaces and in very small channels, Richard M. Hays of the Albert

Einstein College of Medicine and the author have obtained information<sup>12</sup> perhaps pertinent to this discussion. Both theory and experiments support the view that viscosity and self-diffusion in bulk water are largely determined by intermolecular hydrogen-bonding. Deductions regarding the degree of hydrogen-bonding and, therefore, the state of water can be made from the activation energies for diffusion and viscous flow in water. The temperature dependence of both processes has been shown by Wang and associates<sup>13</sup> to be essentially identical, yielding activation energies of 4.6 and 4.59 kilocalories per mole at 25°C., respectively. We have therefore examined the temperature dependence for both diffusion of tritiated water (THO) and net transfers of water through the toad bladder. FIGURE 2

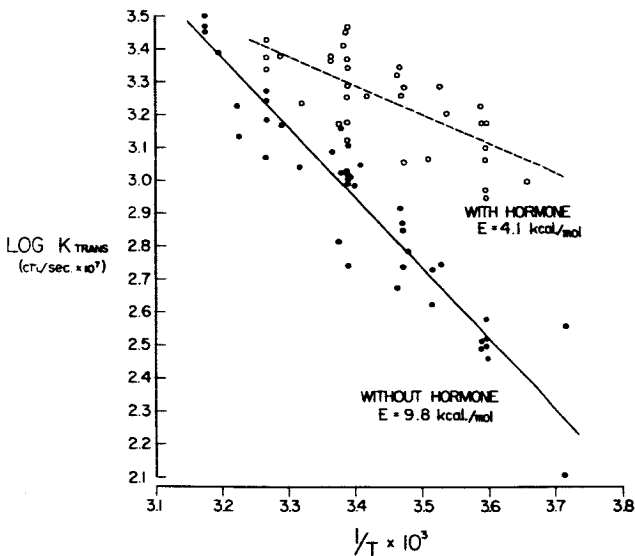


FIGURE 2. Temperature dependence of diffusion of THO through isolated toad bladder.  $K_{trans}$  is the transepithelial permeability coefficient for diffusion of THO and  $1/T$  is the reciprocal of the absolute temperature. (From Hays, R. M. & A. Leaf. 1962. The state of water in the isolated toad bladder in the presence and absence of vasopressin. *J. Gen. Physiol.* 45: 933).

shows Hays' findings on the temperature dependence of THO through the toad bladder in the presence and absence of vasopressin.<sup>12</sup> The results are presented as a familiar Arrhenius plot of the reciprocal of absolute temperature on the abscissa and the logarithm of the rate constant, in this case the transepithelial permeability coefficient for THO, on the ordinate. From the slopes of the experimental lines obtained the activation energies are readily calculated. In the absence of vasopressin a high value of 9.8

kilocalories per mole was obtained for the activation energy for diffusion which dropped to 4.1 kilocalories in the presence of vasopressin. The latter value is sufficiently close to the known value of 4.6 kilocalories for self-diffusion of water to indicate that in the presence of vasopressin the frictional resistance that the diffusing THO encounters is similar to that in bulk water. However, the value of 9.8 kilocalories in the absence of the hormone means that the frictional resistance which the diffusing water molecule meets in the membrane is considerably greater than that encountered during diffusion in bulk water.

This finding in the absence of vasopressin seems consistent with two possible interpretations regarding the nature of the rate-limiting diffusion barrier in the bladder. A continuous nonaqueous barrier, such as the unimolecular lipid layers studied by Archer and La Mer,<sup>11</sup> would necessitate such high activation energies for penetrating water molecules. On the other hand, if continuous aqueous channels perforate the rate-limiting diffusion barrier in the absence of hormone, as they do in its presence, the water molecules in these channels must be bonded more tightly to each other or to the membrane than is the case in bulk water since the frictional resistance is determined by intermolecular hydrogen bonding. The activation energy obtained for bulk transfer of water in the presence of vasopressin was found to be 4.6 kilocalories per mole, in good agreement with the value of Wang and associates<sup>12</sup> for viscous flow in bulk water.

Further studies have excluded, we think, the possibility that this peptide hormone, vasopressin, acts simply by affecting the state of water in aqueous channels.<sup>12</sup> Some change in the porosity of the barrier to bulk transfer of water seems to be an essential part of the hormonal effect as originally suggested by Koefoed-Johnsen and Ussing.<sup>6</sup>

One can not study the temperature dependence of diffusion or bulk transfers of water across a delicate living membrane with the assurance with which one makes such observations on nonliving and synthetic membranes. Many metabolic activities of the cell upon which the structure of its permeability barriers ultimately must depend, will be affected. Also one can not be certain that the temperature dependence of the hormonal interaction with the membrane is not responsible for the observations in the presence of the hormone. However, the fact that "normal values" for the apparent activation energies for both diffusion and viscous flow were obtained in the presence of the hormone lends confidence to the high value of 9.8 kilocalories obtained for the diffusion of tritiated water across the bladder in the absence of the hormone.

The finding that in the presence of vasopressin water seems to traverse pathways through the bladder in which the ordinary bulk properties of water exist, doesn't help us out of our apparent need for large channels through the limiting barrier to accommodate the observed large net trans-



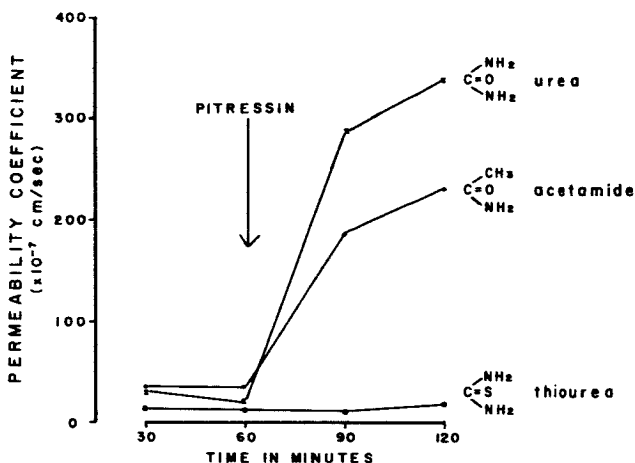


FIGURE 3. Effect of vasopressin on the permeability of the isolated toad bladder to urea, acetamide and thiourea. After two 30 minute control periods vasopressin was added to the medium bathing the serosal side of the bladder. (From Maffly, R. H., R. M. Hays, E. Lamdin & A. Leaf. 1960. The effect of neurohypophyseal hormones on the permeability of the toad bladder to urea. *J. Clin. Invest.* **39**: 630.)

fers of water in response to osmotic driving forces. A brief examination of the permeability of the bladder to small solutes, however, shows the inapplicability of any explanation for the hormonal action or transport of water which requires the presence only of large pores.

The striking feature of the effect of vasopressin on the permeability of the toad bladder to small molecules is its specificity. FIGURE 3<sup>15</sup> contrasts the large increase in permeability to urea and acetamide that followed addition of vasopressin with the absence of an effect on the structurally similar molecule of thiourea. Of the more than 40 compounds tested only in the case of certain small uncharged amides and certain small alcohols is the permeability of the toad bladder increased by vasopressin.<sup>16</sup>

These compounds, like water, penetrate the bladder passively. We have been unable to demonstrate interaction of these molecules with the membrane. However, since the very fact of specificity necessitates interaction with the barrier one suspects the presence of hydrogen bonding, a form of interaction likely to escape detection by the criteria of self-depression or competition. Although the mechanism of the molecular specificity is not yet understood, examination of the permeability coefficients and of the effects of solvent drag support the argument that vasopressin exerts its effect by modifying aqueous channels in the bladder through which these compounds seemingly move.<sup>16</sup>

The evidence from the effect of vasopressin on the penetration of small solutes that seems so irreconcilable with any simple pore hypothesis of the action of vasopressin is the specificity of its effects on the permeability to solutes, just considered, and the high degree of impermeability the bladder retains to small solutes even in the presence of large net transfers of water. The reflection coefficients<sup>1</sup> for thiourea, chloride, and urea were obtained<sup>16</sup> in the presence of large net transfers of water, averaging 200  $\mu\text{l}/\text{cm}^2 \text{ hr}$ . A value of 1.0 for the reflection coefficient means total impermeability of the membrane for the solute whereas a value of zero indicates a completely nonselective membrane. The reflection coefficient for thiourea was 0.995 and for chloride 0.993. Even urea is subject to a retardation in its rate of penetration of some 80 per cent relative to that of water.

We have good reasons to believe that the site of action of vasopressin with respect to all three of its effects — on water, solutes such as urea, and sodium ions, is in or near the plasma membrane lining the mucosal or urinary surface of the single layer of epithelial cells in this tissue.<sup>11,15,17,18</sup> In order to circumvent the apparent paradox of the need for large channels to accommodate the large net movements of water and simultaneously the impermeability to small solute molecules, a compound series barrier has been proposed. A fine diffusion barrier, highly permeable to water, urea, and sodium, but effectively blocking other solutes, such as thiourea, would be located most superficially on the mucosal surface of the bladder, overlying a deeper porous barrier. It is the porous barrier which is affected by vasopressin. In the absence of vasopressin the porous layer acts as the rate-limiting barrier to water and urea, but in the presence of the hormone the porosity increases imparting the characteristics of bulk flow to the transport of water across the bladder. As most solute molecules are blocked by the outer diffusion barrier, changes in porosity of the inner layer have little or no effect upon their passage across the epithelium.

Until recently such a double, series barrier has constituted only a formal description lacking any independent evidence for its existence. Recently, however, Norman Lichtenstein in our laboratory has found that amphotericin applied to the mucosal surface of the bladder will effectively remove the outer diffusion barrier leaving the deeper porous barrier relatively intact.<sup>19</sup> His evidence is that low concentrations of amphotericin in the mucosal bathing medium induce marked permeability increases to potassium, chloride, sodium and thiourea. Very little net transfers of water, however, occur under these circumstances until vasopressin is added. As amphotericin reacts with sterols and its actions on the bladder can be inhibited by cholesterol, it is hoped that this agent may afford a means of chemically dissecting the proposed series barrier and thereby contribute further insight into the actions of vasopressin and the specificity of the permeability characteristics of cellular membranes.

## References

1. STAVERMAN, A. J. 1951. The theory of measurement of osmotic pressure. *Recueil Travaux Chem. Pays-Pas*. 70: 344.
2. KEDEM, O. & A. KATCHALSKY. 1961. A physical interpretation of the phenomenological coefficients of membrane permeability. *J. Gen. Physiol.* 45: 143.
3. FRANK, H. S. 1958. Covalency in the hydrogen bond and the properties of water and ice. *Proc. Roy. Soc. London, Series A*. 247: 481.
4. DEBYE, P. & R. L. CLELAND. 1959. Flow of liquid hydrocarbons in porous vycor. *J. Appl. Phys.* 30: 843.
5. PAPPENHEIMER, J. R., E. M. RENKIN & L. M. BORRERO. 1951. Filtration, diffusion and molecular sieving through peripheral capillary membranes. *Am. J. Physiol.* 167: 13.
6. KOEFOED-JOHNSEN, V. & H. H. USSING. 1953. The contributions of diffusion and flow to the passage of  $D_2O$  through living membranes. *Acta Physiol. Scand.* 28: 60.
7. SOLOMON, A. K. 1960. Pores in the cell membrane. *Sci. Am.* 203: 146.
8. ROBBINS, E. & A. MAURO. 1960. Experimental study of the independence of diffusion and hydrodynamic permeability coefficients in collodion membranes. *J. Gen. Physiol.* 43: 523.
9. SIDEL, V. W. & J. F. HOFFMAN. 1961. Water transport across membrane analogues. *Fed. Proc.* 20: 137.
10. EWER, R. F. 1952. The effect of pituitrin in fluid distribution in *Bufo regularis* Reuss. *J. Exptl. Biol.* 29: 173.
11. HAYS, R. M. & A. LEAF. 1962. Studies on the movement of water through the isolated toad bladder and its modification by vasopressin. *J. Gen. Physiol.* 45: 905.
12. HAYS, R. M. & A. LEAF. 1962. The state of water in the isolated toad bladder in the presence and absence of vasopressin. *J. Gen. Physiol.* 45: 933.
13. WANG, J. W., C. V. ROBINSON & I. S. EDELMAN. 1953. Self-diffusion and structure of liquid water. III. Measurements of the self-diffusion of liquid water with  $H^2$ ,  $H^3$  and  $O^{18}$  as tracers. *J. Am. Chem. Soc.* 75: 466.
14. ARCHER, R. J. & K. LA MER. 1955. The rate of evaporation of water through fatty acid monolayers. *J. Phys. Chem.* 59: 200.
15. MAFFLY, R. H., R. M. HAYS, E. LAMBIN & A. LEAF. 1960. The effect of neurohypophyseal hormones on the permeability of the toad bladder to urea. *J. Clin. Invest.* 39: 630.
16. LEAF, A. & R. M. HAYS. 1962. Permeability of the isolated toad bladder to solutes and its modification by vasopressin. *J. Gen. Physiol.* 45: 921.
17. LEAF, A. 1960. Some actions of neurohypophyseal hormones on a living membrane. *J. Gen. Physiol.* 43(Suppl.): 175.
18. FRAZIER, H. S., E. DEMPSEY & A. LEAF. 1962. Movement of sodium across the mucosal surface of the isolated toad bladder and its modification by vasopressin. *J. Gen. Physiol.* 45: 529.
19. LICHTENSTEIN, N. S. & A. LEAF. 1965. Effect of Amphotericin B on the permeability of the toad bladder. *J. Clin. Invest.* In Press. (August, 1965.)

## DIFFUSION AND THE TRANSPORT OF ORGANIC NONELECTROLYTES IN CELLS\*

Samuel B. Horowitz and I. Robert Fenichel

*Laboratory of Cellular Biophysics,  
Albert Einstein Medical Center, Philadelphia, Pa.*

The observation was made by Overton and has been repeatedly confirmed<sup>1-6</sup> that the passive transport of organic nonelectrolytes in cells is commonly related to the chemical properties of the nonelectrolyte. These studies have shown that a correlation exists between cellular transport rates and the equilibrium distribution of the nonelectrolyte between water and a nonpolar solvent: roughly, the greater the relative concentration of the solute in the nonpolar phase the more rapid the transport process. These observations occupy a central position in the origin of current ideas on cell permeability. It has become customary to view nonelectrolyte transport as involving diffusional and solubility parameters, both determined by a membrane at the surface of cells — the plasma membrane — largely of lipid composition. Modification of ideas on the nature of this membrane has kept step with the experimental disclosure of the complexity of cellular transport, including, for example, the introduction of the idea of aqueous pores as a primary route of penetration of highly polar solutes. However, recent evidence from several areas has suggested alternative models incorporating features which could not have been anticipated by early investigators.

Electron microscopy has shown that the plasma membrane is not the unique membranous structure of the cell. Numerous similar structures have been demonstrated, some bordering cellular inclusions, others distributed in the cytoplasm.<sup>7,8</sup> Other levels of structure have been revealed as well; in muscle, for example, a highly regular though nonmembranous periodicity is seen in most of the cytoplasmic matrix.<sup>9,10</sup>

Secondly, it has been shown that chemical specificity similar to that seen in cellular transport is a general property of diffusion of organic nonelectrolytes in hydrogen bonding solvents.<sup>11,12</sup> Specificity in the latter systems is primarily a result of solute-solvent H-bond interaction, the stronger the interaction, the slower the diffusion. Since solute-solvent H-bond interaction largely determines the equilibrium distribution of nonelectrolytes,  $K_d$ , between water and nonpolar solvents, it is not surprising that the correlation which exists between cellular transport and  $K_d$  also exists between cellular transport and diffusion in H-bonding solvents; see FIGURE 1.

\*This work was supported in part by National Science Foundation Research Grant GB 1794 and by Public Health Service Research Grant GM 11070 from the Division of General Medical Sciences.

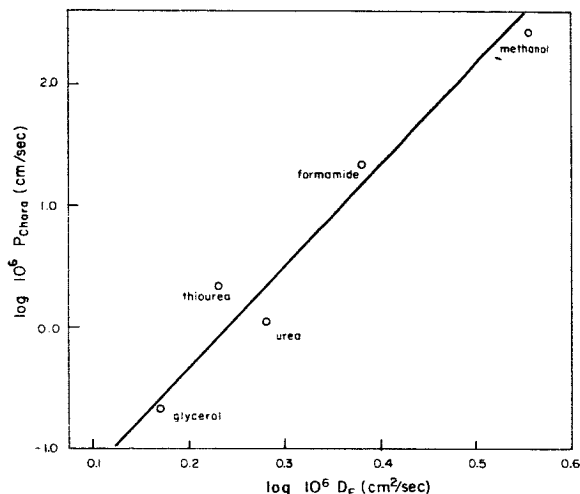


FIGURE 1. Correlation of permeability coefficients,  $P$ , of H-bonding solutes in *Chara* at 18-23°C.<sup>2</sup> with diffusion coefficients,  $D_F$ , in formamide-swollen dextran gel at 15.3°C.<sup>11</sup> Only the first members of homologous series of solutes are included. This correlation should be compared to that of  $P$  with nonpolar solvent/water equilibrium distribution coefficients.<sup>2</sup>

Two questions arise: Is there a single transport barrier at the surface of the cell or is the barrier distributed, and if the latter, does the barrier occur in discrete substructures or is it a continuous, though not necessarily uniform, property of the cell at a finer level of organization? Secondly, does chemical specificity arise from both solubility and diffusional effects, as in classical theory, or is it of purely diffusional origin? The answers to these questions are not unrelated. For example, if the barrier is continuous and uniform, specificity must be entirely diffusional. If the barrier is discrete, both solubility and diffusion must be considered.

A number of different types of models can be formulated:

- I. Classical single barrier at surface of cell.
  - A. Specificity primarily determined by lipid solubility.
  - B. Specificity primarily determined by diffusional specificity.
- II. Multiple discrete barriers distributed through the cell\* (multimembrane model).
  - A. Specificity primarily determined by lipid solubility.
  - B. Specificity primarily determined by diffusional specificity.

\*Part of the emphasis on a single cell surface barrier has been due to other properties attributed to this barrier (eg. "active transport" and electrical activity). These, according to membrane theory, necessarily occur at or near the cell boundary. There is no *a priori* necessity for nonelectrolyte transport to be linked to surface activity, so that a multimembrane model is admissible.

III. Barrier, as a first approximation, distributed uniformly throughout the cell and owing its properties to the predominant constituents of the cell. Specificity primarily determined by diffusional specificity.

From the point of view of theoretical understanding, the most significant difference among the models is not the distribution of the barriers but their composition. A model based primarily on lipid solubility is, because of the small quantity of lipids in most cells, confined to discrete barriers. While the specificity which can arise from lipid solubility is probably adequate to account for the magnitude of cellular transport specificity, the operation of this mechanism in cellular transport places rather stringent requirements on the structure of the barriers. Each barrier must contain a lipid phase which is continuous, except possibly for a small number of pores of molecular dimensions. In addition the lipid must have sufficiently strong intermolecular forces to account for the slow permeation of even highly lipid soluble solutes.

On the other hand, a diffusional mechanism which is based on solute-solvent H-bonding requires that wherever the barrier, it be strongly H-bonding. A high density of H-bonding sites in the barrier is, however, not sufficient in itself, as may be inferred from the low specificity seen in strongly H-bonding liquids.<sup>11,12</sup> In order to account for the high specificity of cellular transport a plausible mechanism must be provided whereby the effect on specificity of the H-bonding in the barrier is enhanced relative to that in liquids. Such a mechanism has been described elsewhere<sup>6</sup> and will be considered in detail below.

In current literature, a lipid solubility mechanism of specificity is generally accepted, and EM evidence is taken as indicating the existence of at least one lipid phase capable of serving as a transport barrier. Some of the physical chemical implications of this model merit enumeration. Using data from the frog *R. pipiens* extensor muscle<sup>6</sup> and *Bufo sp.* bladder,<sup>3</sup> diffusion coefficients for 1-butanol in a 100 Å membrane can be calculated to be about  $10^{-10}$  cm.<sup>2</sup>/sec. at 25°C. In comparison, the diffusion coefficient of a nonpolar solute of similar size, n-pentane, in vulcanized rubber, a dense nonpolar material, is in the range  $10^{-7}$  to  $10^{-8}$  cm.<sup>2</sup>/sec.<sup>13</sup> Only a substantial degree of crystallinity of the cellular membrane lipid could account for such extremely low diffusion coefficients.\* The activation energy for diffusion in vulcanized rubber is on the order of 14-15 kcal.,

\*Danielli<sup>3</sup> has assumed that an oil-like liquid phase of high viscosity would be adequate to give rise to a low diffusion coefficient. That this is incorrect can be appreciated from current knowledge of the very different mechanisms involved in viscous flow and small molecule diffusion in long-chain solvents. Stein<sup>14</sup> has treated membrane permeation in terms of a crystalline lipid phase.

whereas that for 1-butanol transport in muscle is 6.4 kcal.† The direction of this difference is not that to be expected from increased crystallinity, as has been shown by Barrer.<sup>15</sup> Little attention has been paid to the clarification of this type of physical chemical consequence in the formulation of lipid membrane permeation models.

In view of the imperfect theoretical status of lipid barrier models, and of the possibilities of multiple barriers, as well as a diffusional specificity mechanism, EM evidence does not constitute conclusive support for a lipid solubility mechanism. The hypothesis that EM-demonstrable membranes are transport barriers, though reasonable, has not been proved. But even if one accepts this hypothesis, the possibility exists that the membranes may impose specificity by a diffusional mechanism, based perhaps on an ordered protein phase. From this point of view, emphasis on the lipid component of membranes seem disproportionate. For example, Robertson<sup>16</sup> has demonstrated the intimate involvement of the surface membrane of the Schwann cell in the synthesis of the myelin sheath, while Fernández-Morán and Finean<sup>17</sup> showed that extraction of myelin with acetone leads to marked dimensional changes. The generalization of these findings to a universal model of the cell membrane is partly based on classical transport theory. Were there no alternative to the latter, this generalization would be logical and simplifying, but the existence of new alternatives renders the line of reasoning circular. Furthermore, conflicting evidence relevant to membrane ultrastructure exists. Thus, recently it has been shown that solvents, including acetone, which extract cellular lipids, extract large quantities of protein as well.<sup>18</sup> On the other hand, Fleisher *et al.*<sup>19</sup> found that extraction of 80 per cent of the phospholipids and neutral fats from mitochondria, using acetone, left the staining and structural properties of the unit membranes essentially unaltered. Together, these findings seem to counsel caution in the pursuit of an early codification of ultrastructural and physiological models.

Finally, the erythrocyte provides a good example of the pitfalls of deducing the existence of a particular transport barrier from the presence

†A more correct comparison would require a knowledge of  $E_D$ , the activation energy for diffusion in this membrane, rather than  $E_p$ , the activation energy for permeation. These are related by

$$E_p = E_D + \Delta H_K$$

where  $\Delta H_K$  is the enthalpy of distribution of the solute between the membrane and water.  $\Delta H_K$  for the distribution of 1-butanol between various nonpolar and weakly polar liquids (i.e. 2-methylbutane, 1-hexanol and ethyl-n-butyrate) and water is positive (unpublished data). For a crystalline lipid phase  $\Delta H_K$  should be even more positive. The disparity between  $E_D$  in rubber and  $E_p$  in a lipid membrane is, therefore, even greater than that indicated.

of lipids and cellular membranes. Mammalian erythrocytes show a typical surface membrane structure, and Gorter and Grendel<sup>20</sup> concluded that the lipid content is just that required to form a continuous bimolecular surface layer (cf. Ponder<sup>21</sup>). Nevertheless, these cells do not show the specificity to be expected from a lipid transport barrier.<sup>22</sup>

### *The Distribution of Transport Barriers*

The form of the kinetics of flux into or out of the cell is determined by the distribution through the cell of transport barriers. In general, distinctive kinetics will result from each of the barrier distribution models listed above. The extreme models, those of a single surface barrier (I, above) and of the continuously distributed barrier (III) give readily specifiable kinetics.

Consider tracer efflux from a long cylindrical cell into a medium free of tracer. In the single surface barrier model, the thickness of the barrier is usually taken as 75-100Å; this is small in comparison to the total cell thickness, so that the kinetics, to the limit of resolution, are given by

$$\frac{\bar{C}(t)}{C_0} = e^{-\sigma t} \quad (1)$$

where  $C_0$  is the uniform initial concentration in the cell and  $\bar{C}(t)$  is the mean concentration at time  $t$ . The parameter  $\sigma$  is the surface rate constant; for a membrane of permeability  $P$ ,  $\sigma = 2P/r_0$ , where  $r_0$  is the radius of the cell.

In the case of the continuous barrier

$$\frac{\bar{C}(t)}{C_0} = \sum_{j=1}^{\infty} \frac{4}{\gamma_j^2} \exp\left(-D_i \gamma_j^2 t / r_0^2\right) \quad (2)$$

where  $D_i$  is the intracellular diffusion coefficient;  $\gamma_j$  the  $j$ th root of the Bessel function  $J_0(\gamma) = 0$ ; and  $r_0$ , the fiber radius.

The form of the kinetics given by a multimembrane model will depend upon: (a) the spatial distribution of the barrier. Barriers may act in parallel or in series as well as differing in the cellular volumes they enclose. (b) the degree of heterogeneity of the barriers. (c) solubility differences in the cellular volumes compartmentalized by the barriers. In general such models will lead to complex "multicompartment" kinetics, different from those given by Equations 1 and 2. A special case, that of pure series distribution of barriers will, if there is a sufficient number of barriers, closely approximate the kinetics for a continuous barrier, Equation 2. For a uniform spacing of identical barriers,  $D_i$  in Equation 2 is replaced by  $Pd$ , where  $d$  is the interbarrier spacing.

These differences bespeak the need for a careful examination of non-electrolyte flux kinetics to resolve the distribution of barriers. Unfor-



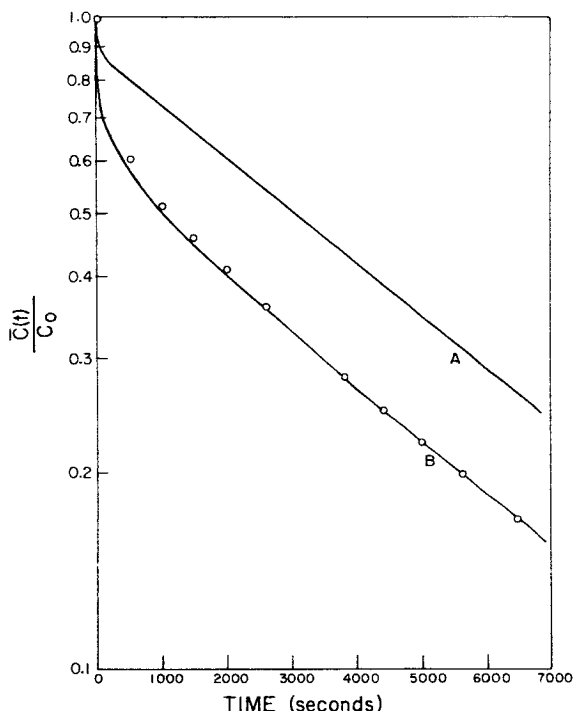


FIGURE 2. Efflux of urea- $C^{14}$  from the sartorius of *R. pipiens* at  $5.6^{\circ}\text{C}$ . Ordinate: mean fractional tissue concentration. Points are experimental. Curve A: theoretical efflux based on surface-limited cellular flux. Curve B: theoretical efflux based on bulk diffusion limited cellular flux. The derivation of the theoretical expressions and a description of the experimental technique are given in Reference 6.

tunately, few studies have been directed toward this object; in most cases it has been assumed that a single surface barrier model is correct.

A recent detailed analysis of the fluxes of a number of nonelectrolytes from frog skeletal muscle has shown this not to be the case. A typical result is shown in FIGURE 2 in which the efflux from *R. pipiens* sartorius of urea- $C^{14}$  is compared with theoretical curves based on Equations 1 and 2 but modified to correct for the influence of extracellular space and other relevant parameters. Details and a number of other examples are given in Reference 6.

The inadequacy of a single, surface barrier model is apparent. The results are consistent with a model in which the barrier is continuously distributed; or, as pointed out above, the kinetics could be produced by

a multimembrane barrier. The latter would be so, provided a suitable distribution existed: either a number of barriers in series, or, if parallel barriers are involved, of such geometry as, by coincidence, to give the appropriate set of first order curves. Present knowledge of the ultrastructure of frog skeletal muscle provides some support for the series barrier alternative. The longitudinally oriented myofibrils are encircled by sheaths of the sarcoplasmic reticulum; this part of the reticulum does not appear to be continuous with the extracellular space.<sup>23</sup> If a solute molecule diffusing radially from within the muscle fiber to the extracellular space had to pass successively through these sheaths, and if the sheaths represented a transport barrier, one would expect kinetics of the form of Equation 2 modified for series membranes. However, examination of the detailed structure of the sheaths does not strengthen this possibility; it indicates that the sheaths are not continuous as is required by the multibarrier model but lacunar, so that extensive free paths exist between the myofibrils.<sup>24,25</sup>

Justification for considering a continuous barrier model derives, at the ultrastructure level, from the high degree of order in the myofibrils.<sup>9,10</sup> X-ray diffraction<sup>26</sup> and nuclear magnetic resonance<sup>27</sup> suggest that order extends to the molecular level as well. This is supported by corollary studies in other cells and macromolecular systems,<sup>6,28-30</sup> some of which are reported at the present symposium. These studies indicate that layers of water molecules in apposition to protein and other macromolecules have reduced freedom of motion, relative to that in bulk liquid water. An investigation, described below, of the diffusional properties to be expected of such layers, suggests that they can account for the features of cellular nonelectrolyte transport.

The reticulum contains protein and water, just as do the myofibrils. If a diffusional mechanism determines cellular transport the distinction between mechanisms operating in the reticulum and the myofibril can be expected to be small — primarily of degree rather than of kind. The model of the diffusional mechanism will be given in terms of a continuous barrier; i.e., with the approximation that the sarcoplasm is homogeneous in respect to nonelectrolyte transport. However, it should be kept in mind that with little modification the treatment is applicable to discrete diffusional barriers as well.

#### *Diffusion in an Ordered Protein-Water Phase*

The underlying premise of this model is that protein molecules having a suitable periodicity of functional groupings can stabilize a lattice of tetrahedrally H-bonded water molecules. As mentioned above, the idea that water in the vicinity of proteins has modified properties is not new, and is well documented. The influence of this modified water on transport, in any given system, will depend on its distribution relative to the average molec-

ular diffusion path. For example, in ovalbumin solutions in which hydration is not extensive, the major diffusional path is through unmodified bulk water, and diffusional coefficients differ little from those in pure water.<sup>31</sup> The applicability to the cell of the model to be described is therefore contingent on the assumption that the distribution of modified water is such as to determine the overall transport behavior of the system. Evidence that this assumption is reasonable has been reviewed elsewhere.<sup>6</sup>

*Pure water systems.* The properties of diffusion in the protein-water system is dependent upon the modified dynamics of the water molecules. To elucidate these dynamics we shall first consider pure water systems. Consider a perfect tetrahedrally H-bonded water lattice as shown schematically in FIGURE 3a. The water molecules execute a variety of motions

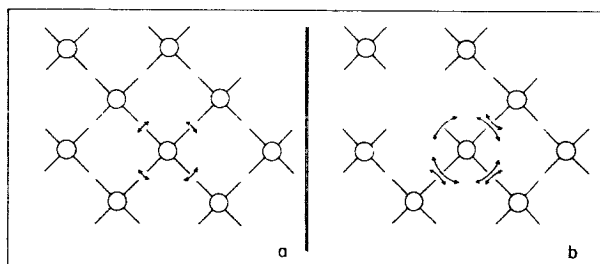


FIGURE 3. A schematic tetrahedrally H-bonded water lattice. a: showing a water molecule oscillating about H-bonding directions in the undisturbed lattice. b: showing the increased amplitude of oscillation of a water molecule in the presence of a lattice vacancy. The increased amplitude is propagated to neighbors but diminishes with distance from the vacancy.

involving, among other things, the bending and stretching of H-bonds. Three factors determine the amplitude and frequency of these intermolecular oscillations: temperature; the inertia of the water molecules — their mass and moment, both of which are small; and the potential energy functions for the oscillations. Restricting attention to the bending of H-bonds (torsional oscillations), the potential energy function is determined by the variation of H-bond energy with the orientation of bonded molecules. This energy falls off rapidly with deviation from a linear nuclear array of the O-H...O group. Because of the small inertia of the water molecule, and the high geometrical specificity of the H-bond, the motion of any water molecule is strongly dependent upon the orientation of H-bonding directions of its neighbors. These, in turn, are dependent upon the first molecule and others around them. In other words the motions of water molecules are cooperatively linked.

The consequences of this become clear when one considers a lattice defect, such as a Bjerrum rotational defect or a vacancy — any with a missing H-bond. A water molecule at the defect no longer sees a spatially specific, fairly deep potential well in the direction of the defect. The potential for torsional oscillation about this direction will be shallow and nondirectional, and the molecule will therefore execute oscillations of greater amplitude. Since the orientations of the other H-bonding directions of the water molecule are relatively rigidly fixed with respect to the defect direction, they also oscillate with greater amplitude. The H-bond directions are, therefore, “smeared out”. This is schematized in FIGURE 3*b*. Because of this, the potential wells seen by neighboring molecules are also shallower and less directional,\* so that these too oscillate with greater amplitude. The effect

\*This effect may be reinforced by differences in the hybridization of the water molecule in the 4-bonded and non-4-bonded states.<sup>32</sup> is transmitted to successive neighbors with damping as distance from the defect increases.

The overall effect of the defect on the lattice is, therefore, a zone of partial lattice disorder. In ice, the concentration of the defects is low; for Bjerrum defects, on the order of  $10^{11}/\text{cm}^3$ , at  $-10^\circ\text{C}$ .<sup>33</sup> As the number of defects in the system increases with rising temperature, the zones of disorder overlap. In the overlap regions, the additional energy required to break H-bonds will be small. We may, for example, consider the melting of ice as occurring when a critical degree of overlap of partially disordered zones is achieved, permitting the formation of large numbers of defects with little expenditure of energy.

In a water lattice the structure of defects can be complex but may be classified by considering their unit components. Excluding ionic defects, three types are recognized: lattice vacancies, interstitial molecules, and orientational defects. Each of these involves one or more unfilled H-bonding sites and/or distorts the lattice, and for reasons similar to those given above, will be associated with a zone of disorder. Diffusion can be mediated by both vacancies and interstitials even if they occur singly. On the other hand, single orientational defects, such as Bjerrum rotational defects, are not conventionally taken as permitting molecular diffusion. However, when the concentration of orientational defects is high, and defect groups are common, as in liquid water, place exchange of defectively oriented molecules — which in the limit tend toward free rotation — is to be expected, particularly in a loosely packed lattice.

Assuming a defect model of diffusion, we may make a rough estimate of the mole fraction of defects permitting the diffusion of water from the self diffusion coefficients in ice and water. These are respectively  $10^{-10}$  and  $10^{-5}$   $\text{cm}^2/\text{sec}$ . near the melting point. From the equation<sup>34</sup>

$$D_1 = ga^2 N_{11} e^{-\Delta G_1^\ddagger/RT} \quad (3)$$

where  $a$  is the jump distance,  $N_1$  is the fraction of defects assuming diffusion can occur at every defect,  $\nu$  is the intermolecular vibrational frequency,  $\Delta G^\ddagger$  is the free energy of activation of diffusion of the defect, and  $g$  is a factor near unity which includes geometrical and correlation effects. Taking, as usual,  $\nu = 10^{12} - 10^{13} \text{ sec}^{-1}$ ,  $a \approx 2.8 \times 10^{-8} \text{ cm}$  (roughly the intermolecular spacing in a water lattice),  $g = 1$ , we get  $N_1 e^{-\Delta G^\ddagger/RT}$  equal to about  $10^{-8}$  in ice and  $10^{-3}$  in water.\* Because of the disordered region around a defect the enthalpy  $\Delta H^\ddagger$ , and free energy,  $\Delta G^\ddagger$ , of activation will be smaller than the corresponding quantities for defect formation. This is supported for the diffusion of rotational defects in ice by the calculations of Jaccard.<sup>35</sup> In liquid water, the sum of the enthalpies is only 4.4–4.6 kcal.,<sup>36</sup> which suggests that  $\Delta H^\ddagger$ , and therefore  $\Delta G^\ddagger$ , is very small (cf.) Zener).<sup>37</sup> The difference of  $N_1 e^{-\Delta G^\ddagger/RT}$  between the two systems, then, probably represents largely a difference of  $N_1$ .

*Protein-water systems.* Let us introduce into the aqueous system protein with the characteristic of having H-bonding sites of a periodicity equal to some small multiple of a characteristic distance between H-bonding positions of a tetrahedral water structure. These H-bonding sites are not subject to the increased oscillational amplitude seen in the case of water molecules when a defect is nearby. This is because the sites are covalently linked to a molecule of immense inertia. The fixed H-bond directions therefore stabilize water molecules against cooperative disordering; the disordered zone, per single defect, is smaller than in a pure water lattice.

We may make a rough estimate of the mole fraction of defects present in the protein-water system of the muscle cell, using the self diffusion coefficient determined for water (see below) of  $10^{-7}$  to  $10^{-8} \text{ cm}^2/\text{sec.}$ ,<sup>†</sup> and Equation 3. This gives a value of  $N_1 e^{-\Delta G^\ddagger/RT}$  of  $10^{-5}$  to  $10^{-6}$ . The protein-water phase, therefore, has some  $10^2$  times as many defects as does ice. Because of this, the overall disorder in the protein-water phase is greater than in ice even though the disorder per defect is smaller. The energy of new defect formation, therefore, will be smaller than in ice, but larger than in liquid water; theory does not yet permit an estimation of the energy.

The diffusion of solutes in the protein-water lattice will be strongly influenced by both the size and chemical nature of the solute. The open nature of the tetrahedral water structure and the resultant possibility of interstitial occupancy, such as occurs in the melting of ice, makes it reasonable to assume that a solute of sufficiently small size can exist in the phase as an interstitial. Such a solute will diffuse relatively rapidly.

\*The physical significance of the factors in Equation 3 when applied to liquid water is subject to the validity of a lattice model. As in the case of other liquids, this validity is inherently limited.

†Cf. the values calculated by Dick.<sup>38</sup>

Let us assume that the diffusion of molecules of the size of water and larger, which must overlap one or more lattice sites, occurs by a vacancy mechanism. The rate will be determined by two factors: the probability of finding one or more vacancies (depending upon the size of the diffusing molecule) next to the molecule; and the activation energy for the subsequent place change. Both of these will be importantly influenced by the chemical nature of the solute. For self-diffusion Equation 3 holds; for solute diffusion we may write

$$D_2 = g a^2 v N_2 e^{\frac{-\Delta G}{RT}} \quad (4)$$

which differs from Equation 3 in that the concentration of vacancies,  $N_2$  and the activation energy,  $\Delta G^\ddagger$ , for the jump are those appropriate to the specific diffusing solute.

*Size specificity.* Let us focus attention on size alone by assuming that  $N_2$  and  $\Delta G^\ddagger$  depend only upon the number of lattice sites occupied by the solute. In an idealized rigid lattice, we will have approximately

$$N_2 = N_1^n \quad (5)$$

and

$$\Delta G_2^\ddagger = n \Delta G_1^\ddagger \quad (6)$$

where  $n$  is the number of lattice sites occupied, taken equal to the number of lattice sites required for diffusion. The potential size specificity from this model is enormous; for example, the values of  $N_1 e^{-\Delta G^\ddagger/RT}$  for ice and the protein-water systems give, for a solute occupying two lattice sites,  $D_2/D_1$  equal to  $10^{-8}$  and  $10^{-5}$  respectively. In a real lattice these numbers would be reduced for several reasons. Because of disordering of the lattice around the defect, diffusion may be possible in the presence of less imperfection than in the examples given above. For example, the combination of a vacancy or an orientation defect may produce sufficient disorder to permit a place exchange with relatively small additional energy beyond that required for single vacancy diffusion. Secondly, when the defect concentration is high, the assumption that  $N_2 = N_1^n$  fails. In liquid water, a high-defect aqueous system, the defects permitting self-diffusion were calculated to be  $10^{-3}$  of the total water molecules; this implies an even larger number of partial defects. The overlap of disordered regions around these defects, and the high collision frequency of the various defects, greatly reduce the size specificity; experimentally this is, roughly,

$$D_2 \approx \frac{D_1}{n} \quad (7)$$

representing a size specificity on the order of that in gases.

Among real solutes, which only rarely exactly fit the water lattice, another effect of size is important. This is distortion of the lattice by collapse

when the solute molecule is too small, and compression when it is too large, to fit an integral number of lattice sites. The effect of either is to increase the diffusion coefficient.

*Chemical specificity.* The chemical nature of the solute will have a profound effect on diffusion in the protein-water system, through changes in both  $N_2$  and  $\Delta G^\ddagger$ . The reason for this can be clarified by considering the effect of the introduction of a non-H-bonding solute into the lattice. Each of the unfilled H-bonds adjacent to the solute represents a lattice defect similar to those around the vacancy in FIGURE 3b. The resulting effect on the lattice will be different in the protein-water system than in liquid water. In the liquid the absence of lattice order much beyond the nearest neighbor permits water molecules to reorientate in such a way as to eliminate these defects, while still forming H-bonds with surrounding molecules, which are free to accommodate themselves to the orientation of the "cage" molecules. On the other hand, in a lattice having long range order such reorientation is only possible if there is a good matching of the reorientated water molecules with the basic lattice structure. This is unlikely in a preordered system; as a result, the defects are permanently associated ("bound") with the solute.\*

The presence of bound defects, together with the resultant disorder, reduces the need for additional defects to permit diffusion, as well as reducing the magnitude of  $\Delta G^\ddagger$ . Diffusion of the solute is therefore rapid, with a small activation energy. The larger the non-H-bonding solute, the greater the defect zone; on the other hand, the greater also is the defect requirement for diffusion and the inertia of the molecule. The opposing influences will, as a result, make for small differences in  $D_2$  among members of an homologous series differing in alkyl chain length.

We have now considered the limiting solute types: those whose size and H-bond interactions permit a perfect fit to the water lattice (probably no real solute approaches this limit) and those having no H-bonds (e.g. the alkanes and noble gases), whose effect on the lattice is disruptive. The vast majority of real solutes fall between these limits. For any given size, they vary in number, strength and geometrical arrangement of H-bonding groups.

While the principles outlined for the limiting cases can be expected to apply generally, the need for knowledge of the detailed structure of the protein-water lattice becomes important when dealing with real H-bonding solutes. One can count the number of potential H-bonding sites on the

\*The potential function for the water molecules neighboring the solute, besides being shallow because of broken H-bonds, may show two minima, one corresponding to the configuration in FIGURE 3b, the second corresponding to a reoriented "cage" configuration, with other H-bonds broken.

solute, and estimate their strength independently, but the steric fit of the solute to the water lattice will depend on the orientation of H-bonding groups in the lattice. A number of crystallographic forms of solid water lattices are possible; for some of these, at least, evidence of tetrahedral H-bonding has been obtained.<sup>39-40</sup> In the protein-water lattice, as in other systems in which water is ordered by a second component, the orientation of water molecules can be expected to depend upon the spacing and configuration of ordering groups. A start towards elucidating these relationship has been made.<sup>41,42</sup> In the absence of detailed information, the following points can be offered as probable. Among solutes of equal size, the one having H-bonding sites of greatest number and strength will form the most H-bonds to the lattice, have as a result the smallest  $N_2$  and largest  $\Delta G_2^\ddagger$ , and therefore diffuse slowest. The presence on a solute of an H-bonding site which is misaligned with lattice sites will be disruptive, the extent of lattice disorder increasing with the number and angular separation of minima in the potential function.

The quantitative predictions which may be made from the model are as yet limited. Using data on water diffusion in the frog extensor as a base line,  $D_1 \sim 10^{-7}$  to  $10^{-8}$  cm<sup>2</sup>/sec, and an activation energy  $E_1 \sim 7$  kcal.,\* we would expect the following:

(1) For solutes which are non-H-bonding, and for solutes which can form an H-bond but have large nonpolar groups,

$$\begin{aligned} D_2 &\sim D_1, \\ E_2 &\sim E_1 \end{aligned} \quad (8)$$

a small size dependence of  $D_2$  and  $E_2$ , either direction being possible.

(2) With increasing number of H-bonding groups relative to nonpolar groups, a sharply decreasing  $D_2$  and increasing  $E_2$ , approaching, in the limit,

$$\frac{D_2}{D_1} \sim (10^{-5})^{n-1} \quad (9)$$

and

$$E_2 \sim nE_1$$

where  $n$  is a size parameter (see above).

(3) The presence of a nonpolar solute in the protein-water phase should increase the diffusion coefficient of an H-bonding solute, in proportion to the collision probability of the latter with the disordered zone around the nonpolar:

$$\frac{D_2'}{D_2} = 1 + kC_n \quad (10)$$

\*These values are for the efflux of tritiated water from the extensor of *R. pipiens*. The techniques have been published previously.<sup>6</sup> The large uncertainty in the values is due to the low precision of the method when  $D$  is large.



where  $D'_2$  and  $D_2$  are, respectively, in the presence and absence of the nonpolar;  $C_n$  is the concentration of nonpolar; and  $k$  is larger, the larger the nonpolar. Potentially, the size of the disordered region is estimable from  $k$ .

*Comparison with experimental data.* In FIGURES 4-6 diffusion coefficients in three different biological systems, calculated assuming uniform resistance throughout the cell are presented for a variety of solutes as a function

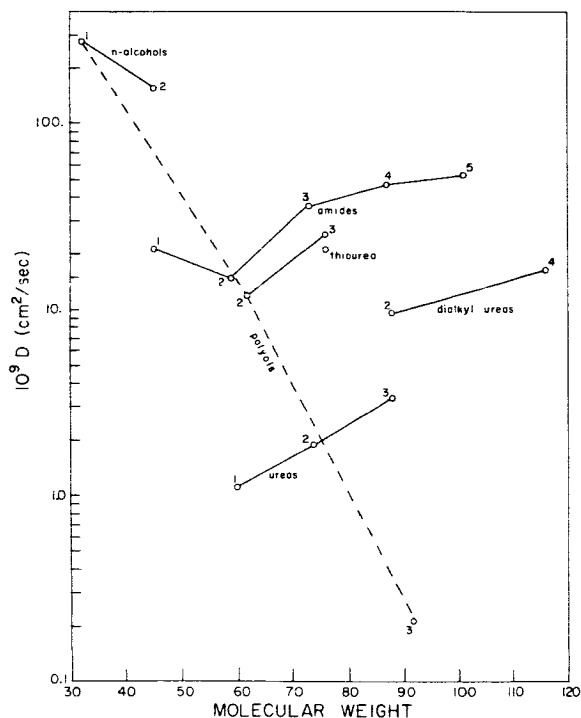


FIGURE 4. Intracellular diffusion coefficients at 18-23°C. in the terminal leaves of *Chara*, as a function of molecular weight. Solid lines connect members of homologous series; dotted lines, the polyhydroxyl alcohols. The diffusion coefficient was calculated from

$$D = \frac{Pd}{3600}$$

in which  $P$  is the permeability coefficient<sup>2</sup> and  $d$  is the width of the limiting barrier,<sup>43</sup> here taken as the protoplasmic tube lying between the cell wall and the central vacuole. In fixed preparations it measures 4 to 6  $\mu$ ; allowing for shrinkage we have taken  $d$  as 10  $\mu$ . An inner layer of cytoplasm is in cyclosis; this may affect the transport but no data are available to permit assessment of the effect. Additional, but probably small, effects on the calculated  $D$  are attributable to imperfect stirring in the vacuole and to the 5  $\mu$  cell wall; the effect of extra-cellular space on this single cell preparation is probably negligible.

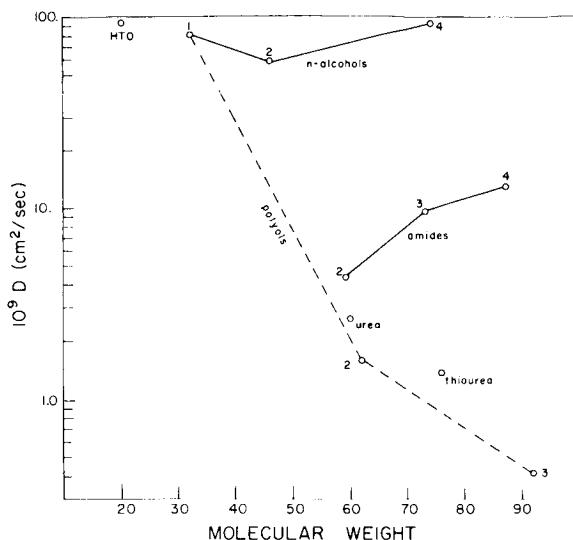


FIGURE 5. Intracellular diffusion coefficients at  $25 \pm 2^\circ\text{C}$ . in the mucosal epithelium of the toad bladder, as a function of molecular weight. Solid lines connect members of homologous series; dotted lines, the polyhydroxyl alcohols. The average thickness of the bladder is about  $50 \mu$ , of which about  $10 \mu$  is mucosal epithelium, an essentially continuous cellular phase.<sup>11,15</sup> The latter was taken as the diffusional barrier, and values of  $D$  were calculated from the permeability coefficients,<sup>5</sup>  $K_{trans}$ , in the absence of vasopressin, and the  $10 \mu$  thickness,  $d$ , by the equation  $D = K_{trans} d$ . The  $40 \mu$  serosa is heterogeneous and contains large extracellular channels. Its influence on trans-bladder fluxes is probably that of an unstirred water layer having a small but significant effect on the calculated  $D$ .

of molecular weight. Points for members of homologous series are connected by solid lines, while a dashed line connects the points for polyhydroxyl alcohols.

The overall specificity among the solutes is large; primarily it reflects the polar group of the solute. In qualitative agreement with the model, at any molecular weight the greater the number and strength of H-bonds that a solute can form the slower is its diffusion. There is virtually no overlap between the various homologous groups; the addition of alkyl groups to an H-bonding radical has a relatively small effect, in most cases to increase  $D_2$ . Furthermore, in agreement with Equation 8,  $D_2$  for the alcohols (the least polar solutes studied) is essentially independent of size and approaches that of water.

The limited data available on activation energies (TABLE 1) support the present model. A sharp increase in  $E_2$  is associated with increasing number of H-bonds among solutes of comparable size, as is expected.

The only series that increases in size while maintaining relatively unchanged composition in respect to the ratio of H-bonding and nonpolar groups is the polyhydroxyl alcohols. The size specificity is very high; a three-fold increase in molecular weight from methanol to glycerol gives

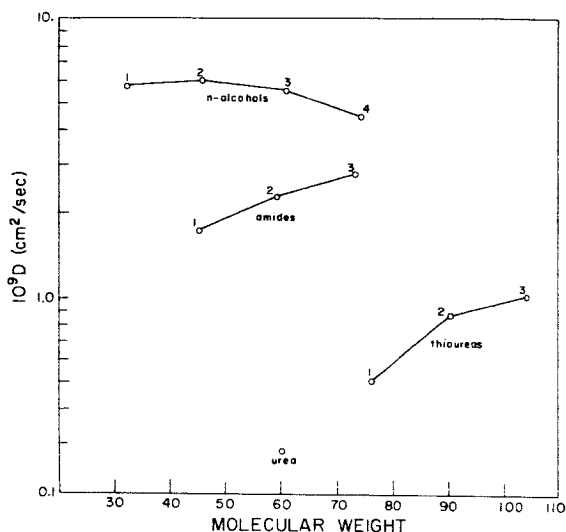


FIGURE 6. Intracellular diffusion coefficients at 5°C. in the sartorius of *R. pipiens*, as a function of molecular weight. Solid lines connect members of homologous series.  $D$  was calculated from the limiting behavior of Equation 2 at large  $t$ ;  $r_0$  was measured to be 34.9  $\mu$ . Of the three preparations described in FIGURES 4-6, the sartorius has the largest noncellular diffusional path; comparison of the sartorius data with that in the much smaller extensor longus digiti IV<sup>6</sup> shows that the values of  $D$  here presented are satisfactory for slowly diffusing solutes, whereas for rapidly diffusing solutes the extracellular diffusion strongly affects the calculated  $D$ .

a 100- to 1000-fold decrease in  $D_2$  (see FIGURES 4 and 5). This does not, however, approach the limit of size specificity given by Equation 9, suggesting both that these solutes, though strongly H-bonding, do not approximate a perfect fit to the lattice, and/or that the lattice itself is far from perfect.

In several instances, the smallest member of a homologous series diffuses more rapidly than the next member, while for subsequent members  $D_2$  increases. The existence of a minimum suggests the possibility of partial interstitial occupancy, and therefore rapid diffusion, of the smallest solutes.

The order of the diffusion coefficients of urea and thiourea varies in the different systems of FIGURE 4-6. Variation of this sort represents a level

TABLE 1  
EXPERIMENTALLY DETERMINED ENERGIES OF ACTIVATION,  $E_2$ , FOR THE  
TRANSPORT OF THREE NONELECTROLYTES OF COMPARABLE MOLECULAR  
WEIGHT IN THE EXTENSOR LONGUS DIGITI VI OF *R. pipiens*.<sup>6</sup>

	$E_2$ (kcal./mole)
1-butanol	6.4
propionamide	8.6
thiourea	15.6

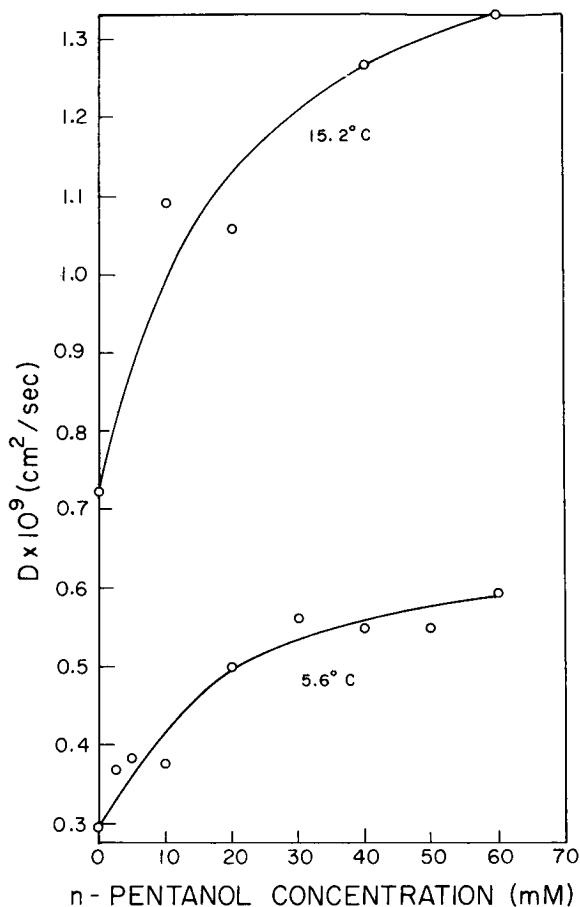


FIGURE 7. Intracellular diffusion coefficient of urea in the frog sartorius, at two temperatures, as a function of intracellular concentration of 1-pentanol.

of detail in respect to specific interactions which is beyond the limits of extension desirable for the present approximation.

Experimental verification of the prediction that the presence of a weakly H-bonding solute will increase the rate of diffusion of a strongly H-bonding solute is presented in FIGURE 7. In FIGURE 7, the diffusion coefficient of urea in muscle is presented as a function of 1-pentanol concentration at two temperatures. Rather than the simple linear relation predicted in Equation 10, a saturation curve is seen, indicating failure of the assumption of independence of disordered zones around nonpolar solutes implicit in Equation 10. It is of interest that the muscle goes into rigor at about the 1-pentanol level (70–100mM) producing saturation of the diffusion-enhancing effect. Following the onset of rigor, the flux rate of urea is smaller than that in the normal state.<sup>16</sup> The enhancement of urea diffusion

by three homologous alcohols was studied, using a constant concentration of 60mM. The ratios  $D_2'/D_2$  of urea diffusion in the presence and absence of alcohols were 1.45, 1.64, and 2.00 for 1-propanol, 1-butanol, and 1-pentanol, respectively, at 5.6°C. The increasing effect with alkyl radical size is in accord with the expectation of increasing lattice disordering. Concentrations of urea and glycerol up to 150mM exert no effect on the diffusion of urea.

An enhancement of the transport rates of urea and other amide-containing solutes, as well as water and small alcohols, by vasopressin has been studied by Leaf and associates.<sup>5,47</sup> One would not expect the mode of action of the polypeptide vasopressin to be the same as that of a largely nonpolar material such as 1-pentanol. In terms of the present model, a suggestion can be offered whereby the observed effect on nonelectrolyte transport will, nevertheless, be the same. As pointed out above, the extent and stability of the water lattice is dependent on matching to the detailed configuration of H-bonding sites of the stabilizing protein. Changes in configuration, resulting from vasopressin-protein interaction, may lead to increased disorder of the water lattice, enhancing diffusion. The incompleteness of this simple picture is made clear by the specificity of the effect of vasopressin: no effect is seen with solutes such as glycerol and thiourea. No model has been offered to explain this specificity. Extension of the present model in the direction of examining the detailed interaction of solutes with the water lattice and protein may shed light on this question.

#### *Cellular Narcosis by Non-polar Solutes*

The disordering effect of nonpolar radicals on the protein-water lattice provides a simple mechanism of cellular narcosis. Cellular narcosis may be defined as the reversible inhibition of cellular function (eg. contraction, luminescence, neural transmission) by any of a wide variety of non-polar and weakly polar solutes. The pertinent interaction is generally taken to be physical rather than chemical. The larger noble gases, such as xenon, and the alkanes (eg. butane), which have virtually no ability to interact chemically under the conditions prevailing in cells, are narcotics; within a series of narcotics, such as the alcohols, potency increases with length of the alkyl chain.<sup>48-52</sup>

Many investigators have suggested that water structure is important in cellular processes.<sup>28,29,53-56</sup> One would then expect disordering of the water lattice by nonpolar radicals, as outlined above, to impair the operation of these processes. The characteristics of this disordering are appropriate to a model of narcosis. It is physical in nature and dependent on the size of the nonpolar radical, but otherwise relatively nonspecific in respect to the chemical structure of the solute. At low solute concentrations, the disordering effect is reversible; as the concentration is increased,

cooperative lattice disordering ("melting") can occur. Similarly, increasing narcotic concentration leads experimentally to irreversible changes.

A number of other theories of narcosis exist. Some have attributed primary importance to a lipid-pore membrane;<sup>4,50</sup> others have focussed on the possibility of these agents inhibiting and denaturing enzymes.<sup>57-59</sup> Recently, two versions of a hypothesis which draws attention to modification of cellular water have appeared.<sup>51,52</sup> This hypothesis attributes narcosis to the formation, in the presence of nonpolar solutes, of intracellular hydrate microcrystals or icebergs, stabilized by cellular proteins. A detailed examination of the various models of narcosis is inappropriate to this paper. However, because the hydrate microcrystal hypothesis and the present "disordering" hypothesis both draw attention to changes in cellular water, a brief comparison is in order.

The basic assumption of the two theories are contradictory. The hydrate microcrystal hypothesis postulates that the intracellular protein-water system is able to stabilize specific water structures associated with nonpolar solutes. The disordering hypothesis postulates, as described above, that the preexisting protein-water lattice is incompatible with the types of water structure which would be required to reduce the number of unfilled H-bonds around the nonpolar solute. Certain testable predictions of these two theories differ.

(1) The presence of microcrystals would tend to slow the transport rate of solutes.<sup>52</sup> In the disordering theory, the rate will be increased by narcotic solutes. The results reported above, for the effect of alcohols, which are cellular narcotics, on urea diffusion support the disordering theory. Similar enhancement of urea transport occurs with other narcotics: chloroform, ethyl ether, and urethane.

(2) Microcrystal formation will be decreased by increasing temperature;<sup>52</sup> on the other hand, lattice disorder will be increased by increasing temperature. Consequently, the theories predict antagonism and synergism, respectively, of narcosis and increased temperature.

A recent paper<sup>60</sup> has purported to show the antagonism of narcosis and temperature. The conclusion drawn, however, is not justified, since no quantitation of the effect of temperature alone was possible in the experimental design, despite clear evidence of a pronounced effect of temperature alone in a direction which could account for the results observed.

The results of a study, in our laboratory, of the effect of temperature and narcotic concentration on the rheobase for electrical stimulation of the frog sartorius is presented in FIGURE 8. The minimum voltage (duration

0.1 sec.) causing contraction, at two temperatures, is plotted against concentration of the narcotic, 1-pentanol, in the muscle water. At any concentration, the narcotic effect is greater at the higher temperature. At low concentration, the temperature coefficient suggests a process having

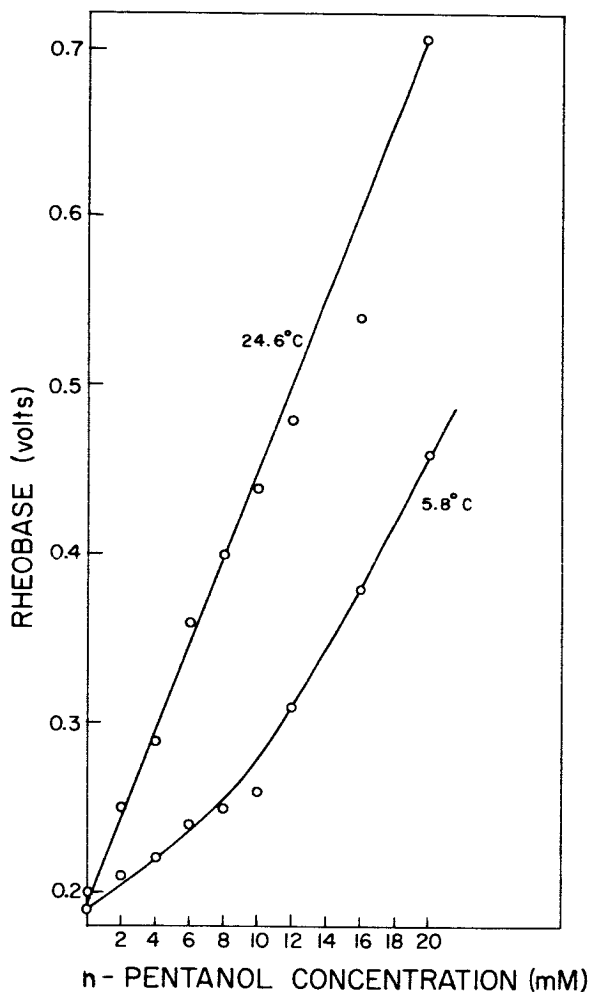


FIGURE 8. Rheobase of *R. pipiens sartorius*, measured as the minimum voltage of 0.1 sec. duration causing contraction, as a function of intracellular concentration of 1-pentanol, at two temperatures. Stimulation was applied with a Grass S4C stimulator and platinum electrodes. Contraction was observed visually.

a  $\Delta H \approx +10$  kcal. These results are consistent with the disordering hypothesis.

In the hydrate microcrystal hypothesis the temperature coefficient of the narcotic effect,<sup>32</sup> at constant partial pressure, is given by the enthalpy of formation,  $\Delta H_1$ , of the hydrate from gaseous agent and pure solvent (i.e., cellular water).  $\Delta H_1$  includes two terms, both negative: that for the

formation of crystalline cages from cellular water, and that for condensation of the vapor in the cage. Using Henry's law, one may express the narcotic effect in terms of the concentration of agent in solution; the temperature coefficient at constant concentration is then given by  $\Delta H_1 - \Delta H_2$ , where  $\Delta H_2$  is the enthalpy of solution of the vapor in the solvent. The enthalpy  $\Delta H_2$  also includes two negative terms: that for condensation of the vapor and that for the formation of certain imperfect structures — the Frank and Evans "icebergs."<sup>61</sup> It is likely that  $\Delta H_1 - \Delta H_2$  will be negative, since it is determined primarily by the difference in enthalpy between the crystalline cage and the less perfectly H-bonded iceberg. In the system hydrate — pure water — gas,<sup>62</sup>  $\Delta H_1 - \Delta H_2$  is on the order of -12 to -20 kcal./mole of solute; the larger value is appropriate to a molecule of the size of 1-pentanol. Thus, the difference between the observed temperature coefficient of narcosis and that for the formation in pure water of a hypothetical 1-pentanol hydrate corresponds to a  $\Delta H$  of 30 kcal. Two factors could reduce this discrepancy: (1) Although unlikely,<sup>62</sup> it is possible that the entry of 1-pentanol into a hydrate cage in the cellular protein-water system requires breakage of its H-bonds to water molecules; the  $\Delta H$  for this is about 8 kcal. (2) The water adjacent to proteins or membranes may be "pre-stabilized" relative to the bulk solvent. To account for the data, the  $\Delta H$  of this stabilization would have to be  $-(30-8) = -22$  kcal., a value greater than the  $\Delta H$  of formation of the hypothetical hydrate in water. The "pre-stabilized" water would be more ice-like than the subsequent hydrate.

#### Summary

Recent advances in knowledge of diffusional specificity in H-bonding systems, of the ultrastructure of cells, and in the analysis of flux kinetics in cells have made appropriate a reexamination of classical explanations of cellular nonelectrolyte transport. A number of alternatives, distinguished by the distribution and nature (solubility or diffusional) of transport barriers are considered. It is shown that none of these is as yet supported by conclusive evidence; on the other hand, in frog muscle, there is strong evidence against one alternative, the single surface barrier.

A model of a diffusional barrier uniformly distributed throughout the cell is considered in detail. This model assumes that the protein and water of the cell form an ordered molecular lattice whose properties are describable in solid-state terms.

The influence of proteins on lattice defects, and thereby on diffusion, is considered. The interactions of solutes with an ordered protein-water lattice are examined, and a satisfactory, though primarily qualitative, agreement with experimental cellular transport data is demonstrated.



The model, furthermore, leads to an hypothesis of cellular narcosis, for which some support has been obtained.

### *Acknowledgments*

We thank B. Bednarek, L. Perin, and V. Wasylyszyn for technical assistance.

### *References*

1. OVERTON, E. 1902. *Pfluegers Arch. Ges. Physiol.* **92**: 115, 346.
2. COLLANDER, R. & H. BÄRLUND. 1933. *Acta Botan. Fennica.* **11**: 1.
3. DAVSON, H. & J. F. DANIELLI. 1943. *The Permeability of Natural Membranes.* Cambridge Univ. Press. Cambridge, England.
4. HÖBER, R. 1950. *Physical Chemistry of Cells and Tissues.* Blakiston Co. New York, N. Y.
5. LEAF, A. & R. M. HAYS. 1962. *J. Gen. Physiol.* **45**: 921.
6. FENICHEL, I. R. & S. B. HOROWITZ. 1963. *Acta Physiol. Scand.* **60** (Suppl. 221): 1.
7. PORTER, K. 1961. *In The Cell.* J. Brachet & A. E. Mirsky, Eds. **2**: 621. Academic Press, New York, N. Y.
8. VOELLER, B. R. 1964. *In The Cell.* J. Brachet & A. E. Mirsky, Eds. **6**: 245. Academic Press, New York, N. Y.
9. HUXLEY, H. E. 1960. *In The Cell.* J. Brachet & A. E. Mirsky, Eds. **4**: 365. Academic Press, New York, N. Y.
10. HODGE, A. J. 1959. *Rev. Mod. Phys.* **31**: 409.
11. HOROWITZ, S. B. & I. R. FENICHEL. 1964. *J. Phys. Chem.* **68**: 3378.
12. FENICHEL, I. R. & S. B. HOROWITZ. 1965. *This Annal.*
13. AITKEN, A. & R. M. BARRER. 1955. *Trans. Faraday Soc.* **51**: 116.
14. STEIN, W. D. 1962. *In Comprehensive Biochemistry.* M. Florkin & E. H. Stoltz, Eds. **2**: 283.
15. BARRER, R. M. 1939. *Trans. Faraday Soc.* **35**: 644.
16. ROBERTSON, J. D. 1960. *In Progr. Biophys. Biophys. Chem.* J. A. V. Butler & B. Katz, Eds. **10**: 344. Pergamon Press. New York, N. Y.
17. FERNÁNDEZ-MORÁN, H. & J. B. FINEAN. 1957. *J. Biophys. Biochem. Cytol.* **3**: 725.
18. MUNRO, H. N. & E. D. DOWNIE. 1964. *Arch. Biochem. Biophys.* **106**: 516.
19. FLEISCHER, S., G. BRIERLEY, H. KLOUWEN & D. B. SLAUTTERBACK. 1961. *J. Biol. Chem.* **237**: 3264.
20. GORTER, E. & F. GREDEL. 1925. *J. Exptl. Med.* **41**: 439.
21. PONDER, E. 1949. *Disc. Faraday Soc.* No. 6. 152.
22. HÖBER, R. & S. L. ORSKOV. 1933. *Pfluegers Arch. Ges. Physiol.* **231**: 599.
23. HUXLEY, H. E. 1964. *Nature.* **202**: 1067.
24. PORTER, K. R. & G. E. PALADE. 1957. *J. Biophys. Biochem. Cytol.* **3**: 269.
25. REGER, J. F. 1961. *J. Biophys. Biochem. Cytol.* **10**: 111.
26. SPIEGEL-ADOLF, M., G. C. HENNY & E. W. ASHKENAZ. 1944. *J. Gen. Physiol.* **28**: 151.
27. BRATTON, C. B., A. L. HOPKINS & J. W. WEINBERG. 1964. *Am. Phys. Soc. abstracts Spring meetings.* Washington, D. C.
28. PRIVALOV, P. L. 1958. *Biofizika.* **3**: 738.
29. KLOTZ, I. M. 1962. *In Horizons in Biochemistry.* M. Kasha & B. Pullman, Eds. : 523. Academic Press. New York, N. Y.
30. CERBÓN, J. 1964. *Biochim. Biophys. Acta.* **88**: 444.
31. WANG, J. H., C. B. ANFINSEN & F. M. POLESTRA. 1954. *J. Am. Chem. Soc.* **76**: 4763.
32. FRANK, H. S. & W. Y. WEN. 1957. *Disc. Faraday Soc.* **24**: 133.

33. GRÄNICH, H. 1963. *Phys. kondens. Materie.* 1: 1.
34. SHEWMON, P. G. 1963. *Diffusion in Solids.* McGraw-Hill Book Co., Inc. New York, N. Y.
35. JACCARD, C. 1959. *Helv. Phys. Acta.* 32: 89.
36. WANG, J. H., C. V. ROBINSON & I. S. EDELMAN. 1953. *J. Am. Chem. Soc.* 75: 466.
37. ZENER, C. 1952. *In Imperfections in Nearly Perfect Crystals.* W. Shockley, J. H. Hollomon, R. Maurer, F. Seitz, Eds.: 289. J. Wiley & Sons, Inc. New York, N. Y.
38. DICK, D. A. T. 1964. *J. Theoret. Biol.* 7: 504.
39. BERTIE, J. E. & E. WHALLEY. 1964. *J. Chem. Phys.* 40: 1646.
40. TAYLOR, M. J. & E. WHALLEY. 1964. *J. Chem. Phys.* 40: 1660.
41. BERENDSEN, H. J. C. & C. MICHÉLSEN. 1965. *This Annal.*
42. WARNER, D. T. 1965. *This Annal.*
43. COLLANDER, R. 1930. *Acta Botan. Fennica.* 6: 1.
44. LEAF, A., J. ANDERSON & L. B. PAGE. 1958. *J. Gen. Physiol.* 41: 657.
45. PEACHEY, L. D. & H. RASMUSSEN. 1961. *J. Biophys. Biochem. Cytol.* 10: 529.
46. FENICHEL, I. R. & S. B. HOROWITZ. 1965. *Science.* 148: 80.
47. MAFFLEY, R. H., R. M. HAYS, E. LAMBIN & A. LEAF. 1960. *J. Clin. Invest.* 39: 630.
48. FERGUSON, J. 1939. *Proc. Roy. Soc. London.* B127: 387.
49. BRINK, F. & J. M. POSTERNAK. 1948. *J. Cellular Comp. Physiol.* 32: 211.
50. MULLINS, I. J. 1954. *Chem. Rev.* 54: 289.
51. PAULING, L. 1961. *Science.* 134: 15.
52. MILLER, S. L. 1961. *Proc. Nat. Acad. Sci. U.S.* 47: 1515.
53. BAIRD, S. L., JR., G. KARREMAN, H. MUELLER & A. SZENT-GYÖRGYI. 1957. *Proc. Nat. Acad. Sci. U.S.* 43: 705.
54. SZENT-GYÖRGYI. 1957. *Bioenergetics.* Academic Press. New York, N. Y.
55. ELEY, D. D. 1962. *In Horizons in Biochemistry.* M. Kasha & B. Pullman, Eds.: 341. Academic Press. New York, N. Y.
56. LING, G. N. 1962. *A Physical Theory of the Living State: The Association-Induction Hypothesis.* Blaisdell Publishing Co. New York, N. Y.
57. JOHNSON, F. H., H. EYRING, R. STEBLAY, H. CHAPLIN, C. HUBER & G. GHERARDI. 1944. *J. Gen. Physiol.* 28: 463.
58. McELROY, W. D. 1947. *Quart. Rev. Biol.* 22: 25.
59. BUTLER, T. C. 1950. *Pharmacol. Rev.* 2: 121.
60. CHERKIN, A. & J. F. CATCHPOOL. 1964. *Science* 144: 1460.
61. FRANK, H. S. & M. W. EVANS. 1945. *J. Chem. Phys.* 13: 507.
62. VAN DER WAALS, J. H. & J. C. PLATTEEUW. 1959. *Advan. Chem. Phys.* 2: 1.

## THE HYDRATE MICROCRYSTAL THEORY OF ANESTHESIA

J. F. Catchpool

*Department of Pharmacology,  
University of California, San Francisco Medical Center,  
San Francisco, Calif.*

Linus Pauling in his paper entitled "A Molecular Theory of General Anesthesia,"<sup>1</sup> first published in the journal *Science* in July, 1961, remarked that this theory was forced on us by the facts about anesthesia. What are these facts?

The phenomenon of anesthesia can be regarded as a state of affairs existing when the application of a physical or chemical stimulus to a living organism produces a reversible depression of biochemical, motor and sensory activity, starting with the most subtle and delicate activity of the nerve cells in the highest centers and proceeding downwards, inhibiting and then arresting activity until the point is reached when the anesthetist decides that the depression of activity is deep enough to permit the surgeon to inflict the trauma contemplated without initiating reflex or voluntary activity, or causing the patient to feel pain or to record in his memory the sensations of pain. Thus the degree of depression of the nervous system at which the organism can be said to be in a state of anesthesia can be any point on a continuum from full reflex activity to a stage near death when practically no reflex activity remains. Of course many poisons and toxins will depress the central nervous system in a manner closely analogous to anesthesia, but anesthetic agents have the distinguishing property of causing a *reversible* depression.

Almost since the beginnings of modern chemistry, chemical substances that could miraculously suspend animation a few moments after administration have been discovered and reported. In 1799, Sir Humphrey Davy<sup>2</sup> reported that the inhalation of nitrous oxide would remove sensations of pain and suggested that the gas be administered for surgical operations. Michael Faraday<sup>3</sup> later wrote a paper on the depressant effects of ether. Both of these great scientists sought a rational explanation for these effects, concluding that the mechanism must be some sort of reversible asphyxiation of the vital centers. However, it was not until 50 years later that Morton,<sup>4</sup> a Boston dentist, launched the introduction of general anesthesia into surgical practice with his classic demonstration at the Massachusetts General Hospital.

Among the many theories of anesthesia which must be mentioned is the theory of reversible coagulation of the substance of nerve cells that was proposed by the great French physiologist Claude Bernard,<sup>5</sup> who gave a

whole series of lectures on the subject of anesthesia. Later came the proposals of Meyer and Overton<sup>6</sup> that the action of anesthetics must depend upon a suitable partition coefficient between the water and lipid materials of the brain; they "proved" their theory by the noticeable correlation of anesthetic potency with solubility in fats and oils. However, these correlations fail to explain the anesthetic action of substances like the inert gas xenon,<sup>7</sup> or the anesthetic action of the only slightly fat soluble magnesium ion, or the fact that many excellent lipid solvents like the detergents are devoid of anesthetic action. Moore and Roaf<sup>8</sup> later noticed that the solubility of anesthetic agents in solutions of proteins was much greater than their solubility in water, and suggested that the high protein and lipid solubility served to transport the anesthetics to the sites where they could leave the lipid to combine with the "protoplasm". For over 50 years these lipid theories were held to be near the truth, and in fact in many places they seem still to constitute the accepted explanation of the mechanism of anesthesia.

So much progress has been made towards the understanding of the molecular structure of biological material in the last 20 years that it must now be possible to make a new attack on this old puzzle of how these simple chemical agents produce these extraordinary physiological effects, although I feel that the answers will not be complete until many of the questions about the structure of water being asked at this conference are finally resolved.

There is an enormous number of chemical substances that fit the description I have just given you of an anesthetic agent, but only a few are used in clinical anesthesia. Others are used only as sedatives to quiet nervous activity, or as hypnotics to promote sleep, or as anticonvulsants to damp down reflex activity as in the treatment of epilepsy; others calm mental disorders, and some are used as tranquilizers or even, as in the case of alcohol, as euphoriants. Many more known anesthetics have undesirable side effects that prohibit their use, toxic effects sometimes appearing before anesthesia can be established. The chemical substances chosen for use in clinical anesthesia are used because they are able to depress vital activity to the desired level quickly and safely. In many cases, their degree of depression is limited because the concentrations obtainable in the body are restricted by such factors as a low aqueous solubility or a rather high vapor pressure. The most commonly used anesthetic agents have been chosen for their chemical inertness, thus effectively reducing the possibilities of toxic chemical reactions that might complicate anesthesia.

Examination of the physical properties of these anesthetic agents has thrown considerable light onto the possible mechanisms of anesthesia. The fact that many dissimilar anesthetic agents have strikingly similar physical properties and often produce equal levels of anesthesia at about equal ther-

modynamic activity, forces one to conclude that anesthesia is being produced in similar ways by dissimilar anesthetic agents.

The list of general anesthetics includes such gases as xenon, argon and even nitrogen, which can produce anesthesia under pressure (as anyone familiar with the dangers of scuba diving knows as "raptures of the deep") and it is impossible to believe that these gases produce anesthesia by taking part in ordinary chemical reactions. Butler<sup>9</sup> in 1950 wrote, "the action of these spherically symmetrical atoms without any permanent dipoles furnishes the most conclusive demonstration that anesthesia need not depend on the specific effects of any structural grouping."

The most surprising group of anesthetic agents are the noble gases such as xenon.<sup>10</sup> Xenon has no ability to form ordinary chemical compounds by covalent or ionic bonding; its only known chemical property, in biological systems, is its ability to form clathrate compounds with water. Xenon, like most of the general physical anesthetics, does not form the hydrogen bonds which are known to play an important part in many physiological processes.

Crystals of xenon hydrate have been shown by x-ray diffraction studies to have the same structure as the hydrates of other small molecules such as chlorine and methane.<sup>11</sup> In 1952, Pauling and Marsh<sup>12</sup> made a thorough study of chlorine hydrate and found it to consist of cages formed by 20 water molecules joined tetrahedrally by hydrogen bonds so as to form twelve sided polygons, each facet being pentagonal. These pentagonal dodecahedra

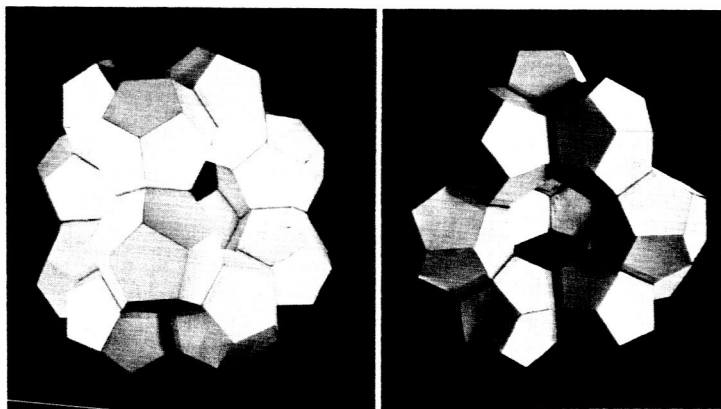


FIGURE 1. Two views of a paper model of the hexakaidecahedron cavity of the 17 Angstrom (Type II) hydrate structure. The cavity is formed by 12 dodecahedra, each contributing one pentagonal face to the cavity. The centers of each hexagonal face would lie at the corners of a regular tetrahedron. Each of the four hexagonal faces of a single hexakaidecahedron will be shared by other hexakaidecahedra.

fill space in such a way that there are slightly larger spaces left between the dodecahedra, each with 14 sides (12 pentagonal faces plus 2 hexagonal faces.) The chlorine molecules were found to be occupying these 14-sided tetrakaidecahedra. The smaller dodecahedra were probably occupied by single water molecules. The repeating cubic unit of structure of the chlorine hydrate has an edge of 11.8 Angstroms, and contains 46 water molecules, each surrounded tetrahedrally by four others with which it forms hydrogen bonds at a distance of 2.75 Angstroms. The hydrate of chloroform first reported by Sir Humphrey Davy<sup>2</sup> has since been found to possess a slightly different arrangement of dodecahedral clusters of water molecules. The cubic unit of structure of the chloroform (type II) hydrate is 17.3 Angstroms on an edge and contains 16 dodecahedra formed by 136 water molecules filling space in such a way that 8 larger cavities are formed, each with 16 sides, 4 of which are hexagonal, the other 12 being pentagonal faces shared with the dodecahedra. Ordinary ice consists of hexagonally arranged water molecules at a distance of 2.76 Angstroms from each other. The volume per water molecule of the 11.8 Angstrom hydrate structure is approximately 16 per cent greater than the volume per water molecule of ordinary ice. The 17 Angstrom chloroform-type hydrate has a volume per water molecule 18 per cent greater than ordinary ice. The stability of these hydrates is partly due to the Van der Waals interactions between the trapped anesthetic molecules and the water molecules forming the framework of their cages, but since the framework is somewhat more open in the hydrates than the framework of ordinary ice, the stabilizing effect of the Van der Waals forces is slightly less for the hydrates than for ordinary ice. The amount of stabilization of the hydrate due to the trapped anesthetic molecules' Van der Waals interactions can be calculated by applying the London equation for the interaction energy between two molecules. In the case of the eight caged xenon molecules in each cubic unit of hydrate I structure, two are trapped in pentagonal dodecahedral chambers with water molecules at a distance of 3.85 angstroms from each xenon atom, and the other six xenon atoms are trapped in tetrakaidecahedral chambers. The average Van der Waals attraction energy of a xenon atom to its neighboring water molecules was calculated by Pauling to be -9.1 kilocalories per mole, and adding the values for interactions with the more distant water molecules this figure becomes -10.3 kilocalories per mole.<sup>1</sup>

There is not much difference between the enthalpies of the empty hydrate frameworks and enthalpy of ordinary ice at 0°. Using the London equation, Pauling calculated these differences to be 0.16 kilocalories per mole for the structure I hydrate, and 0.20 kilocalories for the structure II hydrate. The enthalpy of hydrate formation at 0° of xenon-5<sup>34</sup> H<sub>2</sub>O from gaseous xenon and ice was determined experimentally by von Stackelberg<sup>13</sup> to be 8.4 kilocalories per mole, and the value calculated by Pauling was 9.4 kilocalories



similarly stabilized by filling more of the cavities. Pauling<sup>10</sup> describes how he formulated his theory of general anesthesia on the day that he read that G. A. Jeffrey of the University of Pittsburgh<sup>11</sup> had determined the structure of a crystalline hydrate of an alkylammonium salt which he found to have a clathratelike structure resembling xenon hydrate, decomposing at 25°. He then speculated that if all the small dodecahedral cavities were filled, the hydrate crystal would be stabilized at temperatures above 37°. These alkylammonium salts closely resemble the lysyl side chains of proteins. If hydrate crystals were to involve the protein side chains in the brain by incorporating molecules of anesthetic agent, the hydrates would also interfere with the motion of ions or the electrical charges of the side chains that normally contribute to the electrical oscillations in the brain. These electric oscillations are involved in consciousness and ephemeral memory, and interference or damping-down of the electrical activity might be enough to cause loss of consciousness. Alternatively, it is conceivable that the microcrystals might be masking the active sites of an enzyme molecule.

It is obvious that anesthesia is not simply the formation in the brain of hydrates of the chlorine and chloroform types. Enormous pressures would be necessary to stabilize these hydrates at 37°. For instance, methyl chloride is anesthetic for mammals at a partial pressure of 0.14 atmospheres and at a temperature of 37°, but the hydrate crystals decompose at 37° unless a pressure of 40 atmospheres is maintained. To stabilize the hydrates at 37° and at one atmosphere pressure, Pauling proposed that the side chains of the protein molecules and other solutes in the aqueous medium surrounding neuronal proteins act as stabilizers. If the mechanism of anesthesia involves hydrate formation or further structuring of the water solvent of the proteins and ions, then the anesthetic potency of an anesthetic agent should be proportional to the electric polarizabilities of the anesthetic molecules which determine their ability to stabilize the hydrate crystals, the polarizability being a measure of their effectiveness in stabilizing the hydrate crystals by Van der Waals intermolecular interactions. Pauling plotted the partial pressure of anesthetic agents in equilibrium with their hydrate crystals and water and ice at 0° against their mole refraction. The logarithm of the anesthetizing partial pressure for mice is plotted against the mole refraction of the anesthetizing agent shown on the right in FIGURE 2. The two curves are identical. FIGURE 3 shows the correlation between the partial pressure of some non-hydrogen bonding anesthetic agents necessary to maintain anesthesia and the dissociation pressure of the hydrates of these anesthetic agents at 0°. A short while after Pauling had published his paper, Professor Stanley Miller<sup>12</sup> of the University of California at San Diego published a paper proposing almost exactly the same mechanism for anesthesia, and he also calculated the ratio of anesthetic pressure to hydrate formation at 0°, showing a good correlation. Both Miller and Pauling sur-



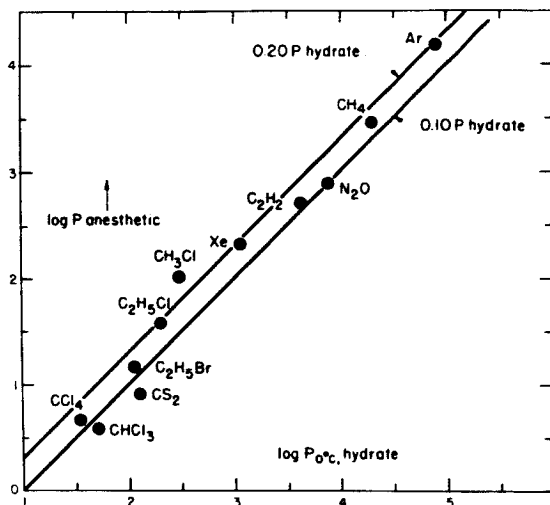


FIGURE 3. The logarithm of the anesthetizing partial pressure of nonhydrogen-bonding anesthetic agents plotted against the equilibrium partial pressure of their hydrate crystals. (From Pauling, *Science* **134**: 19.)

mised that hydrate formation, or "iceberg cover" as Miller preferred to call it, would have the same effect with and without gas molecules encaged in the structured water, and they both suggested that this might explain the anesthetic effects of hypothermia. The ability of the anesthetic agent to stabilize these hydrates would also be enhanced by any lowering of the temperature at which the anesthetics were acting. In order to test this hypothesis, my colleague A. Cherkin and I<sup>16</sup> conducted a series of experiments using goldfish as a test animal. The fish were acclimated at a temperature of 5, 10, 20, or 30° for three or four days and then anesthetized by placing batches of ten fish in a four-liter sealed vessel containing fully aerated tap water at the temperature at which the fish had been acclimated and adding a concentrated aqueous solution of anesthetic calculated to bring the final solution up to the desired concentration. The criterion of anesthesia was taken as the point when the fish were no longer able to escape a small electric shock. The anesthetized fish were counted every minute, starting half an hour after the addition of the anesthetic. The anesthetic dose for 50 per cent of the animals was obtained from the results of several experiments. By comparing the anesthetic potency of a number of anesthetics at different temperatures, we were able to show that reducing the body temperature raises the potency of these anesthetics (FIGURE 4). Our experiments showed that anesthesia occurred in 50 per cent of fish at 1.6° without any anesthetic. The potency of the anesthetic agents steadily decreased from 5 to 30°; extrapolation to 37° showed that our values agreed very

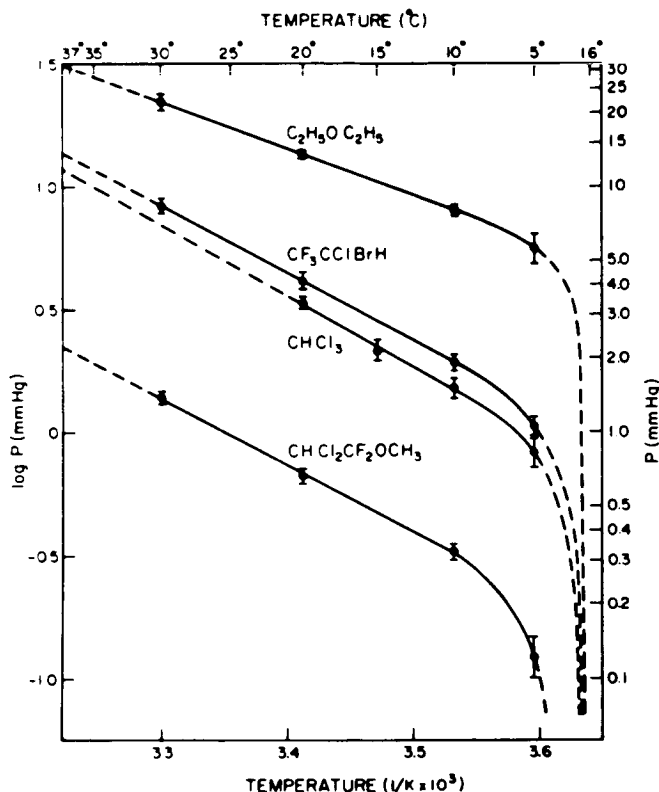


FIGURE 4. Relationship between body temperature and partial pressure anesthetizing 50 per cent of goldfish.<sup>14</sup> Each point represents 50 to 190 fish. Vertical bars indicate the 95 per cent confidence limits. The dashed lines below 5°C. indicate that anesthesia occurs in 50 per cent of the fish at 1.6°C. in the absence of an anesthetic compound ( $P=0$ ;  $\log P = -\infty$ ). The dashed lines above 30°C. permit  $P$  to be extrapolated for comparison with values for other species. (From Cherkin & Catchpool. *Science* 144: 1461.)

closely with the anesthetic potency values for mice. Recovery from the anesthetic was complete in nearly every case within five minutes after transferring the fish to fresh water. Having determined the exact anesthetic dose for our test animals, we then were able to look for synergistic action between anesthetic agents forming type I and II hydrates. We also hope to be able to compare the potencies of anesthetics of branched chain and straight chain types in order to assess the effects of the shape of the molecule on its potency as an anesthetic.

Some of the alcohols, esters, ketones, and aldehydes, substances which contain oxygen, have anesthetic properties. Acetone is known to form a hydrate of the structure II type.<sup>17</sup> There has been a report recently of hy-

hydrate formation by alcohols.<sup>18</sup> It is likely that the narcotic activity of diethyl ether and other ethers is to be attributed to their electron correlation reactions with other molecules (water molecules) and not to hydrogen bond formation.<sup>19</sup> Dielectric measurements at microwave frequencies show an increase in the amount of irrationally bound water in solutions of hemoglobin containing dissolved xenon, indicating that the dissolved xenon does appear to increase the amount of structured water surrounding a protein molecule.<sup>20</sup>

The hydrate microcrystal theory of anesthesia of Pauling and Miller reasserts what was pointed out nearly 100 years ago, that "an anesthetic is not merely a special poison to the nervous system; it anesthetizes all elements, all tissues by numbing them, temporarily blocking their irritability."<sup>21</sup> That this is true has been confirmed by countless papers on the effects of anesthetics on nearly every tissue of the body and nearly every physiological function. Miller<sup>15</sup> proposes that the ice cover "lowers the conductance of the nerve membrane, or stiffens it, or plugs up the pores of the membrane." He also suggests that anesthetics raise the threshold for conduction along a nerve by increasing the capacity of the membrane by altering the structure of the water at its interface with the membrane. Pauling states more simply that in the water surrounding and supporting the protein molecules, microcrystals are formed by the stabilization of hydrate structures already existing among the electrically charged side chains of these proteins. These microcrystals, he argues, would decrease the energy of the electric oscillations in the brain, damping the activity, until the higher centers are disconnected.

We are still a long way from the complete solution to this mystery, but I think that now at least we are pointed in the right direction.

### References

1. PAULING, L. 1961. *Science* **134**: 15.
2. DAVY, H. 1880. *Researches Chiefly Concerning Nitrous Oxide*. J. Johnson. London, England.
3. FARADAY, M. 1818. *Quart. J. Sci. Arts.* **4**: 158.
4. MORTON, W. J. 1905. *Post Graduate* **20**: 333.
5. BERNARD, C. 1875. *Lecons sur les anesthesiques et sur l'asphyxie*. Bailliere et fils. Paris, France.
6. MEYER, H. H. 1899. *Arch. Exptl. Pathol. Pharmacol.* Naunyn-Schiedeberg's **42**: 109.
7. CULLEN, S. C. & E. G. GROSS. 1951. *Science* **113**: 580.
8. MOORE, B. & H. ROAF. 1905. *Proc. Royal Soc.* **77B**: 86.
9. BUTLER, T. 1950. *Pharmacol. Rev.* **2**: 121.
10. FEATHERSTONE, R. M., C. A. MUEHLBAECHER, F. L. DEBON, & J. A. FORSAITH. 1961. *Anesthesiology* **22**: 977.
11. CLAUSSEN, W. F. 1951. *J. Chem. Phys.* **19**: 259, 662, 1425.
12. PAULING, L. & R. E. MARSH. 1952. *Proc. Nat. Acad. Sci. U.S.* **38**: 112.
13. VON STACKELBERG, M. *et al.* 1947. *Fortschr. Mineral.* **26**: 122.
14. McMULLAN, R. K. & G. A. JEFFREY. 1959. *J. Chem. Phys.* **31**: 1231.
15. MILLER, S. 1961. *Proc. Nat. Acad. Sci.* **47**: 1515.

16. CHERKIN, A. & J. F. CATCHPOOL. 1964. *Science* **144**: 1460.
17. FRANK, H. S. & A. S. QUIST. 1961. *J. Chem. Phys.* **65**: 560.
18. GLEW, D. N. 1962. *Nature* **195**: 698.
19. PAULING, L. 1964. *Anal.* **43**: 1.
20. SCHOENBORN, B. P., P. O. VOGELHUT & R. M. FEATHERSTONE. 1964. *Nature* **202**: 695.

# A PROPOSED WATER-PROTEIN INTERACTION AND ITS APPLICATION TO THE STRUCTURE OF THE TOBACCO MOSAIC VIRUS PARTICLE

Donald T. Warner

*The Upjohn Company, Kalamazoo, Mich.*

The elucidation of the primary structures of a large number of naturally-occurring polypeptides and proteins has now been accomplished. These studies have brought to light many special structural features such as disulfide-stabilized rings, closed decapeptide rings, and antibiotics containing a large proportion of N-substituted amino acids. Although these features have frequently been identified with smaller peptides and antibiotics such as insulin, vasopressin and gramicidin S, in at least one instance of a protein, ribonuclease,<sup>1</sup> the presence of an octapeptide portion joined by a disulfide linkage has been indicated.

These special structural features have been examined by various workers in the light of existing concepts of tertiary structure such as the  $\alpha$ -helix or the pleated sheet.<sup>2</sup> Thus Scheraga's model of ribonuclease<sup>1</sup> has formulated the disulfide-stabilized octapeptide ring as a nonhelical portion between helical segments. The cyclic decapeptide, gramicidin S, has been presented in the form of a modified pleated sheet<sup>3</sup> since the  $\alpha$ -helical concept can be applied to this ring system only by severe distortions of the postulated bonding principles. The small six-membered peptide ring of insulin also poses distortion problems for the helical concept as indicated by Lindley and Rollett.<sup>4</sup>

These studies with highly reactive and important biological sequences may indicate that some alternate chain conformation could constitute the preferred "reactive" form for these molecules although it is difficult to deny the possibility that their reactivity may in fact reside in the distortion of the helix (or pleated sheet) which the special structural features seem to require. Nevertheless, our knowledge of protein conformation, especially in aqueous solution, is still so limited that other tertiary building principles deserve to be presented for discussion, particularly if arrangements can be found which accommodate in a fairly uniform manner most of the special primary sequences mentioned above. With this thought in mind, molecular models of various antibiotics and hormones containing such sequences were assembled and other possible peptide chain conformations were examined.

From these model studies a possible conformation began to emerge which seemed to confer at least one common structural feature on all of the compounds studied. This structural feature concerned the possible orderly arrangement of the peptide carbonyl oxygens. Starting with the simplest example studied of the disulfide-stabilized hexapeptide ring in the insulin

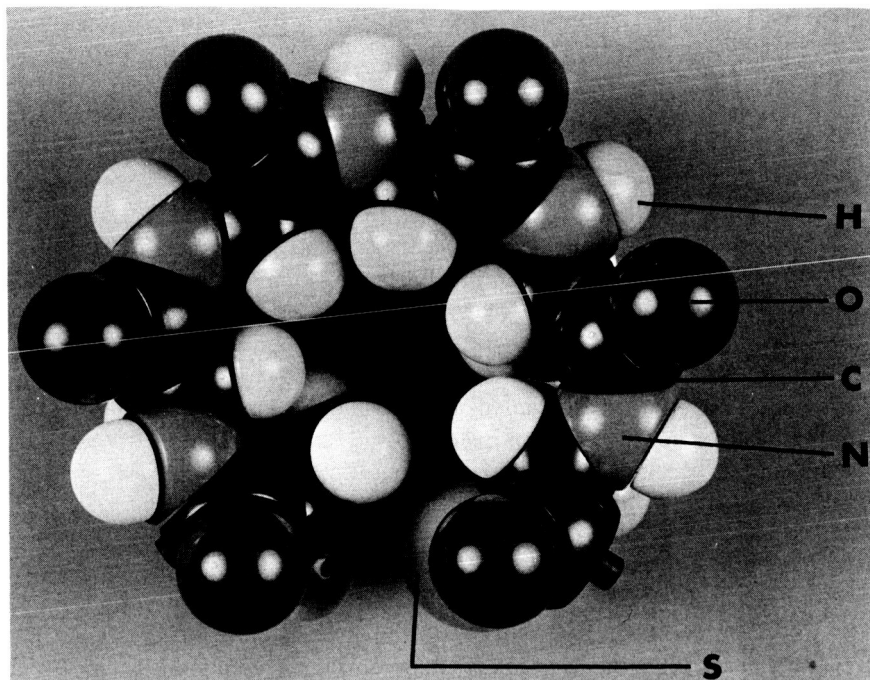


FIGURE 1. Cyclic hexapeptide ring of insulin.

A chain, it could be shown that this peptide ring can be laid out so that the peptide oxygens form a uniform hexagon.<sup>5</sup> In this arrangement the carbonyl oxygens lie in a common plane as indicated in FIGURE 1, and the model of the ring shows all of the peptide linkages and the  $\alpha$ -carbon atoms on one surface, while the other surface of the ring (not illustrated) contains mainly the side chains. The peptide surface is for convenience designated as the "hydrophilic surface" to distinguish it from the side chain or "hydrophobic surface."

The uniform hexagonal arrangement of peptide carbonyl oxygens may be readily extended to the cyclic decapeptide case by laying out the 10 peptide oxygens in the form of two fused hexagons as in FIGURE 2, a result which can be readily achieved without straining the normal bond angles. Although FIGURES 1 and 2 are simplified models with some side chains omitted to emphasize the carbonyl oxygen arrangements in print, several models of known sequences with all the side chains attached were also constructed and studied in detail.<sup>5,6</sup> In the complete models incorporating these hexagonal carbonyl oxygen features, it was readily seen that the available side chain positions for the various amino acid residues also favored a consider-

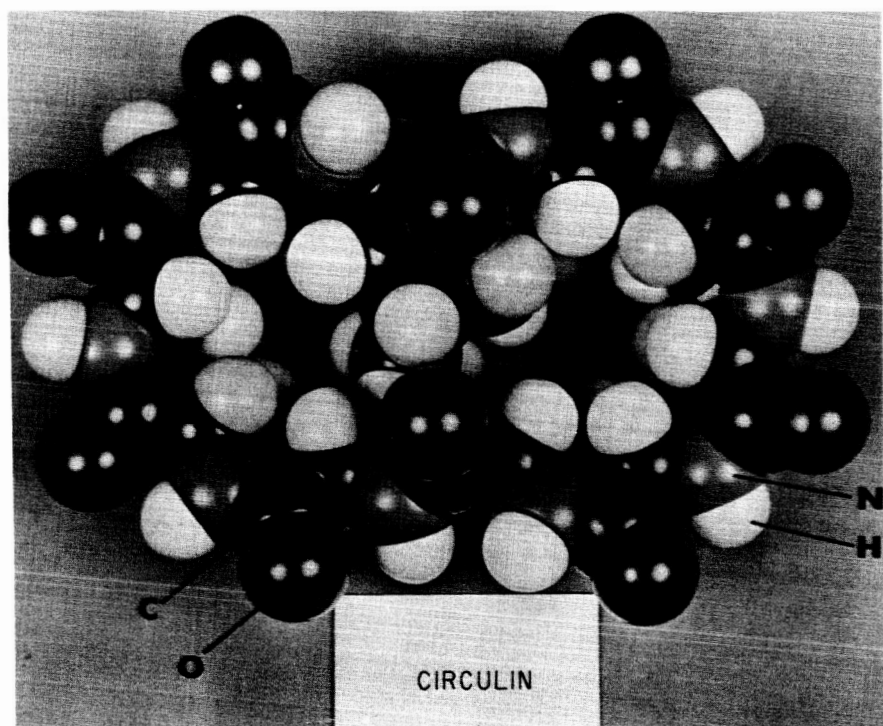


FIGURE 2. Cyclic decapeptide ring.

able number of hydrophobic and polar interactions among the side chains. Particular attention was given to the case of gramicidin S for the sake of comparison with the modified pleated sheet conformation suggested by other workers.<sup>3</sup> In the alternate hexagonal conformation for gramicidin S, this cyclic decapeptide presents a "hydrophilic surface" which is similar to FIGURE 2 except that the open hexagonal centers may be occupied by the  $\delta$ -amino groups of the two ornithine side chains and two of the  $-\text{NH}$  groups are replaced by the  $-\text{NCH}_2-$  of proline residues. By way of contrast the "hydrophobic surface" of this molecule from the model in FIGURE 3 is seen to consist almost entirely of paraffinic or aromatic groups in very orderly and compact contact. The degree of hydrophobic contact is appreciably greater in the fused hexagon model shown here than in the pleated sheet array, and the permissible placement of the aromatic D-phenylalanine rings allows better aromatic interaction in such a way that the hexagonal model suggests a structural preference for the D-isomer.

Further details of other antibiotic and open chain peptide models in the hexagonal conformation are also included in the previous papers.<sup>5,6</sup> I would

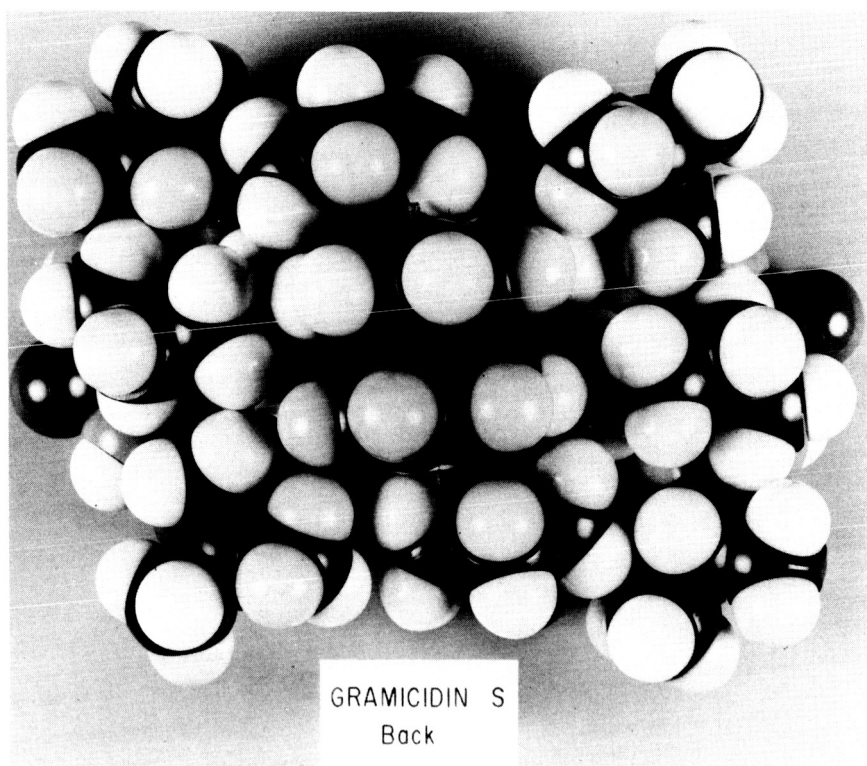


FIGURE 3. Hydrophobic surface of gramicidin S in fused hexagon conformation.

like to emphasize that within the limits of the hexagonal concept as it is applied to the "hydrophilic surface" various placements of the side chains on the "hydrophobic surface" are usually possible because of the free rotations of the various  $\beta$ -carbon atoms around the  $\alpha$ - $\beta$  carbon-carbon linkage; and I certainly would not care to imply that the side chain arrangements there presented are the only possible ones or necessarily the most favored ones. The model studies do indicate unmistakably that the hexagonal conformation applied to known sequences allows excellent side chain interactions on the suggested "hydrophobic surface." A most interesting and perhaps more significant observation about the hexagonal pattern of the "hydrophilic surface" was made, however, while comparing its oxygen pattern with the oxygen pattern in an ordered water structure. It was clearly seen that the second neighbor oxygens of the ice lattice also form a honeycomb pattern of regular hexagons which are also coplanar, and even more striking was the realization that the hexagonal water pattern and the hexag-



onal peptide oxygen pattern are almost identical dimensionally with oxygen-oxygen distances of about 4.8 Å. Thus a water layer lying over a peptide layer in our suggested hexagonal form can be hydrogen bonded to the peptide layer by exactly positioned collinear bonds providing maximum bond strength for each bond and a maximum number of interactions. This presented itself as an exciting way of bringing the water into the protein picture in a useful structural sense, with theoretical possibilities for a mutual water-protein stabilization by way of their common hexagonal oxygen patterns. Therefore, we immediately began the extension of the hexagonal principle of chain conformation to larger peptide sequences.

In our initial efforts with open chain peptide sequences the models contained perhaps one or two hexagons; but as the chain length increased, it was of interest not only to study the side chain interactions on the "hydrophobic" side but also to see whether the hexagonal peptide oxygen pattern on the "hydrophilic" surface could be maintained. The largest complete sequence which I have thus far constructed with actual space-filling models is the B chain of insulin. Starting with the N-terminal end of this peptide chain, the respective carbonyl oxygens are arranged to form first a single hexagon (positions 1 to 6), then an adjoining second hexagon is formed by using carbonyl oxygen positions 7 through 10 together with common positions 1 and 6 of the first hexagon, proceeding in a clockwise manner. By continuing to spiral the chain around the first hexagon additional hexagons are added with some common edges. The complete pattern for the carbonyl oxygen positions of the thirty peptide residues of the B chain of insulin is given in FIGURE 4. It will be noted that the thirty carbonyl oxygens in this

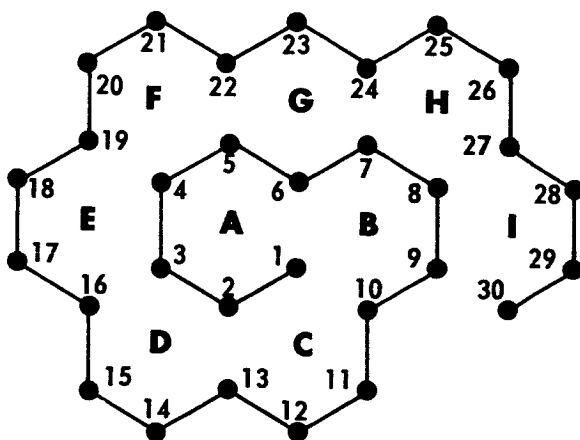


FIGURE 4. Hexagonal form of carbonyl oxygens in insulin B chain.

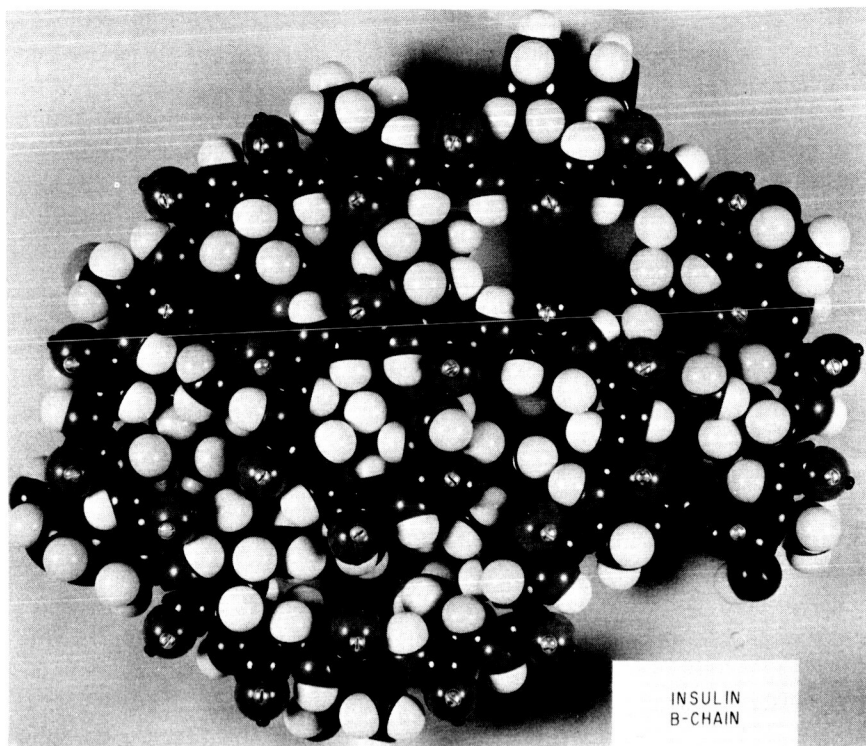


FIGURE 5. Catalin model of B chain of insulin (hydrophilic surface).

hexagonal conformation serve to form the corner positions of nine contiguous regular hexagons of a honeycomb pattern (letters A-I). In FIGURE 5 an actual model of the B chain of insulin as constructed with Catalin models ("hydrophilic surface") is shown in the same relative position as in FIGURE 4. In spite of small discrepancies in the bond angles of some of the model atoms, it is quite feasible to arrange the model chain to conform to the pattern of FIGURE 4. The actual model (FIGURE 5) suggested an interesting possibility about the  $\text{-NH}$  groups of the various peptide bonds. It is readily appreciated that in the second neighbor oxygen pattern of water there will be an oxygen position above the *center* of each hexagon which will not be contacting a peptide carbonyl oxygen. Although in some instances this water oxygen could be contacting polar side chain groups projecting into the hexagonal center, as I have already suggested,<sup>5</sup> the peptide  $\text{-NH}$  groups offer another possible bonding pair. Each of the nine hexagons except A and B has two peptide  $\text{-NH}$  groups pointing into the hexagonal central area to allow the bonding of an additional oxygen of

water there. Hexagon B could employ one amide  $\text{-NH}$  and one N-terminal  $\text{-NH}$  for water bonding in a similar manner, and perhaps the other amino  $\text{-NH}$  could serve a similar function in hexagon A although the angle is not quite so favorable. In any event the hexagonal conformation of FIGURE 5 has inherent possibilities for satisfying all of the bonding requirements for each and every  $\text{-CO-NH-}$  bond by a very orderly interaction with the water structure. Another item of potential importance for water bonding is the position of the  $\text{-CH}$  groups of the  $\alpha$ -carbon atoms of the peptide chain. Judging from their position in a cyclic hexapeptide constructed with Dreiding stereomodels,  $\alpha$ -hydrogens are exactly in the position and at the proper distance to hydrogen bond to a centrally-located water oxygen within each hexagon. Sutor<sup>7</sup> has recently re-emphasized the possibility of  $\text{-C-H} \cdots \text{O}$  hydrogen bonds, especially when the carbon is located next to a hetero atom, and has suggested the importance of such bonds in biological systems.

The favorable results with the B chain of insulin using Catalin models and the possible water stabilization prompted us to extend our study of the hexagonal principle to an actual protein situation, visualizing not only the stabilization of the subunit by water layers but also attempting the study of subunit assembly to form the protein rod, perhaps through the medium of water cementing as a laminating feature. For this purpose the case of tobacco mosaic virus (TMV) was selected. TMV has been studied for many years by chemical, physical chemical and biological techniques. Although no complete x-ray analysis has been done, various data related to the radial electron density distribution and particle size have been collected. An excellent review of the available literature up to about 1960 has been compiled by Klug and Caspar.<sup>8</sup> Chemical studies culminating in the complete amino acid sequence of the TMV protein subunit were published independently by Tsugita *et al.*<sup>9</sup> and Anderer *et al.*<sup>10</sup> The protein subunit contains 158 amino acids in a straight chain in addition to an N-terminal acetyl group for a total of 159 peptide oxygens. In attempting to study the assembly of a large number of protein subunits in forming the TMV rod, for a preliminary effort it was impractical to use actual Catalin models and build complete subunits. A simpler physical representation of the hexagonal array of carbonyl oxygens related to the various amino acid residues was achieved by the use of hexagonally ruled paper. By extending the spiral of hexagons initiated in FIGURE 4 on such paper to 159 positions, the protein subunit of TMV in the hexagonal conformation may be represented by FIGURE 6. Note that the N-terminal acetyl oxygen is given the number "zero" to avoid changes in the established numbering of the amino acid sequence. In the FIGURE each of the 159 carbonyl oxygen positions in the clockwise spiral has been numbered, and through the use of different code symbols for the different amino acids

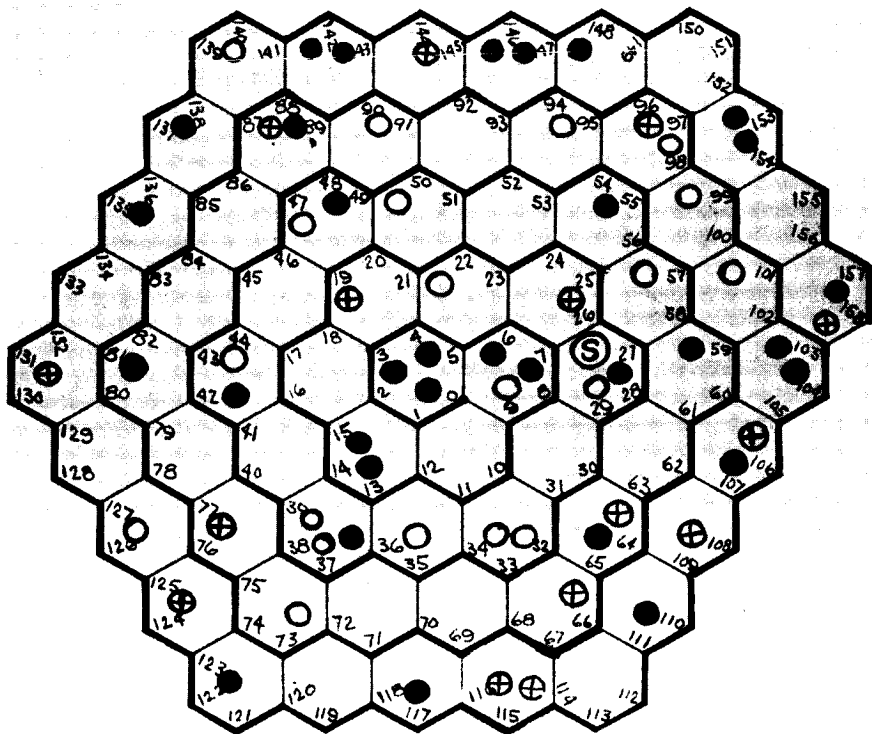


FIGURE 6. Hexagonal conformation of carbonyl oxygens of tobacco mosaic virus subunit. Symbol Code: ● Hydroxy amino acids; ○ Carboxamide; ⊕ Carboxyl; S Cysteine.

the various kinds of side chains could be approximately located. In order to avoid too much complexity this author has selected code symbols for carboxyl, carboxamide and hydroxyl-containing amino acids only and these three types of side chains are indicated by this code throughout the subunit. The single cysteine -SH residue position is also marked.

Several things of interest may be noted about the six-sided TMV subunit representation of FIGURE 6. First of all, since the oxygen positions at the hexagon corners of the "hydrophilic surface" are about 4.8 Å. apart, the overall size of the subunit may be quite accurately determined and turns out to have a maximum length of about 79 Å. This value approximates the TMV particle radius and suggests a possible radial arrangement of subunits having this conformation around a central hole to form the TMV rod. Second, the subunit in this conformation is a thin disc (average thickness about 3.4 Å.) having *hydrophilic* and *hydrophobic* surfaces. Theoretically the hydrophilic surface with its honeycomb array

of carbonyl oxygens, forming exact collinear hydrogen bonds with an equivalent layer of second neighbor oxygens from the aqueous environment, yields a sort of laminated structure capable of mutual stabilization of the two interacting partners, perhaps reminiscent of the structural members of a geodesic dome but in a planar form. The hydrophobic side of the proposed subunit contains nonpolar as well as some polar groups capable of promoting side chain attractions as contributory forces for maintaining the proposed subunit in the suggested flat disc form. Perhaps of equal importance, this surface also constitutes a general hydrophobic plane studded with interacting groups which may have a specific attraction for complementary zones of side chain groups on the hydrophobic surface of other protein subunits. Various minor points about the subunit are elucidated in the complete manuscript describing the TMV model.<sup>11</sup>

We may now ask whether it is feasible to utilize subunits of this general shape and size in constructing a model of the TMV rod. Since the overall dimensions of the subunit clearly allowed a radial assembly around a central core, three of the models are shown in this position in FIGURE 7, with the same point of each subunit oriented toward the central hole. The space between subunits in this FIGURE is a provision for water spacing and bridging of the peptide oxygens of neighboring subunits, which would otherwise repel each other upon close approach. Each subunit in this "combination-of-three" has its own hydrophilic and hydrophobic face, and the problem is, "How may these combinations be further utilized in the formation of rods?" The work of Buzzell<sup>12</sup> suggests that the characteristics of TMV protein dissociation can be accounted for to a considerable extent by the reversal of paired amide, paired carboxyl and amide-carboxyl interactions. Since in our proposed subunit these side chain groups are present on the hydrophobic surface, two combinations such as illustrated in FIGURE 7 have been placed back-to-back with hydrophobic sides in contact to yield the overlap pattern of FIGURE 8. Here the shaded areas represent the hydrophobic contact zones between the two "combinations-of-three" where intersubunit side chain reactions may occur. The choice of this particular mode of overlap is, of course, partly arbitrary but it is one of the possible choices and upon closer examination turns out to have the following points in its favor when compared with the actual TMV protein rod.

- (a) The overall hexagonal shape is consistent with the early electron microscope work of Williams,<sup>13</sup> a result which was substantiated by Matthews, Horne, and Green<sup>14</sup> and reiterated by Mattern.<sup>15</sup>
- (b) The measured model dimensions (maximum radius = 83.5 A., average radius = 78.5 A.) compare closely with the respective experimental values of 84 A. and 77 A. itemized by Klug and Caspar.<sup>8</sup>

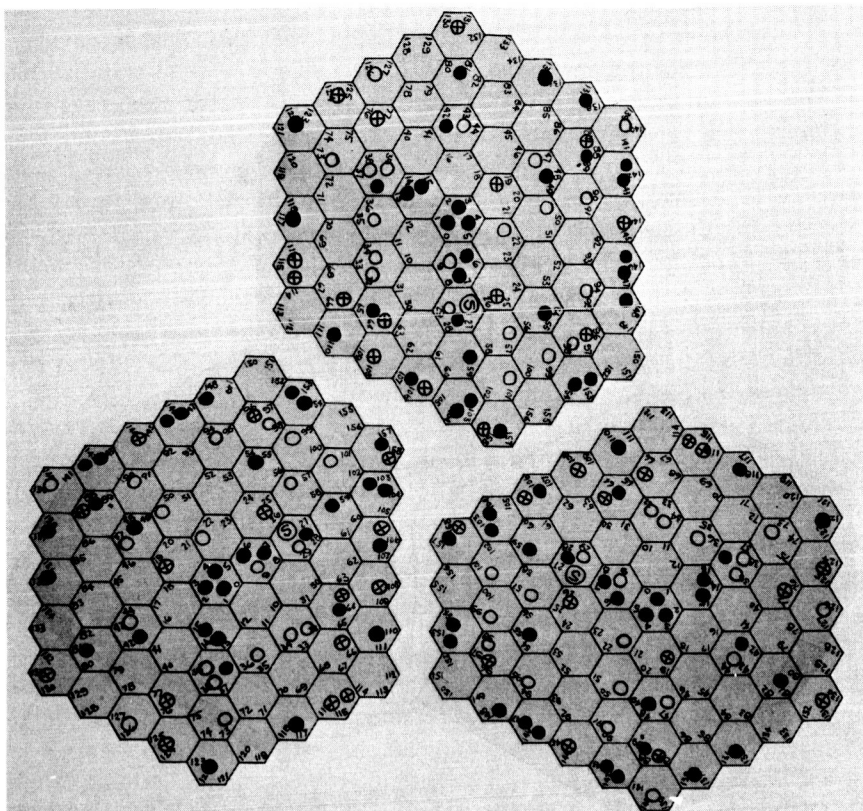


FIGURE 7. Radial combination of three TMV subunits.

- (c) The postulated side chain combinations (amide-amide, amide-carboxyl, etc.) suggested by Buzzell<sup>12</sup> are frequently encountered as indicated by the code symbols in the overlap zones with the hexagonal paper models.<sup>11</sup>
- (d) The total of six subunits in the assembly is consistent with the value for the so-called "A-protein" of Schramm<sup>16</sup> although the possibility that "A-protein" may not be a single entity has recently been presented by Caspar.<sup>17</sup>

If we now take the assembly of six subunits indicated in FIGURE 8 and picture it schematically as in FIGURE 9 to give a slightly exaggerated feeling of the thickness of the individual subunit layers, we arrive at a staggered sandwich model where the hydrophobic surface forces (polar, nonpolar, perhaps some ionic) cement the two slices together, and the upper and lower surfaces are pictured as hydrophilic hexagonal arrays of peptide

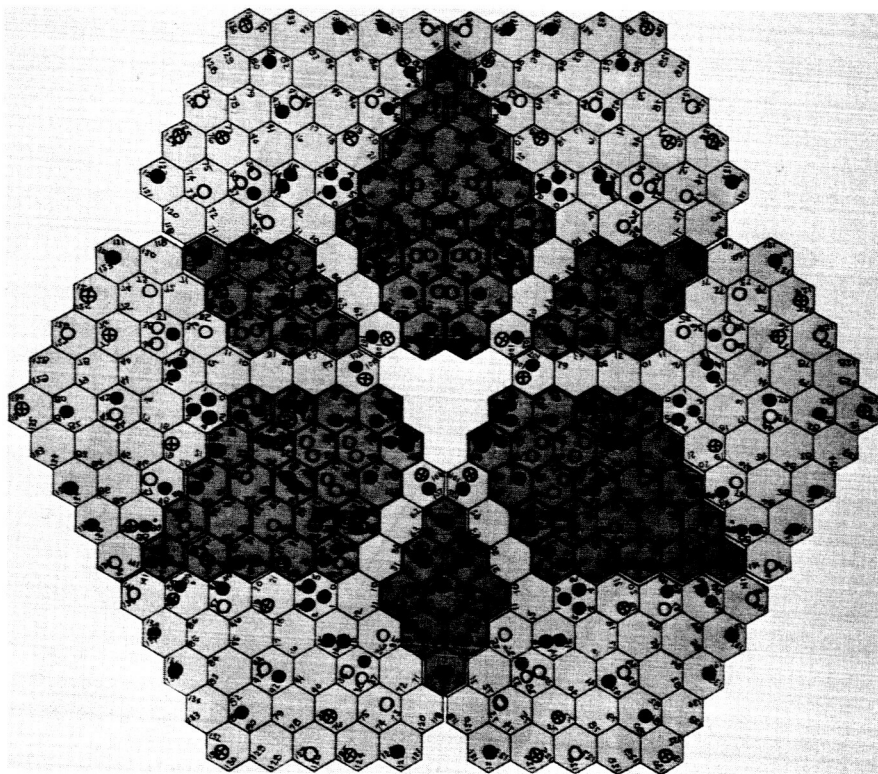


FIGURE 8. Hydrophobic overlap of two radial combinations in schematic "A-Protein" model.

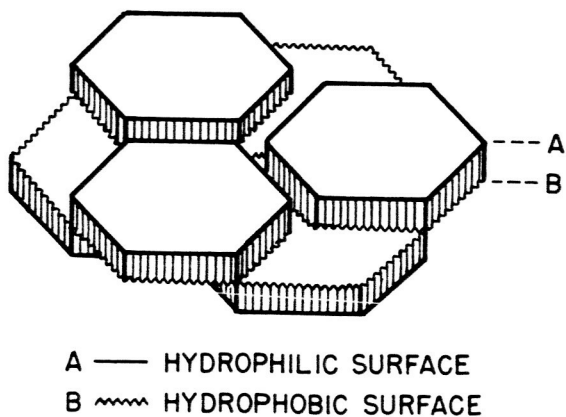


FIGURE 9. Three-dimensional schematic "A-Protein" model.

oxygens which may be water-coated in an aqueous environment. Presuming FIGURE 9 is a working model for "A-protein", how can we postulate the formation of the rod-like particles from such building units? This author has already indicated that the respective peptide carbonyl oxygens are about 4.8 Å. apart, and as a refinement of this distance has stipulated the possibility that this distance may vary between about 4.76 Å. and 4.90 Å. for the *cis* and *trans* forms of the peptide bonds respectively. Since the second neighbor oxygen distance in water should also vary with temperature, water must be warmed to about 25-30°C. to achieve an average second neighbor distance of about 4.76 Å., based on the first neighbor oxygen value of about 2.94 Å. at 30°C. determined by Brady and Krause.<sup>18</sup> Therefore, the hexagonal peptide array of the TMV subunit (FIGURE 6) and the hexagonal second neighbor oxygen pattern of water should begin to be dimensionally similar at about 25-30°. Although water undoubtedly also bonds to proteins at lower temperatures; if the respective hexagonal patterns are not dimensionally similar (with the water pattern theoretically smaller below about 25°) so that the bonds are not exactly collinear, the net effect based on a mechanical analogy would be a tendency to produce a concave surface for the protein subunit. Such a water-layered concave surface would have only a small contact area with other similar concave surfaces, just as the concave surfaces of two water-wet watch glasses make contact only at the edges. However, at temperatures where the water and peptide patterns are dimensionally similar and the cooperative forces might theoretically be expected to yield a planar water-layered peptide surface, one protein subunit can be expected to have a large intimate contact with another similar planar subunit while requiring only a monolayer of ordered surface water between them. A crude analogy would be two glass plates held in close and firm contact by a few drops of water spread in a thin layer between their contacting surfaces. In the case of the protein layers, the analogy would perhaps be further refined to include electrostatic attractions capable of being effective between two planar surfaces in close contact which would not be allowable when the two surfaces were concave and consequently separated by a considerable distance at certain points. These probable electrostatic interactions would also be influenced by the pH of the medium and the isoelectric point in the protein situation.

Going back now to the probable model of the "A-protein" of TMV in FIGURE 9, if this material in aqueous solution at the proper pH and at a relatively low temperature (*ca.* 10°C.) is gradually warmed to about 30°, the average second neighbor water distances will gradually approach the hexagonal peptide distances of about 4.8 Å. At the optimum water temperature the hydrophilic surfaces of the upper (or lower) TMV subunits of the proposed "A-protein" model would be presumably exactly planar and



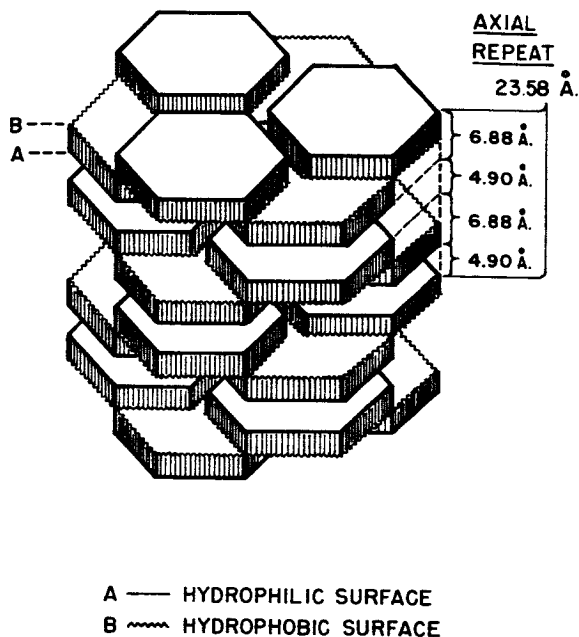


FIGURE 10. TMV protein rod of four "A-Protein" units.

theoretically capable of "cementing" with the hydrophilic surfaces of other "A-protein" aggregates to produce the rod-like structure of FIGURE 10. This FIGURE represents schematically a possible axial layering of the aggregates placing the hydrophilic surfaces of the subunits directly above each other for a maximum water-protein interaction and cementing effect. From the work of Smith and Lauffer,<sup>11</sup> "A-protein" polymerization in buffered aqueous solution at pH 6.5 does proceed rapidly at temperatures above about 20° and approaches completion at about 30°. The polymerization is reversible with cooling. Therefore, the experimental observations with TMV protein are in certain respects consistent with the theoretical possibilities inherent in the schematic "A-protein" model. This model views polymerization in terms of interactions taking place at the hydrophilic surface of the protein subunits by virtue of the bonded water layer at that surface. The schematic rod of FIGURE 10 has a suggested axial repeat of about 23 Å. This value is close to the proposed pitch of the helical rod.<sup>8</sup> The schematic value indicated could conceivably be a pseudorepeat if the subunits were not exactly superposed by the water interaction. It should be pointed out that FIGURE 10 allows 12 subunits in 23 Å., which is in conflict with the currently accepted value of  $16\frac{1}{3}$  subunits in 23 Å.<sup>8</sup> It is equally apparent that the concept of  $16\frac{1}{3}$  subunits per helical turn

is incompatible with the idea of a hexagonal cross section for the virus rod, a discrepancy which suggests that there are many aspects of TMV structure which still need to be resolved and certainly kept in mind while evaluating the possibilities of any model.

In addition to the axial array of the "A-protein" to form rods as in FIGURE 10, it is also possible to envision equatorial interlocking of the edges of the subunits by overlapping at the corners. Apparently the electron micrographs of TMV preparations in some instances have shown interlocking of particles<sup>13,14</sup> although microdensitometer tracings recently carried out by Markham, Hitchborn, Hills and Frey<sup>20</sup> showed little interpenetration of adjacent virus rods in the area examined. This may be a factor which varies with concentration and pH. In any case the interpenetration can be applied to the "A-protein" aggregates for the purpose of our study. The schematic diagram that illustrates the overlaps of the proposed models is a rather complex one and it has already been reproduced in our recent publication<sup>11</sup> for the benefit of those who wish to see it in detail. For the present discussion it is adequate to mention that the water spacings which appear between the subunits in the "A-protein" equatorial overlap occur at definite easily measurable distances from the central holes in the respective rods. These spacings of water in the rod represent zones of lower electron density in the subunit network. If the various distances of these lower electron density zones from the central reference holes are checked against the known radial electron density distribution pattern observed for TMV protein,<sup>8</sup> the distances correspond to known minima in the radial distribution pattern. So in this instance too the initial protein subunit conformation suggested in FIGURE 6 is capable of being fitted into a model which accommodates the known data about TMV protein. This author would emphasize again that this discussion has been confined to the TMV protein and probable rods assembled from it. The role of water in the construction of the model has been emphasized at each step, and every effort has been made to evaluate feasible water-protein interactions as possible structural principles. Certain discrepancies between this model and other proposed models known to me have been pointed out, and I have also submitted many features about this model which I believe argue for its possible validity. There are some aspects of the water-protein reaction which need to be studied in greater detail with this proposed subunit, and every effort is being made to secure more and better models at a reasonable price.

Some of the other studies of other biological compounds and their possible interaction with the ordered water structure will be discussed. These studies were first initiated with the cyclitol, *scyllo*-inositol, and the demonstration that the oxygens on the 1-, 3- and 5-carbons of this compound have the same arrangement in space as three "second neighbor" water

oxygen.<sup>21</sup> Similarly, the oxygens on carbons 2-, 4- and 6- also form a "second neighbor" trio in a different plane. In view of the dimensional flexibility of the water oxygen pattern with temperature and the relatively stable arrangement of the oxygen network in the scyllo-inositol, each of the inositol oxygen trios may be thought of as representing a "built-in" and quite definitely fixed arrangement of three "second neighbor" water oxygens at only one particular water temperature, probably about 37°C. In this sense the inhibiting effect of inositol on dessication damage to life forms observed by Webb<sup>22</sup> and the stabilizing effect of various sugars on freezing-thawing damage<sup>23</sup> are conceivably a partial manifestation of their ability to replace segments of the water structure in contact with protein or nucleic acids under conditions where the rigid "built-in" hydroxyl patterns of the carbohydrates are biologically preferable to the less favorable ambient water oxygen spacings at the prevailing temperature. It is likely that the "inositol" used by Webb<sup>22</sup> was not scyllo-inositol but the more readily available *myo*-inositol. This recalls a very provocative thing about *myo*-inositol which has been observed by other workers in another connection. This particular cyclitol also has six hydroxyl groups, but in this instance five of the hydroxyl groups are equatorial and one hydroxyl is axial. In biological systems *myo*-inositol is specifically oxidized at the axial hydroxyl only. The all-equatorial scyllo-inositol is not oxidized at all.<sup>24</sup> When models of the two compounds are inserted into a water structure it is noted that the six hydroxyls of scyllo-inositol all occupy positions where they exactly bond to water oxygens without appreciably disrupting the oxygen pattern. This form is not oxidized. On the other hand the *myo*-inositol has five equatorial hydroxyls which can bond to water without disturbing the oxygen lattice. However, it also has the single axial hydroxyl which does not coincide with any oxygen position in the water lattice. It is interesting that this "nonconforming" unit is the one that is oxidized to a keto group. In its resulting keto form it ends up considerably closer to a "conforming" water oxygen position.

Since carrying out these early studies on inositol with tedious calculations, the author has had available Dreiding Stereomodels of the water structure (W. Büchi Glasapparatefabrick, Flawil, Switzerland) built on the same scale as the other Dreiding models (1 cm. = 0.4 Å.) and calibrated to water-oxygen distances at about 37°C. With this assembled water lattice, Dreiding molecular models of various active biological compounds may be inserted into the water network. Then the positions of various reactive groups — hydroxyls, aminos, ethers, carbonyls, etc. — in these compounds may be compared directly with the oxygen positions of the water to see whether the positions coincide or differ (as in *myo*-inositol's axial hydroxyl, above). An example of such a comparison is shown in FIGURE 11 for the steroid, hydrocortisone. Particular attention is focused on the

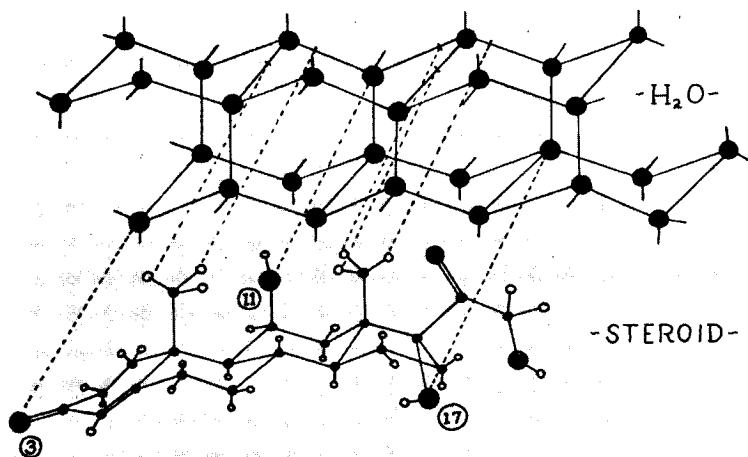


FIGURE 11. Steroid-water interactions.

three oxygen functions of the rigid steroid nucleus in the comparison, since their positions are fixed and therefore less equivocal. Because of their firm positioning on the rigid ring, the close correspondence of the three widely separated oxygen functions with three definite oxygen positions in the water lattice is perhaps at least a mild surprise. Through the use of the models it is theoretically possible to consider the fate of such steroid oxygen functions in the surrounding water-oxygen media, and assess some ways in which their presence upsets the resonance pattern of water and influences its reactivity in subtle directed ways. It is suggested, first of all, that if a steroid oxygen in the model resides at the same place as a water oxygen in the lattice, we will presume that it displaces this water oxygen. With this in mind consider, for example, the hydroxyl at position 11 in the hydrocortisone nucleus. The water oxygen which the 11-hydroxyl displaces was initially in contact with four surrounding water oxygens in the lattice through hydrogen bonds, with each hydrogen (in our poor materialistic representation of it) capable of resonating along each bonding leg within certain proximal and distal limits which are actually marked out on the Dreiding water models. By inserting into this situation the 11-hydroxyl group via a definite covalent bond (coming in from the same direction as the  $\text{-O-H-}\cdots\text{-O}$  bond in the original water situation), one of the resonance freedoms is effectively eliminated, leaving

at best only three degrees of resonance freedom. Further interferences with these remaining resonance freedoms are suggested by the positions of the 18-CH<sub>3</sub> and 19-CH<sub>3</sub> groups. These methyl groups almost certainly interfere with the two near water oxygen positions and, as indicated by the dotted lines of FIGURE 11, the hydrogens of each of these methyl groups insert themselves by their fixed covalent -CH linkages at the *distal* positions of what had been two resonating distal-proximal hydrogen possibilities in the water, thus drastically altering the chance that the hydrogen atom of the 11-hydroxyl group will reside along either of these two resonance pathways. Instead we find two distally fixed hydrogens along these former resonance outlets. (Note: These comparisons are best noted when the steroid is inserted into the diamond cubic ice lattice.<sup>21</sup>) Continuing this comparison the physical models seem to suggest only one remaining degree of allowable resonance freedom for the 11-hydroxyl group of the steroid with a single water position. If a reduction in the number of resonating possibilities does result in higher reactivity along the remaining pathways, then the biological activity of this particular hydroxyl group may be inherent in the environmental influences suggested here. It is undoubtedly true that any reactive molecule has its most telling effect on its immediate surroundings, and its widespread effect will reside in the ability of these surroundings to efficiently communicate these short term perturbations to more distant points. For such long-range communication an ordered water lattice may be exceedingly useful, and perhaps an attempt such as this to understand the possible substrate interaction with its immediate aqueous environment will furnish useful clues about substrate reactivity at the vital molecular level.

Many compounds of biological importance can be readily constructed with Dreiding stereomodels and examined in the water lattice. Some of the earlier examples studied with Catalin space-filling models have been rechecked with the Dreiding stereomodels. For example, a cyclic hexapeptide shows a very exact correspondence between its peptide oxygens and the second neighbor oxygens of the Dreiding water model. For the purpose of this paper this author will confine most of the other presentations to rigid ring systems where the placement of the groups is fairly certain. A few examples of general interest are included in TABLE 1. Most of the interactions are easily seen. In the case of thymine (Example *d.*), the placement of the one and three oxygens at the one and three water positions brings the carbon of the four methyl group at the four water oxygen position given in the TABLE. The hydrogens of this methyl group are able to rotate so that they can reside at the "distal" position of the resonating hydrogen extremities for a water oxygen lying just *above* oxygen four in an adjacent layer of the water structure. This methyl position again suggests a possible interference of this base with the resonance

TABLE 1  
WATER-SUBSTRATE INTERRELATIONSHIPS

Water model*	
Substrate	Formula†
a. Biotin	
b. 1, 4-Quinone	
c. meta-Dihydroxybenzene	
d. Thymine	
e. Triglyceride (R = fatty acid radical)	

\*Water oxygens numbered for identification.

†Numbers in formula indicate interaction points with the corresponding numbered oxygens in the water segment above.

stability of water at a specific location and in a particular way. The one example of a nonring compound in TABLE 1, the triglyceride of Example *e*, is interesting in view of current concepts of membrane structure involving protein-lipid bilayers with water layers between. If triglyceride in this conformation can interact favorably with structured water, and the protein in the hexagonal conformation can also interact favorably with this same structured water, then water should of course be theoretically capable of serving as a structural cement at protein-lipid interfaces as well as at protein-protein interfaces. The fact that the ester carbonyl is perhaps less capable of existing in the enol form than the amide carbonyl of the peptide is worth keeping in mind on a theoretical basis, since the enol form of a carbonyl is potentially capable of interaction with water in a different spacing relation than the keto form.<sup>21</sup> O. Hechter and I are considering the application of these concepts to peptide hormone interactions with specific receptors in the cell membrane and their relation to the molecular organization of the cell membrane. Some of these concepts are discussed by Hechter in his paper.

#### *Summary*

The importance of water in life processes is a factor that is widely recognized but little understood. Although it is well known that protein contains a considerable quantity of bound water, neither the  $\alpha$ -helix nor the pleated sheet models make provision for the incorporation of this water into the model structures. However, the "hexagonal" conformations of polypeptides and proteins presented for discussion in this paper contain structural features which permit the incorporation of water in a uniform manner, implying that the incorporated water is present in an ice-like lattice in hydrogen-bonded contact with each peptide oxygen and probably each  $-NH$  group as well. The hexagonal structure is capable of incorporating small cyclic rings and decapeptide structures which the  $\alpha$ -helix cannot assimilate without distortion. In the case of the TMV protein, the hexagonal principle can be consistently applied to yield a subunit model capable of serving as a "building block" for the TMV rod.

Other biological components such as sugars, steroids and triglycerides have reactive groups which in many instances are also capable of accommodating themselves to the oxygen lattice of the water structure. Some of the possible implications of these close "fittings" are discussed in the light of their biological consequences and importance. The value of models in picturing the relationships has been stressed. It is hoped that these preliminary studies will encourage others to utilize model building in attempting to understand structural relationships, especially of known compounds in their relationship to the water structure.

*Acknowledgment*

I would like to thank the editor of *Nature* for permission to reproduce FIGURES 1-3 and the publishers of the *Journal of Theoretical Biology* for the use of FIGURES 6-10.

*References*

1. HIRS, C. H. W. 1960. *N. Y. Acad. Sci.* **88** (3): 611.
2. PAULING, L. & R. B. COREY. 1952. *Proc. Natl. Acad. Sci.* **38**: 86.
3. SCHMIDT, G. M. J., D. C. HODGKIN & B. M. OUGHTON. 1957. *Biochem. J.* **65**: 744; 752.
4. LINDLEY, H. & J. S. ROLLETT. 1955. *Biochim. Biophys. Acta.* **18**: 183.
5. WARNER, D. T. 1961. *Nature (London)* **190**: 120.
6. WARNER, D. T. 1961. *J. Theoret. Biol.* **1**: 514.
7. SUTOR, D. J. 1963. *J. Chem. Soc.*: 1105.
8. KLUG, A. & D. L. D. CASPAR. 1960. *Adv. Virus Res.* **7**: 225-320.
9. TSUGITA, A., D. T. GISHI, J. YOUNG, H. FRAENKEL-CONRAT, C. A. KNIGHT & W. M. STANLEY. 1960. *Proc. Natl. Acad. Sci. Wash.* **46**: 1463.
10. ANDERER, F. A., E. WEBER, H. UHLIG & G. SCHRAMM. 1960. *Nature (London)* **186**: 922.
11. WARNER, D. T. 1964. *J. Theoret. Biol.* **6**: 118.
12. BUZZELL, A. 1962. *Biophys. J.* **2**: 223.
13. WILLIAMS, R. C. 1952. *Biochim. Biophys. Acta.* **8**: 227.
14. MATTHEWS, R. E. F., R. W. HORNE & E. M. GREEN. 1956. *Nature (London)* **178**: 635.
15. MATTERN, C. F. T. 1962. *Virology* **17**: 76.
16. SCHRAMM, G. 1947. *Z. Naturf.* **2b**: 112, 249.
17. CASPAR, D. L. D. 1963. *In* *Advances in Protein Chemistry*. C. B. Anfinsen, Jr., M. L. Anson, J. T. Edsall, Eds. **18**: 37-121. Academic Press. New York, N. Y.
18. BRADY, G. W. & J. T. KRAUSE. 1957. *J. Chem. Phys.* **27**: 304.
19. SMITH, C. E. & M. A. LAUFFER. 1962. 15th Annual Symp. Fund. Canc. Research, M. D. Anderson Hosp. and Tumor Inst. Univ. of Texas Press. Austin: 184 (Table 1); 192 (Fig. 5).
20. MARKHAM, R., J. H. HITCHBORN, G. J. HILLS & S. FREY. 1964. *Virology* **22**: 342.
21. WARNER, D. T. 1962. *Nature (London)* **196**: 1055.
22. WEBB, S. J. 1961. *Can. J. Microbiol.* **7**: 621.
23. MERYMAN, H. T. 1956. *Science* **124**: 515.
24. MAGASANIK, B. & E. CHARGAFF. 1948. *J. Biol. Chem.* **174**: 173.



# INTRACELLULAR WATER STRUCTURE AND MECHANISMS OF CELLULAR TRANSPORT\*

Oscar Hechter

*Worcester Foundation for Experimental Biology,  
Shrewsbury, Mass.*

## *Preface*

The history of ideas shows that whenever a monistic concept is developed which connects previously unconnected aspects of a large field in a powerful unifying configuration, another monistic concept soon emerges which is its antithesis. The coexistence of these opposing configurations is intolerable; the partisans on both sides, utilizing the "either-or" weapon of Occum's razor, attack with data. In the ensuing struggle evidence accumulates so that one concept is victorious and becomes generally accepted; the other is rejected. As time passes and increased understanding of the overall system is achieved, it then becomes clear that the accepted concept has been based upon an overly simple model of the field encompassed. In the context of new information, some ideas from both poles of opposition are now found to be valid, some invalid. In effect, a resolution of the conflict is achieved, as the *also* and the *and* of pluralism replaces the monolithic dichotomy of *either-or*.

## *Introduction*

From the very beginnings of mechanistic thinking of biology, the nature of water in the cell has figured prominently in certain continuing debates about the nature of fundamental mechanisms of living systems. Of these perhaps the most important has involved the question as to how cells which live in an aqueous ionic environment, high in sodium and low in potassium ions, are able to maintain levels of high potassium and low sodium in the cell interior. Two concepts were developed to answer the specific question relating to  $K^+$  and  $Na^+$  distribution. The universality of high  $K^+$  and low  $Na^+$  in cells was considered to be the expression of a unitary mechanistic principle applicable to all cells and these two concepts have traditionally been presented as mutually exclusive antithetical alternatives. Both have been modified and adapted as new information was obtained, while retaining their essential differences. Both have been expanded so they conceptually accommodate the entire field of selective accumulation and exclusion. Both have been employed to provide explanations for bioelectric potentials, particularly with regard to excitability changes in nerve and muscle.

\*Supported by The Commonwealth Fund, New York, N. Y. and the Ittleson Family Foundation, New York, N. Y.

These concepts differ fundamentally with respect to the importance of the cell interior in control of the transport of substances into and out of the cell. Each concept uses a set of different assumptions concerning the state and structure of water, ions, solutes and macromolecules in the cell interior; they also differ as to how metabolic energy is utilized for transport processes. One of these concepts has been almost universally accepted, the other rejected. The concept which is generally accepted postulates that the selection and exclusion of solutes by cells is determined exclusively, or primarily, by the properties of a thin lipoprotein permeability barrier at the cell surface, first designated as the cell membrane, later as the plasma membrane. The generally rejected alternative is a holistic concept which holds that structural relationships in the cell as a whole, not just in the membrane, determine what substances enter or leave and which substances are excluded or accumulated in the cell.

#### *The Two Concepts of Transport*

*Membrane thesis.* The widely accepted thesis (for partial listing of reviews cf.<sup>1-12</sup>) assumes that the interior of the cell may be considered as one (or more) relatively simple "well stirred" compartment(s) containing ions, small molecules and the polymers of the cell bounded by a cell membrane regarded as the primary permeability barrier limiting the entry and exit of substances. The bulk of the water and monovalent cations within such a cell is assumed to be "free" and in essentially the same state inside and outside of the cell. A small fraction (10–20 per cent) of the total intracellular monovalent cations may be "bound" to structural components; a fraction of cell water corresponding to "bound" ion is likewise "bound" and unavailable as solvent for permeant electrolytes or nonelectrolytes. The intracellular nondiffusible biopolymers, primarily proteins, possess sites potentially available for "binding" permeant solutes (via electrostatic forces, hydrogen-bonding, etc.), but it is categorically assumed that such binding sites are not *selective* in the sense that they are *not* able to discriminate between closely related chemical species, for example as between  $K^+$  and  $Na^+$ , or stereoisomers in the sugar or amino acid series.

Selective binding sites are required to account for the observed selectivity of the transport of various substances in cells; these sites are classically assumed to be localized exclusively in the plasma membrane. The binding sites in the plasma membrane — few in number — serve a catalytic role in two types of transport processes, differentiated thermodynamically in terms of whether the transmembrane flow of solute is *uphill* (active) or *downhill* (passive). The transmembrane flow of specific solutes *with* the gradient is assumed to involve membrane "pores" or "channels" possessing binding sites for appropriate selectivity. Passive processes of this type do not require the obligatory coupling of metabolic

energy with solute flow; metabolic energy may, however, be required for maintaining the membrane or "pores" in an appropriate state for selective solute flow. The inflow of  $\text{Na}^+$  and outflow of  $\text{K}^+$  following electrical stimulation of nerve serves as an example of the flow of ions through the depolarized nerve membrane *with* the gradient. The selective accumulation of substances in the cell represents transmembrane flow of solute against an apparent thermodynamic gradient, and active transport processes of this type are attributed to metabolically energized membrane pumps. The coupled  $\text{Na}^+$ - $\text{K}^+$  pump was the first membrane pump was the first membrane pump to be postulated; this pump is assumed to select and translocate  $\text{Na}^+$  from an aqueous intracellular region high in  $\text{K}^+$  and low in  $\text{Na}^+$  to the external aqueous medium, high in  $\text{Na}^+$  and low in  $\text{K}^+$ ; coupled with  $\text{Na}^+$  translocation external  $\text{K}^+$  is selected and translocated by the pump to the cell interior. Membrane pumps for other cations and for sugars and amino acids were later to be postulated when other substances were observed to be specifically accumulated in various cell types. In general, membrane pumps represent specialized devices for the transduction of metabolic energy into specific osmotic work; the transducing device has componentry for the energetic reactions and selective binding sites for permeant translocation, so arranged spatially that energized directional translocation of specific solute through the membrane phase occurs against an apparent thermodynamic gradient.

*Holist thesis.* The generally rejected holist thesis has been advanced in several different versions, which differ somewhat in specific mechanistic formulation but have certain essential features in common. The most sophisticated and comprehensive of these proposals is to be found in Ling's present association-induction hypothesis described in a recent monograph;<sup>13</sup> other formulations may also be referred to.<sup>14-17</sup> The fundamental assumption in all holistic proposals is that water, ions, and biopolymers within the cell constitute a highly ordered unitized system (or systems), so arranged and organized architecturally that various types of fixed sites on the macromolecular components of the ordered system are available for specific interactions with certain permeant solutes but not others. Fixed negative and positive sites for electrostatic interactions with counterions (cations and anions), as in polyelectrolyte interactions, are assumed to be selective; selective binding sites involving hydrogen bonding, as well as other bonding modes, are likewise envisaged.

The type of ordered intracellular system postulated has properties of a lattice in which the water component is considered to differ fundamentally in structure and properties from ordinary liquid water, the specific mechanistic formulation differing from one holistic proposal to another. Potassium accumulation and sodium exclusion in cells is assumed to occur on the basis that potassium ion is selectively utilized as the counterion for

certain fixed negative sites in the ordered intracellular system, the sodium ion being excluded from the ordered phase. This thesis demands that selective binding sites postulated be present in stoichiometric number to account for the solute accumulated. Thus there must be enough fixed negative sites (carboxyl, phosphate, etc.) present within the cell to interact with the  $K^+$  accumulated within the cell. The idea utilized to account for  $Na^+$  exclusion can be generalized; thus all permeant substances which distribute in only a small fraction of the total water of the cell are assumed to be excluded from a greater or lesser volume of the aqueous regions which comprise the ordered unitized intracellular system.

The holistic proposals envisage a requirement for metabolic energy — primarily for the formation of the ordered selective intracellular system; once formed, maintenance of the ordered system requires only minimal energy expenditure.<sup>13,17</sup> Energy is thus required for *organization* and is not directly coupled to solute flow. The ordered selective intracellular system may be disturbed, so that it becomes disordered (in part or *in toto*) and in this case selectivity of the affected region is altered. Thus, excitation (as in nerve or muscle) can be considered to alter the ordered system, so that certain negative sites lose their selectivity for potassium ions; in this case  $K^+$  would leave and  $Na^+$  enter the cell with the gradient. Reformation of the ordered lattice system requires metabolic energy and  $K^+$ ; upon reformation of the ordered system,  $Na^+$  would leave and  $K^+$  enter the cell. In effect holistic proposals envisage an energized *intracellular* mechanism coupling  $Na^+$  and  $K^+$  translocation as an alternative to a cation pump in the plasma membrane.

#### *Present Status of the Concepts*

There is insufficient space to attempt here a critical review of the data *pro* and *con*, which has been advanced to support one theory as against the other. A voluminous literature of review articles, monographs and proceedings of symposia<sup>1-12</sup> present the record of cogent formidable arguments advanced historically in favor of the membrane concept, and against the data and theoretical proposals of the holists. The monographs of Ling<sup>13</sup> and Troschin<sup>14</sup> provide literature summaries from the minority point of view.

Perusal of the writings bearing on these opposing views reveals that, with a few notable exceptions, discussions of transport resemble the monologues of political or theological controversies, rather than scientific dialogues between the protagonists. Views are stated in monistic "either-or" form together with supporting evidence on a few cell types, extrapolated to cells generally; serious attention has rarely been given to arguments of opponents, or to the possibility of penetrating deeply behind the differ-

ences of interpretation within the concepts to attempt to reach a more profound understanding of the problem.

It is the thesis of this presentation that recent advances in our understanding of the principles of structural and functional organization of the cell provide a basis for the pluralistic resolution of the long-standing conflict between these opposing concepts of transport. These advances — made possible by the concurrent development of electron microscopy, together with techniques for isolation and biochemical study of functional units of characteristic organelles of the cell — have clearly revealed that the principles of the structural and functional organization of cells are characterized not only by uniformity but diversity. The classical transport theories developed their different models of the cell before the advent of electron microscopy; these models have been maintained without substantial modification despite the revolutionary changes in our conceptual model of the cell, produced by electron microscopy. If a sophisticated model of the cell is employed, and diversity as well as uniformity in cell types is taken into account, *certain* ideas advanced by both of the opposing camps of transport are found to be valid. In the context of this model, the antithetical concepts of transport are seen to be complementary — not mutually exclusive antagonists.

As the first step in this attempted reconciliation, we first note that several of the cardinal predictions of the plasma membrane thesis have been definitively established in recent years. The existence of an energized  $\text{Na}^+ - \text{K}^+$  pump in the plasma membrane — denied in principle by the holists — has in fact now been definitively established in erythrocyte ghosts, wherein most of the intracellular hemoglobin has been replaced by simple ionic solutions (for review, cf.<sup>18</sup>). This definitive finding, first indicated in 1954 by Straub's results with erythrocyte ghosts<sup>19</sup> has made it possible to investigate various biochemical aspects of this cation pump. The immediate energy source has been shown to be ATP.<sup>18</sup> The stoichiometric relationship of the energetics of ion translocation in the erythrocyte membrane system has been shown to involve the efflux of 3  $\text{Na}^+$  and the influx of 2  $\text{K}^+$  per molecule of ATP utilized.<sup>20</sup> A membrane-bound enzyme — a  $\text{Mg}^{++}$  ATPase requiring both  $\text{Na}^+$  and  $\text{K}^+$  for activity — first discovered in lobster nerve by Skou<sup>21</sup> has clearly been shown to be an integral component of the pump. The fact that ouabain — known to inhibit cation transport in certain cell types — selectively inhibits this ATPase has served importantly to relate this enzyme to cation transport. The demonstration of similar membrane-bound  $\text{Na}^+ - \text{K}^+ - \text{Mg}^{++}$  ATPases in liver, intestine, heart, muscle, brain, kidney (for references cf. <sup>22</sup>), as well as erythrocytes and nerve, has become widely accepted as evidence for the view, long held, that a coupled cation pump would eventually prove to be present in the plasma

membranes of cells generally. Indeed, this ATPase activity is now widely utilized as a marker for the presumptive presence of plasma membrane fragments in broken cell preparations.

A second cardinal prediction of the plasma membrane thesis concerns the primary importance of the surface membrane relative to the cell interior in the generation of bioelectric potentials; this view, too, may now be regarded as established. Perfused preparations of giant nerve fibers, where the bulk of axoplasm have been removed and replaced by simple aqueous solutions of electrolytes, exhibit resting membrane potentials and action potentials<sup>23</sup> which are in essential accord with the classical membrane theory of Hodgkin and Huxley.<sup>24</sup> Some findings with perfused nerve preparations, however, are difficult to explain and the view is emerging that the origin of membrane potentials may be considerably more complex (cf. <sup>25</sup>), than originally envisaged in the widely accepted classical theory.

Concurrent with these developments, the importance of the cell interior for transport phenomenon — long emphasized by the holists — has likewise been unequivocally demonstrated by biochemists in the course of studying the functional activities of membrane bounded organelles, isolated from disrupted cells. Studies of the nature of "relaxing factor" of muscle led to discovery of a particulate system now considered to be the "microsomal" vesicular membrane fragments derived from the paired membrane system of the sarcoplasmic reticulum. The muscle relaxing factor has been the subject of a recent symposium organized by Gergeley (1964. *Federation Proc.* 23: 885-939). In skeletal muscle this system has *two* components<sup>26</sup>: the sarcoplasmic reticulum proper and a transverse tubular system which represent invaginations of the sarcolemma, the plasma membrane of the muscle fiber. Biochemical investigation of this isolated membrane system has clearly revealed the existence of an ATP-energized system which directionally translocates  $\text{Ca}^{++}$  (and oxalate or phosphate as counterion) across the membrane so that calcium precipitates are accumulated within membrane vesicles (cf. <sup>27</sup>). This  $\text{Ca}^{++}$  sequestering system is now invoked as a coupling system linking excitation with muscle contraction (cf. <sup>28-30</sup>); relaxation is induced when the system removes  $\text{Ca}^{++}$  from the hyaloplasm and the actomyosin contractile system; following excitation, the sarcotubular system is inhibited so that  $\text{Ca}^{++}$  is released and becomes available for the system of actin and myosin filaments inducing contraction.

In similar fashion studies designed to elucidate various functional relationships in mitochondria revealed the existence of a system in the membranes of this organelle for the energized directional translocation of divalent ions (e.g.  $\text{Ca}^{++}$ ,  $\text{Mg}^{++}$ , and  $\text{Mn}^{++}$ ); for reference see the monograph of Lehninger.<sup>31</sup> All typical mitochondria consist of an outer membrane, an inner membrane whose infoldings form the cristae and two aqueous chambers — one between the two membranes, the other on the

interior side of the inner membranes.<sup>32</sup> The accumulation of calcium (or other divalent cations) together with phosphate has been observed to lead to calcium (or  $Mg^{++}$ ) precipitates within the interior chamber of the mitochondrion. The system involved in energized translocation of ions, observed in mitochondria from all cell types studied, is energized by ATP or electron flow through the electron transfer chain; the energetic system is generally considered to be localized in the inner membrane (cf.<sup>33</sup>).

Energized processes leading to the accumulation of  $Na^+$ ,  $K^+$ , and of amino acids in isolated thymic nuclei have been demonstrated;<sup>34</sup> this organelle is likewise membrane bounded. The findings that diverse membrane systems in the cell exhibit so-called active transport properties, has led to the view<sup>35</sup> that cellular membrane systems—as a class—and independent of whether they are at the surface of the cell or in the interior—possess specialized macromolecular assemblies for transducing metabolic energy into osmotic work.

#### *Nature of Membranes in the Cell*

Let us therefore reexamine the fundamental problems of transport in the light of present information about the structural and functional organization principles of the cell (cf.<sup>32</sup>).

Electron microscopy has revealed that animal and plant cells generally exhibit a profusion of membrane systems in the cell interior as well as at the surface. The membrane at the cell surface was often found to infold tortuously into the cell interior. A greater or lesser part of the cytoplasm (depending upon cell type) was found to be filled with a paired membrane system designated as the endoplasmic reticulum (ER); all of the characteristic organelles of the cell—including the nucleus, mitochondria, Golgi apparatus, lysosomes, various plastids, etc.—are bounded by membranes. The membrane system of the ER, in many cell types, is in intimate contact with the membranes of the various organelles and with the plasma membrane. The diversity of cell structure as between various specialized cell types has been amplified by electron microscopy, particularly with respect to the membrane systems of the cell. Concurrent biochemical studies of the isolated organelles from cell fractions then served to establish the now well-known functional specialization of various organelles. From these combined studies it became clear that a fundamental principle of cellular organization in all animal and plant cells (but not bacteria) involved the ample use of membranes to separate the cell interior into discreet segregated compartments and to provide a solid framework for the precise arrangement of active functional units for the energetic and replicative processes of the cell.

The invisible (by light microscopy) plasma membrane, which had been earlier predicted to account for the permeability and transport properties

of cells, was revealed by electron microscopy. It proved to have characteristic morphological features which may now be confidently attributed to a lipoprotein membrane of a general type envisaged in the classical Davison-Danielli model of the plasma membrane.<sup>36</sup> In potassium permanganate-fixed preparations a characteristic trilaminar pattern was observed consisting of two narrow dense lines separated by a band of low density but of similar width, the thickness of the trilaminar unit being about  $75\text{\AA}$ .<sup>37</sup> Later study revealed that most, if not all, of the various membrane systems of the cell exhibited this characteristic trilaminar feature. This morphological uniformity of cellular membranes finds expression in the now widely accepted concept of the *unit-membrane* vigorously promulgated by Robertson.<sup>38-41</sup> This concept holds that all of the various membranes in the cell are built on a single fundamental design principle; the basic plan of structural organization involves two monolayers of lipid sandwiched between two fully spread monolayers of non-lipid components — thought to be protein — differing somehow in structure to produce an asymmetrical unit-membrane. The similarities and differences between the unit membrane concept and the Davison-Danielli model have been discussed by Robertson.<sup>41</sup>

We have already seen that the functional diversity associated with this morphological uniformity is expressed by different types of functional units associated with the various membranes. At the molecular level this diversity is expressed in profound differences in the types of membrane associated enzymes. Each type of membrane in turn exhibits a characteristic enzymatic pattern of uniformity together with distinctive features; thus when a single type of membrane is considered, differences and similarities are observed when one cell type is compared to another in the same organism, or as between species. This association of uniformity with distinctiveness has been most clearly observed for the enzymes associated with membranes of the endoplasmic reticulum (cf. <sup>42</sup>) and of mitochondria (cf. <sup>31</sup>).

Fernández-Móran<sup>43-46</sup> has vigorously promulgated the concept that a laminar hydrated lipoprotein system — similar in all membrane systems — provides a structural framework for specialized unitized transducing units periodically arranged in the matrix of the membrane. Functional differences, as between membranes, would then depend upon the types of transducing units present; the morphological uniformity would be the expression of the ordered lipoprotein matrix. The transducing units are considered to be ordered macromolecular assemblies (consisting of the membrane bound enzymes and other macromolecules coupled spatially and energetically in unitized systems) responsible for energized membrane processes, for example for the vectorial translocation of specific solutes (ions, etc.), contraction, etc. Some very general ideas are available about the nature of the componentry required for energized transduction devices



in the membrane; an encouraging beginning in approaching this fundamental problem has been achieved particularly in mitochondrial membranes, where periodically arranged membrane subunits were first visualized by Fernández-Móran<sup>46</sup> and then by others.<sup>48-50</sup> At this time, neither the chemistry of all of the essential componentry nor the molecular arrangement of the parts of these membrane subunits is known with certainty. The fundamental attempt of H. Fernández-Móran and D. E. Green, together with their associates,<sup>51</sup> to correlate structure with function in the mitochondrial membrane systems has attracted wide interest and several groups are now actively working on this problem. If the energized directional translocation of solutes through a membrane is arbitrarily designated a "pump" (independent of other mechanistic connotations), the rate of progress already achieved in this field suggests that the mitochondrial pump for divalent cations may well turn out to be the first membrane pump to be dissected and fully described at a molecular level.

Functional diversity in membranes may be attributed to factors other than differences in transducing units. It is widely appreciated that functional differences as between membranes may reside in different types of mucopolysaccharide or glycoproteins which may serve as extrinsic coatings at the outermost membrane layers (cf. for example<sup>51</sup>). Indeed, specialized "coatings" of this type have been widely considered as a possible basis for the asymmetrical nature of the unit membrane.

#### *Nature of Water in the Cell*

Given a conceptual picture of the cell where a widespread system of membranes provides segregated compartments and "housing" for various types of functional units, it becomes immediately apparent that the water of the cell exists in heterogenous aqueous regions, which may differ widely from one cell type to another. The concept that cell water exists as a single predominant type of bulk phase in all cell types, be it the simple aqueous compartment of the type envisaged in active transport theory, or "special" water structures of unitized intracellular systems of the holists, is almost certainly untenable. With regard to the nature of cell water, both concepts of transport may be partially valid in that each emphasizes one of several types of water structure present in the heterogenous aqueous regions of the cell.

Several types of morphologically distinctive aqueous regions are present in the "typical" mammalian cell, as revealed by electron microscopy. In each type of region, water molecules find themselves in different environments; accordingly different types of water structures may be envisaged. At a gross level we can distinguish between: (a) water *within* the membrane structure; (b) one or more layers of water directly in contact with extended relatively immobile macromolecular surfaces, be it at the surfaces

of membranes or highly ordered structural components of certain cell types (eg. the contractile system in muscle fibers), or filaments of DNA in the chromosomes of the nuclei; (c) water *between* closely paired systems of unit membranes, as in the aqueous region between the interior and outer membranes of the mitochondria, or in the cisternae of the endoplasmic reticulum; (d) water within interior chambers of an organelle, like the mitochondrion or between the structural nucleoprotein components of the nucleus; (e) water in the hyaloplasm between the various organelles in the cell.

The point to be made is that a sizeable fraction of all the water in the "typical" cell is intimately associated with the membrane systems, whether at the *surface* or *within* the membrane structure proper. Water thus associated with membranes or other "fixed" structural components must be sharply differentiated from the water in the hyaloplasm. In the hyaloplasm most of the water is mobile and may not differ much either in structure or properties from the water structures existent in simple aqueous solutions of water soluble proteins. Part of the water in hyaloplasm is firmly associated with "mobile" solutes, some of which are macromolecules (eg. certain enzymes and certain RNA's) which are translocated from one site to another in the hyaloplasm, eventually to impinge upon a "fixed" macromolecular surface (eg. a membrane). Most of the water in the hyaloplasm, however, would resemble the types of hydrogen-bonded water clusters (cf. Frank, this symposium) thought to exist in ordinary liquid water, which continually change — as hydrogen bonds are broken by thermal energy and then reform — to give a somewhat different structural water polymer. If the "cellular water" advanced by the proponents of the cell membrane theory of transport exists anywhere in the cell, it exists in the hyaloplasm.

Contrariwise, if the types of water structures envisaged in holistic proposals of transport exist anywhere in the cell, the most likely locus for such structures would be the water associated with the system of membranes, and with other extended macromolecular surfaces of the fixed structural elements of the cell. It has long been appreciated that water is a bulk component of membrane systems, comprising 30–50 per cent of the total system, and must therefore figure importantly in the molecular organization of the system (cf. <sup>43-45,52,53</sup>). In an ordered lamellar system of this type, it has long been considered that the water in a highly ordered membrane system must likewise be "highly ordered" in relation to the polar groups of both the protein and lipid components of the membrane. Fernández-Móran,<sup>11-17</sup> in particular, has emphasized the concept that water in the membrane must be highly ordered, whether in "ice-like" or crystal hydrate lattices, to serve an integral role in the structural and functional processes of the membrane. This view can be traced back to Szent-Györgyi's concept of ordered water<sup>21</sup> poetically envisaged as serving an essential role

in various functional processes in the cell. Applied to the membranes, rather than to the cell as a whole, Fernández-Móran<sup>44-46</sup> has indicated how this concept serves as a powerful mechanistic basis for understanding a variety of essential processes in the membrane. Thus, localized reversible phase changes in ordered water structure can be envisaged to provide the mechanistic basis for conformational changes in protein layers and concurrently modify the arrangement of the polar lipids from an ordered bimolecular leaflet to a less tightly packed micellar form. These phase transitions through the various phases of the membrane could "spread" as water structure changes reversibly, and provide a molecular basis for propagation of a local perturbation. Selective permeability might be envisaged in terms of molecular sieves lined with ordered water; the marked permeability changes induced by excitation could be the consequence of the "melting" of water structures in special regions. By providing an interconnected hydrogen bonding medium, ordered water structures could participate in fast protonic charge transport mechanisms of a type demonstrated by Eigen and DeMaeyer,<sup>55</sup> or in electron transport, via hydrogen free radical or hydride ion as suggested by Klotz.<sup>56</sup> There is no question that the idea of ordered water lattices as an integral structural component of the membrane, as promulgated by Fernández-Móran, has great power in providing a conceptual basis for understanding a multiplicity of fundamental mechanisms associated with membrane function. The precise molecular nature of the ordered membrane water is unknown; the question whether this water in the membrane is arranged hexagonally in an "ice-like" lattice or pentagonally in crystalline-hydrate types of water<sup>57</sup> or in yet another form cannot be answered at this time. Nuclear magnetic spectroscopy offers the potential of a non-destructive method for evaluation of water structures<sup>44</sup> but there are profound difficulties in interpreting changes in the proton resonance signal of water in systems of this order of complexity. Despite uncertainties containing the precise structures involved, there is strong evidence from a variety of sources for the structural role of water in the membrane systems. The recent report of Person and Zipper<sup>58</sup> provides exceptionally strong evidence for this concept. These authors have reported that treatment of mitochondrial suspensions with a *dry* zeolite produces the same type of membrane disruption, as achieved by treatment of mitochondrial membranes with detergents; membrane-bound cytochrome oxidase is solubilized and the lipids become separable from the residual membrane fraction. These disruptive results are not achieved if the zeolite preparation is wetted; thus membrane disruption is attributed to the avidity of the zeolite preparation for water, but only in part, because the zeolite may serve to remove divalent cations ( $Mg^{++}$ ?) from key cross-linked mitochondrial sites which are critical for maintenance of structure. Independent of the latter possibility, the findings of Person and Zipper<sup>58</sup>

provide substantial support for the thesis that water serves as a major structural link for the protein and lipid moieties in ordered lipoprotein structures.

Elsewhere I have described<sup>59-61</sup> a model of cellular membranes to illustrate the fundamental molecular organization of the lipoprotein matrix; in effect a variety of ideas dealing with selected aspects of membrane structure and function, developed by others, have been brought together in a unifying configuration. The new model attempts to "fill-in" the molecular details of protein and water structure "missing" from the unit-membrane concept. Starting with Warner's hexagonal principle of peptide and protein structure (discussed by Warner in this monograph), it is possible to conceptually envisage a system of interlocked hexagonal protein discs arranged in a hexameric goeodesic pattern<sup>62</sup> forming a protein layer, two of these layers being "cemented" together by ordered water lattices in a hexagonal ice-like arrangement to form the protein envelopes of a unit-membrane. The hexagonal arrangement of peptide structure visualized by Warner provides an ordered arrangement of the carbonyl oxygens of the amide bonds of polypeptides in a regular hexagonal arrangement which corresponds to a *second neighbor* relationship to the oxygens of the "ice lattice" (4.8 Å). This peptide conformation provides an extensive ordered system of hydrogen bonding sites for water molecules arranged hexagonally as in ice. Warner has reported at this meeting that the carbonyl oxygens of the ester bonds of triglyceride can be "fitted" perfectly into the hexagonal water structure, these oxygens replacing the oxygen in water. Warner and I (unpublished studies) have studied structural models of several typical phospholipids; there appear to be no special difficulties in arranging polar groups of phospholipids, so that they likewise fit the ordered ice-like water structure. In Warner's model of the TMV virus, a hexameric arrangement of protein subunits, three on three, is employed to build a protein coat as discussed at this meeting. Two types of channels emerge in this overlap pattern: upon analysis they turn out to be permselective and available for *either* cations *or* anions.

Using the architectural principles of Warner, it then becomes possible to "fill-in" the protein and water structures of a unit-membrane with the familiar bimolecular leaflet of lipid between protein coats. It then becomes possible to envisage the nature of molecular changes associated with changes in membrane structure and function in terms of this model. To date the model has been utilized to provide a basis for the molecular interaction of peptide hormones with specific receptors in responsive cells<sup>59</sup> and for the changes in the nerve membrane associated with depolarization.<sup>60,61</sup> FIGURES 1 and 2 illustrate some central features of the model, and show in schematic form the neuronal membrane at "rest" and following depolarization. (For an adequate treatment and discussion of the

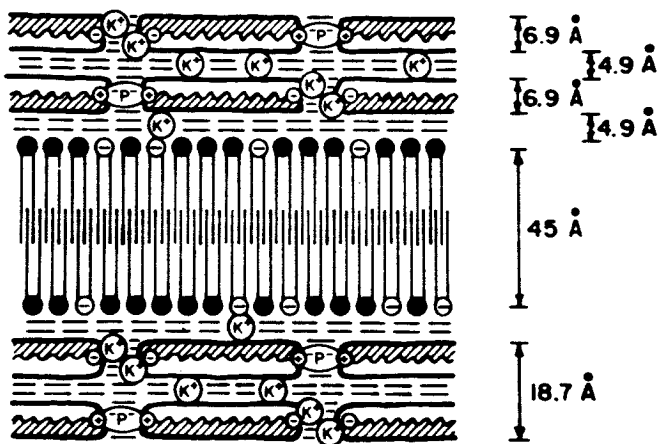


FIGURE 1. A schematic representation of the "resting membrane" where the basic features of the unit-membrane concept are retained and the protein layers are represented as a system of interlocked hexagonal discs "cemented" together by water layers in an ice-like arrangement to form a precisely ordered lattice system. The individual hexagonal subunits are shown as "interlocked" through hydrophobic surfaces to form "disc units" held together by two layers of water in an ice-like state, this type of water being represented as (—). The aqueous channels in the protein layer of the membrane possess fixed charge sites, and are shown in a "staggered" relationship; most of the water in the aqueous channels has an "ice-like" structure. The bilayer arrangement of the mixed lipids, involving interdigitation of fatty acid tails, is assumed to be dependent upon the "ice-like" layers of water which fix the hydrophilic portion of lipid molecules in position in relation to the hydrophilic surfaces of the neighboring protein subunits. Potassium is shown as the principal counterion for fixed negative sites in the resting membrane, phosphate as the counterion for fixed positive sites; but other ions possibly involved are not shown. In this model selectivity for potassium over sodium ion depends upon the organization of the membrane units to form a precise lattice.

proposed model, interested readers are referred to the detailed publications.) The essence of the proposal is that the polarized membrane is envisaged as a precisely ordered lattice involving arrangements of monolayers of protein, lipids, and "ice-like" water, depolarization as the induction of localized "disorder", each component exhibiting a characteristic phase transition which then "spreads" through the membrane phase. We may note in passing that the lattice arrangement envisaged in the membrane bears a remarkable resemblance to the arrangements of macromolecules and water structures in certain holistic proposals of transport.<sup>13,16,17</sup>

Having discussed ordered water lattices in the membrane phase of the cell, it remains to be stated that water may also be ordered in extensive hydrogen-bonded lattices at the surface of extended macromolecules whether at the surfaces of membranes or of structural filaments, such as

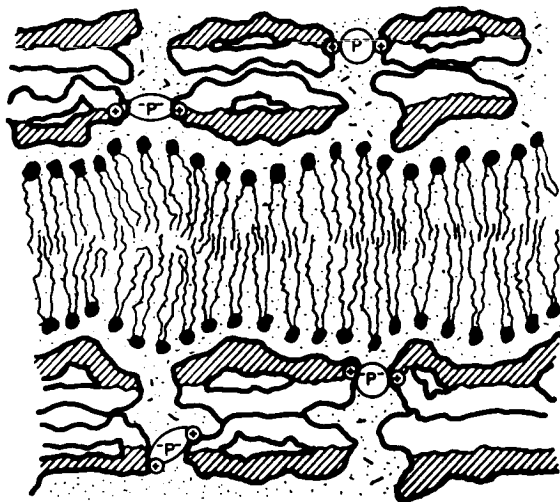


FIGURE 2. A schematic representation of the "depolarized" membrane, where the arrangement of protein subunits, lipids, and of water no longer provide a precisely ordered lattice. For purposes of illustration, the hypothetical changes in the various structural components of the membrane are highly exaggerated. The protein subunits have changed from hexagonal discs to a more globular helical form, the lipid bilayer to a more random micellar arrangement, and the "ice-like" water structures to less ordered water structures. In consequence the fixed negative sites in the depolarized region of the membrane no longer exhibit high selectivity for potassium over sodium. Mobile water molecules, represented as small dots ( $\bullet$ ), thus become available and provide aqueous channels which permit relatively free diffusion of cations *with* the electrochemical gradient. The phosphate cross-links between neighboring fixed positive sites are shown as "undisturbed," to indicate that the membrane structure does not "break down" completely; other links which maintain membrane structure and which provide the basis for reversal to the "resting" membrane state are not illustrated.

actomyosin. The nature of such water structures would here depend upon the polar or nonpolar nature of the surface groups exposed to the aqueous environment. If a large number of polar or hydrogen-bonding sites are exposed and arranged in an ordered manner (as envisaged in our model of membrane) extensive hexagonal ice-like lattices several layers thick may be envisaged. If nonpolar groups of proteins are exposed, pentagonal "cages" of water clathrate might be formed as Klotz<sup>63</sup> has suggested; alternative modes of modifying local water structure in the neighborhood of nonpolar groups have been suggested by Kauzmann<sup>64</sup> and Scheraga.<sup>65</sup>

The important point which emerges from the foregoing discussion is that not one, but several types of water structures appear to be present in the cell. To the degree that a particular cell type exhibits a sparse intracellular membrane system, and accordingly a large relative volume of

hyaloplasm, the intracellular water would resemble the ordinary liquid water assumed in the plasma membrane concept of transport. Contrariwise, if a particular cell type is "loaded" with membrane systems and the relative volume of hyaloplasm is small, intracellular water would be profoundly different in structure and properties from liquid water and resemble the type of water envisaged in holistic proposals.

Given profound diversity in cell structure, particularly with respect to membrane systems, it is apparent that water structure in various cell types may be very different. It has been estimated<sup>35</sup> that in certain cell types, where the endoplasmic reticulum is well developed, the membrane systems of the cell plus attached componentry may account for perhaps as much as 80-90 per cent of the total cell mass. The estimated value for membrane plus componentry in the case of the hepatic parenchymal cell is about 50-60 per cent. In bacterial protoplasts, where subcellular organelles are not present, the cell membrane by itself accounts for about 10 per cent of the mass;<sup>66</sup> the value for the mature erythrocyte would be very much less than 10 per cent. These rough estimates give some idea of the variations in the proportions of hyaloplasm to "membrane" in different cell types. They illustrate the hazard of extrapolating findings relating to the water of one cell type (say erythrocytes) to all cells generally. This is an important, but largely neglected consideration in transport theory. It does not appear to be a coincidence that the proponents of membrane pumps have emphasized studies on the red cell, whereas the proponents of the holistic thesis have emphasized data on muscle.

#### *The Number and Locus of Selective Binding Sites*

It will be recalled that one of the fundamental differences between the plasma membrane concept of transport and its holistic alternatives concerns the locus and number of selective binding sites postulated to be present in the cell. To account for the selective accumulation of  $K^+$  (or amino acids, sugars, etc.), the membrane thesis postulates a catalytic number of selective binding sites associated with solute specific pumps in the plasma membrane; the holistic thesis postulates a stoichiometric number of selective binding sites distributed throughout the cell. If selective binding sites are present in all membrane systems, whether at the cell surface or interior, it would be expected that the diversity in intracellular membrane systems observed in cell types would be associated with wide variations in the number and locus of selective binding sites.

The erythrocyte serves as an example of a cell type where the selective binding sites for transport may be exclusively localized in the plasma membrane; it is very clear, however, that the erythrocyte is a very atypical cell as compared to other mammalian cells which possess characteristic systems of intracellular membranes. The accumulation of a substance by

a more "typical" cell (where the hyaloplasm represents about 20-50 per cent of the cell volume) is more likely to be the resultant of both solute binding to selective sites on membranes distributed throughout the cell, *and* to energized translocation devices in membranes. On this basis, selective binding sites involved in solute accumulation would be present in *neither* catalytic *nor* stoichiometer number, but at some intermediate value which would vary from one cell type to another, depending upon the nature and extent of the intracellular membrane systems present. In effect both types of selective binding sites are present: one type associated with transduction devices serving a catalytic role in solute translocation through the membrane; the other type serving to bind solute selectivity, in a structural sense as envisaged by the holists, not involving translocation through the membrane phase.

Both types of selective binding sites are observed in the studies of calcium accumulation by the isolated sarcotubular membrane vesicles of skeletal muscle. If the vesicles are incubated in presence of  $Mg^{++}$  and ATP, with  $Ca^{++}$  and a calcium precipitating anion (like oxalate or phosphate),  $Ca^{++}$  accumulation involves energized translocation of ions through the membrane phase as demonstrated by calcium precipitates inside the membrane vesicle (cf.<sup>27</sup>). This translocation of ions involves binding sites specific for  $Ca^{++}$  since  $Mg^{++}$ , though required, is not similarly translocated. However, if vesicles are incubated with  $Ca^{++}$  and a counterion which does not serve as a calcium precipitate, ATP dependent calcium accumulation though at a lower level, can likewise be demonstrated; this type of accumulation has been attributed to binding sites on the lipoprotein membrane which are selectively available for  $Ca^{++}$  in the presence of ATP. Thus, for example, Ohnishi and Ebashi<sup>67</sup> have demonstrated considerable binding of  $Ca^{++}$  to the membrane within 30 milliseconds; though this selective binding requires ATP, there is no correlation between  $Ca^{++}$  uptake and ATP breakdown. Indeed, Ebashi<sup>68</sup> believes the  $Ca^{++}$  released in response to excitation is Ca bound to the membrane of the sarcoplasmic reticulum rather than that from inside the vesicles.

To consider the process in isolated sarcotubular vesicles as active transport of  $Ca^{++}$  as in classical membrane transport theory, would require knowledge of the activity coefficients of the transported ions in the two aqueous compartments separated by the membrane. There are no special difficulties in measuring the activity coefficients of the ions in the exterior medium; since calcium oxalate precipitates inside the vesicle, it would appear that the product of the activities of calcium and oxalate inside the vesicle would be identical with the solubility product of calcium oxalate.<sup>27</sup> The latter postulate is correct, however, only if the aqueous region inside the vesicles is a simple aqueous solution. Is this actually the case? It is known that the membranes shrink during the accumulation of calcium



oxalate (or phosphate) forming egg shaped dense bodies;<sup>27</sup> the volume and structure of intervesicular water is completely undefined; so is the pH. One wonders, therefore, how activity coefficients for  $\text{Ca}^{++}$  and oxalate can be estimated in an undefined aqueous system of this type of complexity.

The difficulty in determining whether  $\text{Ca}^{++}$  accumulation in the sarcotubular vesicles actually represents active transport in a classical sense, reappears in the mitochondrial system. A similar vectorial process of energized translation of  $\text{Ca}^{++}$  and phosphate has been observed in mitochondria, leading to the precipitation of calcium salts in the interior chamber of the mitochondrion (cf.<sup>31,69-71</sup>). In addition to the difficulty of determining activity coefficients of ions in the interior chamber of the mitochondrion, another complicating factor arises from vectorial biochemistry<sup>72</sup> and must be taken into account. Mitchell<sup>72</sup> has indicated that the mitochondrial oxidation of pyridine nucleotides, which ultimately gives rise to  $\text{H}_2\text{O}$  involves the asymmetrical discharge of protons ( $\text{H}^+$ ) to the external medium and of  $\text{OH}^-$  to the interior chamber of the membrane system. The effect of hydroxyl ions to facilitate calcium precipitation in solutions of  $\text{Ca}^{++}$  and phosphate (or oxalate) is well known; one wonders to what extent the energized translocation of divalent cations might more appropriately be termed the energized production and asymmetrical discharge of  $\text{H}^+$  and  $\text{OH}^-$  across a membrane. If the  $\text{H}^+$  and  $\text{OH}^-$  required for splitting of ATP by the ATPase in sarcotubular vesicles (because of spatial relationships in the membrane phase) were derived from protons from water *inside* the vesicle, and hydroxyl ions from the external aqueous medium, the net effect would be the production of  $\text{OH}^-$  inside the membrane; the precipitation of calcium with oxalate within the vesicles of the sarcoplasmic reticulum would be expected to be profoundly influenced.

Having discussed problems arising in the active transport of  $\text{Ca}^{++}$  by intracellular membrane systems, we may now return to our initial question of how cells accumulate  $\text{K}^+$  and exclude  $\text{Na}^+$ . Let us immediately grant that  $\text{Na}^+-\text{K}^+$  coupled ion pump exists in the plasma membrane of the erythrocyte and that the ouabain-sensitive  $\text{Na}^+-\text{K}^+-\text{Mg}^{++}$  ATPase is an integral component of this cation pump. Is this pump the prototype of a universal cation pump present in the plasma membrane of all cell types, and exclusively responsible for the universally observed distribution of  $\text{K}^+$  and  $\text{Na}^+$  in tissues and cells generally? Or must we envisage the participation of several types of mechanisms involving not only the plasma membrane, but the system of intracellular membranes as well? Although there is evidence that the effect of ouabain upon  $\text{Na}^+$  and  $\text{K}^+$  transport in some eight tissues is qualitatively similar to the effects of ouabain upon the  $\text{Na}^+-\text{K}^+-\text{Mg}^{++}$  ATPase,<sup>73</sup> definitive evidence to answer this general question is not available. There is enough data available, however, to strongly suggest that a plurality of mechanisms is operative in  $\text{K}^+$  accumu-

lation associated with  $\text{Na}^+$  exclusion. Gamble<sup>74</sup> has shown that selective binding sites for  $\text{K}^+$ , unavailable for  $\text{Na}^+$ , are present in fragmented mitochondrial membranes; the selectivity of these sites depend upon ATP (cf. Discussion of Gamble's studies in<sup>31</sup>). Moreover, it has been shown that during the energized translocation of  $\text{Ca}^{++}$  into mitochondria from liver, kidney, heart, and brain,  $\text{K}^+$  leaves the mitochondrial membrane while external  $\text{Na}^+$  enters;<sup>75</sup> thus an energized coupled  $\text{Na}^+\text{K}^+$  membrane process is widely distributed in the mitochondrial membrane system.  $\text{K}^+$  is specifically required for protein synthesis by ribosomal systems,<sup>76</sup> and other cations are ineffective, suggesting the existence of binding sites selective for  $\text{K}^+$  in this system as well. We have previously discussed the translocation of  $\text{Na}^+$  and  $\text{K}^+$  against apparent thermodynamic gradients in isolated nuclei,<sup>17</sup> where fixed negative sites on polynucleotide polyelectrolytes are available.

Thus intracellular membrane systems do provide selective intracellular binding sites for  $\text{K}^+$ . Depending upon the nature and extent of the membrane systems of a particular cell type (together with extended macromolecular structural components) relative to hyaloplasm, a greater or lesser fraction of the  $\text{K}^+$  accumulated by the cell would be the consequence of selective intracellular binding sites, as proposed by the holists. As the ratio of "hyaloplasm" to "membrane" decreases, the importance of selective binding of  $\text{K}^+$  for accumulation would increase. To the extent that this process is operative, the  $[\text{K}^+]$  in the hyaloplasm would be lower and the  $[\text{Na}^+]$  higher than estimated for the cell as a whole.

While selective binding of  $\text{K}^+$  at sites on mitochondrial, nuclear, and other organellar systems may be envisaged (together with some  $\text{K}^+$  binding on polynucleotides, actomyosin, etc.), the problem remains that  $\text{Na}^+$  must be removed from the cell interior. The membrane system of the endoplasmic reticulum is unique among the intracellular membranes of the cell in that it may directly communicate with the cell exterior. It is apparent that an energized cation pump localized in this intracellular membrane system, which discharges  $\text{Na}^+$  into the cisternal aqueous region between the membranes, would effectively remove  $\text{Na}^+$  from the cell hyaloplasm. In this latter connection it is of interest to note that in many studies (cf.<sup>22</sup>), the  $\text{Na}^+-\text{K}^+$  dependent ATPase in brain and kidney has been localized in the microsomal fraction, but the cytological origin of the activity has not been definitively established. The enzyme from membrane fragments of certain kidney preparations are attributed by Kinsolving et al.<sup>22</sup> to the plasma membrane; on the other hand, Abood<sup>76</sup> believes that the  $\text{Na}^+-\text{K}^+$  dependent ATPase in brain may be associated with membranes of the endoplasmic reticulum as well as the plasma membrane. Thus there is a real possibility that in certain cell types the  $\text{Na}^+-\text{K}^+$  ATPase activity involved in transport may not be exclusively localized in the plasma

membrane but may be present in the endoplasmic reticulum as well. The recent finding of an ATPase in the sarcoplasmic reticulum of skeletal muscle<sup>77</sup> activated by either  $K^+$  or  $Na^+$ , and which is not ouabain-sensitive, serves to remind us that more than one kind of membrane and more than a single type of enzymatic mechanism may be involved in the old problem of  $K^+$  accumulation and  $Na^+$  exclusion. Conway's<sup>78</sup> findings suggesting that the Na pump in frog skeletal muscle appears to involve a redox system pump, where lactic dehydrogenase and not ATPase participates, would be consistent with the above idea.

It must be emphasized that in specialized differentiated cells, the various membrane systems of the cell are likewise differentiated, both in structure and function. We have seen that specialized endoplasmic reticulum of skeletal and cardiac muscle fibers possesses a sequestering system for  $Ca^{++}$  which is highly selective. The endoplasmic reticulum in other cell types, such as liver<sup>72</sup> does not possess this system. In cells other than muscle fibers, the mitochondria appear to be the primary devices utilized to sequester  $Ca^{++}$ , but other divalent cations (such as  $Mg^{++}$ ,  $Mn^{++}$ ) are similarly sequestered. Thus, the mitochondrial system is not as selective for  $Ca^{++}$  (or as fast) as the sarcotubular system in muscle. Given functionally specialized cells, exhibiting uniformity and diversity at all levels, it may safely be predicted that when the molecular mechanisms of maintaining an unequal distribution of  $Na^+$  and  $K^+$  in cells are discovered, once again a pattern of uniformity associated with diversity will emerge.

### *Epilogue*

We have discussed the two opposing classical concepts of transport. Upon analysis, both ideas are shown to be right in part; and both partially wrong. The proponents of the plasma membrane thesis of transport were wrong in that they neglected the role of the cell interior; the holists were wrong in their deemphasis of the plasma membrane and of intracellular membranes generally. If one considers that membrane systems throughout the cell are involved in transport, and that cells exhibit diversity as well as uniformity, a pluralistic resolution is achieved. This conclusion, so obvious to me today, was first presented to me in 1959 by a friend of many years, Theodore Shedlovsky of the Rockefeller Institute. We had been discussing the nature and structure of water in the cell, the polyelectrolyte character of intracellular macromolecules and certain findings in my laboratory, all of which seemed to me to be wholly inconsistent with the plasma membrane thesis. Shedlovsky agreed. However, I also knew of other data which almost forced one, as in chess, to the plasma membrane thesis. Shedlovsky agreed. And then he said: "What if what we call transport involves a membrane system *throughout the cell*, so that what we call the cell membrane is really packed inside the cell as well as at the surface?"

I heard then, but did not really listen. Monistic configurations which are all encompassing are so powerful in attractiveness that it was only after several years that I came to understand what Shedlovsky had said.

### References\*

1. HARRIS, E. J. 1960. *In* Transport and Accumulation in Biological Systems. 2nd Ed. Butterworth Scientific Publications. London, England.
2. CHRISTENSON, H. N. 1962. *In* Biological Transport. W. A. Benjamin. New York, N. Y.
3. HODGKIN, A. L. 1958. *Proc. Royal Soc. (B)* **148**: 1.
4. LEAF, A. 1959. *Ann. N. Y. Acad. Sci.* **72**: 396.
5. GLYNN, I. M. 1959. *Internat. Rev. Cytology* **8**: 449.
6. WILBRANDT, W. 1961. *Internat. Rev. Cytology* **13**: 203.
7. SHANES, A. M. 1959. *Pharm. Rev.* **10**: 59.
8. WHITTAM, R. W. 1959. *Ann. Reports Chem. Soc.* **72**: 396.
9. EDELMAN, I. S. 1961. *Ann. Rev. Physiol.* **23**: 37.
10. WILBRANDT, W. 1959. *J. Pharm. Pharmacol.* **11**: 65.
11. PARK, C. R., D. REINWEIN, M. J. HENDERSON, E. CADENAS & H. E. MORGAN. 1959. *Amer. J. Med.* **26**: 674.
12. RANDLE, P. J. & F. G. YOUNG. 1960. *Brit. Med. Bull.* **16**: 224.
13. LING, G. N. 1962. *In* A Physical Theory of the Ling State: The Association-Induction Hypothesis. Blaisdell Publishing Co. New York, N. Y.
14. TROSCHEIN, A. S. 1958. *In* Das Problem der Zellpermeabilität. Fischer. Jena, Germany.
15. ERNST, E. 1958. *In* Die Muskeltätigkeit; Versuch einer Biophysik des quergestreiften Muskels. :355. Verlag Ungarischen Akad. Wissenschaften. Budapest, Hungary.
16. SIMON, S. E., F. H. SHAW, S. BENNETT & M. MULLER. 1957. *J. Gen. Physiol.* **40**: 753.
17. HECHTER, O. & G. LESTER. 1960. *Recent Progr. Hormone Res.* **16**: 139.
18. HOFFMAN, F. 1962. *Circulation* **26**: 1201.
19. STRAUB, F. B. 1954. *Acta Physiol. Hung.* **4**: 235.
20. POST, R. L. & P. C. JOLLY. 1957. *Biochem. Biophys. Acta* **25**: 118.
21. SKOU, J. C. 1961. *In* Membrane Transport and Metabolism. A. Kleinzeller & A. Kotyk, Eds.: 228. Academic Press, Inc. New York, N. Y.
22. KINSOLVING, C. R., R. L. POST & D. L. BEAVER. 1963. *J. Cell Comp. Physiol.* **62**: 85.
23. BAKER, P. F., A. L. HODGKIN & T. I. SHAW. 1961. *Nature (Lond.)* **190**: 885; 1962. *J. Physiol.* **164**: 355.
24. HODGKIN, A. L. & A. F. HUXLEY. 1952. *J. Physiol.* **117**: 500.
25. TASAKI, I. & T. SHIMAMURA. 1962. *Proc. Nat. Acad. Sci. (U.S.)* **48**: 1571.
26. FRANZINI-ARMSTRONG, C. 1964. *Federation Proc.* **23**: 887.
27. HASSELBACH, W. 1964. *Federation Proc.* **23**: 909.
28. WEBER, A., R. HERZ & I. REISS. 1964. *Federation Proc.* **23**: 896.
29. DAVIES, R. E. 1963. *Nature (Lond.)* **199**: 1068.
30. PODOLSKY, R. J. & I. L. COSTANTIN. 1964. *Federation Proc.* **23**: 933.
31. LEHNINGER, A. L. 1964. *In* The Mitochondrion. : 157. W. A. Benjamin, Inc. New York, N. Y.
32. PALADE, G. 1964. *Proc. Nat. Acad. Sci. (U. S.)* **52**: 613.
33. FERNANDEZ-MORAN, H., T. ODA, P. V. BLAIR & D. E. GREEN. 1964. *J. Cell Biol.* **22**: 63.

\*The references listed in this conceptual survey of transport and accumulation represent a small selection of the voluminous literature bearing on this field. Many important papers and reviews necessarily have had to be omitted in this type of treatment.

34. ALLFREY, V. G., R. MENDT, J. W. HOSKINS & A. E. MIRSKY. 1961. *Proc. Nat. Acad. Sci. (U.S.)* 47: 907.
35. LEHNINGER, A. L. 1964. *Neurosciences Research Program Bull.* 2(2).
36. DAVSON, H. & J. DANIELLI. 1952. *In Permeability of Natural Membranes*. 2nd Ed.: 111. Cambridge University Press. Cambridge, England.
37. ROBERTSON, J. D. 1957. *J. Physiol.* 140: 58.
38. ROBERTSON, J. D. 1959. *Biochem. Soc. Symposium (Cambridge, Eng.)* 16: 3.
39. ROBERTSON, J. D. 1960. *Progr. Biophys.* 10: 343.
40. ROBERTSON, J. D. 1962. *Res. Pub. Assoc. Res. Nervous Mental Disease* 40: 94.
41. ROBERTSON, J. D. 1964. *In Cellular Membranes in Development*. M. Locke, Ed.: 24. Academic Press, Inc. New York, N. Y.
42. SIEKOWITZ, P. 1963. *Ann. Rev. Physiol.* 25: 15.
43. FERNÁNDEZ-MÓRAN, H. 1957. *In Metabolism of Nervous Tissue*. D. Richter, Ed.: 1. Pergamon Press, London, England.
44. FERNÁNDEZ-MÓRAN, H. 1959. *Rev. Modern Phys.* 31: 319.
45. FERNÁNDEZ-MÓRAN, H. 1959. *In Biophysical Science: A Study Program*. J. L. Oncley, Ed.: 319. John Wiley & Sons. New York, N. Y.
46. FERNÁNDEZ-MÓRAN, H. 1962. *Circulation* 26: 1039.
47. FERNÁNDEZ-MÓRAN, H. 1964. *J. Royal Microscop. Soc.* 83: 183.
48. PARSONS, D. F. 1963. *Science* 140: 985.
49. SMITH, D. S. 1963. *J. Cell Biol.* 19: 115.
50. STOECKENIUS, W. 1963. *J. Cell Biol.* 16: 483.
51. FAWCETT, D. W. 1962. *Circulation* 26: 105.
52. SCHMITT, F. O., R. L. BEAR & K. J. PALMER. 1941. *J. Cell. Comp. Physiol.* 18: 31.
53. FINEAN, J. B. 1957. *J. Biochem. Biophys.* 3: 95.
54. SZENT-GYÖRGYI, A. 1957. *In Bioenergetics*. : 32. Academic Press, Inc. New York, N. Y.
55. EIGEN, M. & L. DE MAEYER. 1959. *In The Structure of Electrolytic Solutions*. W. J. Hamer, Ed.: 64. John Wiley & Sons. New York, N. Y.
56. KLOTZ, I. M. 1962. *In Horizons in Biochemistry*. M. Kasha & B. Pullman, Eds.: 523. Academic Press, Inc. New York, N. Y.
57. PAULING, L. 1961. *Science* 134: 15.
58. PERSON, P. & H. ZIPPER. 1964. *Biochem. Biophys. Res. Comm.* 17: 225.
59. HECHTER, O. NATO Conference on Mechanisms of Hormone Action. P. Karlson, Ed. Meersburg, Germany (May, 1964). *In press*.
60. HECHTER, O. 1965. *Federation Proc.* 24: S-91.
61. HECHTER, O. 1964. *Neurosciences Res. Program Bull.* 2(5).
62. CASPAR, D.L.D. & A. KLUG. 1962. *Cold Spring Harbor Sympos. Quant. Biol.* 27: 1.
63. KLOTZ, I. M. 1960. *Brookhaven Symposium in Biol.* No. 25. Brookhaven National Laboratory, Upton, New York.
64. KAUFMANN, W. 1959. *Adv. Protein Chem.* 14: 1.
65. SCHERAGA, H. A. 1961. *J. Phys. Chem.* 65: 1071.
66. MITCHELL, P. 1961. *In Membrane Transport and Metabolism*. A. Kleinzeller & A. Kotyk, Eds.: 113. Academic Press, Inc. New York, N. Y.
67. OHNISHI, T. & S. EBASHI. 1964. *J. Biochem. (Tokyo)* 55: 599.
68. EBASHI, S. 1961. *Progr. Theor. Physics, Suppl.* 17: 35.
69. CHAPPELL, J. B., M. COHN & G. D. GREVILLE. 1963. *In Energy-Linked Functions of Mitochondria*. B. Chance, Ed.: 219. Academic Press, Inc. New York, N. Y.
70. ROSSI, C. S. & A. L. LEHNINGER. 1963. *Biochem. Biophys. Res. Comm.* 11: 441.
71. BRIERLY, G. P., E. MURER & D. E. GREEN. 1963. *Science* 140: 60.
72. MITCHELL, P. 1963. *In Structure and Functions of Membranes and Surfaces of Cells in Biochem. Soc. Symposia No. 22*. 142. Cambridge University Press, Cambridge, England.

- 73. BONTING, S. L. & L. L. CARAVAGGIO. 1962. *Nature (Lond.)* **194**: 1180.
- 74. GAMBLE, J. J. JR. 1962. *Am. J. Physiol.* **203**: 886.
- 75. LEHNINGER, A. L. 1964. Abst. 6th Int. Congr. Biochem. VIII Cellular Organization.: 623.
- 75a. LUBIN, M. 1964. *Federation Proc.* **23**: 994.
- 76. TANAKA, R. & L. G. ABOOD. 1964. *Arch. Biochem. Biophys.* **108**: 47.
- 77. ENGEL, A. G. & L. W. TICE. 1964. *J. Cell Biol.* **23**: 117a.
- 78. CONWAY, E. J. 1963. *Nature (Lond.)* **198**: 760.
- 79. SCHUEL, H., R. SCHUEL & L. LORAND. 1964. *J. Cell Biol.* **23**: 83a.

## RAPID FREEZING AND THAWING OF BLOOD\*

R. R. Sakaida, G. F. Doebbler, R. S. Kibler, A. P. Rinfret

*Union Carbide Corporation, Linde Division,  
Research Laboratory, Tonawanda, N. Y. and  
Roswell Park Memorial Institute,  
Department of Nuclear Medicine,  
Buffalo, N. Y.*

Techniques for the preservation of blood for periods of time measured in years are needed today, more than ever, to insure availability of blood in the event of major disasters and to compensate for the undesirable fluctuations in blood supply. With increasing knowledge of the immunological specificity of blood and the ever-increasing use of transfusion therapy, the banking of sufficient supplies of uniquely typed blood becomes of vital importance. Since presently accepted methods of storage require that blood be used within three weeks after collection, large stores of blood can only be maintained with much difficulty.

For long-term preservation blood must be kept at temperatures at which chemical and biological activity become negligible. Our studies have shown that temperatures below  $-100^{\circ}\text{C}$ . are sufficient in permitting several years of blood storage without evidence of damage. However, in the absence of protective additives and optimal procedures for cooling and warming, freezing is an effective method for destroying erythrocytes.

In order to protect blood, protective additives have thus far been a necessity, whether the cooling operation is carried out rapidly or slowly. Additives which have been extensively evaluated for the long term preservation of blood at sub-zero temperatures for subsequent transfusion can be divided into two general classes: (1) those which function protectively within and outside the cell<sup>1-5</sup> and (2) those which act solely in the medium surrounding the cell.<sup>6-8</sup> Of these the intracellular additives such as glycerol, dimethylsulfoxide and glucose yield cells which are not osmotically stable in a physiological medium. Therefore, the additives must be removed prior to transfusion. On the other hand, an additive which is extracellular in nature and which will not damage cells by excessive dehydration at concentrations that are protective should yield cells which are osmotically more stable after thawing. Since our primary objective has been to provide blood which can be transfused immediately after thawing the use of extracellular additives became mandatory.

\*These studies were aided by Contract Nonr 3003 (00) (NR 105-208) between the Office of Naval Research, Department of the Navy, and the Linde Division of Union Carbide Corporation.

Luyet<sup>9</sup> and Meryman and Kafig<sup>10</sup> first showed that ultra-rapid freezing and thawing of blood in thin films on a microscope cover slip or in droplet form using liquid nitrogen as a coolant allowed substantial recovery of red blood cells with and without additives. These observations were confirmed in our laboratory.<sup>11</sup> Subsequent studies<sup>6,12</sup> showed that less rapid rates of cooling (several degrees per second instead of 100 degrees per second) with small amounts of extracellular protective solutes satisfactorily inhibited cell hemolysis.

Experiments primarily with thin films, droplets and volumes of less than 10 cc. of blood were used to evaluate various aspects of the rapid freezing process. When transfusion grades of polyvinylpyrrolidone (PVP) of mean molecular weights between 25,000 and 40,000 were found to provide protection at concentrations which did not affect the osmotic properties of the red cells, research was directed towards freezing of volumes of blood sufficient for *in vivo* red cell viability studies.

Processing, minimally, 50 cc. of blood in a sterile manner and with reproducible results, involved extensive combined efforts of a biochemical, biophysical, engineering and medical nature. Composition of the blood to be frozen, containers for freezing up to one pint of blood, cryogenic seals for sterile transfer and freezing and thawing methodology were evaluated with respect to the biochemistry, *in vitro* recovery and *in vivo* survival of erythrocytes. These studies have either been presented elsewhere<sup>12-16</sup> or are in the process of being reported. In this communication we intend to show some of the effects of freezing and thawing parameters on erythrocyte recovery and *in vivo* survival using blood protected by PVP.

Using PVP, several processes have been devised for the freezing of blood. These are based on the addition of protective medium (1) to the whole blood as collected, (2) to packed cells after almost complete removal of plasma or (3) to blood with a measured quantity of plasma removed.

In all methods a concentration of PVP in the blood of about 7 per cent wt./vol., which is approximately 10 to 12 per cent in the extracellular fluid, is sufficient for maximal cell protection. With almost complete removal of plasma a small amount of albumin is necessary to maintain maximum *in vitro* recovery and *in vivo* survival of erythrocytes. These process modifications do not significantly affect the freezing and thawing requirements. Thus the data which are presented apply to the several PVP processes mentioned.

Freezing is conducted in liquid nitrogen and thawing in a water bath normally maintained at 45° C. Agitation which is required for both freezing and thawing is accomplished by wrist action shaking at an amplitude of about six inches with the blood-filled container held at the end of a 17-inch rod. The containers made of aluminum are rectangular with a cross sectional width of 19 mm. and a volume approximately double the



quantity of blood to be frozen.<sup>12</sup> For processing 50 cc. of blood a flat-walled container measuring approximately 7 x 8 cm. is used. For half and one pint units of blood the walls are corrugated in order to increase the surface area available for the transport of heat.

#### Freezing

It was determined early in the study with PVP-protected blood that changes in cooling rates only at the interface between the container surface and the liquid nitrogen were not sufficient for optimal recovery of undamaged cells and that agitation of the blood during phase change was a necessity. FIGURE 1 shows the effect of agitation rate on cell recovery. Fifty cc. samples of blood were frozen in rectangular aluminum containers of 110 cc. capacity. Identical thawing conditions were utilized for all samples. This FIGURE shows that direct recovery of the red cells was not significantly affected. Saline resuspension recovery, however, increased

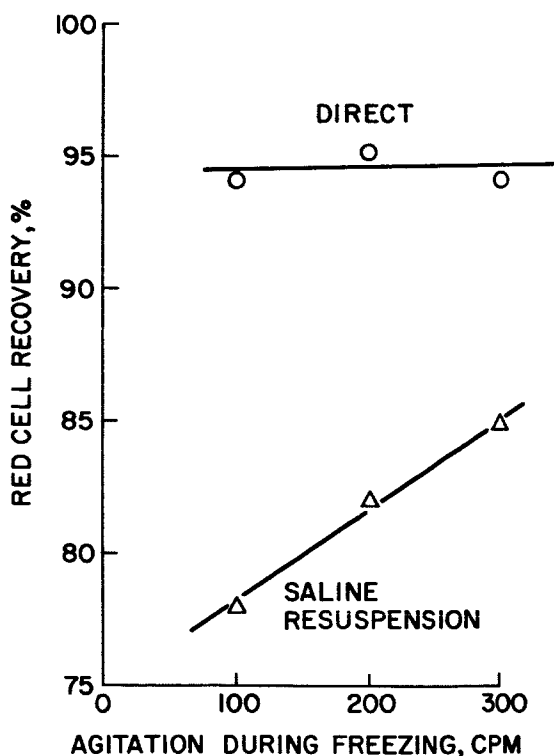


FIGURE 1. Effect of agitation rate of the "Linde" Blood Processing Unit on recovery of 50 cc. samples of blood frozen in a rectangular aluminum container of 110 cc. capacity.

significantly with increase in agitation rate. Saline resuspension recovery is a measure of the cells which remain intact after freezing, storage, thawing and resuspension in an excess volume of physiological (0.85 per cent) saline solution. These data suggest that convection during the freezing process is essential when volumes of blood measured in 10's or 100's of milliliters are frozen in containers of practicable dimensions and also that saline resuspension recovery is not a function of direct cell recovery except as a limiting value.

Container surface modifications to adjust heat transfer rates from the container to boiling liquid nitrogen during cooling were not used in these experiments. With proper control of external heat transfer rates, maximal cell recoveries can be attained by agitating at 200 cycles per minute (cpm.). This is very important in terms of increasing the reliability and service life of the processing equipment by decreasing the stresses imposed by the higher frequency of agitation.

Changes can be made in the rate of cooling of a warm body to the temperature of a boiling cold liquid by use of insulating films applied to the material to be cooled.<sup>15,16</sup> TABLE 1 shows the effect of various insulating films on the cooling rate of a metal probe held stagnantly in a pool of boiling liquid nitrogen. The coatings are applied by dipping the probes into a liquid solution then vaporizing the solvent by air drying a few minutes prior to immersion in the liquid nitrogen. Silica powder is applied by dipping the container coated with glycerol into the powder.

TABLE 1  
EFFECT OF HEAT TRANSFER COATING ON FREEZE-THAW RECOVERY  
OF PVP PROTECTED BLOOD

Coating	Direct recovery %	Saline resuspension %	Relative stagnant cooling rate*
50% glycerol-50% CH <sub>3</sub> OH and Silica powder	80	58	10.0
Polystyrene A-5 resin†	97	90	5.3
Polystyrene A-5 resin	97	88	5.3
1000 cp PVP-CH <sub>3</sub> OH	96	89	2.3
500 cp PVP-CH <sub>3</sub> OH	97	88	2
Uncoated	93	78	1

\*Cooling rates determined by stagnant immersion of coated metal probes in liquid nitrogen then compared with rate for uncoated probe.

†Obtained from Pennsylvania Industrial Chemical Corp.

At this point, let us digress and clarify the reasons for obtaining increased cooling rates by actually increasing resistance to heat transfer by the use of insulating films. Several stages exist in the transfer of energy from a warm surface to a boiling liquid. At very small temperature differences between the surface and liquid heat transfer is similar to that between a cold surface and a warm liquid. As the temperature difference is increased and boiling occurs heat flux increases much more rapidly due to the agitation of the liquid. At the point of critical temperature difference, nucleate boiling provides maximum heat flux. Beyond this temperature difference a highly insulating layer of vapor begins to form and results in lowered rates of heat transfer. The effect of an insulating film in blood freezing, therefore, is to lower the surface temperature rapidly to the nucleate boiling range. Cooling then occurs and is controlled at these higher allowable rates of heat transfer.

To obtain the recovery data shown in TABLE 1, 50 cc. of blood were frozen in aluminum containers using an agitation rate of 200 cycles per minute. As shown there exists an optimum cooling rate between that obtained without a coating and the maximum rate attainable using a powder coating. Available techniques do not allow accurate measurement of the freezing and cooling rates in the various regions of a bulk volume of blood under conditions of agitation. Hence such data are not presented. Although cooling rates are critical, these data show that some variation is allowable in obtaining maximal *in vitro* red cell recovery.

To determine whether rapid attainment of a minimum temperature above that of liquid nitrogen might be advantageous, blood was frozen by agitation in liquid halocarbon baths at temperatures from  $-10$  to  $-108^{\circ}\text{C}$ . After equilibration at these temperatures, the blood was further reduced to liquid nitrogen temperatures prior to thawing. Almost complete hemolysis of unprotected whole blood occurred in all tests. With PVP blood, as shown in FIGURE 2, recoveries increased with decreasing bath temperatures to  $-90^{\circ}\text{C}$ . In the  $-90$  to  $-108^{\circ}\text{C}$ . range the results are comparable to those attainable by cooling in liquid nitrogen. Need for cooling to an intermediate point prior to further reduction of the temperature of blood is not indicated. Since cooling rate is increased by lowering the bath temperature, we can also see that red cells with PVP can be cooled at rates provided by maintaining bath temperatures of  $-90$  to  $-110^{\circ}\text{C}$ . with no difference in recoveries.

Several practical problems exist in the use of aluminum for blood containers. Primary problems of corrosion, opacity and cryogenic sealing might be avoided by the use of the plastic films. Plastics which could sustain agitation in liquid nitrogen were found. Methods were then developed whereby half pint units of blood can now be frozen and thawed by our

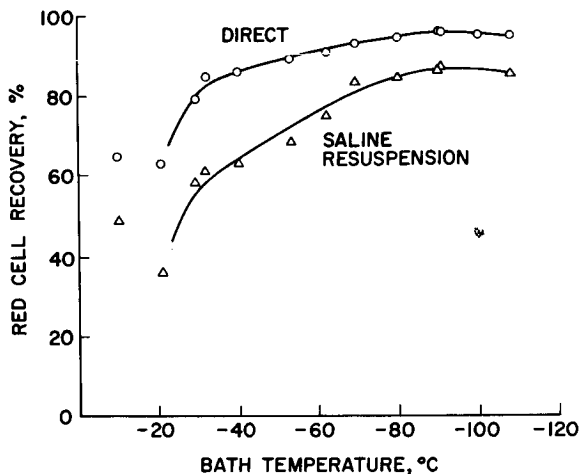


FIGURE 2. Recovery of red cells frozen by agitation of 50 cc. samples of blood in a liquid, nonboiling refrigerant maintained at various subzero temperatures. Thawing conditions were all identical.

conventional procedure in transparent packs made of films down to a thickness of half mil (0.0005 inch).

Using polycarbonate, Kel-F or Teflon FEP films of various thicknesses in single or multilayers, blood was frozen and thawed under optimum conditions. FIGURE 3 presents erythrocyte recovery data as a function of the container wall conductance during freezing. Conductance is the thermal conductivity of the film divided by the wall thickness. Conductance thus decreases with increasing wall thickness. Under normal conditions such as thawing increased conductance will increase the rate of heat transfer. For cooling, however, indications from a very few tests are that overall cooling rates are lowest for the point at the highest conductance value used. This would be an effect of boiling heat transfer.

As shown in FIGURE 3, an increase in conductance from 0.04 to 0.16 cal./cm.<sup>2</sup> sec. °C. results in a linear decrease in the saline resuspension recovery of the red cells. Direct recoveries are also similarly affected except at the two lower conductance values. These two poorer recovery values can be attributed to mechanical lysis of the damaged but nonhemolyzed cells because of the extended agitation required during the thawing process.

To simulate our standard procedures with aluminum containers on which a readily water-soluble, insulating coating is applied for freezing, experiments were run using packs constructed of multilayers of thin films. For freezing of blood the pack was used as fabricated but for thawing the outer layers of film were removed. As can be seen in the FIGURE at the 0.06 con-

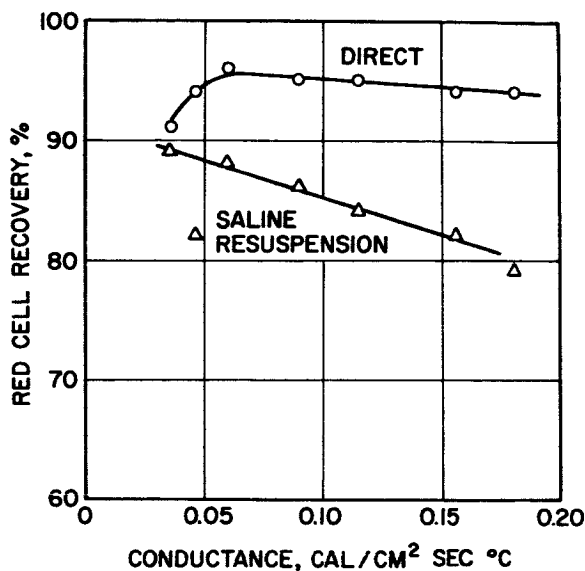


FIGURE 3. Recovery of red cells frozen in plastic containers of differing wall thickness and resistance to heat transfer. Wall thicknesses can be reduced for thawing thus reducing the resistance of the container wall to energy transport.

ductance value, the best direct recovery was attained using these procedures.

In addition to its use as a practical blood container for long-term preservation, it would appear that the proper use of multilayers of thin plastic films can provide engineers and biophysicists with control of bulk cooling and warming rates in a variety of cryobiological operations.

#### Thawing

Unless blood is overheated or subjected to excessive agitation during thawing, this operation is least critical of the processing conditions as measured by *in vitro* red cell recovery. In fact, many of our studies have shown that maximal red cell recoveries are normally attained by using stagnant thawing in a water bath at temperatures between 37 and 45°C. FIGURE 4 shows the effect of thawing and warming to a final bulk temperature of approximately 38°C. of half pint units of PVP protected blood which were frozen optimally in a metal container. Between 275 and 300 cc. of blood were processed in rectangular corrugated aluminum containers of 500 cc. capacity and warmed in a 45°C. water bath using conditions specified on the FIGURE. The first number beside each point is the direct recovery of red cells and the number following in the parenthesis is the saline resuspension recovery. These *in vitro* recovery data as a function

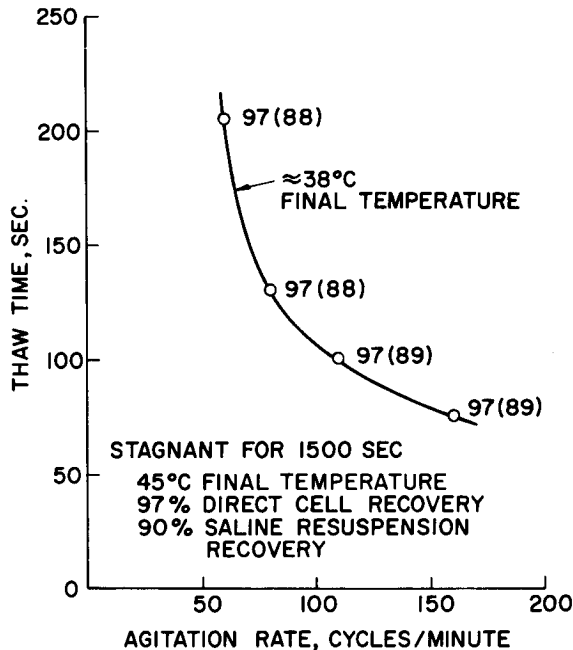


FIGURE 4. Effect of thawing and warming rate on red cell recovery. All samples were frozen in half-pint volume under identical conditions using a corrugated rectangular aluminum container.

of warming rates are effectively identical. Trying to warm stagnantly to a given final bulk temperature below that of the bath temperature was not attempted. We found that once stagnant thawing is completed the immediate red cell recovery will not be affected by additional standing of up to 30 minutes in the thaw bath. Recovery data from the stagnant thawing studies as shown in the FIGURE further reflect the insensitivity of *in vitro* results to variations in warming rates.

As a final evaluation of a laboratory nature prior to study of the clinical efficacy and effect of bulk transfusions of preserved blood, the red cell survival is determined *in vivo*. We have measured red cell survival by the use of the sequential chromium technique.<sup>17,18</sup> Fresh, autologous, unfrozen red cells are tagged with a small amount of chromium-51 and injected to determine the relative red cell volume of the recipient. This injection, which is used as the baseline for subsequent measurements, is followed by the transfusion of test red cells tagged with a three-fold larger quantity of chromium-51. Comparative radioactivity data are then obtained at given intervals from which *in-vivo* red cell survival is calculated. Autologous transfusions (control and test cells) of 10 cc. volumes of tagged

TABLE 2  
EFFECT OF THAWING RATE ON CELL SURVIVAL

Thawing conditions	No. tests	Direct recovery (%)	Survival %	
			1/2 hr.	24 hr.
machine—150 cpm.	6	96 ± 1	94 ± 4	79 ± 4
machine—75 cpm.	2	96 ± 0	88 ± 1	81 ± 11
manual—gentle	3	96 ± 1	88 ± 3	70 ± 3

Specimens thawed in 45° C. water.

blood have resulted in survival data with a standard deviation of less than five per cent for the testing of a given process parameter.

TABLE 2 presents data showing the effect of thawing conditions on *in vivo* red cell survival. Fifty cc. quantities of blood were frozen identically in 110 cc. rectangular aluminum containers. Thawing rates were varied by the use of different agitation conditions and these are listed in order of decreasing rates of heat transfer. All direct red cell recoveries are identical. However, *in vivo* survival of the thawed cells does vary. Excluding the average value for the 24-hour survival of the sample thawed at 75 cycles per minute, the more rapid thawing condition gave the better result. Only two samples were studied at 75 cycles per minute and the spread of the 24-hour data is indicated by the large standard deviation. Actual values of 89 and 73 per cent suggest that the former is in error and the average survival should more nearly be represented by the samples thawed by gentle manual agitation.

TABLE 3 briefly presents data of blood frozen and thawed in containers of different material. Metal refers to standard aluminum containers. For

TABLE 3  
RESISTANCE TO HEAT TRANSFER DURING THAWING AND EFFECT ON CELL SURVIVAL

Container	No. tests	Direct recovery (%)	Survival %	
			1/2 hr.	24 hr.
Metal	2	96 ± 2	93 ± 3	74 ± 3
Plastic	3	96 ± 1	78 ± 5	59 ± 6

Specimens thawed in 37°C. water with blood processing unit operating at 150 cycles per minute.

plastic, commercially available containers of low density polyethylene were used. These were rectangular with walls of variable thickness. A thorough study of processing parameters was made using the plastic bottles and *in vitro* results equivalent to the best attainable in metal containers were reproducibly obtained. Of course the warming rates were considerably lower in the plastic than the metal containers. Again we see that red cell recovery values were identical while the *in vivo* survival values were much impaired with the slower thawing.

#### Discussion

The long-term preservation of blood by rapid freezing and thawing, in the presence of extracellular additives only, requires attention to processing detail if useful yields of viable erythrocytes are to be obtained. When volumes of blood which approach those employed in transfusion are frozen, we find that simple scale-up of experiments involving volumes measured in fractions of a ml. up to 50 ml. is unsatisfactory in terms of the yield of intact red cells. At the same time increasing volume adds to experimental difficulty in obtaining information on the thermal and other events occurring in the different regions of a specimen during freezing and thawing. Empirical methods were thus used in the development of freezing and thawing procedures.

We have presented here a few results which emphasize the problems one faces in the study of cryobiologic processes and the need for close interrelationship between medical, biophysical and engineering groups. For instance, much time can be spent in improving *in vitro* red cell recoveries and in simplification of procedures while maintaining these maximal *in vitro* results. However, as shown with the thawing data rapidly frozen blood can be warmed at various rates with no change in *in vitro* red cell recovery but with substantial reduction in the *in vivo* survival of these cells.

The freezing data show that there need be no correlation between direct recovery of the red cell and its saline resuspension recovery. Both recovery values are of importance in providing a minimum quality standard for the frozen and thawed blood. For example, the direct recovery provides a measure of the free hemoglobin in the blood and a low saline resuspension recovery indicates a blood preparation of osmotically unstable cells. Beyond these *in vitro* minima, the only present criterion for a successful process is the *in vivo* evaluation of red cell viability.

Data obtained in studies of the type presented have led to control of processing techniques such that pint volumes of blood protected with PVP can now be rapidly frozen and thawed with an *in vitro* red cell recovery of 97 per cent. Transfusion of up to pint units of this blood have resulted in the *in vivo* survival of approximately 85 per cent of the cells 24 hours after infusion.



## References

1. BLOOM, M. L., A. P. RINFRET, E. WITEBSKY, H. STEINBERG, J. LAWROW & T. M. BOW. 1962. Frozen and thawed blood: studies in rabbit and man. *Proc. 8th Congr. Int. Blood Transf. (Tokyo, 1960)*. 443-446.
2. HAYNES, L. L., J. L. TULLIS, H. M. PYLE, M. T. SPROUL, S. WALLACH & W. C. TURVILLE. 1960. Clinical use of glycerolized frozen blood. *JAMA* 173: 1657-1663.
3. HAYNES, L. L., W. C. TURVILLE, M. T. SPROUL, J. W. ZEMP & J. L. TULLIS. 1962. Long term blood preservation — a reality. *J. Trauma* 2: 3.
4. HUGGINS, C. E. 1963. Prevention of hemolysis of large volumes of red blood cells slowly frozen and thawed in the presence of dimethyl sulfoxide. *Transfusion* 3(6): 483-493.
5. HUGGINS, C. E. 1963. Preservation of blood for transfusions by freezing with dimethyl sulfoxide and a novel washing technique. *Surgery* 54(1): 191-194.
6. DOEBBLER, G. F., R. G. BUCHHEIT & A. P. RINFRET. 1961. Recovery and *in vivo* survival of rabbit erythrocytes. *Nature* 191(4796): 1405.
7. RINFRET, A. P., C. W. COWLEY, G. F. DOEBBLER & H. R. SCHREINER. 1964. The preservation of blood by rapid freezing. *Proc. 9th Congr. Int. Soc. Blood Transf. (Mexico, 1962)*. 80-88.
8. SLOVITER, H. A. & R. G. RAVDIN. 1962. Recovery and transfusion of human erythrocytes after freezing in polyglycol solutions. *Nature* 196(4857): 899-900.
9. LUYET, B. J. 1949. Effects of ultra-rapid and slow freezing and thawing on mammalian erythrocytes. *Biodynamica* 6(121): 217-223.
10. MERYMAN, H. T. & E. KAFIG. 1955. Rapid freezing and thawing of whole blood. *Proc. Soc. Exptl. Biol. Med.* 90(3): 587-589.
11. RINFRET, A. P. & G. F. DOEBBLER. 1960. Observations on the freezing and thawing of blood in droplet form. *Biodynamica* 8(165): 181-193.
12. RINFRET, A. P. 1963. Some aspects of preservation of blood by rapid freeze-thaw procedures. *Fed. Proc.* 22(1): 94-101.
13. DOEBBLER, G. F. & A. P. RINFRET. 1962. The influence of protective compounds and cooling and warming conditions on hemolysis of erythrocytes by freezing and thawing. *Biochim. Biophys. Acta* 58: 449-458.
14. RINFRET, A. P. 1960. Factors affecting the erythrocyte during rapid freezing and thawing. *Ann. N. Y. Acad. Sci.* 85(2): 576-594.
15. COWLEY, C. W., W. J. TIMSON & J. A. SAWDY. 1961. Ultra rapid cooling techniques in the freezing of biological materials. *Biodynamica* 8(170): 317.
16. COWLEY, C. W., W. J. TIMSON & J. A. SAWDY. 1962. A method for improving heat transfer to a boiling fluid. *Ind. Eng. Chem., Process Des. Dev.* 1(2): 81-84.
17. DOEBBLER, G. F., R. F. DWYER & A. P. RINFRET. 1962. A simple comparative method of measuring red cell viability. *Nature* 195(4855): 912-913.
18. DOEBBLER, G. F., R. S. KIBLER & R. F. DWYER. Determination of *in-vivo* survival of red cells by consecutive chromium-51 labeling. In preparation.

# THE ROLE OF CELL MEMBRANES IN THE FREEZING OF YEAST AND OTHER SINGLE CELLS\*

Peter Mazur

*Biology Division, Oak Ridge National Laboratory, Oak Ridge, Tenn.*

Much of the damage in cells that are subjected to subzero temperatures appears ascribable to two physical factors: the concentration of solutes that accompanies ice formation, and the formation of large ice crystals within the cell (Mazur, 1965). However, low-temperature exposure is by no means invariably lethal, for a wide variety of cells can survive cooling to  $-190^{\circ}\text{C}$ . and below under appropriate conditions. Whether or not damage occurs under a particular set of conditions depends on a number of parameters, among the most important of which are the permeability properties of the plasma membrane. The properties of the membrane strongly influence the likelihood of intracellular freezing. Furthermore, when cells are killed by freezing and thawing, their permeability barriers are almost invariably disrupted. There are suggestions that this damage is a direct consequence of freezing, and not just a postmortem effect.

## *The Cell Membrane as a Barrier to Nucleation*

The freezing point of most nonhalophilic cells is above  $-2^{\circ}\text{C}$ . (Mazur, 1965). This means that at temperatures below  $-2^{\circ}\text{C}$ . the cytoplasm is supercooled; nevertheless, most cells freeze only at temperatures below  $-5^{\circ}\text{C}$ . and often only below  $-10^{\circ}\text{C}$ ., even when the external medium contains ice (TABLE 1).

Ice and supercooled water can coexist only if there is a barrier between them, and this barrier must be the cell wall or the plasma membrane. However, the plasma membrane is permeable to water, more permeable in fact to water than to nearly any other solute (Davson & Danielli, 1952), and this high permeability raises the question of how the membrane can be a barrier to the passage of ice.

In considering possible answers, an additional fact must be kept in mind: namely, below a certain temperature, usually between  $-5^{\circ}\text{C}$ . and  $-15^{\circ}\text{C}$ ., the membrane loses its barrier properties. As shown in TABLE 1, most cells freeze internally between  $-5^{\circ}$  and  $-15^{\circ}\text{C}$ . The available evidence indicates that the freezing is not spontaneous but is the result of seeding of the supercooled cytoplasm by the external ice. Thus, if cells are cooled under conditions that minimize the likelihood of external ice, they remain unfrozen at lower temperatures than when external ice is present (TABLE 1).

\*Research sponsored by the U. S. Atomic Energy Commission under contract with Union Carbide Corp.

TABLE 1  
 SUPERCOOLING OF CELLS IN THE PRESENCE AND ABSENCE OF EXTERNAL ICE\*

Cell, tissue, or organism	Extent of supercooling of cell water (°C.)		References
	External ice present	External ice absent	
(1) Guinea pig testis	- 6 to -10	-18 to -20	Smith and Smiles (1953)
(2) Rabbit corneal tissue	- 5 to -10	- 5 to -10	
(3) <i>Amoeba</i>	- 5 to - 8		Chambers and Hale (1932) Smith, Polge and Smiles (1951)
(4) Sea urchin eggs	- 8	<-15	Asahina (1961)
(5) Various plant cells	- 7	-20	Asahina (1956)
(6) Insect larvae	-10 to -15	-20 to -30	Salt (1950, 1963)
(7) Cabbage leaf	-13		Sakai (1961)
(8) Yeast	-10†	<-16	Mazur (1961a)
(9) Vesicles of lemon	<-7	-12 to -18	Lucas (1954)
(10) Muscle fibers (frog)	-10	<-15	Chambers and Hale (1932)

\*External ice was eliminated (or reduced) by mounting the cells in silicone or paraffin oil (1, 2, 4, 5, 10), by supercooling the whole suspension (8), or by cooling the animal or fruit in air (6, 9).

†Based on evidence that cell death is caused by intracellular freezing (cf. text and FIGURE 1).

The difference in the temperature at which freezing occurs is especially striking in insects. Many insects remain unfrozen at  $-30^{\circ}\text{C}$ . or lower when surrounded by air, but undergo freezing at  $-10^{\circ}\text{C}$ . when they are in contact with ice (Salt, 1963).

The problem, then, is to explain why the plasma membrane blocks the passage of ice crystals above a certain temperature but permits their passage at lower temperatures. There are three possibilities: (1) the membrane comes in contact with ice only below the critical temperature; (2) the ability of ice to permeate the membrane increases with lowered temperature; or (3) the permeability properties of the membrane change with lowered temperature. These possibilities require discussion.

*Contact with ice.* Even if the suspending medium is originally deionized water, it will soon contain solutes as a result of leakage from the cells. For example, the concentration of solutes in the extracellular water in a sus-

pension of  $4 \times 10^9$  yeast cells/ml. is about 0.003 osmolar (Mazur, 1963a). Thus, since the external medium is always a solution, it will contain some liquid water during freezing at all temperatures above the eutectic point. The proportion of liquid ( $q$ ) will be roughly

$$q \approx \frac{1.86_v m_i}{273-T} \quad (1)$$

where  $m_i$  is the concentration of the solution before freezing,  $v$  is the number of species into which the solute ionizes, and  $T$  the temperature (Mazur, 1963a, 1965); 1.86 is the molal freezing point lowering in water. In the example cited  $v m_i = 0.003$ , and  $q$  is about 0.11 per cent at  $-5^\circ\text{C}$ . and 0.06 per cent at  $-10^\circ\text{C}$ .

If intracellular freezing occurred whenever the cell came in contact with ice, one would expect that the lower the percentage of liquid water, the greater would be the likelihood of contact with ice and the greater the probability of intracellular freezing. This is not the case in yeast. The evidence is strong that death in rapidly cooled yeast is due to intracellular freezing (Mazur, 1961a; 1963a, 1963b; Nei, 1960; Araki & Nei, 1962), but death is related to temperature and not to the fraction of the suspension frozen. As shown in FIGURE 1, survival drops abruptly between  $-10^\circ$  and  $-20^\circ\text{C}$ . in solutions ranging in concentration from 0.0006 to 0.3 osmolar. The percentage of unfrozen water at  $-10^\circ\text{C}$ . in such solutions would range from 0.01 to 6 per cent. Furthermore, it can be seen that the lethal temperature range is independent of the eutectic points of the suspending solutions, which vary from  $-2.7$  to  $-50^\circ\text{C}$ .

Intracellular freezing of eggs of the sea urchin *Strongylocentrotus nudus* also appears unrelated to the eutectic point of the suspending medium. The former occurs around  $-8^\circ\text{C}$ .; the latter is below  $-22^\circ\text{C}$ . (Asahina, 1961). On the other hand, internal freezing of eggs of the sea urchin *Hemicentrotus pulcherrimus* is closely correlated with the eutectic point of the suspending medium, at least at temperatures above  $-30^\circ\text{C}$ . (Asahina, 1962). Why the two species behave so differently is uncertain.

*Growth of ice through unaltered membranes.* If intracellular supercooled water is inoculated by external ice, an organized crystalline surface must be passing through the cell membrane. Therefore, water-filled channels wide enough to permit this passage must either be normally present in the plasma membrane or they must be formed at subzero temperatures. Many (although by no means all) students of permeability believe that plasma membranes normally do contain aqueous channels. (Solomon, 1960; Whitembury, 1962; Villegas, 1963; but see Shanes, 1963 for an opposing viewpoint). The equivalent radius of these channels or pores has been estimated to be 3 to 8 Å on the basis of the rate of flow of water under osmotic gradients and on the basis of the rates of permeation of graded

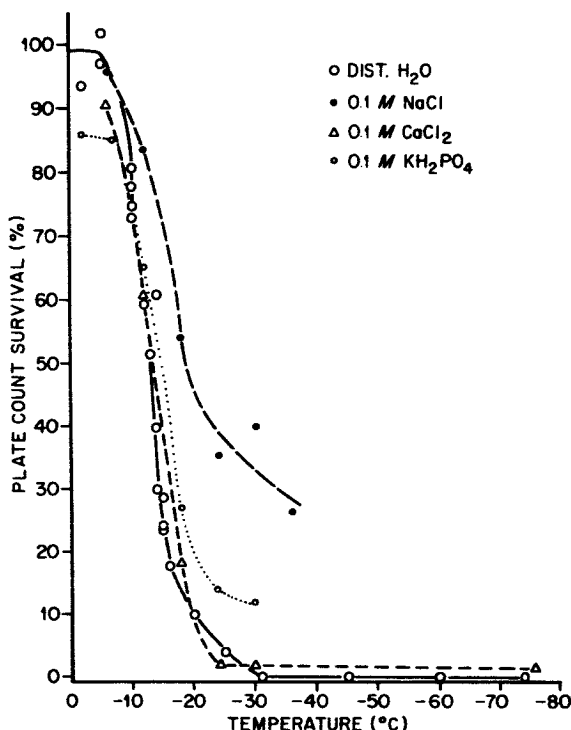


FIGURE 1. Survival of yeast suspended in distilled water or in indicated 0.1M solutions, cooled to indicated temperatures for 10 minutes and warmed at 1°C./minute. [From data published previously (Mazur, 1961a).] The eutectic points of KH<sub>2</sub>PO<sub>4</sub>, NaCl, and CaCl<sub>2</sub> are -2.7, -21.1, and -50°C., respectively.

sizes of nonionic solutes. Furthermore, Solomon (1960) indicates that all the pores must have about the same diameter.

It has been suggested that the existence of such minute pores might account for the barrier properties of the plasma membrane (Mazur, 1960). If an external ice crystal attempted to grow through a cylindrical pore like that depicted schematically in FIGURE 2, the ice-water interface would have the indicated configuration. The contact angle  $\theta$  would have a value to satisfy the relation

$$\cos \theta = \frac{\sigma_{SC} - \sigma_{LC}}{\sigma_{SL}} \quad (2)$$

where  $\sigma_{SC}$ ,  $\sigma_{LC}$ , and  $\sigma_{SL}$  are the interfacial energies between ice and the capillary wall, between water and the capillary, and between ice and water, respectively. One can determine the relation between the melting point of this crystal with its curved surface and the pore radius ( $a$ ) by deriving an

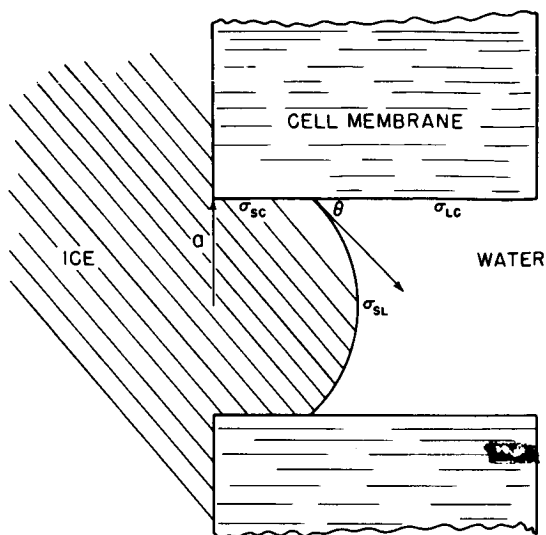


FIGURE 2. Schematic diagram of the growth of ice through a capillary pore in a cell membrane. See text for details.

expression for the change in free energy associated with the transfer of ice from the external ice to the ice in the pore, a transfer that enlarges the ice-capillary interface, and by deriving a comparable expression for the change in free energy associated with the transfer of water to the water in the pore (Mazur, 1965). The relation turns out to be the Kelvin equation:

$$\Delta T = \frac{2v_1 T_f \sigma_{sl} \cos \Theta}{a L_f} \quad (3)$$

where  $v_1$  is the molar volume of water,  $T_f$  is the freezing point of planar water, and  $L_f$  the molar heat of fusion.

Although  $\sigma_{sl}$  cannot be measured directly, it has been estimated indirectly to be around 20 erg/cm.<sup>2</sup> for the ice-water interface (Fletcher, 1962, p. 207). When this value and numerical values for  $v_1$ ,  $L_f$ , and  $T_f$  are substituted into Equation 3, the relation becomes:

$$\Delta T \approx \frac{300 \cos \Theta}{a} \quad (4)$$

if  $a$  is expressed in Angstrom units.

Assume for the moment that  $\Theta$  is  $0^\circ$ , so that  $\cos \Theta$  is 1 (an assumption that means complete wetting of the pore wall by water). Then, Equation 4 indicates that the melting point of ice in a capillary of 30A-radius would be  $-10^\circ\text{C}$ . It also indicates that an ice crystal could not pass through a pore with a radius of 30A at temperatures above  $-10^\circ\text{C}$ ., for in trying to do so

it would melt, but that it could pass through at temperatures below  $-10^{\circ}\text{C}$ . Although the lower melting point of ice in a capillary pore thus can qualitatively account for the barrier properties of the plasma membrane, there is a large quantitative discrepancy. The evidence suggests that the plasma membrane ceases to be a barrier at approximately  $-10^{\circ}\text{C}$ . On the basis of Equation 4, the critical pore radius at  $-10^{\circ}\text{C}$ . is  $30A$ , whereas the estimated pore size from permeability studies is 3 to  $8A$ . What is responsible for the discrepancy? One possibility is that the ability of a plasma membrane to block nucleation above certain temperatures has nothing to do with capillary pores. Another is that the value of 300 in Equation 4 is wrong. This would imply that the values of  $\sigma_{sl}$  and  $L_i$  obtained from macroscopic systems are erroneous in micro systems, and there is some evidence that this is so (Van Hook, 1961, p. 76). But there is a third possibility, and that is that  $\Theta$  is not  $0^{\circ}$ . If, for example,  $\Theta$  were  $80^{\circ}$ ,  $\cos\Theta$  would be 0.17, Equation 4 would become

$$\Delta T \approx \frac{52}{a} \quad (4a)$$

and the pore radius at  $-10^{\circ}\text{C}$ . would become  $5A$  in agreement with the values derived from permeability studies.

Although there is no evidence whatsoever that  $\Theta$  is  $80^{\circ}$ , there are cogent reasons to believe that  $\Theta$  is greater than zero and, therefore, that  $\cos\Theta$  is less than 1. Plasma membranes are believed to be composed chiefly of lipoproteins, with nonpolar hydrophobic groups buried in the interior of the membrane. If the walls of the water-filled pores are lined predominantly with nonpolar groups, it follows from the work of Frank and Evans (1945), Kauzmann (1959), and Némethy and Scheraga (1962) that the water in contact with the pore walls will be more ordered or "ice-like" than normal water. Measurements of the activation energy for the permeation of water into and out of cells tend to support this supposition. As shown in TABLE 2, these activation energies are two to three times greater for most cells (the red cell being an exception) than for the self-diffusion of water. Hempling (1960) and Hays and Leaf (1962) have suggested that these high activation energies are a reflection of a large and positive entropy of activation; and they have further suggested that the positive entropy could mean that the permeation of water involves the "melting" of structural water normally in the pore. If the pore water is "ice-like," it seems likely that the tension at the pore-water interface would be closer in value to the tension at the pore-ice interface than it would if the water were not "ice-like." And from Equation 2 it can be seen that as  $\sigma_{lc}$  approaches  $\sigma_{sc}$ ,  $\cos\Theta$  approaches zero and  $\Theta$  approaches  $90^{\circ}$ .

Although the Kelvin equation appears capable of accounting for the ability of a porous membrane to block the growth of ice crystals, a word

TABLE 2  
ACTIVATION ENERGIES FOR THE PERMEATION OF WATER IN CELLS AND TISSUES

Cell or tissue	Activation energy (kcal./mole)	Temperature range (°C.)	Reference
<i>Arbacia</i> eggs (unfertilized)	13-17	10-24	McCutcheon and Lucké (1932)
<i>Asцитes</i> tumor	9.6	10-37	Hempling (1960)
Toad bladder:			
(- vasopressin)	9.8	5-35	Hays and Leaf (1962)
(+ vasopressin)	4.1	5-35	
Human red cells	5.7	0-20	Jacobs, Glassman, and Parpart (1935)
Self-diffusion and viscous flow of water	4.5	10-50	Wang (1951 <i>a,b</i> )
	6.4	0	

of caution is in order. Interfacial tensions, contact angles, and radii of curvature apply to assemblages of many molecules. Their meaning becomes blurred in microscopic systems of the dimensions considered here. After all, a pore 15 Å in diameter would contain only five water molecules abreast. It would probably be possible to derive an equation analogous to the Kelvin equation that would give the chemical potential of such a small assemblage of molecules, but perhaps this would be premature in view of the complete lack of knowledge of the value of  $\sigma_{sc}$  even in macroscopic systems.

*Growth of ice through altered membranes.* Another explanation of the loss of the barrier properties of cell membranes is that they become altered below certain temperatures. Small pores might enlarge; or large perforations might be formed. Such alterations could come about either because of the lowered temperature or because of the increasing concentration of solutes that occurs as the temperature of a partially frozen solution is lowered. Both these factors have been found to alter the chemical and physical properties of cell membranes and model membranes. Lovelock (1954), for example, found that red cells lose phospholipid upon exposure to 1 M NaCl, and that this loss makes them susceptible to lysis upon cooling to temperatures below 20° C. Davson and Danielli (1952, pp. 112-116) have reviewed the effects of ions on the permeability of cells to water. Leitch and Tobias (1964) observed that the concentrations of  $Ca^{++}$  and  $K^+$  in the medium affected the permeability of a model phospholipid-cholesterol membrane.



There is a question whether these or comparable alterations can occur rapidly enough to account for the nucleation of cells in which only a few seconds elapse between the onset of cooling and the occurrence of intracellular freezing. The evidence is meagre. However, Asahina's studies (1962) suggest that intracellular freezing of eggs of the sea urchin *Hemacentrotus* is due to alterations of the cell membrane produced either by the precipitation of salts or by the complete solidification of the external medium. On the other hand, studies on yeast suggest that if alterations occur during cooling, they are not great enough to markedly increase the permeability of the plasma membrane to intracellular solutes (cf. Mazur, 1963a, 1965, and below).

One might think that cell membranes could be damaged by the mechanical forces produced by the formation of external ice itself, but this seems generally not to be the case. This point is discussed in more detail elsewhere (Mazur, 1965), so let me just mention here that 50 to 100 per cent of yeast can survive external ice formation without damage to membranes if the temperature remains above  $-10^{\circ}\text{C}.$ , or if cooling to lower temperatures is either slow ( $1^{\circ}\text{C}./\text{minute}$ ) or very rapid ( $\sim 10^4^{\circ}\text{C}./\text{minute}$ ).

#### *The Plasma Membrane and Cellular Dehydration*

As long as the plasma membrane is preventing the nucleation of intracellular supercooled water, the higher chemical potential of the supercooled water will cause it to flow out of the cell and freeze externally. If the water leaves the cell rapidly enough to reduce the chemical potential of the remaining cellular water to that of ice before the membrane ceases to be a barrier, then intracellular freezing will be precluded. On the other hand, if the cell still contains supercooled water at the temperature at which the membrane ceases to be a barrier, intracellular freezing and consequent death will occur. One of the important factors affecting the rate of water loss is the permeability of the plasma membrane to water. Thus,

$$-\frac{dV}{dt} = \frac{kAT}{v_1} \ln (p_i/p_e) \quad (5)$$

where  $V$  is the volume of intracellular water,  $t$  is time,  $k$  is the permeability constant of the cell to water,  $A$  is the area of the cell surface, and  $p_i$  and  $p_e$  the vapor pressure of the internal supercooled water and the external ice, respectively (Mazur, 1963b).

The permeability constant  $k$  is actually not constant; it decreases approximately exponentially with decreasing temperature; i.e.,

$$k = k_g e^{b(T-T_g)} \quad (6)$$

where  $k_g$  is the permeability constant at temperature  $T_g$ , and  $b$  is the temperature coefficient of the permeability constant. The relation between

b and  $Q_{10}$  is

$$\ln Q_{10} = 10b \quad (7)$$

Investigators usually give the temperature characteristics of the permeability constant in terms of an Arrhenius equation of the form

$$k = k_g e^{-E/R(1/T - 1/T_g)} \quad (6a)$$

when  $E$  is the activation energy in cal./mole.

Over a restricted temperature range, Equations 6 and 6a are nearly equivalent. Between  $+20$  and  $-30^\circ\text{C}$ ., the relation between  $b$  and  $E$  is closely described by

$$E \approx 1.5 \times 10^5 b \quad (8)$$

The driving force for the loss in water is the ratio of the internal to external vapor pressures. As shown previously (Mazur, 1963b), this ratio increases with decreasing temperature, according to the relation

$$\frac{d \ln(p_i/p_e)}{dT} = \frac{nv_1}{V(V + nv_1)} \frac{dV}{dT} - \frac{L_f}{RT^2}, \quad (9)$$

where  $n$  is the number of osmoles of solute in the cell.

If  $T$  and  $t$  are equated by means of the cooling velocity ( $dT/dt = B$ ), Equations 5, 6, and 9 can be combined to give an equation that relates the amount of supercooled water in a cell to temperature and the several parameters (Mazur, 1963b), namely,

$$T e^{b(T_g - T)} \frac{d^2 V}{dT^2} - \left[ (bT + 1) e^{b(T_g - T)} - \frac{ARk_g n}{B(V + nv_1)} \cdot \frac{T^2}{V} \right] \frac{dV}{dT} = \frac{L_f Ak_g}{Bv_1} \quad (10)$$

Numerical solutions to this equation give an estimate of the effect of various parameters on the likelihood of intracellular freezing. FIGURE 3, for example, shows the calculated effect of cooling velocity on the water content of a  $6\mu$  diameter cell. The curve Eq. shows the equilibrium water content as a function of temperature; i.e., it shows the water content the cell would have to maintain in order to avoid supercooling. It can be seen that cells cooled at  $1^\circ\text{C./minute}$  are no longer supercooled at  $-10^\circ\text{C}$ . or below; therefore, they should not freeze internally. On the other hand, cells cooled at  $100^\circ\text{C./minute}$  are supercooled below  $-10^\circ\text{C}$ . and should, therefore, undergo intracellular freezing.

The permeability of the cell profoundly affects the water content and hence the likelihood of freezing. The solutions for the curves in FIGURE 3 used a permeability constant of  $0.15 \mu \text{ minute}^{-1} \text{ atm}^{-1}$  and a temperature coefficient  $b$  of the permeability constant of 0.0325 ( $Q_{10} = 1.4$ ; activation energy 4900 cal./mole). FIGURE 4 shows the large effect of varying the temperature coefficient and activation energy. The value of 4900 cal./mole is about that found for blood cells, while the value of 15,000 cal./mole is that characteristic of sea urchin eggs (cf. TABLE 2).

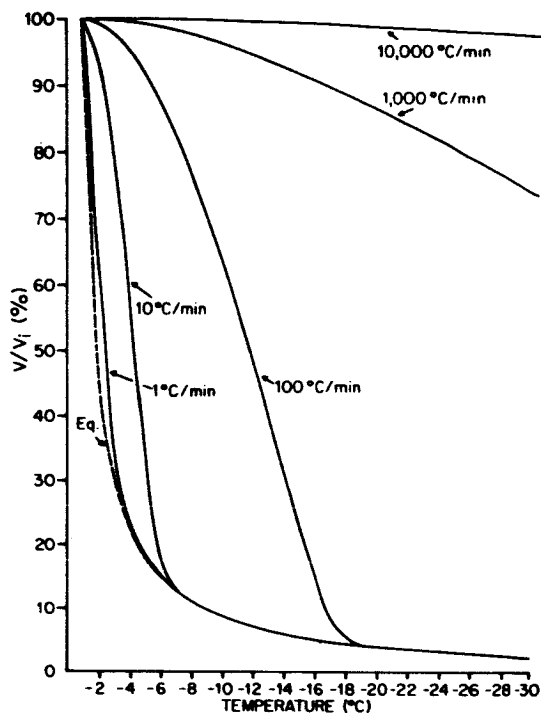


FIGURE 3. Calculated percentage of cell water remaining in a  $6\mu$ -diameter spherical cell as a function of temperature and cooling velocity. The calculation used the values  $k_g = 0.15$  and  $b = 0.0325$ . Curve Eq. is the equilibrium percentage of intracellular water. From Mazur (1963*b*) by permission of the Rockefeller Institute Press (J. Gen. Physiol. 47: 347-369).

The effect of varying the permeability constant  $k_g$  is shown in FIGURE 5. (The activation energy was assumed to be 4900 cal./mole.) The values of  $k_g$  used represent the range of values reported for various cells. Thus  $k_g$  is 0.02, 0.2, 0.5, and 5 in *Amoeba*, *Arbacia* eggs, lymphocytes, and human red blood cells, respectively (Dick, 1959). The curves show that when cells are cooled at a given velocity (100°C./minute in this case), their permeability to water will determine whether they dehydrate and thus avoid internal freezing (e.g. red blood cells), or whether they remain highly hydrated, extensively supercooled, and therefore certain to undergo intracellular freezing (sea urchin eggs, *Amoeba*). It should be noted that a 10-fold increase in  $k_g$  has the same effect on water content as a 10-fold decrease in cooling velocity.

The high sensitivity of the water contents to the permeability of the cell to water emphasizes that the values of  $k_g$  and  $b$  probably constitute

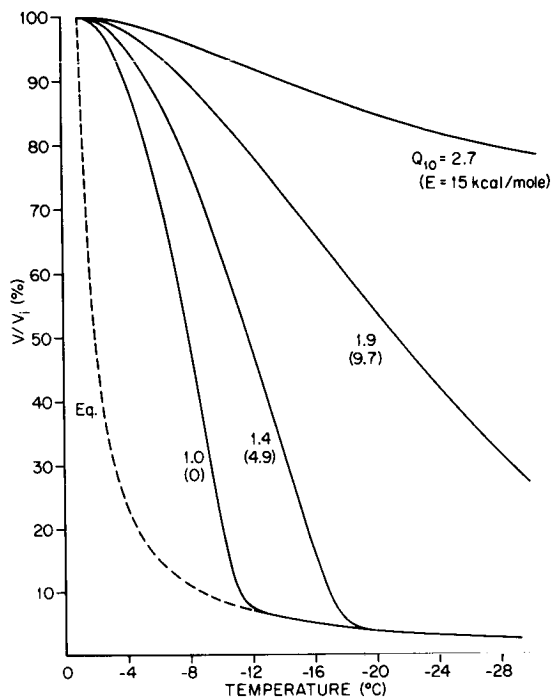


FIGURE 4. Calculated percentage of cell water remaining in a  $6\mu$ -diameter spherical cell as a function of temperature and the temperature coefficient of the permeability constant,  $k_g$ . The calculation assumed a cooling rate of  $100^\circ\text{C./minute}$  and a value of  $k_g = 0.15$ . The values of the other parameters are given elsewhere (TABLE 1 from Mazur, 1963b).

the greatest source of inaccuracy in the solutions to Equation 10 [the likely errors introduced by the various simplifying assumptions used to derive Equation 10 have been discussed previously (Mazur, 1963b)]. In the first place, the value of  $k_g$  is known for only a limited number of cells, and in only a small fraction of these is the value of the temperature coefficient of  $k_g$  known. Thus, if we apply Equation 10 to cells for which  $k_g$  and  $b$  are not known, the likelihood of large errors is high. Second, even when the value of the temperature coefficient is known, it is known only at  $0^\circ\text{C.}$  and above. This author has assumed that the same value applies at subzero temperatures, and this is a perilous assumption. The activation energies tend to increase with lowered temperatures. Furthermore, the formation of ice in the external medium introduces a factor other than temperature; namely, a progressive increase in the concentration of extracellular solutes. As mentioned in the previous section, the concentrated solutes could affect the permeability characteristics of the membrane.

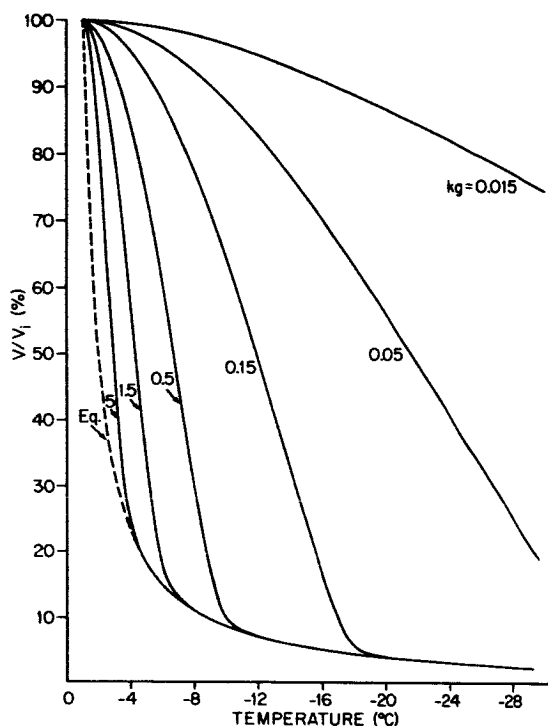


FIGURE 5. Calculated percentage of cell water remaining in a  $6\mu$ -diameter spherical cell as a function of temperature and of the permeability constant for water. The calculation assumed a cooling rate of  $100^{\circ}\text{C./minute}$  and a value of  $b = 0.0325$ .

In spite of these uncertainties, the numerical solutions to Equation 10 agree with experimental observations to an order of magnitude. TABLE 3 compares the calculated cooling rate required for intracellular ice formation in several cells with those observed experimentally. It should be emphasized that the experimental values are also subject to considerable error; for example, the cooling velocities have usually not been measured accurately and are nonlinear, whereas Equation 10 assumes a linear cooling velocity. The values for the various parameters in Equation 10 are probably best known for the red cell, and the best agreement between theory and experiment is with the red cell.

#### *Cell Membranes as a Site of Freezing Damage*

As shown in TABLE 4, large quantities of intracellular solutes leak out of yeast cells that have been killed by freezing and thawing. The fact that the dead cells lose 80 per cent of their intracellular molarity but only 31

TABLE 3  
MINIMAL COOLING VELOCITIES FOR THE FORMATION OF INTRACELLULAR ICE

Organism	Cooling velocity		Observer
	Calculated* (°C./min.)	Observed (°C./min.)	
<i>Amoeba</i>	<1	<1	Smith <i>et al.</i> (1951)
Sea urchin egg ( <i>Strongylocentrotus nudus</i> , unfertilized)	1	1 to 9	Asahina (1961)
Yeast ( <i>S. cerevisiae</i> )	20	10 20-50	Mazur (1961a, 1961b) Araki and Nei (1962)
<i>Escherichia coli</i>	~ 500	> 100	Rapatz and Luyet (1963)
Red cells (mammalian)	5000	4000	Luyet, Rapatz, and Gehenio (1963)

\*The calculated cooling rate was considered to be that for which the cell still contained 20% of its intracellular water at -12°C., according to solutions to Equation 10. Known values for the parameters are referenced by Mazur (1963b). Assumed values were used in other cases, viz. (a) sea urchin eggs:  $b = 0.1034$  (the measured value for *Arbacia* [cf. TABLE 2]; (b) yeast:  $b = 0.065$ ; (c) *E. coli*:  $k_g = 0.3$ ,  $b = 0.0325$ .

TABLE 4  
LEAKAGE OF SOLUTES INTO SUSPENDING MEDIUM FROM YEAST CELLS KILLED  
BY FREEZING AND THAWING

Measurement	Technique*	% of Cell solids in external medium	% of Cell molarity in external medium	Reference
Optical retardation	Interference microscopy	31		Mazur (1961c)
Conductance	Conductivity		82	
Melting point	Differential thermal analysis		80	Mazur (1963a)
Heat absorption			80	

\*The interference microscopy measurements were made on cells cooled at 50°C./minute to -30°C. and warmed at 1°C./minute. The other measurements were made on cells cooled at 300°C./minute to -196° and warmed at 1°C./minute.

per cent of their total solids suggests that most of the solutes lost are of low molecular weight, for low molecular weight materials in cells are responsible for most of the molarity. This conclusion is supported by measurements of the rate at which the solutes in the extracellular medium dialyze. The solutes escape through dialysis tubing more rapidly than raffinose, which has a molecular weight of 595 (Mazur, 1961c). It is also supported by direct chemical analyses of the external medium (see references in Mazur, 1965).

The quantity of escaping solutes is roughly proportional to the percentage of cells that are killed (TABLE 5). The microscopic appearance of the frozen-thawed cells suggests that the permeability damage tends to be all-or-none; that is, it suggests that a greater loss of solutes is not due to a greater loss from all cells, but to maximal loss from a greater proportion of the cells. Normal viable yeast cells contain a large vacuole, and it can be seen from TABLE 5 that the percentage of cells that lack a vacuole parallels the percentage of cells that are dead after freezing and thawing. Other evidence comes from examining the frequency distribution of the diameters of unfrozen and frozen-thawed cells (FIGURE 6). That of the unfrozen cells appears to be normal with a single mode at about  $6\mu$ . The distribution of the rapidly frozen cells (more than 99 per cent of which are dead) also appears to be normal with a single mode at a lower value of around  $4.5\mu$ . But the distribution of the cells cooled slowly to  $-30^{\circ}\text{C}$ . appears to be bimodal. There appears to be one mode at  $4.5\mu$ , the same as

TABLE 5  
EFFECT OF VARIOUS FREEZING TREATMENTS ON THE SURVIVAL AND MORPHOLOGY OF CELLS OF *S. cerevisiae* AND ON THE CONCENTRATION OF SOLUTES LEAKING INTO THE MEDIUM

Treatment	Killed* (%)	Relative cell volume* (%)	Cells lacking vacuoles* (%)	Relative concentration of cell solutes in external medium†
Untreated	0	100	7	0.00
Cooled to $-10^{\circ}\text{C}$ .	25	90	44	0.3
Slow cool to $-30^{\circ}\text{C}$ .	55	65	54	0.5
Rapid cool to $-30^{\circ}\text{C}$ .	>99	54	99.4	—
Rapid cool to $-78$ to $-196^{\circ}\text{C}$ .	>>99†	55	100	1

\*From Mazur (1961a, 1961b).

†From Mazur (1963a).

‡Based on conductivities, melting points, and refractive indices of suspensions and supernatant fluid. (Mazur, 1961c, 1963a, and Mazur, unpublished data).

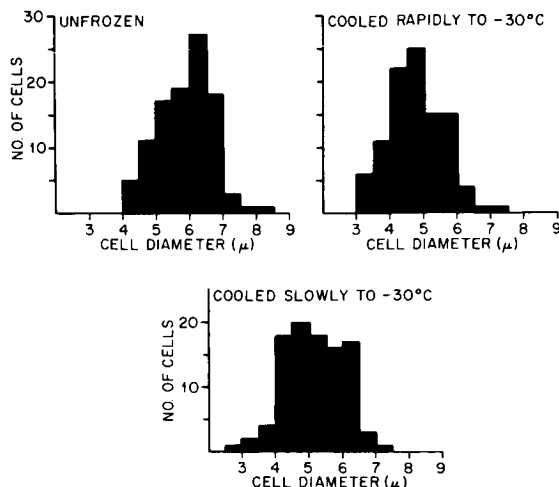


FIGURE 6. Frequency distribution of the diameters of cells of *Saccharomyces cerevisiae* subjected to indicated treatments. More than 99 per cent of the cells were killed by rapid cooling; about 60 per cent were killed by slow cooling. Treated cells were warmed at  $1^{\circ}\text{C./minute}$ . The procedures followed in culturing, freezing, and measuring the cells by micrometry are published elsewhere (Mazur, 1961*b*).

that of the dead cells, and a second mode at about  $6\mu$ , the same as that of the untreated cells. Furthermore, the two modal values contain approximately equal numbers of cells, which is consistent with the fact that slowly frozen samples contain approximately equal numbers of dead and living cells. The shrinkage of the dead cells can be explained on the basis of loss of internal osmotic pressure (Mazur, 1961*c*).

An important question is when did the permeability damage occur: during freezing, during warming, during thawing, or after thawing had been completed? Measurements of the electrical conductivity of suspensions before and after freezing tend to rule out the last of these (FIGURE 7). Before freezing, the conductivity is low because the measuring current does not detect the solutes compartmented within an intact plasma membrane (Mazur, 1963*a*). (The progressive rise in conductivity presumably reflects slow leakage of solutes from cells.) But immediately after thawing it jumps to a value 10 or more times higher than the value before freezing. (In the experiments, the tubes containing the suspensions were transferred to a  $25^{\circ}\text{C}$ . water bath as soon as the last traces of ice had disappeared. The temperature of the suspension at that time was  $0^{\circ}$  to  $5^{\circ}\text{C}$ . Ionic conductivity has a temperature coefficient of about  $2\frac{1}{2}$  per cent/ $^{\circ}\text{C}$ . Thus, the low value of the conductivity two minutes after thawing is due



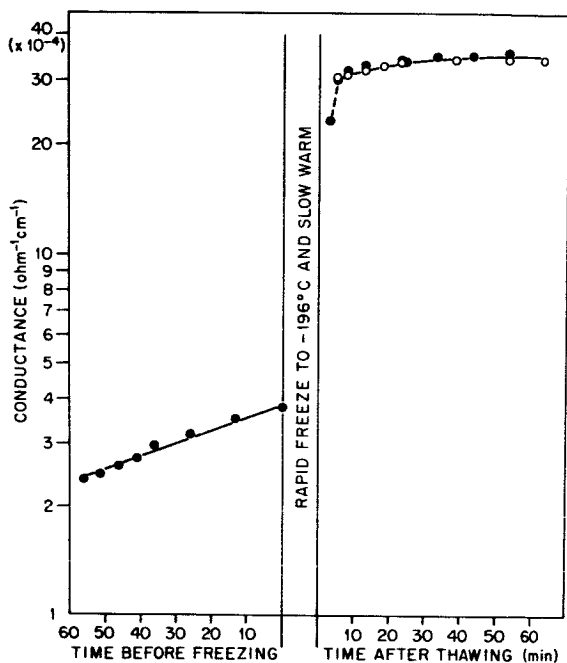


FIGURE 7. Conductance of unfrozen and of frozen-thawed suspensions of *S. cerevisiae* as a function of time. The survival after thawing was about  $10^{-5}$  per cent. The procedures followed have been described previously (Mazur, 1963a).

to the fact that the temperature of the suspension had not yet reached  $25^{\circ}\text{C}$ .) The fact that the conductivity of the thawed solution immediately reached a high value strongly indicates that membrane damage occurred before or at the completion of thawing.

Further information on the time of occurrence of membrane damage comes from measurements of the electrical resistivity of frozen suspensions during warming and thawing (Mazur, 1963a). Several facts are evident from the data in FIGURE 8. The curve labeled "after second freezing" shows the resistivity of a suspension in which the intracellular solutes are known to be distributed throughout the extracellular medium. The permeability barriers of the cells in this suspension are thus definitely damaged, and it can be seen that the resistivity of the suspension begins to drop above  $-35^{\circ}\text{C}$ . On the other hand, the resistivity of a suspension subjected to only a single freezing remains high from  $-35^{\circ}$  to about  $-4^{\circ}\text{C}$ . I have interpreted this fact to mean that the cell membranes are still sufficiently intact after a single freezing to prevent the outflow of intracellular solutes (Mazur, 1963a). However, above  $-4^{\circ}\text{C}$ ., the resistance of the initially frozen

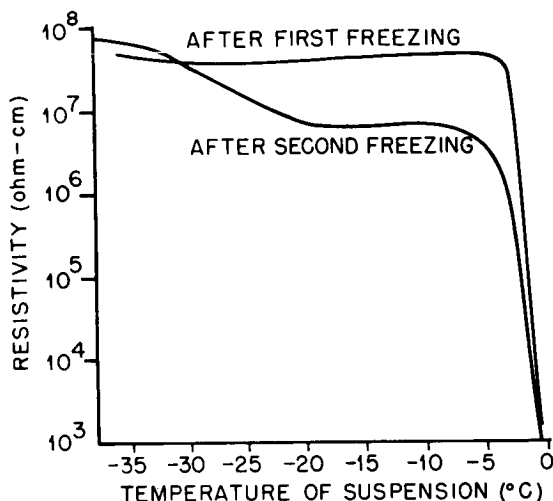


FIGURE 8. Resistivity of frozen suspensions of *S. cerevisiae* as a function of temperature during warming and thawing. Suspensions were frozen rapidly in liquid nitrogen at 300°C./minute, and the resistance measured during slow warming at 1°C./minute (upper curve). The thawed suspension was then re-frozen and the resistance measured during the second warming. The measuring frequency was 1000 cps. From Mazur (1963a) by permission of the Rockefeller Institute Press (Biophys. J. 3: 323-353).

suspensions drops abruptly, and reaches a value below that of a suspension in which the cell membranes are intact, well before the ice has disappeared from the suspension. As shown in TABLE 6, the freezing of yeast cells to a minimum of  $-2^{\circ}\text{C}$ . produces little or no alteration in the resistivity of the suspension after thawing, an observation that indicates that the cell membranes have not been irreversibly damaged. Yet the resistivity of this suspension of intact cells while it is partly frozen at  $-1^{\circ}\text{C}$ . is 30 times or more higher than that of a suspension frozen rapidly to  $-196^{\circ}\text{C}$ . and warmed to  $-1^{\circ}\text{C}$ . This difference indicates that solutes are leaking out of the rapidly frozen cells and into the surrounding medium even before the completion of thawing.

In conclusion, the permeability barriers of yeast cells are definitely damaged when the cells are killed by rapid freezing and slow thawing. The damage apparently occurs during freezing or thawing and appears, therefore, to be closely associated with intracellular ice formation. Although one cannot state unequivocally that the formation of large internal ice crystals is the direct cause of membrane damage, such a conclusion is reasonable. A suggested mechanism by which the formation and growth of ice crystals could lead to damage is presented elsewhere (Mazur, 1965).

TABLE 6  
RESISTIVITIES OF *Saccharomyces cerevisiae* AFTER BEING SUBJECTED TO  
VARIOUS LOW TEMPERATURE TREATMENTS

Suspension cooled to minimum of -2°C.*		Suspension frozen rapidly to -196°C. and warmed slowly†	
Treatment	Resistivity at indicated temperatures‡ (ohm-cm.)	Treatment	Resistivity at indicated temperatures‡ (ohm-cm.)
Untreated at 25°C.	4600	Untreated at 25°C.	5000
Supercooled to -1.0°C.	7500	Frozen once;	
Frozen at -2°C.; equilibrated at -1°C.	250,000	warmed to -1.0°C.	8700
Thawed; supercooled again to -1°C.	6870	warmed to -0.9°C.	5200
		thawed at 25°C.	290
		Frozen twice;	
		warmed to -1.0°C.	2130
		warmed to -0.9°C.	1420
		thawed at 25°C.	230

Suspensions contained  $4 \times 10^9$  cells/ml. in distilled water (Mazur, 1963a).

\*Unpublished data. Survival exceeds 90 per cent with these treatments.

†Survival is less than 0.0001 per cent (Mazur, 1963a).

‡Measured at 1000 cps. See Mazur (1963a) for details.

It is clear that the outer permeability barrier of a cell plays an important role in the response of that cell to low temperatures. It is one of the important factors determining whether or not the cell will freeze internally, and it appears to be one of the important loci of freezing damage. Knowledge of these facts should be of pragmatic importance in selecting optimal procedures for freezing cells, tissues, or organs. Possibly the emphasis can also be reversed. That is to say, knowledge of the changes in the properties of cell membranes as a result of the conversion of water to ice may be helpful in determining the ultrastructure and organization of membranes.

#### Acknowledgment

The computer program for obtaining numerical solutions to Equation 10 was devised by Mr. M. T. Harkrider, Mathematics Division, Oak Ridge National Laboratory.

## References

- ARAKI, T. & T. NEI. 1962. *Low Temp. Sci. Ser. B (Sapporo)* **20**: 57-68.
- ASAHINA, E. 1956. Contributions from the Institute of Low Temperature Science, No. 10 : 83-126. Hokkaido University. Sapporo, Japan.
- ASAHINA, E. 1961. *Nature* **191**: 1263-1265.
- ASAHINA, E. 1962. *Nature* **196**: 445-446.
- CHAMBERS, R. & H. P. HALE. 1932. *Proc. Roy. Soc. (London)*, Ser. B. **110**: 336-352.
- DAYSON, H. & J. F. DANIELLI. 1952. *The Permeability of Natural Membranes*. 2nd Ed. Cambridge University Press. Cambridge, England.
- DICK, D. A. T. 1959. *Intern. Rev. Cytol.* **8**: 387-448.
- FLETCHER, N. H. 1962. *The Physics of Rain Clouds*. Cambridge University Press. Cambridge, England.
- FRANK, H. S. & M. W. EVANS. 1945. *J. Chem. Phys.* **13**: 507-532.
- HAYS, R. M. & A. LEAF. 1962. *J. Gen. Physiol.* **45**: 933-948.
- HEMPLING, H. G. 1960. *J. Gen. Physiol.* **44**: 365-379.
- JACOBS, M. H., H. N. GLASSMAN & A. K. PARPART. 1935. *J. Cellular Comp. Physiol.* **7**: 197-225.
- KAUZMANN, W. 1959. In *Advances in Protein Chemistry*. C. B. Anfinsen, Jr., *et al.*, Eds. **14**: 1-63. Academic Press, Inc. New York, N. Y.
- LEITCH, G. J. & J. M. TOBIAS. 1964. *J. Cellular Comp. Physiol.* **63**: 225-232.
- LOVELOCK, J. E. 1954. *Nature* **173**: 659-661.
- LUCAS, J. W. 1954. *Plant Physiol.* **29**: 245-251.
- LUYET, B. J., G. L. RAPATZ & P. M. GEHENIO. 1963. *Biodynamica* **9**: 95-124.
- MAZUR, P. 1960. *Ann. N. Y. Acad. Sci.* **85**: 610-629.
- MAZUR, P. 1961a. *Biophys. J.* **1**: 247-264.
- MAZUR, P. 1961b. *J. Bacteriol.* **82**: 662-672.
- MAZUR, P. 1961c. *J. Bacteriol.* **82**: 673-684.
- MAZUR, P. 1963a. *Biophys. J.* **3**: 323-353.
- MAZUR, P. 1963b. *J. Gen. Physiol.* **47**: 347-369.
- MAZUR, P. 1965. In *Cryobiology*, H. T. Meryman, Ed. Academic Press, Inc. London (In press).
- MCCUTCHEON, M. & B. LUCKÉ. 1932. *J. Cellular Comp. Physiol.* **2**: 11-26.
- NEI, T. 1960. In *Recent Research in Freezing and Drying*, A. S. Parkes & A. U. Smith, Eds. Blackwell Scientific Publ. Oxford, England.
- NÉMETHY, G. & H. A. SCHERAGA. 1962. *J. Chem. Phys.* **36**: 3401-3417.
- RAPATZ, G. & B. LUYET. 1963. Abstracts of the Biophysical Society 7th Annual Meeting. New York, N. Y.
- SALT, R. W. 1950. *Can. J. Research (D)* **28**: 285-291.
- SALT, R. W. 1963. *Can. Entomologist* **95**: 1190-1202.
- SAKAI, A. 1961. *Low Temp. Sci. Ser. B (Sapporo)* **19**: 1-16.
- SHANES, A. M. 1963. *Science* **140**: 824-825.
- SMITH, A. U., C. POLGE & J. SMILES. 1951. *J. Roy. Microscop. Soc.* **71**: 186-195.
- SMITH, A. U. & J. SMILES. 1953. *J. Roy. Microscop. Soc.* **73**: 134-139.
- SOLOMON, A. K. 1960. *J. Gen. Physiol.* **43** (Suppl.): 1-15.
- VAN HOOK, A. 1961. *Crystallization: Theory and Practice*, A. C. S. Monograph Series No. 152, Reinhold Publ. Corp. New York, N. Y.
- VILLEGAS, L. 1963. *Biochim. Biophys. Acta* **75**: 131-134.
- WANG, J. H. 1951a. *J. Am. Chem. Soc.* **73**: 510-513.
- WANG, J. H. 1951b. *J. Am. Chem. Soc.* **73**: 4181-4183.
- WHITTEMBURY, G. 1962. *J. Gen. Physiol.* **46**: 117-130.

# NEW APPROACHES IN MEASURING THE LINEAR RATE OF ICE CRYSTALLIZATION IN WATER AND AQUEOUS SOLUTIONS\*

Maxim D. Persidsky and Victor Richards

*Presbyterian Medical Center  
San Francisco, Calif.*

The problem of measuring the crystallization rates of water and its solutes has occupied the interest of many scientists since the end of the 19th century, in particular, Tammann and his students.<sup>1-15</sup> Although the main importance of this problem lies in the realm of physical chemistry, more recent studies in the field of low temperature biology stimulated additional interest<sup>16</sup> and opened another aspect of this problem. Since it is well accepted now in cryobiology that the main assault on the living system at low temperatures occurs during the phase change, the rate of crystallization is of profound importance in the fate of the living system. The information available on the rate of ice-crystal growth is, however, very limited, and a systematic study of this problem in a wide temperature range is lacking. The only method used in earlier studies<sup>1-16</sup> for measuring the linear crystallization velocity was direct observation of the growth of ice, within a demarked distance, in a u-shaped glass tube which was immersed in a cooled alcohol bath. The liquid in the tube was brought to equilibrium with the cooling bath and remained in a supercooled state for some time before ice was initiated by seeding. The use of this method is limited both by the temperature of spontaneous crystallization and by the accuracy of reading, particularly at lower temperatures, where the velocity of ice growth becomes too rapid for accurate visual tracking. More recently,<sup>17</sup> high speed microcinematography was introduced for such measurements. The solution was frozen in a thin layer between cover slips by rapid immersion into the cooling bath of a low temperature microscope. Although very high freezing velocities were recorded at low temperatures, the determination of the actual temperature at which freezing occurred was practically impossible.

This paper will deal with a new approach to the problem of measuring the linear crystallization velocity in aqueous solutions, within a wide temperature range. New instruments will be described, and the preliminary results obtained will be discussed.

\*This work was carried out under the Office of Naval Research Contract No. 105-235.

## MATERIALS AND METHODS

*Instruments*

The main limiting factor of previous methods is the temperature of spontaneous crystallization of the solution being studied, below which no measurements were possible. If, however, the solution is supercooled for a very brief period of time in a region close to the advancing ice front, a much greater degree of supercooling is achieved and ice forms at a much lower temperature than was previously possible. This is accomplished by freezing in a thin-walled glass capillary tube which is immersed vertically into a cooling bath. The ice is initiated by seeding at the lower end of the tube and grows in an upward direction as the tube is immersed. The velocity with which the tube is being immersed is adjusted to equal the velocity of the ice growth, so that the ice front remains stationary in respect to the level of the fluid in the cooling bath. The distance of the ice front from this level at any given bath temperature determines the degree of supercooling of the liquid in the tube, and should be kept at its maximum. The measurements of the immersion velocity of the tube represent, then, the linear crystallization rate of the solution being frozen under these conditions. More detailed discussion of the thermal conditions inside the tube will follow later.

The velocity with which the capillary tube is being immersed in the cooling bath can be controlled either manually or automatically.

For automatic control of the immersion velocity we have utilized a Honeywell Class 15 strip chart recorder which was especially adapted for this purpose. The pen mechanism of this recorder was used to drive the glass tube into a cooling bath. Since the pen mechanism in this recorder travels in a horizontal plane, it was necessary to rotate the instrument 90° from its normal position. In order to overcome possible inking problems, the pen was replaced with a hot stylus. Although this recorder was not designed to operate in such a position we have not encountered any irregularities in its performance even after continuous use for many hours per day.

The recorder is also used in another unusual way, in that it is not connected as a potentiometric recorder. The pen drive motor amplifier has its input connected to a signal source only. Whenever there is no input signal, the pen drive motor stops. As long as there is an input signal of one polarity, the pen will move downward, the rate of travel being determined by the magnitude of the input signal. If the signal polarity reverses, the pen will move upward, the rate of travel again dependent on signal amplitude.

It was desired to control the immersion speed of the glass tube at the same rate as the advancing ice front. This was accomplished by projecting the image of the ice front, by means of a microscope, onto a photocell.

Light will pass through the unfrozen solution, but is partially blocked by the frozen portion of the solution.

Based on light intensity measurements a photocell circuit was designed to provide the sensing signal to the pen drive motor amplifier. A cadmium-sulfide cell, RCA type 7163, was chosen. It has the proper spectral response needed, good fast time constant, and other satisfactory specifications. Calculations indicated the output voltage would be many-fold greater than needed by the amplifier of the Honeywell recorder. This assured us of all the sensitivity that would be required. A Wheatstone Bridge circuit was designed, using the photocell as one arm. Characteristic curves on the photocell indicated it should have a resistance of approximately 100 K ohms at the light levels to be encountered. Thus the bridge was designed to have an impedance of 100 K ohms. The power supply for the photocell bridge was a 1- 1½ volt dry cell. Due to the high impedance of the bridge, the battery life will be essentially its shelf life. Due to the tremendous sensitivity it was possible to connect a voltage divider across the photocell bridge. The divider consisted of a 100 ohm resistor in series with a one megohm resistor. The output fed to the pen drive motor amplifier was the voltage across the 100 ohm resistor. The voltage divider also provided a low loading factor on the photocell bridge, thus assuring a maximum linear voltage output with respect to light changes. In addition, the 100 ohm source of signal voltage provided a low impedance so there was no problem with stray pickup between the signal source and the Honeywell recorder. The balance arm of the Wheatstone Bridge consisted of two linear taper potentiometers which were both connected as variable resistors. The 250 K potentiometer provided a coarse, while the 50 K potentiometer provided a fine balance. The use of coarse and fine controls allows the circuit to function over a wide range of light intensities. The balance controls in the bridge circuit must be adjusted so as to provide just the right amount of light reaching the photocell to maintain the ice front at a constant level as seen through the microscope. If incorrectly adjusted, the ice front and the glass tube will be driven into or out of the cooling bath too fast, which is followed by "jittering" of the tube.

The mechanical arrangement of this instrument is illustrated in FIGURE 1. It consists of a chart recorder (1), having the pen mechanism equipped with a special arm (2) and a clamp to hold the glass tube (3). The container for the cooling bath is a Dewar flask (4) with a clear window through which the glass tube is viewed. The liquid of the bath is either alcohol or isopentane cooled by aspiration of liquid nitrogen (5) through a copper coil within the flask. The liquid of the bath is agitated by air which is first passed through a drying column and then bubbled through the liquid (6). The temperature of the bath is sensed by a thermocouple and is controlled by means of a Brown Pulse Pyro-O-Vane Controller (7)

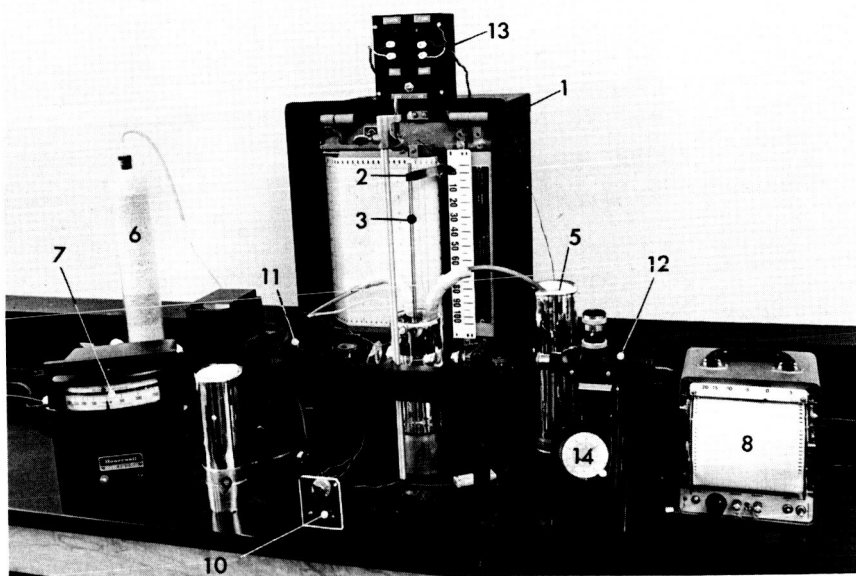


FIGURE 1. The instrument for measuring the rate of crystallization velocity in aqueous solutions. (See text for details.)

which opens and closes a solenoid valve on the aspirating line. In addition, the temperature of the bath is also recorded with a Varian chart recorder, (8) type G-11A, by which it can be read with an accuracy of  $\pm 0.2^\circ$ . The accuracy of these readings is improved by periodically adjusting the  $0^\circ\text{C}$ . reading by means of an ice water bath in a Dewar flask (9) using a selective switch (10) for the various thermocouples. A Bausch and Lomb horizontal microscope (11) with a  $2\times$  magnification objective was used to project the image of the moving ice front onto the photocell (12). The fine and coarse adjustments controlling the movement of the capillary tube are located on the Wheatstone Bridge (13).

A record of the tube travel versus time is made either directly on the chart of the Honeywell recorder (1) or by using an electrical timer (14). The timer is activated automatically by a microswitch which is attached to the pen mechanism and is turned on during the 10 cm. travel distance of the glass tube. The temperature inside the capillary tube was measured during freezing by means of a 0.003 inch thick thermocouple, and was recorded with the Varian recorder (8). The capillary tubes used for measurements with this instrument had an O.D. of 2.0 mm., an I.D. of 1.5 mm. and an overall length of 30 cm.



The instrument with manual controls was designed for measurements of the linear crystallization velocities of water, since the ice is too transparent to obtain the required response from the photocell; also, the use of polarized light was not practical with the photocell because of frequent changes of the crystalline orientation in the ice. As with the previous instrument the linear crystallization velocity was determined by the rate a capillary tube was immersed vertically into a cooled bath, and the advancing ice front was kept at a constant position in respect to the liquid level of the bath. The tube was attached to a carriage which moves along a vertical plane. The carriage was connected by a cable to a gear train to allow smooth manual movements. The capillary tubes used with this instrument had an O.D. of 1.0, an I.D. of 0.5 mm. and a length of four feet. A three and one-half foot long Dewar flask, the upper part of which was not silvered, was used for the cooling bath. The bath was cooled by aspirating liquid nitrogen through a copper coil in the flask, while the liquid of the bath was agitated by bubbling dry air throughout it. The temperature was controlled and measured the same way as with the previous instrument. To maintain the ice front at a constant position, the tube was viewed in polarized light through a binocular microscope while the carriage holding the tube was driven downward by hand. The velocity of ice crystallization was determined by measuring the time necessary for the tube to travel a 65 cm. distance which was demarked by two electrical contacts, which controlled the operation of a stop watch. The temperature inside the tube was measured and recorded by a Varian recorder.

The third method for measuring the crystallization velocity used in this study was a modification of the old method, utilizing a u-shaped capillary tube, in which some improvements were introduced. The visual tracking of the ice movement was substituted by an automatic sensing arrangement. Two, 3 mil thermocouples were inserted in both arms of the u-shaped tube. Both thermocouples were in parallel connection with a Varian recorder so that the signals received from them at any time interval were recorded consecutively. The manually controlled apparatus described above was used to immerse the tube into a cooling bath; after 30 to 60 seconds the temperature of the liquid inside the tube reached the same temperature as the bath and ice was initiated at one of its arms by seeding with a cold metal rod. The ice front was traveling a distance of 64 cm. between the two thermocouples, and the distance between the two signals recorded was used to calculate the velocity of the ice growth.

#### *Preparations*

The solutions used were: sucrose in 1.0, 2.5 and 5.0 per cent concentrations, polyvinylpyrrolidone K-30 in 2.5, 5.0, 10, 20, 30, 40 and 50 per cent concentrations, and 0.1 and 0.2 N-NaCl. All solutions were prepared in

glass distilled water. The capillary tubes used were first thoroughly cleaned, then filled with a solution and then, with the exception of those used with the third method, had one end sealed with a flame.

#### OBSERVATIONS

The performance of the first instrument, with automatic controls, was studied by making a record of the movement of the capillary tube during its immersion into a cooling bath. Five concentrations of PVP were used, which gave a wide range of freezing velocities. FIGURE 2 shows a photograph of an original record made with this instrument. The varying degrees of line slope indicates different linear velocities of ice propagation which are characteristic of given solutions in respect to concentration and bath temperature. The straight lines indicate the uniformity of movement with which the tubes were immersed into the cooling bath. The use of these chart records was, however, found to be impractical for a large number of measurements, therefore an electrical timer was incorporated which made it possible to make these measurements much faster.

Measurements were made with this instrument with various solutions and some of the results obtained are illustrated in FIGURE 3. Three sets of curves represent the changes of the velocity of crystallization with different

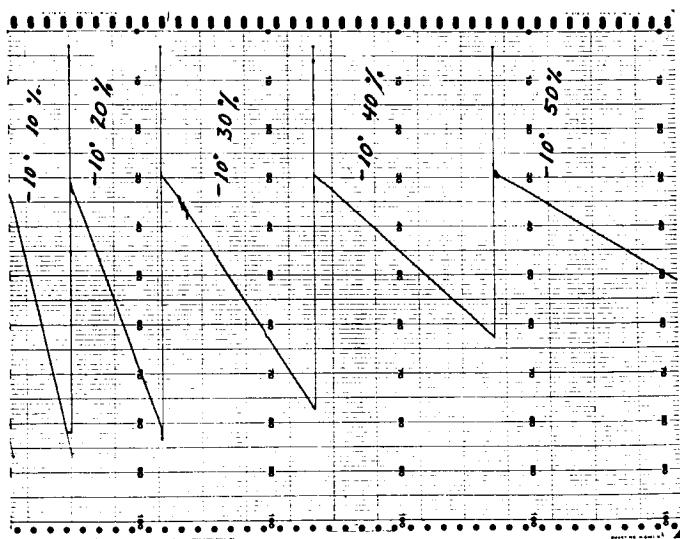


FIGURE 2. Five lines with a different slope are the record of the immersion velocity versus time of the capillary tubes containing solutions of 10, 20, 30, 40 and 50 per cent concentrations of PVP, the linear rates of crystallization of these solutions being 18.4, 13.1, 1.8, 4.6 and 3.0 cm./min. respectively.

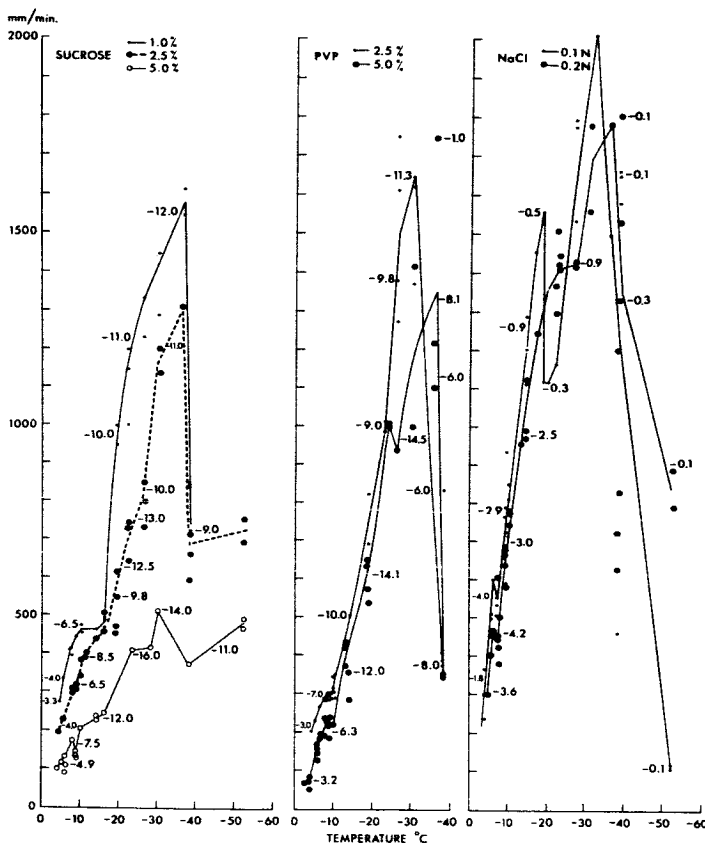


FIGURE 3. Three sets of curve represent measurements of the rate of linear crystallization velocity at different temperatures in solutions of sucrose, PVP, and NaCl at different concentrations, and obtained by using the instrument with automatic controls.

concentrations of sucrose, PVP and NaCl, occurring when the bath temperature is lowered. All these curves are characterized by an abrupt change of the crystallization velocity occurring in the temperature range between  $-8$  and  $-10^{\circ}\text{C}$ . and by a peak at  $-36$  to  $-38^{\circ}$  which is then followed by a sudden decrease of velocity. The degree of supercooling of the solution measured inside the tube, at different bath temperatures, are shown at certain points along the curves. In NaCl solutions, almost no changes were detected in this internal temperature which remains quite high throughout all temperature ranges measured. This can perhaps be explained by too great a thermal lag of the thermocouple making detection of very rapid

temperature changes impossible. (See discussion for possible ways of determining the temperature in the capillary tube.)

It is important to point out that when lowering the temperature of the bath below  $-20^{\circ}\text{C}.$ , it was necessary to reduce the distance between the level of the bath and the advancing ice front, in order to prevent spontaneous crystallization.

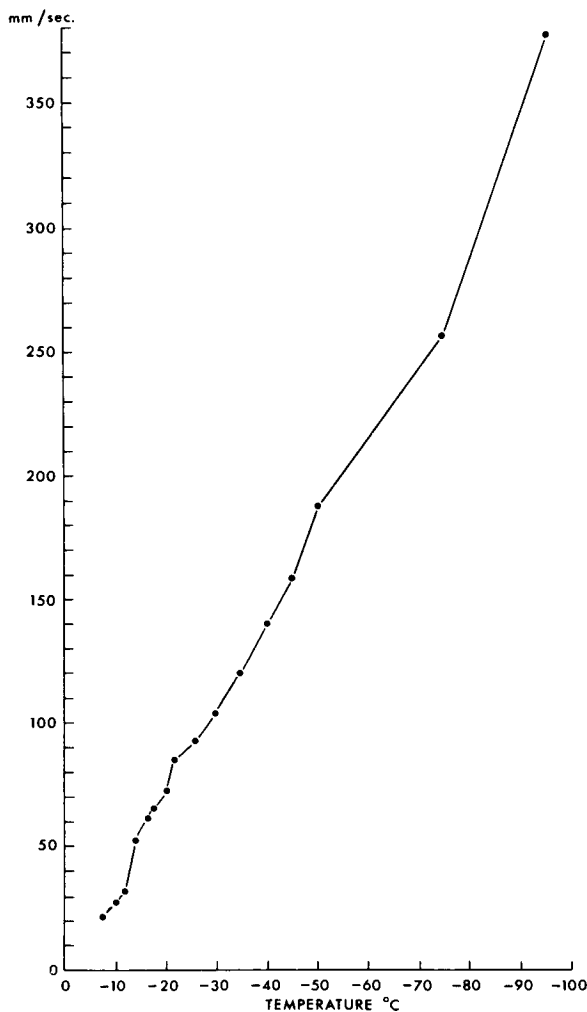


FIGURE 4. The curve represents the measurements of the rates of the linear crystallization velocities in water at different temperatures and is obtained with the hand controlled instrument.

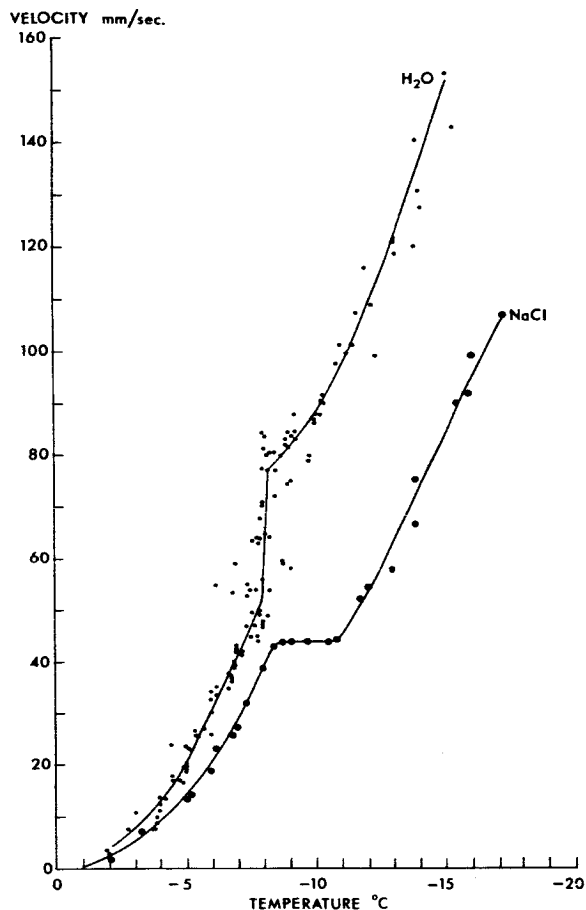


FIGURE 5. Two curves shown represent the measurements of the rate of linear crystallization velocities at different temperatures in water and in 0.1 N NaCl, and are obtained with the third method.

The study of the freezing velocity in water in a wide temperature range was attempted with the second apparatus, where the immersion speed of the tube is controlled by hand. The results of one experimental series is shown in FIGURE 4. When the bath temperature is close to  $-100^{\circ}\text{C}.$ , the freezing velocity reaches 25 meters per minute.

The third method, which is an improvement of a classical method utilizing u-shaped capillary tubes, was used in this study for comparative reasons, and the results are illustrated in FIGURE 5. Two curves are shown, one representing the freezing velocities in water, and the other in a 0.1 N solution of NaCl. The crystallization velocities in both cases are not uni-

form. While in water, the velocity of crystallization undergoes a sudden increase at approximately  $-8^{\circ}\text{C}.$ , which was well verified by numerous measurements, the velocities with NaCl solution, at  $-8^{\circ}\text{C}.$ , reaches a plateau which persists for several degrees. These measurements with NaCl compare well with the results obtained by using the first method with automatic controls. The liquid inside the capillary tubes in the third method was supercooled to the temperature of the bath after being immersed for a period of 30 to 60 seconds.

#### DISCUSSION

In evaluating the validity of the first method for measuring the velocities of linear crystallization in aqueous solutions, it is necessary to analyze first, the thermal condition produced inside the tube during freezing. The automatic adjustment of the velocity of the tube by the rate of ice growth creates a state of dynamic equilibrium which can be characterized by several parameters:

1. The distance of the ice front from the surface of the cooling bath or the depth of the immersion at which freezing takes place is constant after having been determined experimentally.
2. The length of time the tube is exposed to the temperature of the bath is constant at any given distance from the level of the bath, and is determined by the immersion velocity of the tube.
3. The thermal gradient created across the wall of the tube at any given distance from the level of the bath is constant.
4. The degree of supercooling of the liquid inside the tube during its freezing is also constant.

The situation, however, is complicated by the fact that the surface of the ice front in the capillary tube is not a flat but a concave one, as observed under the microscope. The degree of curvature of the surface increases with an increase in the rate of ice growth. At very rapid rates, such as in the case of freezing pure water, the ice front at the center of the tube advances so much slower than at the periphery that a long channel is formed. Our measurements refer only to the ice front at the surface of the tube where it advances at its fastest rate. The temperature in this layer should be very close to that of the surface of the glass. Therefore, the calculation of the thermal gradient across the wall of the glass tube and the amount of the heat of crystallization released at the ice-liquid interphase would give us the approximate temperature at which the crystallization velocity is being measured. The mathematical treatment of the thermal conditions during the freezing of the water in a capillary tube after supercooling is presented in the work of Förster.<sup>12</sup>

It is important to mention here that this apparatus enables continuous measurement of the temperature of the solution at a point very close to

the advancing ice front. This is made possible by attaching a one mil thermocouple wire to a holder above the capillary tube so that the wire is withdrawn from the tube during its immersion. The position of the thermal junction with respect to the ice-liquid interphase will be stationary and its distance from the ice front made adjustable. Thus, the thermocouple will remain for a sufficient period of time in this region, thereby reaching thermal equilibrium with it, and making measurements of the temperature possible. This study is now in progress and the results will be reported elsewhere.

The second method using manually controlled immersion gives less reproducible results than the first method, but with the development of skill better reproducibility can be achieved.

The preliminary data obtained in this study has importance mainly in the evaluation of a new method for measuring the velocity of ice growth. A few comments, however, can be made concerning some aspects of the curves shown in FIGURES 3, 4 and 5. There is a definite change in freezing velocity, occurring between  $-8^{\circ}$  and  $-10^{\circ}\text{C}$ . In water the velocity increases in this temperature region very rapidly, while in the solutions studied, a small decrease in velocity was observed. Among the factors which could affect the velocity of crystallization are the change of crystal habit or the change in orientation of crystalline axis. It is interesting to note that the measurement of crystallization rate in water made by Hartmann,<sup>8</sup> Tammann and Büchner<sup>14</sup> indicates a decrease of the velocity of crystallization at  $-8^{\circ}$ . A sharp decline of the rate of crystallization at  $-38^{\circ}$  observed in our study was also noticed previously by Volmer and Marder<sup>10</sup> and was interpreted as due to an increase in viscosity of the solution.

#### SUMMARY

1. A new method and an instrument is described for measuring the rate of linear crystallization velocity in water and aqueous solutions. The velocity is measured by the speed with which a glass capillary tube, containing solution, is immersed into a cooling bath while the advancing ice front is kept stationary with respect to the level of the cooling bath. Two methods of control of the rate of immersion, automatic and manual, are described.

2. An improvement of an older method utilizing u-shaped capillary tubes was made, and is described.

3. The evaluations of new methods and analysis of some results obtained in this study are presented.

#### ACKNOWLEDGMENT

The authors wish to express their gratitude to Mr. K. C. Rock for his help in adapting the Honeywell recorder for measuring the velocity of ice

propagation. The authors also wish to thank Mr. James Leef for his technical assistance.

## REFERENCES

1. TAMMANN, G. 1897. Ueber die Erstarrungsgeschwindigkeit. *Z. Phys. Chem.* **23**: 326–328.
2. FRIEDLÄNDER, J. & G. TAMMANN. 1897. Ueber die Krystallisationsgeschwindigkeit. *Z. Phys. Chem.* **24**: 152–159.
3. TAMMANN, G. 1898. Ueber die Krystallisationsgeschwindigkeit. II. *Z. Phys. Chem.* **26**: 307–316.
4. BOGOJAWLENSKY, A. 1898. Ueber die Krystallisationsgeschwindigkeit. *Z. Phys. Chem.* **27**: 585–600.
5. TAMMANN, G. 1899. Herrn F. W. Küsters Bemerkungen über die Krystallisationsgeschwindigkeit. *Z. Phys. Chem.* **28**: 96–98.
6. TAMMANN, G. 1899. Ueber die Krystallisationsgeschwindigkeit. III. *Z. Phys. Chem.* **29**: 51–76.
7. WALTON, J. H., JR. & R. C. JUDD. 1914. The velocity of the crystallization of undercooled water. *J. Phys. Chem.* **18**: 722–728.
8. HARTMANN, R. 1914. Über die spontane Kristallisation des Eises aus wässrigen Lösungen. *Z. Anorg. Chem.* **88**: 128.
9. FREUNDLICH, H. & F. OPPENHEIMER. 1925. Ueber die Krystallisationsgeschwindigkeit unterkühlter wässriger Sole. *Ber.* **58**: 143–148.
10. VOLMER, M. & M. MARDER. 1931. Zur Theorie der linearen Kristallisationsgeschwindigkeit unterkühlter Schmelzen und unterkühlter fester Modifikationen. *Z. Phys. Chem.* **154**: 97–112.
11. KAISCHEW, R. & I. N. STRANSKI. 1934. Zur Theorie der linearen Kristallisationsgeschwindigkeit. *Z. Phys. Chem.* **170**: 295–299.
12. FÖRSTER, T. 1936. Ueber die experimentelle Bestimmung der linearen Kristallisationsgeschwindigkeit. *Z. Phys. Chem.* **175**: 177–186.
13. TAMMANN, G. & A. BÜCHNER. 1935. Die Unterkühlungsfähigkeit des Wassers und die lineare Kristallisationsgeschwindigkeit des Eises in wässrigen Lösungen. *Z. Phys. Chem.* **222**: 371–381.
14. TAMMANN, G. & A. BÜCHNER. 1935. Die lineare Kristallisationsgeschwindigkeit des Eises aus gewöhnlichem und schwerem Wasser. *Z. Phys. Chem.* **222**: 12–16.
15. CAMPBELL, A. N. & A. J. R. CAMPBELL. 1937. The velocity of crystallization from supersaturated solutions. *Trans. Faraday Soc.* **33**: 299–308.
16. LUSENA, C. V. 1955. Ice propagation in systems of biological interest. III. Effect of solutes on nucleation and growth of ice crystals. *Arch. Biochem. Biophys.* **57**: 277–284.
17. PERSIDSKY, M. D. & B. J. LUYET. 1960. Periodicity in the freezing of aqueous solutions. *Biodynamica* **8**: 165–180.



# ENZYME PATTERNS OF TUMORS DEMONSTRATED HISTOCHEMICALLY IN CRYOSTAT SECTIONS

P. J. Melnick

*Associate Clinical Professor of Pathology, University of California Medical Center, San Francisco; and Chief, Laboratory Service, Veterans Administration Hospital, Martinez, Calif.*

## *Introduction*

This report concerns a histochemical study of the enzyme patterns of about 195 human malignant tumors, chiefly surgically resected but also including fresh autopsy material, as well as a number of normal animal and human tissues as controls. It began in 1958 with a histochemical enzyme study of a group of about 25 breast cancers to learn if their enzyme patterns might give some hint as to which were hormone dependent and which were autonomous, since the histologic type fails to give this information.<sup>1</sup> TABLES 1*a* and 1*b* summarize the results, and indicate that the differentiated breast cancers generally contained the enzymes characteristic of their normal tissue cells of origin, but that enzyme defects were frequently encountered in the undifferentiated cancers.

This study was extended to include a group of 31 carcinomas of the lung.<sup>2</sup> TABLES 2*a* and 2*b* summarize the enzyme profiles of this group, and again demonstrate that the differentiated lung cancers tended to contain the enzymes of their cells of origin, but the undifferentiated cancers presented many enzyme defects. The highly undifferentiated small round cell and oat cell carcinomas especially, showed an impressive number of enzyme defects, much like embryonal tissue. Further, in both the breast cancers and lung cancers there was considerable and generally unpredictable variation of the enzyme patterns between different specimens of each histologic type, as well as much variation in degree of activity of each enzyme in different tumors.

Aided by U.S.P.H.S. Research Grant CA-07468, and a Veterans Administration Research appropriation.

## *Enzyme Deletions*

The central problem that presented itself was the need to determine if the observed enzyme deletions or of diminished enzyme activity may have been artefactually induced by nonoptimal freezing of the tissue in the course of making the cryostat sections. Cryostat sections were used exclusively in this study, since the dehydrogenases can only be identified in frozen sections of the fresh tissue, and for convenience and uniformity the hydrolases were studied in the same set of cryostat sections also, because they are excellent for these enzymes. Should chemotherapy become

TABLE 1a  
 ENZYME PATTERNS OF CARCINOMAS OF THE BREAST  
 (1958-1961, 25 CASES)

	Hydrolases						
	Esterase	Cholinest.	Lipase	Acid Phos.	Alk. Phos.	Beta-Gluc.	Leuc. Amino.
Adenoca. 8 Cases	8	5	8	8	8	8	8
Scirr. Ca. 9 Cases	9	2	5	8	3	8	7
Medull. Ca. 4 Cases	2	0	0	4	0	3	3
Mucin Ca. 2 Cases	2	0	2	2	2	2	1
Fibroad. 2 Cases	2	2	2	2	2	2	0

a reality, pathologists may in the future be requested to determine enzyme profiles of malignant tumors in addition to the histologic diagnosis. The large literature on cancer chemotherapy indicates that empirical programs of clinical evaluation, the animal screen, the tissue culture screen, the hamster cheek pouch, and similar screens, are slow and cumbersome and present complex problems. The fresh tissue in the hands of the pathologist may become the strategic opportunity, and perhaps the only opportunity before the tumor is altered by therapy, to determine which enzymes they contain and which enzymes are missing, and the effect of various agents on their activity.<sup>3</sup> It would be important, therefore, to determine their enzyme patterns accurately.

#### *Plan of Study*

Since January, 1962, a histochemical enzyme study has been made on 140 malignant tumors to compare the effect of various freezing rates on the histochemical demonstration of enzyme activity in cryostat sections. The basic study and the detailed descriptions of the technics have been reported elsewhere.<sup>4,5</sup> Summarized briefly, when blocks of tissue were quenched rapidly in isopentane cooled to  $-160^{\circ}\text{C}.$  by liquid nitrogen, the full intensity of the enzyme activity present was demonstrated in the cryostat sections by the histochemical technics for the various enzymes. How-



TABLE 2a  
 ENZYME PATTERNS OF CARCINOMAS OF THE LUNG  
 (1958-1961, 31 CASES)

	Hydrolases						
	Esterase	Cholinest.	Lipase	Acid Phos.	Alk. Phos.	Beta-Gluc.	Leuc. Amino.
Diff. squ. cell ca. 6 Cases	6	3	3	4	3	6	5
Undiff. squ. cell ca. 9 Cases	8	4	3	8	2	6	9
Undiff. adenoca. 5 Cases	5	2	5	4	3	5	6
Undiff. small cell & oat cell ca. 5 Cases	1	0	0	2	1	3	1
Adeno-squamous ca. 2 Cases	2	2	2	2	1	2	2
Diff. adenoca. 4 Cases	4	2	1	4	3	4	1

ever, slow freezing of aliquot tissue blocks in the range of  $-1^{\circ}\text{C.}$  per minute often resulted in marked diminution of the histochemical enzyme reaction product, and often in its complete absence. Standard cryostat sections, in which the freezing rate of the tissue block varies from  $-7^{\circ}\text{C.}$  to  $-12^{\circ}\text{C.}$  per minute, generally gave results resembling those in the slowly frozen sections.

An exception was cytochrome C oxidase, which was generally completely inactive in the rapidly frozen blocks, but was usually fairly active in the slowly frozen tissues. Addition of cytochrome C to the incubating system resulted in full activity at all freezing rates, which presents an interesting principle to be discussed later. Another exception was seen when the ac-

TABLE 2b  
 ENZYME PATTERNS OF CARCINOMAS OF THE LUNG  
 (1958-1961, 31 CASES)

	Dehydrogenases									
	DPNH Diaph.	TPNH Diaph.	Succ. Dehy.	Succ. D. Syst.	Malic Dehy.	Isocit. Dehy.	Glut. Dehy.	B-Hyd But. D.	Lact. Dehy.	Cyto Oxid.
Diff. squ. cell ca. 6 Cases	5	2	3	1	4	5	6	6	6	6
Undiff. squ. cell ca. 9 Cases	9	6	5	1	8	6	9	8	7	9
Undiff. adenoca. 5 Cases	5	2	5	4	2	3	4	5	5	5
Undiff. small cell & oat cell ca. 5 Cases	3	0	1	0	0	2	2	5	4	5
Adeno- squamous ca. 2 Cases	2	1	1	0	1	1	2	2	2	2
Diff. adenoca. 4 Cases	4	4	4	3	4	4	4	4	4	4

tivity of any given enzyme was very intense such as acid phosphatase in prostatic carcinomas; in such cases the enzyme was usually visualized at all freezing rates.

### *Results*

The findings of this cryogenic study of the 140 tumors examined during the past three years are summarized in TABLES 3*a* and *b*, 4*a* and *b*, 5*a* and *b*, and 6*a* and *b*. Without giving the large number of details involved, for purposes of simplification the tables indicate the number of tumors in each group in which activity was found for each enzyme without specifying their degree of activity, since even feeble activity may have significance for chemotherapy. The number of cases in which true enzyme deletions were encountered, that is, in which no activity whatever was observed are thereby more clearly indicated. The details of the technics in the comparative study of freezing rates by which these findings were determined are given in the reference cited.<sup>4</sup>

The significant findings were again found to be similar to those observed in the series of breast and lung cancers studied between 1958–1961. For almost all of the enzymes there was considerable variation of the enzyme profiles in the different types of tumors. The differentiated tumors had more of the enzymes of their tissue cells of origin, and the undifferentiated cancers often had many enzyme defects, especially well seen among the undifferentiated lung cancers (TABLES 3*a* and 3*b*). Again, there was the unpredictable variation of enzyme patterns between different specimens of each histologic type, as well as much variation in degree of activity of each enzyme in different tumors. As already stated, the latter point is not indicated in the TABLES, but is summarized in the references cited.<sup>4</sup>

### *"Pseudo" Enzyme Deletions*

The results of the comparative study of various freezing rates may help to avoid wrong interpretations of enzyme deletions. However, many complexities and problems present themselves, some of which can be discussed under the following headings.

*Induced enzyme "deletions".* The avoidance of pseudodeletions is probably the largest and most difficult problem to be dealt with by pathologists in the future. In the present study, examination of the standard cryostat sections, or sections of the slowly frozen tissues alone, may have led to the wrong interpretation of many more enzyme deletions in these tumors than were actually present. Various forms of fixation and embedding procedures often diminish or abolish enzyme activity and this has been studied by several investigators.<sup>6</sup> For this reason it is possible that cryostat sections of rapidly frozen tissues may become a standard method. Other sources of false negative and false positive reactions encountered have been described in detail elsewhere reporting other aspects of this study.<sup>4,5</sup>

TABLE 3a  
 ENZYME PATTERNS OF CARCINOMAS OF THE LUNG  
 (1962-1964, 31 CASES)

	Hydrolases											
	Esterase	Chol. est.	Lipase	Acid Ph.	Alk. Ph.	5'-Nuc.	G-6 Ph.	ATP ase	Beta Gluc.	Leuc. Amin.	Ala. Amin.	Sulfat.
Diff. squ. cell ca. 6 Cases	6	6	3	6	3	5	6	6	6	6	5	6
Undiff. squ. cell ca. 11 Cases	11	5	4	10	6	7	8	8	6	9	6	10
Undiff. adenoca. 3 Cases	3	0	2	1	0	2	1	2	1	2	2	2
Undiff. small cell & oat cell ca. 3 Cases	1	0	0	0	0	1	1	1	0	0	0	2
Adeno-squamous ca. 2 Cases	2	1	1	2	1	2	2	2	2	2	1	2
Diff. adenoca. 6 Cases	6	3	5	5	4	5	6	6	6	6	3	6

TABLE 3b  
ENZYME PATTERNS OF CARCINOMAS OF THE LUNG  
(1962-1964, 31 CASES)

	Dehydrogenases													
	DPNH Dia.	TPNH Dia.	Succ. Dehy.	Succ. Syst.	Isoc. Dehy.	Malic Dehy.	Glut. Dehy.	B-Hyd. But. D.	Lact. Dehy.	Glyc.- Ph. D.	Eth. Deh.	G6P Deh.	6PG Deh.	Cyto Oxid.
Diff. squ. cell ca. 6 Cases	5	4	6	5	5	6	5	4	6	6	0	6	6	6
Undiff. squ. cell ca. 11 Cases	8	6	3	2	5	4	3	3	4	4	3	5	6	11
Undiff. adenoca. 3 Cases	1	2	2	1	1	1	0	0	0	0	2	0	0	3
Undiff. small cell & oat cell ca. 3 Cases	1	0	2	2	2	2	2	1	2	1	0	2	2	3
Adeno- squamous ca. 2 Cases	2	2	2	2	2	2	2	1	1	2	0	1	1	2
Diff. adenoca. 6 Cases	6	5	5	5	5	5	5	4	6	4	0	5	5	6



TABLE 4a  
 ENZYME PATTERNS OF MALIGNANT TUMORS  
 (1962-1964)

	Hydrolases											
	Esterase	Chol. est.	Lipase	Acid Ph.	Alk. Ph.	5'-Nuc.	G-6 Ph.	ATP ase	Beta-Gluc.	Leuc. Amin.	Ala. Amin.	Sulfat.
Colon: adeno-ca. 25 Cases	25	15	14	22	12	18	14	20	20	22	13	25
Stomach: adeno-ca. 6 Cases	6	6	5	6	5	6	6	6	6	5	4	6
Pancreas: adeno-ca. 4 Cases	4	2	4	4	2	3	2	3	3	1	1	3
Prostate: ca. 13 Cases	13	1	0	13	3	4	4	9	7	3	0	13
Skin: squ. cell ca. 13 Cases	13	7	1	12	2	6	6	6	8	12	4	13
Skin: basal cell ca. 3 Cases	3	2	2	2	2	1	1	3	1	1	0	3

TABLE 4b  
 ENZYME PATTERNS OF MALIGNANT TUMORS  
 (1962-1964)

	Dehydrogenases													
	DPNH Dia.	TPNH Dia.	Succ. Dehy.	Succ. D. Syst.	Isoc. Dehy.	Malic Dehy.	Glut. Dehy.	B-Hyd. But. D.	Lact. Dehy.	Glyc.- Ph. D.	Eth. Deh.	G6P Deh.	6PG Deh.	Cyto. Oxid.
Colon: adeno-ca. 25 Cases	25	23	22	20	20	20	19	17	18	19	5	16	18	25
Stomach: adeno-ca. 6 Cases	6	6	6	4	4	4	5	6	4	4	1	6	6	6
Pancreas: adeno-ca. 4 Cases	4	3	3	3	3	3	3	3	4	4	2	4	4	4
Prostate: ca. 13 Cases	10	9	9	7	6	6	7	5	6	4	0	5	7	13
Skin: sq. cell ca. 13 Cases	9	10	9	6	10	11	10	8	10	7	1	10	11	13
Skin: Basal cell ca. 3 Cases	3	3	2	1	2	1	3	2	2	1	0	2	2	3



TABLE 5b  
ENZYME PATTERNS OF MALIGNANT TUMORS  
(1962-1964)

Dehydrogenases														
	DPNH Dia.	TPNH Dia.	Succ. Dehy.	Succ. D. Syst.	Isoc. Dehy.	Malic Dehy.	Glut. Dehy.	B-Hyd. But. D.	Lact. Dehy.	Glyc.- Ph. D.	Eth. Deh.	G6P Deh.	6PG Deh.	Cyto. Oxid.
Hepatocellular ca. 5 Cases	2	1	4	4	0	2	2	1	5	2	3	4	3	5
Thymomas 3 Cases	3	3	2	2	1	1	3	0	3	2	0	3	3	3
Brain: gliomas 3 Cases	3	3	3	3	1	1	1	1	3	1	0	3	3	3
Bladder: tran- sitional cell ca. 4 Cases	4	2	1	1	2	3	4	2	4	1	0	4	4	4
Gall bladder ca. 1 Case	1	1	1	1	1	1	1	1	1	1	0	1	1	1
Parathyroid adenoma 1 Case	1	0	0	0	0	1	1	0	1	1	0	1	1	1
Kidney: hypernephroma 2 Cases	2	0	1	1	1	1	1	1	1	0	0	2	2	2
Testis: seminoma 1 Case	1	1	1	1	1	1	1	1	1	1	0	1	1	1

**TABLE 6a**  
**ENZYME PATTERNS OF MALIGNANT TUMORS**  
**(1962-1964)**

TABLE 6b  
ENZYME PATTERNS OF MALIGNANT TUMORS  
(1962-1964)

	Dehydrogenases													
	DPNH Dia.	TPNH Dia.	Succ. Dehy.	Succ.D. Syst.	Isoc. Dehy.	Malic Dehy.	Glut. Dehy.	B-Hyd. But. D.	Lact. Dehy.	Glyc.- Ph. D.	Eth. Deh.	G6P Deh.	6PG Deh.	Cyto. Oxid.
Parotid: Mixed tumors 5 Cases	5	2	5	3	2	5	5	5	5	2	0	5	5	5
Thyroid ca. 1 Case	1	1	1	1	1	1	1	1	1	1	0	1	1	1
Mesenchymal Tumors:														
(a) Mesothelioma (2 Cases)	2	2	2	0	0	1	2	0	2	0	0	2	2	2
(b) Giant cell tumor, (stroma: tend. sh. (g. cells: (2 Cases)	2 2 2	2 2 2	2 2 2	0 0 2	2 2 2	2 2 2	2 2 2	0 0 2	2 2 2	0 0 2	0 0 0	2 2 2	2 2 2	2 2 2
(c) Fibrosarcoma (2 Cases)	2	0	2	0	2	2	2	0	2	0	0	2	2	2
(d) Rhabdomyosa. (1 Case)	1	1	1	1	1	1	1	1	1	1	0	1	1	1
(e) Liposarcoma (1 Case)	0	1	1	1	0	0	0	1	1	1	1	1	1	1
(f) Hibernoma (1 Case)	1	1	1	1	1	1	1	1	1	1	0	1	1	1
(g) Lipoma (1 Case)	1	0	1	0	1	1	1	1	1	1	0	0	0	1
(h) Leiomyoma (1 Case)	1	1	1	0	1	1	0	0	1	0	0	1	0	1
Lymphomas:														
(a) Lymphocytic (7 Cases)	7	2	5	3	5	3	5	5	5	5	0	5	5	7
(b) Hodgkins (1 Case)	1	0	1	1	1	1	1	1	1	0	0	1	1	1
(c) R-E Sarcoma (1 Case)	1	0	1	0	1	0	1	1	1	1	0	1	1	1

*Latent enzymes.* Unmasking of histochemical enzyme activity by rapid freezing suggests that other mechanisms of unmasking possible latent enzyme activity should be investigated. In a study with my colleague S. H. Lawrence,<sup>7</sup> application of histochemical enzyme methods to blood serum in immunoelectrophoretic preparations disclosed that beta lipoprotein was the carrier for all of the serum enzymes. Purified beta lipoprotein however showed feeble or no enzyme reactivity *in vitro*, until it was either sonicated, or treated with ether or detergents, or frozen and thawed repeatedly. Another well-known example is the unmasking or increased activity of acid hydrolases and cathepsins in degenerating lysosomes. Aside from such matters as the availability and concentration of substrates and the competitive activities of closely related enzymes, the control mechanisms that release enzyme activity under physiological and pathological conditions, about which so little knowledge has until now been accumulated, will probably present a central problem for biological research for a long time to come.

*Abnormal enzymes.* The often great chromosomal variability of tumors understandably can result in the failure of synthesis of enzymes if the DNA and RNA templates are abnormal or missing. Another mechanism considered by some is binding by toxic agents or by viruses, of these templates or other cell organelles, or perhaps the enzymes themselves, so that they become eliminated in daughter cells.

Another possibility that should be considered is that the apparently missing enzymes are in reality present but have been formed abnormally by any of the mechanisms described above, so that they can not react with their normal substrates. Investigation of such apparent enzyme deletions with analogues of their normal substrates is indicated. It is planned to extend the present study to test this hypothesis in tumors where enzyme deletions are encountered that appear not to be artefactual, by the use of analogues of DPN and TPN and of other substrates, to possibly detect abnormal enzymes if present.

*Nonspecific substrates.* Enzymes exist in multiple molecular forms some of which may react with one or more substrates, but not with others. Vice versa, various molecular forms of an enzyme, or even a group of often unrelated enzymes, may act upon the same substrate. For example, the naphthyl acetates, the naphthol AS acetates, the indoxyl acetates, thiol-acetic acid, and the thiocholine and other choline substrates can almost all be hydrolyzed by carboxylic acid esterases as well as by choline esterases, occasionally by some peptidases, and perhaps by other enzymes. Differential inhibitors have been used, but the many isozymes demonstrable by electrophoresis in starch gel and similar media reveal a complexity that may not become resolved by means of differential inhibitors alone.

*Enzyme Patterns*

The purpose of the present study was specifically to find out what enzymes tumor cells contain and how active they are, without relation to problems of viability. Slow freezing rates generally protect the viability of cells, and rapid freezing is generally destructive and lethal as Waravdekar *et al.*<sup>8</sup> and others have demonstrated. Increased histochemical activity of enzymes in rapidly frozen tissues may therefore be related to injury of cell organelles in the course of rapid freezing, that may release or unmask active sites of enzymes which in the living cell perhaps are held inactive until needed. As mentioned, an example is the increased activity of acid hydrolases in degenerating lysosomes. However, inactivity or feeble activity in the slowly frozen tissues was often more accentuated in autopsy tissue even only a few hours postmortem, and in surgical specimens that had been separated from their blood supply several hours before being processed, and which therefore had presumably sustained more anoxic injury than fresh specimens. Levitt<sup>9</sup> has indicated that ice crystal formation in slowly frozen tissues compresses cytoplasm, thereby approximating sulfhydryls to form disulfide bonds that tend to obscure and mask reactive sites. Such a mechanism may explain the diminished activity found in the slowly frozen tissues, and it is planned to investigate this material further with histochemical methods for disulfide and sulfhydryl. However, Shikama<sup>10</sup> believes that freezing injury resulting in enzyme inactivity may result from a change of the normally found cubical arrangement of water molecules that are tightly bound to ultrastructural lipoprotein membrane surfaces, into a hexagonal structure. It is planned to extend the present study to see what role additives such as dimethyl sulfoxide or glycerin may have in preventing such a destructive rearrangement of the molecular structure of bound water, and what the histochemical results may be.

The attached TABLES give summaries of the enzyme patterns of the 195 tumors that were studied, extracted from the large amount of detailed data recorded for the total project. Twelve hydrolases and 14 oxidative enzymes were studied. For most of the enzymes many different substrates and couplers were tested, the details of which have been described in the technical report cited.<sup>1</sup> For the purpose of this report a positive result was recorded for each enzyme under a single heading, even if only one of several different substrates that may have been used had given a result. In similar studies in the future it may be of significance to record results for each substrate separately, as was mentioned in relation to isozymes some of which show specific as well as general reactivity. It was often necessary to test out a range of conditions to find the optima for the realistic conditions of medical practice on human tissues. Most histochemical technic were



developed on normal fresh animal tissues, which are genetically different and therefore understandably require different optima. It is interesting to observe the different electrophoretic mobilities of enzymes in different animal species.<sup>11</sup> Furthermore, animal tissues can be processed very quickly before hypoxic and other degenerative conditions can get under way, which is not usually possible in human surgical and autopsy material. Also, and perhaps of prime importance, in human tissues the many variables introduced by disease will require close attention and most careful consideration in histochemistry. Discussion of the findings observed in the 195 tumors studied as recorded and summarized in the attached TABLES, can be conveniently grouped under the following headings.

*Hydrolases.* (1) Among the hydrolases, esterase (tested with five substrates), and acid phosphatase, ATPase, beta-glucuronidase, and sulfatase, tested with two substrates each, were almost ubiquitous, yet occasionally and unpredictably acid phosphatase and beta-glucuronidase were inactive. Examination of the slowly frozen sections or the standard cryostat sections alone would have resulted in the false interpretation of many enzyme deletions for these enzymes, or at least of feeble activity. It was only in the rapidly frozen tissue quenched at  $-160^{\circ}\text{C}$ . in isopentane that the full range of enzyme activity was observed. These statements apply to every enzyme studied (with the exception of cytochrome C oxidase to be discussed in more detail below), so that there is no need to repeat them in the discussions of the other enzymes below.

(2) Lipases studied with three substrates were active in carcinomas of the liver, most carcinomas of the digestive tract (pancreas, stomach and colon), and in many breast, lung and skin cancers. It was interesting that some liver cell carcinomas did not react to Tween 80 whereas the adjacent normal liver parenchyma reacted strongly to it.

(3) Cholinesterase studied with five substrates was active in gliomas of the brain, thymomas, and occasionally tumors whose normal cells of origin are subject to cholinergic influence such as carcinomas of the pancreas, stomach, colon and liver. Acetylcholinesterase was occasionally uniquely seen in carcinomas of the stomach.

(4) Alkaline phosphatase studied with two substrates was prominent in mesenchymal tumors and in stroma and capillaries of tumors in general. It was also often active in tumors of the digestive tract such as stomach and colon; occasionally it was demonstrated only with naphtholic substrates in the more differentiated portions of carcinomas of the prostate and breast. In such tumors the rapidly frozen tissue showed the enzyme active throughout.

(5) Glucose-6-phosphatase and adenosine-5'-monophosphatase (generally known as 5' nucleotidase) were active in many tumors yet were also unpredictably inactive in a number of tumors of various kinds. The role

of these two enzymes is often obscure and it is hoped that histochemical correlations in material such as this may help elucidate their functions.

(6) Leucine aminopeptidase studied with two substrates was also active in most tumors, but was also unpredictably inactive in many tumors of various kinds. Alanine aminopeptidase was active in fewer than half the tumors examined, chiefly in carcinomas of the liver, pancreas and digestive tract. Aside from the hormone-producing endocrine tumors and mucinous and keratinizing tumors, the subject of biosynthetic function in tumors such as those that contain peptidases has been obscure and difficult to examine. It may be that histochemical enzyme techniques may in the future aid in probing problems of function and specialization in tumor cells, aside from the opportunities they furnish to examine bioenergetic and biosynthetic pathways.

*Dehydrogenases.* Bioenergetic mechanisms in living cells have occupied the best efforts and intense interest of many biologists for a long time, since the controlled release of chemical energy is essential for the life of the cell. For this reason the enzyme defects in tumors among the glycolytic and oxidative pathways have attracted much attention. As will be seen from the TABLES, these are especially prominent in the undifferentiated cancers, but also occur unpredictably in all of the groups of tumors. The possible hypotheses for this phenomenon, varying from the chromosomal variability of tumors, to the inactivation of their DNA and RNA templates, have already been discussed.

The same principles of cryoenzymology that were described for the hydrolases also apply to the oxidative enzymes. In the slowly frozen blocks the enzyme reaction product was often feeble or absent, and in the parallel block frozen rapidly the full extent of enzyme activity was visualized. True enzyme deletions could be identified with more confidence, therefore, provided factors as yet unknown are not involved.

It is quite possible, therefore, that histochemical methods may be able to supplement, confirm, or enhance the work in this area that has been done chiefly by biochemists for some years. Histochemical methods furnish accurate localization, while biochemical methods furnish accurate quantitation, and the two supplement one another significantly. Of course, the most important problem that is presented is to trace the possible alternate pathways of the metabolism of glucose in these tumors when enzyme defects block the usual routes.

At this point it seems important to cite an important paragraph in a brilliant review by LePage and Henderson<sup>12</sup> entitled: "Unity and Diversity in Cancer — The Deletion Hypothesis". They state: "In recent years students of the biochemistry of cancer have tended to become mesmerized by metabolic likenesses among tumors. These findings have been formulated in the "convergence" hypothesis of Greenstein (1954, 1956), and have

been widely accepted. At the same time, those primarily interested in the chemotherapy of cancer and those who observed tumor growth and biology have always been profoundly impressed by the great differences observed among tumors. This is indicated by the fact that no one definition of the words "cancer" or "neoplastic" is entirely satisfactory. Even Greenstein (1956) recognized this diversity in the biology of tumors, while citing the apparent biochemical similarities among them. It seems possible to reconcile the unity and diversity in cancer by the application of the "deletion" hypothesis of carcinogenesis. Such a concept of the origin of neoplastic cells from normal cells appears to have more experimental support than other theories of carcinogenesis and to have wider application to the problems of cancer...."

The results of the present study take on logical meaning when interpreted in the light of the deletion hypothesis of Potter, Miller and Miller, LePage and Henderson, and others; and the discussions of the various oxidative enzyme groups in these tumors will reflect this viewpoint. The variable enzyme patterns seen in these tumors are actually not new in nature, but are seen in an endless variety of microorganisms, plants and animals. Yeasts prefer to ferment carbohydrate to alcohol; lactic acid bacilli contain no Krebs cycle but prefer to go no further than terminate glycolysis with lactic acid; a host of microorganisms can be induced to acquire or lose many different enzymes by giving them or withholding the proper substrate; and the diabetic or starving mammalian organism loses temporarily or even permanently a number of oxidative enzymes.<sup>13,14</sup>

With respect to the dehydrogenases found in the 195 tumors of the present study, it is understandable that the Pasteur effect will be seen in those that contain few or no enzymes of the Krebs cycle; and the Warburg effect (aerobic glycolysis), too, for the same reason, no matter how much oxygen may be available. The Crabtree effect can also be understood if highly active glycolytic enzymes reduce and appropriate DPN so that it becomes removed from weakly active respiratory enzymes. The highly active pentose phosphate shunt in very many of these tumors is understandable because in many of them the glycolytic as well as respiratory pathways were seriously impaired by enzyme defects. The Entner-Doudoroff pathway<sup>15</sup> may become still another avenue for glucose metabolism through glucuronic acid formation, in tumors whose enzymic structure is seriously impaired. Perhaps this is the reason for the frequent occurrence of beta glucuronidase in these 195 tumors, tested with two substrates. It seems hopeful that histochemical methods may contribute realistic support to these areas of knowledge that have so far been almost purely biochemical.<sup>16</sup>

It can be stated, however, that in general, in the more differentiated tumors, the various group of dehydrogenases were reasonably complete,

resembling in this way their normal tissue cells of origin. However, in the undifferentiated cancers many were missing.

*Glycolytic pathway.* The enzymes of the glycolytic pathway tend to be soluble and to dissolve rapidly into the incubating solution, so that successful histochemical technics have so far been developed for only a few of them. However, lactic dehydrogenase can be readily demonstrated, and as the TABLES indicate, it was very active in many of the undifferentiated cancers. The Pasteur, Warburg and Crabtree effects can be readily understood in such cancers in which the Krebs cycle is impaired; and indeed, in many of them succinic, malic and isocitric dehydrogenases were inactive. Ethanol dehydrogenase was completely inactive in most of the tumors. Apparently the human organism prefers not to convert acetaldehyde to ethanol as does yeast. It would be interesting to see what cirrhotic livers could do with this enzyme. Alpha glycerophosphate dehydrogenase was active in a number of tumors, so that it may be significant in lipid metabolism, and perhaps the Pasteur effect.

*Tricarboxylic acid cycle.* One of the impressive findings was the frequent impairment of the Krebs cycle in many tumors of all varieties. Succinic, malic and isocitric (DPN) dehydrogenases were frequently inactive. At the same time lactic, beta hydroxybuteric, and glutamic dehydrogenases, which bring materials to the Krebs cycle from carbohydrate, lipid and protein respectively, were frequently active in the same tumors (although occasionally also inactive). To trace alternate pathways of electron transport presents an intriguing problem and histochemical methods may become rewarding in the future in this area. Succinic dehydrogenase, incidentally, was one of the enzymes most frequently found inactive in the slowly frozen tissues. Had the latter alone been examined an incorrect interpretation of many more deletions would have been made.

*Pentose phosphate shunt.* The first two enzymes of the oxidative shunt, glucose-6-phosphate dehydrogenase and 6-phosphogluconic dehydrogenase, were both often found to be very active in many of the tumors. The pentose shunt is a most important source of biosynthetic pathways of various kinds, for example, as a source for synthesis of nucleic acid pentoses for growing tissues such as tumors. The pentose shunt is also almost the only source for TPNH. The TPNH (NADP) formed by this system is a most important reducing agent not only in biological synthesis of various kinds, but as an electron acceptor in the absence of oxygen. Still further, the pentose shunt is important in the breakdown of glucose when other enzymes that perform this function are inactive or missing.

*DPNH and TPNH diaphorases.* Both of the diaphorases were often found intact and very active in the tumors, yet again, they were often unpredictably inactive. It is impressive to find deletions of these two key enzymes

which transfer electrons from so many enzymes to an enzyme of such central importance as cytochrome C oxidase. It is probable that these are also tumors in which glycolysis is so prominent and in which the Pasteur effect is seen.

It may also be possible that tumors vary in their bioenergetic mechanisms under different circumstances. The vascularity of many tumors is often greatly impaired (i.e., bulky tumors often show ischemic necrosis in their centers), and such impaired vascularity may activate glycolysis when oxygen tension is severely diminished. Just as in diabetes or starvation, enzymes concerned with glucose metabolism may disappear and fail to become synthesized, so tumors that are ischemic may lose enzymes of oxidative metabolism although they may have originally contained them. Histochemical methods may help to elucidate such problems, as evidenced by the range of enzyme activity in various portions of a tumor at the various distances from its blood supply.

*Cytochrome C oxidase.* The experience with cytochrome C oxidase in all of the tumors and normal tissues examined was diametrically opposite to that observed for the hydrolases and dehydrogenases. In the rapidly frozen tissues quenched in isopentane at  $-160^{\circ}\text{C}$ . the enzyme was invariably totally inactive or at most showed only feeble activity. In the slowly frozen tissues and in the standard cryostat sections the enzyme was generally feebly to moderately active in many tumors, although inactive in others. This puzzling reversal was seen even in normal tissues as a general rule with the exception of the myocardium; but even in the myocardium mitochondrial cytochrome C was inactive in the rapidly frozen blocks.

The clue to the solution of the problem was presented by a well-known phenomenon ordinarily present in all sections processed for cytochrome C oxidase and well known to histochemists for many years, namely, the presence of scattered nucleations or nidations of activity scattered haphazardly throughout the section and unrelated to formed elements in the tissue. These nucleations generally consist of scattered localized deposits of reaction product that obscure even the best preparations. In the rapidly frozen tissues these curious clusters of reaction product were all that was observed.

It became evident that freezing the tissue resulted in sequestration and crystallization of the intrinsic cytochrome C so that it became unavailable as the substrate for the enzyme. This process of crystallization became much accentuated by rapid freezing. In the focal areas where the cytochrome C was sequestered enzyme activity took place and focal deposits of reaction product occurred. In the remainder of the section however no activity was seen because there was no substrate present.

The reaction for cytochrome C oxidase was therefore repeated in a second set of sections of the tumors, with the addition of extrinsic cytochrome C to the incubating solution in a concentration of one milligram

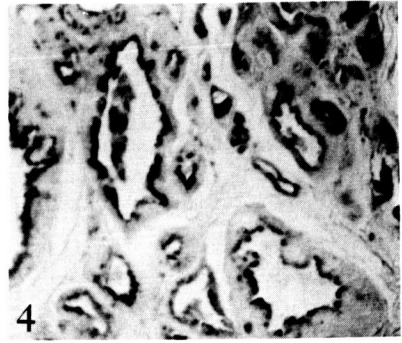
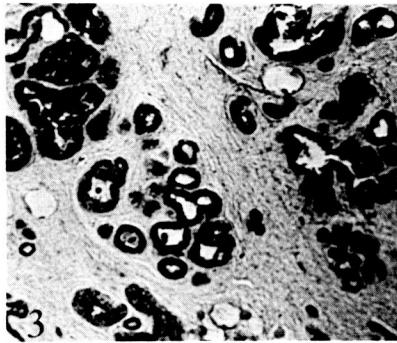
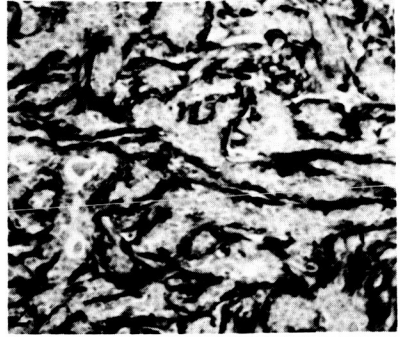
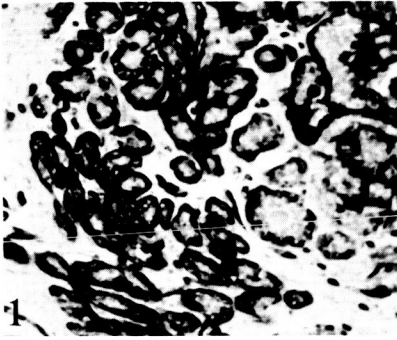


FIGURE 1. Differentiated adenocarcinoma of the breast (H-3-59;  $\times 225$ ). Alkaline phosphatase, Gomori method. Enzyme reaction product is seen throughout the cytoplasm of the tumor cells.

FIGURE 2. Differentiated adenocarcinoma of the breast (H-10-59;  $\times 225$ ). Alkaline phosphatase, Gomori method. Enzyme activity is present only in the myoepithelial layer.

FIGURE 3. Differentiated adenocarcinoma of the breast (H-10-59;  $\times 225$ ). Esterase, azo dye method. Enzyme reaction product is seen in this example throughout the cytoplasm of the tumor cells.

FIGURE 4. Differentiated adenocarcinoma of the breast (H-3-59;  $\times 350$ ). Esterase, azo dye method. Enzyme reaction product is seen only in the luminal border of the cells of this tumor.

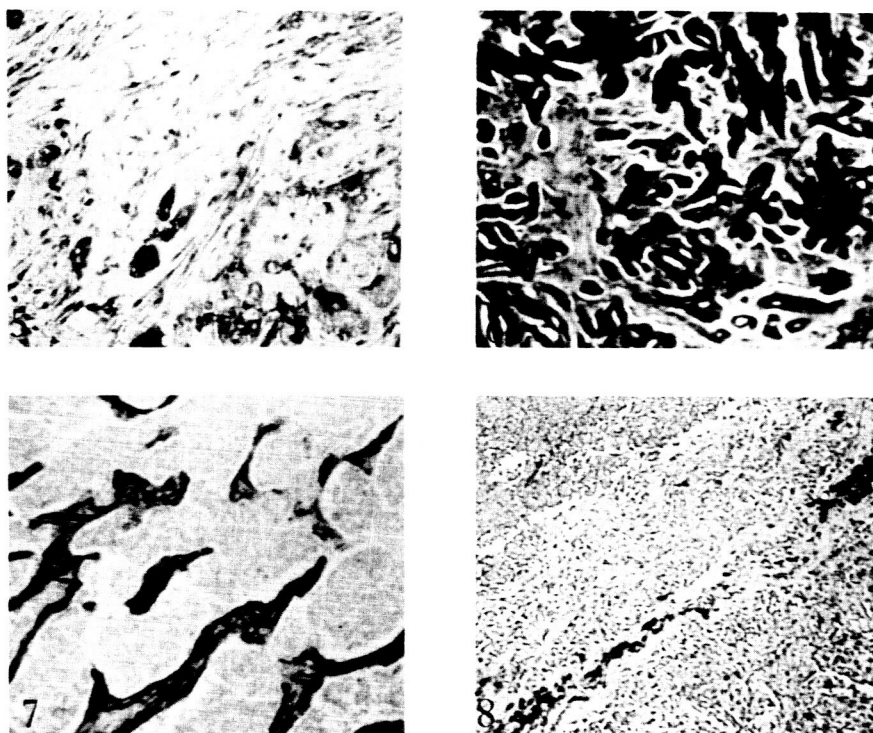


FIGURE 5. Scirrhus carcinoma of the breast (H-12-59;  $\times 250$ ). Alkaline phosphatase, Gomori method. Enzyme reaction product is seen in an occasional ductule, but the cords of tumor cells contain no enzyme activity.

FIGURE 6. Scirrhus carcinoma of the breast (H-12-59;  $\times 400$ ). Esterase, azo dye method. Enzyme activity is seen throughout the cytoplasm of the tumor cells.

FIGURE 7. Undifferentiated medullary carcinoma of the breast (H-4-59;  $\times 175$ ). Alkaline phosphatase, Gomori method. No enzyme activity is present in the tumor cells, but is seen in the stromal fibroblasts.

FIGURE 8. Undifferentiated medullary carcinoma of the breast (H-4-59;  $\times 225$ ). Esterase, azo dye method. No enzyme activity is seen in the tumor cells, but is seen in clumps of histiocytes in the stroma.

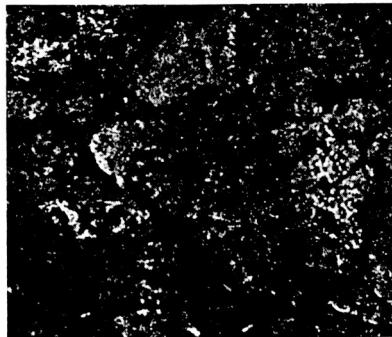
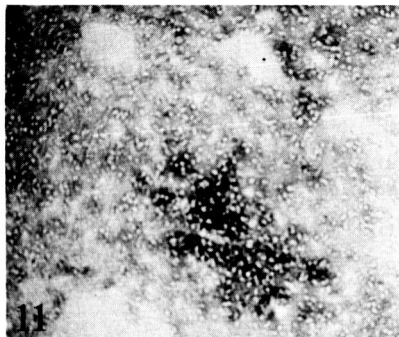
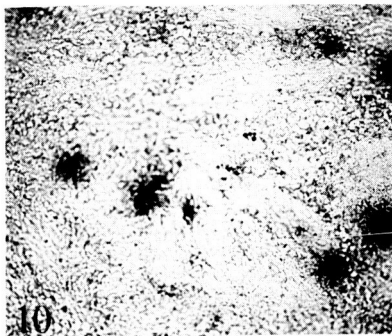
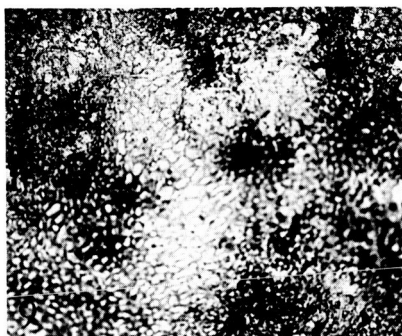


FIGURE 9. Undifferentiated squamous cell carcinoma of the larynx (H-59D-64;  $\times 275$ ). Cytochrome C oxidase, Burstone method. Slowly frozen section. Enzyme activity is seen in some tumor cells, but not in others where, instead, clumps of reaction product are seen unrelated to formed elements.

FIGURE 10. Undifferentiated squamous cell carcinoma of the larynx (H-59E-64;  $\times 250$ ). Cytochrome C oxidase, Burstone method. This section is from the rapidly frozen block and demonstrates that freezing, especially rapid freezing, crystallizes and thus sequesters intrinsic cytochrome C, rendering it unavailable as the substrate for the reaction except in the localized areas where it is present. By adding cytochrome C to the incubating mixture the reaction is uniform throughout, in both the rapidly frozen and slowly frozen blocks (not illustrated). This demonstrates that this enzyme is apparently not affected by freezing, in contrast to all the other enzymes examined.

FIGURE 11. Glioma of the brain (H-18D;  $\times 300$ ). Cholinesterase, Gomori method. Slowly frozen block. Moderate amounts of enzyme reaction product is seen in the cytoplasm of some of the tumor cells, but in the majority there is only feeble enzyme activity in this slowly frozen block.

FIGURE 12. Glioma of the brain (H-18E-64;  $\times 250$ ). Cholinesterase, Gomori method. In this section from the rapidly frozen block enzyme activity is intense.



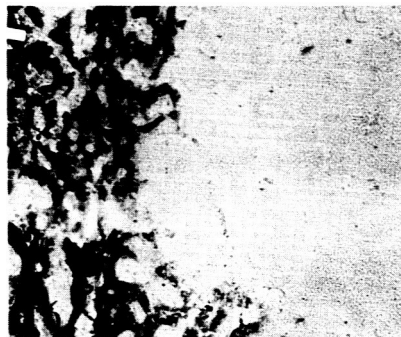
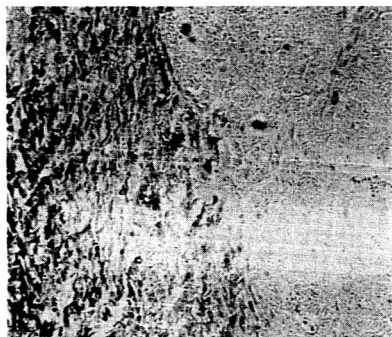
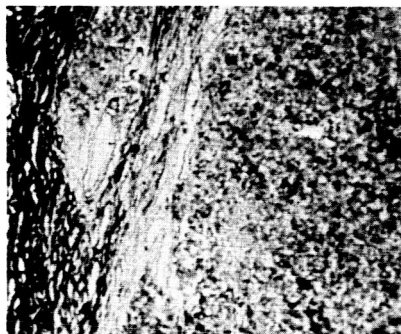
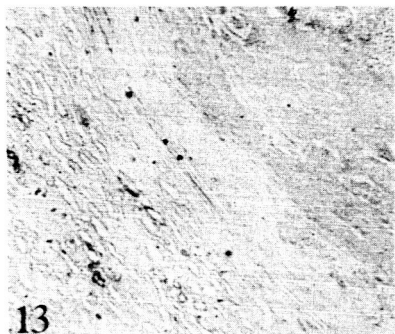


FIGURE 13. Metastasis of an undifferentiated carcinoma of the lung to the kidney (H-65D-64;  $\times 150$ ). Succinic dehydrogenase. Slowly frozen block. Histochemical enzyme activity is not present in the tumor, and is very feeble in the kidney in this section from the slowly frozen block.

FIGURE 14. Metastasis of an undifferentiated carcinoma of the lung to the kidney (H-65E-64;  $\times 200$ ). Succinic dehydrogenase. Rapidly frozen block. Enzyme activity appears in the tumor, and is greatly enhanced in the kidney. (FIGURES 15 and 16 illustrate an example of what is probably a true enzyme deletion in a tumor.)

FIGURE 15. Metastasis of an undifferentiated carcinoma of the lung to the liver (H-52D-64;  $\times 175$ ). Beta-hydroxy-butyric dehydrogenase. Slowly frozen block. Histochemical enzyme is absent in the tumor, and is feeble in the adjacent liver parenchyma.

FIGURE 16. Metastasis of an undifferentiated carcinoma of the lung to the liver (H-52E-64;  $\times 225$ ). Beta-hydroxy-butyric dehydrogenase. Rapidly frozen block. In this section the enzyme activity in the liver can be seen greatly intensified, but is absent in the tumor.

per ml. This is immediately reduced by the naphtholic component of the incubating system so that ample reduced cytochrome C was available for the procedure, that had not been sequestered by previous freezing. The result was that the enzyme was found active at all freezing rates in all tissues. Even so, in the rapidly frozen tissues with its focal areas of more intense concentration of cytochrome C, the focal concentrations of reaction product often persisted in addition to the diffuse normal activity of the enzyme throughout the section.

Cytochrome C oxidase is an ubiquitous enzyme present in all living forms. Its active site has an identical structure in all organisms, even in yeast which is 600 million years old in the course of evolution, although the apo-enzyme varies in different species. It is therefore of great interest that this enzyme was found active in every tissue examined, since it is the key enzyme that receives electrons from every source and transfers them to molecular oxygen. It is therefore of great interest that no deletions of this enzyme were found.

A number of troubling questions immediately present themselves. If cytochrome C oxidase is always present why does it not invariably carry out oxidative metabolism. One possible answer is the fact that in a number of tumors it has been found that no reduced cytochrome C may be formed to act as a substrate because of the competitive need for DPNH and TPNH by the defective enzyme patterns of the tumor. Another possible answer may be found in those tumors in which DPNH and TPNH diaphorases are absent. Still other answers may be related to direct ATP synthesis from glycolytic enzymes that may become greatly activated under anaerobic conditions. It is hoped that the many intriguing problems thus presented can be probed with histochemical technics in combination with biochemical methods.

Although water is the universal menstruum in which all life exists, the above described experience with cytochrome C oxidase may justify our turning our attention also to other substances in cells that may be affected by freezing and by other cryogenic modalities.

#### *Acknowledgments*

The technical assistance of Pauline Heizer, Ph.D., the late Carl W. Howell and the cooperation of the Linde Co., are gratefully acknowledged.

#### *References*

1. MELNICK, P. J. & W. BULLOCK. Histochemical study of breast neoplasms. *Am. J. Pathol.* 35: 706, 1959.
2. MELNICK, P. J. 1962. Histochemical study of undifferentiated lung cancers. *Proc. 21st Annual Res. Conf. Pulm. Dis. VA-Armed Forces.* : 151-154.
3. BURSTONE, M. S. 1962. *Enzyme Histochemistry.* : 563-573. Academic Press. New York, N. Y.

4. MELNICK, P. J. 1965. Effective of various freezing rates on the histochemical identification of enzyme activity. *Proc. Fed. Am. Soc. Exptl. Biol.* (Washington). **24**: S259-S268.
5. MELNICK, P. J. Histochemical identification of enzyme activity in frozen tissues and tumors. *Cryobiology* **1**: 11.
6. STOWELL, R. E. 1964. (Chairman). Conferences on comparison of different fixation methods and their significant for histochemistry. *In Proc. 2nd Int. Congress of Histo- and Cytochem.* T. H. Schiebler, A. G. E. Pearce & H. H. Wolff, Eds. : 111-112. Berlin, Germany.
7. LAWRENCE, S. H. & P. J. MELNICK. Enzymatic activity related to beta-lipoprotein in immunoelectrophoresis. *Proc. Soc. Exptl. Biol. Med.* **107**: 998-1001.
8. WARAVDEKAR, V. S., P. J. GOLDBLATT, B. F. TRUMP, C. C. GRIFFIN & R. F. STOWELL. 1964. Effect of freezing and thawing on certain nuclear and mitochondrial enzymes of mouse liver. *J. Histochem. Cytochem.* **12**: 498-503.
9. LEVITT, J. 1964. Cryobiology as viewed by the botanist. *Cryobiology* **1**: 9-10.
10. SHIKAMA, K. 1963. Denaturation of catalase and myosin by freezing and thawing. *Science Rep. Tohoku Univ. 4th Series. Biology* **29**: 91-106.
11. LAWRENCE, S. H., P. J. MELNICK, & H. E. WEIMER. 1960. A species comparison of serum proteins and enzymes by starch gel electrophoresis. *Proc. Soc. Exptl. Biol. Med.* **105**: 572-575.
12. LEPAGE, G. A. & J. F. HENDERSON. 1960. Biochemistry of tumors. *In Progress in Experimental Tumor Research.* F. Homburger, Ed. 440-476. J. B. Lippincott Co. Philadelphia, Pa.
13. GREENBERG, D. M., Ed. 1960. *Metabolic Pathways*, 2nd Ed. **1**. Academic Press. New York, N. Y.
14. THANNHAUSER'S TEXTBOOK OF METABOLISM AND METABOLIC DISORDERS. 1962. 2nd Ed. N. Zollner, Ed. Trans. by S. Estren. Grune & Stratton. New York, N. Y.
15. HOLLMAN, S. 1964. Nonglycolytic Pathways of Metabolism of Glucose. Trans. by O. Touster. : 81-82. Academic Press. New York, N. Y.
16. AISENBERG, A. C. 1961. *The Glycolysis and Respiration of Tumors.* Academic Press. New York, N. Y.

## CHEMICAL AND MORPHOLOGIC CHANGES IN THE PROSTATE FOLLOWING EXTREME COOLING

Maurice J. Gonder, Ward A. Soanes, Vernon Smith  
*Veterans Administration Hospital, Buffalo, N.Y.*

The prostate in man is an accessory sex gland located at the outlet of the bladder. It forms the first portion of the urethra and circumscribes the urethra. Normally, during micturition, the prostatic urethra becomes intravesicalized as the detrusor muscle of the bladder contracts, thereby markedly reducing urethral resistance. The prostate is subject to pathologic changes which prevent this reduction in resistance making it difficult to void and ultimately ending in bladder decompensation, renal failure or intolerable symptoms. These pathologic changes are scarring secondary to inflammation of the prostate. All operative procedures designed to eliminate obstruction create the intravesiculization of the prostatic urethra by removing portions of the prostate gland.

Thirty years ago, the operative intervention into this area carried a mortality rate as high as 15 per cent. Better operative techniques, adequate blood replacement, and antibiotic therapy has reduced this mortality to two per cent or less. However, mortality is still considerable, and combined with the heritage of a much higher mortality, operative intervention, for the most part, has been confined to those patients with bladder decompensation, kidney failure, and intolerable symptoms. These rather terminal indications for intervention suggest that there is room for improvement in our approach to this problem. Indeed the symptoms of moderate difficulty voiding, night-time voiding, etc., has been assumed by our older population to be a burden they must assume with years.

The controlled application of extreme cold to tissue has been made possible by modern engineering advances, primarily, the development of vacuum insulation. The instrument we employ to effect surgical freezing is the Linde CE 2 Cryosurgical equipment developed initially for use of the Cooper cryosurgical system. The CE 2 is a completely integrated unit capable of furnishing cold down to  $-200^{\circ}$  to the tip of the probe. The unit consists of a vacuum-insulated liquid nitrogen container, feed line, and probe assembly, and is equipped with appropriate temperature control devices. The vacuum insulation allows all but the heat transfer surface of the probe tip to remain at room temperature.

For our first studies, the dog prostate was selected because it is readily accessible and undergoes a hypertrophy in aging canines somewhat similar to that found in human beings. The anterior half of one side of the prostate was frozen. The rest was used as a control. The probe temperature was

dropped to  $-150^{\circ}$  and freezing continued for four minutes. The animals were then sacrificed at intervals, the prostate serially sectioned, and the pathologic changes studied.

*Pathology*

*Gross.* After thawing, there was immediate swelling of the prostate gland with hemorrhage (FIGURE 1). By the 14th day, the prostate was



FIGURE 1. Swelling of the gland with hemorrhage.

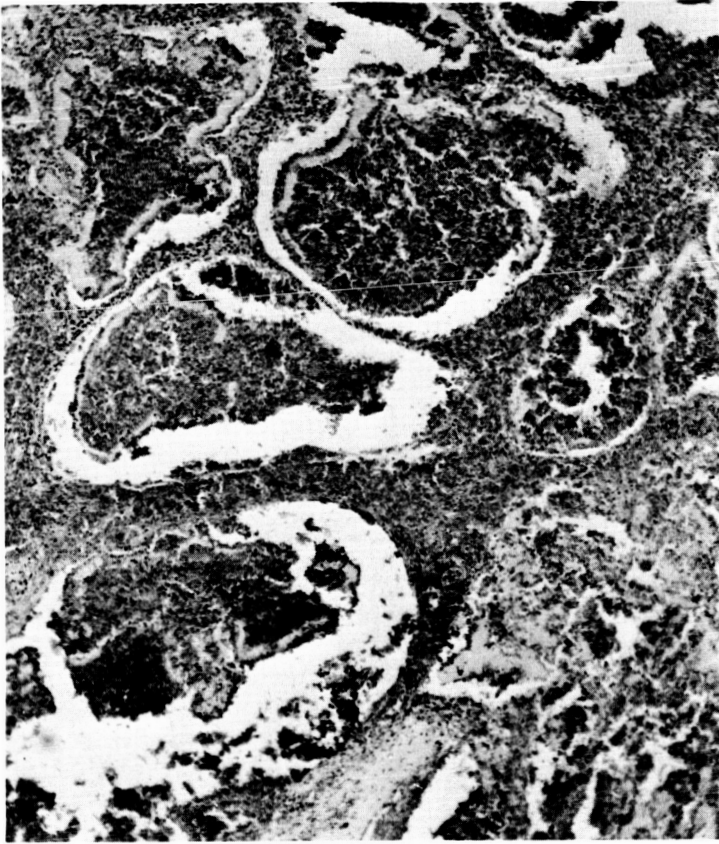


FIGURE 2. Necrosis and hemorrhage noted at five days. Nuclear detritus in lumen of glands. Ghost outline of glands remain but cellular membrane destroyed.

definitely decreased in volume. By the 22nd day, there was gross diminution in size but no other visible abnormality.

*Microscopic.* Microscopically, there was immediate necrosis (FIGURE 2) which progressed with ghost cells apparent and breakdown in cellular membranes and collections of nuclear detritus. Hemorrhage into the tissue is marked. This is from the area which was cooled to the lowest temperature. As we progressed towards the periphery of the injury, glandular structures are damaged (FIGURE 3), but noticeably spared to a degree. By nine days there is distinct fibroblastic activity around the periphery of the injury. There is still hemorrhage noted and only ghost outlines of glandular and stromal substance. There was marked histiocytic activity seen and hemosiderosis demonstrated. By the 14th day, microscopic ne-

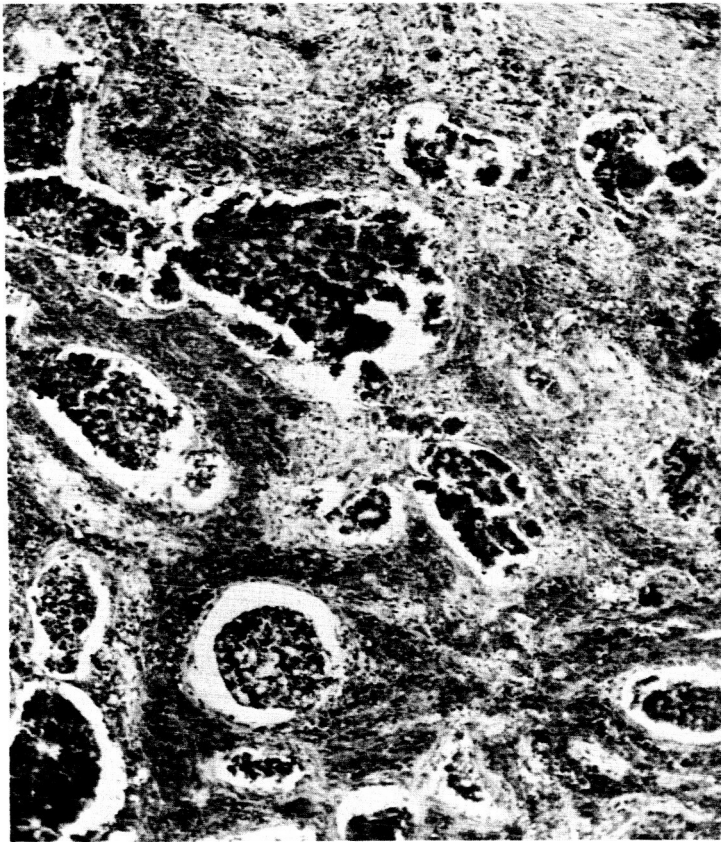


FIGURE 3. Periphery of damaged area at five days. Some cells at basement membrane of gland survive.

crisis was still evident. There is still evidence of some nuclear detritus. Hemorrhage is less evident and collections of hemosiderin are prominent. It is noted at this point, that there is beginning regrowth of tubules in an immature fashion, at the periphery of the injury (FIGURE 4). The periphery of the injury, likewise, shows well-advanced fibrosis with some remaining hemorrhage and hemosiderosis. In several specimens at this stage, there was evidence of squamous metaplasia in the glands surrounding the necrotic area. Inflammation per se was still quite minimal. At 22 days, the microscopic picture is that of maturation of the glandular regeneration. There is modest scar formation and minimal inflammatory reaction. Histiocytic activity and hemosiderosis continue. At 28, 35 and 45 days, the regrowth of tissue continues with distinct budding and branch-

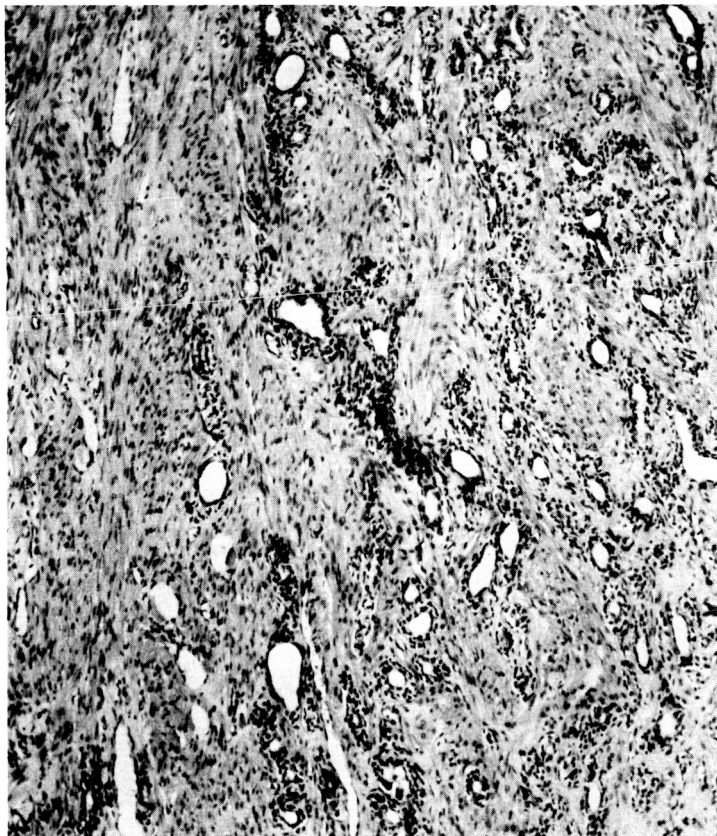


FIGURE 4. Periphery of lesion at 14 days. Demonstrating beginning regrowth of tubules.

ing noted (FIGURE 5). The epithelial cell is more typical. FIGURE 6 demonstrates the reduction in size and obvious alteration of the histologic pattern grossly apparent at 13 days.

We feel that these experiments demonstrated that freezing causes cellular breakdown which was ultimately resorbed with minimal inflammatory reaction. Cellular destruction was most complete when the temperature was the lowest and where freezing occurred the fastest. In those areas at the periphery of the lesion where freezing was slower and the temperature less cold, there was considerable fibrosis seen. There was minimal inflammatory reaction early and late, and this suggested to us that there was a minimal amount of denaturization of protein. Grossly, the prostate was definitely smaller where frozen, by the second week. Due to the fact the





FIGURE 5. Histology at 45 days; glands are beginning to branch.

degree of cold could be carefully controlled and simple freezing did not cause total necrosis, we felt we could begin to study the effects on human prostate with safety.

Before and during this study, we had anticipated certain problems which needed resolution before and while the treatment of prostatic urethral obstructions in man was carried out by this method:

1. Toxicity of the patient post-treatment due to tissue necrosis. Denaturation of protein might cause a foreign protein-type of reaction.
2. Initially, the equipment available for freezing tissues, particularly in organs with a large blood supply, presented a technical problem.
3. We thought that bleeding might be a problem due to the obvious histologic hemorrhage.

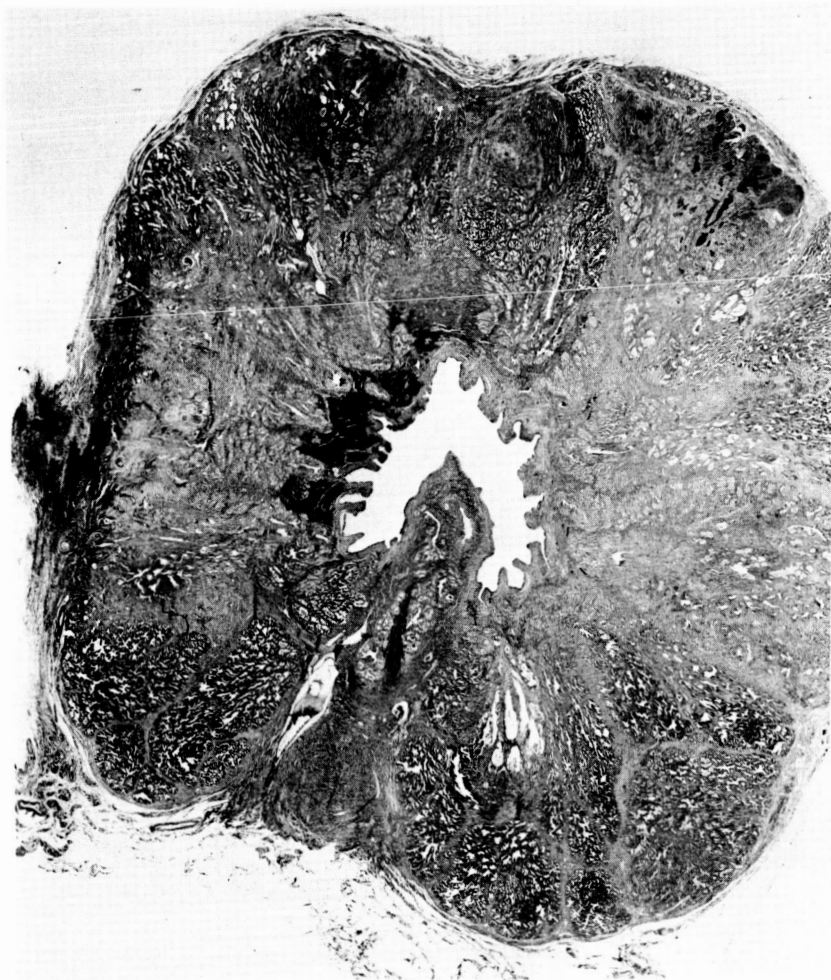


FIGURE 6. Reduction in size apparent by 13 days.

4. The length of time required for relief of the obstruction after treatment. There was considerable swelling secondary to the freezing injury, and the patient might require catheter drainage for an inordinate period of time.

5. There is a critical relationship between bladder function and urethral resistance, and there was a danger of damaging either the external urethral sphincter, bladder or rectum due to the anatomic relationships of these structures to the enlarged prostate.

6. The fibrosis occurring at the periphery of the injury could result in a marked narrowing of the prostatic urethra during the healing phase.

7. Almost all enlargements of the prostate are associated with infection and the necrotic tissue would be vulnerable to this infection.

8. It appears that some cells might resist freezing more than others, and inadequate destruction of the mixture of stromal and glandular cells making up the prostate, might be a possibility.

9. It was essential that we have a simple method to facilitate a wider application of this procedure.

With these considerations in mind, we began to create cold lesions, study pathologic changes and to develop the technical equipment required. It was apparent that *that* tissue cooled the fastest resulted in the most complete destruction, whereas the slower freezing at the periphery noted the survival of certain cells. The injured but surviving tissue was stimulated to produce granulation tissue. This encouraged us from several aspects; primarily, it indicated that if the majority of the freezing was applied to the urethral surface, then the possibility of fistula and damage to adjacent structures would be minimized.

The *enlarged* prostate in man is fitted snugly in a firm, fibrous capsule which has a separate blood supply from the adjacent membranous urethra and bladder. As freezing continues, the prostate enlarges, increasing the pressure between the frozen area and this firm, fibrous capsule, thus de-

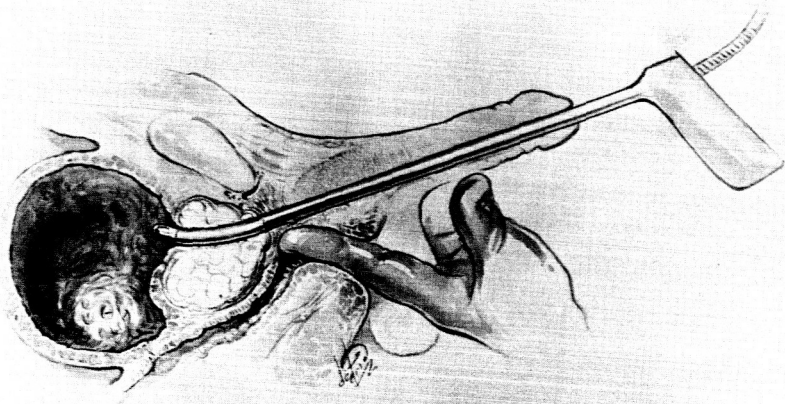


FIGURE 7. Freezing probe in place in urethra.

creasing the blood supply and accelerating the freezing process. Those adjacent structures with separate blood supply were cooled but not frozen. Definitely within the survival range.

We ascertained that we could advance from a rather complicated procedure, using relatively small probes, to a larger instrument allowing increased freezing capabilities. This enables us to freeze larger amounts of prostatic tissue colder with little damage to adjacent structures.

#### *Method*

The bladder is filled with air, holding the bladder walls away from the prostatic urethra (FIGURE 7). The freezing surface is  $2\frac{3}{8}$ " long, located at the end of the probe. One cm. from that freezing surface, there is a

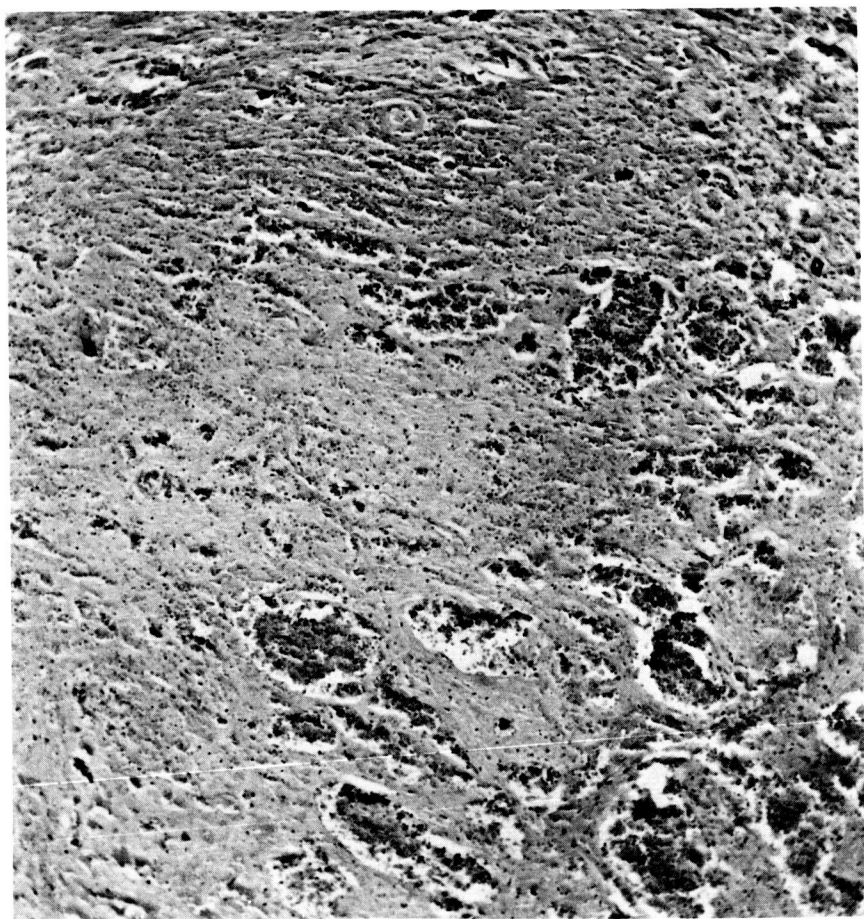


FIGURE 8. Necrosis at five days.

button which is palpable rectally and this is placed at the apex of the prostate gland. Any extra length projects into the bladder, and the bladder is insulated by the air. The prostate is palpably and visibly frozen within 30 seconds. The temperature of the probe tip is reduced to  $-190^{\circ}$  and the freezing process continued for five minutes. As cooling starts, the prostate becomes adherent to freezing surface. As the temperature is reduced, there is obvious expansion within the frozen prostate. The lesions produced resemble those noted in the animal experimentation. The necrosis apparent (FIGURE 8) at five days in that area adjacent to the urethra was complete. Towards the periphery, there was partial survival. At the very edge of the prostate, there was tissue that seemed histologically near-normal.

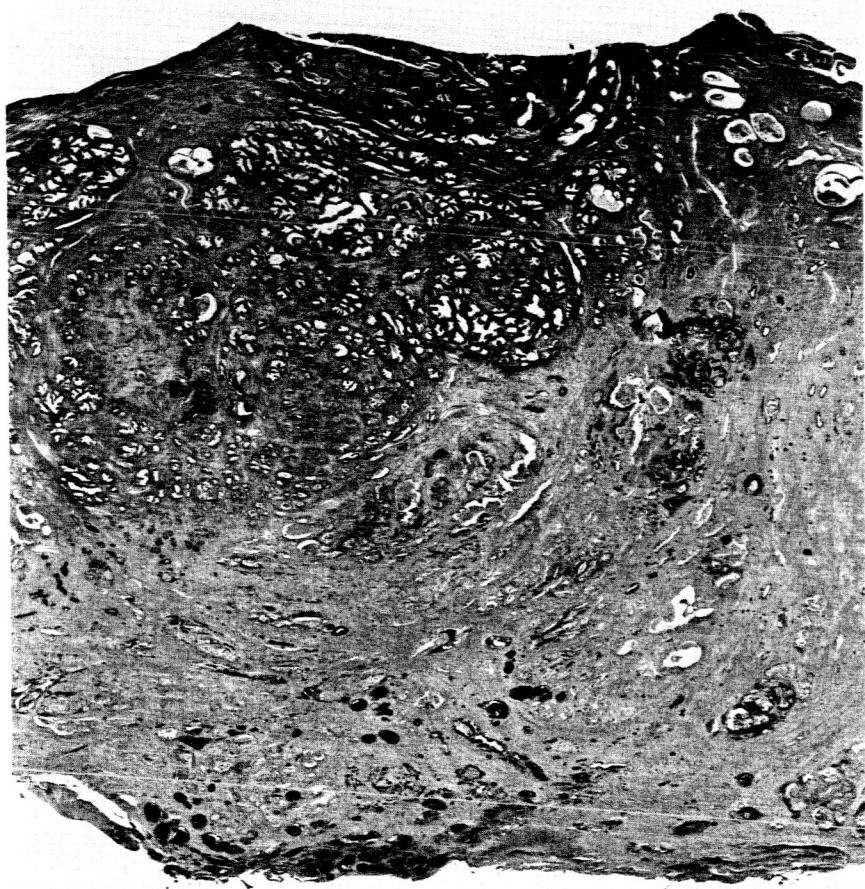


FIGURE 9. Full thickness prostate gland.

Utilizing a Gomori histologic technique, there is, histologically, no acid phosphatase activity in this tissue. Apparently, the rather sophisticated function of the prostate epithelium to produce enzymes is suspended, at least temporarily by the freezing process. The whole thickness of the prostate gland is shown (FIGURE 9). Much of the necrotic portion has been discharged in the urine. Some remains, and the more normal hypertrophied prostate remaining is demonstrated. This elimination of necrotic prostate within five days is illustrated (FIGURE 10) by these x-ray pictures on the left showing the air-filled bladder with the probe in place, and the hypertrophied prostatic impinging on the floor of the bladder, and on the right upper, a preoperative urethrogram, and on the lower picture, the urethrogram taken at five days, clearly demonstrating rather marked widening of the bladder and intravesicalization of the bladder neck.

Several prostatic carcinomas have been frozen rather thoroughly. FIGURE 11 demonstrates tissue removed at 14 days for biopsy purposes. Extensive necrosis is seen. Squamous metaplasia is present in a malignant gland.

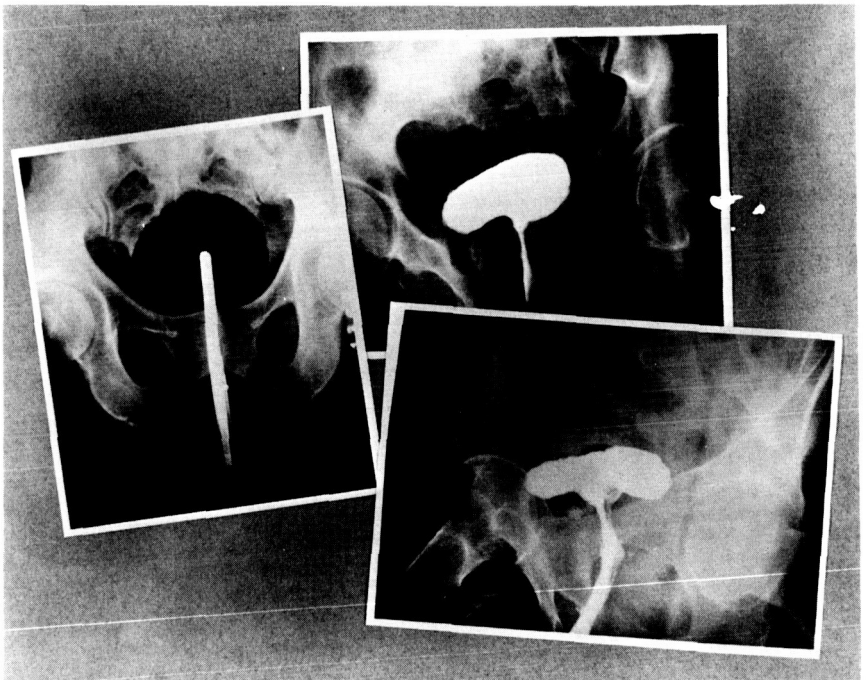


FIGURE 10. Left, air-filled bladder with probe in place, hypertrophied prostatic impinging on floor of bladder. Right upper, preoperative urethrogram. Lower, urethrogram taken at five days, demonstrating rather marked widening of bladder and intravesicalization of bladder neck.



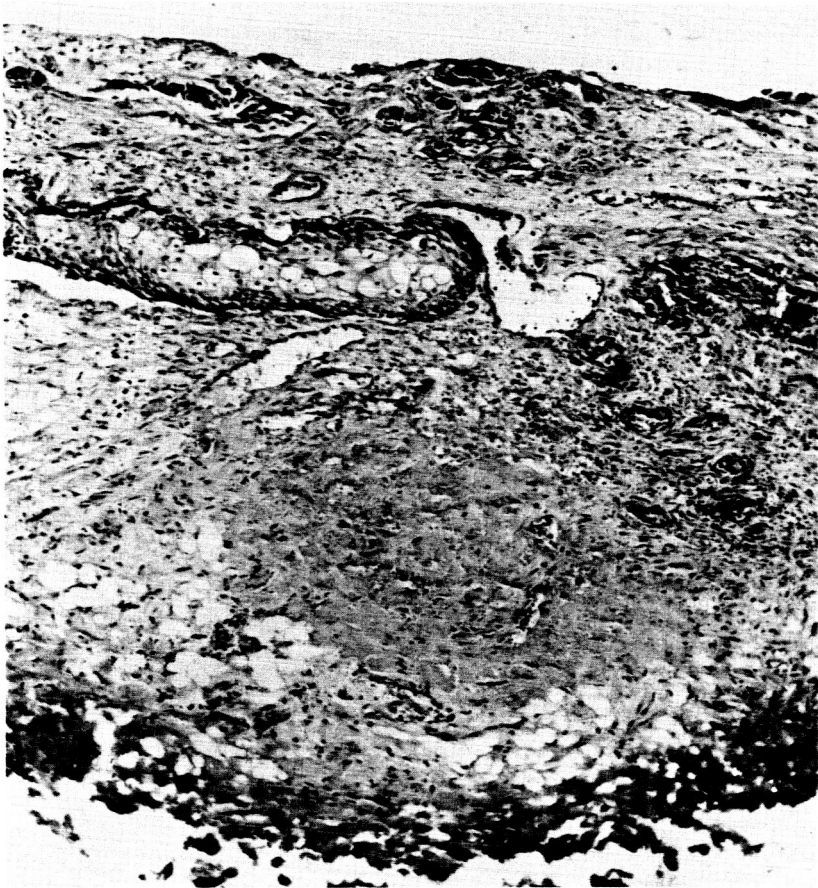


FIGURE 11. Necrosis and squamous metaplasia in prostatic carcinoma, 14 days.

There are scattered cells which may represent nuclear detritus or may represent remaining malignancy. Other sections of the biopsy specimen revealed only empty spaces where that glandular epithelium had been with stromal fibrosis and little resemblance to the earlier picture. FIGURE 12 demonstrates the reaction produced within the prostate when the gland is frozen to  $-20^{\circ}$  and no colder. There is necrosis to a less marked degree. There is severe fibrosis and squamous metaplasia seen. This is a typical reaction of the prostate to injury of any sort.

We have now treated 15 patients with prostatism entirely by this method. To recapitulate our parameters:

1. None of the patients have run a fever or been otherwise ill post-treatment.



FIGURE 12. Squamous metaplasia and little necrosis seen when temperature only  $-20^{\circ}\text{C}.$ ; 14 days.

2. We now feel that we have adequate equipment to destroy the prostate by freezing.

3. There has been transient hematuria. In every case, this has cleared within 12 hours, thus far presenting no clinical problem.

4. In most cases, catheter drainage was not required after five days. In all cases, the catheter had been removed in 14 days.

5. There has been no damage to the bladder function or to the external urethral sphincter or rectum. This is apparently due to the fact that these structures have a separate blood supply which is unaffected by the freezing of the prostate by this technique.



6. Although fibrosis in the remaining prostate undoubtedly occurs, we are dealing with a structure of such wide diameter that even though mild contracture of the urethra occurred, it should not effect the ability to void.

7. Bacterial infections of the necrotic tissue have thus far not been clinically apparent.

8. Adequate destruction of the prostate to alleviate the obstruction has occurred in all cases.

9. The method is simple and safe, requires minimal anesthesia and has caused no significant blood loss.

We are now proceeding in an orderly fashion, offering this method of treatment to all patients presenting with bladder neck obstruction.

#### *Summary*

We have presented a description of pathologic changes induced by freezing in the canine and human prostate. We have included a description of equipment adapted for clinical use. It appears the method is an improvement on those currently available and should allow the treatment of patients with mild and incipient difficulties. No longer need treatment be deferred until the patient's condition is nearly terminal.

## SUMMATION AND GENERAL DISCUSSION

H. S. FRANK (*University of Pittsburgh, Pittsburgh, Pa.*): The proposed procedure was that the discussion of this paper would be included with the discussion of the other papers, which will follow the initial part of this morning's program. The arrangement is that Fernández-Móran and I will make some preliminary statements preceding the general discussion, perhaps giving some further background for the general discussion, and then there will be the free-for-all to which some of you have been looking forward all week. Fernández-Móran and I are supposed to act as moderators.

As the next item I have an exceedingly pleasant duty to perform. The Steering Committee had tried to secure the participation in this Conference of Professor J. D. Bernal. This turned out to be impossible. They then thought that a next best thing would be to dedicate the volume of the proceedings of the Conference to Professor Bernal and therefore the following cable was sent to him by the Executive Director of The New York Academy of Sciences. "Professor J. D. Bernal, Birkbeck College, University of London, London, England. Sorry you were unable to join us, Conference on Forms of Water in Biologic Systems. Dr. Saunders and Steering Committee desire that published proceedings be dedicated to you as pioneer in this important field. Academy concurs. If acceptable to you, please advise by cable, so that announcement can be made Thursday Morning Session."

After the appropriate length of time, the following reply was received: "E. T. Miner, Executive Director, The New York Academy of Sciences. Very much appreciate quite undeserved honor proposal dedicate to me published proceedings your Conference, Forms of Water in Biologic Systems. Accept with pleasure. Look forward receiving papers read there."

So the proceedings will be dedicated to Professor Bernal and this is, I think, a very fitting tribute and I think it would be appropriate if those present were to greet this announcement with a round of applause.

Now, I am not sure that everyone present realizes how very appropriate this dedication is. In fact, the modern discussion of water structure began with the paper of Bernal and Fowler, which, appropriately enough, was in Volume 1 of the *Journal of Chemical Physics*, in 1933. This is the first treatment of water structure in which the idea of structure is used in its crystallographic sense, where you are trying to say where individual molecules are and what their geometry is. It is also the first treatment which made the attempt, and a very successful attempt, at a comprehensive interdisciplinarity. Bernal and Fowler started with the necessity of satisfying the requirements of x-ray scattering data, basing their treatment on the structure of ice, which had just then become well known, but they also included calculations of the dielectric constant of water and of the be-

havior of water as a solvent, computing the partial molal volumes of salts in solution, discussing the influence of salts on the viscosity of water, and giving the first quantum-mechanical discussion of the extra mobility of the hydrogen ion in acid solutions. So this was a truly interdisciplinary effort and in this regard is still a model to be emulated.

Again, for those who may wish to know more about Professor Bernal, he is now Professor of Crystallography at Birkbeck College, University of London. He is a Fellow of the Royal Society, and is also a fellow of a number of other distinguished societies. (Fowler is the late Sir Ralph Fowler, of Cambridge University, one of the distinguished theoretical physicists of the last generation. He made important contributions to the formal parts of the joint paper, but the beginning of the project, and the carrying through in respect of water, was Bernal's work.)

Another respect in which a dedication of these proceedings to Professor Bernal is particularly appropriate is that one of the subjects in which he has been active is the discussion of the origin of life. It was in 1948 that his first big paper on *The Physical Basis of Life* appeared in the *Proceedings of the Physical Society* (1948. 62: 537). He is a man of infinite resource; had he been present here, the discussions would have been even more interesting than they have been, and we would have been even more crowded for time. We are grateful to him for accepting this dedication.

As a starting point for some introductory remarks to precede the general discussion we are going to have, the first thing I want to do is to emphasize again the necessity for the interdisciplinary approach. If we are going to entertain any theory seriously, then we must show we are taking it seriously by seeing what it implies on contexts other than the particular set of experiments which happen to be before us. For unless one has looked to this side and to that to see what the implications are of what one has said, one is not really taking seriously the proposals which are being made. In the case, in particular, of a theory of water, we have to see how compatible its proposals are, not only with experimental data from a wide variety of fields, but also with the best theoretical thinking which can be brought to bear on any of the features of the model which is being discussed. This is not easy. I have a couple of slides, which perhaps we can look at now.

There are a dozen fields of experimental work from which evidence has been obtained which is relevant to water structure or structures of solutions in water. Among these are x-ray scattering, thermodynamics, spectroscopy, nuclear resonance, diffusion, viscosity, sound-absorption, thermal conductivity, dielectric constant and its relaxation, surface and interfacial tensions, neutron scattering, and solubility in ternary systems. Within the last month there has been a paper in which inferences about water

structure are drawn from light scattering, which should therefore be added to this list.

Wetlaufer and his associates in the Medical School of the University of Minnesota, interested in denaturation of proteins by urea, have studied model systems (1964. J. Am. Chem. Soc. **86**: 509) and the models they chose in this work were the simple hydrocarbons which furnish the tails that are found on the amino acids of which proteins are composed. They measured the solubility of these hydrocarbons in water and then, by the same method, in seven-molar urea and you will see that whereas methane is less soluble in the urea than it is in water, butane is more soluble and more so at high temperatures (FIGURE 1). This produces the result shown in TABLE 1, namely, that the transfer of these hydrocarbons (except methane) from water to a seven-molar urea solution is endothermic but spontaneous.  $\Delta H^\circ$  is positive, but  $\Delta G^\circ$  is negative. That means that the hydrocarbons, so to speak, swim upstream. There is no question of com-

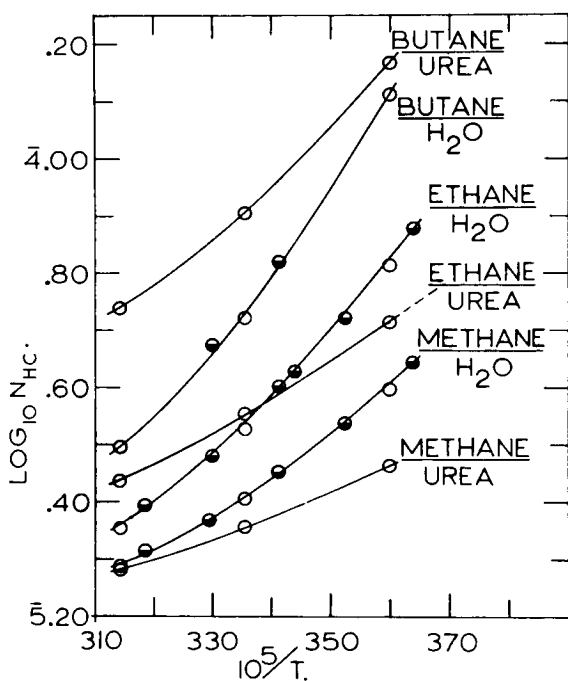


FIGURE 1. Solubility of three aliphatic hydrocarbons in water and 6.96 M aqueous urea;  $N_{HC}$  is the mole fraction of hydrocarbon in equilibrium with 760 mm. hydrocarbon pressure;  $T$  is the absolute temperature. The butane curves have been displaced upward by the addition of 0.400 to the ordinate of each point. The half-shaded points are those of Claussen and Polgase.

TABLE 1  
THERMODYNAMIC FUNCTIONS FOR TRANSFER FROM WATER TO 7M AREA

Solute	$\Delta H^\circ$	$\Delta S^\circ$	$\Delta G^\circ$
	kcal./mole	e. u.	kcal./mole
Methane	1.3	4.1	+0.07
Ethane	1.9	6.5	-0.04
Propane	1.7	6.3	-0.13
Butane	1.9	7.2	-0.25
Isobutane	1.5	7.1	-0.23
Neopentane	1.7	6.6	-0.29

pound formation, because that would have made the transfer exothermic. The hydrocarbons tend to go where they are less favored energetically and they must do so for reasons connected with the entropy of transfer.

Clearly, then, there is something here that needs discussion. It is an entropy effect. It has presumably to do with water structure, and Felix Franks and I have worked during the past year on a way of accounting for this in terms of a structure hypothesis. We think we can do so, but the attempt has required enlarging some of the notions that we have previously had about the influence of solutes on water structure. Among other things, it turns out that urea is a structure-breaker and that this can be shown to be essential to the Wetlaufer effect.

Another point about this paper, though, is that its title does not mention the word "water," and had I not attended a Gordon Conference a year ago last June I might never have come across this work at all. This exemplifies one of the difficulties of the state that the question of water structure is now in. Work bearing on water structure is being done on a large scale in a large number of fields, and in a large number of places, and sometimes one can find out about it and sometimes not. So it is quite possible to be saying something which right now can be disproved on the strength of the experimental results that somebody has in his notebook or in his publication, which you have not seen. In this connection one might make a plea for more comprehensive titling of papers, so that when a paper has implications for water structure, the word "water" will appear in the title so that it may be listed in "Chemical Titles" and so that the indexing and abstracting people will know how to cross-reference it.

The need for looking here, there and yonder for evidence which will confirm or disconfirm ideas about water structure is thus clear and needs to be emphasized. This may be taken as a moral that we can draw from the Bernal and Fowler paper.

Another of the things that makes the study of water difficult has been abundantly obvious in the earlier sessions this week, namely, that water does different things in different contexts. Pure water has a certain type of behavior which it imposes upon itself. When you dissolve things in it to make dilute solutions, you get a little bit of modification of the water structure in this direction or that direction. When the solutions become more concentrated the modifications can not only become more intense, but can change in kind, and when the solution becomes quite concentrated and you have the water against a membrane or included in a biological structure, then what the water does will be different again. It is all water, but under different influences. But, in order to understand as fully as we want to what water does in any one context, it is highly desirable for us to know as much as we can about what it does in every other context and this is something else which should be kept in mind.

Except for this interrelationship, I should be apologizing for being here. I am the interloper at these sessions, for I do not know any biology. I am grateful, however, for the opportunity to be here, because I have been learning things during the week which will become grist to my own mill as a physical chemist.

If the present state of the study of water is in such a bad state, what do we look for now? What should we at present be trying to do about it? Well, we should be trying to make a conceptual model which will be, on the whole, consistent with all of the information from all of the various kinds of work that we can lay our hands on, and which shall also have the best promise of being amenable to the alterations, adjustments, improvements, refinements, which are going to be necessary; because there is one thing about water which I can state with perfect assurance, and that is that no single idea that any person in this room now has about it is free from the likelihood that this idea will need either to be recast or perhaps even rejected, in the course of the next five or ten years, and possibly in the course of the next five days. So that one of the features that a model should have is a kind of plasticity and amenability to the kind of revision which is sure to be necessary as time goes on.

Accepting this point of view, what is the current best guess about water? The answer to this depends on the guesser, and as we have mentioned earlier this week, there are people who will have none of the notion of water as a mixture of distinguishable species. To them an average is an average is an average, and whatever one molecule is doing another molecule is also doing, on the average and without reference to what the first one was doing. This is one point of view, and papers are being published, making use of this explicit hypothesis. There is one by Woessner on deuteron quadrupole resonance relaxation in  $D_2O$ , in the *Journal of Chemical Physics*, (1964: 40: 2341) fine work, and interpreted on the assumption that

there is no cooperativeness between what one water molecule does and what a neighboring water molecule does.

The opposite explicit assumption is that there is cooperativeness, and that if there is cooperativeness, then whatever water molecules do they will do in patches. There will, instantaneously, be structured patches and unstructured patches and these patches will be of different sizes and shapes and so on. They will also be forming and breaking down, continually, and at a very high frequency. We speak of "flickering clusters." Now is not the time to go into a lengthy discussion of why this is an attractive hypothesis on theoretical grounds, but to me it is and to H. A. Scheraga it certainly is. It is also attractive on experimental grounds. On this basis you can account for the maximum of density, the fact that as you squeeze water its viscosity goes down, and a whole group of other properties, including some recent spectroscopic ones which again we do not have time to refer to in any detail. At any rate, I think the best guess is a mixture model. But, do not ever forget that somebody may tell you differently and give you quite convincing arguments which may leave you persuaded that mixtures are "for the birds." This is a case where "you pays your money and you takes your choice."

I, as you see, have plunked my money on the mixture model, and said that I think water consists of flickering clusters. This is part of the interdisciplinarity, you see. Water is a statistical thermodynamic system and  $kT$  is always there. Thermal fluctuations are always taking place. Thus, when we talk about dielectric relaxation, it is not the flopping of the electric field which makes the molecules flip back and forth. The experimental devices used produce only a tiny fraction of a volt per Ångström, so we cannot create a strong enough field to make a molecule flip. If molecules were not flipping anyhow, nothing that we could do would produce flipping. They are doing it spontaneously all the time, through the flickering of the clusters, and what we do is to probe their flipping, to see what frequency gets to be too high for the flipping to respond to. The frequency turns out to be about  $10^{-11}$  seconds. Even in ice there are always flips taking place. C. Jaccard told us about the excellent work that has been done on dielectric relaxation in ice. What causes flipping there? Well, some kind of defect structure. There are probably Bjerrum faults of one sort or another, but the detailed description of the Bjerrum faults may need revision, as was pointed out a couple of days ago.

At any rate, these flips are always taking place, whether we are looking at them or not. The Atlantic Ocean has waves in it whether I am there to see the waves or not, and it is these waves that our methods probe, and not these waves which our methods produce. This is an important point of view which I recommend be kept more firmly in mind than is sometimes done.

We assume, then, that water is made up of flickering clusters, and that a thermal fluctuation will cause some molecules to jump to attention in a structured chunk here, which will then melt down, and a structure chunk there that will melt down. This is happening all over the place very rapidly. In that case we must try to see what these species are like. How do you describe the bulky species? One species has to be bulky, otherwise you do not get the maximum of density. Well, in the case of the bulky species we have an embarrassment of riches, because there are so many bulky structures of water molecules which are known. There is hexagonal Ice I and cubic Ice I and there are the structures of the clathrates, which we saw yesterday. Solid water can do all of these things, and this produces an embarrassment of riches in speculating about liquid water, which I think may have something to do with Drost-Hansen's embarrassment with the liquid seeming to behave differently in different temperature ranges. This would be because there are so many different kinds of structures which could exist, and the fact that there is no reason why the one which is most favored in one set of circumstances (temperature and pressure) should also be most favored in another.

When we come to the dense species the embarrassment is of a different sort, because it is the existence of the dense species which is denied by the physicists who do not like mixture models, and one must not minimize the difficulties. What is this dense species like? How can water be close-packed when its molecule has so large a dipole moment? Well, a quantum mechanical argument can be advanced which I think is pretty good, making use of the fact that when a water molecule is rotating in certain states its dipole moment gets washed out. Quantum mechanics indicates that this does indeed happen. In such states you might be able to have rotating molecules which could be close packed, and then you would be able to have one of the dense species that has been proposed by a number of people. Or the dense species may be one in which hydrogen bonds are bent, and Scheraga has essentially taken the Lennard Jones-Pople water model and allowed the LJP water to be the dense species that surrounds, and changes places with, the structured clusters. At any rate, this is something which is on the agenda for further elucidation, what can be the nature of the dense species.

Then, what kind of an equilibrium can there be between the dense and bulky species? This might be a simple mass-action equilibrium, as a lot of people have written, or it could be a more complicated mass action equilibrium in which an exponent is put in for the polymer-number of the clusters. There could also be an entirely different equilibrium constant such as is obtained when you do the statistical thermodynamics for an interstitial model, in which the dense species consists of separate monomers inside of clathrate cages. In this model liquid water could be called a "water hydrate"



in the same way that we have xenon hydrate or propane hydrate. Each of these possible equilibrium constants would predict a different response to a change in temperature, a change in pressure, a change of electric field, etc. This is therefore also on the agenda of unfinished business. Actually there are probably several simultaneous equilibria. There might be four species with three equilibria among them. Something of this sort would offer an interpretation of the phenomena that Drost-Hansen was telling us about.

Again, whatever we say that water does, it must be able to make sense of the behavior of aqueous solutions, and here, very briefly, there are four kinds of solutes: ionic solutes all have a structure-breaking tendency. Some of them, if the ions are small and have a big charge, also produce a local lining-up of the water molecules, but out at the periphery they are structure-breaking. This is easy to understand because the radial field of the ion tries to orient the water one way, whereas the rest of the water wants to orient another way, and there is a conflict between these tendencies and this will produce a region of breaking.

Then there are the hydrogen bonding solutes. These can enter into water structure reasonably well, so that a solution of ammonia in water, for instance, is not very nonideal. In general OH groups and NH<sub>2</sub> groups like water pretty well, and behave normally in it. One exception to this is urea. Urea has NH<sub>2</sub> groups, and has an oxygen with a negative partial charge, but it has a triangular shape, which is incompatible with the tetrahedral coordination of whatever the clustered species of water is, and so urea is a structure-breaker. Franks and I had to invoke that notion in accounting for the Wetlaufer results which were on the screen a moment ago.

Chemically inert solutes are structure-makers. They cause the water to form extra structure and this can be clathrate-like, but probably only approximately clathrate-like, because this structure-making is often produced by larger molecules than can go inside of the normal clathrate cages. If one believes in flickering clusters then the obvious picture is that a cluster, a part of a cage, will form around part of a hydrocarbon tail and will last a little longer than an ordinary cluster, but then go away again. This will produce fragmentary and transitory cages, and the effect of the hydrocarbon tail will be to increase the statistical degree of structuredness, and such a statistical increase is what the thermodynamics of these solutions shows. Here, I would comment on what Catchpool was telling us about in connection with Pauling's model for anesthesia. You need not have actual crystallites, in the sense of complete cages. All you need is a greater statistical degree of structuredness in the neighborhood of the nerve tissues to account for the Pauling results if this is, indeed, the framework within which an account can be given.

Then we have polyfunctional solutes. Alcohols are an example. An alcohol molecule has an OH group and it has a tail. Franks told us about alcohols the other morning. Amino acids are another example. They break structure on the zwitter-ion end and make structure on the tail end, and this making of structure dominates the thermodynamics of the aqueous solutions (but not the dielectric properties). As solutions of polyfunctional solutes get more concentrated, the effects of the functions cease being simply additive and we get some quite complicated interactions. This, of course, is what this meeting is all about, because we have been talking about what water does in rather concentrated solutions of these polyfunctional solutes.

There are several outstanding puzzles. W. A. Senior the other day was telling us about the change in the chemical shift of water protons in NMR when hydrocarbon tails are put into the water. It looks as though hydrogen bonds were being broken. He followed his colleague, B. A. Pethica, in inventing a euphemism for this, saying that it looks as though the hydrogen bonds were becoming more nonpolar in character. I do not know exactly what happens there. On the face of it, it looks as though hydrogen bonds were being broken, because the same effect is produced as if the temperature were being raised, but this is just the opposite of what all our thermodynamic information tells us. It is also the opposite of the information obtained from the relaxation time studies. However, nuclear magnetic resonance is a subject of its own that has traps of its own and we must be on guard against making interpretations from a field of this sort unless we have some expert in the field standing over our shoulders and advising us. At any rate, this is a place where there is an outstanding puzzle.

A new question has also arisen in connection with the extra entropy loss when a hydrocarbon dissolves in water. Some of that comes from a shift in the structure equilibrium. Marjorie Evans and I proposed this almost 20 years ago (1945. *J. Chem. Phys.* **13**: 507). But, some entropy loss can come from other sources also, in particular an Eley effect, which I am naming for D. D. Eley who proposed it in 1939 (1939. *Trans. Faraday Soc.* **35**: 1281), that some of the water is not available as solvent because of the existence of structure, and this, by itself, can cause extra entropy loss. How much of the observed entropy deficit, then, is a Frank and Evans effect and how much is an Eley effect? I do not know, but would earnestly like to, and this is another of the pieces of unfinished business.

There were a dozen of the items on the program of the last three days which I either especially enjoyed, or was especially instructed by, or would have had special comments to make about. I have already referred to several of these and I will take time only for one more. This is the very nice discussion we heard yesterday about tobacco mosaic virus, Warner's

model. Here, I would suggest that an interdisciplinary check be applied. It happens that in Pittsburgh my colleague, Max A. Lauffer, has been studying the equilibrium in TMV protein between the rods and the subunits which make up the rods. At a pH of 6.5 in a 0.1 N phosphate buffer at the ice point there are no rods, but when the solution is warmed to 25°C. rods are formed. You can see this by turbidity, and you can see it with electron microscopy, and it is a reversible equilibrium, which can be carried up and down as often as one wants. This means that raising the temperature has caused agglomeration of the subunits. But agglomeration is supposed to mean a loss in entropy, because there is not as much freedom for the subunits. On the other hand, if it goes forward at higher temperatures this means that there has been a gain in entropy. What has obviously happened, therefore, is that when you raise the temperature, and the subunits come together, they release some water which had been fastened to the subunits, and the release of water produces the increase in entropy which then drives the reaction forward. The constants of that equilibrium have been determined within modest limits, and Stevens, who is attending these meetings, has done some measurements which tell something about the amount of water released when the rods are formed. Now any model of tobacco mosaic virus protein which purports to say how the rod is built up of subunits is going to have to be able to say something about the degrees of hydration of the separate subunits and of the completed rods. This is therefore a place where another discipline gives information which must be brought to bear on one of the problems that this conference has discussed. Many other examples could be given, but I have already used as much time as — perhaps more than — your patience will allow and so I will now surrender the microphone to Fernandez-Moran.

HUMBERT FERNÁNDEZ-MORÁN (*The University of Chicago, Chicago, Ill.*) \*: It has been my privilege to attend this symposium which is unique in many ways. If by general consensus we have agreed to dedicate the volume of the proceedings of this Conference to Professor J. D. Bernal, I believe it would also be fitting if we were to include in this dedication Professor Henry Frank and Professor Albert Szent-Györgyi. For, while it is true that the first treatment of water structure in its crystallographic sense dates back to the classic paper of Bernal and Fowler,<sup>1</sup> it is actually to Henry Frank,<sup>2,3</sup> that we owe the original concept which has provided the most fruitful working hypothesis that water is a "flickering mixture of

\*This work was supported by U.S. Atomic Energy Commission contract AT(30-1)-2278, by Grants B-2460, C-3174, and NB-04267 from the National Institutes of Health, and by NASA Grant NsG 441-63 from the National Aeronautics and Space Administration.

instantaneously distinguishable species" which may prove to be of key operational value to the biologist. It is equally appropriate to recall the stimulating and challenging ideas propounded by Albert Szent-Györgyi,<sup>4</sup> who with remarkable foresight many years ago pointed out that "water is not only the *mater*, mother, it is also the matrix of life." One could actually paraphrase the title of this symposium to: "Biologic Systems as Formed by Water." We, as biologists, are well acquainted with the fact that all biological systems are composed mostly of water, that life originated and is maintained in a watery medium. But it was only when we began to consider water as more than just a mere filling agent, as a structured matrix, that as Szent-Györgyi so aptly put it "we began to enter a fantastic and fascinating world." What I witnessed during the past years and particularly during these past few days is the phenomenon that this concept of "structured-water" is now beginning to be taken seriously by the biologist. This is in large measure due to the accumulating evidence presented by physicists and physical chemists that water does indeed have a number of unique properties which places it far beyond the mere role of a filling agent.

Even though it is evident from this broad and representative interdisciplinary approach that the study of the structure of water is right now in a difficult stage, one cannot help but be impressed by the experimental evidence in support for a mixture model. Thus, on the basis of data derived from neutron scattering,<sup>5</sup> and other studies of water, we are able to envisage a sample of liquid water as being made up of "flickering clusters" (of about 100 molecules) with an average lifetime of the order of  $10^{-11}$  seconds, therefore long enough for the structure to have a distinguishable existence. One can imagine what consequences this will have for the essential water component forming an integral part of the biological membranes<sup>6,7</sup> and the paracrystalline membrane derivatives such as myelin<sup>8</sup> and photoreceptors.<sup>9-11</sup> We, as biologists, can no longer afford to relegate these considerations to the realm of interesting speculations. Instead, we must begin to take seriously the concept of organized water as an integral structural component of membranes<sup>7,10,12</sup> and of cytoplasmic water viewed as a biological lattice-ordered matrix. This would have significant implications for charge-transfer, selective permeability, energy storage and transduction, localized reversible phase changes, and other processes essential to life.

Specifically, we may try to formulate some of the following important questions: (a) what forms of "structured" or "ordered" water are conceivable in biological systems in the light of our present knowledge; (b) what role would such ordered water structures play; (c) what would be the interrelationship with the organized macromolecular systems<sup>13</sup> which we consider to be one of the most distinctive features of life; (d) how can

we detect "ordered" water in biologic systems and what methodological approaches are feasible?

Obviously, these questions have been the leitmotiv of the numerous stimulating and original papers that have been presented here. As Frank has reminded us, water does many different things in many different situations. If we are to conceive of ordered water as part and parcel of the highly differentiated mosaic of organized three-dimensional structures at the macromolecular and molecular level which constitutes the fabric of living systems, it is only natural to assume that organized water will be specifically tailored to its molecular environment. Hence, there will be ample opportunity for good use to be made of the over-abundance of possibilities of the bulky species in constituting the warp and woof of the living cell: from the crystalline hydrate structures to the numerous other possibilities of frameworks of approximately tetrahedral fourfold coordination, and the particularly appealing concept of the flickering clusters.<sup>3,14</sup> Fortunately, today we have at our disposal a wide variety of powerful tools, such as nuclear magnetic resonance, neutron-scattering, neutron diffraction, x-ray scattering and diffraction, etc., which permit us to study the state of water in biological systems in a nondestructive way. For example, the beautiful studies on the hydration structure of fibrous macromolecules by H. J. Berendsen<sup>15</sup> and C. Migchelsen using nuclear magnetic resonance are already yielding very valuable information.

However, precisely because of this diversity of configurations, one would wish to be able to investigate the forms of water in biological systems in a more direct and straightforward fashion. That is to say, with methods which are above the level of statistical uncertainties inherent in most of our physical and physical-chemical analytical techniques. We have, to date, in electron microscopy, a tool that permits us to deal with a selected, specific domain and, despite its many shortcomings, is nevertheless capable of giving us information on a limited number of molecules or atoms.<sup>16,17</sup> Recent advances in electron microscopy are now gradually making it possible to achieve direct visualization of the fine structure of biological systems under conditions approaching the native hydrated state.<sup>12,16,18,19</sup> Whereas previously the objects to be examined in the high requisite vacuum of the electron microscope were completely dried out, it is now possible, by a combination of techniques, to preserve part of this water structure. This includes the use of special vacuum-tight microchambers, of a few hundred Angstroms thickness, microbeam illumination of low intensity, and cooling of the specimen.<sup>9-12,16,18-22</sup>

On this occasion, I would like to give a brief account of some of the more promising approaches which are opening up in this field. High resolution electron microscopy, which permits direct visualization of crystal lattice structure, combined with electron diffraction, as a powerful analytical tool

for accurate determination of the hydrogen positions is uniquely suited for detailed investigations of the lattice structure and imperfections in isolated ice crystals. Recent technical improvements, which overcome the limitations set hitherto by vacuum sublimation, electron bombardment and contamination, have made it possible to carry out direct studies of ice crystal structure and growth by low temperature electron microscopy.<sup>19,21,22</sup> Thus, electron micrographs and electron diffraction patterns have been recorded from minute ice crystals, which have been stabilized by cooling, and protected from contamination by special shielding devices. Confirming and extending the results of previous electron diffraction studies, the ice crystals formed by deposition of water vapor on cold, thin carbon films were found to be mixtures of hexagonal and cubic ice. At least the two structural forms of ice, hexagonal and cubic ice, have been confirmed by these studies. However, much more work remains to be done. In particular, a critical investigation is needed to determine unequivocally the existence of the amorphous or vitreous ice modification at the lowest temperatures. At the present stage of our knowledge, it is still impossible to say whether the diffuse ring patterns obtained are actually due to very small ice crystals or to "vitreous" ice. This is more than an academic question. It is of the greatest importance for the state of water in frozen material, and is intimately linked with the preservation of biological systems at low temperatures.

Of particular interest are present attempts to investigate the existence of organized water structures of the crystalline hydrate type, particularly in membranes and in lipoprotein systems. The open structure of water favors the formation of crystalline hydrates<sup>23-25</sup> which are clathrate compounds with a hydrogen-bonded, icelike framework defining cavities, able to enclose molecules of noble gases, liquids, ions, protein side chains, etc., provided they are of appropriate size (4 to 6.9 Å) (FIGURE 1a). In contrast to ordinary ice, the hydrogen-bonded lattice of these microcrystalline hydrates, which are about 12 to 24 Å, is stabilized by van der Waals interaction. In favorable cases, involving double hydrate formation and the stabilizing effects of protein side chains, the hydrate crystals may remain stable in the range of normal body temperatures. In fact, this marked stability was one of the main reasons for earlier suggestions that crystalline hydrate structures of this type could supplement, or partly substitute for, the concept of icelike hydration shells to provide an interconnected hydrogen-bonded framework permeating the ordered lipoprotein systems.<sup>19,22,26</sup> These polyhedral structures with numerous built-in cavities, could effectively enclose ions, form closely fitting "replicas" around protein side chains, and adapt in a more differentiated way to the specific macromolecular configurations by three-dimensional interpenetration.

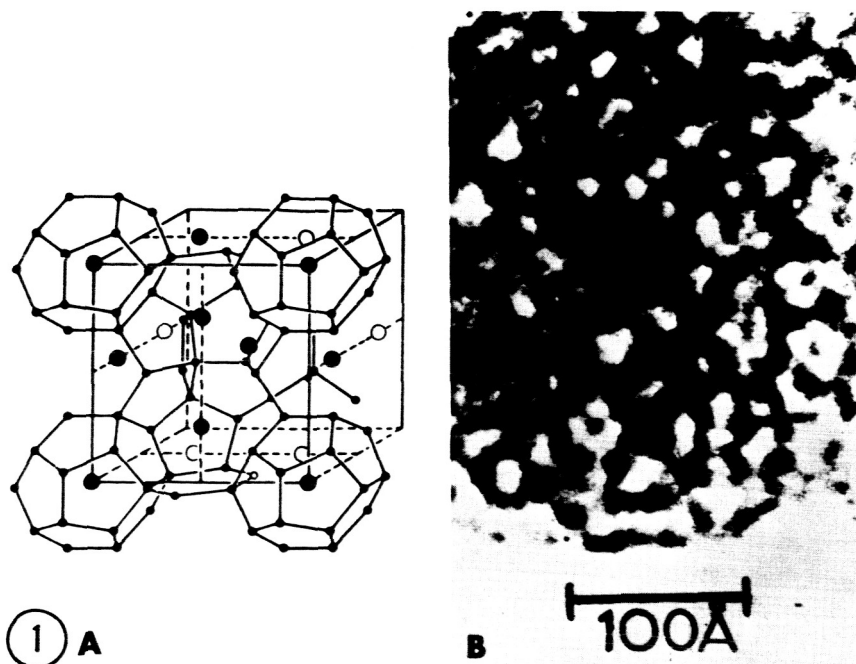


FIGURE 1a. Model of arrangement of water molecules in crystalline nonpolar hydrates according to von Stackelberg *et al.*

FIGURE 1b. High resolution electron micrograph of microcrystalline hydrates of tetra-n-butyl ammonium tungstate enclosed in vacuum-tight microchamber.  $\times 2,300,000$ .

Using the described experimental approach of low temperature electron microscopy, we have been examining the hydrates of tetra-n-butyl ammonium tungstate (which was kindly supplied by Richard K. McMullan). Ions instead of molecules occupy the cavities within the icelike lattice of the quaternary ammonium salt hydrates, and the n-butyl compounds have tetragonal crystal structures with a unit cell,  $a=23.6 \text{ \AA}$ ;  $c=12.4 \text{ \AA}$ .<sup>27</sup> As shown in FIGURE 1b electron microscopy of these compounds, suitably prepared in special vacuum-tight microchambers and examined at low temperature, reveals typical cuboidal-shaped microcrystals giving characteristic single-crystal electron diffraction patterns. At higher magnifications, the microcrystals exhibit an exceptionally regular polyhedral structure, with periodic subunits of 10 to 20  $\text{\AA}$  resembling the general arrangement in the postulated models of crystalline hydrates, in a form not unlike so-called negative staining, due to the built-in heavy tungstate ions (FIGURE 1b).

Continuing earlier work, we have been engaged in attempts to provide direct experimental verification of organized water structures of the postulated crystalline hydrate type through local formation of microcrystalline, noble gas hydrates in selected lipid, lipoprotein complexes and cell membranes. By application of argon and xenon under controlled high pressure (approximately 1500 pounds per square inch) and temperature in special specimen chambers, one can produce characteristic electron-dense microcrystalline hydrates (about 10 to 20 Å) in which the chemically completely unreactive noble gas atoms occupy polyhedral cavities in a hydrogen-bonded framework of water molecules.<sup>9,10</sup> This either contributes further to stabilize and make electron-optically visible any pre-existing organized water structures of the hydrate type in lipoprotein systems, or alternatively, to bind available free water molecules in the process of entrapping the noble gas atoms. This technique has been successfully employed in combination with negative embedding procedures, to visualize argon or xenon hydrate microcrystals of 10 to 20 Å, localized mainly in the hydrophilic regions of isolated lipoprotein layers (FIGURES 3, 4) and cell membranes. When this

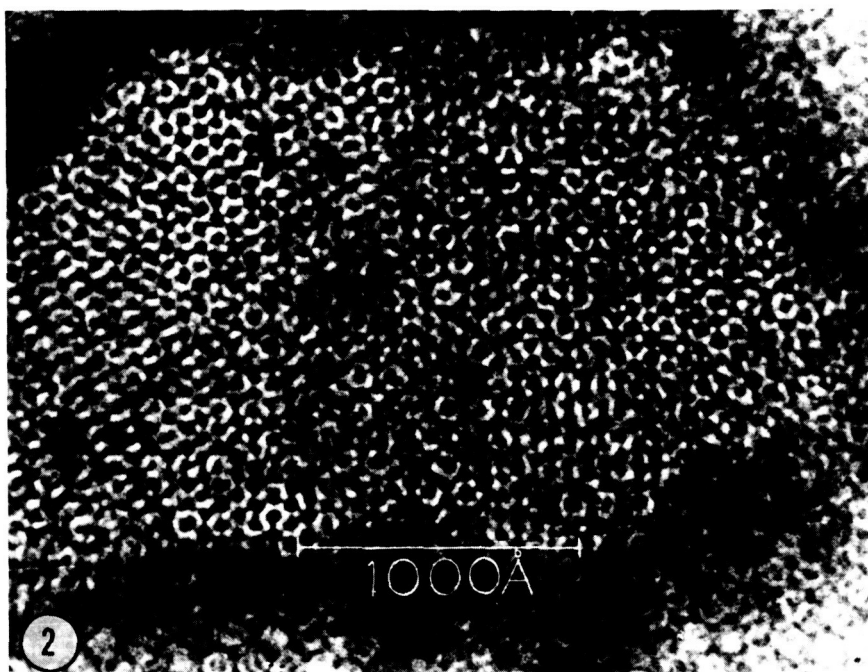


FIGURE 2. Electron micrograph of Ferritin/PTA microdroplet exposed to argon gas under pressure showing ordered ferritin aggregates.  $\times 360,000$ .



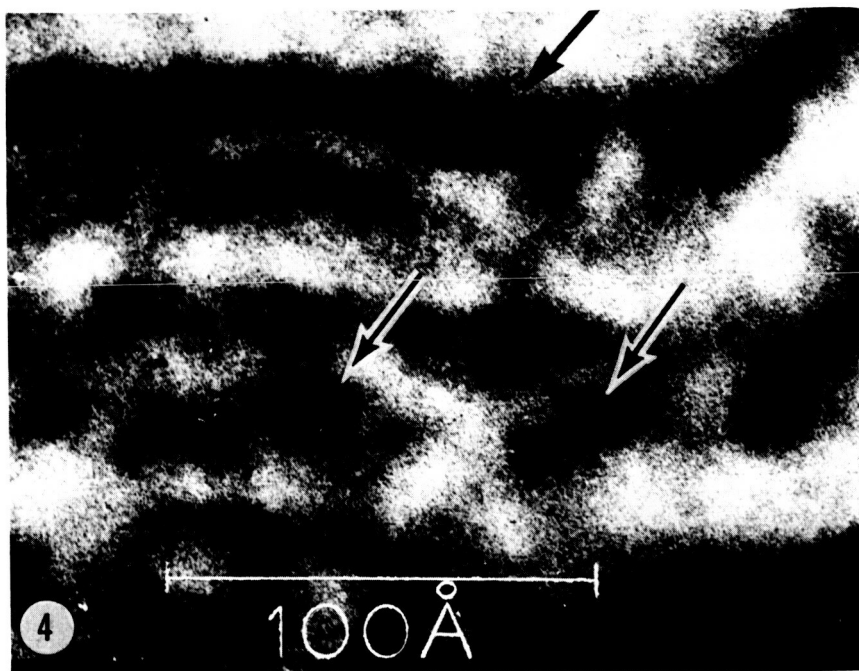


FIGURE 4. Low-temperature electron micrograph of lecithin micelles embedded in thin phosphotungstate film exposed to argon gas under pressure showing dense aggregate (arrows) presumably induced by the formation of argon hydrate microcrystals.  $\times 5,600,000$ .

These experiments are of relevance to the molecular theory of general anesthesia, postulated by Pauling and his associates. Pauling<sup>28</sup> and subsequently Miller, postulated that formation by anesthetic agents, including noble gases, of clathrate-like structures in the aqueous portion of nervous tissues could cause anesthesia by modifying the electrical activity through entrapment of ions and electrically charged side chains of protein molecules, due to increased amounts of structured water in these regions. The described techniques for direct electron microscopical visualization of noble gas hydrates, particularly of xenon which has high electron density, could provide direct experimental proof of the existence of these hydrate microcrystals forming reversibly in membranes. In fact, one might even go beyond this theory of Pauling, which has certain features in common with the hypothesis of anesthesia as propounded by Claude Bernard.<sup>29</sup> According to Claude Bernard's theory of anesthesia, anesthetics would produce a reversible coagulation of the constituents of the nerve cell and of other less sensitive tissues. If, indeed, such reversible "coagulations" or

phase changes can occur in the nerve membranes, the logical site for this would be the synaptic membranes. And it might not be unreasonable to suppose that these transformations are not only associated with anesthesia, but perhaps with certain rhythmic changes, such as, for example, sleep. In any event, reversible modifications of the molecular organization of the highly complex structures in the central nervous system, must inevitably take into account the structure and cooperative ordering of water. Particularly in biological lamellar systems which are concerned with energy transfer, hydrate structures of this type permeating the ordered lipoprotein layers would provide an interconnected H-bonded substrate for fast protonic charged-transport mechanisms.<sup>10,22,30</sup>

We come next to the problem of attempting to study water in biological systems in the native hydrated state. For many years the problem was considered to be insuperable. This was mainly owing to the fact that electron microscopy has to be carried out in a high vacuum. Also, it was considered impossible to get sharp pictures for any structures, such as suspensions of particulate components in water, because of Brownian motion. Actually it has proven to be less difficult than initially supposed. Recently, it has been possible in our laboratories.<sup>16,22</sup> in Russia by Stoianova *et al.*, and, in a more thorough fashion, in France by Dupuoy and Perrier<sup>31</sup> to build special vacuum-tight microchambers in which one can enclose a liquid or an aqueous suspension of bacteria and spores. We have built vacuum-tight microchambers that have single-crystal windows, only 50 to 100 Å thick.<sup>21,22</sup> The liquid layers sandwiched between these two lamellae are thin enough to considerably restrict motion, and if we add the refinement of cooling it is possible to "freeze" any existing motion and to study the structure in considerable detail. Thus in FIGURE 5, a negatively stained T-2 bacteriophage tail fiber, which appears as a smooth thin filament only 20 Å thick, can be compared with the corresponding picture of a "wet" phage tail examined in such a microchamber, using low-intensity microbeam illumination. A characteristic thickening and indications of a helical type of structure are discernible in the filaments of the tail complex (FIGURE 6). Only when we are able to examine wet structures by electron microscopy, will we be really in a position to establish the true configuration of native biological systems. Part of the remarkable success of negative staining in revealing the fine structure of viruses is probably due to the fact that the embedding medium, a phosphotungstate glass, preserves part of the hydrated structure. One might even conceive that the prevalent icosahedral structure of certain spherical viruses may ultimately be related to the special polyhedral type of structure encountered in the crystalline hydrates. Dupuoy in France has gone one step further and actually demonstrated that one can take pictures of bacteria by high voltage electron

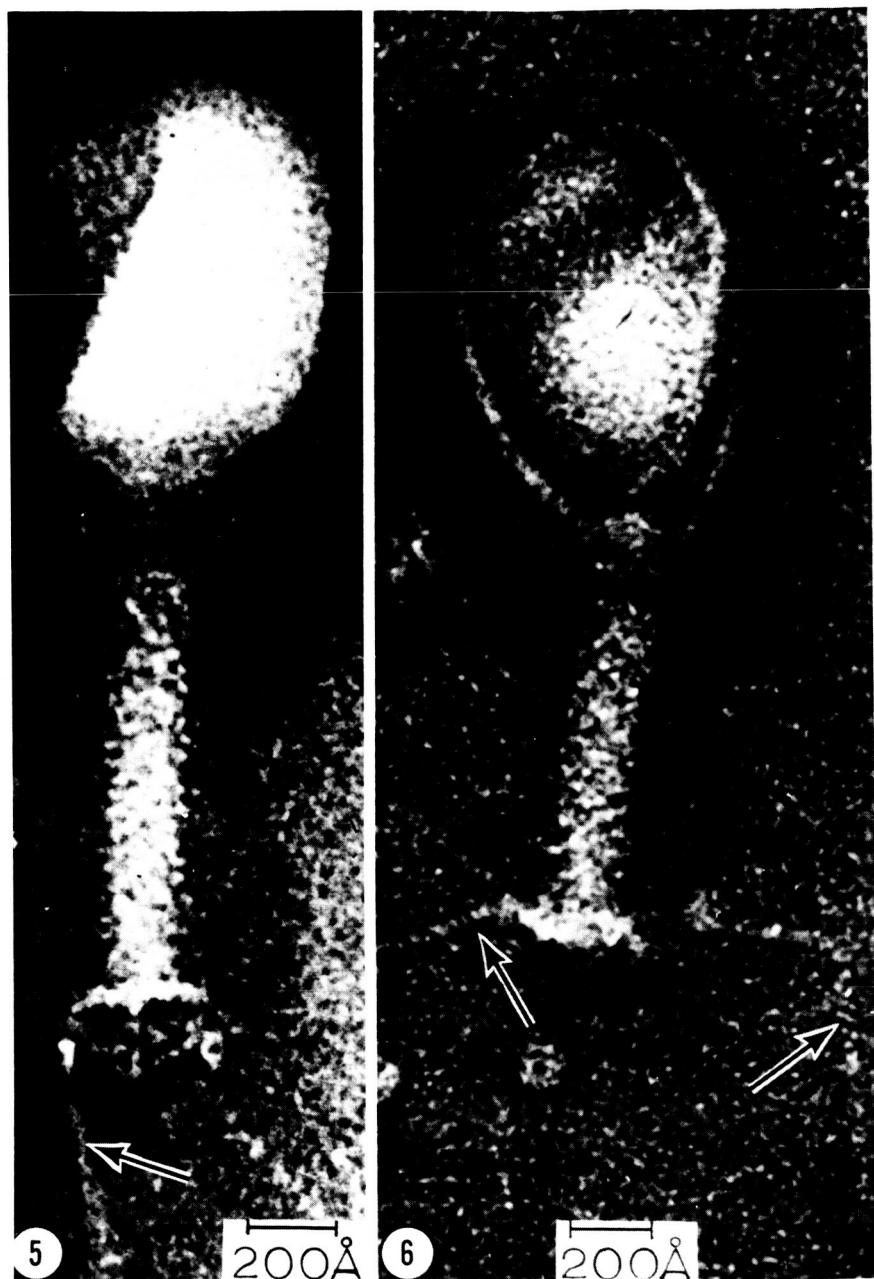


FIGURE 5. Electron micrograph of T2 bacteriophage negatively stained with PTA.  $\times 575,000$ .

FIGURE 6. Low-temperature electron micrograph of partially hydrated T2 bacteriophage enclosed in vacuum-tight microchamber.  $\times 525,000$ .

microscopy, proving by subsequent culturing that the bacteria have not been killed and are still viable.

Modern electron microscopes are capable of resolving directly the array of atoms in crystalline lattices of the order of a few angstroms (FIGURE 8). Beyond this there are certain characteristic electron-optical phenomena, such as moiré patterns which are particularly suitable to the study of organized water and of ice crystals. Thus, when two ice crystals overlap the electron microscope images display regular fringe patterns, that may be interpreted as a moiré pattern arising from the coincidence of the projected planes of atoms in the overlapping lattices. By means of such moiré patterns, indirect resolution of the atomic array in crystalline lattices has been achieved and the lattice imperfections can also be studied.<sup>18</sup> When ice crystals are grown at  $-90^{\circ}\text{C}$ . on mica or graphite single crystals, (FIGURE 7), it is possible to detect, in suitably oriented ice crystals, a series of dense fringes with regular spacings from 15 Å upward. The corresponding electron diffraction pattern show the typical arrangement of double

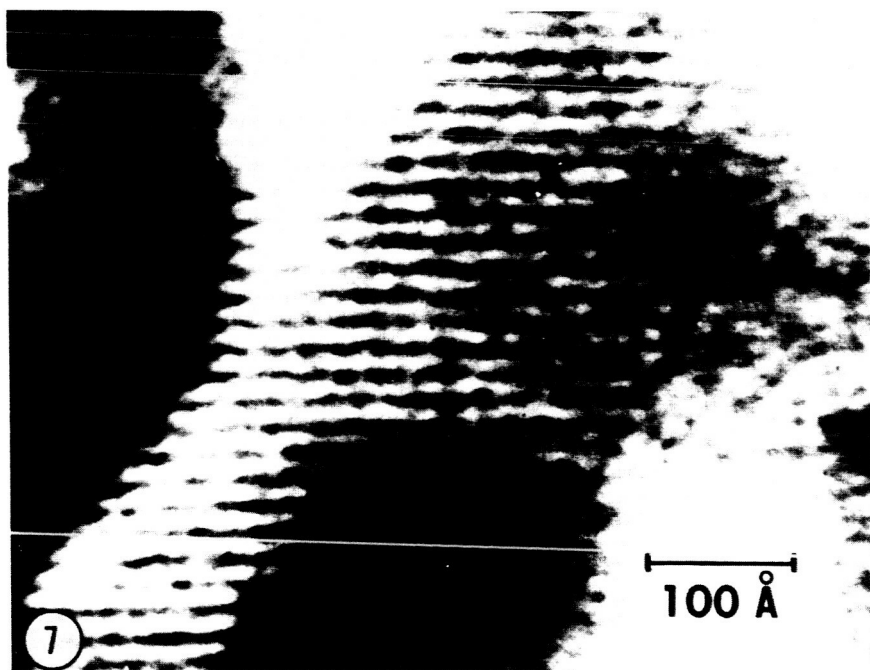


FIGURE 7. Low-temperature electron micrograph of moiré pattern exhibited by ice crystals grown on a single-crystal mica film at  $-80^{\circ}\text{C}$ ., with a regular period of 18 Å.  $\times 2,000,000$ .

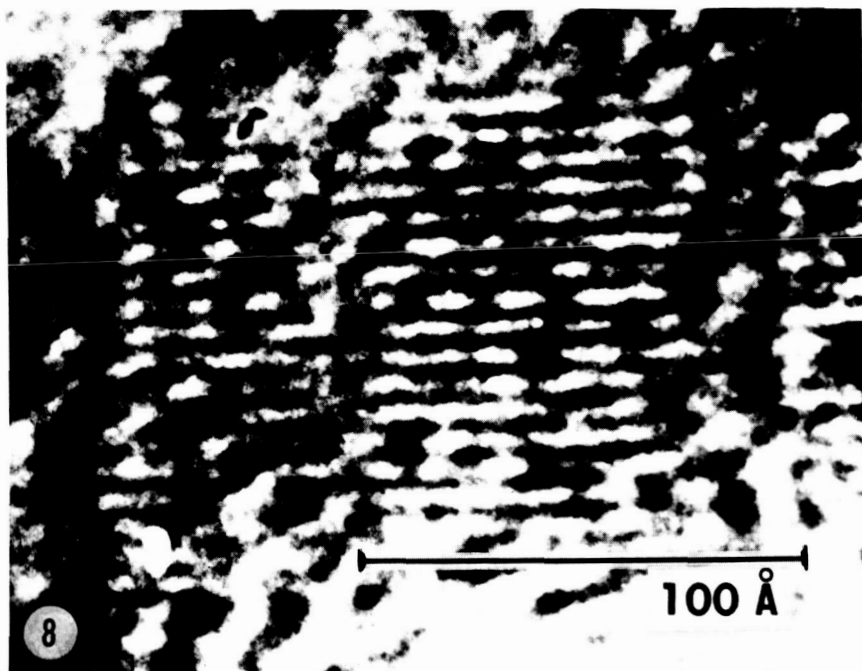


FIGURE 8. Low-temperature electron micrograph of  $K_2PtCl_6$  microcrystal showing lattice spacing of (100) planes. Spacing resolved by direct illumination method is 6.99 Å.  $\times 5,900,000$ .

diffraction spots around the primary diffraction spots. Although interpretation of these moiré patterns is still at a preliminary stage, it is hoped eventually to observe patterns that are related more directly to the lattice structure of the ice crystals. It may also be possible to recognize lattice dislocations and other modifications by combining high resolution electron diffraction patterns with the corresponding electron micrographs. Rapid changes in the moiré patterns and associated modifications of the diffraction patterns of ice crystals subjected to irradiation at low temperatures have also been recorded in motion picture sequences. Direct observation of ultra-rapid processes occurring in microseconds or even shorter intervals may eventually be possible by using stroboscopic illumination obtained through pulsed-T-F emission from pointed filaments in combination with high speed photography.<sup>16,21,22</sup> By virtue of this inherent capacity for achieving both high spatial and high temporal resolution, improved electron optical methods can be expected to play a key role in the elucidation of the structure of ice and other phases of water, including organized water in biological systems.

Beyond its fundamental role as a structured matrix of life, water may be endowed with an equally important, and yet more subtle role, namely as the mediator of information and energy transfer at the molecular level in biological systems. I am reminded here of the fascinating simile made by Frank in explaining the flickering clusters. Frank, in referring to the flips which are always taking place whether we are looking at them or not, points out that the Atlantic Ocean has waves in it whether we are there to see the waves or not. One wonders whether these waves of incredibly short duration ( $10^{-11}$  seconds) and involving clusters of only 100 molecules of water might not be playing an essential role in sustaining the incessant movement that we all witness when we examine living cells. Could it not be that one of the unique attributes of living protoplasm is that its molecular constituents are able to respond, to "resonate" harmoniously with the flickering clusters in water, "riding" in synchrony with these molecular waves during life, and bobbing around at random like an inert cork of dead matter once they have lost this capability? Moreover, we can ask ourselves, what role does water play in the basic functions of living organisms, which according to Schrödinger,<sup>32</sup> maintain their organization by extracting 'order' from the environment? Is water the entropy drainage system par excellence? These and many other questions will be more meaningfully posed in the years to come.

We come back full cycle to Szent-Györgyi's definition that "research is to see what everybody has seen and to think what nobody has thought before." Thanks to present advances in concepts and methodology, our generation of biologists is now able to start thinking about water and its cardinal role as no other generation has been able to do before. Ultimately, we will probably have far deeper reason than Thales of Miletus in acknowledging the full truth of his cryptic saying that "Water is best." I feel that the problem of water is not only of critical importance to an understanding of terrestrial systems, but water or equivalent compounds may very well play a great role in understanding extraterrestrial phenomena, as Miller,<sup>33</sup> has already suggested.

To conclude with a humorous note, some years ago *The New Yorker* had a cartoon depicting an obviously very far off planet with a wrecked space ship, from which a weird, alien creature emerged, with drooping antennae, straggling away, gasping for "ammonia, ammonia!"

#### References

1. BERNAL, J. D. & R. H. FOWLER. 1933. Theory of water and ionic solution with particular reference to hydrogen and hydroxyl ions. *J. Chem. Phys.* 1: 515.
2. FRANK, H. S. & WEN, W. 1957. Ion-solvent interaction: structural aspects of ion-solvent interaction in aqueous solutions, a suggested picture of water structure. *Disc. Farad. Soc.* 24: 133.

3. FRANK, H. S. 1958. Covalency in the hydrogen bond and the properties of water and ice. *Proc. Roy. Soc. A* **247**: 481-492.
4. SZENT-GYÖRGYI, A. 1957. *Bioenergetics*. Academic Press. New York, N. Y.
5. EGELSTAFF, P. A. 1962. *Advances Phys.* **11**: 203.
6. FERNÁNDEZ-MORÁN, H. 1959. Fine structure of biological lamellar systems. *Revs. Modern Phys.* **31**: 5.
7. HECHTER, O. 1964. On the role of water structures in the molecular organization of nerve cell membranes. Presented at American Cancer Society Conference on Cryobiology. Rye, New York, October 9, 10, 1964. In press.
8. FERNÁNDEZ-MORÁN, H. 1960. Improved pointed filaments of tungsten, rhenium and tantalum for high resolution electron microscopy and electron diffraction. *J. Appl. Phys.* **31**: 1840.
- 9a. FERNÁNDEZ-MORÁN, H. & J. B. FINEAN. 1957. Electron microscope and low-angle x-ray diffraction studies of the nerve myelin sheath. *J. Biophys. Biochem. Cytol.* **3**: 725.
- 9b. FERNÁNDEZ-MORÁN, H. 1962. New approaches in the study of biological ultrastructure by high-resolution electron microscopy. Paper presented at Symposium of the International Society for Cell Biology, Berne (September, 1961). In *Symposia of the International Society for Cell Biology*: **1**: 411-427. R. J. C. Harris, Ed. Academic Press, Ltd. London, England.
10. FERNÁNDEZ-MORÁN, H. 1962. Cell membrane ultrastructure. *Circulation* **26**: 1039.
11. FERNÁNDEZ-MORÁN, H., T. ODA, P. V. BLAIR & D. E. GREEN. 1964. A macromolecular repeating unit of mitochondrial structure and function. *J. Cell Biol.* **22**: 63.
12. FERNÁNDEZ-MORÁN, H. 1961. The fine structure of vertebrate and invertebrate photoreceptors as revealed by low temperature electron microscopy. In *The Structure of the Eye*: 521-556. G. K. Smelser, Ed. Academic Press. New York, N. Y.
13. SCHMIDT, F. O. 1959. Molecular biology and the physical basis of life processes. *Revs. Modern Phys.* **31**: 5.
14. NEMETHY, G. & H. A. SCHERAGA. 1962. *J. Chem. Phys.* **36**: 3382, 3401.
15. BERENDSEN, H. J. C. 1960. The structure of water in tissue, as studied by nuclear magnetic resonance. *Biol. Bull.* **119**: 287.
16. FERNÁNDEZ-MORÁN, H. 1964. New approaches in correlative studies of biological ultrastructure by high-resolution electron microscopy. *J. Roy. Microsc. Soc.* **83**: 183-195.
17. HAINE, M. E. & V. E. COSSLETT. 1961. *The electron microscope*. Interscience. New York, N. Y.
18. FERNÁNDEZ-MORÁN, H. 1960. Low temperature preparation techniques for electron microscopy of biological specimens based on rapid freezing with Helium II. *Ann. New York Acad. Sci.* **85**: 689.
19. FERNÁNDEZ-MORÁN, H. 1961. High resolution electron microscopy of hydrated biological systems. *Proc. Internat. Biophys. Congr.* **324** Stockholm, Sweden.
20. FERNÁNDEZ-MORÁN, H. 1959. Cryofixation and supplementary low-temperature preparation techniques applied to the study of tissue ultrastructure. *J. Appl. Phys.* **30**: 2038.
21. FERNÁNDEZ-MORÁN, H. 1960. Direct study of ice crystals and of hydrated systems by low-temperature electron microscopy. *J. Appl. Phys.* **31**: 1841.
22. FERNÁNDEZ-MORÁN, H. 1960. Low temperature electron microscopy of hydrated systems, in fast fundamental transfer processes in aqueous biomolecular systems. :33. Massachusetts Institute of Technology, Department of Biology. Cambridge, Massachusetts.
23. CLAUSSEN, W. F. 1951. Suggested structures of water in inert gas hydrates. *J. Chem. Phys.* **19**: 259, 1425.

24. PAULING, L. & R. E. MARSH. 1952. The structure of chlorine hydrate. *Proc. Nat. Acad. Sci.* 38: 112.
25. STACKELBERG, M. v. & H. R. MÜLLER. 1954. Feste Gashydrate. II Struktur und Raumchemie. *Ztschr. Elektrochem.* 58: 25.
26. KLOTZ, I. M. 1960. Protein molecules in solution. *Circulation* 21: 828.
27. MCMULLAN, R. & G. A. JEFFREY. 1959. Hydrates of the tetra n-butyl and tetra i-amyl quaternary ammonium salts. *J. Chem. Phys.* 31: 1231.
28. PAULING, L. 1961. A molecular theory of general anesthesia. *Science* 134: 15.
29. BERNARD, C. 1875. *Leçons sur les anesthésiques et sur l'asphyxie*. Paris, Bailliere, France.
30. EIGEN, M. & L. DEMAYER. 1959. Hydrogen bond structure, proton hydration, and proton transfer in aqueous solution. *In the Structure of Electrolytic Solutions*: 64-85. W. J. Hammer, Ed. John Wiley & Sons, Inc. New York, N. Y.
31. DUPUOY, G. & F. PERRIER. 1962. *J. Microsc.* 1: 167; 1963. *Ann. Phys.* 8: 251.
32. SCHRÖDINGER, E. 1948. *What is life?* Cambridge University Press.
33. MILLER, S. L. 1961. The occurrence of gas hydrates in the solar system. *Proc. Nat. Acad. Sci.* 47: 1798.



## GENERAL DISCUSSION

FINNEMA (*University of Wisconsin, Madison, Wis.*): I would like to make a few comments on the clathrate theory of anesthesia. I have done some work in the area of clathrate compounds. There are some discrepancies that I have observed with the characteristics of clathrate compounds and with the theory as we have seen it presented here.

I would like to cite several examples of such discrepancies. First, we consider the formation of the clathrate compound in simple fluid systems, consisting solely of water plus the hydrate or clathrate former only. We find it is not particularly easy to form clathrate crystals in systems of this sort, at least in the systems with which I am familiar. It is necessary to have the clathrate former present in abundance, that is, the water must be saturated or nearly saturated, with the clathrate former.

Second, the system must be undercooled with respect to the decomposition temperature of the clathrate with which we are dealing. This involves several degrees undercooling. The more we undercool the faster the clathrate will form.

Another condition which generally must be imposed upon the system is that of agitation. If we do not agitate we are faced with extremely long times of clathrate formation. In some systems in which it is particularly difficult to form clathrates, we sometimes have to seed the system either with ice or with a crystal of the clathrate with which we are dealing.

We can see that it is not an easy task to form clathrate crystals. If we leave this simple fluid system and move into solid systems, such as we would find in gels or in plant or animal tissue, we face even a more difficult task. We have been completely unsuccessful in forming clathrate compounds in animal tissue; animal muscle was the particular example with which I have worked. We have had one or two successes in gels and plant tissue. The plant tissue which we used was apple tissue which was exceedingly open, has great amounts of voids in the tissues, and crystals form in these voids. When we were successful in forming clathrate crystals in these solid systems, a period of many hours was involved. On the basis of these observations it would appear extremely unlikely that clathrate crystals in a true sense could penetrate into a tissue system and form in blood, for example. Let us look for a moment at the decomposition temperatures of clathrate compounds in general. The critical decomposition temperature is that above which the clathrates are unstable regardless of the pressure imposed upon them. If we look at the whole series of clathrate compounds which are common to us today, we find that most of them are stable at room temperature or below — most of them below.

By adding gases such as hydrogen, carbon dioxide, nitrogen, oxygen, and ingredients of this sort, we can improve the stability of the clathrate compounds slightly. It has been my observation that you have to impose rather severe pressures on the system to improve stability.

It is suggested then that if there are other components in the system such as proteins or other colloidal constituents, these may improve stability of the clathrate compounds and allow them to exist at higher temperatures.

We have formed clathrates in aqueous systems containing high percentages of protein, lipid, and carbohydrate. In every instance we have found very little difference between the decomposition temperatures of these clathrates as compared to systems in which these constituents were absent.

If we look at the whole pattern of the effect of solutes on clathrate, sodium chloride or sugar for example, and their effect on the decomposition temperature of clathrates, we find that, in general, they will lower the critical decomposition temperature of clathrate compounds. If we should add salt to a clathrate, we find that it lowers the decomposition temperature to a magnitude which is nearly identical to the freezing point depression that this material would have. It is parallel to it.

If you try to take a clathrate like xenon, which has a high pressure requirement, again formation of a true type clathrate compound in blood is unlikely to be due to the temperature of the body and to the lack of pressure that we have there.

If we look at tables listing the properties of the commonly known clathrate compounds, we see that each clathrate compound has its own decomposition temperature and decomposition pressure. There are only a few that are stable at atmospheric pressure. Most of them require high pressure. Xenon in water, for example, requires a quite high pressure. If we go to hydrates of oxygen and nitrogen, we are speaking of pressures in excess of 100 atmospheres.

When we look at their decomposition temperatures, we find that they vary considerably, usually from room temperature downward. If for a moment we would assume that this clathrate theory of anesthesia is in fact true, and if we would look at the particular anesthetics with which we are working, we should find that each of these anesthetics has a pressure and temperature condition under which it will function. If we exceed this temperature or go below this pressure, then it will no longer function as an anesthetic.

These are some of my observations and there seem to be some gross inconsistencies between general properties of clathrates — the macrocrystals, not these microcrystals — and with the general theory of anesthesia which has been presented. Perhaps it will turn out that this discrepancy should be resolved by saying that these really aren't clathrates but rather half

clathrates, like half hydrogens in water structure. I do not know, however, they do seem to be quite different.

H. FERNANDEZ-MORAN (*University of Chicago, Chicago, Ill.*): Listening to what we just heard, we are quite amazed at the ease with which Faraday over 100 years ago made clathrates and with the ease with which any student really can produce clathrates. It is true that many of the variables you have enumerated hold, but it is by no means necessary to fulfill all of them.

You have to define very rigorous criteria for establishing whether you have clathrates or not. What you are talking about are crystals of clathrates for x-ray diffraction study. This is quite a different order of problem than forming microcrystals, which you can only detect with polarization optics, electron microscopy and electron diffraction.

H. A. SCHERAGA (*Cornell University, Ithaca, N. Y.*): I just want to speak to only one aspect of the many that the speaker raised, that is, the stability of the clathrate. He referred to the concentrations. In the theory of hydrocarbon solutions, which Nemethy and I developed, we did not use the concept of a complete clathrate cage around the hydrocarbon, but rather a partial cage. The origin of this partial cage was a shift in energy levels of those occupied by the water molecules. One of these levels, namely the lowest one which corresponded to tetrabonded water, was shifted downward because the hydrocarbon could interact with the tetrabonded water species via Van der Waals type interaction so that the water in effect became pentacoordinated. In hydrocarbons you have a very dilute solution so that a particular tetrabonded water species is going to have only one hydrocarbon molecule. If you are in a concentrated system such as in the crystalline hydrates, you have the possibility of a cooperation such that a water molecule in one cage may see a hydrocarbon inside that cage and there may be a hydrocarbon in the next cage. In other words, the hydrocarbons are filling neighboring polyhedral cages and you are getting greater stability in that more water molecules can interact with hydrocarbons and thereby stabilize complete cages as you have in acrySTALLINE hydrates. In aqueous solution where these are dilute and, of course, in anesthesia, you do not have the hydrocarbons near enough to each other because the solubilities are too low to provide this cooperation. Thus we cannot stabilize complete cages.

I would agree with the speaker in the sense that in a microcrystalline range, I do not think you would expect to find complete polyhedral cages encapsulating or enclosing hydrocarbons as, I believe, was postulated in the anesthesia case. If you want to say that the partial cages which we have talked about can function in the anesthesia case, that is another possibility. But, I do not think that you can have complete cages in dilute

aqueous solution as you do have in the more concentrated system in the crystalline hydrate.

H. S. FRANK (*University of Pittsburgh, Pittsburgh, Pa.*): We must not be too literal in talking about a theory as it was worded by the person who first stated it. What Scheraga has said just now is certainly correct, if you say microcrystals. The statistical degree of structureness can be increased and this would produce the same effect. This, I believe, is what the discussant mentioned at the very end. If we are not too literal in repeating the words of the theory, but consider what might have been said, then we have something really good.

O. HECHTER (*The Worcester Foundation for Experimental Biology, Shrewsbury, Mass.*): My understanding of the Pauling-Miller clathrate theory of anesthesia is that it arises primarily from the fact that a group of agents, which are chemically nonreactive, are able to produce a totally unexpected biologic effect. I do not believe there is any suggestion on the part of Pauling or Miller that other agents — hydrogen bonding agents — which might effect metabolic reactions at one point or another, might in other ways influence ionic fluxes. This theory, I believe, attempts to account for an unexpected biologic finding. In so doing, it provides a unique conceptual base with which to operate, wherein the water structures of the membrane assume great importance in both the normal generation of the excitability properties that are being studied and with respect to the whole problem of anesthesia.

I. R. FENICHEL (*Albert Einstein Medical Center, Philadelphia, Pa.*): Regarding this question of anesthesia and clathrate formation, the Pauling model, I would like to reiterate a point that I made very quickly in my presentation. I feel it is very difficult to make it compatible with the Pauling clathrate model. If you study the movement of urea out of the cell (whether you regard this as membrane permeability or as bulk diffusion), with the addition of nonpolar solutes which are known anesthetics (the alcohols, chloroform, ether, urethane), you find that in each case the rate of movement of urea out of the cell is increased, almost directly in proportion to the concentration. If these agents act by stabilizing a water structure cooperatively with the membrane structure, I find it difficult to understand how they can increase the rate of diffusion of urea through this material. This is particularly true, if one used a urea flux (as most people now seem to do) as moving through aqueous channels because of its very low solubility in the lipid phase. Would anybody care to offer an idea as to how this might be brought into agreement?

H. S. FRANK: One way would be that the hydrocarbon makes the water more structured and makes the water less available as solvent and, therefore, raises the escaping tendency of the urea and increases the driving

force. Unless you are going to say that water inside the cells acts entirely differently from the way in which it can be shown to act in other contexts, then I do not believe what you have said is true.

A. LEAF (*Massachusetts General Hospital, Boston, Mass.*): I think it is very important to point out again that in these experiments to which Fenichel was referring, these poor solvents destroy cell membrane. Cell membranes are highly lipid and all these solvents damage the membrane thus permitting the urea to leak out more rapidly. I do not really think his evidence has anything to do with the problem under discussion.

I. R. FENICHEL: I was certainly not referring to the question of whether the action of a nonpolar solvent is on the lipid component of the membrane. I was simply referring to the Pauling model in which this action is purportedly on the aqueous phase of the membrane.

H. A. SCHERAGA: You have a very complicated structure here and I am sure there are many effects involved. In his initial presentation, Frank raised a very fundamental question about the role of urea. I would like to ask him if he has some picture as to what urea in both dilute and concentrated solutions is doing to water structure?

H. S. FRANK: The idea is that if water is a mixture of a structured and unstructured species, then urea or anything else dissolving in water will dissolve one way in the structured species and another way in the unstructured. In the structured species it is a kind of quasiclathrate whereas in the unstructured it is a kind of regular solution. Because of its triangular geometry, urea cannot enter into the structured species at all. Therefore, you add this and it dilutes the unstructured material and shifts the equilibrium in the direction of the structured material by ordinary mass action alone. It produces a structure breaking effect. Felix Franks and I have made some calculations on the basis of this. We can account for the activity coefficient of urea-water mixtures and the heat of dilution of urea-water mixtures quite accurately. Those data are well known. This then would be a statistical influence of urea just because of its shape.

H. A. SCHERAGA: In this sense, why is urea different from a salt which is also a structure breaker?

H. S. FRANK: The salt ions have strong electrostatic fields which will produce strong orienting effects which are not present in water itself. The urea, presumably, hydrogen bonds much as though it were water and the other influence predominates.

H. A. SCHERAGA: Does your theory take account of possible dimerization of urea as was proposed some years ago?

H. S. FRANK: If you are talking about urea-water alone, the thermodynamic properties of those solutions can be accounted for without any dimerization whatever.

O. HECHTER: It is important to remember that when you translate simple aqueous solutions to the cell, this is an extrapolation which has no meaning for a biologist. You know that urea, for example, has an effect on some proteins. It might be breaking hydrophobic bonds, as well as having effects on hydrogen bonding systems. In the context of the cell interior where you have an agent that acts both on proteins as well as on water, the effects in some cases are much more mysterious than simple aqueous solutions.

G. N. LING (*Pennsylvania Hospital, Philadelphia, Pa.*): I have heard so much about structure breaking and structure forming. For my own information I would very much like to hear to what structure are we referring? It seems to me that there are all kinds of structures. One kind is the clathrate and the other kind is what is referred to as the bound water. Warner has produced another kind of water which seems to be related to the water lattice in ice. We have been learning about these in this Conference. When we begin to talk about structure breaking, I would like to see if it is a single and unidirectional process. Does this mean that it applies to all. I would like to hear further comments, because it seems to me that an agent which may be structure breaking in one case might be doing just the opposite when the structure is different.

S. B. HOROWITZ (*Albert Einstein Medical Center, Philadelphia, Pa.*): Ling made an extremely important point and the last comment of Frank cast some light on some of the confusion that may be existing here. Frank, in summarizing what we had previously said, said it is either aqueous solution inside the cell or it is acting in a way which is very different from aqueous solution, as we understand it, on the outside. That is precisely the point we are making here. The point again ties into Ling's observation. Inside the cell we are maintaining that a nonpolar solute acts to disorder, just as in my original talk we showed the inverse, namely, that a nonpolar solute in aqueous solution must be producing order to explain the diffusional properties. So the very point here is the question of the states of water in these two phases and whether we can really so blithely extrapolate from the properties of urea in aqueous solution to the properties of urea intracellularly.

H. S. FRANK: We cannot discuss problems of this sort without postulating models. What you do is specify the properties of the model, account for those properties, and then show how those properties account for the phenomena under discussion. If you are making a model in which urea inside the cell does something very different from what it does outside, then it is incumbent upon you to specify how this can be expected to come about. In the absence of such specification I would suggest that the model is very incomplete.

LUCK: Drost-Hansen has shown that we have four anomalous temperatures in water. These were 15, 30, 45 and 60 degrees and it may be possible

to say something about the point of 60 degrees. We know from the technique by Fonteil and Pimentel that the cyclic hydrogen bonding has its own infrared band and it is possible, I think, in the infrared band of pure water to show that the optical densities in the region of this band will have a maximum near 65 degrees.

The optical density in pure water in the region of the band of cyclic hydrogen bonding is maximal in the region of 65 degrees. The infrared analysis has some difficulties because our assumption was that during melting you have clusters — it may be 100 or 300 molecules — and these clusters have some subunits which are combined with cyclic hydrogen bonding. It may be that the cyclic hydrogen bonding is increasing the temperatures and with higher temperatures the clusters become smaller and smaller. In this case we have more linear hydrogen bonding and it may be that the data shown by Drost-Hansen make this point of view more probable. It is necessary, however, to make the infrared analysis more exacting.

W. DROST-HANSEN (*Jersey Production Research Co., Tulsa, Okla.*): There is other evidence from infrared and raman spectroscopy for the reality of this.

H. FERNANDEZ-MORAN: These are new data to me. The thermophilic bacteria and other organisms exist at temperatures above 65 degrees. I wonder whether this might have any biologic significance.

W. DROST-HANSEN: There is a group of bacteria which we refer to as the thermophilic bacteria which ordinarily have maxima in the vicinity of 55 degrees and even temperatures ranging from 60 to 62 degrees. There are also a few strains of bacteria and indeed some algae which may tolerate considerably higher temperatures. I am not attempting to explain these, nor to explain them away. They are there and I do not know what they mean. They certainly do not seem to fit into the scheme that I am proposing.

H. A. SCHERAGA: The thermophilic bacteria may also involve another phenomenon which may have nothing to do with the kinks that Drost-Hansen mentioned. The enthalpy of formation of a hydrogen bond is positive at low temperatures, but it is temperature dependent. As you raise the temperature to the neighborhood of 50 to 60 degrees, the magnitude of  $\Delta H$  becomes zero and at higher temperatures becomes negative. This is perfectly rationalized in the terms of properties of aqueous hydrocarbon solutions on which the whole theory is based. It is the phenomena which are involved in hydrocarbon solubility which may be playing the role in the thermophilic bacteria and not these structural transitions.

O. HECHTER: Regarding Frank's comment pointing out that the water in the cell might be different, I believe it is quite fair to recognize that Berendsen presented evidence that a typical macromolecule, collagen, had water that was highly structured. The structured water in that system was clearly different than those obtained in simple aqueous solutions. Per-

haps Berendsen could comment a few moments on this. This forces us to consider very clearly that the extrapolation of concepts in simple aqueous solution into cell is not without danger.

H. S. FRANK: I could not agree with you more on what you last said, but structure ideas now are something like the word "catalysis" was 75 years ago. Whenever anything showed up that people did not understand, they said "catalysis" and everyone was satisfied. There has been a tendency to use the word structure in the same way, and a kind of explanation which can explain anything cannot explain anything at all. It is necessary to try to specify what the differences are between the two contexts in which the different behavior is alleged. I agree with you.

H. A. SCHERAGA: I believe, however, you should have restated the comments you made before Dr. Frank. If there are differences in behavior in aqueous solution versus behavior in the cell, then there are other kinds of phenomena which must be built into the model of the cell, which we have not as yet put in aqueous solution.

O. HECHTER: We are not talking about a cell. We are talking about collagen.

H. A. SCHERAGA: Whether it is a cell or a macromolecule, whatever the system is, you have to have a model. There is no difference in terms of the idea that you must have a model for whatever system you are talking about, which will incorporate all the phenomena which you can demonstrate in very simple systems.

H. J. C. BERENDSEN (*Groningen University, Groningen, The Netherlands*): We see a logical difference when you take out about half of the water in systems like collagen. If you have them in the native state, you still get the same kind of thing, but not as pronounced as when you take out half of the water. We see these chain-like structures when humidity is of the order of 80 per cent but we do not see them anymore at humidity of 100 per cent. I believe that what you measure at these lower humidities might be the basis of the structures existing at the higher humidities. They are just built further out, though they are much more labile. You can easily get an order of magnitude of how long lifetimes are. They turn out to be of the order of microseconds at the humidity rates of 80 per cent. The chain-like structures go to much shorter times,  $10^{-8}$  and  $10^{-9}$ , while liquids go up to  $10^{-11}$  for humidities which are much higher.

The structures, then, are imposed by collagen and look a little like ice. The same chains occur in ice along an axis and they have the same repeats. There are many possibilities in using structures induced by macromolecules and this is just only one of them. We should compare the kind of structure that can be induced with the structures which are possible in water. I would like to bring out one possible structure which has been overlooked thus far and which is a very probable structure in water.



This is a kind of cage that is different from the ones that we have seen before. It contains two pentagonal faces and six hexagonal ones. The two pentagonal planes are behind each other at a distance of 4.7 angstroms and if you build a space filling model of this cage, there is just enough room inside for one water molecule. Then, if you look at the x-ray diffraction pattern that one would get from this kind of structure when the hole is filled, this agrees with what is found experimentally in water. There is a difficult point in the x-ray diffraction of water that one finds at peak 2.9 Å and certainly not at 2.74 Å, as in ice, or at 2.76 Å. This 2.9 may be either due to two peaks at something around 2.7, 2.8 and a higher peak, or it may be due to a lengthening of the hydrogen bonds. This is not very likely because 2.9 Å hydrogen bond is too low in energy to account for the energy of the water itself. I believe there is a difficulty and this model could give an explanation, because if you look at the model, you find there are two distances and you will get two peaks in x-ray diffraction which emerge to a peak at an average of 2.9 Å.

You can build normal ice structures on the edge of this structure and this will fit very nicely. It also fits around collagen.

From these cages you can build structures around a macromolecule like collagen. Such structures have a 10-fold symmetry as the collagen molecule has, and it has the repeating distance in the actual direction, which fits to this 28.6 Å of the collagen fiber. The amount of water that is present is equivalent to the amounts that you have at 100 per cent humidity and the native state. Thus, this structure could be there, but in a very labile form.

H. FERNANDEZ-MORAN: This model, Dr. Berendsen, as well as the other model that you propose, can actually be tested by electron microscopy and electron diffraction and I would highly encourage you to do so. We know it is possible to isolate collagen fibrils, to produce ice and to study the ice configuration around the collagen directly, both by direct transmission electron microscopy and electron diffraction and by the replica technique. Certainly this type of model that you suggest is within the range of our present techniques.

H. J. C. BERENDSEN: There is probably a great difficulty in doing this. This structure is very labile, and if you freeze it, you might well produce other structures of ice instead of this one which is more stable at lower temperatures. I am not sure that you will preserve this structure at low temperatures.

H. FERNANDEZ-MORAN: That holds true to a certain point only. Collagen happens to be one of the most hardy materials as far as freezing goes and there are already in the literature a number of pictures taken of rapidly frozen collagen that has been replicated and studied. Although I can see the difficulty, I believe an attempt should be made. Anything that can lead to a verification or a refinement of a model is welcome.

D. T. WARNER (*The Upjohn Co., Kalamazoo, Mich.*): We have found the stereo models of the water permit very free rotation around the various bonds. As we look at Berendsen's model we see that it has really five inter-fused boats of near neighborhood oxygens. In the stereo models, if you make the near neighbors oxygens, (six of them), in the boat form you find there is a lot of flexibility in this structure and this free rotation around each one of the bonds. On the other hand, if you take these six near neighbor oxygens and convert them over into the chair arrangement, then we have a completely rigid and stable mechanical form, no longer with a free rotation. Whether this has any significance in our thoughts about protein structure in the water relation, I am not sure.

One of the things that we can see in the ice structure is that in ordinary ice you have planes running in one direction all of which are chairs. When you look at the planes which run in the opposite direction, they are all boats. Ordinary ice is a mixture apparently of these two types, whereas in stable low temperature ice, each one of the arrangements of the six near neighbors is in the chair form exclusively. This will require a little thinking in terms of stability of chair and boats as applied to the cyclohexane system.

I have one other comment concerning our general thinking about the relation of centrally located oxygen which has four oxygens around it in tetrahedral configuration. Perhaps I tend to look at these things in too simplified a form, but let us just take that central oxygen which in the water structure is associated with two free hydrogens and two hydrogen-bonded hydrogens. When we replace that particular oxygen with a nitrogen we would find a situation in which the nitrogen furnishes no hydrogens to that arrangement of oxygens around it. In the case of HF it would furnish one hydrogen; in the case of water, two; in the case of ammonia, three, and in the case of methane, four. It seems to me that from our study of the interaction of these various components and the inserting of them in the water structure, some of the things that we see may be important. When we have water in contact with a biologic system, the possibility of draining off this resonant disturbance is always there. When we are dealing simply with a component in water, there may be no possibility of draining off this resonant disturbance thereby compelling us to do tremendous things like cooling it down or putting a tremendous pressure on it in order to achieve some sort of a crystalline form.

P. MAZUR (*Oak Ridge National Laboratory, Oak Ridge, Tenn.*): If one takes precautions to eliminate external ice, it is possible to supercool cells, many to minus 15 degrees and some to minus 30. This seems to me to indicate that cells do not contain effective nucleating agents since the cloud physicists and others who have studied the subject find that silver iodide will nucleate at  $-2^{\circ}$ ; in many compounds it will nucleate above  $-10^{\circ}$ . If the cell does not contain effective nucleating agents, does this not mean

that if ordered water exists, the lumps or patches in which it exists must be very small because the nucleating efficiency depends on the size of the particle and only large particles are effective nucleating agents at higher temperatures? If one does not have effective nucleating agents that are present, it means that they are either small, with radial curvatures, or else it means that the material has little crystallographic affinity to ice. Apparently there is also correlation between the nucleating ability of a substance and its crystallographic affinity to ice. One question I have in regard to this is, can clathrates nucleate supercooled water?

H. FERNANDEZ-MORAN: The point that Mazur raises is a very important one and we have puzzled about it a great deal. Could it not be that the moment you cool slowly, you do get instead of the diffused rings some sharpening of the diffraction rings. Could it not be that instead of getting ice, we still would get organized water, but not in domains but rather in sheets? This is a problem that I would like to pose to the physical chemists. Is it that supercooling enhances the organization of the water, but not necessarily in the direction of ice crystal formation?

P. MAZUR: All I can say about supercooled water is that it is supercooled in the sense that it gives up the full length of heat of fusion when it finally does freeze.

O. HECHTER: In the model of the cell membrane that we proposed previously, you notice that the ice was sandwiched between layers of macromolecules. This kind of ice might not readily be available for nucleating agents.

Recently, we have been looking at the water in mitochondrial membranes furnished by David Green. In effect we are trying to get at this problem with higher dilution NMR spectroscopy. We have made two preliminary findings that are interesting. We know the amount of water in the system by weight and when we do high resolution NMR spectroscopy, part of the water that should be registering as a proton signal just does not do so. Maybe it is highly structured. Quantitatively we cannot put a number on this, but there seems to be part of that.

Secondly, when we take mitochondrial membranes in sucrose and then begin to wash out the sucrose, using 98 per cent  $D_2O$  - 2 per cent  $H_2O$  and 0.1 M tetramethylammonium chloride, we are able to see two proton signals, one from the methyl group and one from the  $H_2O$  proton. We noticed at first that this is at least a three compartment system. There is water outside. There is water in the interior chamber and in the membrane phase. We noticed at first that most of the interstitial water is instantaneously replaced with  $D_2O$ . Despite seven washings of these mitochondria membranes with this salt mixture over a four-hour period, we still have a sizable fraction of water represented by  $H_2O$  protons that are still registering. It is very difficult to wash out all of the proton water from this

system. Despite this our evidence forces us to the fact that the methyl protons enter into the interior chamber and we are left with water in a membrane phase that just does not seem to exchange. We know the exchange reaction would be almost instantaneous; if the environment permitted. I am very hopeful that by pursuing this evidence we might be able to approach some aspects of this water in the membrane.

H. FERNANDEZ-MORAN: May I call on Dr. Meryman to speak about this problem of residual water that seems to be vital for the viability of a system?

H. T. MERYMAN (*Naval Medical Research Institute, Bethesda, Md.*): What is residual water? I would call this an unanswerable question unless you would consider speculation an answer. I would rather avoid that by making a general observation that has troubled me a little bit about the discussions that have been going on. The physical scientists are accustomed to measuring simple systems and the biologists are accustomed to describing complex systems. The term "interdisciplinary science" has become very popular and the assumption is that you can take these two groups, assemble them, and they will solve each other's problems. The trouble is that it is not possible to make a meaningful measure of a system once it gets too complex, because you do not really know what to assay. We have all seen examples of models which have attempted to model systems of somewhat more complexity than the physicist is accustomed to seeing. These models, from the biologist's point of view, bear no relationship to reality. On the other hand, we see biologists who are attempting to measure their complex systems without knowing what they are measuring. I believe that we have to be very guarded in our assumption that the great age of interdisciplinary science has arrived. We are going to have to approach it from both ends. The physical scientist has to make his measurements and in the long run we would hope to be able to measure the complex biological systems. I would not want to imply that the use of models is without value. On the contrary, I believe this is an extremely potent approach, but the models have to be restricted to a degree of simplicity that is meaningful. When the biologist attempts to quantitate, he has to know what his assay means. As an excellent example, almost all of the biologic measurements that have been made have used death of an organism as an index. Now what is death of an organism? As a practical example I can cite that no one has yet been able *in vitro* to freeze a mammalian tissue and bring it back without using additives. If you take a rabbit's foot, freeze it and thaw it, the foot dies. However, it has been shown quite recently that the cause for the majority of this injury in the intact animal is an interference with the circulation. If you maintain the circulation in the frozen rabbit's foot, the tissues will survive. In other words, it was the circumstances following thawing that determined whether

it would die or survive and not necessarily the freezing and thawing itself. We must say, therefore, that when something is killed, not that it has been killed, but that we have been unable to restore it to life under the circumstances of the experiment since we are dealing with a complex system that involves healing as well as deleterious reactions.

The word which I believe is of the greatest significance is the word 'systems.' The purpose of research is to understand nature and this implies function. We are not going to be completely satisfied by describing the shape of things because in the long run it is their function that we wish to understand.

H. FERNANDEZ-MORAN: Thank you very much for these salutary remarks, but you still have not answered the question of the residual water.

FELIX FRANKS (*Bradford Institute of Technology, Bradford, England*): I should like to come back to the transition temperature, the 60° which Luck discussed. This brings out one of the paradoxes. Recently, there have been some measurements made by George Walrafen at Bell Telephone Laboratories on the Raman spectrum of water. He arrived at the amazing conclusion that at about 60° there is hardly any hydrogen bonding left in water. That mainly poses the question, "What holds water together from there on?" Luck has presented infrared frequency data which are due to the cyclic hydrogen bond. This then shows that there is still considerable hydrogen bonding at the critical temperature of water. This is the other side of the paradox.

It seems that we do not know everything yet. We have the intensities and we have the frequencies, but we do not know exactly what they mean.

I have heard a lot to the effect that the water in biologic systems may not necessarily be the water that we recognize as coming out of the tap or down the drain. I believe there are certain properties which this water must show, and when we talk about structured water, there must be certain terms of reference within which this water can only be structured. One of them I would submit is this tetrahedral hydrogen bonding. Another is that if we believe in mixture models, there will still be flickering clusters of one kind and another. I believe just to shrug it off and say that water is different in the membrane or the cell, is not good enough.

H. FERNANDEZ-MORAN: I agree, and regarding the tap water of most cities, you would be surprised at the number of biologic systems it does contain.

PACKER: I wish to point out how seemingly insignificant alterations of the ionic composition of the freezing medium can effect the study of the effects of freezing and thawing of microorganisms, and perhaps tissues as well. This discussion reverts to yesterday's discussion by Mazur, who mentioned the extent of killing these by freezing and thawing was not altered by freezing different concentrations of yeast cells, but from the concentration

of solutes in which the yeast cells are frozen. He also mentioned that the concentrated suspensions of bacterial cells are more resistant to freezing and thawing than are dilute cell suspensions.

Previous investigators have found that the physiologic state of bacterial cells, for example *Escherichia coli* which grow in a complex, undefined nutrient broth in the experiments, affected the sensitivity to repeated freezing and thawing. Exponentially grown *E. coli* were approximately five times more sensitive than were resting stationary cells. Anaerobically regrown cells were 5 to 10 times more sensitive than the aerobically grown cultures. Ingraham and I have just shown that under strictly controlled conditions the rate of repeated freezing and thawing is not a function of initial concentration of cells frozen, nor is it a function of variation of the physiological state of the cells. These controls include, as Mazur indicated, freezing and thawing at a constant rate, keeping the time before plating constant, freezing and thawing in a medium, and thawing at a temperature that precludes rapid growth or increases in cell numbers. This is most critical and it is not usually observed.

We grew *E. coli* in buffered basal salts medium with glucose and carbon compounds under anaerobic conditions. Samples were obtained during exponential growth and during the stationary phase.

Cells were frozen to  $-78^{\circ}$  and thawed to  $11^{\circ}$ . There was no statistically significant differences in the slopes of the growth curves. Death by complete freezing and thawing is not due to lysis alone.

Unless one controls the ionic composition of the freezing medium you can get all kinds of killing rates and cannot quantitatively study this effect. One way is by washing. Another way is by nonionic composition, but you have to know the extent of washing.

O. HECHTER: Previously we talked about the possible significance of water structures in the cell and their implications for active transport. I wonder, Dr. Ling, what in your opinion has evolved from this Conference concerning active transport, and whether there has been any reconciliation anywhere along the line with regard to the subject?

G. N. LING: As to the physical state of water in the living cell, I believe the great weight of discussion has centered around the cell membrane, which is usually considered about 100 Angstrom units thick. For example, a muscle cell which is 60  $m\mu$  across, constitutes 1000th of the total protoplasm. Consequently the question still remains, what is the state of water in the living cell? I mean, the remainder of the cell.

The theses which we have presented very rapidly have not reached very many people. It is asking too much. But, basic issues can be discussed somewhat more clearly and without a great deal of controversy. If one assumes the water inside the cell to be free water, then one has to provide energy for all the parts of the cell and so far the question of the demand

for energy of total metabolism of the cell has never been answered. This question has been raised since 1951. I still have not seen a paper which has answered this question. Therefore, I once more make a plea for those people who do not want to accept an idea which has been proposed to please come out and answer it. Have we done it wrongly or are there some "loop-holes" in our argument? Perhaps we can work it out. I am very conciliatory in every sense. In fact, I have never been otherwise in this regard.

The other side of the picture showed that the cell membrane which contains proteins with ionic groups follows a certain behavior. This behavior can be entirely duplicated by the ionic behavior of a piece of ion exchange resin, of sheep's wool, and dried collodion. None of these contain, of course, living processes. Yet, kinetically, the ion behavior pattern is entirely identical. In fact, from these kinetics one can derive that this arises from the association of these ions and nonelectrolytes with surface sites. The behavior of these surface sites quantitatively again matches with the total equilibrium distribution patterns of the entire protoplasm, which I showed yesterday. Quantitatively as well as qualitatively there is accord between the behavior of the cell membrane and the inside of the cell.

If we accept a picture which Hechter showed yesterday, the negative ionic side chains would have something to do with the ionic property of the cell surface. The ionic side chains bearing negative charge can only belong to the beta and gamma carboxyl groups of the proteins in the membrane. The same gamma carboxyl groups must be found also in the living cell bulk. In fact, since the analysis of muscle now is almost complete, we know exactly how many carboxyl groups can be counted in the cell cytoplasm. This amounted to about 300 millimoles per kilogram of fresh weight. The actual maximum number of sites which is determined from our equation is that typical of Langmuir's adsorption isotherm. The total number of maximum sites determined is 250. So, there is a good concordance both qualitatively and quantitatively.

Up to now the model, for example, of sheep's wool, contains all the characteristics — although not exactly quantitatively the same, but qualitatively — equivalent to the behavior of the living cells. I am making this plea to the people who have taken the opposite view, in the hope they will consider this proposal and look into what pattern bothers them in the energetic aspect, and perhaps answer us.

O. HECHTER: I would like to call on Dr. Fernandez-Moran to make a few comments about the transducing devices in membranes, because I think that with his techniques he has opened a way at least to begin to approach the ultrastructure arrangement of these devices, and I think it is very appropriate that he make several comments about it.

H. FERNANDEZ-MORAN: I had envisaged a real discussion between the two opponents, if I may call them such, G. N. Ling and A. Leaf, because

more is really at issue than just the active transport in the membrane. We have merely made some preliminary excursions in association with David Green and his associates who really have done the biochemistry.

Essentially what it boils down to is this. We have evidence both from the biochemical and ultrastructural side that in the membranes, at least in one type of membrane that we have studied extensively, namely the mitochondrial membrane, there are multienzyme complexes which in the process of playing a major role in the production of ATP, electron transport and oxidative phosphorylation, also mediate and in effect act as ion pumps. This means that the membrane is much more active than we thought, and I am sure that this will shed light on many problems.

This is a fragment of a much greater problem, one that is at the center of research and controversy in nerve physiology and in so many other fields. Personally, I am sorry that we do not have either the time or the participants to bring this out. My own view is that like everything it will be neither black nor white, but gray. In fact, it will be watery gray. Water will play a very significant role in this whole theory of energy transduction.

D. T. WARNER: I would just like to mention one aspect about our model that is delaying water between protein layers. It has to do with the possible mechanics, shall we say, on the molecular level. I believe the way we would like to look at this is that the carbonyl oxygen in the peptide linkage is not a completely nonionic situation. It has the possibilities of going from, shall we say, keto to an enol form. We have pointed out these possibilities in the paper dealing with carbohydrates and they may have been overlooked by some of the people in the protein field.

If you take a layer of water and attach it to a peptide surface, with carbonyl oxygens in the enol form, you have the possibility of having an upper peptide layer and a lower peptide layer with two layers of water between. The distance is about 6.8 Angstrom units. If you convert this carbonyl oxygen into the keto form, then the water will rearrange itself. You will still have two layers between the two peptide layers, but the distance between the peptide layers now becomes about 4.8–4.9 Å. In our model we have the possibility for a sort of a contraction phenomena, which would simply be brought about by pH changes, which might be at local sites due to local acidity such as the release of phosphate groups.

I believe when we are talking about membrane openings and things that might produce membrane openings, we have to begin to think about the mechanics on the molecular level. Similarly, we must do this in the case of some of the sugars where we have these rigid cyclohexane rings with hydroxyls in either the equatorial or the axial position. In the case, for example of myoinositol, which has only one axial hydroxyl not being capable of making contact with one of the oxygens of the water structure in the water model, the axial hydroxyl is preferentially oxidized in the



system. As a result it becomes a keto-oxygen which comes much closer to fulfilling a favorable interaction with the water structure. By the consequence of having oxidized it, we have introduced not only an energy into that system, but also a different ordering of the water molecules around it. I believe some of these things should be begun to be thought of in the terms of the mechanics at the molecular level, if we are going to be molecular biologists.

H. FERNANDEZ-MORAN: Thank you, Dr. Warner. I could not agree with you more. In fact, the work I alluded to previously on the multienzyme complexes that we are working on with Green, and on a newly isolated contractual protein, go precisely in this direction.

COLACICCO (*Albert Einstein College of Medicine, Bronx, N.Y.*): I should like to ask Henry Frank with regard to the concept of structure meeting and structure breaking of urea. We know that if we go from water to ice, the dielectric constant increases. We also know that if we take a urea solution, urea increases the dielectric constant of water. Have you any comment on or any explanation for this increase in the dielectric constant of water by urea with respect to the structure making and structure breaking?

H. S. FRANK: I do not think they are directly connected. When you have a mixture in an electric field, there are contributions from all of the species which are present. In pure liquid water some of the dielectric constants come from the reorientation of the unstructured material and some come from the flickering of Bjerrum salts in the structured material. When you have urea present, some will come from urea orientation of water. Urea happens to have a pretty big dipole moment. If I am right, it is in the midst of a region where there is no structure. It would be very free to rotate and this would fit in nicely enough with the high dielectric constant.

DR. COLACICCO: The importance of dipole-dipole and charge-charge interactions in water has strongly been overlooked by the students of the structure of water who have put tremendous emphasis on hydrophobic bond theory.

I have mentioned to H. A. Scheraga that I have landed on the other extreme end of the molecule that is on the head charge or on the head group. In that respect, I incline to visualize the iceberg structure of water not so much around the nonpolar site of the molecules, but around the polar site of the molecule. Phenomenal electrostriction, I believe, is worthy of investigation. Kauzmann has initiated some studies in that direction but we have not heard much more in the sense that probably work in that direction will bring some conflict between the hydrophobic bond theory and the possibility of a hydrofluoric bond theory. I wonder if H. Frank would be generous enough to comment on this possibility?

H. S. FRANK: You have these polyfunctional solutes. It is quite true that what one end of the molecule does with water may be different from what

the other end of the molecule does. In concentrated solutions these will interact in ways that are exceedingly complicated. I agree with you that we have not reached the place of being able to make a really clear picture of all these interactions, in particular about electrostriction.

On the molecular level, I am very far from being sure that I understand what is means, but it obviously takes place.

R. STOWELL (*Armed Forces Institute of Pathology*): I would like to ask several questions of P. J. Melnick for purposes of clarification of his presentation.

First, it was not clear to me to what extent his results showed the variability between different tumors in their enzyme content, which is the well known phenomena, and to what extent he showed the effect of freezing alone with control of other variables upon the enzyme content.

I would like to know whether he can clarify for us his comment that the histochemical results are well known to not be highly quantitative as compared with biochemical results. Does he have controls which would include free substitution, freeze drying, chemical fixation or biochemical determination in his work? This would give us a better idea as to how much of the variation might be due to the techniques which he was employing.

Along a similar line, what is his estimation of the extent of variability which might be introduced into his work of uncontrolled things, such as the postmortem interval, the storage under frozen conditions such as 79°, the rate of thawing, and the repeated freezing and thawing, if it were employed? All of these are known to make very substantial reductions in certain enzymes under certain conditions.

P. J. MELNICK (*Veterans Administration Hospital, Oakland, Calif.*): The pathologist is in a difficult position, being in the middle, between the clinician and the basic scientist. He must interpret one to the other and when he tells a clinician that a method has a factor of error of plus or minus 10 per cent, this is often acceptable in a dynamic system such as the human organism. But, a physicist may be quite shocked, because he can make fantastic measurements accurately.

In response to Stowell's questions, time will not permit going into detail, but the basic finding was that the tissues, tumors, frozen slowly showed either a diminished or absent reactivity by the application of histochemical implant techniques. Those frozen rapidly by being dropped into isopentane at -160°C. showed the full range of activity.

I made use of a number of controls, fresh animal tissues, human tissues, surgical specimens, and autopsy material, varying lengths of time and so forth. The one variable was the difference in the freezing rate. It was impressive to see how intact enzyme activity was in tissues even many hours after — in postmortem tissues, for example, as long as 18 and even 24 hours after death, as long as the tissue was kept at 5°C.

What I have told you is true for both the hydrolases and the dehydrogenases, but exactly the opposite is true for cytochrome oxidase. Freezing crystallized and sequestered cytochrome C so that it was unavailable as the substrate for the enzyme.

By adding cytochrome C to the incubating system the full activity resulted and this is, of course, understandable with such a key enzyme. May I suggest that although water is the universal medium in which all life exists, we would also be justified to turn out attention to other substances in living cells that are also effected by cryogenic modalities.

H. FERNANDEZ-MORAN: Thank you very much. Unless there is a very pressing point that remains to be discussed I thank the field. Much as I would like to continue, I understand that the cryobiologists will have a meeting tomorrow and they will have a chance to continue their discussion.

May I now turn the meeting over to J. Flynn.

JOHN FLYNN: (*Office of Naval Research Branch Office, New York, N. Y.*): Now that the moment of adjournment is finally reached, I would like on behalf of the conveners of this Conference to express to all of you a very warm appreciation for all that you have accomplished in the last three and a half days. It has more than met our expectations. It has confirmed amply our belief that a Conference on the Forms of Water in Biologic Systems, dealing as this has done with fundamental issues of physics and physical chemistry and biological sciences, would be instructive and profitable.

I would like also to say a word of thanks to all of those whose support and generosity has made this Conference possible, to The New York Academy of Sciences which carried the major financial load, to its supremely effective, efficient Executive Director, Mrs. Miner, and to Admiral Schantze, who for a number of years has been doing an admirable job in managing conferences, for their many courtesies and for the fine and efficient manner in which they handled all the innumerable details, to the National Aeronautics and Space Administration which contributed heavily. I must say, also, a word of appreciation and thanks to my colleagues in the Office of Naval Research, who have responded generously to my request for participation; to the Session Chairmen, who have done a marvelous job; to the speakers, and I wish there had been more time and more of them; and to all participants.

In a moderately long and largely misspent life, filled with too many conferences, I think I have never in my life attended a conference in which the general level of interest remained as high as in this. The ball was kept bouncing at all times. There was always something of interest to discuss.

I leave it with the profound conviction that the influence of this Conference will be felt in biological sciences for years to come. To all of you, I thank you, and auf Wiedersehen.